



**SUMMER SCHOOL IN ELEMENTARY PARTICLE PHYSICS**  
**Theories of Strong Interactions at High Energies**

**Held at**

**Brookhaven National Laboratory**

**July 22 - August 29, 1969**



**BROOKHAVEN NATIONAL LABORATORY**  
**ASSOCIATED UNIVERSITIES, INC.**

under contract with the

**UNITED STATES ATOMIC ENERGY COMMISSION**

**SUMMER SCHOOL IN ELEMENTARY PARTICLE PHYSICS**  
**Theories of Strong Interactions at High Energies**

Held at

Brookhaven National Laboratory

July 22 - August 29, 1969

**RONALD F. PEIERLS, EDITOR**

**BROOKHAVEN NATIONAL LABORATORY**  
**UPTON, NEW YORK 11973**

## LEGAL NOTICE

This report was prepared as an account of Government sponsored work. Neither the United States, nor the Commission, nor any person acting on behalf of the Commission:

A. Makes any warranty or representation, expressed or implied, with respect to the accuracy, completeness, or usefulness of the information contained in this report, or that the use of any information, apparatus, method, or process disclosed in this report may not infringe privately owned rights; or

B. Assumes any liabilities with respect to the use of, or for damages resulting from the use of any information, apparatus, method, or process disclosed in this report.

As used in the above, "person acting on behalf of the Commission" includes any employee or contractor of the Commission, or employee of such contractor, to the extent that such employee or contractor of the Commission, or employee of such contractor prepares, disseminates, or provides access to, any information pursuant to his employment or contract with the Commission, or his employment with such contractor.

Printed in the United States of America

Available from

Clearinghouse for Federal Scientific and Technical Information  
National Bureau of Standards, U.S. Department of Commerce  
Springfield, Virginia 22151

Price: Printed Copy \$3.00; Microfiche \$0.65

February 1970

920 copies

## FOREWORD

A theoretical physics summer school on "Strong Interactions at High Energies" was held at Brookhaven National Laboratory from July 23 through August 29, 1969. This was the first such summer school to be held at Brookhaven and these notes are the written version of its contents.

Two major aims of the school were to restrict the subject matter to a well defined area which could be covered in depth, and to obtain a small, homogeneous class which would interact strongly with the lecturers. Accordingly the number of students was restricted to 20, and closed circuit TV and videotapes were used to allow others and any non-students, to observe the lectures, without diluting the small class. This procedure appeared to work successfully, due in no small measure to the high calibre and enthusiasm of the students and lecturers.

These notes have been edited and in some cases extensively revised by the lecturers from notes taken by students in the school. Much gratitude is due to them for the amount of work put into the preparation and the gallant efforts of most to get the job done quickly. The herculean task of organising the preparation of the manuscript, as well as carrying out much of the actual typing, was tackled by Mrs. Patricia Towey with an appearance of effortlessness completely belying its magnitude.

## CONTENTS

<u>LECTURE I</u>	1
Some Experimental Topics in High Energy Interactions	
D. Hywel White, Cornell University	
<u>LECTURE II</u>	73
Rigorous Properties of Amplitudes at High Energies	
N. N. Khuri, Rockefeller University	
<u>LECTURE III</u>	121
Dynamical Models Based on Classical Limits	
Richard C. Arnold, Argonne National Lab	
<u>LECTURE IV</u>	159
Formalism and Phenomenology of Complex Angular Momentum	
Kerson Huang, MIT	
<u>LECTURE V</u>	249
Dynamical Models Based on Unitarity and Analyticity	
W. R. Frazer, Univ. of California, La Jolla	
<u>LECTURE VI</u>	287
Multiperipheral Dynamics	
Geoffrey F. Chew, Univ. of California, Berkeley	
<u>LECTURE VII</u>	385
Recent Developments	
Haim Harari, Weizmann Institute of Science	

LIST OF ATTENDEES

Aldins, Janis	Cornell University
Boyer, Charles	Pennsylvania State University
Budny, Robert V.	University of Maryland
Campbell, David K.	Churchill College, Cambridge, England
Derman, Emanuel	Columbia University
Farrar, Glennys	Princeton University
Grammar, Garland	Virginia Polytechnic Institute
Green, Michael B.	University of Cambridge, England
Hacinliyan, Avadis	University of Chicago
Hari Dass, N.D.	University of California, Santa Barbara
Holm, Darryl D.	University of Michigan
Krinsky, Samuel	Yale University
Paige, Frank E.	Massachusetts Institute of Technology
Pardee, William J.	University of Illinois
Rosenzweig, Carl	Harvard University
Simon, Barry	Princeton University
Sukhatme, Uday P.	Massachusetts Institute of Technology
Yang, Tsih-Chiang	University of Rochester
Yesian, Harry J.	University of California, La Jolla
Yu, Loh-ping	University of California, Berkeley
Zarmi, Yair	Weizmann Institute of Science



SOME EXPERIMENTAL TOPICS IN HIGH ENERGY INTERACTIONS

Lectures by:

D. Hywel White  
Cornell University





## INTRODUCTION

We have chosen a number of topics in high energy interactions in which, in our opinion, the experiments are capable of unambiguous interpretations and moreover are fairly precise. The topics we have chosen are:

1. Total Cross Sections
2. Forward Elastic Scattering
3. Backward Elastic Scattering
4. Two body Inelastic Processes
5. Multiparticle Production

They have formed the body of five lectures and our mandate was taken as that we should try to describe the experimental data with real emphasis on its strengths and weaknesses. It is not intended as a review but as a starting point in the study of high energy processes. In this vein we would write down here some appropriate expressions valid at high energy which are useful in thinking about these experiments. We shall use units in which masses and momenta are measured in GeV.

When the incident particle has a momentum  $p_{\text{LAB}}$ , and the target is a proton, the c.m. energy squared

$$s \approx 2m_p p_{\text{LAB}}$$

the term we miss is the sum of the squares of the masses. So even better

$$s = 2p_{\text{LAB}}^2 \quad (1)$$

is quite accurate in our momentum range.

The momentum of either particle in the c.m. system

$$K^2 = \frac{[s+(m_i-m_p)^2][s-(m_i+m_p)^2]}{4s} \approx \frac{s}{4} \quad (2)$$

For elastic scattering the invariant 4 momentum transfer

$$-t \approx \frac{s}{2}(1-\cos\theta) \quad (3)$$

The invariant crossed 4 momentum transfer

$$u \approx \left(\frac{s}{2}-m_p^2\right)(1+\cos\theta_{\text{c.m.}}) - \frac{m_p^4}{2s} \quad (4)$$

If you check you will find that  $s+t+u \neq \Sigma m^2$ , that is because these approximate expressions are only valid where  $\Sigma m^2$  is not important.

At small angles

$$|t| \approx \frac{s \cdot \theta^2}{2 \cdot 2} = k^2 \theta^2 = (p_{\perp})^2$$

$$p_{\perp} \approx (-t)^{\frac{1}{2}} . \quad (5)$$

This little expression accounts in part for the difficulty in choosing the appropriate argument against which to plot cross sections.

The velocity of the c.m.,

$$\gamma_{\text{c.m.}} = \frac{W+m_p}{(s)^{\frac{1}{2}}} \quad \begin{array}{l} W \text{ the total energy of the} \\ \text{incident particle} \end{array} .$$

At high energies

$$\approx \frac{(s)^{\frac{1}{2}}}{2m_p} . \quad (6)$$

To transform angles from c.m. to the laboratory system

$$\tan \theta_{\text{LAB}} = \frac{p \sin \theta_{\text{c.m.}}}{\gamma (\beta W + p \cos \theta_{\text{c.m.}})} \quad \begin{array}{l} p \text{ the momentum of the} \\ \text{particle in the c.m. system.} \end{array}$$

at high energies and small angles

$$\theta_{\text{LAB}} \approx \frac{\theta_{\text{c.m.}}}{2\gamma} . \quad (7)$$

Many of the original expressions are contained in the Rosenfeld tables. We have simply adapted them to the high energy, small angle limit.

## I. TOTAL CROSS SECTIONS

The total cross section is undoubtedly the most accurate measurement in high energy physics. This being so, we become more preoccupied with the systematic errors in the experiment for the statistical errors are usually very small. We shall try to indicate the problems in assessing the systematic accuracy. Measurements have been made on all the "stable" particles that can be made at an accelerator and a start has been made on one of the unstable particles, namely the  $\rho$ . The particles that are made in beams and have their cross sections measured at high energies are

proton, antiproton  
neutron  
pion (+ and -)  
K (+ and -).

We shall discuss some of the experiments in detail, and we plot a selected set of accurate measurements by incident particle.

Figure 1 represents a typical experiment. It is taken from reference 11. Notice that the diagram is not to scale in the sense that portions of the dimension

parallel to the beam are omitted. The counters  $S_1$ ,  $S_2$  and  $S_3$  define the beam. That is, a signal appears when a particle traverses both counters within a short time, the resolving time of these two counters. We hypothesise in analysing the experiment that there is one particle only present at a time in the apparatus, and we ask if the particles leaves the beam before it reaches  $S_4$  to  $S_{12}$ . The criterion for an interaction is that the particle suffers some angular deviation and of course that means that we include some of the Coulomb interaction and we have to correct for this. Because the counters  $S_4$  to  $S_{12}$  subtend different solid angles at the target we can extrapolate to zero angle of deflection. In order to correct for the Coulomb interaction we have to know the angular divergence of the beam and its spatial density distribution at  $S_3$ . Although  $S_1$ - $S_3$  are called defining counters and  $\bar{G}$  assures us that there is no particle in the halo associated with the beam, in fact the density distributions for particles at  $S_3$  are primarily determined by the optics of the beam transport system and these must be understood. These problems which are difficult in detail are coped with in part because the corrections can be made small by designing the sizes of the counters with care. An example of the extrapolation technique is shown in Fig. 2.

The slope of this curve comes from the angular distribution of both the elastically scattered particles and the particles produced inelastically in the target. Typically this curve is fitted to a quadratic in the solid angle and the constant in this polynomial gives the attenuation by strong interactions. Corrections have been made for single and multiple Coulomb scattering and for Coulomb-nuclear amplitude interference. The real part is estimated from dispersion relation calculations. Examples of the estimates are given in Fig. 3.

Given the attenuation ( $t_e/t_f$ ) the cross section is given by

$$\sigma_T = \frac{1}{N \cdot l} \ln(t_e/t_f).$$

The fact that  $N$ , the number of nucleons/sqcm, and  $l$ , the length of the target, appear directly in this formula means that they must be known to comparable accuracy to produce a total cross section.  $N$  is controlled by controlling the pressure of the liquid and  $l$  must be measured cold.  $t_e$ , the attenuation of the empty target must be the same as  $t_e$  for the full target when empty; this is checked in these experiments. The reason for the three interchangeable targets is so that conditions in a particular target vessel are stable and so the time spent in waiting for stability is saved when the target can be moved.

The counter C is a Cerenkov counter which is sensitive to the angle  $\theta$  of the Cerenkov radiation. A particular  $\theta$  is selected by a diaphragm in the optical system and the effect of moving that diaphragm is shown in Fig. 4. It is clear that when set to the K meson position the contamination of pions is very small. The Cerenkov counter technology is such that all the stable particles, with the exception of muons

and electrons, can be separated to sufficient precision in our energy region. Remember that the Cerenkov angle  $\theta$  is given by

$$\cos\theta = \frac{1}{n\beta}$$

$n$  is the refractive index of the radiating material, and  $\beta$  the velocity of the particle. The difference in velocity of pions and muons is so slight at high energies that separation is too difficult. The muon and electron contamination in the beam is measured separately and since they do not interact strongly a correction is made. Frequently the muon contamination is measured by passing the beam through many strong interaction lengths of material, only the muons emerge to be counted.

We are ready to review the cross section data, at least as far as the charged particle cross sections are concerned.

#### 1. Proton-Proton

References 1, 2, 8, 9.

The first reference, Barashenkov and Maltsev, is a suitable introduction and represents the state of the art in 1961. Bugg et al.<sup>3</sup> have made measurements up to 8 GeV/c; Foley<sup>8</sup> and Galbraith<sup>9</sup> have measured up to 30 GeV/c. The graph of Fig. 5 is a composite plot of all the pp data of superior accuracy with cross section plotted against the logarithm of  $s$ , the c.m. energy squared. The only feature that stands out is the rapid rise at about 500 MeV/c followed by a levelling off to about 38 mb. Between 16 and 22 GeV/c incident momentum the cross section is flat within the errors of the Galbraith<sup>9</sup> experiment. The rapid rise has been associated with the opening of the inelastic channels, particularly  $N^*(1236)$  production. The total cross section is essentially constant above about 15 GeV/c, and as far as anybody has been able to see there are no high mass dibaryon resonances.

#### 2. Pion-Proton

References 4, 5, 7, 9.

Here the situation is quite different. The composite cross sections are plotted in Figs. 6 and 7. At low energies there is a good deal of structure corresponding to the excitation of baryon resonances, this has been a very fruitful method of finding these. However, above 5 GeV/c there is little evidence for bumps in the total cross section and the energy dependence becomes smooth. The experiments of Foley et al.<sup>7</sup> are very accurate and show a cross section still falling slowly at 30 GeV/c. Moreover the positive and negative pion cross sections are still different by  $\sim 1.6$  mb and not showing signs of becoming equal very rapidly. By fitting their data Foley et al. came to the conclusion that the pion cross sections became energy independent and equal at very high energies indeed. Preliminary data from Serperkov on  $\pi^-p$  are also shown in Fig. 7 and seem to indicate a rather dramatic flattening of the cross section in disagreement with the fit. It is clear that the

total cross sections at Serperkov will be very interesting indeed.

Before we leave pion-proton cross sections we should note that Foley et al. used a method for getting the total cross section that is, in principle, more reliable than the method we have already described. The method is described in reference 7 and we shall discuss it in detail when we discuss the measurement of the real part of the forward scattering amplitude. Suffice to say that although the agreement is not exact, the data of Galbraith et al.<sup>9</sup> and Foley et al. seems to indicate the cruder method is reliable, at least to the accuracy claimed by Galbraith.

### 3. Antiproton-Proton

There is discernible structure to the  $\bar{p}$ -p cross section at lower energies that is attributed to the formation of boson resonances. The low energy situation is summarised in Abrams et al.<sup>12</sup> and the composite plot is in Fig. 8. The high energy data comes from Galbraith<sup>9</sup> and seem to be steadily decreasing from 10 to 20 GeV/c. The cross section is  $\sim 50$  mb in this region compared to 38 mb for pp. One will need to go to very high energies indeed for these two cross sections to become equal from the rate at which they are converging in this energy region.

### 4. Kaon-Proton

The  $K^-p$  system is known to resonate through the  $Y^*$ , strangeness -1 baryon states. This is reflected in the low energy structure in Fig. 9. This structure dies away and with the new Serperkov data is seen to be quite flat above 20 GeV/c. Again as in  $\pi^-p$  the previous Regge pole fits would not expect the cross section to level off as it does. The  $K^+p$  system does not have strongly coupled resonances and the data in Fig. 10 are reminiscent of the pp case. There has been a good deal of discussion of a bump at  $\sim 1.2$  GeV/c incident momentum, or about  $1.9$  GeV/c<sup>2</sup> total c.m. energy. It is referred to as the  $Z^*$ , we shall mention it again in the context of the energy dependence of backward elastic  $K^-p$  scattering. Apart from this structure the  $K^+p$  system settles down at a very low energy.

### 5. p-n

We should now discuss how to get cross sections using a deuterium target. Since free neutrons are hard to find, many total cross sections are measured using the neutron in deuterium. There are two difficulties.

a) There is a screening correction, originally due to Glauber, modified by Wilkin. We mean by this that both the incoming and outgoing particles can interact with the spectator proton and this effect reduces the effective amplitude associated with the incoming beam.

b) Fermi motion of the nucleons. The neutron bound in a deuteron is not at rest so that the c.m. energy of the incident particle-neutron system is not well defined. It is equivalent to an experiment with a less well defined incident beam momentum. This effect is not important at high energy where the cross section is

slowly varying but it is important where there is structure. Kriesler et al.<sup>10</sup> observe that this energy spread is comparable to the energy resolution they have achieved in a neutron beam in a direct n-p total cross section experiment. This seems to come down in favour of a direct experiment, at least in the np case. It is more time consuming to do a n-p experiment to the same accuracy as p-n.

The screening correction appears approximately in the form

$$\sigma(c,d) = \sigma(x,p) + \sigma(x,n) - \frac{1}{4\pi} \langle r^{-2} \rangle (\sigma(x,p) \times \sigma(x,n) - \frac{4\pi}{k^2} \text{Re}f_{xp}(0)\text{Re}f_{xn}(0)) .$$

At high energies the term involving the real part is negligible.

$\langle r^{-2} \rangle$  is a parameter that describes the average spacing of the two nucleons in the deuteron. This can be calculated assuming various wave functions giving results which vary from 0.020 to 0.035 mb<sup>-2</sup>. If we measure  $\pi^+p$  and  $\pi^+D$  cross sections and assume charge independence then since we have only two amplitudes we can deduce a value of  $\langle r^{-2} \rangle$  from experimental data. Such a curve is shown in Fig. 11, taken from reference 4. It is clear that the variation of the screening parameter with energy leaves one uncertain about the validity of the theory, but it is probably alright to use this correction for other reactions at the same energy, particularly if we can perform the p-n and n-p experiments separately and check the answer.

The p-n experiment is done by measuring the p-d total cross section exactly as we have described previously. The n-p experiments we now describe.<sup>6,10</sup> The experiment of Kriesler et al. is shown in layout in Fig. 12. A neutral beam is made by making a carefully aligned hole in the shielding wall of the accelerator facing the target. Charged particles are swept out and a neutron and  $K_L^0$  beam of wide energy spectrum emerges. The  $K_L^0$  contamination is negligible for our purposes. To measure the cross section it is necessary to measure the neutron energy. Kriesler et al. do this with a calorimeter, this device samples the energy deposited between slabs of iron by the strongly interacting shower. By adding together the energy deposited in all 5 counters T<sub>1</sub>-T<sub>5</sub> we have a measure of the neutron energy. They claim that the uncertainty in neutron momentum gives a comparable uncertainty in s to that introduced by the Fermi-momentum in the "p-n" case.

Figure 13 shows a comparison of the "p-n" and n-p measurements. The situation is satisfactory, but more accurate measurements of n-p cross sections are probably called for. In the region above 5 GeV/c p-p, p-n and n-n total cross sections are equal.

#### 6. $\bar{p}n$

This cross section has not been plotted separately, for up to the uncertainty

of the screening correction the "pn" cross section is equal to pp at momenta above 5 GeV/c.

#### SUMMARY

With the exception of the nucleon-nucleon cross sections and antinucleon nucleon cross sections, all total cross sections are slowly varying above 10 GeV/c incident momentum and  $\pi^-p$  appears to be quite flat between 30 and 60 GeV/c. It is true that in this energy region we do not appear to have particle-antiparticle cross sections equal and it may be that this never becomes true. In the case of pions, if we believe the present data very funny things must happen for this equality to be met. In an even more pronounced way the  $K^+p$  cross sections do not become equal even though they seem energy independent.

#### REFERENCES

1. V.S. Barashenkov, V.M. Maltsev, Fortschr. Phys. 9, 549 (1961).
2. D.V. Bugg, D.C. Salter, G.H. Stafford, R.F. George, K.F. Riley and R.J. Tapper, Phys. Rev. 146, 980 (1966).
3. D.V. Bugg, R.S. Gilmore, K.M. Knight, D.C. Salter, G.H. Stafford, E.J.N. Wilson, J.D. Davies, J.D. Dowell, P.M. Hattersley, R.J. Homer, A.W. O'Dell, A.A. Carter, R.J. Tapper and K.F. Riley, Phys. Rev. 168, 1466 (1968).
4. A.A. Carter, K.F. Riley, R.J. Tapper, D.V. Bugg, R.S. Gilmore, K.M. Knight, D.C. Salter, G.H. Stafford, J.D. Davies, J.D. Dowell, P.M. Hattersley, R.J. Homer and A.W. O'Dell, Phys. Rev. 168, 1457 (1968).
5. A. Citron, W. Galbraith, T.F. Kycia, B.A. Leontic, R.H. Phillips, A. Rousset and P.H. Sharp, Phys. Rev. 144, 1101 (1966).
6. J. Engler, K. Horn, J. Konig, F. Monnig, P. Schludecker, H. Schopper, P. Sievers, and H. Ullrich, Physics Letters 27B, 599 (1968).
7. K.J. Foley, R.S. Jones, S.J. Lindenbaum, W.A. Love, S. Ozaki, E.D. Platner, C.A. Quarles and E.H. Willen, Phys. Rev. Letters 19, 330 (1967).
8. K.J. Foley, R.S. Jones, S.J. Lindenbaum, W.A. Love, S. Ozaki, E.D. Platner, C.A. Quarles and E.H. Willen, Phys. Rev. Letters 19, 857 (1967).
9. W. Galbraith, E.W. Jenkins, T.F. Kycia, B.A. Leontic, R.H. Phillips, A.L. Read and R. Rubinstein, Phys. Rev. 138, B913 (1965).
10. M.N. Kriesler, L.W. Jones, M.J. Longo and J.R. O'Fallon, Phys. Rev. Letters 20, 468 (1968).
11. R.L. Cool, G. Giacomelli, T.F. Kycia, B.A. Leontic, K.K. Li, A. Lundby, J. Tieger and C. Wilkin, Phys. Rev. (to be published).
12. R.J. Abrams, R.L. Cool, G. Giacomelli, T.F. Kycia, B.A. Leontic, K.K. Li and D.N. Michael, Phys. Rev. (to be published).



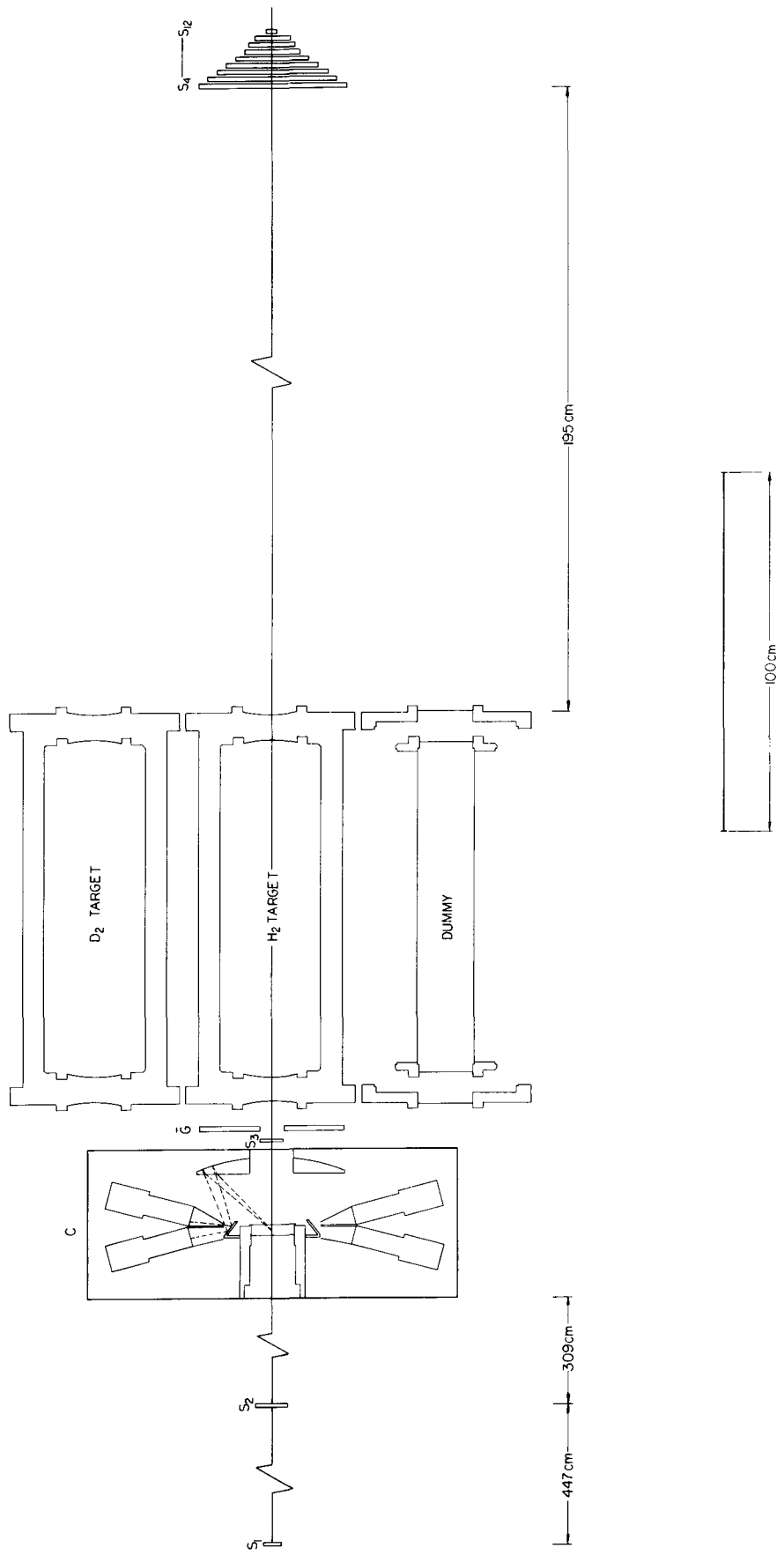
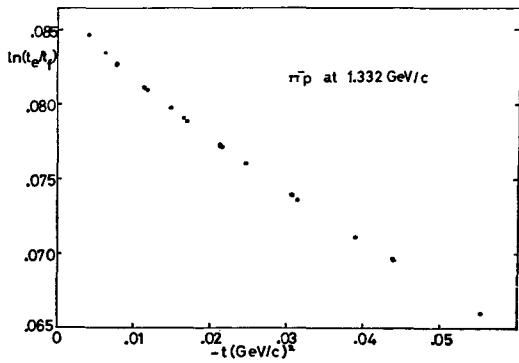


Figure 1.



The form of the extrapolation to zero solid angle over an extended range at 1.332 GeV/c. A small correction has been applied to the value obtained from each counter to allow for the absorption of scattered particles in preceding counters.

Figure 2.

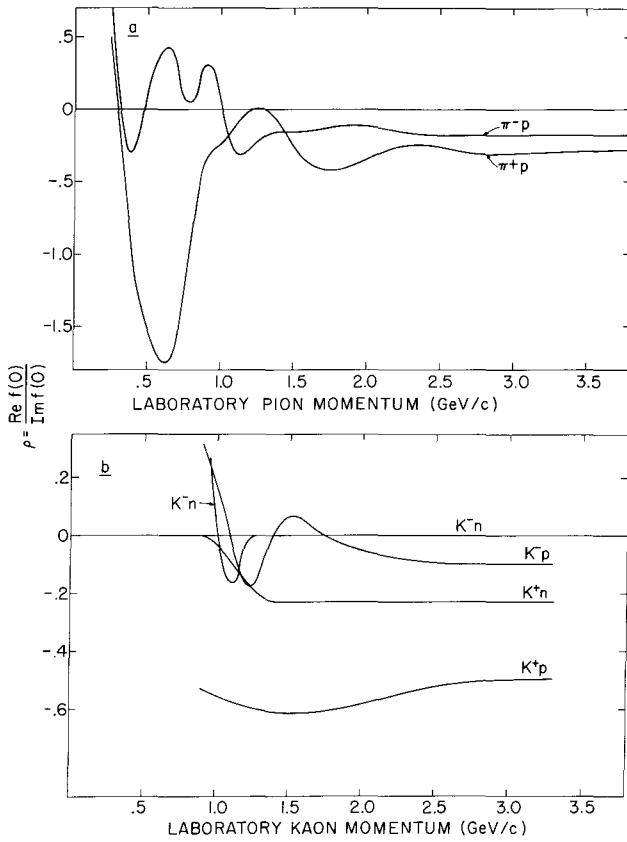


Figure 3.

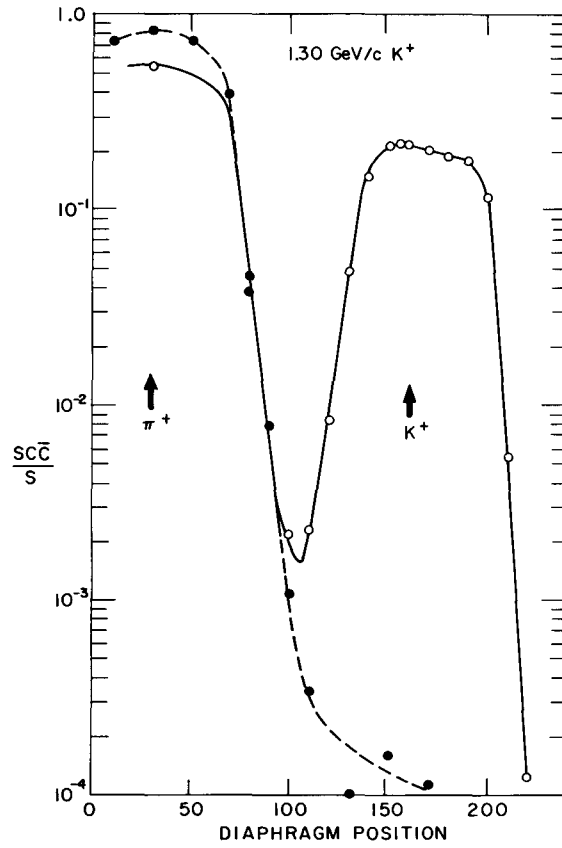


Figure 4.

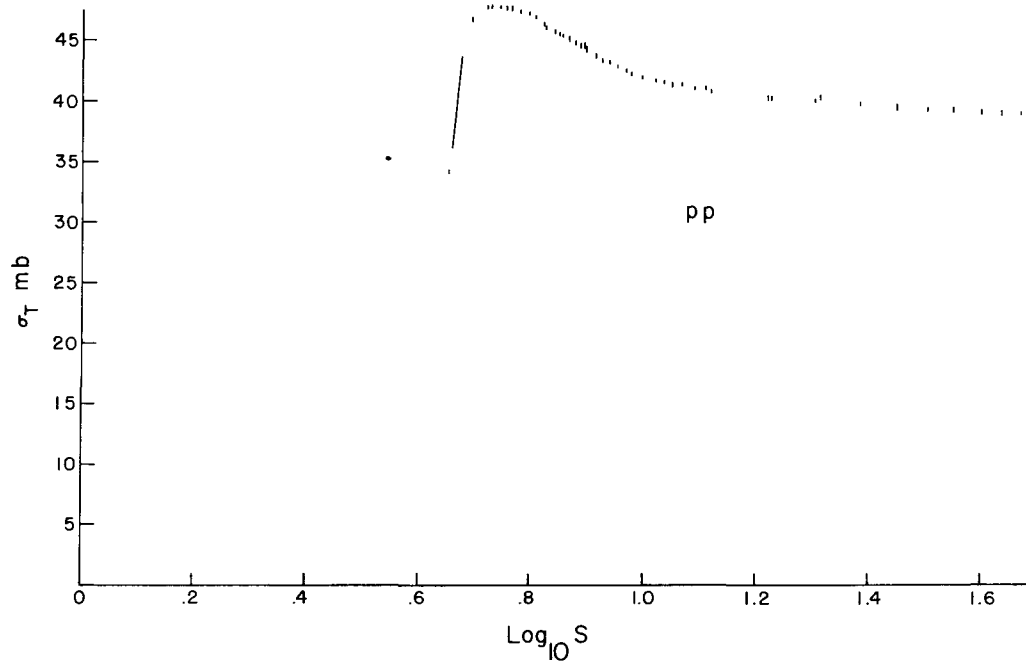


Figure 5.

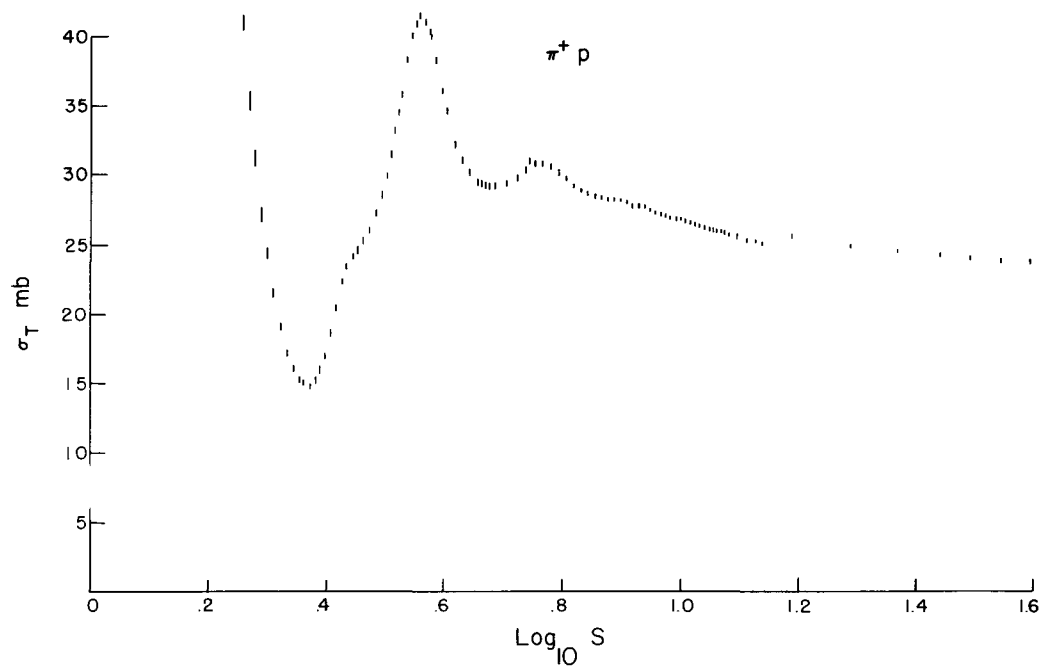


Figure 6.

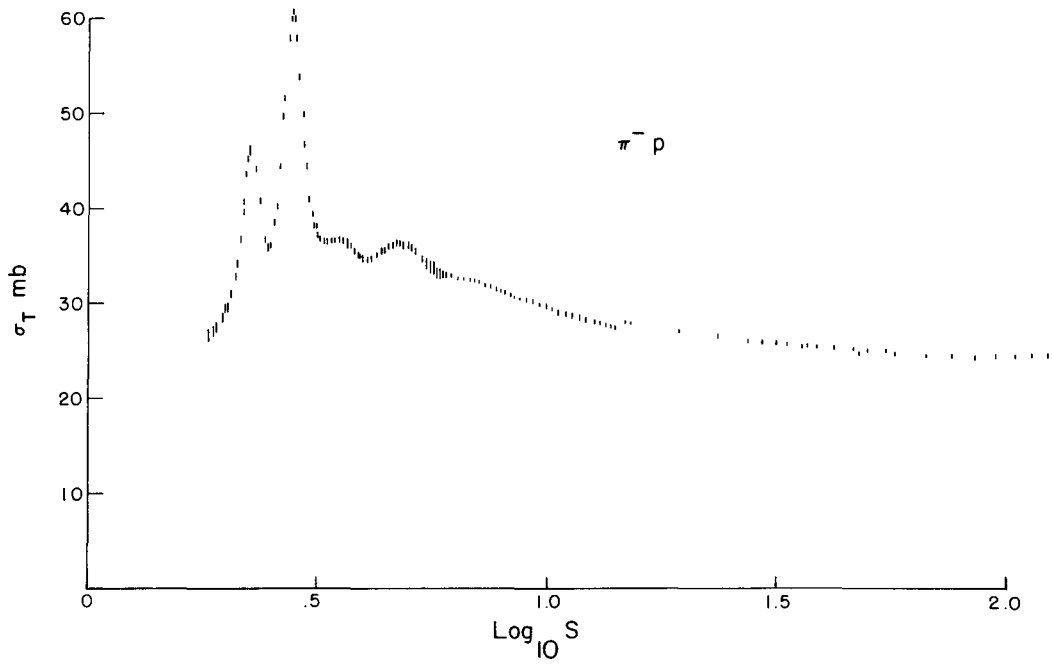


Figure 7.

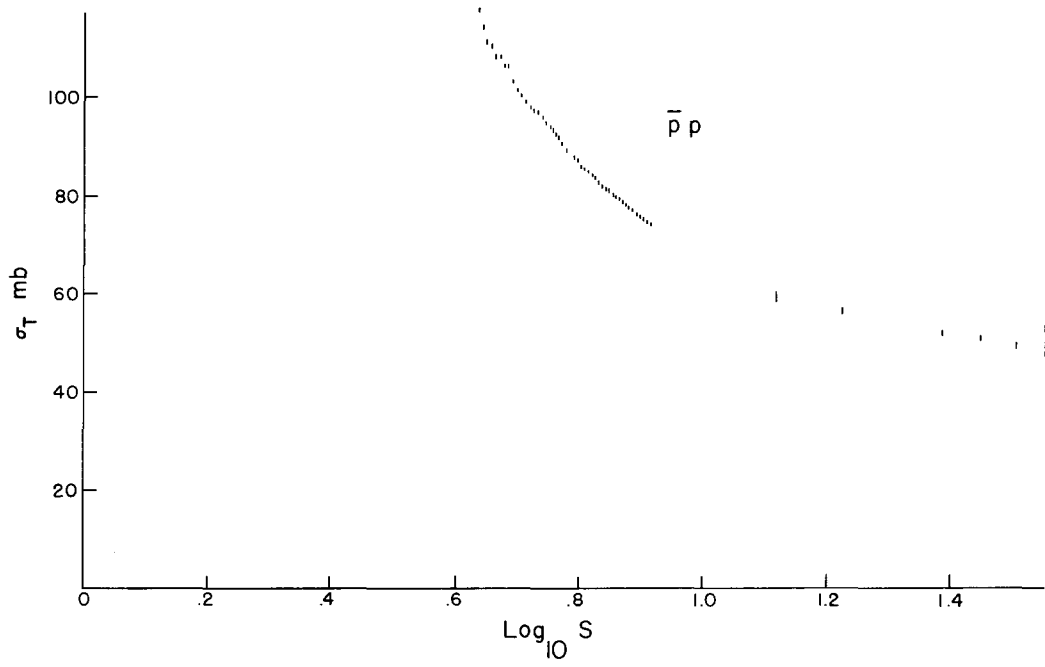


Figure 8.

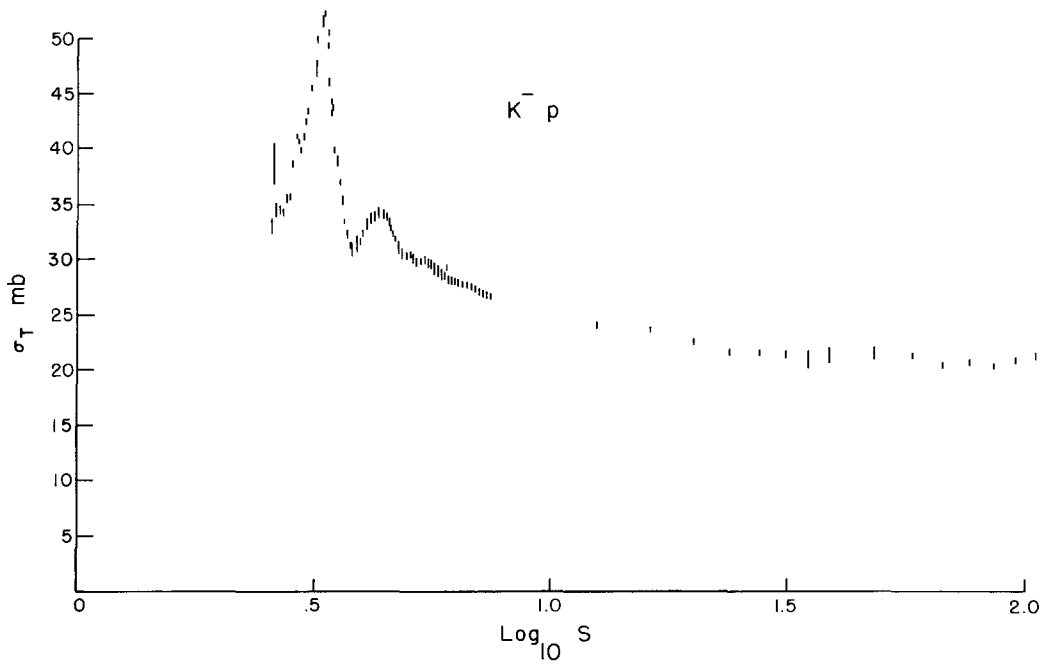


Figure 9.

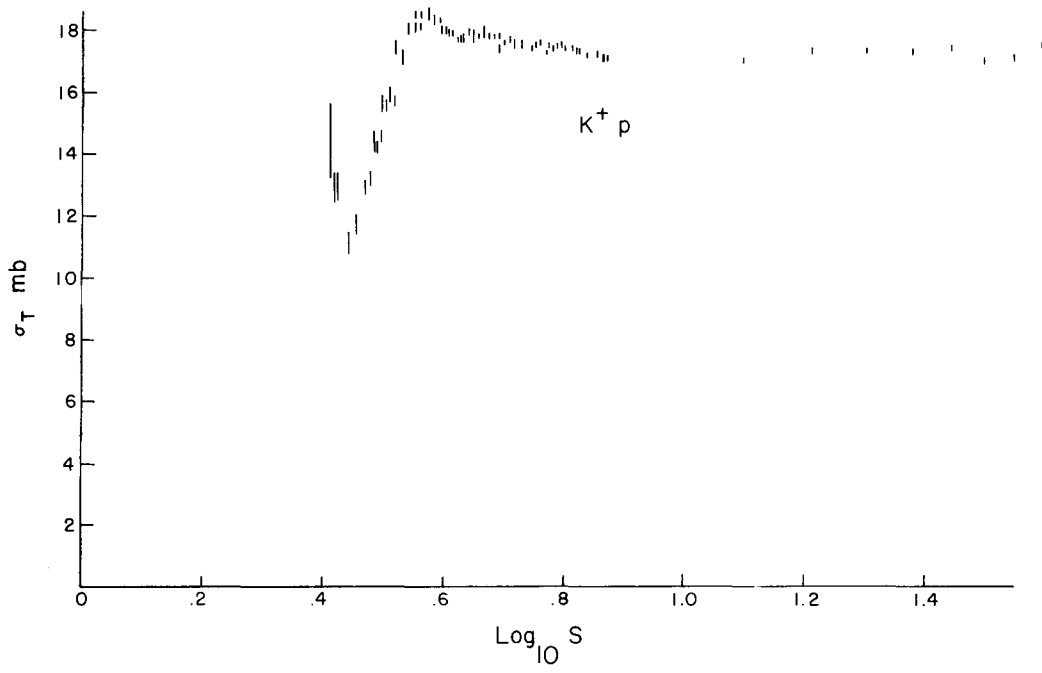
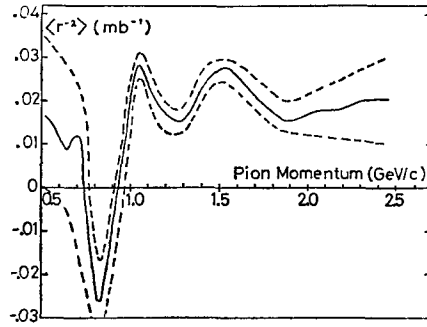


Figure 10.



The parameter  $\langle r^{-2} \rangle$  of the Glauber theory as a function of momentum. The dashed lines indicate estimated limits of experimental error.

Figure 11.

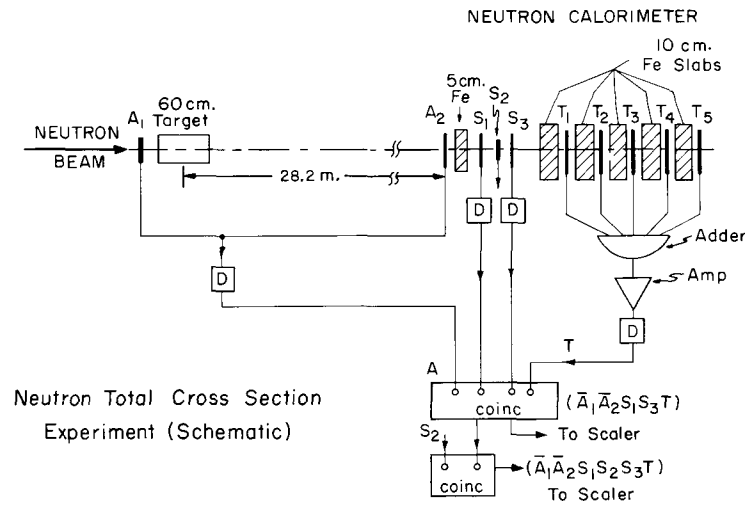
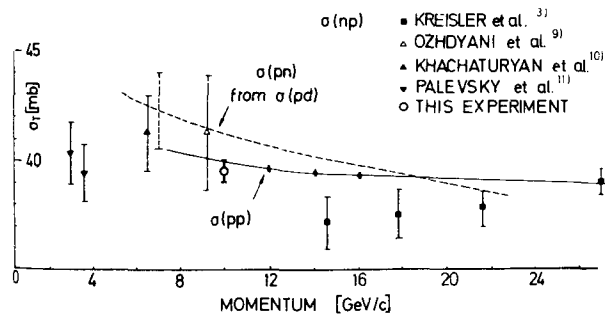


Figure 12.



$\sigma_t(pp)$  and  $\sigma_t(np)$  total cross-sections at various incident momenta. The dashed line was fitted to  $\sigma_t(np)$  cross-sections. The solid line shows the results from  $\sigma_t(pp)$  measurements. The accuracy of these data is represented by some typical errors. All other points are taken from direct  $\sigma_t(np)$  measurements.

Figure 13.

## II. FORWARD ELASTIC SCATTERING

The elastic scattering of hadrons at high energy is naturally divided into two regions. Near the forward direction the cross section is large and peaked at  $t=0$ . The cross section for all the particles falls exponentially against  $t$  for many decades until at  $-t \approx 0.5$  some deviation from this simple behavior is seen. The cross section near  $90^\circ$  in the c.m. system is typically very small indeed and very energy dependent. Near  $180^\circ$  the cross section rises again but is a much smaller value than in the forward direction (about  $10^{-3}$  of the forward cross section). We shall discuss in this section the forward and high momentum transfer region and reserve the backward peak for the next section.

The optical theorem says

$$\text{Im}f(0) = \frac{k\sigma_T}{4\pi} \quad ,$$

$k$  the momentum of the particles in the c.m. system,  $\sigma_T$  the total cross section. If the cross section is nearly imaginary we can say

$$f^2 \approx \frac{k^2 \sigma_T^2}{16\pi^2}$$

or

$$\frac{d\sigma}{d\Omega} = \frac{k^2 \sigma_T^2}{16\pi^2}$$

Since

$$\begin{aligned} -t &= 2k^2(1-\cos\theta) \\ dt &= \frac{k^2}{\pi} d\Omega \quad \text{and} \quad \frac{d\sigma}{dt} = \frac{d\sigma}{d\Omega} \frac{\pi}{k^2} \quad ; \end{aligned}$$

and now we must take care of the units. If we measure  $k^2$  in  $(\text{GeV}/c)^2$  then

$$\frac{d\sigma}{dt} = \frac{d\Omega}{dt} \frac{k^2 \sigma_T^2}{16\pi^2} \times 2.55$$

where  $\sigma_T$  is in mb,

$$\frac{d\sigma}{dt} = \frac{2.55}{16\pi}, \sigma_T^2 = 0.051 \sigma_T^2 \quad .$$

Then  $\frac{d\sigma}{dt}$  is in  $\text{mb}(\text{GeV}/c)^2$ .

Since, as we have seen, the total cross section is almost constant, the forward cross section is also constant, measured as  $\frac{d\sigma}{dt}$ .

The other general comment to repeat is that in the diffraction peak the cross sections fall exponentially against  $t$  so that the parametrisation

$$\frac{d\sigma}{dt} = \frac{d\sigma}{dt}(0) \exp At$$

is often used.

A is a slowly varying parameter, if A gets larger as the energy increases, this is referred to as shrinkage. For most all the elastic peaks A is of the order of  $10 \text{ (GeV/c)}^{-2}$  but we shall discuss this in detail later on.

1. The real part of  $f(0)$ .

When the forward scattering amplitude is calculated using the optical theorem it is found that the measured cross section is larger than this value. The difference is accounted for by a real part. It is possible to measure the real part this way, but a method that is not only more accurate than this, but also determines the sign of the real amplitude involves Coulomb interference. At very small angles the Coulomb amplitude and the elastic scattering amplitude are comparable and so the interference term is detectable with a careful measurement of the scattering cross section.

Foley et al.<sup>1</sup> and Belletini et al.<sup>2,3</sup> have performed such measurements and Fig. 1 shows the experimental layout of the Foley experiment. The momentum resolution of the beam was better than 0.5% and pions were identified by the Cerenkov counters  $CT_1$  and  $CT_2$ . The direction of the incident pion was measured by the hodoscopes  $HO_1$  and  $HO_2$ . The outgoing particles were measured in angle and momentum to about 0.1 mrad and  $\frac{\Delta p}{p}$  better than 0.5%. This momentum resolution allows the elastically scattered particles to be identified and the momentum transfer calculated from the angular deviation. In addition the total cross section was measured defining an interaction as either an angular or momentum change of the incoming particle. With the extra constraint of momentum and the improved angular accuracy the systematic problems of extrapolation should be minimized compared to the more traditional methods of total cross section measurement described in Lecture 1. Figures 2 and 3 show typical angular distributions with the single and multiple Coulomb scattering subtracted. The real part is the same sign for positive and negative pions since we have reversed the sign of the Coulomb amplitude and the change of interference is clear.

The counters which identify the pion include muons also. Since muons have a Coulomb interaction it is necessary to exclude them from the experiment and they are identified as these particles which traverse the  $\pi$  absorber in Fig. 1. The electron contamination in the beam is very small and is corrected separately.

In fitting the data Foley et al. chose a form for the nuclear amplitude of

$$|f(s,t)|^2 = |f(s,0)|^2 \exp(bt+ct^2).$$

c was fixed from measurements at wider angles than in this experiment and then



the data fitted for  $b$  and for  $\alpha = \frac{\text{Re}f}{\text{Im}f}$ . The forward imaginary amplitude was calculated from the total cross section and the optical theorem and  $\chi^2$  minimized to obtain  $a$  and  $b$ . The fit was good and consistent with a fit in which the forward imaginary amplitude was not constrained. It is worth noting that since the spin flip amplitude contains a term in  $\sin\theta$  this amplitude will have very little effect in the small angles used in this experiment. ( $\approx 22$  mrad) The values of  $\alpha$  are plotted against the incident momentum in Fig. 4. These authors consider the systematic errors in some detail and observe that they tend to cancel when the sum of  $\alpha^+$  and  $\alpha^-$  is considered and become relatively large in the difference. The total cross sections are included in the plot in Figs. 6 and 7 of Lecture 1. Since the magnitude and phase of the forward amplitude are known under the assumption of charge independence it is possible to calculate the charge exchange cross section. The agreement is satisfactory although the errors are fairly large so that this is not a stringent list of charge independence since the I spin amplitudes are almost equal.

The problem in p-p scattering is that there are two nuclear amplitudes, singlet and triplet. So a measurement of small angle scattering does not provide enough information to determine the phase of both. Under the assumption that the amplitude is spin independent Belletini et al.<sup>2,3</sup> have measured the ratio  $\text{Re}f/\text{Im}f$ . The results are plotted in Fig. 5 together with other measurements of the same quantity. Belletini et al. also try to fit the cross section by assuming different angular dependencies for imaginary singlet and triplet parts only and conclude that some real part is necessary although some compromise position between these two extremes is allowed. It is amusing to notice that the sign of the real part really changes sign at the same energy that the inelastic channels affect the total cross section behavior.

The forward peak.

We have already mentioned that up to a momentum transfer  $t$  of  $-0.5$   $(\text{GeV}/c)^2$  the forward peak has a primarily exponential behavior. Foley et al.<sup>4,5</sup> have measured the values of the exponent for pions, kaons and nucleons between 7 and 20  $\text{GeV}/c$ . These papers give values of the constants together with an elastic cross section integrated out to  $-t=1$ . This restriction in integration involves a possible error of  $\sigma_{el} < 1\%$ . The Fig. 6 shows some typical curves. In most of the diffraction region the angular dependence is dominated by the  $b$  term, the energy dependence of which is of interest. The general tendencies are summarized below.

p-p	$b$	Increases from 9.78 to 10.48 from 7 to 20 $\text{GeV}/c$
$\pi p$	$b$	Does not change in this region $\pi^+ p \approx 8.9$ $(\text{GeV}/c)^2$ $\pi^- p \approx 9.7$ $(\text{GeV}/c)^2$
$k p$	$b$	Does not change $k^+ p \approx 7.0$ $(\text{GeV}/c)^2$ $k^- p \approx 10.0$ $(\text{GeV}/c)^2$
$\bar{p} p$		If anything $b$ decreases in this region. $b \approx 12.0$ $(\text{GeV}/c)^2$ .

Figure 7 shows some recent Serperkhov data (reported at the Lund Conference) which shows the slope of pp elastic continuously increasing up to 60 GeV/c. This discussion illustrates the fact that these diffraction peaks have little energy dependence, and such as is present has no ready explanation.

#### Elastic Scattering at high momentum transfers

##### 1. proton-proton

Elastic scattering has been measured by measuring the momentum and angle of either one or both of the scattered particles. The conservation of momentum both transverse to the incident beam and along the beam provides the constraints which allow the separation of the elastic scattering from the other channels even at the very low cross sections that have been measured. Figure 1 is a good example of a "one arm" spectrometer, when the momentum transfer is small this is the only way, since the momentum of the recoil proton is too small to detect. When the momentum transfer is high the two arm spectrometer experiment has the advantage that the momentum resolution needed in each arm becomes very much less for adequate separation of elastic and inelastic events. Figure 9a shows a two arm spectrometer used by Akerlof et al.<sup>7</sup> A nice feature of this layout is the two C magnets "Left" and "Right". For a given momentum transfer and incident energy the momenta of the two scattered particles are known. These two magnets are used to change the angle of the scattered particles so that they always fall on the same line. To perform an angular distribution it is only necessary to change the current in the magnets and not move these very heavy objects around on the floor.

Allaby et al.<sup>6</sup> have made a spectacular set of measurements in the 10-20 GeV/c region and they are shown against  $t$  in Fig. 8. The rather featureless behavior of the forward region gives way to a striking energy dependence as  $t$  becomes large. In addition a structure at  $t \sim -1.0$  (GeV/c)<sup>2</sup> is apparent at the highest energies and is reminiscent of diffraction minima. A number of people have tried to reduce the three dimensional quality of this presentation by suitable choosing an independent variable against which to plot the cross sections. Orear suggested  $\frac{d\sigma}{dt}$  against  $p_{\perp} = p \sin\theta$ , Krisch  $\frac{d\sigma}{dt}$  against  $\beta^2 p_{\perp}^2$  where  $\beta$  is the proton velocity in the c.m. system. It is fair to say that the success of these approaches has varied inversely with the accuracy of the data although Krisch's plot given in Fig. 9b is the most successful. There are discrepancies of about a factor of two between the data and the lines drawn in this figure, of course they don't show up in a logarithmic plot with this many decades. One can also see how breaks are found in an experiment which measures at a fixed angle in the c.m. as is done by Akerlof et al.<sup>7</sup> It is most interesting to see how this distribution changes at even higher energies. It has been suggested that there is an asymptotic angular distribution, independent of energy, and the structure that is appearing near  $-t=1$  is a part of this.

Whenever a model is suggested to explain scattering the most sensitive prediction turns out to be the polarisation. If there are two amplitudes involved the interference between these accounts for polarisation if it exists at all. Recently targets have been made where the free protons have their spins aligned. The most popular has been a crystal in which the free protons are contained in H<sub>2</sub>O molecules within the lattice. When the crystal is cooled and a very uniform magnetic field applied the energy levels of states with proton spin up or down are split. The population of these two states is affected by an applied R.F. field and these "free" protons are polarised by as much as 60%. This polarisation is defined as

$$P = \frac{N_+ - N_-}{N_+ + N_-} .$$

To reverse the polarisation of these protons it is necessary to change the R.F. frequency only, so that the opposite spin state becomes more populated. The experiment has to distinguish between scattering off the "free" protons and those in the nuclei forming the crystal. An additional disadvantage is that the crystal dimensions are those corresponding to the wavelength of the R.F. needed to populate the polarised states, typically one inch instead of the tens of inches used in a liquid hydrogen target. The densities of the free hydrogen in the crystal are comparable with those of liquid hydrogen. It is a bonus that the magnetic field does not have to be changed when the polarisation is changed so that scattered particle trajectories are unaltered on changing the polarisation.

The limited number of free protons and the difficulties of separation of free proton scattering vs quasi elastic scattering on the protons in the nuclei has meant that polarisation measurements have been performed mainly at lower energies. Measurements at low momentum transfers (0.8 (GeV/c)<sup>2</sup>) have been made up to 12 GeV/c by Borghini et al.,<sup>8</sup> Fig. 10. At lower energy (5.15 GeV/c) Booth et al.<sup>9</sup> have made measurements out to -t=2.0 GeV.c, Fig. 11, complementing the measurements of Grannis et al.<sup>10</sup> The broad conclusions are that the maximum polarisation decreases with measuring energy, and that near -t=0.6-0.8 (GeV.c)<sup>2</sup> there appears to be some structure corresponding to that in the elastic scattering at high energies. Many models have been proposed, both Regge and more classical, but a clear decision seems impossible at this stage.

## 2. Antiproton-proton

The cross section measurements for  $\bar{p}p$  elastic scattering are not nearly so extensive as for  $pp$ . The flux of antiprotons at an accelerator is small, and experimentally, measurements are more difficult when each antiproton in the beam is accompanied by 100 negative pions. The antiprotons in the beam are identified with Cerenkov counters and measurements have been made up to 16 GeV/c.

Figure 12a shows data taken with a one arm spectrometer by Birnbaum et al.<sup>11</sup> at 8 and 16 GeV/c. Figure 12b shows data at 6 and 10 GeV/c in a higher momentum transfer region reported by Owen et al.<sup>12</sup> It is immediately clear that there is a great deal more structure in the antiproton data than with a proton beam. As before almost all the energy dependence appears at  $-t > 0.6$  (GeV/c)<sup>2</sup>. It is observed by Birnbaum et al. that the cross section in the vicinity of  $-t=1$  divided by the cross section at  $t=0$  has become almost energy independent above 6 or 7 GeV/c. Perhaps this feature of the cross section is part of the "asymptotic" cross section that should emerge even more clearly at higher energies. In Fig. 12c we show various values for the slope of the forward peak and it looks as if  $b$  is a steadily decreasing number (antishrinkage) up to the highest measured energies.

### 3. n-p

At high energies it is necessary to measure n-p scattering by detecting both particles. Since as with all other hadrons almost all of the cross section is concentrated in the forward peak, then the neutron after scattering is still of high energy. Experimentally the neutron is detected by observing the interaction in some dense material in the form of spark chamber plates. There is little energy information and really the only quantitative measurement is one point, the conversion point, on the neutron trajectory. Hence the experiments have<sup>13,14</sup> also measured the proton direction as a constraint, and as a way of determining the incident neutron momentum. The neutral beam from an accelerator contains neutrons and a very few  $K_L^0$  with a momentum spectrum that is wide and peaked below the protons that produce the beam. This energy loss depends upon the production angle. Experiments are performed with a relatively wide acceptance in angle for the neutron and recoil proton detectors so that data is taken simultaneously over a wide range of  $s$  and  $t$ .

If the scattering is elastic, then the plane defined by the neutron and proton has within it the incident neutron direction. In addition, in the experiment of Engler et al.,<sup>14</sup> the proton velocity was measured giving an extra constraint on the elasticity of the event. Figure 13 shows the experimental setup of Engler et al.,<sup>14</sup> Fig. 14a,b typical angular distributions. It is clear that this data is less accurate and complete than the p-p data. A comparison that is easy to make is that of the equality of slope of the forward peak using incident neutrons and protons or hydrogen. This comparison is shown in Fig. 15. The error flags are large but it seems that the two slopes are substantially equal and moreover the n-p data shrinks in the same way that the p-p data does. These experiments are much more painful to do than the p-p scattering experiments and for the foreseeable future we expect that we must be content with the conclusion that n-p scattering is remarkably like p-p scattering within a fairly wide uncertainty.

But there is one difference. Since the pp system is symmetrical it is

meaningless to talk of a backward peak. However, in n-p scattering, there is a discernable backward peak where the particle that emerges with small momentum transfer is the proton. The experiment of Manning et al.<sup>15</sup> is an excellent high energy measurement of the n-p charge exchange cross section whose principal feature is the very narrow peak at small angles. This peak is the source of a good deal of theoretical wonderment although its narrowness has led to interpretation concentrating on pion exchange. Here more data is clearly needed.

#### 4. $\pi p$

We have already discussed the substantial real part of the forward scattering amplitude of pions and pointed out that the real part has the same sign for both charges. With a lifetime of  $10^{-16}$  or so no scattering experiments are performed on neutral pions. The shape of the forward peak for the charged pions is exponential and the exponent does not seem to vary with  $s$  at all.<sup>4</sup> The exponent is slightly different for positive and negative particles, and since the total cross sections are a little different ( $\sim 2$  mb out of 25 mb) then the scattering is therefore different in the  $I = 1/2$  and  $3/2$  states at the energies we have reached as yet. This is reflected in the finite charge exchange  $|\pi^- p \rightarrow \pi^0 n|$  cross section; we shall discuss this.

As  $-t$  increases above  $0.5 (\text{GeV}/c)^2$  some non-exponential structure appears which is quite energy dependent. Coffin et al.<sup>16</sup> show a plot reproduced in Fig. 16 which displays nicely the way that the secondary maximum dies away as the energy of the incident pion increases. Owen et al.<sup>9</sup> have measured a nearly complete angular distribution at 6 and 10 GeV/c incident momentum; it is reproduced in Fig. 17. The experimental method is also discussed in some detail in this paper. It is clear that the whole of the cross section outside  $-t=1 (\text{GeV}/c)^2$  is very energy dependent, the dip at  $-t \sim 0.7 (\text{GeV}/c)^2$  diminishes to a shoulder at high energies and the dip at  $-t = 3 (\text{GeV}/c)^2$  becomes quite prominent. It is probably that this dip is prominent everywhere when  $-t=3$  is in the physical scattering region. Booth has observed that near where  $t=3$  is at  $180^\circ$  in the laboratory (an incident momentum of  $\sim 2 \text{ GeV}/c$ ) there is a violent change in the cross section as we shall see in the next section. When we have a "map" of the cross section as we do in p-p then we shall be able to check this conjecture. There is a real debate about which is the physically most appropriate variable to plot the cross section. Notice that the structures seem to remain constant against  $t$ . These dips tend to be at small angles so that  $-t=p_\perp$  and so we cannot decide that the constancy against  $t$  is significant. The Booth remark may be relevant to this discussion.

The interpretations of the pion scattering experiments are many and varied; it is fair to say that semi-classical diffraction, Regge, and the quark model incorporating the possibility of multiple scattering of the quarks are all

possibilities. As always, a strong constraint on the theory is the polarisation dependence. Borghini et al.<sup>8</sup> show measurements at 6, 8, 10 and 12 GeV/c. Figure 18 shows their results. The simplest models ask that the polarisation is equal but opposite for  $\pi^+$ , this does not seem to be the case. Recall that the measurement of the polarisation of the protons in the target crystal is a little hard to determine, but since these polarisations have been measured with the same apparatus we are inclined to believe that this discrepancy is real.

We have finally remarked that since  $\pi^+p$  and  $\pi^-p$  scattering is different then there should be a small charge exchange cross section. Figure 19 shows a plot of this cross section from Sonderegger et al.<sup>17</sup> The cross section is quite energy dependent and shows the dip that was apparent in the elastic scattering at  $-t = 0.6$ . This cross section has been the focus of a good deal of attention from the Regge fitters, largely because of the hypothesis that only one trajectory is important, the rho. The absence of a diffraction like amplitude leads to real simplification in the analysis. Moreover, the rho trajectory goes through a wrong signature point at  $-t = 0.6$  so the major structure is fitted naturally. As we might expect with the parameters available an impressive fit was produced. This edifice has collapsed with the detection of a non-zero polarisation in the small t region. This handsome experiment, although lacking in accuracy, indicated a non zero polarisation which moreover did not seem to have any energy dependence. Their results are shown in Fig. 20. The single trajectory model cannot cope with this and another trajectory or cuts have to be invoked spoiling the pristine nature of the earlier ideas.

Experimentally, the forward charge exchange experiment does not turn out to be as hard as it appears at first sight. There is a good signature, in that a charged particle comes into the target and no charged particle emerges. At 6 GeV/c the "all neutral" cross section amounts to about 450  $\mu\text{b}$  and the charge exchange ( $n\pi^0$ ) final state accounts for 100  $\mu\text{b}$  of this. So the rejection factor needed is not too large after the first criterion is met. The method relies on measuring the conversion points of the  $\gamma$ 's from the decay of the  $\pi^0$  in a spark chamber made from a hi Z material, for example stainless steel or lead. Then since the velocity of the  $\gamma$ 's is known the experimenter can transform the events to the c.m. system where all "elastic" events have a common momentum for the  $\pi^0$ . Then the events cluster near the minimum opening angle as, for example, in Wählig and Mannelli et al.<sup>19</sup> in Fig. 21. When this distribution is understood by the experimenter, cross sections are extracted.

## 5. Kp

These cross sections, in Fig. 22, resemble the  $\pi p$  cross sections as do the experiments.<sup>9</sup> There has been little structure observed (there may be a small effect near  $-t = 0.8$ ) and the small t exponent does not vary much with s. Possibly the cross section shrinks if anything. The experiments are lacking in accuracy because

of the lack of high flux separated K beams. The short lifetime of the K is a real experimental handicap in designing high intensity beams. One can imagine a considerable improvement in high energy elastic K data as the beam technology improves since at low energies 1-2 GeV/c the data is already fairly extensive.

#### REFERENCES

1. K.J. Foley, R.S. Jones, S.J. Lindenbaum, W.A. Love, S. Ozaki, E.D. Platner, C.A. Quarles and E.H. Willen, Phys. Rev. 181, 1775 (1969).
2. G. Bellettini, G. Cocconi, A.N. Diddens, E. Lillethun, I. Pahl, J.P. Scanlon, J. Walters, A.M. Wetherell and P. Zanella, Physics Letters 14, 164 (1965).
3. G. Bellettini, G. Cocconi, A.N. Diddens, E. Lillethun, J.P. Scanlon and A.M. Wetherell, Physics Letters 19, 705 (1966).
4. K.J. Foley, S.J. Lindenbaum, W.A. Love, S. Ozaki, J.J. Russell and L.C.L. Yuan, Phys. Rev. Letters 11, 425 (1963).
5. K.J. Foley, S.J. Lindenbaum, W.A. Love, S. Ozaki, J.J. Russell and L.C.L. Yuan, Phys. Rev. Letters 11, 503 (1963).
6. J.V. Allaby, F. Binon, A.N. Diddens, P. Duteil, A. Klovning, R. Meunier, J.P. Peigneux, E.J. Sachardis, K. Schlupmann, M. Spighel, J.P. Stroot, A.M. Thorndike and A.M. Wetherell, Physics Letters 28B, 67 (1968).
7. C.W. Akerlof, R.H. Hieber, A.D. Krisch, K.W. Edwards, L.G. Ratner and K. Ruddick, Phys. Rev. 159, 1138 (1967).
8. M. Borghini, G. Coignet, L. Dick, K. Kuroda, L. di Lella, P.C. Macq, A. Michalawicz and J.C. Olivier, Physics Letters 24B, 77 (1966).
9. N.E. Booth, G. Conforto, R.J. Esterling, J. Parry, J. Scheid, D. Sheriden and A. Yokosawa, Phys. Rev. Letters 21, 651 (1968).
10. R. Grannis, J. Arens, F. Betz, O. Chamberlain, B. Dieterle, C. Schultz, G. Shapiro, H. Steiner, L. Von Rossum and D. Welson, Phys. Rev. 14B, 1297 (1966)
11. D. Birnbaum, R.M. Edelstein, N.C. Hien, T.J. McMahon, J.F. Mucci, J.S. Russ, E.W. Anderson, E.J. Bleser, H.R. Blieden, G.B. Collins, D. Garelick, J. Menes, and F. Turkot, Phys. Rev. Letters 23, 663 (1969).
12. D.P. Owen, F.C. Peterson, J. Orear, A.L. Read, D.J. Ryan, D.H. White, A. Ashmore, C.J.S. Damerell, W.R. Frisken and R. Rubenstein, Phys. Rev. 181, 1794 (1969).
13. J. Cox, M.L. Perl, M.N. Kreisler, M.J. Longo and S.T. Powell, III, Phys. Rev. Letters 21, 641 (1968).
14. J. Engler, K. Hoarn, J. König, F. Münnig, P. Schludecker, H. Schapper, P. Sievers, H. Ullrich and K. Runge, Physics Letters 29B, 321 (1969).
15. G. Manning *et al.*, Nuovo Cimento 41A, 167 (1966).

16. C.T. Coffin, N. Dikmen, L. Ettliger, D. Meyer, A. Saulys, K. Terwilliger and D. Williams, Phys. Rev. 159, 1169 (1967).
17. P. Sonderegger, J. Kirz, O. Quisar, P. Falk-Vairant, C. Bruneton, P. Borgeaud, A.V. Stirling, Physics Letters 20, 75 (1966).
18. P. Bonamy, P. Borgeaud, C. Bruneton, P. Falk-Vairant, O. Quisar, P. Sonderegger, C. Caverzasio, J.P. Guillaud, J. Schneider, M. Yvert, I. Mannelli, F. Sergiampietri and L. Vincelli, Physics Letters 23, 501 (1966).
19. M.A. Wahlig and I. Mannelli, Phys. Rev. 168, 1515 (1968).

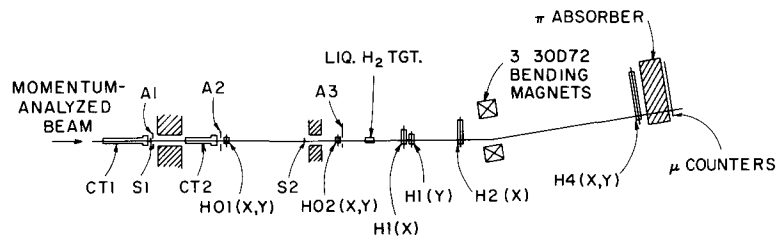


Figure 1.



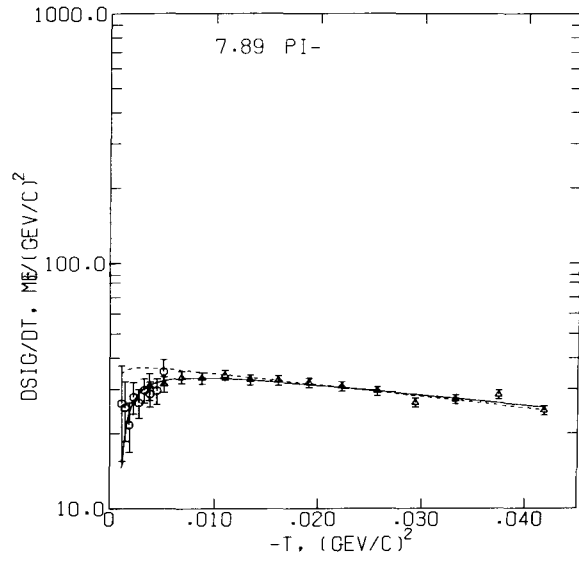


Figure 2a.

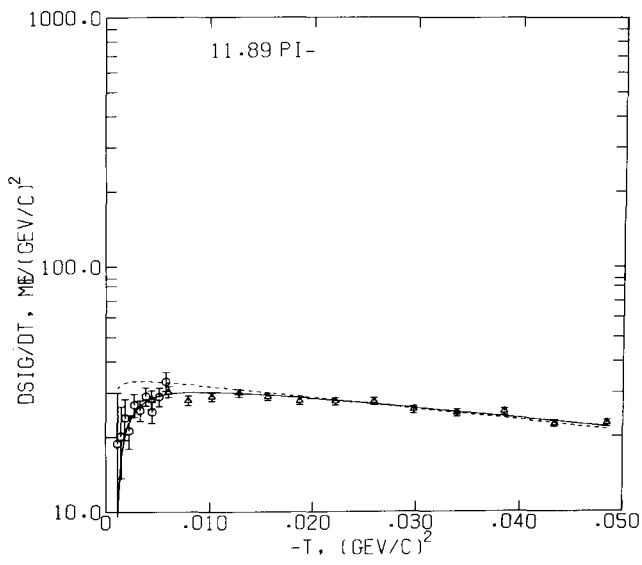


Figure 2b.

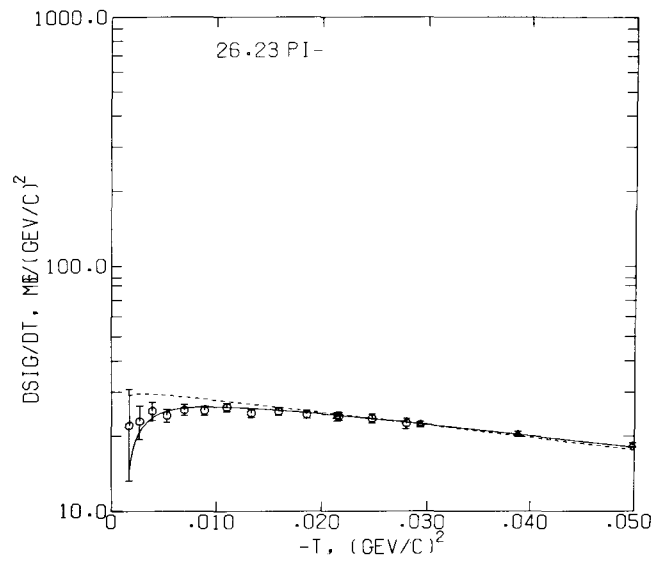


Figure 2c.

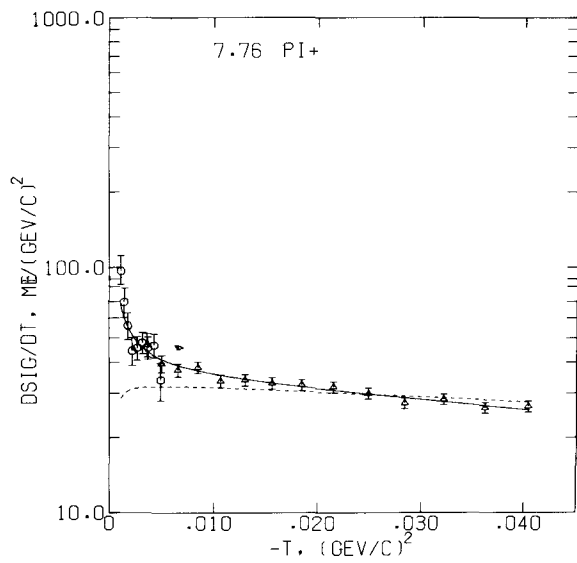


Figure 3a.

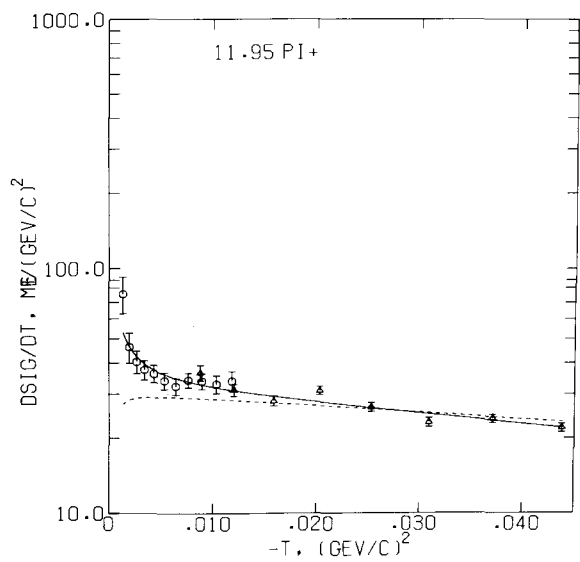


Figure 3b.

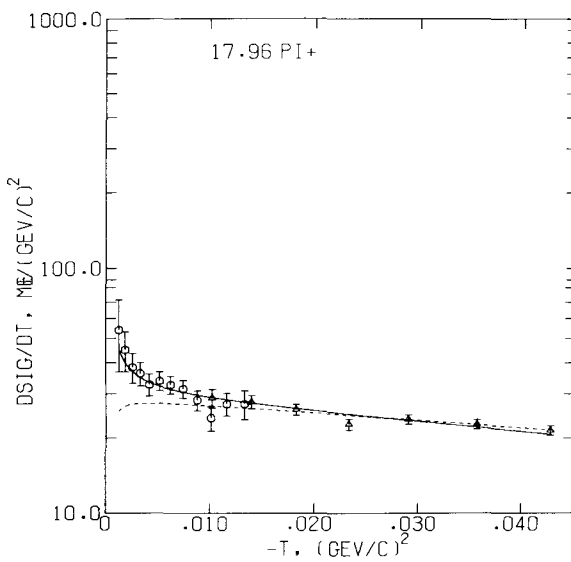


Figure 3c.

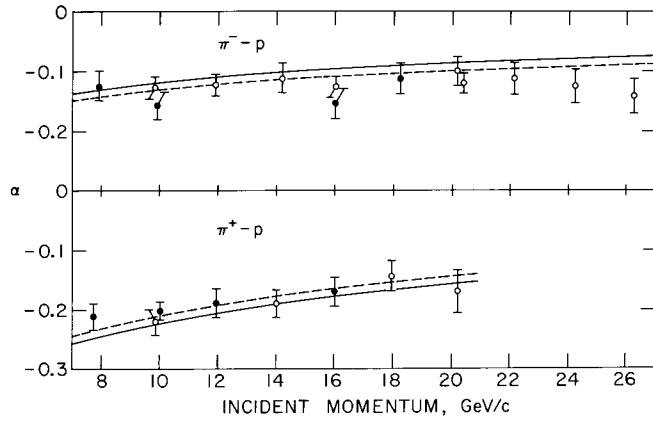


Figure 4.

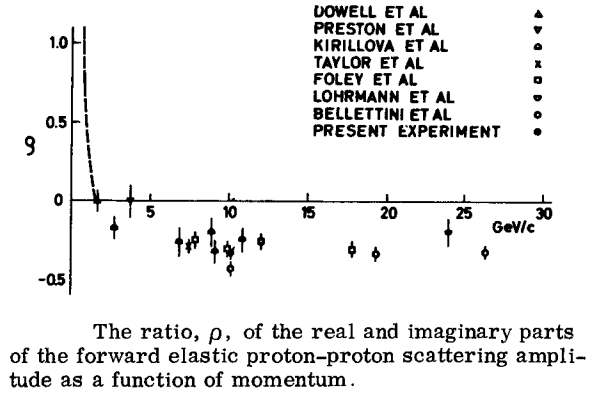
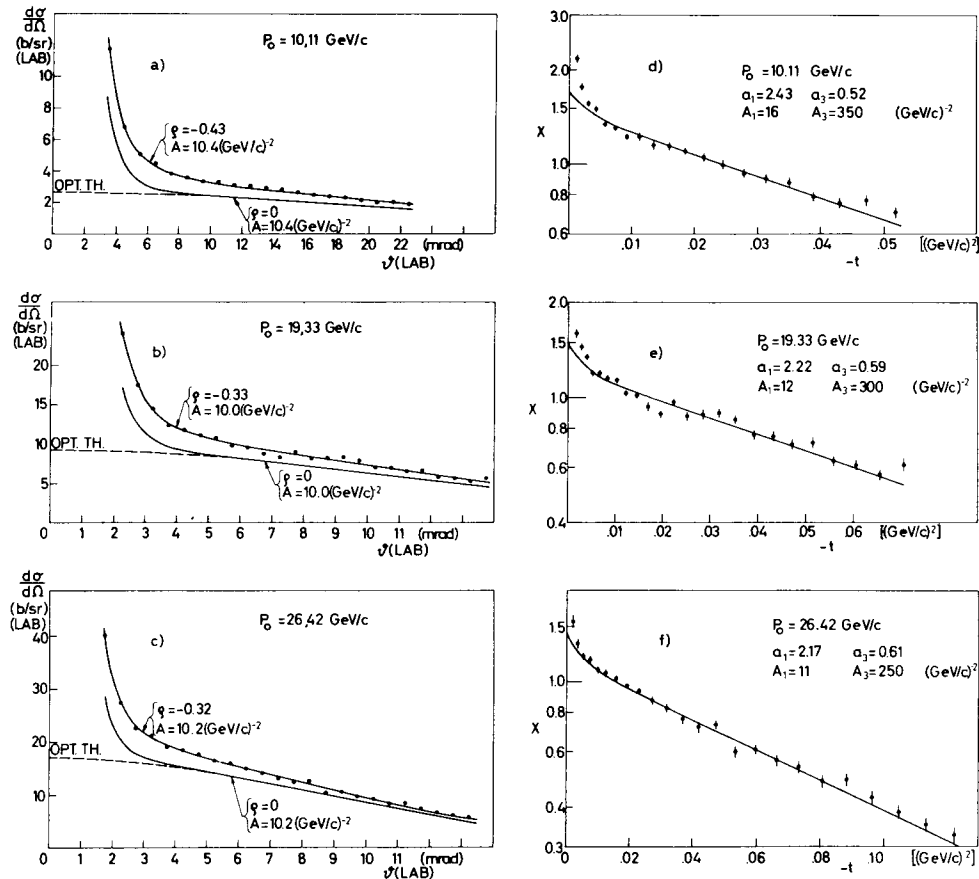


Figure 5b.



Proton-proton elastic scattering angular distributions at 10.1, 19.3 and 26.4 GeV/c. Sections (a), (b) and (c) give the scattering angular distributions plotted against scattering angle and show fits made using a complex spin independent amplitude. In (d), (e) and (f)  $X$  is the difference between the experimental and Coulomb cross sections, normalized to the optical theorem value  $(k\sigma_{tot}/4\pi)^2$ .  $X$  is shown as a function of the square of the 4-momentum transfer  $t$ . Attempts at singlet-triplet imaginary amplitude fits are shown.

Figure 5a.

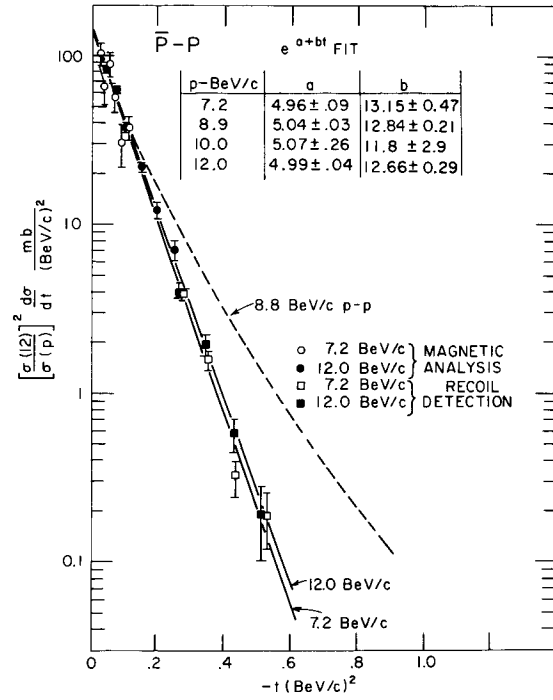


Figure 6a.

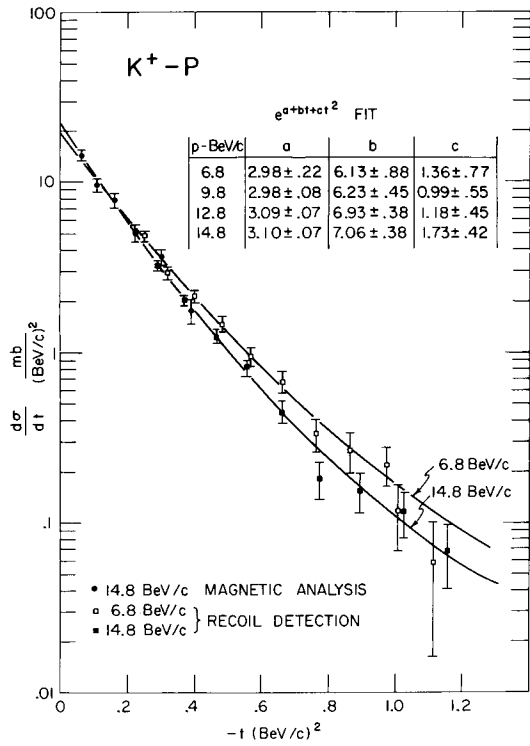


Figure 6b.

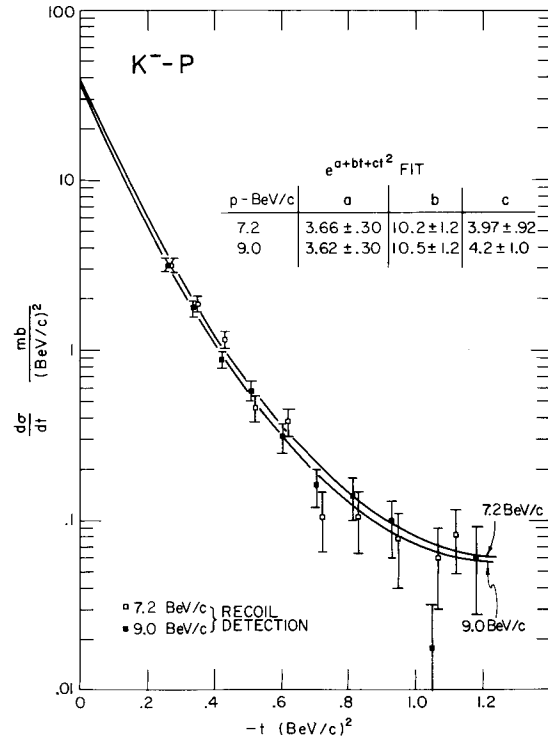
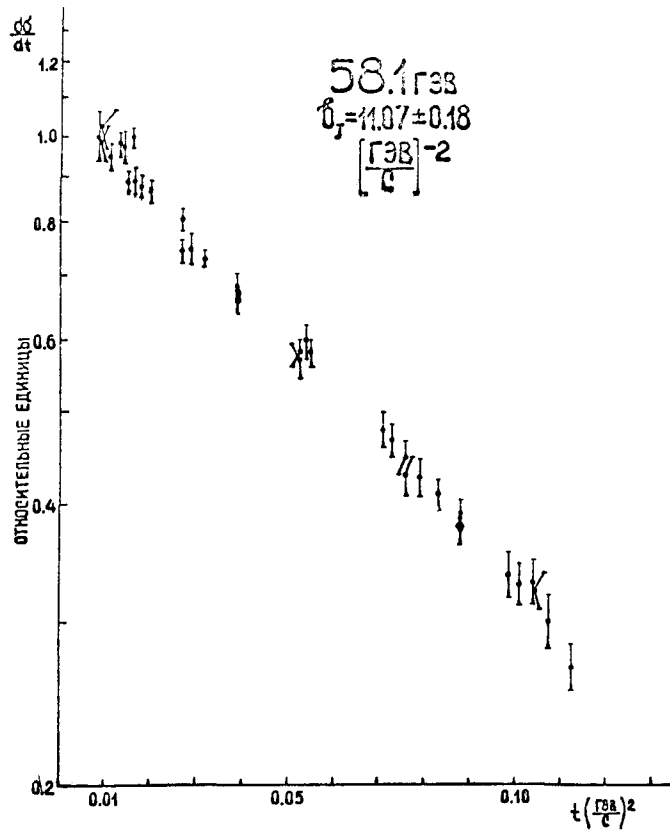
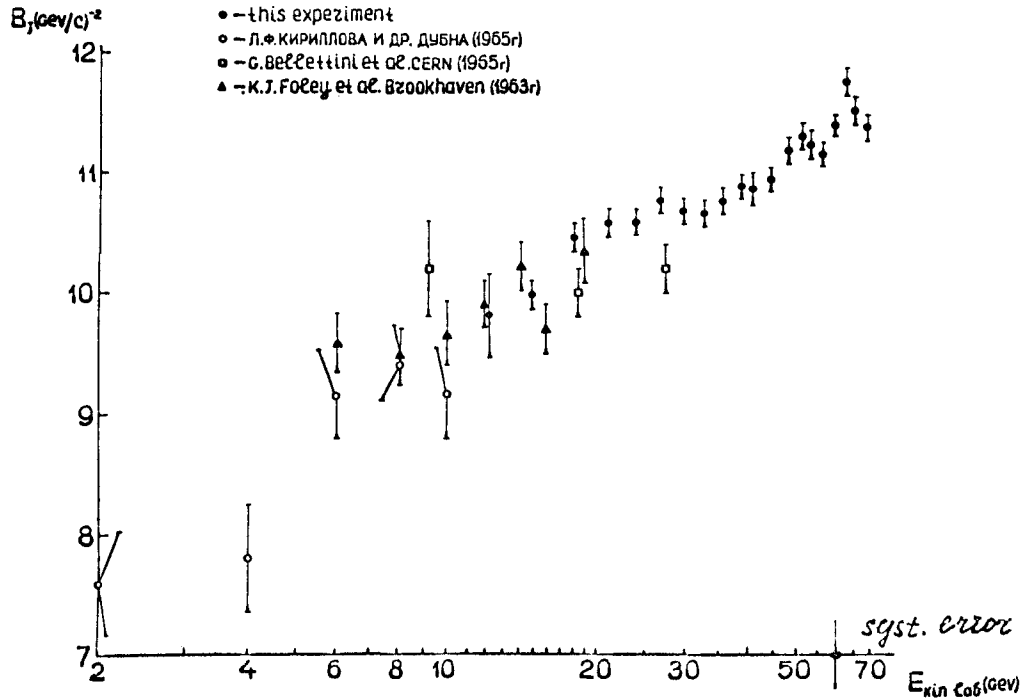


Figure 6c.

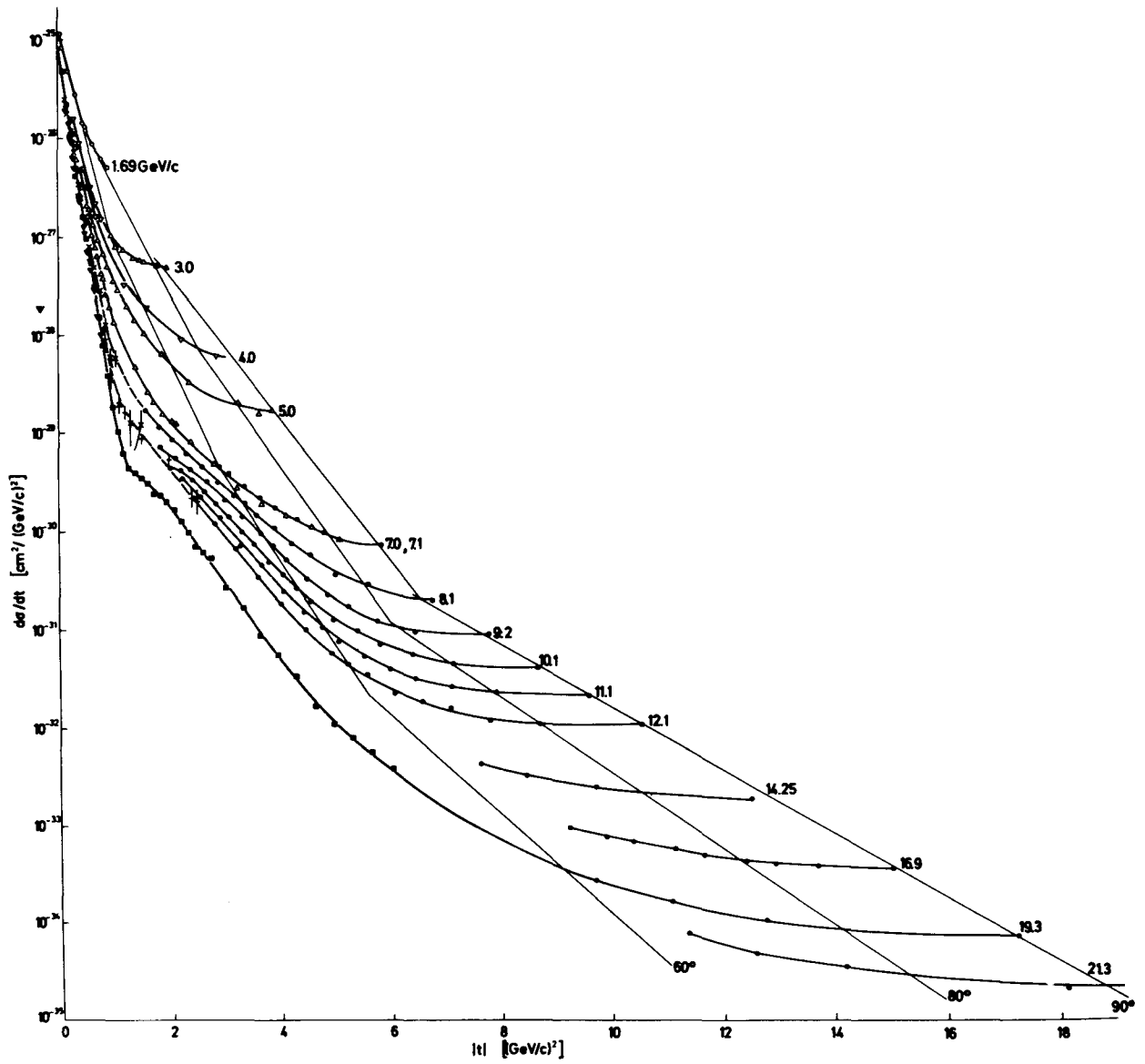


The differential elastic cross-section in the arbitrary units at 58.1 Gev.



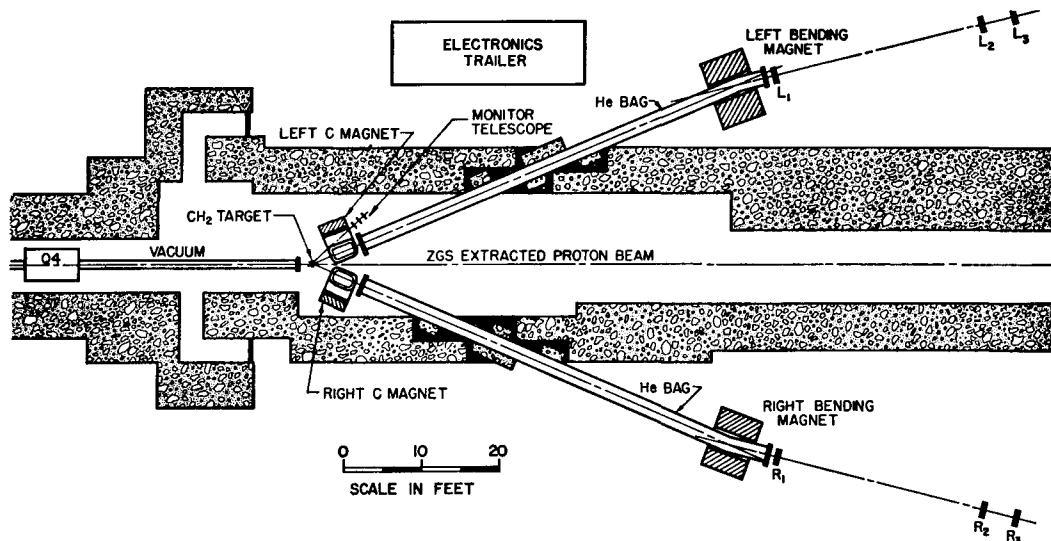
The results of the measurements of the slope parameter.

Figure 7.



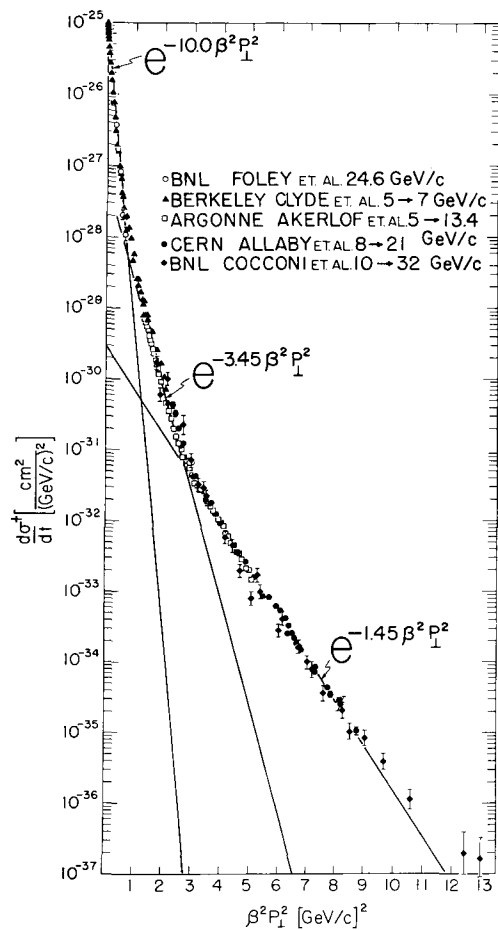
Proton-proton elastic scattering cross sections  $d\sigma/dt$  as functions of  $|t|$ . The curves joining the experimental points are hand-drawn to guide the eye. The loci of cross sections for fixed c.m.s. scattering angle are indicated for  $60^\circ$ ,  $80^\circ$  and  $90^\circ$ .

Figure 8.



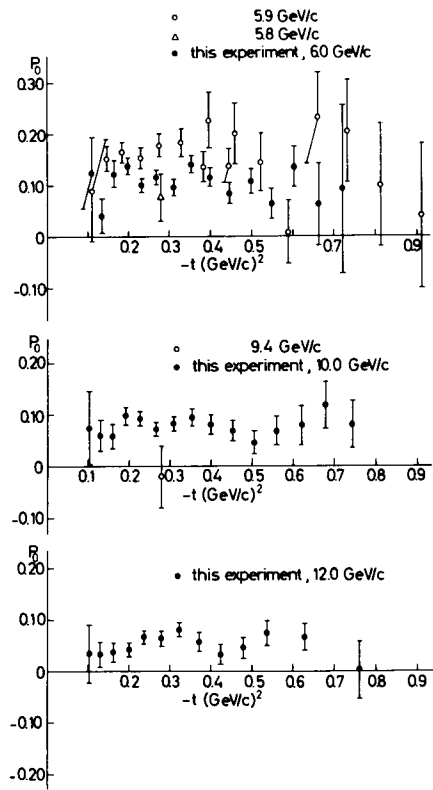
Experimental layout; the incident protons come down the extracted beam and strike the target. The scattered protons pass out through the magnets and scintillation counters.

Figure 9a.



Plot of  $d\sigma^\dagger/dt$  vs  $\beta^2 P_\perp^2$  for all high-energy proton-proton elastic-scattering data. Not all small-angle data are shown on this plot to avoid crowding. The lines drawn are straight-line fits to the data.

Figure 9b.



The polarization parameter  $P_0$  versus  $t$  in pp elastic scattering.

Figure 10.

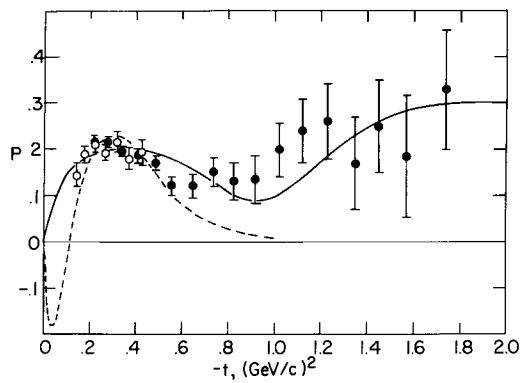
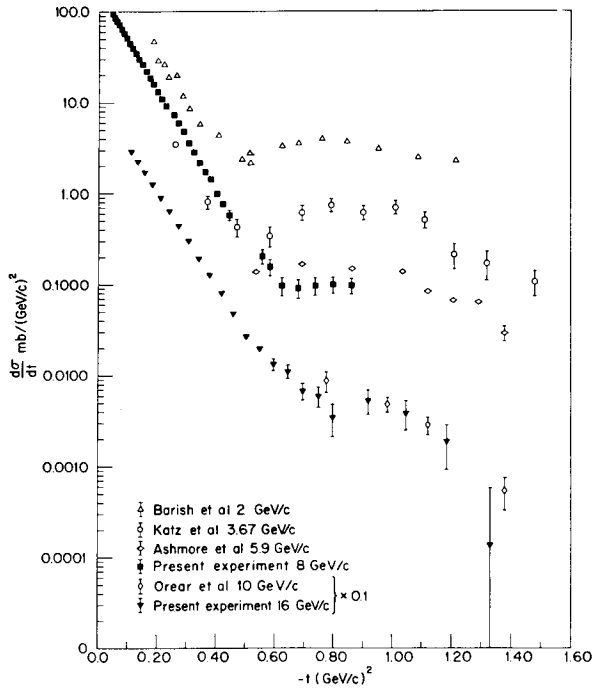


Figure 11.





Differential cross sections for  $\bar{p}$ - $p$  elastic scattering. For purposes of clarity, the data of Orear et al. at 10 GeV/c and the present 16-GeV/c data have been scaled by a factor of  $\frac{1}{10}$ .

Figure 12a.

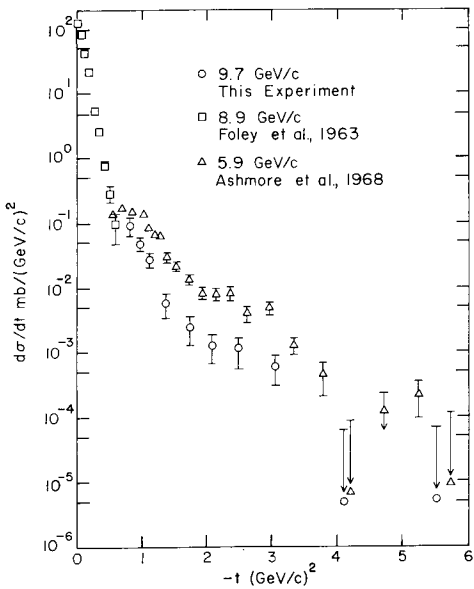
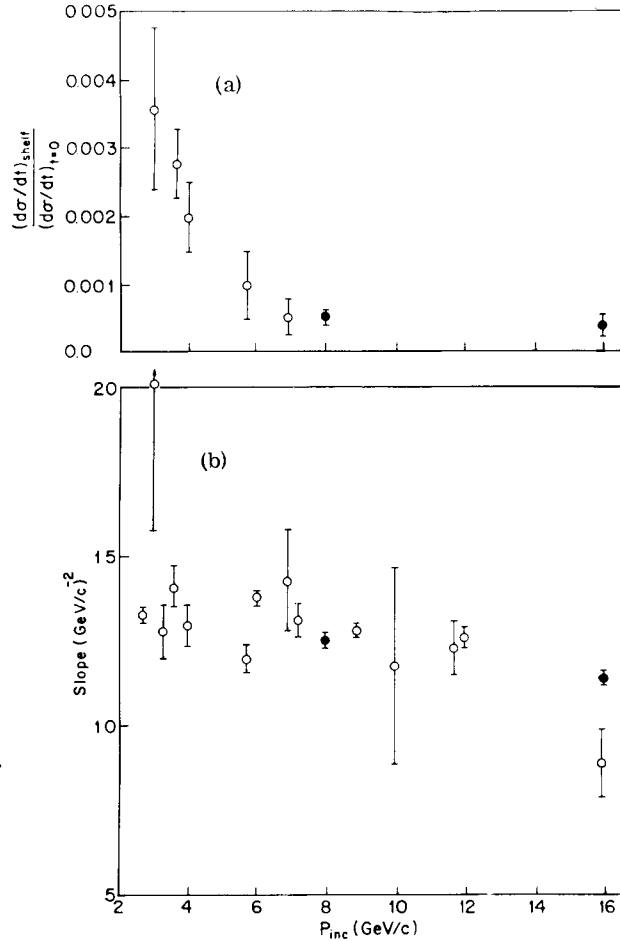
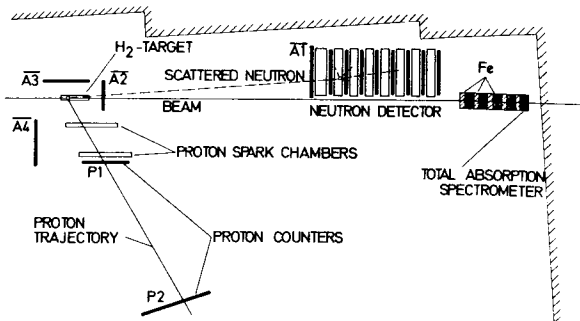


Figure 12b.



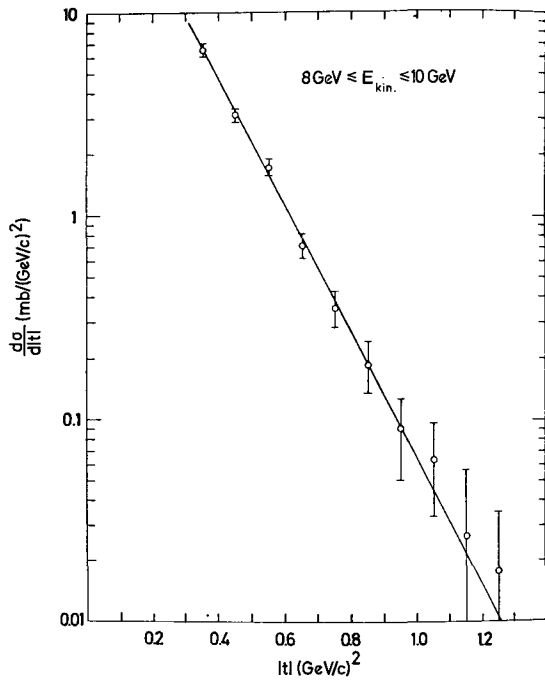
(a) Ratio of the  $\bar{p}$ - $p$  elastic differential cross section at the secondary maximum to that at  $t=0$  as a function of incident momentum. Solid circles are our data; (b) Logarithmic slope of the  $\bar{p}$ - $p$  elastic differential cross section as a function of incident momentum. Solid circles are our data.

Figure 12c.



The experimental set-up.

Figure 13.



The differential cross sections  $d\sigma/d|t|$  versus  $|t|$  for primary-neutron kinetic energy of 8-10 GeV. The cross section at  $t = 0$  is normalized to the optical theorem point. The straight line represents the fit to  $\exp(A + Bt)$ .

Figure 14a.

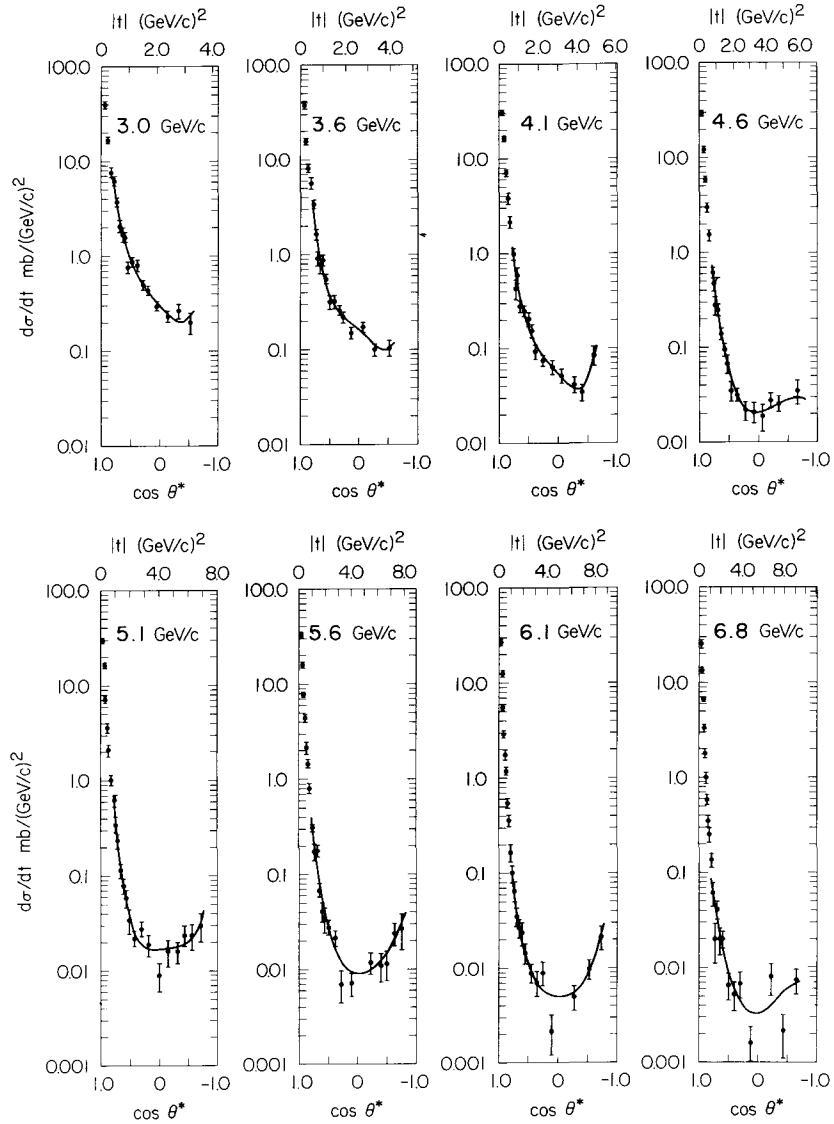
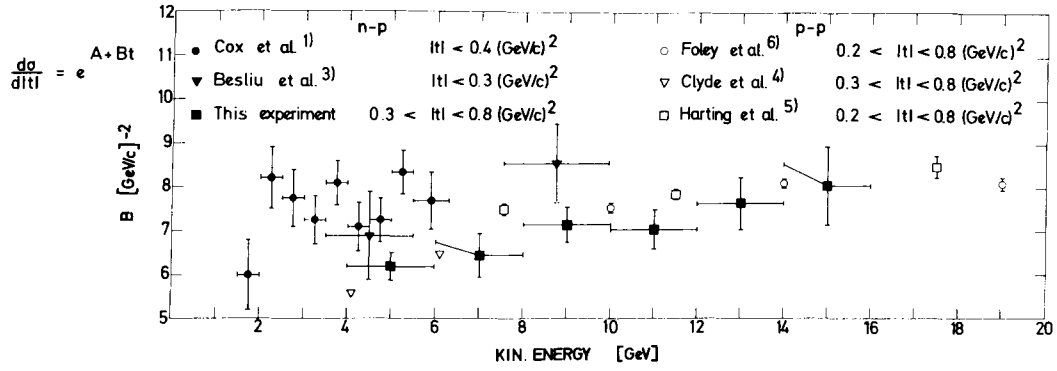
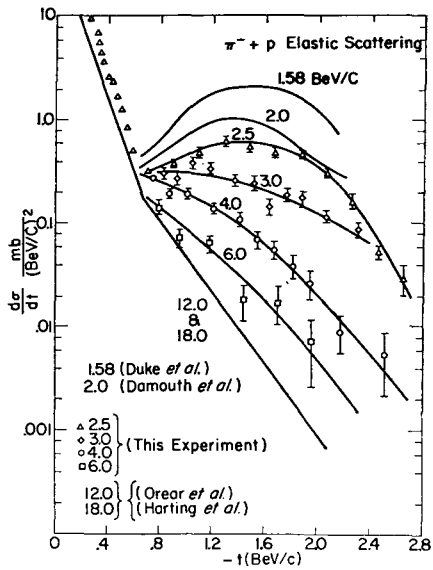
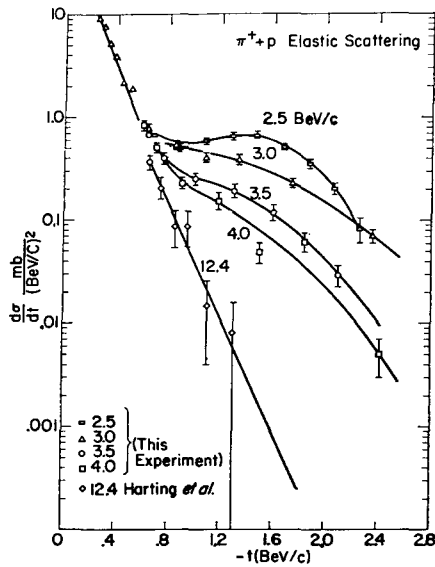


Figure 14b.



The slope  $B$  as obtained by fitting the differential cross sections by  $\exp(A+Bt)$  versus primary-neutron kinetic energy. The range used for the fit is given.

Figure 15.



Momentum dependence of the secondary peak in  $\pi^+ + p$  and  $\pi^- + p$  scattering.

Figure 16.

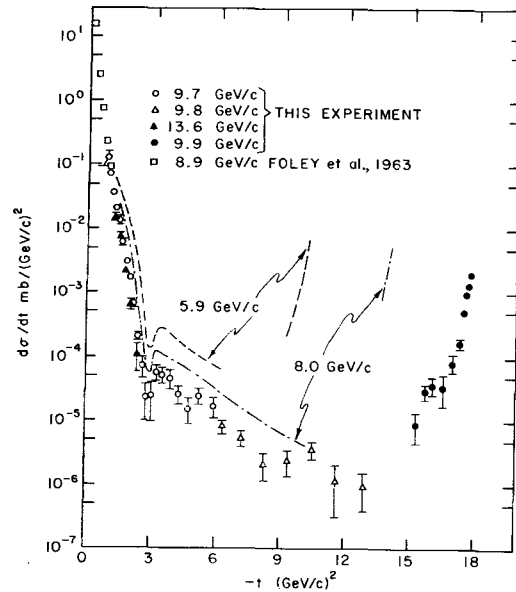
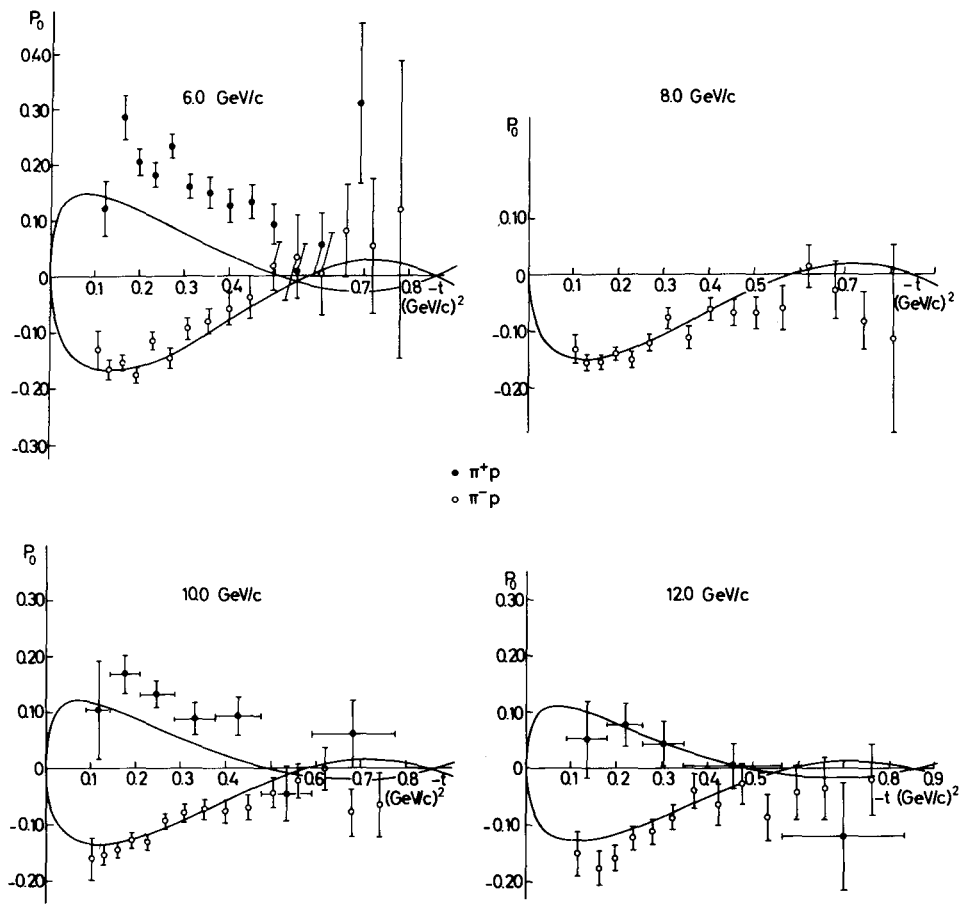
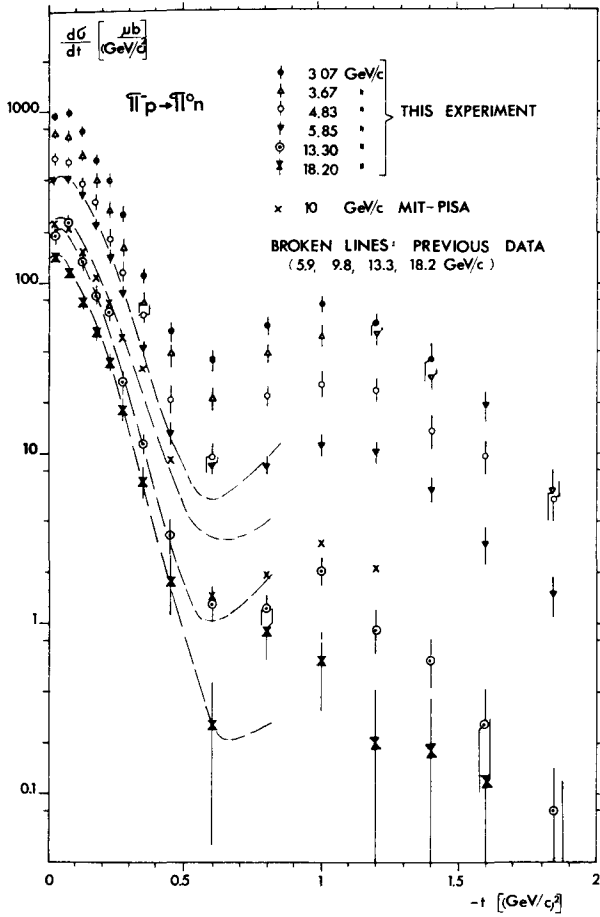


Figure 17.



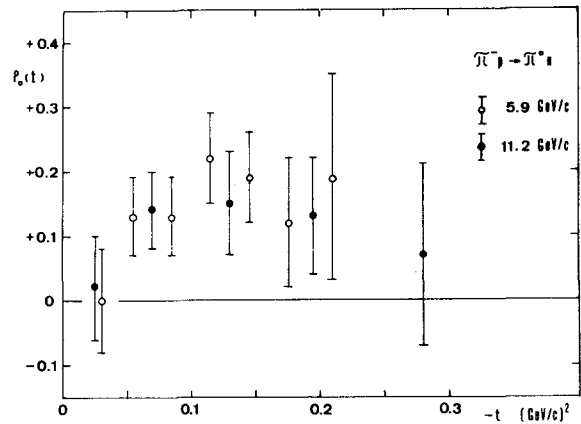
The polarization parameter  $P_0$  versus  $t$  in  $\pi^\pm p$  elastic scattering. The curves represent the theoretical predictions of Chiu et al.

Figure 18.



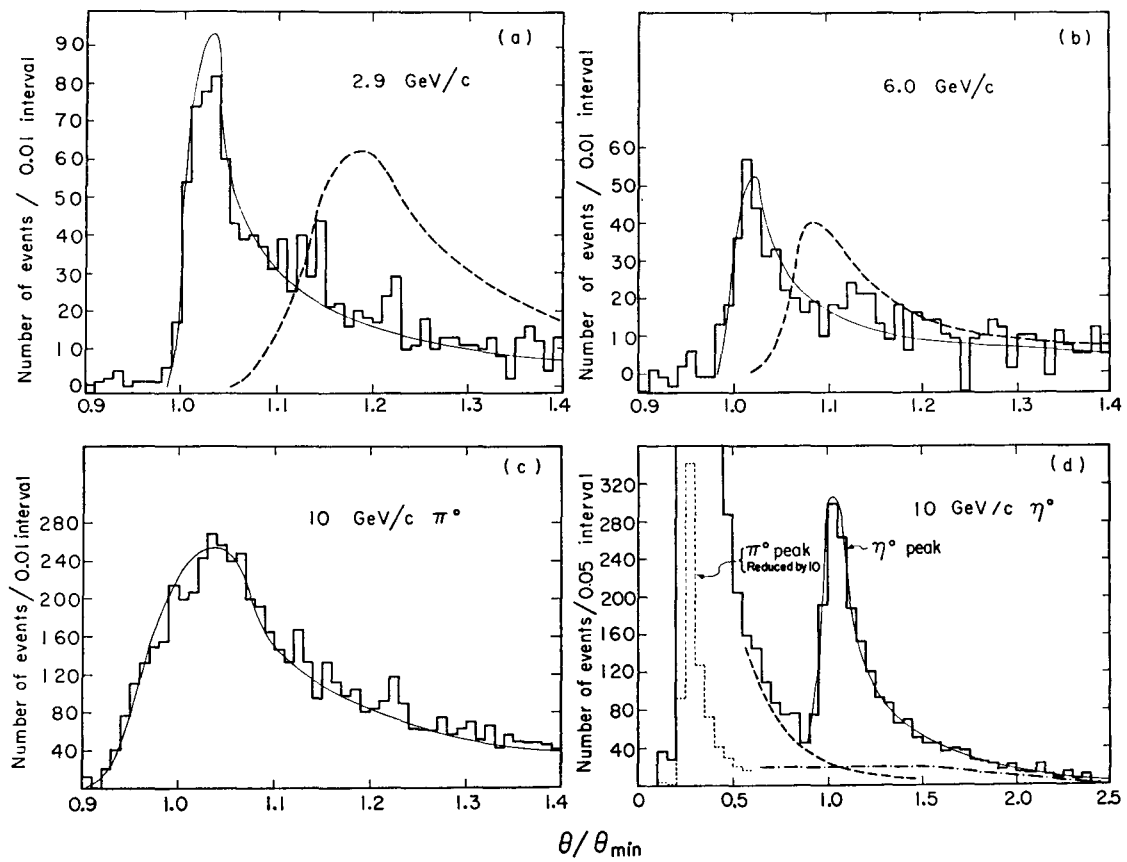
Differential cross sections for  $\pi^- p \rightarrow \pi^0 n$ . The MIT-Pisa results at 10 GeV/c. The broken lines are smooth lines through the results.

Figure 19.



Polarization parameter  $P_0(t)$  at 5.9 GeV/c (open circles) and 11.2 GeV/c (black dots).

Figure 20.



Distributions of the  $2\gamma$  opening angles  $\theta$  in the  $\pi^-p$  c.m. system, normalized to the minimum allowed opening angle  $\theta_{\min}$  for each momentum. Note that the sharpness in the opening-angle distribution is masked here by the expanded scale and buried zero in  $\theta/\theta_{\min}$ . The solid lines are the Monte Carlo predicted distributions, normalized to the number of experimental events in the interval  $0.965 \leq \theta/\theta_{\min} \leq 1.165$ . The dashed lines in (a) and (b) are the Monte Carlo predicted distributions for the  $\pi^0$  in the reaction  $\pi^- + p \rightarrow N^{*0}(1236) + \pi^0$ , and are arbitrarily normalized. (a) The 2.9-GeV/c distribution is typical of all those between 2.4 and 3.8 GeV/c. (d) The  $\eta^0 \theta/\theta_{\min}$  distribution has two backgrounds—the tail of the  $\pi^0$  distribution which extends under the  $\eta^0$  peak (dashed line) and a residual flat background from multi- $\gamma$  events (shown by dash-dot line). The  $\eta^0$  Monte Carlo calculated distribution (solid line) includes these two backgrounds.

Figure 21.

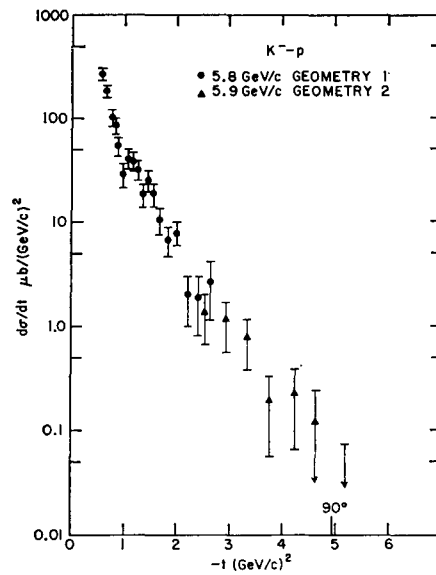


Figure 22.

### III. BACKWARD PEAKS

The motivation behind the study of the cross section near  $180^\circ$  has derived largely from the fact that if exchange diagrams are postulated as the major contribution, the number of particles or trajectories that contribute is small. This represents a satisfyingly small number of parameters available (for example, in a Regge fit) so that careful experiments are expected to reveal some understanding of the dynamics. First we would like to show why the assumption of dominance of the exchange diagrams is reasonable at the energies that are accessible presently. Baryons exist of strangeness -1 and strange states with baryon number +1 do not appear. The question of the existence of the  $Z^*$  we set on one side for the moment. In this case if s channel contributions dominate, we would expect  $K^-p$  scattering to be much larger than  $K^+p$  scattering and if there is peaking at  $180^\circ$  it would be thought as reflecting the high spin of the compound states of the high mass  $K^-p$  system. As is shown in Fig. 1<sup>1</sup> even at 3.5 GeV/c the backward cross section is much greater for  $K^+p$  than  $K^-p$ . This, which combined with the fact that the  $K^+p$  cross section is, as we shall see, comparable with  $\pi^+p$  leads us to claim that at momenta above 5 GeV/c say, the baryon exchange diagrams are dominant.

There is another feature which has made this field attractive experimentally and that is illustrated in Fig. 2.<sup>2</sup> Here  $\pi^+p$  and  $\pi^-p$  scattering are plotted on the same graph and we see that  $\pi^+p$  near  $180^\circ$  has a higher cross section than  $\pi^-p$ . Since  $\pi^-p$  scattering involves the exchange of a doubly charged baryon, we can deduce that it proceeds by  $\Delta$  exchange only.  $\pi^+p$  on the other hand can be either nucleon exchange or  $\Delta$  exchange and if the  $\Delta$  were dominant this would make the  $\pi^+p$  1/9 the  $\pi^-p$  cross section. Clearly the nucleon is dominant and this helps us to simplify the analysis of these experiments. Conversely, there is less the theorist can do to fix the correspondence of theory to experiment.

It is not our place to explain the phenomenology of these data but we must remark that the energy dependence of the cross section is a crucial parameter and since the dip in  $\pi^+p$  at  $-u = 0.2$  (GeV/c)<sup>2</sup> is explained by a zero in the  $\Delta$  exchange amplitude it is also important to understand the experimental behavior in the dip region. After describing the experiments we shall try to focus on these features.

#### $\pi p$ Elastic Scattering

Perhaps the most complete measurements of  $\pi p$  elastic scattering at high energy is made by Owen et al.<sup>3</sup> Measurements of useful accuracy were made on both charges at 6 and 10 GeV/c and on negative pions at 14 GeV/c. In the lower u region accurate measurements have been made for negative pions by Anderson et al.<sup>4</sup> at 8 and 16 GeV/c. These data are particularly impressive in view of the small cross sections involved, typically, the cross section integrated over the entire peak is less than 1  $\mu$ barn.

The most salient problem in these experiments is that of removing background processes. Figure 3 shows the momentum spectrum of the forward going proton in the experiment of Anderson et al.,<sup>4</sup> the signal is clear and subtraction is minimal. This experiment is shown schematically in Fig. 4, the method consists of comparing the momentum of the incoming pion to the outgoing proton and calculating the missing mass. That the peak at  $m_{\pi}^2$  is so prominent is gratifying indeed. Remember that at high energies the dependence in the momentum of the outgoing proton and the incident pion is

$$p_{\text{out}} - p_{\text{in}} = \frac{m}{2} \quad .$$

The outgoing proton is slightly above the beam momentum. Owen et al used the two arm spectrometer technique illustrated in Fig. 5 where the momenta of the scattered pion and the recoil proton are measured. In this experiment there are a number of parameters determining the elastic events, 5 in fact. Figure 6 illustrates the technique.

The angle of the scattered pion in the laboratory even after passage through the magnet  $M_1$  of Fig. 5 is monotonically related to the c.m. scattering angle for an elastic event. It is possible to make an algorithm which gives a c.m. scattering angle when the angle of the track is measured in  $sc_1 - sc_4$ . With this information the momentum of the pion is known and the trajectory can be extrapolated back through magnet  $M_1$  to the target T. The interaction point is taken as the point of closest approach of this trajectory to the center of the beam. Then, the recoil proton trajectory can be calculated and compared with the proton track in  $sc_{5,6}$ . We can insist that the slope of the proton track and its spatial position in two dimensions must coincide with the expected coordinates. We insist also that the interaction point is in the hydrogen target,  $\Delta x_p$ . In Fig. 6 we show the difference in the horizontal displacement of the proton that is measured and that is expected from the pion. The upper curve is this difference in all the events, the lower curve when the other four parameters are constrained to be near their elastic values. Again the elastic peak is gratifying and the subtraction minimal. The tail when  $\Delta x_p$  is positive is accounted for by the emission of a  $\pi^0$  or heavier mesons of relatively low energy. The experiment of reference 2 is performed in a similar way to this one. Although this method is not general, it illustrates the technique that all the parameters that can be measured may not be in a particular experiment, if the event signal to background is adequate.

Figure 7 shows typical data for  $\pi^+ p$  background scattering. Two features are clear. The first is that there is a considerable energy dependence at all values of  $u$ . The second is the very pronounced dip at  $-u \approx 0.15 \text{ (GeV/c)}^2$ . Figure 8 shows the  $\pi^- p$  cross section, and although the energy dependence is still pronounced, there is no very obvious structure as there is with positive pions. As we have discussed,



since there is a good case for the dominance of the nucleon trajectory in exchange for  $\pi^+p$  scattering, the fact that there is a singular point  $\alpha(u) = -\frac{1}{2}$  near  $-u = 0.15$   $(\text{GeV}/c)^2$  allows us to jump to the obvious conclusion that this point is associated with the structure here. A linear nucleon trajectory is consistent with this. Unhappily the singular point in  $\pi^-p$  scattering occurs near  $u = -1.2$   $(\text{GeV}/c)^2$  and nothing so spectacular is here. The simple Regge description needs some amendment. It should be observed that at lower momenta where  $t$  and  $u$  channel effects are more closely intermingled the dip appears. Whether this is significant remains to be seen. In Fig. 9 we show the energy dependence of the cross section at  $u = 0$  for  $\pi^-p$  scattering. We have argued that a single trajectory is dominant so that the energy dependence of the cross section is then simply given by  $s^{2\alpha(0)-2}$ . The graph illustrates one of the difficulties of the field. It is clear that one would expect this to be a smooth curve, in fact linear, even though the experimental errors allow some leeway, there does seem to be an inconsistency. The slope of this curve in rough terms corresponds to a linear trajectory, but some adjustment in the normalization between the experiments would improve the  $\chi^2$ .

It is not hard to see how some of this discrepancy comes about. If we look at Fig. 3 the projected slope of the background can be seen. The experimentalists concerned have many good reasons to believe the shape of the non-elastic distribution that is sketched in the diagram. If we return to Fig. 6 we see the background in the experiment of reference 3 and here the experimentalists have a different prescription, the background varies smoothly under the peak. Both points of view are defensible and only experiments which are capable of greater precision can tell which is correct. In the meantime this parable is intended to convince those who fit theoretical curves to a number of experiments that naivete in regarding the experiments can give nonsense for conclusions.

These two experimental groups have also enjoyed themselves discussing the existence of a possible dip near  $180^\circ$ . If it exists it is clearly small and near the limit of precision of both experiments. This author feels that at best the question is undecided and so the theorists can feel free to speculate. However, at lower energies the dip near  $180^\circ$  certainly exists and it is very clearly demonstrated by Carroll et al.<sup>5</sup> in Fig. 10. It seems like a feature of the data which depends slowly on  $s$  and hence not dependent on the details of the resonant states involved. Kormanyos et al.<sup>6</sup> have used the two-arm spectrometer technique to measure very carefully the variation of the  $180^\circ$  cross section against  $s$  in  $\pi^-p$  elastic scattering. The motivation was that resonances in the  $s$  channel might be more apparent this way. The data is shown in Fig. 11. The structure is splendid, although Booth has observed that the dip at 2.1 GeV/c momentum may be associated with the forward dip at  $-t=3$   $(\text{GeV}/c)^2$  and not a resonance effect at all. This subject is

still cloudy. The peak at 5.1 GeV/c was hailed on Voice of America, but despite this public relations effort, its absence in the charge exchange reaction (Fig. 14) leaves us with fears for statistical fluctuations. More work is needed.

In summary, above 3-4 GeV/c the backward cross section becomes sufficiently large compared with that at  $90^\circ$  c.m. say, that the peak is clear and we can argue that u and t channel processes are separate. Moreover some of the high energy features (for example, the dip in  $\pi^+p$  at  $-u = 0.2$  (GeV/c)<sup>2</sup> can be seen in the data at lower energies than these. The fitting of these data into simple models has been quite successful and the measurement of the polarisation at high energies would be very interesting indeed.

The reaction that provides a strong constraint on the theory is the backward charge exchange. Since it is almost true that  $\pi^+p$  is pure I=1/2 exchange and  $\pi^-p$  is pure I=3/2 exchange then the measurement of  $\pi^-p \rightarrow n\pi^0$  measures directly the relative phase of these two amplitudes. These experiments<sup>7,8</sup> have been done up to about 5 GeV/c and we describe the method. The experiment of Chase et al.<sup>7</sup> is shown schematically in Fig. 12. The target is surrounded by shower chambers or shower veto counters except in the forward direction where there is a veto system for forward showers backed up by a set of neutron converting chambers. The experimental method consists of insisting that no charged particles leave the target region and then that a particle appear in the neutron chamber. The  $\gamma$  rays from pizero decay appear in the shower chamber so that their opening angle in the c.m. system can be calculated just as it is done for forward charge exchange. Again the bisector of these  $\gamma$  ray angles is used as the direction of the pion. The cross sections are shown in Fig. 13. The solid lines are the predicted cross sections using a particular Regge model that fits the charged pion data very well. The general features are described but the details of the cross section do not seem well fit.

An experiment analogous to that of Kormanyos et al.<sup>6</sup> has been done by Kistiakowsky et al.,<sup>8</sup> the cross section at  $180^\circ$  has been measured as a function of the incident pion momentum at closely spaced intervals from 2 to 6 GeV/c. The data is shown in Fig. 14. Since the experiment only measures near  $180^\circ$  and the pizero momentum is essentially independent of the momentum of the beam, then this group were able to make an annular counter hodoscope that detected the gamma rays. The data are quite accurate and should be very useful in the understanding of the s channel effects in particular. There is one difficulty, and that is the data between these two experiments do not seem to agree too well at the lower energies. Patience is called for.

Kp

We have mentioned backward scattering of kaons as a justification of the absence of large s channel effects above a few GeV/c. Baker et al.<sup>2</sup> have measured

$K^+p$  at 5.2 and 6.9 GeV/c, these data are shown in Fig. 15. The peaks are clear but it is hard to make very quantitative remarks about them. Figure 16 shows the energy dependence at  $u=0$  for  $K^+$  and  $K^-$ , it is strikingly different. The slope of the  $K^+$  energy dependence ( $S^{-4}$ ) is entirely consistent with the value of the  $\Lambda_\alpha$  trajectory at  $u=0$ .

$K^-p$  scattering at  $u=0$  falls approximately as  $S^{-10}$ . It has been remarked that this could be consistent with a  $Z^*$  trajectory of conventional slope corresponding to the bump observed in the total  $K^+p$  cross section.

For the future, higher intensity K beams can be made, but there are serious technological problems with doing better K experiments with them at present. It will be some time before this data can be made as accurate as the present pion data.

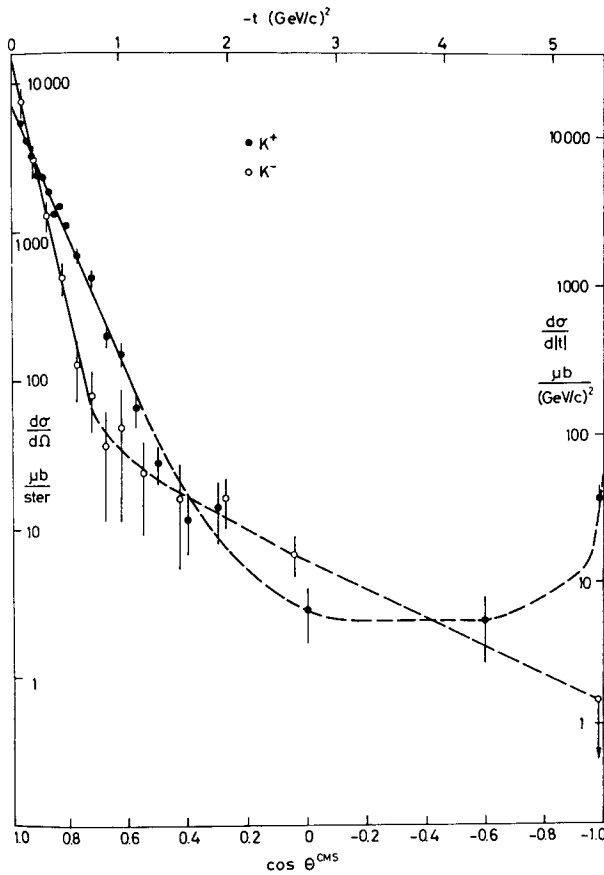
$\bar{p}p$

For the same reasons as in  $Kp$ , the  $\bar{p}p$  data is not available at high energies. At 8 GeV/c, Birnbaum et al.<sup>9</sup> quote an upper limit of  $0.18 \mu\text{b}/(\text{GeV}/c)^2$ . This upper limit is very much smaller than the pion cross section at the same energy. At lower energies this cross section has been measured between 1 and 3 GeV/c. The structure is very pronounced due presumably to the boson states that can be produced and it is hard to say much about the high energy behavior.

#### REFERENCES

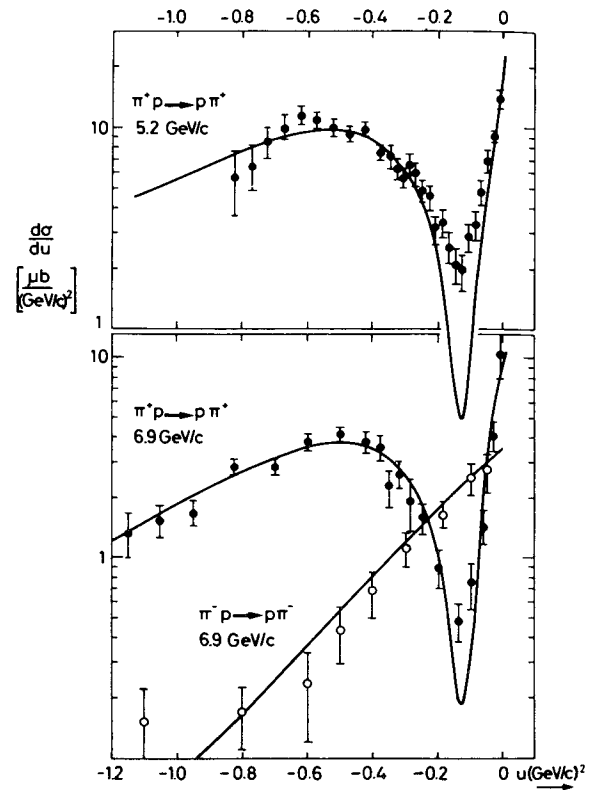
1. J. Banaigs, J. Bergo, C. Bonnel, J. Duflo, L. Goldzahl, F. Plouin, W.F. Baker, P.J. Carlson, V. Chabraud and A. Lundby, Physics Letters 24B, 317 (1967).
2. W.F. Baker, K. Berkelman, P.J. Carlson, G.P. Fisher, P. Fleury, D. Hartill, R. Kalbach, A. Lundby, S. Mukhin, R. Nierhaus, K.P. Pretzl and J. Woulds, Physics Letters 28B, 291 (1968).
3. D.P. Owen, F.C. Peterson, J. Orear, A.L. Read, D.J. Ryan, D.H. White, A. Ashmore, C.J.S. Damerell, W.R. Frisken and R. Rubinstein, Phys. Rev. 181, 1794 (1969).
4. E.W. Anderson, E.J. Bleser, H.R. Blieden, G.B. Collins, D. Garelick, J. Menes, F. Turkot, D. Birnbaum, R.M. Edelstein, N.C. Hien, T.J. McMahon, J. Mucci and J. Russ, Phys. Rev. Letters 20, 1529 (1968).
5. A.S. Carroll, J. Fischer, A. Lundby, R.H. Phillips, C.L. Wang, F. Lobkowitz, A.C. Melissinos, Y. Nagashima and S. Tewksbury, Phys. Rev. Letters 20, 607 (1968)
6. S.W. Kormanyos, A.D. Krisch, J.R. O'Fallon, K. Ruddick and L.G. Ratner, Phys. Rev. Letters 16, 709 (1966).
7. R.C. Chase, E. Coleman, H.W.J. Courant, E. Marquit, E.W. Petraske, H. Romer, and K. Ruddick, Phys. Rev. Letters 22, 1137 (1969).
8. V. Kistiakowsky, R.K. Yamamoto, R.D. Klem, P. Marcato, I.A. Pless, I. Spirm, E.F. Anelli, C.N. DeMazo, A. Romano, D.G. Crabb, A.C. Meyers III and J.R. O'Fallon, Phys. Rev. Letters 22, 618 (1969).

9. D. Birnbaum, R.M. Edelman, N.C. Hien, T.J. McMahon, J.F. Musci, J.S. Russ, E.W. Anderson, E.J. Bleser, H.R. Blieden, G.B. Collins, D. Garelick, J. Menes and F. Turkot, Proceedings of the XIV International High Energy Physics Conference (Vienna (1968)). No. 719.



The angular distributions of  $K^\pm p$  elastic scattering. The non-backward parts are taken at  $3.5 \text{ GeV}/c$ . The dotted curves indicate the gross features of the angular distributions.

Figure 1.



Backward  $\pi p$  elastic scattering angular distributions. The solid curves are Regge exchange fits using the  $N_\alpha$  and  $\Delta_\delta$  trajectories

Figure 2.

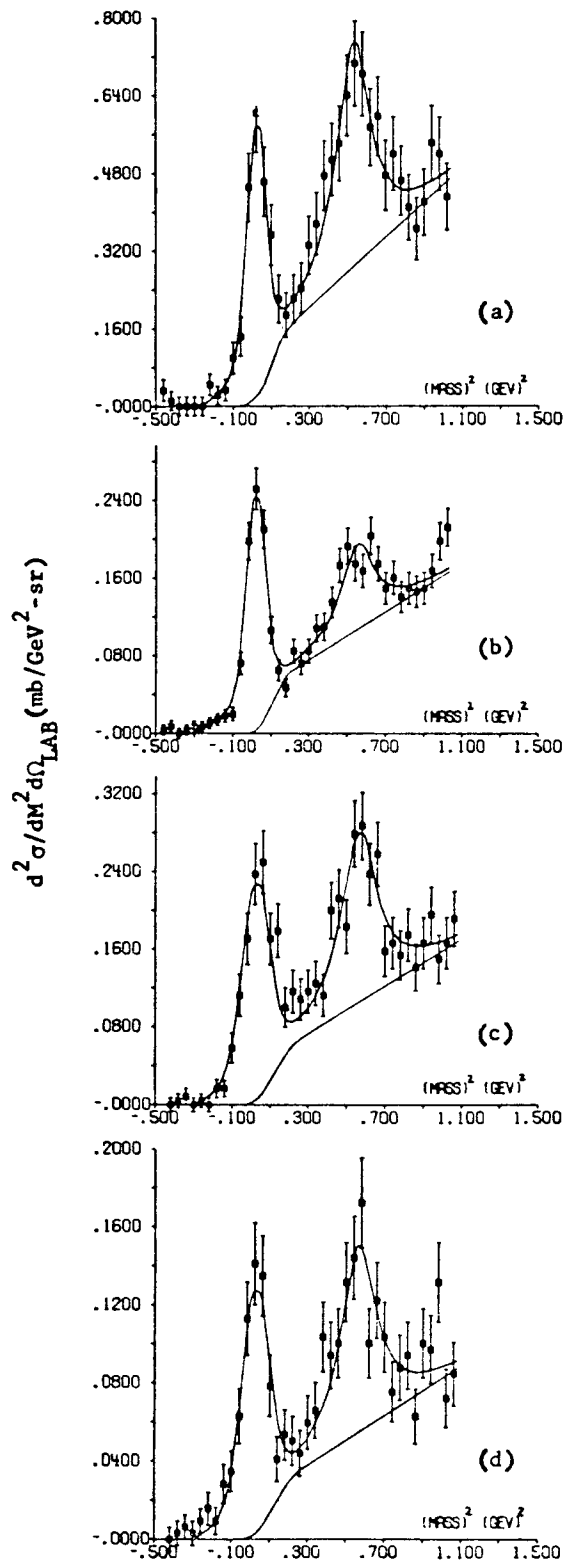


Figure 3.

(a) Missing-mass spectrum in the reaction  $\pi^- p \rightarrow p X^-$  for  $M_{X^-} \leq 1.0$  GeV at 8 GeV/c. The laboratory proton angle  $\theta_p = 20-26$  mrad and  $\langle u_p \rangle = -0.02$  (GeV/c)<sup>2</sup>. (b) Same spectrum as (a) but  $\theta_p = 58-76$  mrad and  $\langle u_p \rangle = -0.29$  (GeV/c)<sup>2</sup>. (c) Same spectrum as (a) except at 16 GeV/c,  $\theta_p = 20-26$  mrad, and  $\langle u_p \rangle = -0.13$  (GeV/c)<sup>2</sup>. (d) Same spectrum as (c) but  $\theta_p = 30-38$  mrad and  $\langle u_p \rangle = -0.30$  (GeV/c)<sup>2</sup>. In these figures the solid lines are the results of the least-squares fits described in the text.

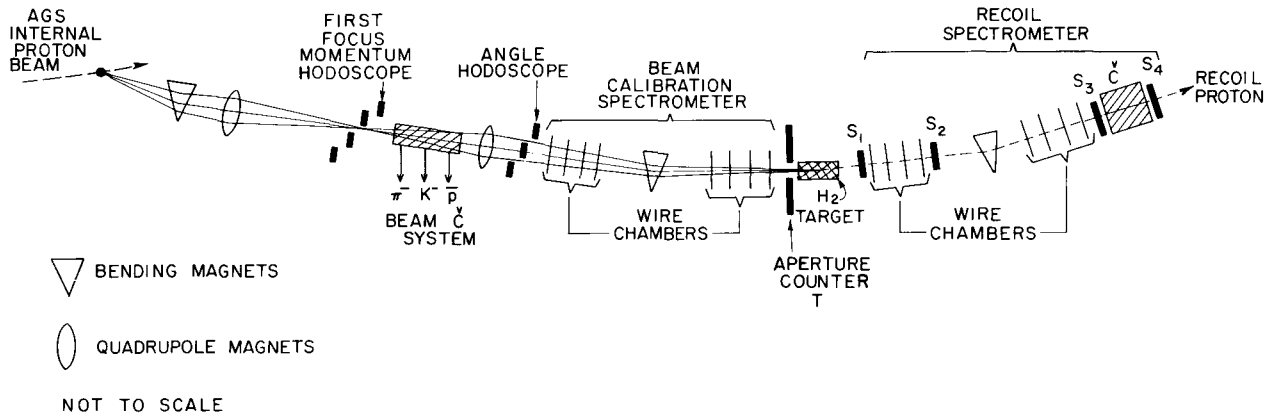


Figure 4.

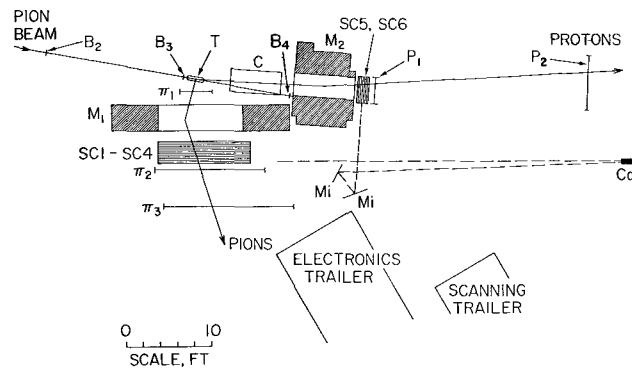


Figure 5.

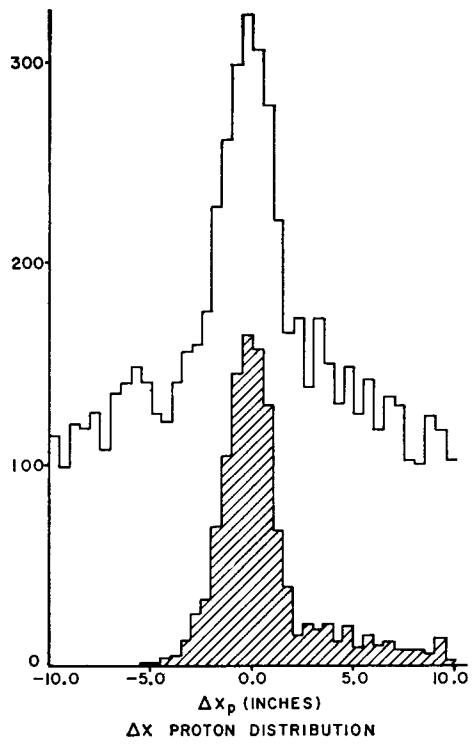


Figure 6.

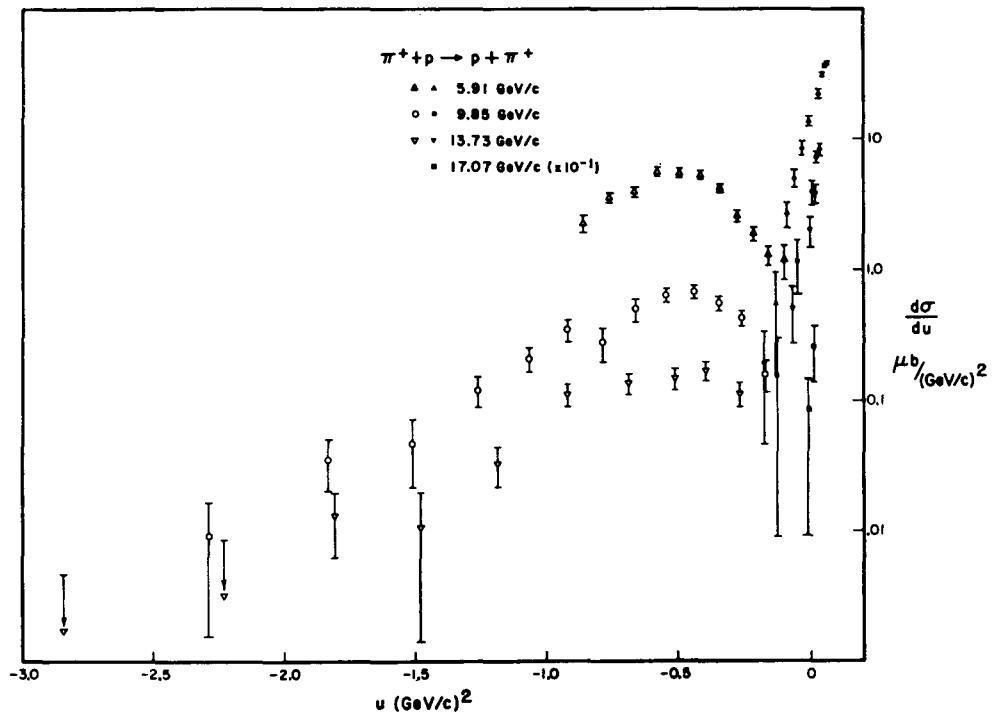


Figure 7.

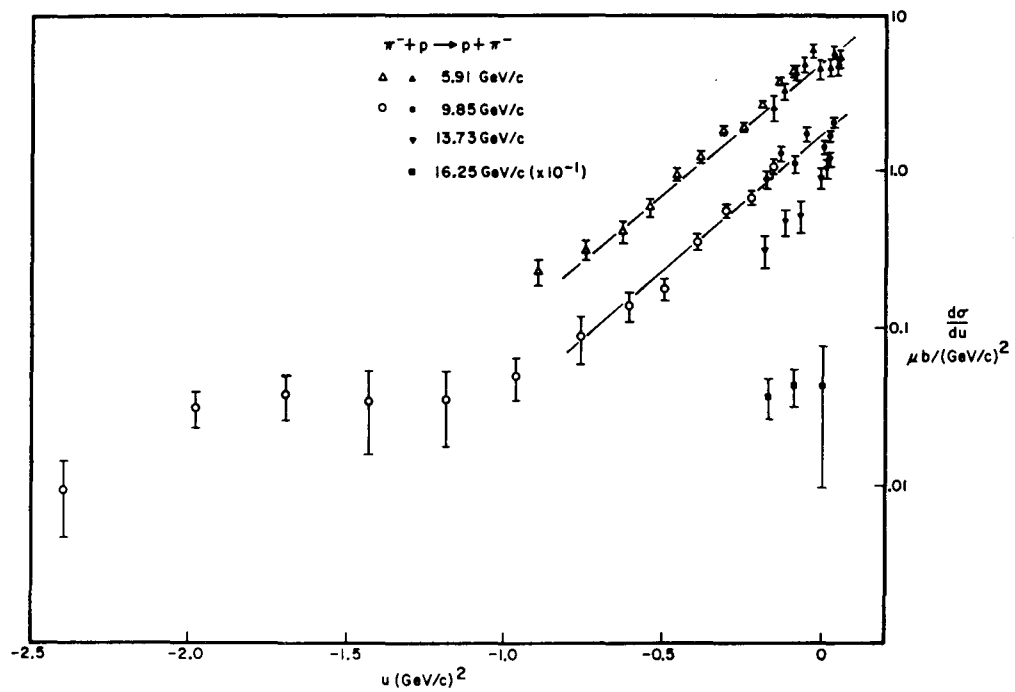


Figure 8.



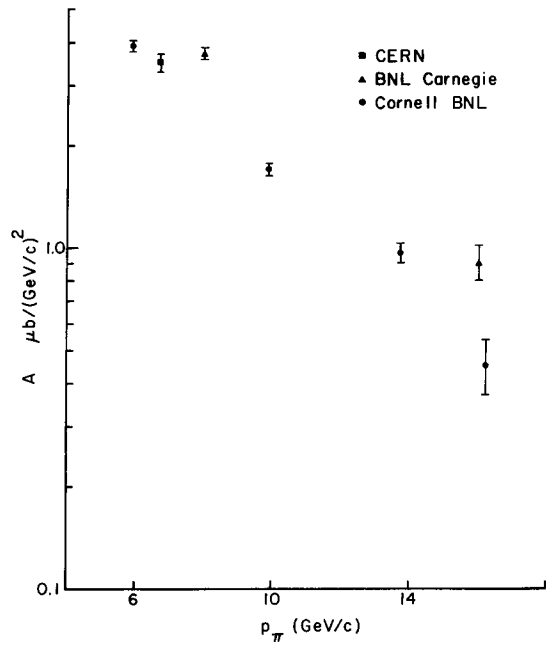


Figure 9.

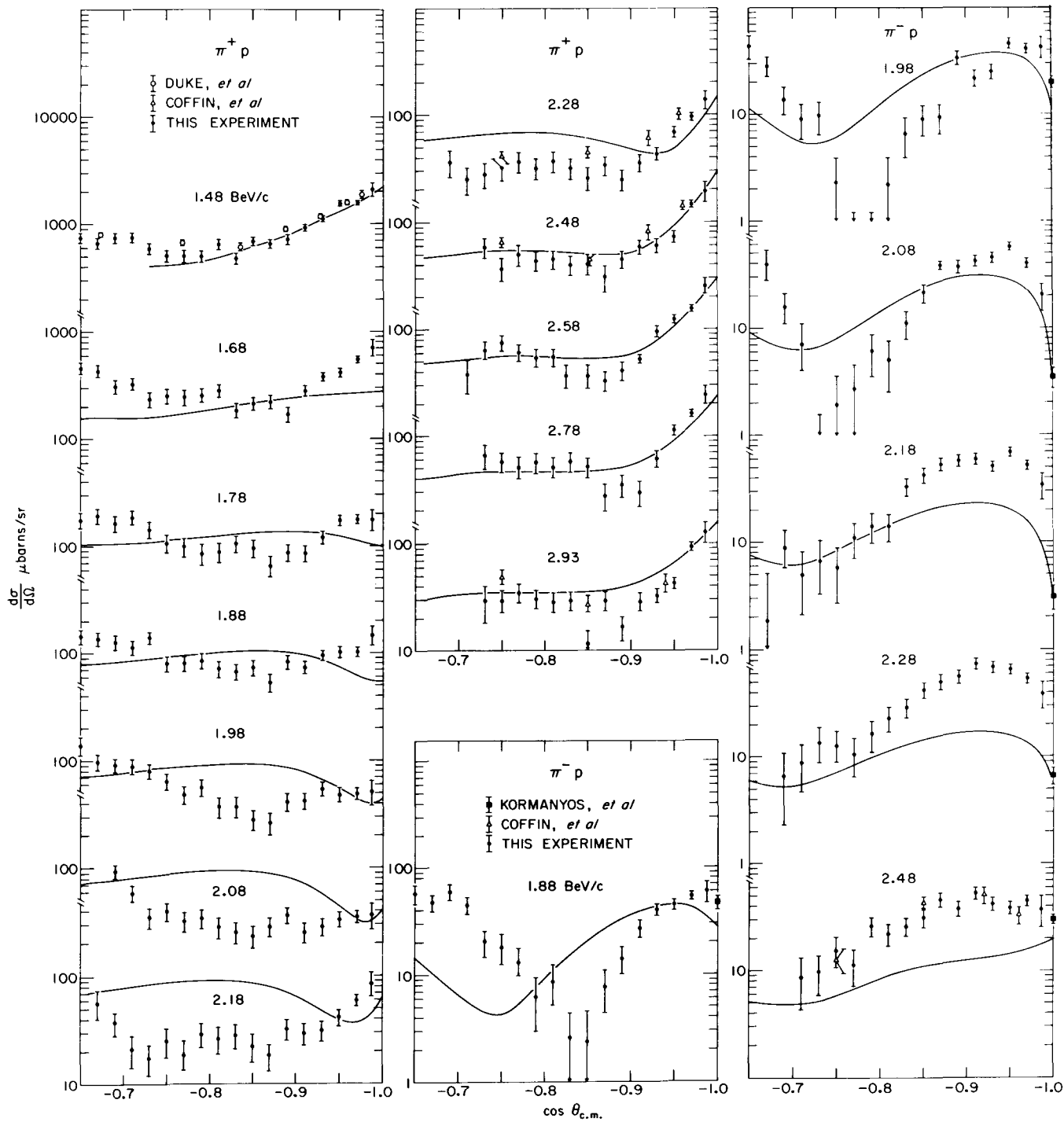
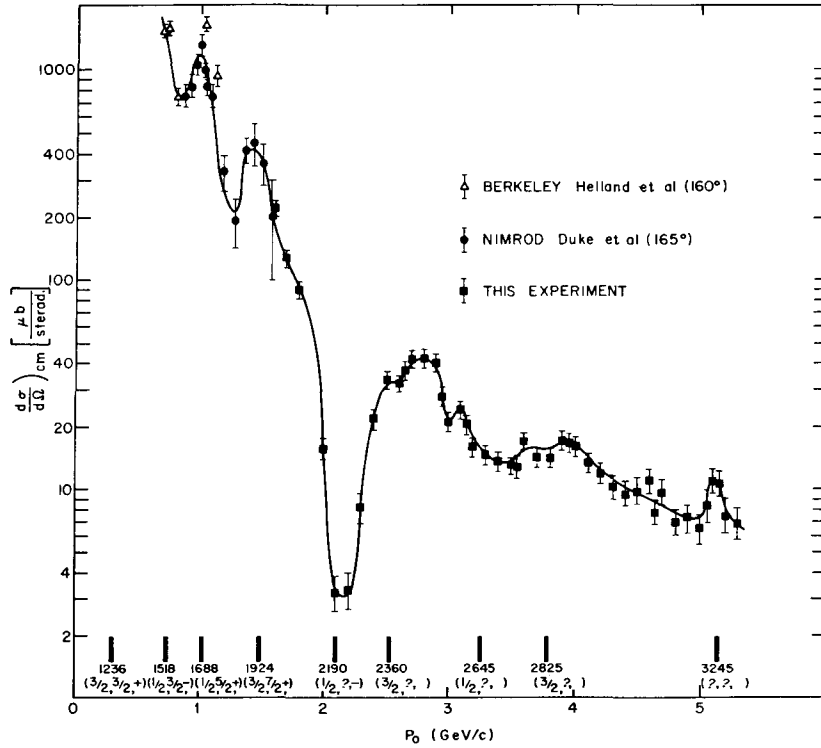


Figure 10.



Plot of  $d\sigma/d\Omega$  against  $P_0$ , the incident  $\pi^-$  laboratory momentum, for  $\pi^-p$  elastic scattering at  $180^\circ$ . The positions and properties of the  $N^*$  resonances are shown. The line drawn is a freehand fit to the data. The error bars shown are statistical. There is also a 12% normalization uncertainty.

Figure 11.

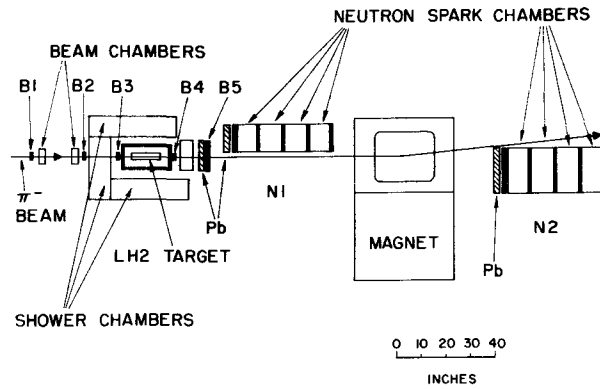


Figure 12.

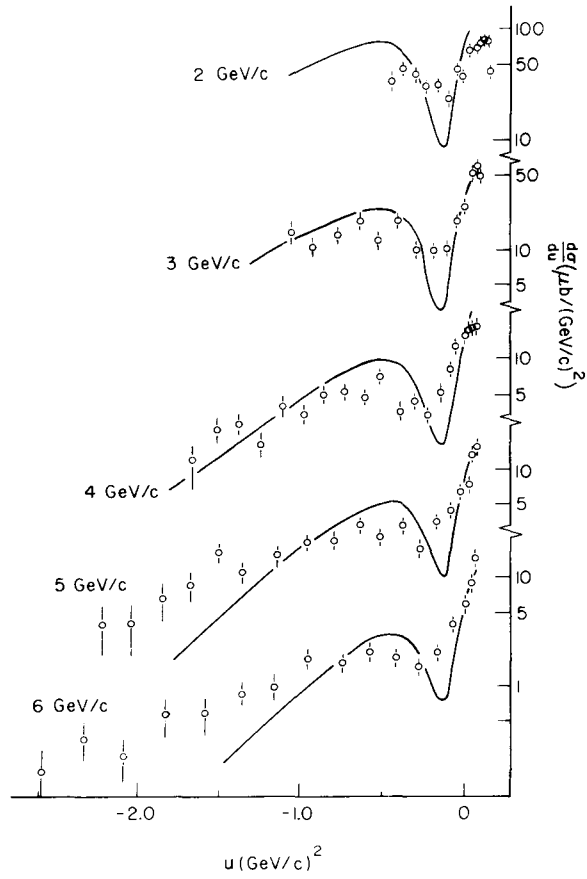


Figure 13.

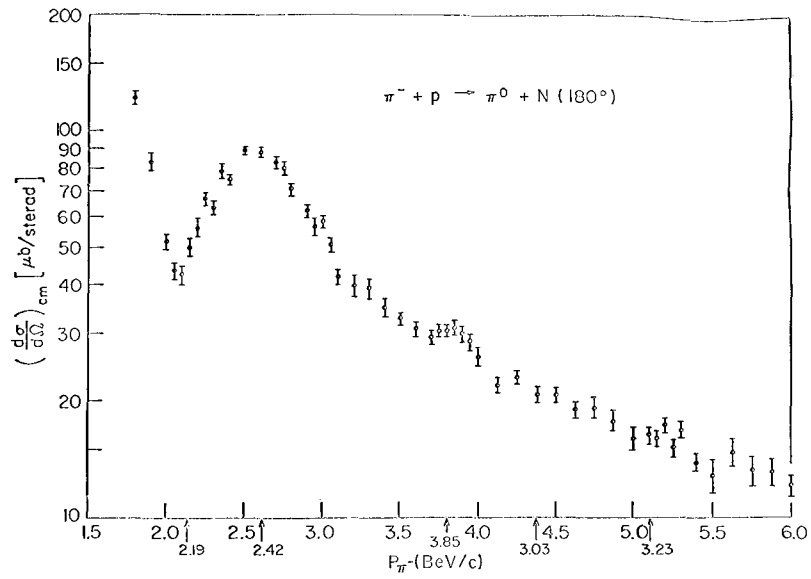
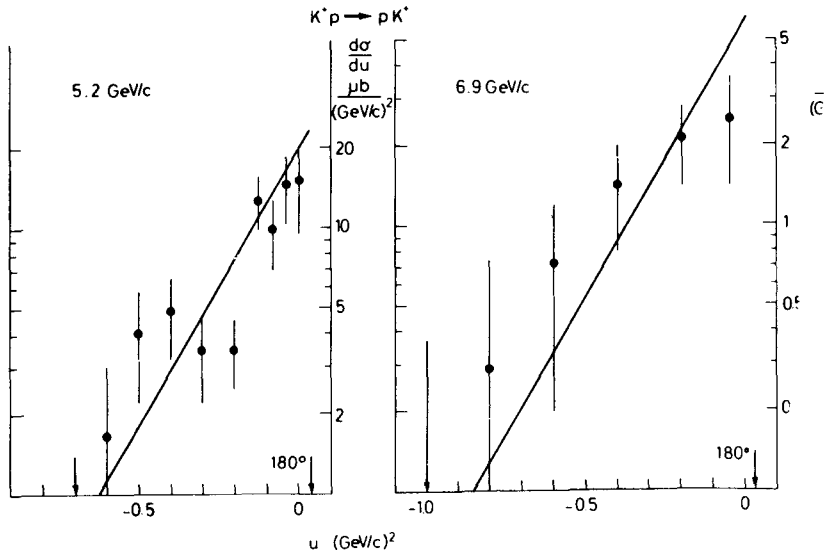
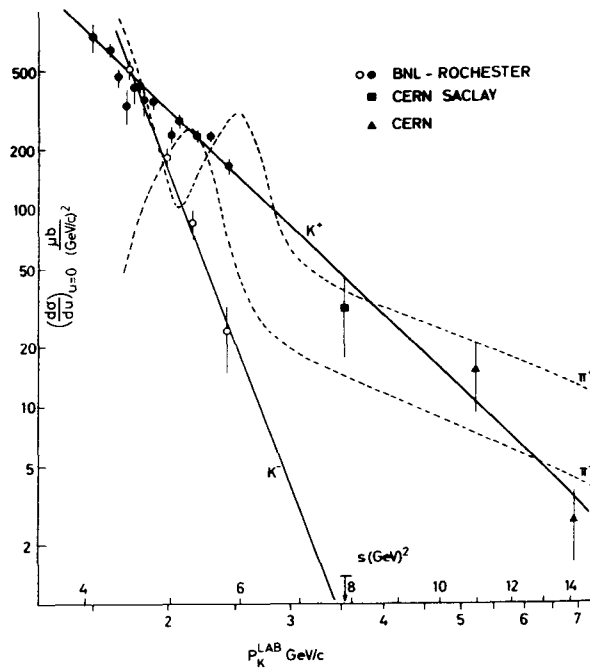


Figure 14.



Backward  $K^+p$  elastic scattering angular distributions. The solid lines indicate the slope of the forward elastic peak for comparison.

Figure 15.



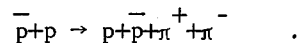
Energy dependence of  $d\sigma/du$  at  $u = 0$  for  $Kp$  elastic scattering. The CERN data are from this experiment. The dashed lines give the  $\pi p$  energy dependence (for sources see ref. 12).

Figure 16.

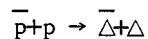
#### IV. TWO BODY INELASTIC REACTIONS

##### Isobar Production.

The data on two body reactions are generally less accurate than the data that we have discussed previously. There are two separate reasons for this. First, the direct observations that are made are of the "stable" particles that are emitted in an interaction. In a bubble chamber all the charged particles are customarily observed and measured. Then by balancing energy and momentum the mass and momentum of the missing object is deduced. If this is a known stable object (for example, neutron, pion) then the reaction is determined. It is often true that a neutral decays in the chamber ( $\Lambda$ ,  $K_S^0$ ) and then these events also are determined as well as if the neutral were a charged particle. After this identification of reaction is done the experimenter calculates the invariant mass for various combinations of these stable particles to see if there are states of defined mass from which the stable particles have come. Bockmann et al.<sup>1</sup> is a typical example in which a  $\bar{p}$  beam is used in a hydrogen bubble chamber. Figure 1 shows the Dalitz plot where the events are plotted against the mass of  $p\pi^+$ ,  $\bar{p}\pi^-$  in a two dimensional array from the reaction



It is easy to see the cluster in mass near the  $\Delta(1236)$  in both states so that we can argue that the primary reaction in most of the cases was



both  $\Delta$ 's being charged.

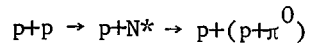
Using the events in the right mass region allows a plot of cross section against momentum transfer to be made as is shown in Fig. 2. Notice there is a minimum momentum transfer even at  $0^\circ$  because of the masses of the  $\Delta$ . The relative paucity of events is explained by the following calculation. A reasonable bubble chamber exposure is  $10^5$  pictures with perhaps ten particles per picture. In a fiducial volume of 30 cm(1) then 1  $\mu$ barn ( $\sigma$ ) of cross section gives

$$\begin{aligned} N_{\text{events}} &= 1 \times \rho \times 6 \times 10^{23} \times \sigma \times N_{\text{particles}} \\ &= 30 \times 0.07 \times 6 \times 10^{23} \times 10^{-30} \times 10^6 \\ &= 1.2 \text{ events}/\mu\text{b} \end{aligned}$$

Now, it is imaginable that we can increase this by a factor of ten but not much more. This is one of the major reasons that we have not discussed many bubble chamber experiments so far since 1  $\mu$ b is a reasonable level of cross section for many of the processes at high energy.

The second reason that these inelastic reactions are generally less accurate,

is that the counter-spark chamber experiments have relied on the one arm spectrometer technique. This means that in a reaction where one of the products is stable, for example



then if we measure the momentum spectrum of protons from this reaction we shall see a peak corresponding to the mass of the  $N^*$  together with a continuum from the protons resulting from  $N^*$  decay. In addition there is a non-resonant background where the mass of the  $p\pi^0$  system lies under the  $N^*$  peak. The experimental problem is typified by the curves in Fig. 3. A smooth curve must be subtracted and the cross section for the peaks deduced. The cross sections are rather dependent on the form of the background and the widths that are assumed; this reflects into the large systematic normalization error quoted although the  $t$  dependence and to a lesser extent the energy dependence of these cross sections should not be so uncertain. Foley et al.<sup>3</sup> show data from pions as well as protons, and at least to the untutored eye they look very similar. Figure 4 shows the integrated cross section for the production of the various isobars as a function of incident momentum. The remarkable fact is that they are rather energy independent with the exception of the  $N^*(1236)$  which decreases with incident momentum.

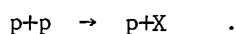
There is an empirical rule, suggested by Morrison,<sup>16</sup> for those reactions which appear to be constant with energy. The rule is that if there is a change of spin  $\Delta J$  from the initial to the final state then for these "allowed" reactions the change in parity is given by

$$p = (-1)^{\Delta J}$$

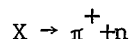
and moreover there cannot be a change in  $I$  spin. This is explained by the diagram in Fig. 5 where the exchanged particle is a pomeron and the mechanism of production is that the incident particle dissociates into a nucleon and a pion and the pion elastically scatters through the pomeron and recombines forming the isobar. Morrison refers to these reactions as quasi elastic scattering. In the Anderson et al.<sup>2</sup> experiment the  $N^*_{1/2}$  isobars that are seen with constant cross sections are thought to have  $J^P = 1/2^+, 3/2^-, 5/2^+$ , so that the quasi elastic rule is satisfied, but the  $N^*_{3/2}(1236)$  clearly does not satisfy the rule as does the  $N^*_{1/2}(1570)$  with  $J^P = 1/2^-$ . This description is typical of the understanding and state of the experimental art in isobar production. The experimental difficulties are real in terms of the understanding of the cross section data itself and so far the crude phenomenology is successful in classifying the reactions that keep their share of the total cross section and those that don't. The energy dependence of those reactions we hypothesize as one particle exchange are consistent with the Regge picture with  $S^{2\alpha-2}$ , but the tests are not stringent.

Recently, there have been two very careful experiments in the higher  $t$  region.<sup>4,5</sup> The  $N^*(1518)$  and  $N^*(1688)$  are two of the quasi-elastically produced resonances that have been studied at high  $t$ . Figures 6 and 7 show their behavior. The very flat angular distribution at low energies seems to give way to a distribution that resembles p-p elastic at the highest energy. Belletini<sup>6</sup> speculates that we may be seeing an energy independent angular distribution which resembles the elastic cross section but one order of magnitude smaller at momenta about 20 GeV/c. The resemblance between the distributions of the two isobars is impressive.

It is interesting to see how the I spin of a peak is established, and a nice example is given by a 28.5 GeV/c bubble chamber exposure by Ellis et al.<sup>7</sup> They look at the missing mass distribution calculated from the proton in the reaction



Then they divide the X sample into 1 prong and 3 prong decays. From the 1 prong sample they separate



from the rest by identifying the neutron missing mass. Additionally the 3 prong decays have no enhancement at 1400 (MeV/c) as expected. Then if we assume that the rest of the one prong decays are  $X \rightarrow \pi^0 + p$  we can compare the rates

$$\begin{aligned} R_1 &= \pi^+ + n \\ R_2 &= \pi^0 + p \quad . \end{aligned}$$

If  $I = \frac{1}{2}$  these are

$$\frac{R_1}{R_2} = 2 \quad .$$

If  $I = 3/2$

$$\frac{R_1}{R_2} = 1/2 \quad .$$

The first is the only solution consistent with the data establishing that there is an  $I = \frac{1}{2}$  state in this peak. This enhancement though, is a complicated structure and more work is needed to completely resolve the situation.

#### Meson-Nucleon Inelastic Scattering

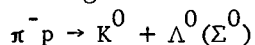
This subject is confused partly because the conclusions have been based on data of limited statistical accuracy. This experimental situation is improving and the confusion is increasing. A fine example of what we mean is shown in Fig. 8. This data is from reference 8. Two mesons are studied  $K^*(890)$  and  $K^*(1420)$  in production by  $K^-$  at 10 GeV/c. It has been thought that reactions where there is charge exchange between incident and final kaon state then pion exchange dominates but if there is no charge exchange than  $\omega$ 's are responsible. This hypothesis is generated to explain



the fact that these cross sections have either a dip near  $t_{\min}$  or a sharp peak depending on whether charge is exchanged or not. These structures are illustrated in the plot for small  $t$  in Fig. 9. Analysis of the decays of the reaction product however, do not seem to bear out the simple dominance picture. A similar situation exists in pion initiated reactions, Fig. 10 is a fine example, from reference 9.

The difficulty in this field is that there is a great deal of data on many reactions much of which has limited statistical accuracy. The conclusion that one can draw, however, is that the kind of detailed structure present in elastic scattering is present here also and the motivation for obtaining really accurate data for understanding the dynamics is strong.

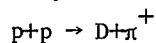
Strange Particle Exchange



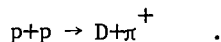
This kind of reaction, where the inelastic products are "stable" is typified by the data in Fig. 11. The experimental resolution is unfortunately not sufficient to separate  $\Lambda^0$  from  $\Sigma^0$  in the final state. Do not be confused by the ordinate, the cross section really decreases with energy. The rate of decrease is consistent with a simple Reggeized exchange picture. The conclusions that these reactions give angular distributions with many structural features in common is reinforced by the Stony Brook<sup>10</sup> data which we shall see in the Stony Brook conference report by Kirz.

Another gross feature of these reactions is illustrated in Fig. 12, where the slope of the forward cross section is quite different for  $\Sigma$  and  $\Upsilon^*$  production from  $\bar{K} p$ .

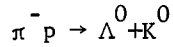
Baryon Exchange



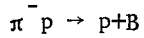
The one arm spectrometer technique has been used to study the reaction



The cross section has been measured near  $0^\circ$  for the deuteron by Anderson et al.<sup>12</sup> and is shown in Fig. 13. The momentum of the deuteron was measured and the particle identified. This point is worth making because of that solitary point in the figure at high energies which relied on measuring the pion. Unfortunately this will not do because the neutron and proton tend to go off with a low relative momentum even when they do not bind in the deuteron so the experiment does not distinguish between these two situations unless the deuteron is identified. Figure 14 shows a typical missing mass distribution together with an angular distribution in Fig. 15. It is remarkable how the slopes of these two curves are the same even though the cross section has changed by two orders of magnitude in going from 6 GeV to 20 GeV. This kind of violent energy dependence is characteristic of baryon exchange processes.



This reaction involving a high momentum  $\Lambda$  is typical of a baryon exchange involving a hyperon trajectory. Fairly accurate data is available on the angular distribution together with the polarisation of the  $\Lambda$  from its decay angular distribution. The data is shown in Figs. 16 and 17 from reference 13. The Reggeized baryon exchange model with the  $\Sigma_\alpha$  and  $\Sigma_\delta$  trajectories can explain these data with much the same parametrization as in  $\pi p$  backward elastic.



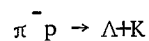
The experiment of Anderson et al.<sup>14</sup> shows very clearly the  $\rho^-$  production near  $180^\circ$ . The experiment as we know measures the momentum of the forward proton and then the expression

$$\Delta p = \frac{m_p^2 - m_x^2}{2m_p}$$

gives the change in momentum between the beam and the proton.  $m_x$  is deduced thereby for each event and the plot is shown in Fig. 18. The systematic error is still involved with the background under the peak, it is more difficult than the elastic reaction, as you can see from this figure. Figure 19 shows the cross section plotted against  $u$  for both 8 and 16 GeV/c incident momentum. In addition, Anderson et al.<sup>15</sup> have evidence for  $A_1$  and  $A_2$  production near  $180^\circ$  in reference 15. It seems that all mesons are produced in the backward peak with the  $A_1$  having a very sharp angular distribution. Shih<sup>16</sup> has explained the  $\rho$  cross sections with a Regge parametrisation that is similar to that needed for elastic scattering.

#### SUMMARY

It is hard to summarise the field of two body inelastic scattering because, as we have seen, there is a vast multiplicity of reactions that share the total cross section, with rather few being measured well. The backward cross sections seem presently to be well explained on the Regge model although the accuracy of the data is such that the constraints are generally not so severe as in elastic scattering. The presence and shape of the polarisation of the  $\Lambda$  produced backwards in



is a gratifying "prediction" of this model.

In the forward direction the situation is more complicated, the possible exchanged particles are more diverse but again the gross features are explained on the exchange picture. The energy dependence of the integrated cross sections fall into 3 categories,

- a) Pomeron exchange (quasi-elastic scattering)
- b) non-strange meson exchange

c) strange meson exchange.

Broadly speaking, the energy dependence of each of these categories fits with the first category being nearly constant given the rule that the parity change

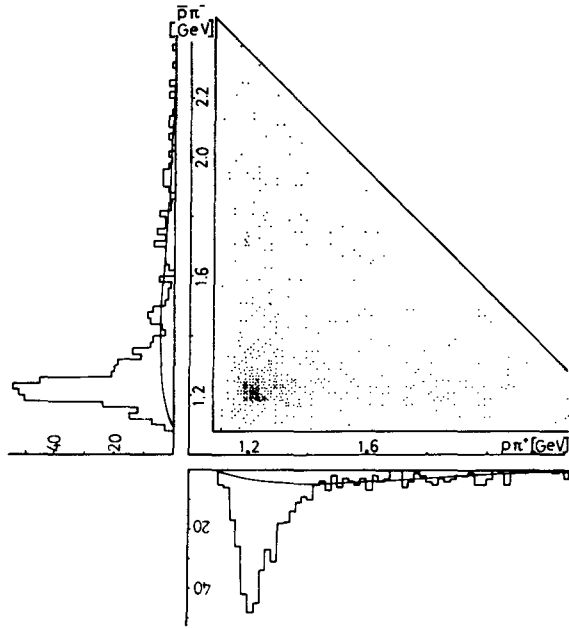
$$\Delta P = (-1)^{\Delta l} .$$

$\Delta l$  the spin change between the two high momentum objects. The structure that appears (forward dip or peaks) seems to hint at an explanation and further data should allow quantitative understanding of these processes. It would seem that this area will develop experimentally a great deal in the next few years with the planning of two arm spectrometers to improve the systematic understanding of the reaction cross sections.

#### REFERENCES

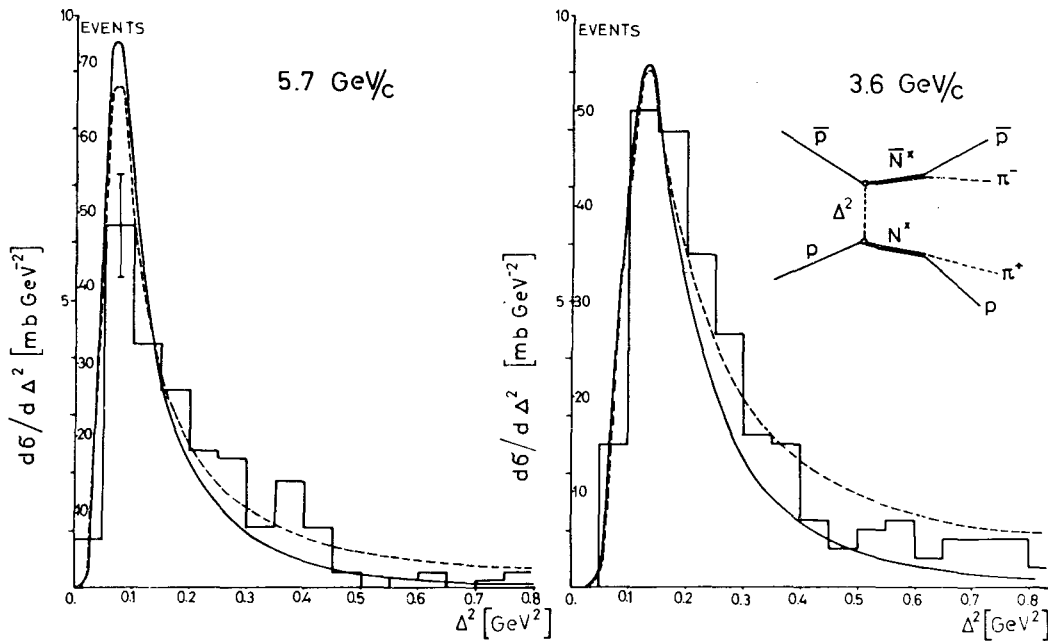
1. K. Bückmann, B. Nellan, E. Paul, I. Borecka, J. Diaz, U. Heeren, U. Liebermeister, E. Lohrmann, E. Raubold, P. Söding, S. Wolff, S. Coletti, J. Kidd, L. Mandelli, V. Pelosi, S. Ratti and L. Tallone, *Physics Letters* 15, 356 (1965).
2. E.W. Anderson, E.J. Bleser, G.B. Collins, T. Fujii, J. Menes, F. Turkot, R.A. Carrigan, Jr., R.M. Edelstein, N.C. Hien, T.J. McMahon and I. Nadelhaft, *Phys. Rev. Letters* 16, 855 (1966).
3. K.J. Foley, R.S. Jones, S.J. Lindenbaum, W.A. Love, S. Ozaki, E.D. Platner, O.A. Quarles and E.H. Willen, *Phys. Rev. Letters* 19, 397 (1967).
4. C.M. Ankerbrandt, A.R. Clock, B. Cork, T. Elioff, L.T. Kerth and W.A. Wenzel, *Phys. Rev.* 170, 1223 (1968).
5. J.V. Allaby, F. Binon, A.N. Diddens, P. Duteil, A. Klovning, R. Meunier, J.P. Peigneux, E.J. Sachardis, K. Schlupmann, M. Spighel, J.P. Stroot, A.M. Thorndike and A.M. Wetherell, *Physics Letters* 29E, 198 (1969).
6. G. Bellettini, Two Body Processes, *Proceedings of the XIV International Conference on High Energy Physics, Vienna (1968)*.
7. W.E. Ellis, D.J. Miller, T.W. Morris, R.S. Panvini and A.M. Thorndike, *Phys. Rev. Letters* 21, 697 (1968).
8. ABCL(IC) Collaboration. Total and differential cross-sections in 10 GeV/c  $k^- p$  interactions. *Nucl. Phys.* (to be submitted).
9. ABC Collaboration. Structure in differential cross-section distributions of quasi two-body reactions in 8 GeV/c  $\pi^+ p$  interactions. *Nucl. Phys.* (to be submitted).
10. Pisa-Orsay Collaboration, reported by Belletini in the Vienna Conference Report (1968).
11. *Proceedings of the International Conference on Two Body Reactions at Stony Brook (1969)*.

12. H.L. Anderson, M. Dixit, H.J. Evans, K.A. Klare, D.A. Larson, M.V. Sherbrook, R.L. Martin, K.W. Edwards, D. Kessler, D.E. Nagle, H.A. Thiessen, C.K. Hargrove, E.P. Hincks and S. Fukui, Phys. Rev. Letters 21, 853 (1968).
13. W. Beusch, W.E. Fischer, R. Frosch, P. Mühlemann, M. Pepin, E. Polgar, J. Codling, M. Green and D. Websdale, Angular distribution and polarisation in the backward peak of  $\pi^+p \rightarrow \Lambda^0 K^0$  at 4 and 6/2 GeV/c, Proceedings of XIV International Conference of High Energy Physics, Vienna (1968).
14. E.W. Anderson, E.J. Bleser, H.R. Blieden, G.B. Collins, D. Garelick, J. Menes, F. Turkot, D. Birnbaum, R.M. Edelstein, N.C. Hien, T.J. McMahon, J. Mucci and J. Russ, Phys. Rev. Letters 22, 102 (1969).
15. E.W. Anderson, E.J. Bleser, H.R. Blieden, G.B. Collins, D. Garelick, J. Menes, F. Turkot, D. Birnbaum, R.M. Edelstein, N.C. Hien, T.J. McMahon, J. Mucci and J. Russ, Phys. Rev. Letters 22, 1390 (1969).
16. C.C. Shih, Phys. Rev. Letters 22, 105 (1969).



Distribution of the  $(p\pi^+)$  mass versus the  $(\bar{p}\pi^-)$  mass for the reaction  $pp \rightarrow pp\bar{\pi}^+\pi^-$  at 5.7 GeV. The curves represent the phase space, normalized to the number of events with masses  $> 1.4$  GeV.

Figure 1.



Distribution of the square of the four momentum transfer  $\Delta^2$  between incident  $\bar{p}$  and outgoing  $(\bar{p}\pi^-)$  system. Only events in the double isobar region are plotted (193 events at 5.7 GeV/c, 270 events at 3.6 GeV/c), with  $1.13 \text{ GeV} < M(\pi^+p)$  and  $M(\pi^-p) < 1.33 \text{ GeV}$ . The full curves are the one pion exchange prediction with Ferrari-Selleri form factors, the dashed curves with the form factor used by Goldhaber et al.

Figure 2.

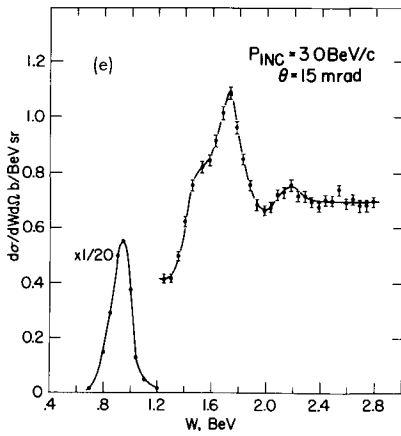
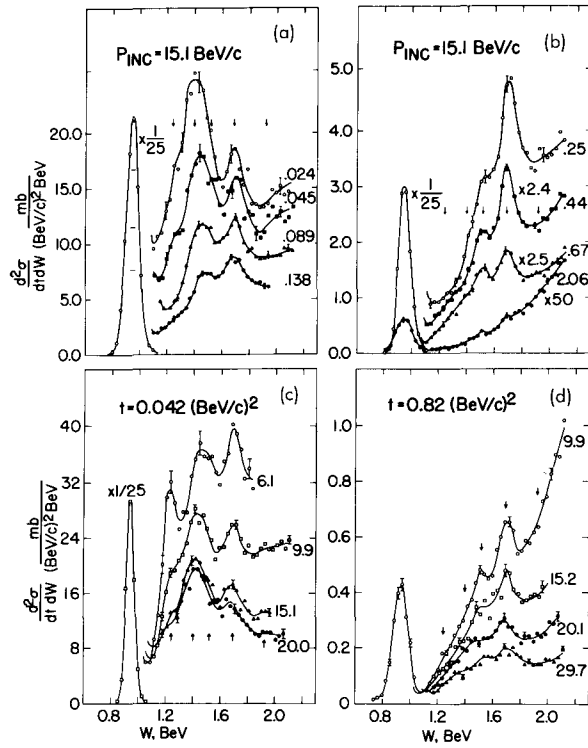


Figure 3.

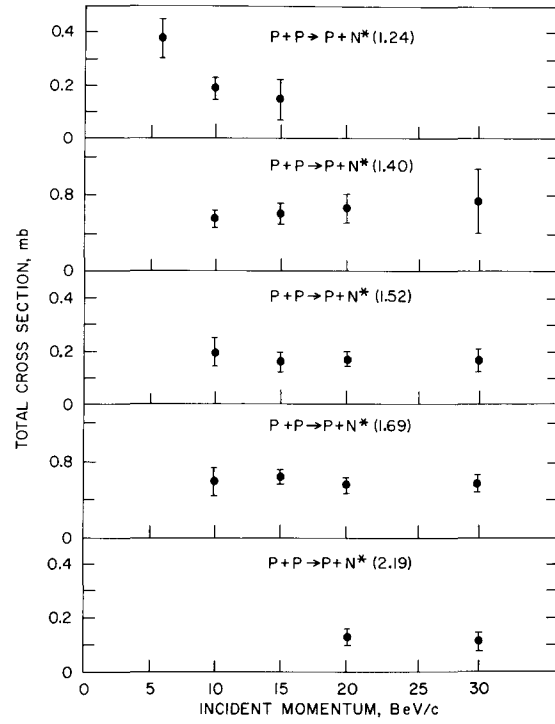


Figure 4.

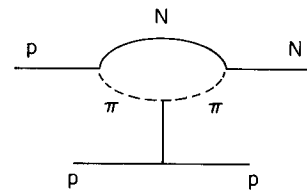
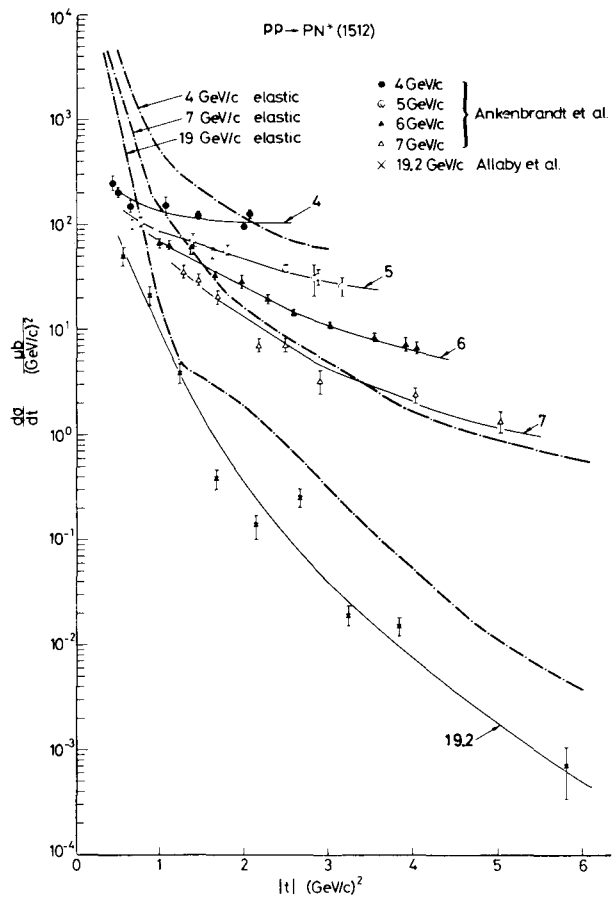
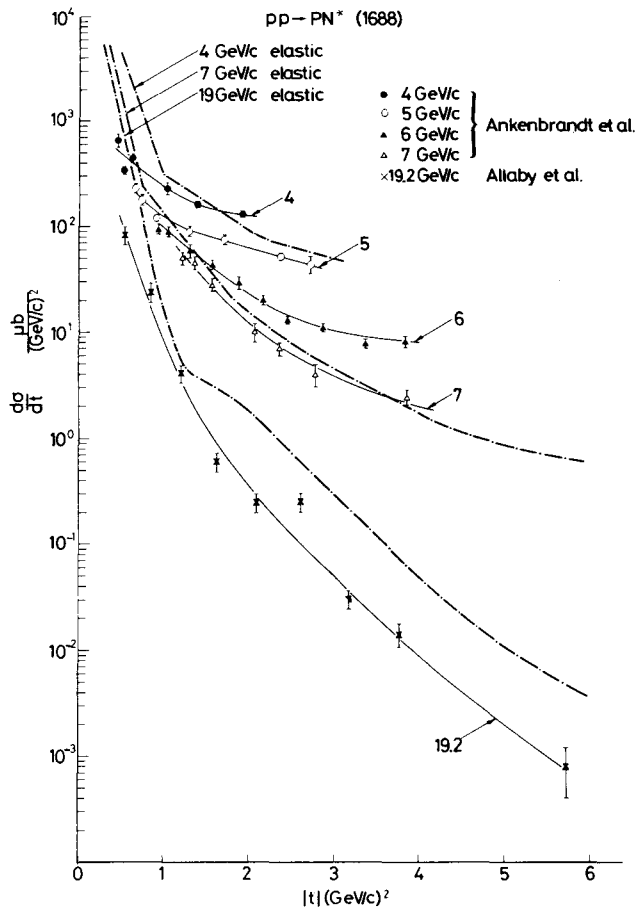


Figure 5.



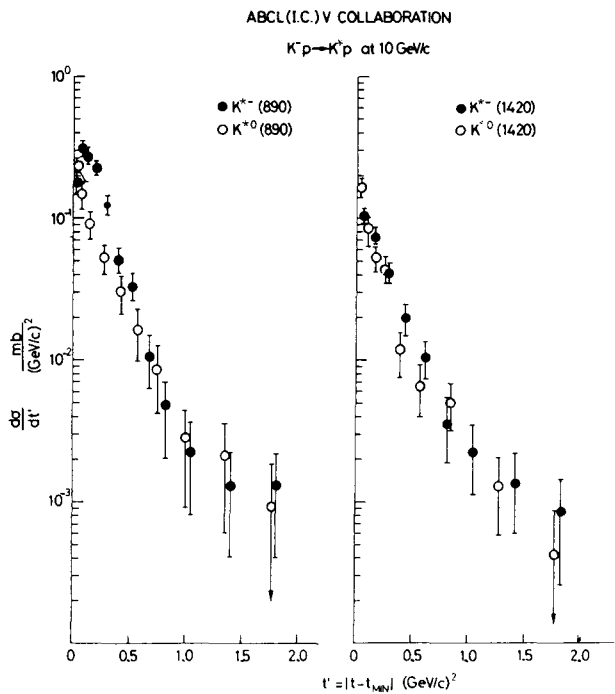
Differential cross-section for the reaction  $pp \rightarrow pN^*(1512)$  at 4, 5, 6, 7, and 19.2 GeV/c, and at large  $[|t| \gtrsim 0.5 \text{ (GeV/c)}^2]$  momentum transfers. The behaviour of the  $\sim 4$ ,  $\sim 7$ , and  $\sim 19 \text{ GeV/c}$  pp elastic scattering cross-section is also shown for comparison.

Figure 6.



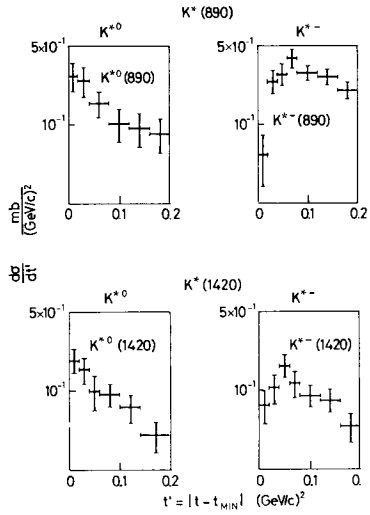
Differential cross-section for the reaction  $pp \rightarrow pN^*(1688)$  at 4, 5, 6, 7, and 19.2 GeV/c, and at large  $[|t| \gtrsim 0.5 \text{ (GeV/c)}^2]$  momentum transfers. The behaviour of the  $\sim 4$ ,  $\sim 7$ , and  $\sim 19 \text{ GeV/c}$  pp elastic scattering cross-section is also shown for comparison.

Figure 7.



Differential cross-sections for the reactions  $K^{*-} + p \rightarrow K^{*0} + n$  for  $K^*(890)$  and  $K^*(1400)$  at 10 GeV/c

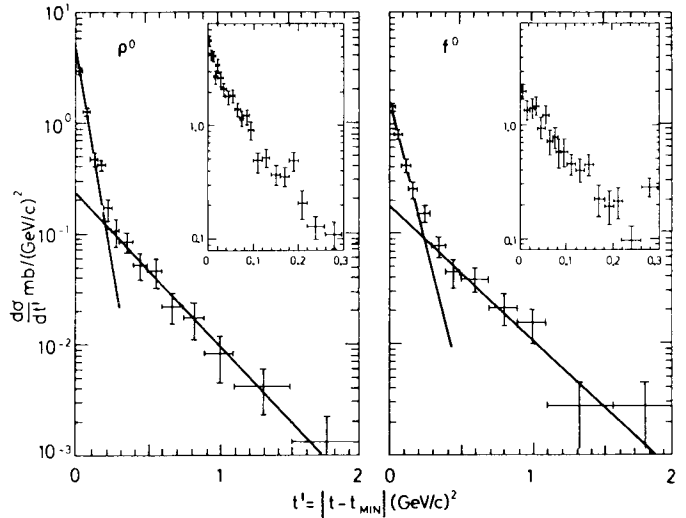
Figure 8.



Differential cross-sections at  $t' < 0.2 \text{ (GeV/c)}^2$  for  $K^*(890)$  and  $K^*(1420)$  excitation in  $K^\pm + p \rightarrow K^*N$  reactions at  $10 \text{ GeV/c}$ .

Figure 9.

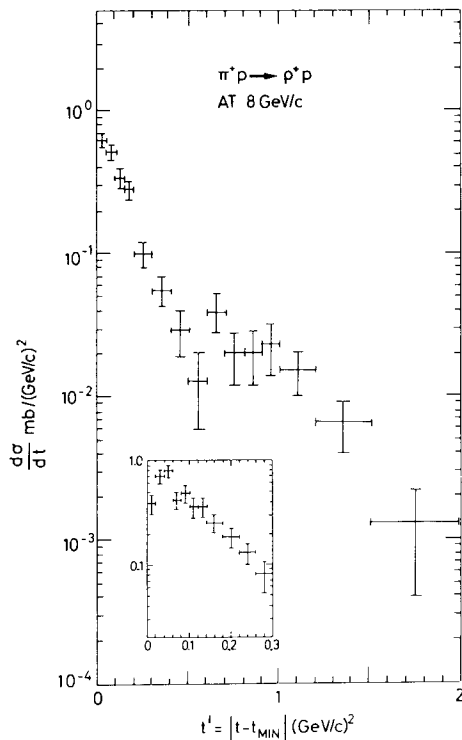
ABC COLLABORATION  
 $\pi^+ p \rightarrow \rho^0(f^0) \Delta^{++}$  at  $8 \text{ GeV/c}$



Differential cross-sections for the reaction  $\pi^+ + p \rightarrow \rho^0(f^0) + \Delta^{++}$  at  $8 \text{ GeV/c}$ . The insert shows the small  $t'$  region in detail.

Figure 10a.

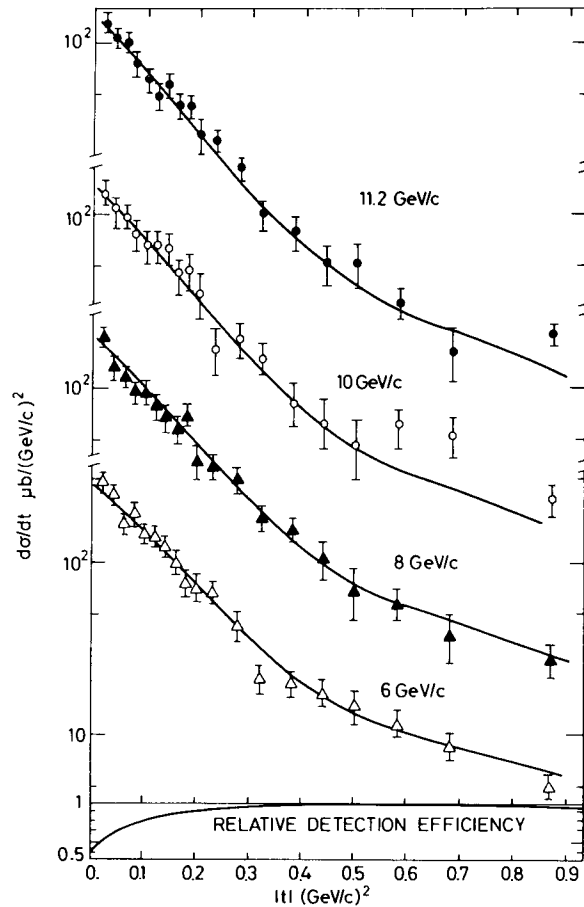
ABC COLLABORATION



Differential cross-section for the reaction  $\pi^+ + p \rightarrow \rho^+ + p$  at  $8 \text{ GeV/c}$ . The insert shows the small  $t'$  region in detail.

Figure 10b.

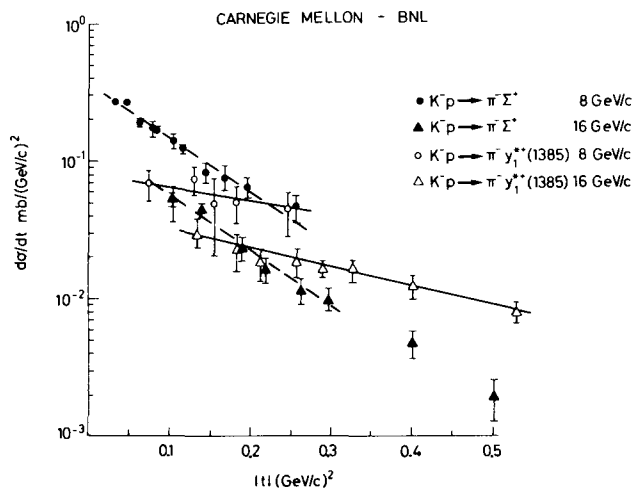
PISA - ORSAY COLLABORATION  
 $\pi^- p \rightarrow K^0 \Lambda(\Sigma^0)$



Differential cross-sections for the reaction  $\pi^- + p \rightarrow K^0 + \Lambda$  (or  $\Sigma^0$ ) at  $|t| \lesssim 1 \text{ (GeV/c)}^2$ . The theoretical curves are fitted to the data and have been calculated in the model by Reeder and Sarma.

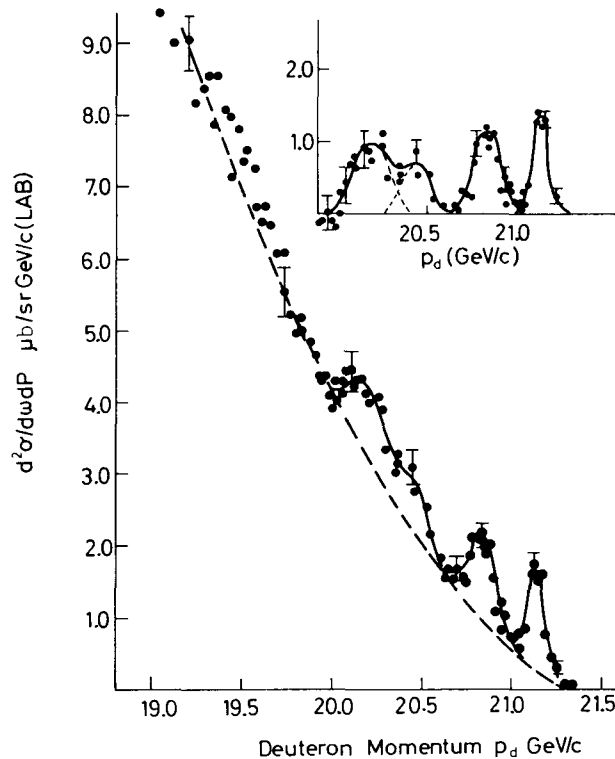
Figure 11.





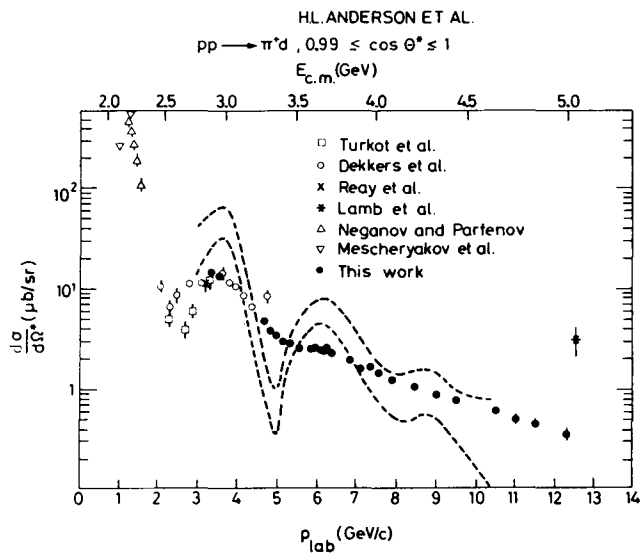
Forward differential cross-sections for the reactions  $K^- + p \rightarrow \pi^- + \Sigma^+$  and  $K^- + p \rightarrow \pi^- + \gamma_1^+(1385)$  at 8 and 16 GeV/c. Figure 12.

J.V. ALLABY et al.  
 $p p \rightarrow d X$  at 21.1 GeV/c  
 $(\theta_{LAB}=40\text{mrad})$



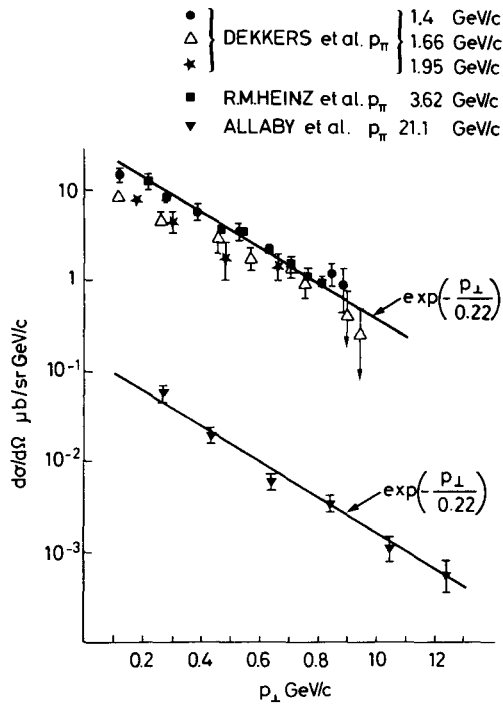
Deuteron momentum spectrum obtained in the experiment of Allaby et al. at a laboratory angle of 40 mrad. The broken line indicates the hand-drawn fit to the smooth continuum used to extract the two-body differential cross-sections. The insert shows the spectrum after subtraction of this continuum.

Figure 14.



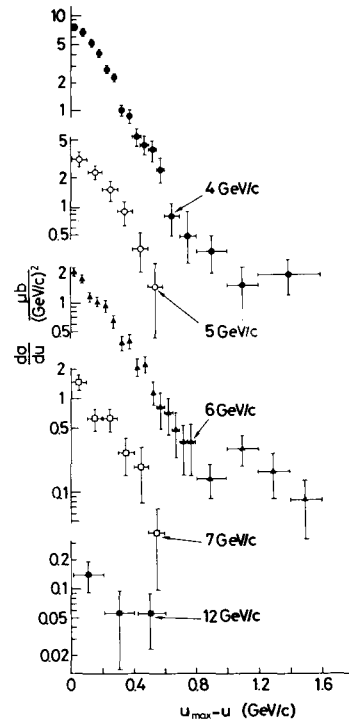
Forward ( $0.99 < \cos \theta^* < 1$ ) differential cross-section for the reaction  $p + p \rightarrow d + \pi^+$  as a function of the incident momentum  $p_{lab}$  and of the total c.m. energy ( $E_{c.m.}$ , upper scale). The dashed curves are calculated according to the model of Yao. The upper and lower bounds correspond to the lack of knowledge on the pion charge-exchange cross-section.

Figure 13.



A comparison by Allaby et al. between their data on the  $p + p \rightarrow d + \pi^+$  reaction at 21.1 GeV/c and the data by Heinz et al. at 3.62 GeV/c. The data of Dekkers et al. on the inverse reaction  $\pi^+ + d \rightarrow p + p$  are also displayed.

Figure 15.



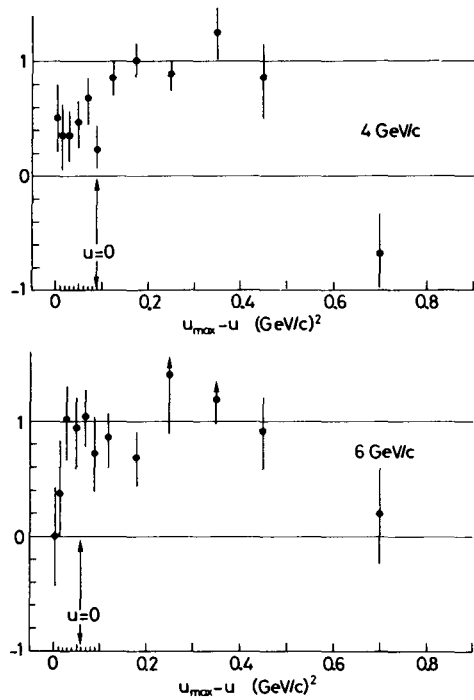
Differential cross-sections for the associated production reaction  $\pi^- + p \rightarrow K^0 + \Lambda$  in the backward region between 4 and 12 GeV/c incoming momentum.

Figure 16.

CERN - ETH - IMPERIAL COLLEGE

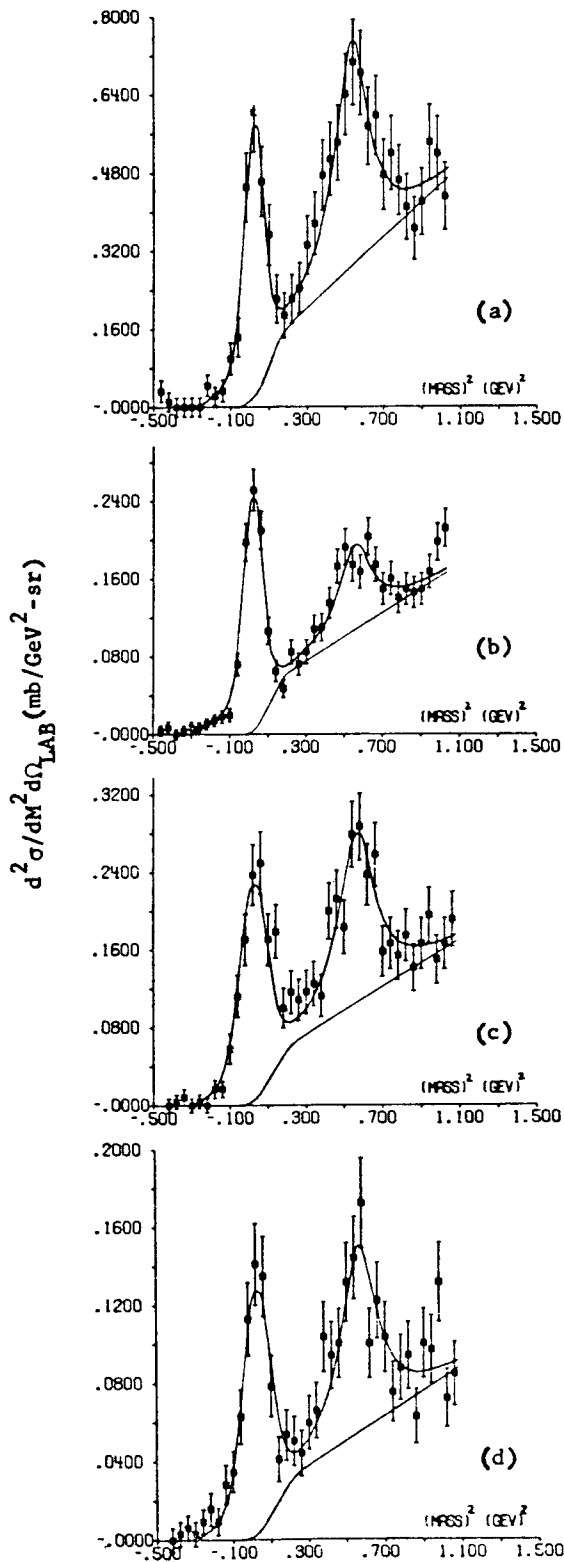
$\pi^- p \rightarrow K^0 \Lambda$

$\Lambda$  POLARIZATION IN THE BACKWARD PEAK



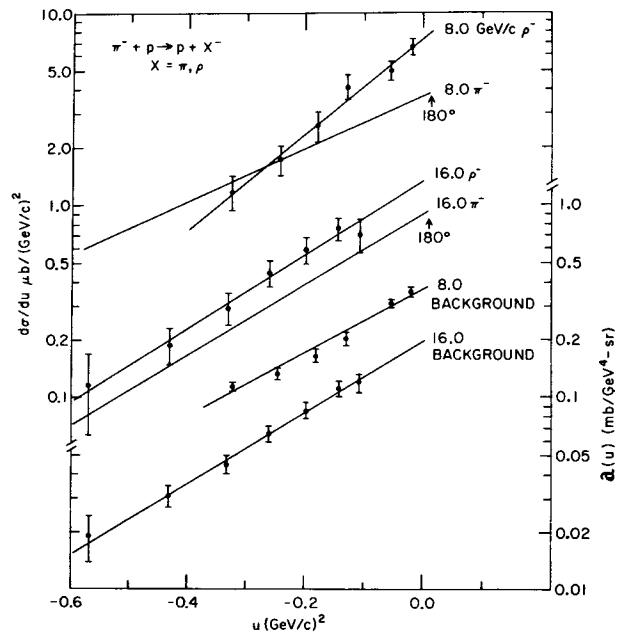
Polarization in backward associated production, at 4 and 6 GeV/c.

Figure 17.



(a) Missing-mass spectrum in the reaction  $\pi^- p \rightarrow p X^-$  for  $M_{X^-} \leq 1.0$  GeV at 8 GeV/c. The laboratory proton angle  $\theta_p = 20-26$  mrad and  $\langle u_\rho \rangle = -0.02$  (GeV/c)<sup>2</sup>. (b) Same spectrum as (a) but  $\theta_p = 58-76$  mrad and  $\langle u_\rho \rangle = -0.29$  (GeV/c)<sup>2</sup>. (c) Same spectrum as (a) except at 16 GeV/c,  $\theta_p = 20-26$  mrad, and  $\langle u_\rho \rangle = -0.13$  (GeV/c)<sup>2</sup>. (d) Same spectrum as (c) but  $\theta_p = 30-38$  mrad and  $\langle u_\rho \rangle = -0.30$  (GeV/c)<sup>2</sup>. In these figures the solid lines are the results of the least-squares fits described in the text.

Figure 18.



$d\sigma/du$  for  $\rho^-$  production near  $180^\circ$ . For comparison the least-squares fit to the  $\pi^-$  elastic data are indicated as  $8.0 \pi^-$  and  $16.0 \pi^-$ . The  $\rho^-$  data points and fitted lines are indicated as  $8.0 \rho^-$  and  $16.0 \rho^-$ . Data points and fitted lines for  $a(u)$ , the background parameter are indicated as  $8.0$  and  $16.0$  BACKGROUND. The units for  $d\sigma/du$  are  $\mu\text{b}/(\text{GeV}/c)^2$  (left-hand scale) and for  $a(u)$  are  $\text{mb}/\text{GeV}^4 \text{sr}$  (right-hand scale).

Figure 19.

## V. MULTIPARTICLE PRODUCTION

One could be forgiven for believing that the principal reason for studying this subject is that physicists hate to see good data go to waste. In most of the bubble chamber work there are a large number of events left over after the two body events have been extracted. A large number of people have tried to understand the dynamics of these left over events. In addition, the one arm spectrometer experiments have a spectrum of "background" when the bumps are skimmed off, this too should reflect some dynamics. Since our prejudice has become clear by now, we shall simply try to pick out representative sets of data, so that in case you get interested then you will know where to start. In particular, the article of Czyzewski<sup>1</sup> is a recent review of the field.

The salient features of non resonant production are these:

- a) Most of the momentum is carried off by the "leading" particle.
- b) The transverse momentum is independent of the multiplicity.
- c) The longitudinal momentum is strongly dependent on multiplicity, being highest when the multiplicity is lowest.

Before we discuss each of these points in detail we need to mention the Peyrou plot, an indispensable aid to visualisation in this field. Each particle has a transverse momentum  $p_{\perp}$  and a longitudinal momentum in the c.m. system  $p_L^*$ . The plot consists of taking each particle for a given reaction and making a two dimensional distribution as in Fig. 1. The semicircle is then the kinematic limit for the reaction.

a) In Fig. 1 we have a typical reaction  $k^- p \rightarrow p k^- \pi^+ \pi^-$ . The "leading particle" concept is nicely demonstrated by the first diagram all the protons have a high and negative value of  $p_L^*$ , i.e., the same as they had before the interaction in the c.m. system. The other "leading particle", the  $k^-$ , has the opposite  $p_L^*$  but this effect is not so pronounced as for the proton. Then the pions in this reaction are primarily of low  $p_L^*$ , although the  $\pi^-$  is less concentrated than the  $\pi^+$ .

b) The assertion that the transverse momentum distribution is independent of the multiplicity is a well documented empirical fact. The number of particles tends to fall exponentially with an exponent of  $-p_{\perp}/0.16$ . In order to quantify this, a function  $F(t)$  has been defined. Figure 2 shows a diagram for  $\pi p \rightarrow pM$  where  $M$  is the mass of the multipion state. At a particular momentum transfer there is a definite phase space available for an object of mass  $M$  and  $F(t)$  is defined as the fraction of particles observed compared to the phase space available. Figure 3 shows such an  $F(t)$  distribution, it resembles remarkably the elastic scattering cross section as you might expect.

c) The fact that the longitudinal momentum depends on multiplicity is hardly surprising at finite energy. The distribution of the number of particles produced



RIGOROUS PROPERTIES OF AMPLITUDES AT HIGH ENERGIES

Lectures by: N. N. Khuri

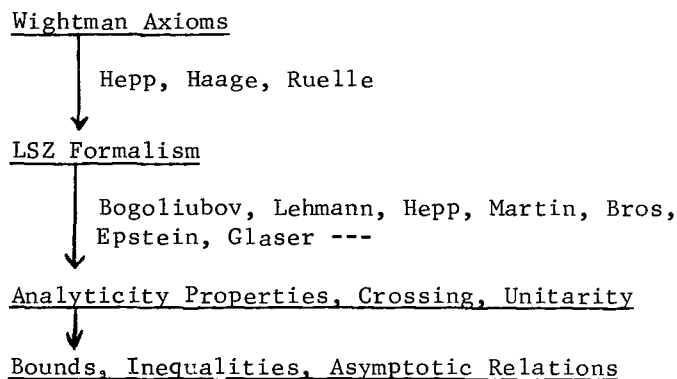


## I. INTRODUCTION

The purpose of this summer school is to survey the present theories of strong interactions at high energies. My task in these lectures is limited specifically to a review of the rigorous bounds and other asymptotic properties of scattering amplitudes at high energies. The word 'rigorous' sometimes evokes strong reactions from many down-to-earth theorists and it would perhaps be wise to state in a few words in what context we are using this term. By rigorous I mean generally results that follow without any further assumptions from the Wightman axioms. One recalls that these axioms in a direct and mathematically precise way embody the general physical principles of relativistic invariance, causality, positivity of energy, and certain technical assumptions which are general features of most local field theories.

It is important to keep in mind that these axioms are not God given. In fact some of the general properties or inequalities derived from them might well turn out to disagree with experiment. If that should happen in the future it would consist of a very important contribution. For example, if the forward dispersion relation is violated at high energies, we would have to face at least as fundamental a change as that involved in CP violation. On a much less ambitious level one can say that it is useful to follow this approach since it tells us that certain results are very much model independent.

The logical (but not the historical) structure of a complete chain of argument would be:



In these lectures we shall only concentrate on the last arrow in the diagram. We shall only state the known analyticity and crossing results without going into their proofs. From there we proceed to derive bounds, inequalities, and asymptotic relations for scattering amplitudes. In both the work related to this last arrow and the crucial analyticity results needed for this work, much of the credit goes to A. Martin.

## II. KINEMATICS AND DEFINITIONS

In the general results derived in these lectures, spin presents us only with a



technical problem. So unless we specify otherwise we will always be dealing with two body collisions involving equal mass, zero spin, and neutral particles shown schematically below.

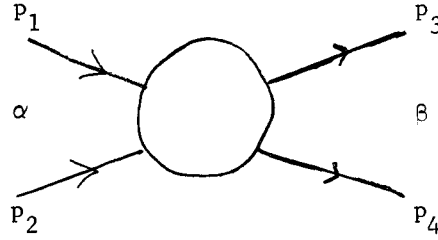


Fig. 1

Here we set  $p_i^2 = m^2$  and define the Mandelstam variables in the usual way,

$$\begin{aligned} s &= (p_1 + p_2)^2, \\ t &= (p_1 - p_3)^2, \\ u &= (p_1 - p_4)^2. \end{aligned} \quad (2.1)$$

The center of mass momentum  $k$  and the scattering angle  $\theta$  are given by

$$\begin{aligned} s &= 4m^2 + 4k^2, \\ t &= -2k^2(1 - \cos\theta), \\ u &= -2k^2(1 + \cos\theta) \end{aligned} \quad (2.2)$$

The S-matrix element for the transition shown in Fig. 1 is defined as

$$S_{\beta\alpha} = \langle p_3 p_4 \text{ out} | p_1 p_2 \text{ in} \rangle = \langle p_3 p_4 \text{ in} | S | p_1 p_2 \text{ in} \rangle \quad (2.3)$$

Its relation to the T matrix is

$$S_{\beta\alpha} = \delta_{\beta\alpha} + i(2\pi)^4 \delta^4(p_3 + p_4 - p_1 - p_2) T_{\beta\alpha}. \quad (2.4)$$

We now define our elastic scattering amplitude as

$$F(s, t) = \langle p_3 p_4 \text{ out} | T | p_2 p_1 \text{ in} \rangle. \quad (2.5)$$

With this normalization the relation between  $F$  and the elastic differential cross section is

$$\frac{d\sigma}{dt} = \frac{1}{16\pi s(s - 4m^2)} |F|^2, \quad (2.6)$$

and the total elastic cross section is

$$\sigma_{el} = \frac{1}{16\pi} \int_{4m^2-s}^0 dt \frac{|F|^2}{sk^2}. \quad (2.7)$$

It is sometimes convenient to work with an amplitude normalized in a slightly different way and which we denote by  $f(s,t)$ . This amplitude is chosen so that

$$\frac{d\sigma}{d\Omega} = |f|^2, \quad (2.8)$$

and clearly we have

$$f(s,t) = F(s,t)/8\pi(s)^{\frac{1}{2}}. \quad (2.9)$$

The optical theorem for our amplitudes has the form

$$\begin{aligned} \text{Im}F(s,0) &= 2k(s)^{\frac{1}{2}} \sigma_{tot}, \\ \text{Im}f(s,0) &= \frac{k}{4\pi} \sigma_{tot}. \end{aligned} \quad (2.10)$$

Finally, we write down the partial wave expansion for  $f(s,t)$ :

$$\begin{aligned} f(s,t) &= \frac{1}{k} \sum_{\ell=0}^{\infty} (2\ell+1) f_{\ell}(s) P_{\ell}(\cos\theta) \\ &= F(s,t)/8\pi(s)^{\frac{1}{2}}. \end{aligned} \quad (2.11)$$

The convergence of this expansion even for nonphysical values of  $\theta$  is a consequence of the analyticity of the amplitude in an ellipse in the  $\cos\theta$ -plane.

The partial wave amplitudes  $f_{\ell}(s)$  in the elastic region have as a consequence of unitarity the simple form

$$f_{\ell}(s) = \frac{e^{2i\delta_{\ell}} - 1}{2i} = e^{i\delta_{\ell}} \sin\delta_{\ell}, \quad (2.12)$$

with real  $\delta_{\ell}$ 's. In the inelastic region  $\delta_{\ell}$  becomes complex but unitarity still gives us the restriction that

$$|S_{\ell}^{el}| = |1 + 2if_{\ell}(s)| \leq 1. \quad (2.13)$$

From this it is trivial to show that

$$0 \leq |f_{\ell}(s)|^2 \leq \text{Im}f_{\ell}(s) \leq 1. \quad (2.14)$$

Thus, both in the elastic and inelastic regions,  $\text{Im}f_{\ell}$  is positive and bounded above by unity. This simple consequence of unitarity will turn out to be the most crucial and important input for most of the bounds that we shall derive.

### III. RIGOROUS ANALYTICITY PROPERTIES

We briefly review the main analyticity properties of  $F(s,t)$  that follow rigorously from the Wightman axioms. No effort is made here to state the best possible results but only to give what is needed and relevant for the derivation of bounds.

#### A. Lehmann Ellipse<sup>1</sup>

We will write  $F(s,t)$  and  $F(s,\cos\theta)$  interchangeably and set  $z=\cos\theta$ . For fixed physical  $s$ ,  $F(s,z)$  is analytic in  $z$  in an ellipse with foci at  $z=\pm 1$  and a semi-major axis  $z_0(s)$  given by

$$z_0(s) = \left[ 1 + \frac{(m^2 - M^2)^2}{k^2 s} \right]^{\frac{1}{2}}. \quad (3.1)$$

Here  $M$  is the smallest mass for which  $\langle 0 | j(x) | M \rangle \neq 0$  and  $j(x)$  is the source current for our colliding particles,  $(\square + m^2)\phi(x) = j(x)$ . Thus  $M = 2m$  for scalar bosons and  $M = 3m$  for pions. For  $\text{Im}F(s,z)$  one has analyticity in a larger ellipse. However, the crucial property of both ellipses is the rate at which they shrink to the line  $-1 \leq z \leq 1$  as  $s \rightarrow \infty$ . In both cases we have, for large  $s$ ,  $[z_0(s) - 1] \sim s^{-2}$ . In the  $t$ -plane,  $t = 2k^2(z-1)$ , the foci of the ellipse are at  $t=0$  and  $t = -4k^2$  and the distance between the focus at  $t=0$  and the turning point shrinks like  $s^{-1}$  for large  $s$ , (see Fig. 2 below).

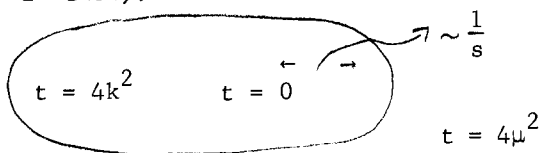


Fig. 2

On the other hand, perturbation theory suggests that the nearest a singularity could be in the  $t$ -plane is at  $t = 4\mu^2$  for any value of  $s$ . The existence of a finite region of analyticity near the origin in the  $t$ -plane with minimum size independent of  $s$  was established by Martin<sup>2</sup> in 1965.

#### B. Martin Analyticity<sup>2</sup>

The input for Martin's work consisted of i) dispersion relations at fixed  $t$ , ii) positivity and iii) the analyticity properties obtained by Bros, Epstein, and Glaser<sup>3</sup>.

Martin proved that for fixed  $s$  near a physical point,  $F(s,t)$  is analytic in  $t$  for  $|t| < R$ , where  $R$  is independent of  $s$ . For pion-pion scattering  $R=4m^2$ .

This result also holds for  $\text{Im}F(s,t)$ . We also know that  $\text{Im}F(s,t)$  is analytic in the Lehmann ellipse with foci at  $t = -4k^2$  and  $t=0$  and expandable in Legendre polynomials of  $\cos\theta$ . The Legendre expansion of  $\text{Im}F$  has positive coefficients as a consequence of (2.14). Therefore this expansion must have a

singularity at the extreme right of the largest ellipse of convergence. But  $\text{Im}F(s,t)$  has no singularities for  $0 < t < 4\mu^2$  and consequently  $\text{Im}F(s,t)$  must be analytic in an ellipse  $E_1(s)$

$$E_1(s): \quad \begin{array}{ll} \text{foci} & t=0, \quad t = 4m^2 - s \\ \text{extremities} & t=4m^2, \quad t = -s. \end{array} \quad (3.2)$$

This region of analyticity can be further enlarged as is shown in Ref. 2., but the results stated so far are sufficient for our purposes which are limited here to the derivation of upper and lower bounds.

#### C. Dispersion Relations and Polynomial Boundedness<sup>4</sup>

For fixed  $t$ ,  $-t_1 \leq t \leq 0$ ,  $F(s,t)$  satisfies a dispersion relation in  $s$  with a fixed number of subtractions.

The crucial fact is that for  $-t_1 \leq t \leq 0$ , and all  $|s| > 1$  we have a bound

$$|F(s,t)| \leq c|s|^N. \quad (3.3)$$

Martin<sup>2</sup> showed that this was true for all  $t$  such that  $|t| \leq R$  and that  $N \leq 2$ . We shall derive these results again below. Polynomial boundedness is to some extent technically built into the Wightman axioms and related to the fact that the Wightman functions are taken to be tempered distributions. However, both Jaffe's axioms and theories based on local observables which do not require temperedness lead to on-shell scattering amplitudes which are polynomially bounded.<sup>5</sup>

### IV. FROISSART AND GREENBERG-LOW BOUNDS

#### A. Intuitive Argument

Suppose we consider scattering by a potential  $V(r) = g(E) e^{-\kappa r}/r$ . A particle with impact parameter 'a' has an interaction of order  $g e^{-\kappa a}$ . Thus the interaction is negligible when  $|g e^{-\kappa a}| \ll 1$ . An estimate of the cross-section is given by the value of a for which  $g e^{-\kappa a} \simeq 1$ , or

$$a \sim \frac{1}{\kappa} \log|g|, \quad (4.1)$$

and

$$\sigma_t \sim \frac{1}{2} \log^2|g|. \quad (4.2)$$

Now if  $g(E)$  is polynomially bounded in  $E$  for large  $E$ ,  $|g(E)| \leq E^N$ , then

$$\sigma_t \leq \frac{c}{2} \log^2 E. \quad (4.3)$$

If  $\kappa_{\min}$  is independent of energy this is just the Froissart bound. The existence of a finite analyticity region in  $t$  near  $t=0$  independent of energy is of course closely related in the language of potential scattering to the fact that the range,  $\kappa_{\min}$ , is independent of  $E$ .

B. Derivation of the Froissart and Greenberg-Low Bounds<sup>6,7</sup>

From (2.11) we have

$$\text{Im}f(s, z) \equiv A(s, z) = \frac{1}{k} \sum_{\ell=0}^{\infty} (2\ell+1) a_{\ell}(s) P_{\ell}(z) , \quad (4.4)$$

where we have set  $\text{Im}f_{\ell} = a_{\ell}$ . From the results summarized in Chapters II and III we know that

i)  $0 \leq |f_{\ell}|^2 \leq a_{\ell} \leq 1.$

ii)  $|A(s, z_1)| < s^N$  for large  $s$  and  $z_1$  inside the Martin or Lehmann ellipse.

iii)  $A(s, z)$  is analytic in  $z$  in the Lehmann ellipse or the Martin ellipse. Both ellipses have foci at  $z = \pm 1$ . The semi-major axis is given by

$$z_0(s) = 1 + \frac{t_0(s)}{2k^2} , \quad (4.5)$$

with the following property for large  $s$

$$t_0(s) \sim \frac{c}{s} \quad (\text{Lehmann}),$$

$$t_0(s) \sim c \quad (\text{Martin}) . \quad (4.6)$$

We now pick a  $z_1(s)$  of the form  $z_1 = 1 + (t_1(s)/2k^2)$ , such that  $0 < t_1(s) < t_0(s)$ . Using the fact that  $P_{\ell}(x) \geq 0$  for  $x > 1$  and the positivity property i) we easily get a bound on  $a_{\ell}(s)$ ,

$$s^N \geq \sum_{\ell=0}^{\infty} (2\ell+1) \frac{a_{\ell}}{k} P_{\ell}\left(1 + \frac{t(s)}{2k^2}\right) \geq (2\ell+1) \frac{a_{\ell}(s)}{k} P_{\ell}\left(1 + \frac{t(s)}{2k^2}\right) , \quad (4.7)$$

and hence for all  $\ell$

$$0 \leq a_{\ell}(s) \leq \frac{s^N \cdot k}{(2\ell+1) P_{\ell}\left(1 + \frac{t(s)}{2k^2}\right)} . \quad (4.8)$$

At the end of this chapter we shall prove the following inequality for  $x > 1$  (see also reference 7):

$$P_{\ell}(x) \geq \frac{c}{(2\ell+1)^{\frac{1}{2}}} (x + (x^2 - 1)^{\frac{1}{2}})^{\ell} > \frac{c}{(2\ell+1)^{\frac{1}{2}}} (1 + (2(x-1))^{\frac{1}{2}})^{\ell} . \quad (4.9)$$

Thus the bound (4.8) with (4.9) gives us

$$a_{\ell}(s) \leq \frac{C s^N k}{(2\ell+1)^{\frac{1}{2}} \left(1 + \frac{(t(s))^{\frac{1}{2}}}{k}\right)^{\ell}} . \quad (4.10)$$

As  $s \rightarrow \infty$ ,  $(t(s)/k) \rightarrow 0$ , and we get

$$a_{\ell}(s) \leq C s^{N \cdot k} e^{-\ell \frac{(t(s))^{1/2}}{k}}, \quad s > s_0 \quad . \quad (4.11)$$

We can now consider two distinct cases depending on the choice of  $t(s)$ .

Case (i): (Greenberg and Low)

Here one uses the analyticity in the Lehmann ellipse only and  $t(s)$  must decrease like  $s^{-1}$  as  $s \rightarrow \infty$ . We choose  $t(s)$  such that

$$t(s) = \frac{c}{s} \quad . \quad (4.12)$$

Hence for  $s > s_0$ ,

$$a_{\ell}(s) \leq C s^{N+\frac{1}{2}} e^{-\frac{c'\ell}{s}} \quad . \quad (4.13)$$

We define  $L(s)$  to be the value of  $\ell$  for which the right hand side of (4.13) is of order unity. Then we have

$$L(s) \cong C \ln s ; \quad (C=C(N)) \quad . \quad (4.14)$$

For fixed large  $s$  and  $\ell < L(s)$  the unitarity bound,  $a_{\ell}(s) \leq 1$ , is a better bound than (4.13). However, for  $\ell > L(s)$ , (4.13) gives a smaller upper bound and in fact  $a_{\ell}(s)$  is negligible for  $\ell \geq L(s)+1$ . Thus  $L(s)$  gives us the number of partial waves that effectively contribute to the amplitude at large  $s$ .

Let  $\hat{L}$  be the smallest integer greater than  $L(s)$ , then we can write

$$A(s, z) \leq \frac{1}{k} \sum_{\ell=0}^{\hat{L}} (2\ell+1) |P_{\ell}(\cos\theta)| + \frac{1}{k} \sum_{\ell=\hat{L}+1}^{\infty} (2\ell+1) C s^{N+\frac{1}{2}} e^{-\frac{c'\ell}{s}} |P_{\ell}(\cos\theta)| \quad . \quad (4.15)$$

In the first sum above we have used the unitarity bound  $a_{\ell}(s) \leq 1$ . In the second sum we have used (4.13).

For the forward case,  $\theta = 0$ ,  $|P_{\ell}(\cos\theta)| = 1$ , and one obtains

$$A(s, 1) \leq \frac{1}{k} \sum_{\ell=0}^{\hat{L}} (2\ell+1) + \text{Remainder} \quad . \quad (4.16)$$

The remainder term can be easily shown to be negligible compared to the first term, and we get

$$A(s, 1) \leq \frac{(\hat{L}+1)^2}{k} (1+\epsilon) \quad . \quad (4.17)$$

Substituting our estimate for  $\hat{L}(s)$  we finally have

$$A(s,1) \leq \frac{C s^2 \ln^2 s}{k} . \quad (4.18)$$

Since unitarity gives us also the bound  $|f_\ell| \leq (a_\ell)^{\frac{1}{2}}$  we can easily follow the same method as above to get a bound similar to (4.18) for the full amplitude

$$|F(s,1)| \leq \frac{C s^2 \ln^2 s}{k} . \quad (4.19)$$

The Greenberg-Low bound for  $\sigma_{\text{tot}}$  follows from (4.18),

$$\sigma_{\text{tot}} = \frac{4\pi A(s,1)}{k} \leq \text{Const.} \ln^2 s . \quad (4.20)$$

For the non-forward case,  $\theta \neq 0$  and  $\theta \neq \pi$ , one has

$$|P_\ell(\cos\theta)| \leq \left( \frac{2}{\pi \ell \sin\theta} \right)^{\frac{1}{2}} . \quad (4.21)$$

Using this bound, and the inequality  $|f_\ell| < (a_\ell)^{\frac{1}{2}}$  and proceeding as before, we get

$$\begin{aligned} |A(s, \cos\theta)| &\leq |f(s, \cos\theta)| \\ &\leq \frac{c}{k(\sin\theta)^{\frac{1}{2}}} \sum_{\ell=0}^{\hat{L}} \frac{(2\ell+1)}{(\ell)^{\frac{1}{2}}} + \text{negligible terms} . \end{aligned} \quad (4.22)$$

For large  $s$  this gives the bound

$$|A(s, \cos\theta)| \leq |f(s, \cos\theta)| \leq \text{Const.} \frac{s \ln^{3/2} s}{(\sin\theta)^{\frac{1}{2}}} . \quad (4.23)$$

Case (ii): (Froissart bound)

For this case we have analyticity in the Martin ellipse defined in (3.2) and one can choose  $t(s)$  to be a constant independent of  $s$ ,

$$t(s) = t_0 . \quad (4.24)$$

Proceeding as in case (i) we get

$$|f_\ell|^2 \leq a_\ell(s) \leq C s^{N \cdot k} e^{-c\ell/(s)^{\frac{1}{2}}} . \quad (4.25)$$

Hence instead of (4.14) we now have

$$L(s) \cong C (s)^{\frac{1}{2}} \ln s . \quad (4.26)$$

With this improved estimate of the number of significant partial waves we get following the same steps as in case (i) for  $s > s_0$

$$A(s,1) \leq |f(s,1)| \leq \frac{\text{Const. } s \ell n^2 s}{k} , \quad (4.27)$$

$$\sigma_{\text{tot}} \leq \text{Const. } \ell n^2 s , \quad (4.28)$$

and

$$|f(s, \cos\theta)| \leq \text{Const.} \frac{s^{3/4} (\ell n s)^{3/2}}{k(\sin\theta)^{1/2}} , \quad \theta \neq 0, \pi . \quad (4.29)$$

These bounds can be easily translated to bounds for  $|F(s,t)|$  for fixed physical negative  $t$ . We use  $\cos\theta = 1 + t/2k^2$  and  $F = 8\pi(s)^{1/2}f$  and obtain from (4.29)

$$|F(s,t)|_{t \text{ fixed, physical}} \leq \text{Const. } s \ell n^{3/2} s , \quad t \neq 0. \quad (4.30)$$

By a Phragmen-Lindelof type of argument one can show that the bound (4.20) holds in all directions in the  $s$ -plane. Thus the maximum number of subtractions needed for fixed  $t$  dispersion relations is 2 as long as  $t$  is negative.

We close our discussion of the Froissart bounds by making two related remarks.

1) The non-forward bound (4.29) cannot be reached for a finite interval  $\theta_1 < \theta < \theta_2$ . For recalling that  $d\sigma/d\Omega = |f|^2$ , we would then have

$$\frac{d\sigma}{d\Omega} \cong \frac{s^{1/2} \ell n^3 s}{\sin\theta} , \quad \theta_1 < \theta < \theta_2 .$$

This would give a  $\sigma_{e1} \gg \sigma_{\text{tot}}$  for large  $s$  and an obvious contradiction. So the bound can only be reached at isolated peaks in  $\theta$ . At this point one immediately is led to the suspicion that (4.29) could and should be improved.

2) Kinoshita, Loeffel and Martin<sup>8</sup> considered the problem of improving the Froissart bounds by assuming analyticity in a domain larger than the Martin ellipse. They assumed:

- (i) Unitarity,  $0 \leq a_l \leq 1$
- (ii) Analyticity in the cut  $z$ -plane
- (iii) Polynomial boundedness for  $z$  inside analyticity domain.

Their main results were:

- (a) In the forward case no improvement is possible. An explicit counter-example satisfying (i), (ii), and (iii) was constructed.
- (b) For  $\theta \neq 0$  or  $\pi$  an improvement of (4.29) is possible and they obtained

$$|F(s, \cos\theta)| \leq \frac{\text{Const.} (\ell n s)^{3/2}}{\sin^2 \theta} . \quad (4.31)$$

This bound gives us a more acceptable bound on the differential cross-section, which vanishes as  $s \rightarrow \infty$ ,



$$\frac{d\sigma}{d\Omega} \leq \frac{C(\ell ns)^3}{s \sin^4 \theta} \quad (4.32)$$

However, translating (4.31) back to a fixed  $t$  bound does not lead to a change in (4.30).

Actually, as is clear from ref. 8, it is not necessary to assume full cut plane analyticity in the  $z$ -plane to obtain (4.31). For more detail on this point the reader should read ref. 8.

Before proceeding to the next chapter we still have the task of proving the inequality (4.9) for  $P_\ell(x)$ , with  $x > 1$ . The second inequality in (4.9) follows trivially from the first. To prove the first we introduce the variable  $y \equiv x + (x^2 - 1)^{\frac{1}{2}}$  for which  $y + y^{-1} = 2x$ , or  $x = \cos \theta$ ,  $y = e^{+i\theta}$ . Then we can write

$$P_\ell(x) = \sum_{n=-\ell}^{+\ell} C_n^{(\ell)} y^n. \quad (4.33)$$

The coefficients  $C_n^{(\ell)}$  have two properties: (a)  $C_n^{(\ell)} \geq 0$ ; (b)  $C_\ell^{(\ell)} = \frac{(2\ell)!}{2^{2\ell} (\ell!)^2}$ . The property (b) follows immediately from the fact that  $C_\ell^{(\ell)}$  is  $2^{-\ell}$  times the coefficient of  $x^\ell$  in the expansion of  $P_\ell(x)$ . From (a) and (b) we have

$$P_\ell(x) \geq C_\ell^{(\ell)} y^\ell > \frac{c}{(2\ell+1)^{\frac{1}{2}}} [x + (x^2 - 1)^{\frac{1}{2}}]^\ell. \quad (4.34)$$

A simple proof of property (a) due to Martin follows from some elementary properties of rotation group. One can write

$$\begin{aligned} P_J(\cos \theta) &= C \langle J, J_z=0 | e^{iJ_y \theta} | J, J_z=0 \rangle \\ &= C \langle J, J_z=0 | \cos J_y \theta | J, J_z=0 \rangle. \end{aligned} \quad (4.35)$$

Introducing a complete set of states in (4.35), we get

$$\begin{aligned} P_J(\cos \theta) &= C \sum_{M=-J}^J \langle J, J_z=0 | J, J_y=M \rangle \langle J, J_y=M | \cos(J_y \theta) | J, J_z=0 \rangle, \\ &= C \sum_{M=-J}^J \cos M \theta |\langle J, J_z=0 | J, J_y=M \rangle|^2. \end{aligned} \quad (4.36)$$

But  $\cos M \theta = \frac{1}{2}(e^{iM\theta} + e^{-iM\theta}) = \frac{1}{2}[y^M + y^{-M}]$  and that completes the proof of (b).

## V. BOUNDS FOR UNPHYSICAL VALUES OF $t$ AND MAXIMUM NUMBER OF SUBTRACTIONS IN DISPERSION RELATIONS

For negative (physical) values of  $t$  we have the bound (4.30),

$$|F(s, t)| \leq C s \ln^{3/2} s. \quad (5.1)$$

In this chapter we shall derive a fixed  $t$  bound for unphysical values of  $t$ . More specifically we shall be interested in the region  $0 < t < 4\mu^2$  and the region  $|t| < 4\mu^2$ . The dispersion relations are valid for any  $t$  in the Martin ellipse and this unphysical bound will give us the maximum number of subtractions needed in the fixed  $t$  dispersion relations. It will also give us a determination of the constant that appears on the right in the Froissart bound (4.20). We follow the method of Jin and Martin,<sup>9</sup> although many of the results of this paper can be also obtained as a byproduct of the proof in reference 2.

Let us, to be slightly more general consider an unequal mass collision  $a+b \rightarrow a+b$ , and allow the following kinematics: (i)  $s+t+u = 2m_a^2 + 2m_b^2$ ; (ii)  $2\mu$  is the lowest mass in the crossed  $t$  channel; (iii) no states in the  $s$  or  $u$  channels with mass less than  $(m_a + m_b)$ ; (iv)  $\mu \leq m_a$ ;  $\mu \leq m_b$ .

The amplitude,  $F(s,t)$ , for fixed  $t$ ,  $|t| < 4\mu^2$ , is analytic in the cut  $s$ -plane. The right hand cut starts at  $s = (m_a + m_b)^2$  and the left hand cut at  $s = (m_a - m_b)^2 - t$ . We further assume that as  $|s| \rightarrow \infty$ ,  $|t| < 4\mu^2$ ,  $F$  is polynomially bounded,

$$|F(s,t)| \leq |s|^N . \quad (5.2)$$

We shall prove by making use of the Froissart bounds that, in fact

$$\lim_{|s| \rightarrow \infty} \left| \frac{F(s,t)}{s^2} \right| = 0 , \quad |t| < 4\mu^2 . \quad (5.3)$$

From the analyticity of  $F$  and the bound (5.2) we can write an  $N+1$  subtracted dispersion relation

$$F(s,t) = \sum_{n=0}^N C_n(t) s^n + \frac{s^{N+1}}{\pi} \int_{(m_a + m_b)^2}^{\infty} ds' \frac{A_s(s',t)}{s'^{N+1}(s'-s)} + \frac{u^{N+1}}{\pi} \int_{(m_a + m_b)^2}^{\infty} du' \frac{A_u(u',t)}{u'^{N+1}(u'-u)} . \quad (5.4)$$

It is easy to see from the partial wave expansion that

$$A_s(s',t) \geq 0, \quad 0 \leq t \leq 4\mu^2 . \quad (5.5)$$

In the  $s$ -channel,  $A_s \equiv \text{Im}F$ . Similarly,  $A_u$  is the absorptive part for the  $u$ -channel reaction  $a+\bar{b} \rightarrow a+\bar{b}$  and by unitarity

$$A_u(u',t) \geq 0; \quad 0 \leq t \leq 4\mu^2 . \quad (5.6)$$

For complex  $s$  and  $\text{Re}s$  large enough the integrals in (5.4) are uniformly convergent for any  $t$  such that  $|t| < 4\mu^2$ . Therefore both integrals define functions

analytic in  $|t| < 4\mu^2$ . The function  $F(s,t)$  is also analytic in the disc,  $|t| < 4\mu^2$ . Hence  $C_n(t)$  are analytic in  $t$  in the same disc, since  $\sum_{n=0}^N C_n(t)s^n$  is analytic for at least  $(N+1)$  distinct values of  $s$ .

From the Froissart bound we have,

$$|F(s,0)| \leq C s \ln^2 s .$$

At the end of this chapter we shall show that using the techniques of Chapter IV, we can always choose an  $\epsilon > 0$  and find a  $t_0$ ,  $0 < t_0 < 4\mu^2$ , such that

$$|F(s,t)| \leq c s^{1+\epsilon}, \quad 0 \leq t \leq t_0 . \quad (5.7)$$

We choose  $\epsilon < 1$ , and thus for  $0 \leq t \leq t_0$  we need only two subtractions in our dispersion relations. We obtain

$$\begin{aligned} F(s,t) = a(t)+b(t)s + \frac{s^2}{\pi} \int \frac{A_s(s',t)}{s'^2(s'-s)} ds' \\ + \frac{u^2}{\pi} \int \frac{A_u(u',t)}{u'^2(u'-u)} du' ; \quad 0 \leq t \leq t_0 . \end{aligned} \quad (5.8)$$

Then using the identity,

$$\frac{s^{N+1}}{s'^{N+1}(s'-s)} = \frac{s^2}{s'^2(s'-s)} - \frac{s^2}{s'^3} - \dots - \frac{s^{N-1}}{s'^N} - \frac{s^N}{s'^{N+1}} , \quad (5.9)$$

and comparing (5.8) with (5.4) we get

$$\sum_{n=0}^N C_n(t)s^n = a(t)+b(t)s + \sum_{n=2}^N \left[ \frac{s^n}{\pi} \int ds' \frac{A_s(s',t)}{s'^{n+1}} + \frac{u^n}{\pi} \int du' \frac{A_u(u',t)}{u'^{n+1}} \right] . \quad (5.10)$$

This last equation is at this stage only valid for  $0 \leq t \leq t_0$ . Two cases have to be treated separately depending on whether  $N$  is even or odd.

(i)  $N$  even  $> 2$ .

Comparing the coefficients of  $s^N$  for large  $s$ , (5.10) gives us

$$C_N(t) = \frac{1}{\pi} \int ds' \frac{A_s(s',t)}{s'^{N+1}} + \frac{1}{\pi} \int du' \frac{A_u(u',t)}{u'^{N+1}} . \quad (5.11)$$

This equation is again only true at this stage for  $0 \leq t \leq t_0$ . From unitarity we know that

$$\left. \frac{d^n}{dt^n} A_s(s',t) \right|_{t=0} \geq 0 ,$$

$$\left. \frac{d^n}{dt^n} A_u(u', t) \right|_{t=0} \geq 0 \quad . \quad (5.12)$$

These positivity requirements follow from the partial wave expansion and the fact that

$$\left. \frac{d^n P_\ell(\cos\theta)}{d(\cos\theta)^n} \right|_{\cos\theta=1} \geq 0 \quad . \quad (5.13)$$

To prove this last inequality easily one can use the expansion (4.36) and the positivity of the coefficients in that expansion.

Returning to (5.11) we can expand both  $A_s$  and  $A_u$  in power series

$$A_s(s', t) = \sum_{n=0}^{\infty} A_s^{(n)}(s') t^n \quad ,$$

$$A_u(u', t) = \sum_{n=0}^{\infty} A_u^{(n)}(u') t^n \quad . \quad (5.14)$$

The coefficients in both series are positive. Now, for  $0 \leq t \leq t_0$ , we can exchange the summation and integration in (5.11) and get

$$C_N(t) = \sum_{n=0}^{\infty} t^n \left[ \int \frac{A_s^{(n)}(s')}{s'^{N+1}} ds' + \int \frac{A_u^{(n)}(u')}{u'^{N+1}} du' \right] \quad . \quad (5.15)$$

The function  $C_N(t)$  is analytic for  $|t| < 4\mu^2$ . The right hand side of (5.15) is a power series expansion and therefore it must also converge for all  $|t| \leq 4\mu^2$ . Then reversing the order again in (5.15) we conclude that

$$\int \frac{A_s(s', t)}{s'^{N+1}} ds' \quad \text{and} \quad \int \frac{A_u(u', t)}{u'^{N+1}} du'$$

are finite for all  $t$  such that  $|t| \leq 4\mu^2$ . It is easy to show using (5.4) that if these integrals are finite, then

$$\lim_{|s| \rightarrow \infty} \left| \frac{F(s, t)}{s^N} \right| = 0 \quad , \quad (5.16)$$

and we can undo one subtraction in (5.4).

(ii)  $N \text{ odd} \geq 3$

In this case an analogous argument shows that we can reduce the number of

subtractions by two.

Repeating the argument as many times as necessary we prove that

$$\int \frac{A_s(s', t)}{s'^3} ds' \quad \text{and} \quad \int \frac{A_u(u', t)}{u'^3} du'$$

converge absolutely for all  $|t| < 4\mu^2$ . Hence it is easy to show that (5.3) follows.

In closing we still have to prove the inequality (5.7). Namely, we have to show from the estimates of the previous chapter for  $|f_\ell(s)|$ , that for any  $\epsilon$  there exists a  $t_0$  such that for  $0 \leq t \leq t_0$ ;  $|F(s, t)| \leq C|s|^{1+\epsilon}$ .

From the partial wave expansion we have

$$|F(s, t)| \leq C \sum_0^{\hat{L}} (2\ell+1) |P_\ell(1 + \frac{t}{2k^2})| + C \sum_{\hat{L}+1}^{\infty} (2\ell+1) s^N e^{-\frac{2\mu\ell}{s}} |P_\ell(1 + \frac{t}{2k^2})| \quad (5.17)$$

Here in the first sum we used the unitarity bound for  $|f_\ell|$  and in the second sum we used (4.11) with  $t(s) \cong 4\mu^2 - \epsilon$ . In (5.17) we have convergence for  $0 \leq t < 4\mu^2$ . We choose  $t_0$  such that  $(t_0)^{\frac{1}{2}} \ll \mu$ , then in the second sum in (5.17) the decreasing exponential will damp the increasing exponential behavior of  $P_\ell(1 + t/2k^2)$ , for  $0 \leq t \leq t_0$ . In fact, one has the bound

$$|P_\ell(\cosh\xi)| \leq C \frac{e^{(\ell+\frac{1}{2})\xi}}{(2\ell+1)^{\frac{1}{2}} (\sinh\xi)^{\frac{1}{2}}}; \quad \xi \neq 0 \quad (5.18)$$

where

$$\cosh\xi = 1 + t/2k^2 \quad ,$$

or

$$\xi = \ell \ln \left[ 1 + \frac{t}{2k^2} + \left( \left( 1 + \frac{t}{2k^2} \right)^2 - 1 \right)^{\frac{1}{2}} \right] \quad (5.19)$$

For large  $s$

$$\xi \cong \frac{2(t)^{\frac{1}{2}}}{(s)^{\frac{1}{2}}} \quad .$$

We then get for large  $s$

$$|P_\ell(1 + \frac{t}{2k^2})| \leq \frac{C}{(2\ell+1)^{\frac{1}{2}}} \frac{s^{\frac{1}{4}}}{t^{\frac{1}{4}}} e^{\ell \frac{2(t)^{\frac{1}{2}}}{(s)^{\frac{1}{2}}}} \quad (5.20)$$

Now as long as  $0 < t \leq t_0 \ll \mu$ , the second sum in (5.17) is negligible compared to the first. Hence, we get

$$\begin{aligned}
 |F(s, t)| &\leq C \sum_{l=0}^{\hat{L}_1} (2l+1) \frac{s^{\frac{1}{4}}}{t^{\frac{1}{4}}} \frac{e^{2l(t)^{\frac{1}{2}}/(s)^{\frac{1}{2}}}}{(l)^{\frac{1}{2}}} \\
 &\leq C e^{-\bar{c} \frac{(s)^{\frac{1}{2}} \ln s(t)^{\frac{1}{2}}}{(s)^{\frac{1}{2}}}} \sum_{l=0}^{\hat{L}_1} \frac{s^{\frac{1}{4}}}{t^{\frac{1}{4}}} \frac{(2l+1)}{(l)^{\frac{1}{2}}} \\
 &\leq \frac{C'}{t^{\frac{1}{4}}} s^{1+\bar{c}(t)^{\frac{1}{2}}} (\ln s)^{3/2}; \quad t \neq 0 \quad . \quad (5.21)
 \end{aligned}$$

Here we have used the fact that  $\hat{L}(s) \cong (s)^{\frac{1}{2}} \ln s$ . Thus by choosing  $t_0$  small enough (5.7) will follow from (5.21). It is interesting to note the vague similarity between (5.21) and Regge like terms.

The knowledge that in the region  $0 \leq t \leq 4\mu^2$  we have no more than two subtractions in the dispersion relation enables us to determine the constant in the Froissart bound. We have derived the bound  $\sigma_t \leq \text{Const.} \ln^2(s/s_0)$ ; we shall calculate an upper bound for the constant. We have

$$\sigma_t = \frac{4\pi}{k^2} \sum_{l=0}^{\infty} (2l+1) a_l(s) \quad . \quad (5.22)$$

From (4.10) we get

$$a_l(s) \leq \frac{C s^{N'} \cdot k}{(t_0)^{\frac{1}{2}} \left(1 + \frac{k}{k}\right)^l} \quad . \quad (5.23)$$

From the results of this chapter we know that  $|F| \leq C(s/s_0)^2$  and hence  $|\hat{F}| \leq C(s/s_0)^{2-\frac{1}{2}}$ , and  $N' = 3/2$ . This gives us

$$a_l(s) \leq C \left(\frac{s}{s_0}\right)^2 e^{-\frac{2\mu l}{k}} \quad , \quad (5.24)$$

and

$$L(s) \cong \frac{(s)^{\frac{1}{2}}}{2\mu} \ln(s/s_0) \quad . \quad (5.25)$$

From (5.22) we get the bound

$$\begin{aligned} \sigma_t &\leq (1+\epsilon) \frac{4\pi}{k^2} L^2 \quad , \\ &\leq (1+\epsilon) \left(\frac{4\pi}{\mu}\right) \ln^2(s/s_0) \quad , \end{aligned} \quad (5.26)$$

where  $\epsilon$  can be as small as we like.

## VI. UNITARITY BOUNDS

In this chapter we shall derive some very simple bounds which follow mainly from unitarity. The additional input we use is that only  $L(s)$  partial waves are significant.

A. . Lower Bounds on  $\sigma_{\text{elastic}}$ <sup>10</sup>:

By definition we have

$$\sigma_{\text{el}} = \frac{4\pi}{k^2} \sum_{\ell=0}^{\infty} (2\ell+1) |f_{\ell}|^2 \quad . \quad (6.1)$$

Hence we write

$$\sigma_{\text{el}} \geq \frac{4\pi}{k^2} \sum_{\ell=0}^L (2\ell+1) a_{\ell}^2 \quad . \quad (6.2)$$

Using the Cauchy-Schwartz inequality we obtain:

$$\left[ \sum_{\ell=0}^L ((2\ell+1)^{\frac{1}{2}} a_{\ell})^2 \right] \left[ \sum_{\ell=0}^L (2\ell+1) \right] \geq \left[ \sum_{\ell=0}^L (2\ell+1) a_{\ell} \right]^2 \quad . \quad (6.3)$$

Hence

$$\sigma_{\text{el}} \geq \frac{\frac{4\pi}{k^2} \left[ \sum_{\ell=0}^L (2\ell+1) a_{\ell} \right]^2}{\sum_{\ell=0}^L (2\ell+1)} \quad . \quad (6.4)$$

If  $\sigma_{\text{tot}} \geq C s^{-N}$ , then (6.4) gives us

$$\sigma_{\text{el}} \geq \frac{k^2}{4\pi} \frac{\sigma_t^2}{(L+1)^2} \geq \text{Const.} \frac{\sigma_t^2}{\ln^2 s} \quad . \quad (6.5)$$

We recall that for  $L \cong C(s)^{\frac{1}{2}} lns$ ,

$$\begin{aligned} \sum_{l=0}^L (2l+1) a_l &= \sum_{l=0}^{\infty} (2l+1) a_l + O(s^{-M}) \\ &= \frac{k^2}{4\pi} \sigma_t + O(s^{-M}) \end{aligned} \quad (6.6)$$

B. Lower Bound on Width of Diffraction Peak

We define the "width" of the diffraction peak,  $\Delta$ , as

$$\Delta \equiv \frac{F(s,0)}{\left| \frac{dF(s,t)}{dt} \right|_{t=0}} \quad (6.7)$$

In Regge theory for large  $s$

$$\Delta \cong \frac{1}{c lns} \quad (6.8)$$

From the partial wave expansion we have

$$\left. \frac{dF(s,t)}{dt} \right|_{t=0} = \frac{8\pi(s)^{\frac{1}{2}}}{k} \sum_{l=0}^{\infty} (2l+1) \frac{f_l(s)}{2k^2} \frac{l(l+1)}{2} \quad (6.9)$$

Therefore,

$$\begin{aligned} \left| \frac{dF(s,t)}{dt} \right|_{t=0} &\leq \frac{C(s)^{\frac{1}{2}}}{k^3} \sum_{l=0}^L (2l+1) \frac{l(l+1)}{2} \\ &\leq C s l n^4 s \end{aligned} \quad (6.10)$$

Since  $|F(s,0)| \geq |\text{Im}F(s,0)| \cong c s \sigma_t$ , one concludes that

$$\Delta \geq \frac{C \sigma_t}{(lns)^4} \quad (6.11)$$

Thus if  $\sigma_t \rightarrow \text{const.}$  the diffraction peak width cannot be rapidly decreasing.

C. Bound on Regge Trajectories

The Froissart bound gives us immediately a bound on Regge trajectories at  $t=0$ ,  $\alpha(0) \leq 1$ . However, if one assumes that the asymptotic behavior of  $F(s,t)$  is dominated by a Regge pole it is possible to prove directly from unitarity, and without using the analyticity input necessary for the Froissart bound, that  $\alpha(0) \leq 1$ . We go through this proof which is due to Leader<sup>11</sup> just to demonstrate how powerful a restriction unitarity gives us.



We start by writing down the expression for  $\sigma_{e1}$ ,

$$\sigma_{e1} = \frac{1}{32\pi} \int_{-4k^2}^0 dt \frac{|F(s,t)|^2}{2k^2 s} . \quad (6.12)$$

From this we have the obvious inequality

$$\sigma_t \geq \sigma_e \geq \frac{1}{32\pi s} \int_{-T}^0 dt \frac{|F|^2}{2k^2} , \quad (6.13)$$

where T is a constant such that  $T \ll 4k^2$ . Let F have Regge asymptotic behavior

$$F(s,t) \sim \beta(t) s^{\alpha(t)} ; \quad (6.14)$$

where we assume that  $\beta(t)$  and  $\alpha(t)$  are continuous in t for  $-t_1 \leq t \leq 0$ . Given any  $\epsilon > 0$  we can choose  $T(\epsilon)$  small enough so that  $\alpha(t)$ , for  $-T(\epsilon) \leq t \leq 0$ , is greater than  $\alpha(0) - \epsilon$ , i.e.,

$$\alpha(t) > \alpha(0) - \epsilon , \quad -T(\epsilon) \leq t \leq 0 . \quad (6.15)$$

The optical theorem for large s gives us  $\text{Im}F \sim C s \sigma_t$ . Substituting this on the left in (6.13) and using (6.15) and continuity on the right we get

$$C s^{\alpha(0)-1} \geq \frac{C'}{k^2 s} s^{2\alpha(0)-2\epsilon} . \quad (6.16)$$

As  $s \rightarrow \infty$  we obtain

$$\alpha(0) - 1 \geq 2\alpha(0) - 2 - 2\epsilon ,$$

or

$$\alpha(0) \leq 1 + 2\epsilon . \quad (6.17)$$

But  $\epsilon$  can be made arbitrarily small, hence

$$\alpha(0) \leq 1 . \quad (6.18)$$

This result follows only from unitarity, continuity, and Regge behavior - no analyticity need be assumed.

#### D. Unitarity Bound on the Diffraction Peak

MacDowell and Martin<sup>12</sup> derived a lower bound for the logarithmic derivative of  $\text{Im}F(s,t)$  at  $t=0$ . Again only unitarity is used. This bound also has the advantage that it can be compared with experiment even at non-asymptotic energies.

Let us write

$$A(s,t) \equiv \text{Im}F(s,t) , \quad (6.19)$$

and

$$A(s,t) = \frac{8\pi(s)^{\frac{1}{2}}}{k} \sum (2\ell+1) a_\ell(s) P_\ell\left(1 + \frac{t}{2k^2}\right) .$$

We also write the definitions

$$\sigma_t = \frac{4\pi}{k^2} \sum (2\ell+1) a_\ell \quad , \quad (6.20)$$

$$\sigma_{e1} = \frac{4\pi}{k^2} \sum (2\ell+1) |f_\ell|^2 \quad , \quad (6.21)$$

$$\sigma_{e1.im} = \frac{4\pi}{k^2} \sum (2\ell+1) a_\ell^2 \quad , \quad (6.22)$$

and

$$\left. \frac{dA(s,t)}{dt} \right|_{t=0} = \frac{8\pi(s)^{\frac{1}{2}}}{2k^3} \sum (2\ell+1) \frac{\ell(\ell+1)}{2} a_\ell(s) \quad . \quad (6.23)$$

The problem is to find a minimum for this last series for a given fixed  $\sigma_t$  and  $\sigma_{e1.im}$ .

Using the method of Lagrange multipliers we get from (6.20), (6.22), and (6.23)

$$\sum_{\ell=0}^{\infty} \left[ \frac{(s)^{\frac{1}{2}}}{k} \frac{\ell(\ell+1)}{2} - p - 2qa_\ell \right] (2\ell+1) \delta a_\ell = 0 \quad . \quad (6.24)$$

The Lagrange multipliers  $p$  and  $q$  are picked to make the bracket zero for  $\ell = 0, 1$  and the  $a_\ell$ 's for  $\ell = 2, 3, \dots$ , are taken to be independent variables. Hence an extremum is reached for

$$a_\ell = \alpha - \beta \ell(\ell+1) \quad , \quad (6.25)$$

where  $\alpha$  and  $\beta$  are functions of  $s$ . It is clear from the case  $\ell=0$  that  $\alpha$  has to be positive. On the other hand taking  $\beta$  negative in (6.25) will obviously not give the minimum we are seeking and  $\beta \geq 0$ .

In addition to (6.25) unitarity gives us the restriction

$$0 \leq a_\ell \leq 1 \quad . \quad (6.26)$$

There are two cases to consider  $\alpha > 1$  and  $\alpha < 1$ .

a)  $\alpha > 1$

The minimum is reached when

$$\begin{aligned} a_\ell &= 1 \quad ; \quad \ell < L_0 \quad ; \\ a_\ell &= \alpha - \beta \ell(\ell+1) \quad ; \quad L_0 \leq \ell < L_1 \quad ; \\ a_\ell &= 0 \quad ; \quad \ell > L_1 \quad ; \end{aligned} \quad (6.27)$$

where  $L_0$  is the smallest integer such that  $\alpha - \beta L_0(L_0+1) \leq 1$  and  $L_1$  is the largest integer for which  $\alpha - \beta L_1(L_1+1) > 0$ .

Using (6.27) in (6.20) and (6.22) we get  $\sigma_t$  and  $\sigma_{e.i}$  as functions of  $\alpha$  and  $\beta$ . Inverting these functions we can write  $\alpha = \alpha(\sigma_t, \sigma_{e.i})$  and  $\beta = \beta(\sigma_t, \sigma_{e.i})$ . With

these values of  $\alpha$  and  $\beta$  in (6.27) we calculate the minimum of (6.23). The algebra is tremendously simplified by converting all sums to integrals and errors are only of order  $1/k^2$ . The result is

$$\left. \frac{d}{dt} \ln A(s, t) \right|_{t=0} \geq \frac{1}{8} \frac{\sigma_t}{4\pi} \left[ 1 + 3 \left( 1 - \frac{\sigma_{e.i}}{\sigma_t} \right)^2 \right] + O\left(\frac{1}{k^2}\right). \quad (6.28)$$

However, the case  $\alpha > 1$  corresponds to small inelasticity and is unphysical. One can check that for  $\alpha > 1$  we have

$$\sigma_{el} > \sigma_{el.im} \geq \frac{2}{3} \sigma_t, \quad (6.29)$$

which is in disagreement with present data.

b)  $\alpha < 1$

In this case the minimum is reached when

$$\begin{aligned} a_l &= \alpha - \beta l(l+1) & l \leq L_1, \\ a_l &= 0 & l > L_1. \end{aligned} \quad (6.30)$$

Using this expression in (6.20), (6.22), and (6.23) one gets, after some algebra,

$$\left. \frac{d}{dt} \ln A(s, t) \right|_{t=0} \geq \frac{1}{9} \left[ \frac{\sigma_t}{4\pi} \frac{\sigma_t + (\sigma_t^2 + 12\pi \sigma_{e.i}/k^2)^{\frac{1}{2}}}{2\sigma_{e.i}} - \frac{3}{2k^2} \right]. \quad (6.31)$$

The bracket has a close lower bound,  $\left[ \frac{\sigma_t}{4\pi} \left( \frac{\sigma_t}{\sigma_{e.i}} \right) - \frac{1}{2} \right]$ . We have then

$$\left. \frac{d}{dt} \ln A(s, t) \right|_{t=0} > \frac{1}{9} \left( \frac{\sigma_t}{4\pi} \frac{\sigma_t}{\sigma_{e.i}} - \frac{1}{2} \right). \quad (6.32)$$

The algebra in going from (6.30) to (6.31) is quite involved. To get a quick derivation correct to order  $1/k^2$  one takes leading orders in  $l$  and converts all sums to integrals. In that case (6.30) becomes

$$\begin{aligned} a_l &\cong \alpha - \beta l^2, & l \leq L_1, \\ a_l &\cong 0, & l > L_1; \end{aligned} \quad (6.33)$$

where now  $\alpha - \beta L_1^2 = 0$  and  $L_1 = (\alpha/\beta)^{\frac{1}{2}}$ . From (6.20) we obtain

$$\sigma_t = \frac{2\pi}{k^2} \frac{\alpha^2}{\beta}, \quad (6.34)$$

and from (6.22)

$$\sigma_{e.i} = \left( \frac{2\pi}{k} \right) \cdot \frac{2}{3} \frac{\alpha^3}{\beta}. \quad (6.35)$$

Note now that for  $\alpha < 1$ ,  $\sigma_{e.i} < 2/3 \sigma_t$ . From (6.23) we obtain

$$\left. \frac{dA}{dt} \right|_{t=0} \geq \frac{\pi(s)^{\frac{1}{2}}}{3k^3} \cdot \frac{\alpha^3}{\beta^2} \quad (6.36)$$

Hence finally one gets

$$\left. \frac{d}{dt} \ln A(s,t) \right|_{t=0} \geq \frac{1}{12k^2} \frac{\alpha}{\beta} = \frac{\sigma_t^2}{36\pi\sigma_{e.i}} \quad (6.37)$$

which is the same as (6.32) when one ignores terms  $O(1/k^2)$ .

It is interesting to note how close (6.37), with  $\sigma_{e.i}$  replaced by  $\sigma_{e1}$ , is to the experimental situation. From Dr. White's lectures we learned that a good fit to the pp data is obtained with the form  $\frac{d\sigma}{dt} \cong A \exp(bt)$ ,  $b \cong 9(\text{GeV})^2$ . One also learns that, ignoring spin,  $\text{Re}f$  and  $\text{Im}f$  have approximately the same  $t$ -dependence. One usually computes  $\sigma_{e1}$  as

$$\sigma_{e1} \cong \int_{-\infty}^0 A e^{+bt} dt \cong \frac{A}{b} \quad (6.38)$$

and

$$A = |f(0)|^2 \frac{2\pi}{2k^2} \quad (6.39)$$

From the fact that  $|\text{Re}f|$  and  $|\text{Im}f|$  have the same  $t$  dependence we get

$$\left. \frac{d \ln f}{dt} \right|_{t=0} = \frac{b}{2} \quad (6.40)$$

Substituting this in (6.37) we obtain

$$\frac{b}{2} \geq \frac{1}{9} \left[ \frac{4\pi(\text{Im}f(0))^2}{k^2} \cdot \frac{b}{A} \right] \quad (6.41)$$

where we have used the optical theorem  $\sigma_t = 4\pi \text{Im}f(0)/k$ . Finally (6.39) gives us

$$\frac{1}{2} \geq \frac{4}{9} \left( \frac{\text{Im}f(0)}{|f(0)|} \right)^2 \quad (6.42)$$

The bound is rather close when  $\text{Re}f/\text{Im}f$  is small.

## VII. LOWER BOUND ON THE FORWARD AMPLITUDE

The results on lower bounds are so far much weaker than one would like. In this chapter we prove the Jin-Martin<sup>13</sup> lower bound of the form

$$|F(s,0)| \geq Cs^{-2} \quad . \quad (7.1)$$

More precisely we only show that there exist a sequence  $\{s_n\}$ ,  $s_n \rightarrow \infty$  as  $n \rightarrow \infty$ , such that

$$|F(s_n,0)| \geq Cs_n^{-2} \quad . \quad (7.2)$$

Although a more direct proof<sup>14</sup> of (7.2) for either large positive or large negative  $s$ , but not both, is possible, we shall here follow the proof of Jin and Martin which uses Herglotz functions. We do this for pedagogical reasons since Herglotz functions are quite useful in scattering theory and they will come up again in later lectures.

Let us start then by giving the definition of Herglotz functions and listing a few of their properties.

Definition: a function  $H(z)$  is called a Herglotz function if  $H(z)$  is analytic in the upper half plane and if  $\text{Im}H(z) > 0$  for  $\text{Im}z > 0$ .

Any Herglotz function has the representation

$$H(z) = A+Bz + \frac{1}{\pi} \int_{-\infty}^{+\infty} \frac{\text{Im}H(x)(1+zx)}{(1+x^2)(x-z)} dx \quad , \quad (7.3)$$

with  $B \geq 0$ ,  $A$  real, and  $\text{Im}H(x) \geq 0$ . Also we have the convergence condition

$$\int_{-\infty}^{+\infty} \frac{\text{Im}H(x)}{(1+x^2)} dx < \infty \quad . \quad (7.4)$$

Another property that is easy to verify is that if  $H(z)$  is a Herglotz function then

$$F(z) \equiv - \frac{1}{H(z)} \quad , \quad (7.5)$$

is also in the Herglotz class. From the defining representation (7.3) one can easily show that, for all  $z$  such that  $\epsilon < \arg z < \pi - \epsilon$ , the following bounds hold:

$$C|z|^{-1} \leq |H(z)| \leq C|z| \quad . \quad (7.6)$$

For the physical amplitudes we want lower bounds on  $|H(x)|$  for real  $x$  and (7.6) is not directly applicable. However one has the following lemma due to Martin.<sup>15</sup>

Lemma 1:

Given a Herglotz function,  $H(z)$ , satisfying (7.6), and such that  $H(z)$  is analytic in the cut  $z$ -plane with right hand cut from  $z=a$  to  $z=+\infty$  and left hand cut from  $z=-b$  to  $z=-\infty$ , and any positive number  $C'$  larger than  $C$ ; one can find an infinite real sequence  $\{x_n\}$ ,  $x_n \rightarrow +\infty$ , such that

$$|H(x_n)| \leq C'|x_n| \quad . \quad (7.7)$$

Similarly, one can find a sequence  $\{x_n\}$ ,  $x_n \rightarrow -\infty$ , along the negative real axis such that (7.7) holds.

Since  $(-1/H(z))$  is also Herglotz, it follows from (7.8) that there also exists a sequence  $\{x_n\}$ ,  $x_n \rightarrow \pm\infty$ , such that

$$|H(x_n)| \geq C'' |x_n|^{-1} \quad (7.8).$$

Proof of Lemma 1:

Let  $F(z)$  be  $H(z)$  minus the contribution of the left hand cut in (7.3), i.e.,

$$F(z) \equiv A+Bz + \frac{1}{\pi} \int_a^{\infty} \frac{\text{Im}H(x)(1+zx)}{(1+x^2)(x-z)} dx \quad (7.9)$$

$F(z)$  is regular in the cut  $z$ -plane with a right hand cut only. It is bounded by  $C|z|$  in any complex direction including the negative real axis. Let us now assume that on the right hand cut for large  $x$

$$|F(x)| \geq C'x, \quad C' > C \quad (7.10)$$

We show that (7.10) leads to a contradiction. This is obtained by first applying the Phragmen-Lindelof theorem to the function  $1/F(x)$ . Since  $(1/F(z))$  is analytic outside the right hand cut and a finite circle around the origin we get for large  $|z|$

$$\left| \frac{1}{F(z)} \right| \leq \frac{1}{C'} |z|^{-1} \quad (7.11)$$

in all directions. Hence we get for all directions

$$|F(z)| \geq C'|z| \quad (7.12)$$

which contradicts the bound given below (7.9) for  $C' > C$ . Thus for any  $C' > C$  there must exist a sequence  $\{x_n\}$ ,  $x_n \rightarrow \infty$  on the positive real axis such that

$$|F(x_n)| < C'x_n \quad (7.13)$$

The integral over the left hand cut in (7.3) when divided by  $|x|$  tends to zero as  $x_n \rightarrow +\infty$ . This gives us for the same sequence  $\{x_n\}$  as in (7.13), as  $x_n \rightarrow +\infty$

$$|H(x_n)| < C'x_n \quad (7.14)$$

An analogous result is obtained by interchanging the roles of the left and right hand cuts. This completes the proof of the lemma 1.

In order to use the lemma 1 and (7.8) to obtain lower bounds we have first to get Herglotz functions from the scattering amplitudes. In general, scattering amplitudes are not Herglotz. We shall need the following second lemma.

Lemma 2:

Let  $F(z)$  be analytic in the cut  $z$ -plane with a right hand cut extending from  $z=a$  to  $z=+\infty$  and a left hand cut from  $z=-\infty$  to  $z=-b$ . Also let  $F(z)$  have the following properties:

$$(i) \quad |F(z)| \leq \text{Const.} |z|^N, \quad |z| > z_0.$$

(ii)  $\text{Im}F(x+i0) > 0$ .

(iii)  $F(z) = F^*(z^*)$ . (reality in gap).

Then  $F(z)$  has only a finite number of zero.

Proof of Lemma 2:

Complex zeros occur in pairs  $z_i, z_i^*$ , and real zero  $x_i$  occurs in the gap  $-b \leq x_i \leq a$ . If the number of zeros is infinite we can take  $p$ -pairs of complex zeros and  $2q$  real zeros and define a new function,  $G(z)$ :

$$G(z) = \frac{F(z)}{\prod_{i=1}^p (z-z_i)(z-z_i^*) \prod_{j=1}^{2q} (z-x_j)}, \quad (7.15)$$

where we take  $2p+2q > N+2$ . Hence from (i) we have for large  $|z|$

$$G(z) \leq \frac{1}{|z|^2}. \quad (7.16)$$

By construction  $\text{Im}G(z) > 0$  on the real axis, and we write the an unsubtracted dispersion relation for  $G$ ,

$$G(z) = \frac{1}{\pi} \int_{-\infty}^{-b} dx \frac{\text{Im}G(x)}{x-z} + \frac{1}{\pi} \int_a^{\infty} dx \frac{\text{Im}G(x)}{x-z}. \quad (7.17)$$

But the positivity of  $\text{Im}G(x)$  implies that  $|G(z)|$  cannot decrease faster than  $|z|^{-1}$  which contradicts (7.16). Hence the number of zeros must be finite and one can easily show that

$$\text{number of zeros} \leq N+2. \quad (7.18)$$

This ends the proof of lemma 2.

Next we want to construct a Herglotz function from an  $F(z)$  satisfying the conditions of lemma 2. Here two cases occur:

(a) Number of Real Zeros Even:

In this case we remove all the zeros and define a function  $\Phi$  as

$$\Phi(z) = \frac{F(z)}{\prod_{i=1}^p (z-z_i^*)(z-z_i) \prod_{j=1}^{2q} (z-x_j)}. \quad (7.19)$$

Now  $\Phi(z)$  has no zeros. Furthermore on the cuts  $\text{Im}\Phi(x+i0) > 0$ , and for large  $|z|$

$$\Phi(z) \leq \text{Const.} |z|^{N-2p-2q}. \quad (7.20)$$

In lemma 3 below we show that such a function is a Herglotz function. Hence there exist a sequence  $\{x_n\}$ ,  $x_n \rightarrow \infty$ , such that

$$|\Phi(x_n)| \geq \bar{C} x_n^{-1}. \quad (7.21)$$

This is a consequence of lemma 1. From (7.21) and (7.19) we now get

$$|F(x_n)| \geq \bar{C} x_n^{2p+2q-1} \geq \bar{C} x_n^{-1}, \quad (7.22)$$

for the same sequence.

(b) Number of Real Zeros Odd:

We remove all complex zeros and all real zeros except one, writing

$$\psi(z) = \frac{F(z)}{\prod_{i=1}^p (z-z_i^*) \prod_{i=1}^{2q} (z-z_i)} \quad (7.23)$$

In this case  $\psi(z)$  still has only one real zero at  $z = x_0$  but it has no complex zeros. The treatment of the remaining zero depends on the sign of the derivative of  $F$  at the remaining zero. A simple modification of the previous argument (see ref. 13) will still give a sequence  $\{x_n\}$ ,  $x_n \rightarrow \infty$ , such that

$$|\psi(x_n)| \geq \bar{C} x_n^{-1}, \quad (7.24)$$

which gives again

$$|F(x_n)| \geq \bar{C} x_n^{-1}. \quad (7.25)$$

To apply (7.22) and (7.25) to scattering amplitudes we still have to consider the situation where  $\text{Im}F(x+i0)$  changes sign  $\nu$ -times from  $-\infty$  to  $+\infty$ . If this happens then we write

$$G(z) = \prod_{k=1}^{\nu} (z-\tilde{x}_k) F(z), \quad (7.26)$$

where the  $\tilde{x}_k$ 's are chosen so that  $\text{Im}G(x+i0) > 0$  on both cuts. Proceeding in the same way for  $G$  as we did for  $F$  we get a sequence  $\{x_n\}$ ,  $x_n \rightarrow +\infty$  such that

$$|G(x_n)| \geq \text{Const.} x_n^{-1}, \quad (7.27)$$

and hence

$$|F(x_n)| \geq \text{Const.} x_n^{-1-\nu}, \quad (7.28)$$

where  $\nu$  is the number of times  $\text{Im}F(x+i0)$  changes sign in  $-\infty < x < +\infty$ .

If we now consider the scattering process  $a+b \rightarrow a+b$ ,  $\text{Im}F(s,0) > 0$  for  $S > (M_a + M_b)^2$ , and  $\text{Im}F(s,0) < 0$  for  $-\infty < s < (M_a - M_b)^2$ . Hence for an actual scattering process all the conditions on  $F$  are satisfied with  $\nu = 1$ . We conclude that there exist a sequence  $\{s_n\}$ ,  $s_n \rightarrow +\infty$ , and a constant  $C$  such that

$$|F(s_n, 0)| \geq C s_n^{-2}. \quad (7.29)$$

In closing we state and prove lemma 3 which we have used to assert that  $\Phi(z)$  was Herglotz.



Lemma 3:

Given a function  $\Phi(z)$  regular in the upper half plane and satisfying the following properties:

- (a)  $|\Phi(z)| < C|z|^N, |z| > z_0$  ,
- (b)  $\Phi(z)$  has no zeros for  $\text{Im}z \geq 0$  ,
- (c)  $\text{Im}\Phi(x+i0) > 0$  on the real axis, (i.e.,  $0 \leq \arg\Phi(x+i0) \leq \pi$ ).

Then  $\Phi(z)$  is a Herglotz function.

Proof of Lemma 3:

Take an integer  $N' > N$  with  $N' \geq 2$ . The function  $(\Phi)^{1/N'}$  will also be analytic in the upper half plane because of (b). Furthermore it is clear that  $\text{Im}[\Phi^{1/N'}]$  will also be positive on the real axis as a consequence of (c). We consider the function

$$W(z) = \exp[i\Phi^{1/N'}] \quad (7.30)$$

This function is regular for  $\text{Im}z > 0$ . On the real axis  $|W(x+i0)| < 1$  holds. Now the Phragmen-Lindelof principle tells us that only one of the following two possibilities holds

(i)  $|W(z)| < 1$  everywhere in the upper half plane

OR (ii) There exists a sequence of points  $\{z_n\}$ ,  $|z_n| \rightarrow \infty$  along some direction in the upper half plane such that

$$|W(z_n)| \geq e^{\alpha|z_n|}, \quad \alpha > 0 \quad (7.31)$$

Alternative (ii) implies that along some direction  $(\text{Im}\Phi^{1/N'})$  blows up at least linearly to  $-\infty$ . Hence we get

$$|(\Phi(z_n))^{1/N'}| \geq \alpha|z_n|,$$

and

$$|\Phi(z_n)| \geq \alpha|z_n|^{N'} \quad (7.32)$$

This contradicts assumption (a) of our lemma. Only alternative (i) can hold, and that implies

$$\text{Im}(\Phi)^{1/N'} > 0 \text{ for } \text{Im}z > 0. \quad (7.33)$$

Let  $\arg\Phi^{1/N'} \equiv u+iv$ . The function  $v(x,y)$  is a harmonic function and  $v \equiv \arg\Phi^{1/N'}$ .

From (7.33) we know that  $0 \leq v \leq \pi$  for all points in the upper half plane and therefore  $v(x,y)$  is bounded for  $y \geq 0$ . However, from our original construction we know that on the x axis

$$0 \leq \arg(\Phi(x+i0))^{1/N'} \leq \frac{\pi}{N'},$$

or

$$0 \leq v(x,0) \leq \frac{\pi}{N'} \quad (7.34)$$

Since  $v(x,y)$  is harmonic and bounded for  $y > 0$  then it follows from (7.34) that for all  $y \geq 0$ ,

$$0 \leq v(x,y) \leq \frac{\pi}{N'} \quad (7.35)$$

or

$$0 \leq \arg(\Phi(z))^{1/N'} \leq \frac{\pi}{N'} \quad (7.36)$$

and

$$0 \leq \arg \mathbb{D}(z) \leq \pi, \quad \text{Im}z \geq 0; \quad (7.37)$$

we conclude that  $\mathbb{D}(z)$  is Herglotz. Q.E.D.

The lower bound obtained above is as we mentioned earlier rather weak. The question of improving it is an immediate challenge.

It is clear from (7.22) that we can immediately improve (7.2) by one power of  $s$  if we know the amplitude has a real zero and by two powers if we know the amplitude has a pair of complex zeros. However, to guarantee the existence of such zeros requires more detailed information about the signs of the scattering lengths and the relative magnitudes of subtraction terms as compared to dispersion integrals over the low energy region. Such conditions are given in Ref. 13.

Another possibility for improvement occurs in the case of a symmetric amplitude, i.e.  $\bar{b}=b$ , if one knows in advance that the scattering length is negative. To show how this happens it is convenient to use the variable  $E$ , the laboratory energy, instead of  $s$ , where for  $\pi^0 K \rightarrow \pi^0 K$  for example

$$s = \mu^2 + M_K^2 + 2M_K E. \quad (7.38)$$

The amplitude  $F(E)$  is even in  $E$  and satisfies the dispersion relation

$$F(E) = F(0) + \frac{2E^2}{\pi} \int_{\mu}^{\infty} \frac{\text{Im}F(E')}{E'(E'^2 - E^2)} dE'. \quad (7.39)$$

We define a new variable  $z=E^2$ , write  $F(E)=G(z)$ , and get

$$G(z) = G(0) + \frac{z}{\pi} \int_{\mu^2}^{\infty} \frac{\text{Im}G(z')}{z'(z'-z)} dz'. \quad (7.40)$$

First note that  $G(z)$  is a Herglotz function of  $z$ , ( $\text{Im}F(E') > 0$ ). Next it is evident from (7.40) that  $G(x)$  is real and monotonically increasing in the interval  $-\infty < x \leq \mu^2$ ;  $dG/dz > 0$  for  $z < \mu^2$ . If the scattering length is negative,

$$G(\mu^2) \equiv F(\mu) < 0, \quad (7.41)$$

then for  $-\infty < x < \mu^2$ ,

$$G(x) \leq G(\mu^2) < 0. \quad (7.42)$$

We can therefore construct another Herglotz function  $H(z)=G(z)/z$ . This is trivial to check from (7.40). Hence we have a real sequence  $\{z_n\}$  such that,

$$\begin{aligned} |H(z_n)| &\geq C |z_n|^{-1}, \\ |G(z_n)| &\geq C, \\ |F(E_n)| &\geq C. \end{aligned} \quad (7.43)$$

This improves (7.2) by two powers of  $s$ .

So far we have only derived lower bounds for the full amplitude. The question of lower bounds for  $\text{Im}F$  or  $\sigma_t$  is also relevant. We need such a lower

bound to complete the proof of (6.5).

We show that

$$\text{Im}F(s_n, 0) \geq C s_n^{-5} (\ln s_n)^{-2} . \quad (7.44)$$

From Chapter IV we write

$$|F(s, 0)|^2 = \left| \sum_0^{L(s)} (2\ell+1) f_\ell(s) \frac{8\pi\sqrt{s}}{k} + O(s^{-N}) \right|^2 . \quad (7.45)$$

Using the Cauchy-Schwartz inequality we get,

$$\begin{aligned} |F(s, 0)|^2 &\leq \frac{s}{k^2} (8\pi)^2 \left( \sum_0^L (2\ell+1) \right) \left( \sum_0^L (2\ell+1) |f_\ell|^2 \right) , \\ &\leq C^2 s \ln^2 s \text{Im}F(s, 0) . \end{aligned} \quad (7.46)$$

This with (7.2) gives us (7.44).

### VIII. POMERANCHUK THEOREMS

#### A. Historical Remarks

The Pomeranchuk theorem<sup>16</sup> in its original form states that asymptotically the total cross section for the scattering of a particle on a target is equal to the total cross section for the scattering of the antiparticle on the same target, i.e.  $\lim_{E \rightarrow \infty} \sigma_+(E) = \lim_{E \rightarrow \infty} \sigma_-(E)$ . The total cross sections were assumed to reach a constant limit.

This theorem is not purely a rigorous consequence of analyticity and polynomial boundedness alone. Other assumptions had to be made. These assumptions have been considerably weakened by succeeding authors as shown below. The only extra input now needed concerns the relative magnitude of  $\text{Re}F$  to  $\text{Im}F$ .

We consider the processes

$$\begin{aligned} a + T &\rightarrow a + T , \\ \bar{a} + T &\rightarrow \bar{a} + T , \end{aligned} \quad (8.1)$$

with forward amplitudes,  $F_\pm(E)$ , respectively and  $E = \text{lab. energy}$ . We set  $m_a = \mu$  and  $m_T = M$ .

Pomeranchuk<sup>16</sup> assumed that:

i)  $F_\pm(E)$  are such that:

$$\lim_{E \rightarrow \infty} \frac{\text{Im}F_\pm(E)}{\sqrt{E^2 - \mu^2}} = \text{const.} \quad (8.2)$$

and for large  $E$ ,

$$\left| \frac{F_\pm(E)}{\sqrt{E^2 - \mu^2}} \right| \leq \text{const.} \quad (8.3)$$

ii)  $F_\pm(E)/(E^2 - \mu^2)$  satisfies an unsubtracted dispersion relation.

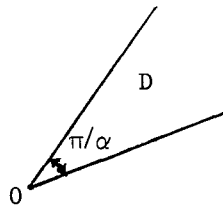
Weinberg<sup>17</sup> weakened the condition  $\sigma_\pm \rightarrow \text{const.}$  as  $E \rightarrow \infty$  and replaced it by the condition that for large enough  $E$ ,  $\Delta\sigma \equiv \sigma_+ - \sigma_-$  should have one sign. He also

showed that if one assumes that for large  $E$ ,  $\sigma_{\pm} \sim C_{\pm} (\ln E)^m$ ,  $0 < m < 1$ , then  $C_{+} = C_{-}$ . In that case one has  $\lim(\sigma_{+}/\sigma_{-}) = 1$ .

Amati, Fierz, and Glazer<sup>18</sup> proved that  $\int^{\infty} \frac{\Delta\sigma}{E} dE$  converges.

A simple and elegant proof of the Pomeranchuk theorem in a slightly weakened form was given by Meiman.<sup>19</sup> We shall follow it here in section C. Before we do that we have to discuss some mathematical preliminaries related to the Phragmén-Lindelöf principle. We have used this principle several times in these lectures and for the sake of completeness should state it somewhere.

B. Mathematical Preliminaries: Phragmén-Lindelöf



(a) Phragmén-Lindelöf Theorem: (Classical Form)

Let  $f(z)$  be analytic in  $z$  regular in a sector,  $D$ , defined by two straight lines intersecting at  $0$  with an angle  $\pi/\alpha$ . Further let  $f(z)$  be continuous in  $\bar{D}$ . As  $r \rightarrow \infty$ , let

$$\text{Max}_{\theta \in \text{sector}} |f(re^{i\theta})| = O(e^{r^{\beta}}), \quad \beta < \alpha \quad . \quad (8.4)$$

If now  $|f(z)| \leq M$  on the straight lines, then  $|f(z)| \leq M$  for all  $z \in D$ .

We specialize this theorem to the case of the half-plane which is of interest to us and we will use in this chapter only the following version of (a).

Theorem (a'):

If  $f(z)$  is analytic in  $z$ , regular in  $\text{Im}z > 0$ , continuous in  $\text{Im}z \geq 0$ , and  $|f(x)| \leq M$  on the real axis, then:

- either  $|f(z)| \leq M$  for all  $z$ ,  $\text{Im}z \geq 0$ ,  
or There exists a constant  $\alpha > 0$  such that

$$M(R_n) \geq e^{\alpha R_n},$$

for an infinite sequence  $\{R_n\}$ ,  $R_n \rightarrow \infty$  as  $n \rightarrow \infty$ , where

$$M(R) = \text{Max}_{0 < \theta < \pi} |f(Re^{i\theta})| \quad .$$

A corollary of this theorem states that if  $f(z)$  satisfies the conditions of theorem (a') and has a bound sufficient to exclude exponential growth in any direction, and if

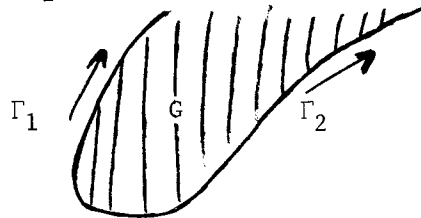
$$\begin{aligned} \lim_{x \rightarrow +\infty} f(x) &= L_1 \quad , \\ \lim_{x \rightarrow -\infty} f(x) &= L_2 \quad , \end{aligned} \quad (8.5)$$

then  $L_1=L_2$  and  $f(z) \rightarrow L_1$  uniformly in all directions.

Another more general form of the Phragmén-Lindelöf principle which we shall use below is contained in the following theorem.

Theorem (b):

We are given a domain  $G$  bounded by two curves  $\Gamma_1$  and  $\Gamma_2$  which extend to infinity in such a way that in going to infinity along  $\Gamma_2$   $G$  is to the left, and as one moves to infinity along  $\Gamma_1$   $G$  lies to the right.



Consider a function  $f(z)$  analytic in  $G$  and continuous and bounded on boundary. Let  $\mathcal{E}_1$  be the manifold of limit values of  $f(z)$  as  $z \rightarrow \infty$  along  $\Gamma_1$  and  $\mathcal{E}_2$  the manifold of limit values as  $z \rightarrow \infty$  along  $\Gamma_2$ . ( $\mathcal{E}_1$  and  $\mathcal{E}_2$  each consist of either one point or a continuum.) If  $\mathcal{E}_1$  and  $\mathcal{E}_2$  have no points in common and if one of them does not surround the other, then  $f(z)$  cannot be bounded in  $G$ .

If  $G$  is the half plane, then it follows from theorem (a') that if  $f(z)$  is unbounded it increases faster than  $\exp(\alpha|z|)$  in some direction. We note also that theorem (a') is valid for a region obtained from the half plane by deforming a finite part of the real axis. We do not need analyticity in the full upper half plane to apply these theorems and we can easily exclude a region that lies inside a semicircle centered at the origin.

C. Meiman's Proof of Pomeranchuk's Theorem

We start with functions  $F_{\pm}(E)$  with the following properties:

- i)  $F_{+}(E+io) = F_{-}(-E-io)$ .
- ii) Analytic in cut plane with cuts  $E=\mu$  to  $E=\infty$  and  $E=-\infty$  to  $E=-\mu$ .
- iii)  $F_{+}(E+io) = F_{+}^{*}(E-io)$ .
- iv) For an arbitrary  $\epsilon > 0$ , and  $|E| > E_0(\epsilon)$   
 $|F(E)| \leq \exp(\epsilon|E|)$ , in all directions. (8.6)
- v)  $F_{\pm}(E)/\sqrt{E^2-\mu^2}$  bounded on real axis as  $E \rightarrow \pm\infty$ .

Properties i)-iv) are consequences of local field theory. In fact iv) can be replaced by polynomial boundedness in local field theory. However, v) has not been proved rigorously, and although one can only make the original Pomeranchuk statement about cross sections that do tend to constants, still as we shall see below there is no guarantee that the real parts are bounded as in v).

We now prove that i)-v) imply that there exists a sequence,  $\{E_n\}$ ,  $E_n \rightarrow +\infty$  as  $n \rightarrow \infty$ , such that

$$\lim_{n \rightarrow \infty} [\sigma_+(E_n) - \sigma_-(E_n)] = 0. \quad (8.7)$$

To do this we define,  $g(E)$ , as

$$g(E) = \frac{F_+(E) - F_-(E)}{\sqrt{E^2 - \mu^2}}. \quad (8.8)$$

The optical theorem gives us

$$\text{Im}g(E) = 2M[\sigma_+(E) - \sigma_-(E)]. \quad (8.9)$$

From the crossing condition i) and the reality condition iii) we obtain

$$g(-E+i0) = g^*(E+i0), \quad (8.10)$$

and

$$g(-E-i0) = -g(E+i0). \quad (8.11)$$

Using theorem (b) of section B with  $G$  corresponding to the upper half plane,  $\Gamma_2$  is the positive real axis and  $\Gamma_1$  is the negative real axis. Let  $\mathcal{E}_2$  be the manifold of limit values as  $E \rightarrow +\infty+i0$  and  $\mathcal{E}_1$  the manifold of limit values of  $g(E)$  as  $E \rightarrow -\infty+i0$ . From (8.10) it is clear that  $\mathcal{E}_2$  and  $\mathcal{E}_1$  should be symmetric with respect to the real- $g$  axis in the  $g$ -plane. These manifolds must intersect the real axis, for if they do not one of them would lie in the upper half plane and one in the lower half plane and they will have no points in common. If they have no points in common  $g(E)$  is unbounded by theorem (b), and hence by theorem (a'),  $g(E)$  increases faster than some exponential ( $\exp|E|$ ) along some sequence of points in the upper half plane. This is excluded by the bound (8.6). Therefore there must exist at least one real point,  $u_0$ , which is in both  $\mathcal{E}_2$  and  $\mathcal{E}_1$ , and thus there exists a sequence  $\{E_n\}$ ,  $E_n \rightarrow +\infty$  as  $n \rightarrow +\infty$ , such that  $g(E_n) \rightarrow u_0$  as  $n \rightarrow \infty$ , or

$$\lim_{n \rightarrow \infty} \{\text{Im}g(E_n)\} = 0, \quad (8.12)$$

and

$$\lim_{n \rightarrow \infty} [\sigma_+(E_n) - \sigma_-(E_n)] = 0. \quad (8.12)$$

This is a weaker statement than the original Pomeranchuk theorem, but an experimentally meaningful statement.

However, if the limit of  $\Delta\sigma(E)$  as  $E \rightarrow \infty$  exists then it immediately follows from (8.12) that

$$\lim_{E \rightarrow \infty} \Delta\sigma(E) = 0. \quad (8.13)$$

Meiman's method can also be used to study the case where the cross-sections do not tend to a constant but increase or decrease like some power of  $\log E$  or  $\log \log E$ .

For example let us assume that for large E along the cut,

$$\Delta\sigma(E) \cong C|\varphi(E)| \quad . \quad (8.14)$$

The function  $\varphi(E)$  is assumed analytic in the upper half plane and satisfies the conditions: 1) for any  $\epsilon > 0$  and large  $|E| > E_0(\epsilon)$  we have  $|E|^{-\epsilon} < |\varphi(E)| < |E|^\epsilon$ ; 2) along the real axis  $(\text{Im}\varphi(E)/|\varphi|) \rightarrow 0$  as  $E \rightarrow \infty$ , and  $\frac{\varphi(-E)}{\varphi(E)} \rightarrow 1$  as  $E \rightarrow \infty$ . An example of such functions is  $\varphi(E) \equiv (\log E)^P (\log \log E)^Q$ .

If now in addition to (8.14) we assume that  $g(E)/\varphi(E)$  is bounded as  $E \rightarrow +\infty$  on the real axis, then by applying theorem (b) to this ratio we get

$$\lim_{n \rightarrow \infty} \left( \frac{\Delta\sigma(E_n)}{|\varphi(E_n)|} \right) = 0 \quad , \quad (8.15)$$

hence  $C=0$  in (8.14). More precisely, if  $\sigma_+(E) \sim C_+|\varphi(E)|$  and  $\sigma_-(E) \sim C_-|\varphi(E)|$  as  $E \rightarrow \infty$ , then  $C_+ = C_-$  and

$$\lim_{E \rightarrow \infty} \left[ \frac{\sigma_+(E)}{\sigma_-(E)} \right] = 1 \quad . \quad (8.16)$$

The only input going into the Pomeranchuk theorem which is not a direct consequence of local field theory is, as we mentioned earlier, condition v). Thus even when the total cross sections tend to constants at infinity, there is no guarantee that the ratio  $\text{Re}F_{\pm}/E$  is bounded as  $E \rightarrow \infty$  along the real axis. Martin<sup>20</sup> was able to weaken v) and replace it by

$$\lim_{E \rightarrow \infty} \left| \frac{F_{\pm}(E)}{E \log E} \right| = 0 \quad . \quad (8.17)$$

With this and the assumption that  $\Delta\sigma(E)$  has a limit as  $E \rightarrow \infty$  he showed that  $\Delta\sigma(\infty) = 0$ .

Thus the main gap remains to find a bound on the growth of the real parts. To close this gap Eden<sup>21</sup> and Kinoshita<sup>22</sup> have shown that using unitarity and analyticity in the Martin ellipse in  $\cos\theta$  one gets the inequality

$$\frac{|\text{Re}F(E)|}{|\text{Im}F(E)|} \leq \frac{C \sqrt{E} \ln E}{[\text{Im}F(E)]^{\frac{1}{2}}} \quad , \quad (8.18)$$

for sufficiently large E. One can easily check that for any process for which  $\sigma(E) \rightarrow \infty$  as  $E \rightarrow \infty$ , (8.18) implies

$$\lim_{E \rightarrow \infty} \frac{|\text{Re}F(E)|}{(\text{Im}F(E)) \ln E} = 0 \quad . \quad (8.19)$$

Unfortunately, (8.19) does not help us in the most interesting case, namely when  $\sigma_{\pm}(E)$  tend to constants. In that case we are still faced with the counter example,

$$F_{\pm}(E) = -AE \ln(\mu-E) + BE \ln(\mu+E) \quad , \quad (8.20)$$

where A and B are real and positive  $A \neq B$ .

For this example we have

$$|\sigma_+(\infty) - \sigma_-(\infty)| = \frac{1}{2M}|A-B| \neq 0, \quad (8.21)$$

also

$$\lim_{E \rightarrow \infty} \frac{\sigma_+(E)}{\sigma_-(E)} = \frac{A}{B} \neq 1. \quad (8.22)$$

The real part of course grows like  $E \ln E$ , a behavior which seems in contradiction with the measurements of the Lindenbaum group.

Finally, using the remark at the end of section B, we stress the fact that neither the Meiman proof nor the Martin proof need full analyticity in the upper half E-plane. It is clear that all the results of this chapter are true even if  $F_{\pm}(E)$  is only analytic outside some large but finite semicircle centered at the origin. In Ref. 20 Martin points out that this minimal analyticity and the crossing property used are known to hold for all collisions of the type  $a+b \rightarrow a+b$  as a result of the work of Bros, Epstein, and Glaser, Ref. 3.

## IX. ASYMPTOTIC RELATIONS BETWEEN PHASES AND TOTAL CROSS-SECTIONS

### A. Motivations and Examples

In deriving upper bounds we have so far barely used the analyticity in energy. In general it is not yet clear how to fully incorporate this information into the derivation of upper bounds. In this chapter we shall show that there is a strict correlation between the behavior of the ratio  $\text{Re}F/\text{Im}F$  as  $E \rightarrow \infty$  and that of  $\sigma(E)$  as  $E \rightarrow \infty$ . Of course, the dispersion relations in principle determine  $\text{Re}F$  from  $\sigma_{\text{tot}}$ . But because of the principal value integrals in the dispersion relations, it is easier to use either geometric methods or the phase representation to determine what certain assumptions on  $(\text{Re}F/\text{Im}F)$  imply about the asymptotic behavior of  $\sigma(E)$ .

In this chapter we restrict ourselves to studying the symmetric amplitude  $F(E)$ :

$$F(E) = \frac{1}{2}[F_+(E) + F_-(E)] - \text{pole terms}. \quad (9.1)$$

Let us first write down a few simple examples to give an idea of the kind of relation we are seeking.

#### (a) $\text{Re}F/\text{Im}F \rightarrow \text{const.}$

An example in this case would be

$$F(E) = \frac{C}{\sin \pi \alpha} [(E-\mu)^{\alpha} + (-E-\mu)^{\alpha}] ; 0 < \alpha \leq 1. \quad (9.2)$$



For this example

$$\lim_{E \rightarrow \infty} \frac{\operatorname{Re}F(E)}{\operatorname{Im}F(E)} = \cot \frac{\pi\alpha}{2} , \quad (9.3)$$

and for large E,

$$\sigma(E) \sim E^{\alpha-1} . \quad (9.4)$$

Thus one feature of this example is that if  $\operatorname{Re}F/\operatorname{Im}F \rightarrow \text{constant}$  as  $E \rightarrow \infty$ , then  $\sigma(E)$  goes to zero like an inverse power and this power is determined by the constant in (9.3). We shall see below that this feature is quite general and can be made more precise.

(b)  $\operatorname{Re}F/\operatorname{Im}F \sim C(\ln E)^{-1}$

Here we take

$$F(E) = iCE[\ln E - i\frac{\pi}{2}]^{\gamma} . \quad (9.5)$$

This gives us

$$\sigma(E) \sim (\ln E)^{\gamma}$$

$$\frac{\operatorname{Re}F(E)}{\operatorname{Im}F(E)} \sim \frac{C}{\ln E} . \quad (9.6)$$

(c)  $\frac{F(E)}{E} \rightarrow \text{const.}$

If  $(F(E)/E) \rightarrow C$  as  $E \rightarrow +\infty$ , it is easy to show that  $\operatorname{Re}F(E)/E \rightarrow 0$ . For by Phragmén-Lindelöf  $(F(E)/E) \rightarrow C$  also as  $E \rightarrow -\infty$ , but  $F(E)/E$  has an odd real part and hence  $C$  must be purely imaginary.

To make some of the features of these examples more general, we follow the techniques used by Khuri and Kinoshita.<sup>23</sup> Similar results can be obtained by using the phase representation method.<sup>24</sup>

#### B. Mathematical Preliminaries

We first state an inequality due to Meiman.<sup>19</sup>

Let  $g(E)$  be analytic in  $\operatorname{Im}E > 0$  and continuous in  $\operatorname{Im}E \geq 0$ . Furthermore, we assume that  $g(E)$  has the symmetry property

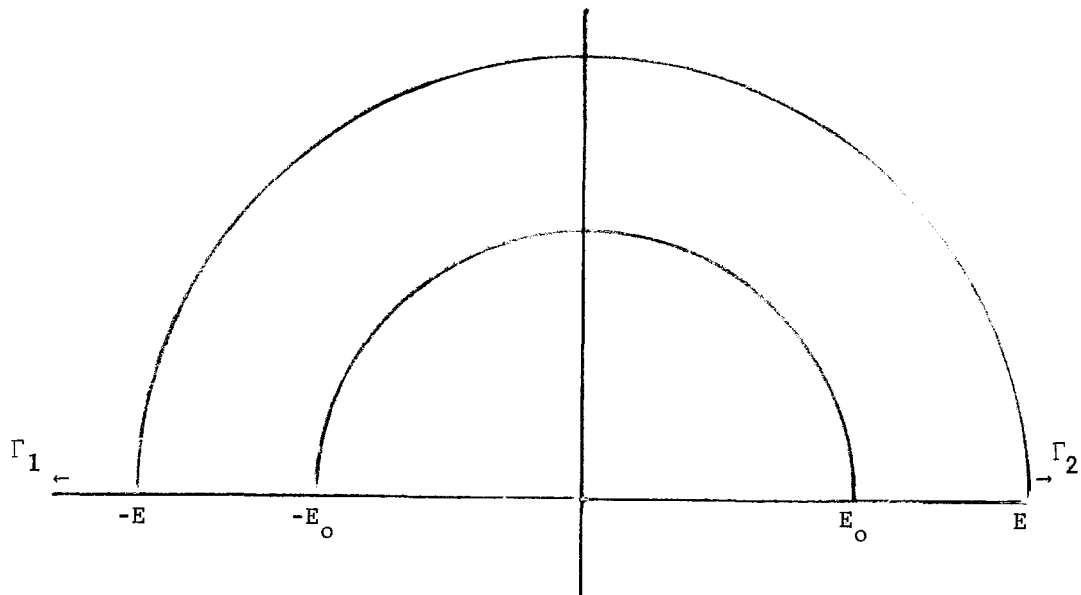
$$g(-E + i0) = g^*(E + i0). \quad (9.7)$$

Also we assume that

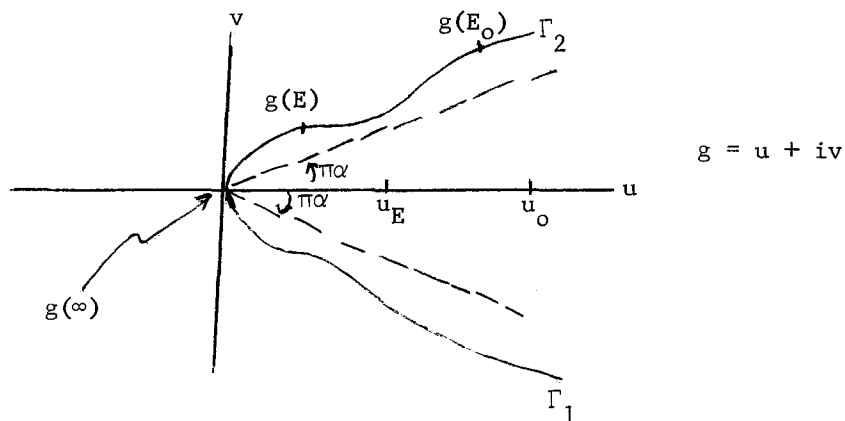
$$\lim_{|E| \rightarrow \infty} g(E) = 0 \quad (9.8)$$

The function  $g(E)$  maps the upper half  $E$ -plane into a certain domain of the  $g$ -plane. In particular the upper edges of the semi real axis  $(0, -\infty)$  and  $(0, +\infty)$  are mapped onto two curves  $\Gamma_1$  and  $\Gamma_2$  symmetrically located with respect to the real  $g$ -axis. In this mapping a sufficiently distant upper-half neighborhood of the point  $E = \infty$  is mapped onto a certain neighborhood (perhaps many sheeted) of the point  $g=0$ . To be more specific we take two large real values  $E$  and  $E_0$ , such that  $E, E_0 \gg E_1$ ;

$E_1$  being a large positive constant. We consider a domain in the  $E$ -plane bounded by two semi-circles centered at the origin with radii  $E$  and  $E_0$  as shown below.



Let us assume that for  $|E| > E_1$ ,  $\Gamma_1$  and  $\Gamma_2$  have no points in common. The image of the above region in the  $g$ -plane is shown below



We let  $u_0$  be the nearest point of intersection of the map of the smaller semi-circle with the positive  $u$ -axis. Similarly, we let  $u_E$  be the farthest point of intersection of the map of the large semi-circle with the positive  $u$ -axis.

Meiman's inequality can now be stated as

$$\int_{u_E}^{u_0} \frac{du}{\rho(u)} \geq \frac{1}{2} \ln \frac{E}{E_0} \quad , \quad (9.9)$$

where  $E \gg E_0$  and  $\rho(u)$  is the shortest distance from the point  $u$  to the curve  $\Gamma(E, E_0)$ . For a proof of this inequality, see Ref. 23 or for more detail

Nevannlina's book.

Using this inequality we state and prove the following two theorems due to Meiman. For simplicity we ignore violent oscillations in the functions  $g(E)$ .

Theorem I:

Let  $g(E)$  satisfy (9.7) and (9.8) and be analytic in  $\text{Im}E > 0$ . Furthermore, let  $g(E)$  have no zeros for  $|E| > E_1$ . If in addition for large real  $E > E_1$ , we have the inequality

$$\left| \frac{\text{Im}g}{\text{Re}g} \right| \geq \tan \pi\alpha, \quad 0 < \alpha \leq \frac{1}{2}, \quad (9.10)$$

then starting with some  $E_0 \gg E_1$ , we have for  $E \gg E_0$ ,

$$\left| g(E)/g(E_0) \right| \leq C \left( \frac{E_0}{E} \right)^{\alpha/2}, \quad (9.11)$$

(actually when we have oscillations, (9.11) holds only on a sequence of intervals extending to infinity).

Proof:

In this case if we draw straight lines through the origin (in the previous figure) with slope  $\tan \pi\alpha$  and  $-\tan \pi\alpha$ , then  $\Gamma_2$  will lie above one line and  $\Gamma_1$  below the other as shown.

It suffices to consider the case  $\alpha = \frac{1}{2}$  since other cases can be reduced to it by considering the function  $g' = g^{\frac{1}{2\alpha}}$ .

For  $\alpha = \frac{1}{2}$  we have

$$\rho(u) \geq (u^2 + |g(E)|^2)^{\frac{1}{2}}, \quad (9.12)$$

with  $u_E \leq u \leq u_0$ . Thus we have

$$\int_{u_E}^{u_0} \frac{du}{\rho(u)} \leq \int_0^{u_0} \frac{du}{(u^2 + |g(E)|^2)^{\frac{1}{2}}} = \ln \left[ \frac{u_0 + (u_0^2 + |g(E)|^2)^{\frac{1}{2}}}{|g(E)|} \right] \quad (9.13)$$

Combining this with (9.9) we get

$$\frac{|g(E)|}{u_0 + (u_0^2 + |g(E)|^2)^{\frac{1}{2}}} \leq C \left( \frac{E_0}{E} \right)^{\frac{1}{2}}, \quad (9.14)$$

and hence

$$|g(E)| \leq C \left( \frac{E_0}{E} \right)^{\frac{1}{2}}. \quad \text{Q.E.D.} \quad (9.15)$$

Remark:

Even though we always choose  $E \gg E_0$  and  $E_0$  large, it is still possible that for some real  $E'$ ,  $E_0 \ll E' < E$ , we have

$$|g(E')| \leq |g(E)|; \quad (9.16)$$

i.e.  $E'$  is the point at which  $|g(E)|$  takes its minimum value. In this case (9.12) reads  $\rho(u) \geq (u^2 + |g(E')|^2)^{\frac{1}{2}}$ . One then gets instead of (9.15) the inequality

$$|g(E')| \leq C \left( \frac{E_0}{E} \right)^{\frac{1}{4}}, \quad (9.17)$$

hence since  $E' < E$ , we get

$$|g(E')| \leq C \left( \frac{E_0}{E'} \right)^{\frac{1}{4}}. \quad (9.18)$$

We see here that if  $|g(E)|$  oscillates (9.15) holds only on a sequence of points.

Theorem II:

If  $g(E)$  satisfies the same conditions as in theorem I but instead of (9.10) we have,

$$|\operatorname{Im} g(E)| \geq C |\operatorname{Re} g(E)|^\nu, \quad C > 0, \nu > 1, \quad (9.19)$$

for large real  $E$ ; then starting with some  $E_0$  we have,

$$|\operatorname{Im} g(E) / \operatorname{Im} g(E_0)| \leq \left( 1 + \frac{1}{4} C' (\nu-1) \ln \frac{E}{E_0} \right)^{-\frac{\nu}{\nu-1}}, \quad (9.20)$$

where  $C'$  is a constant.

For a proof see the Appendix of Ref. 23.

C. Applications to the Even Amplitude

We now show how the two theorems just stated can be used to derive phase relations for the even amplitude  $F(E)$  defined in (9.1).

First we recall the rigorous properties of  $F(E)$ .

- (i) Analyticity in cut  $E$ -plane and continuity on boundary.
- (ii)  $F(E+i0) = F^*(E-i0)$ ; (reality).
- (iii)  $F(-E-i0) = F(E+i0)$ ; (crossing).
- (iv)  $|F(E)| \leq C |E| \ln^2 |E|$ ; (Froissart Bound).

Theorem A:

If  $F(E)$  satisfies i) - iv) and if for large real  $E$

$$\left| \frac{\operatorname{Re} F}{\operatorname{Im} F} \right| \geq \tan \pi \alpha; \quad 0 < \alpha \leq \frac{1}{2}; \quad (9.21)$$

then for large enough  $|E|$ ,

$$|F(E)| \leq C |E|^{1-\alpha/2} (\ln |E|)^2. \quad (9.22)$$

Proof:

We define the function  $w(E)$  as

$$w(E) = \frac{F(E)}{iE \left[ \ln E - \frac{i\pi}{2} \right]^\gamma}, \quad \gamma > 2; \quad (9.23)$$

and  $0 \leq \arg E \leq \pi$ .

By construction  $w(E)$  is analytic in the upper half  $E$ -plane excluding the unit half disc around the origin. Furthermore,  $w(E) \rightarrow 0$  as  $|E| \rightarrow \infty$  in all directions. It also follows from iv) and the dispersion relations for  $F(E)$  that  $F(E)/E$  has no zeros for  $|E|$  greater than some constant  $E_1$ . Thus  $w(E)$  has no zeros for sufficiently large  $|E|$  in the upper half plane and also  $\operatorname{Re} w \geq 0$  in that region. From unitarity we have  $\operatorname{Im} F(E) > 0$  for  $E \geq \mu$ ; hence along the positive real axis  $\operatorname{Re} w(E)$  is positive for large  $E$ .

The reality condition (ii) and the crossing relation (iii) give us

$$\begin{aligned} \operatorname{Re} w(E+i0) &= \operatorname{Re} w(-E+i0) , \\ \operatorname{Im} w(E+i0) &= -\operatorname{Im} w(-E+i0) . \end{aligned} \quad (9.24)$$

For large  $E$  we have,

$$\frac{\operatorname{Im} w(E)}{\operatorname{Re} w(E)} \sim - \frac{\operatorname{Re} F}{\operatorname{Im} F} , \quad (9.25)$$

and hence

$$\left| \frac{\operatorname{Im} w(E)}{\operatorname{Re} w(E)} \right| \geq \tan \pi\alpha . \quad (9.26)$$

Thus  $w(E)$  satisfies all the conditions of theorem I of Meiman, and we get for large enough real  $E$

$$\left| \frac{w(E)}{w(E_0)} \right| \leq C \left( \frac{E_0}{E} \right)^{\alpha/2} . \quad (9.27)$$

This gives us

$$|F(E)| \leq C |E|^{1-\frac{\alpha}{2}} (\ln|E|)^\gamma ; \quad \gamma > 2 . \quad (9.28)$$

For the total cross section we have

$$\sigma_{\text{tot}}(E) \leq C E^{-\alpha'/2} ; \quad \alpha' < \alpha . \quad (9.29)$$

This completes the proof of theorem A. If the cross section tends to a nonvanishing value or decreases more slowly than any negative power of  $E$  as  $E \rightarrow \infty$ , then  $|\operatorname{Re} F/\operatorname{Im} F|$  must tend to zero in that limit.

Again for the mathematically afflicted we stress that (9.28) and (9.29) hold only on a sequence of points in general.

The cases where  $|\operatorname{Re} F/\operatorname{Im} F| \rightarrow 0$  as  $E \rightarrow \infty$  have been treated in detail in Ref. 23. We state here one more theorem to give a flavor of the results.

Theorem B:

If  $F(E)$  satisfies (i) - (iv) and if for large real  $E$

$$|\operatorname{Re} F/\operatorname{Im} F| \geq \frac{C}{(\ln E)^a} , \quad 0 < a < 1 , \quad (9.30)$$

then for large  $|E|$

$$|F(E)| \leq C |E| (\ln|E|)^{-\lambda}, \quad \lambda > 0. \quad (9.31)$$

Here  $\lambda$  can be chosen arbitrarily large.

In this case the total cross section decreases faster than any inverse power of  $\ln E$ . The proof of this theorem depends on using theorem II of Meiman. The details are in Ref. 23, where also more theorems of this type are given.

## X. ASYMPTOTIC PHASE RELATIONS AND UNIVALENT FUNCTIONS

The theorems and inequalities proved in the previous chapter could be improved and strengthened if the symmetric amplitude,  $F(E)$  is also univalent. However, one can easily show that this is not true in general, namely  $F(E)$  is not necessarily univalent. On the other hand as we shall see below, we can easily construct from  $F(E)$  functions that are univalent in the upper half  $E$ -plane. We then use the strong restrictions on univalent functions to derive some asymptotic phase relations for these new functions. The details of this chapter can be found in Ref. 25.

### A. Mathematical Preliminaries

A function,  $f(z)$ , analytic in a domain  $D$  is called univalent in  $D$  if  $z_1 \neq z_2$  implies  $f(z_1) \neq f(z_2)$  for any  $z_1, z_2$  in  $D$ . Locally any analytic function  $f(z)$  is univalent in some neighborhood of a point  $z_0$  if  $f'(z_0) \neq 0$ . A theorem on univalent functions states that if  $f(z)$  is regular for  $z$  in a simple domain  $D$ , and  $f'(z) \neq 0$  for all  $z$  in  $D$ , and if the simple boundary curve of  $D$  is mapped by  $f(z)$  into a simple boundary curve (i.e., with no double points) of the image domain in the  $f$ -plane, then  $f(z)$  is univalent in  $D$ .

We now wish to construct a univalent function from the function  $F(E)$  defined by Eq. (9.1) and satisfying the properties i)...iv) given above theorem A of Chapter IX.

We write a twice subtracted dispersion relation for  $F(E)$ ,

$$F(E) - F(0) = \frac{2E^2}{\pi} \int_{\mu}^{\infty} dE' \frac{\text{Im}F(E')}{E'(E'^2 - E^2)} \quad (10.1)$$

We define the new function  $H(E)$  as,

$$H(E) = \frac{F(E) - F(0)}{E} \quad (10.2)$$

This function  $H(E)$  has the following properties:

- a)  $H(E)$  is regular for  $\text{Im}E > 0$  and continuous for  $\text{Im}E \geq 0$ .
- b)  $H(E)$  is a Herglotz function, i.e.,  $\text{Im}H(E) > 0$  when  $\text{Im}E > 0$ .
- c)  $H(i\lambda)$ ,  $\lambda > 0$  is purely imaginary and positive.
- d)  $\text{Re}H(E+i0) = -\text{Re}H(-E+i0)$ , and  $\text{Im}H(E+i0) = \text{Im}H(-E+i0)$ . Thus the function  $H(E)$  maps the upper half  $E$ -plane into a domain in the upper half  $H$ -plane. This mapping is of course not necessarily one to one.

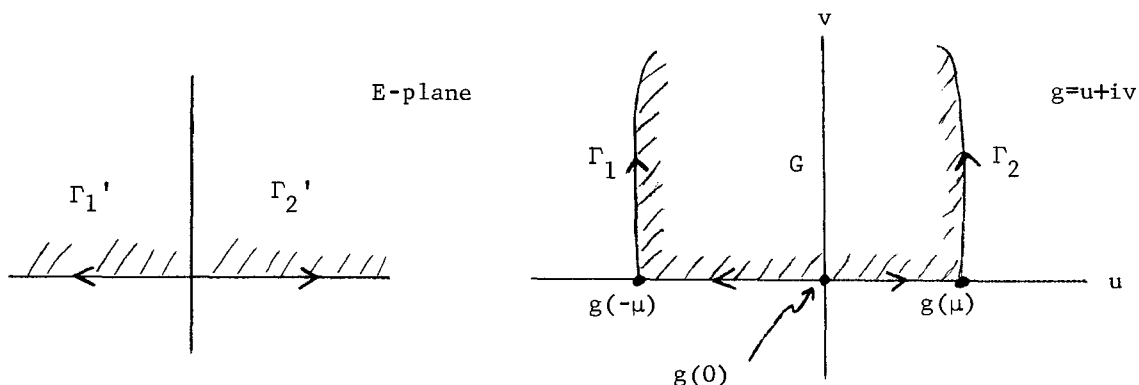
To get a univalent function we write

$$g(E) = \int_0^E \frac{H(E')}{E'} dE' ; \quad \text{Im}E \geq 0 ; \quad (10.3)$$

where the integration contour is taken to be in the upper half  $E$ -plane. The integral is convergent at  $E'=0$  since crossing tells us that  $F'(0) = 0$ .

One can easily check that  $g(E)$  has the following properties: (a)  $g(E)$  is regular in  $\text{Im}E > 0$  and continuous in  $\text{Im}E \geq 0$ , (b)  $\text{Im}g(E) > 0$  if  $\text{Im}E > 0$ , (c)  $dg/dE \neq 0$  for all  $E$  such that  $\text{Im}E > 0$ , (d)  $\text{Im}g(-E+i0) = \text{Im}g(E+i0)$  and  $\text{Re}g(E+i0) = -\text{Re}g(-E+i0)$ , (e) for  $E \geq \mu$ ,  $\text{Im}g(E+i0)$  is non-negative and increases monotonically with  $E$  as  $E$  increases along the positive real axis, (f)  $\text{Re}g(E+i0)$  is non-negative and increases monotonically in the interval  $0 \leq E \leq \mu$ .

As is seen from (b),  $g(E)$  maps the upper half  $E$ -plane into a domain  $G$  located in the upper half  $g$ -plane. We know from (c) that this mapping is locally one-to-one everywhere in the upper half  $E$ -plane. The mapping will be globally univalent if the boundary curve of  $G$  does not have double points. Let us denote by  $\Gamma_1$  and  $\Gamma_2$  the images of the negative and positive real  $E$ -axes respectively. We know from (f) that the part of  $\Gamma_2$  corresponding to  $0 \leq E \leq \mu$ , does not intersect with itself and lies on the positive real  $g$ -axis as shown in the figure below.



For  $E > \mu$ ,  $g(E)$  becomes complex and the corresponding part of  $\Gamma_2$  goes away monotonically from the real  $g$ -axis according to (e). Thus  $\Gamma_2$  cannot have any double points. The same holds for  $\Gamma_1$ . Hence the only remaining possibility is that  $\Gamma_1$  and  $\Gamma_2$  have some common points. Because of the monotonicity and the symmetry the only possible common points of  $\Gamma_1$  and  $\Gamma_2$  can be found only on the imaginary  $g$ -axis. One can easily show from (10.1) that  $\text{Re}g(E+i0) > 0$  for  $E > \mu$ . Hence the only possible common point is  $g(\infty)$ . If  $g(\infty)$  is finite  $\Gamma_1$  and  $\Gamma_2$  meet on the  $v$ -axis. If  $g(\infty)$  is infinite they continue going up. Thus the boundary curve of  $G$  has no double point which proves the univalence of  $g(E)$  in the upper half  $E$ -plane. (Actually, to handle the behavior at infinity properly requires a few more detailed arguments. Those interested should consult Ref. 25).

One may ask what does one gain by going from  $F(E)$  to the univalent function  $g(E)$ ? We give a few examples of the sort of restrictions on the possible behavior of  $g(E)$  which are imposed by some theorems on univalent functions.

For this purpose we introduce the new variable  $z$  defined by



$$z = \frac{E-i\lambda}{E+i\lambda} ; \quad \lambda > 0 \quad . \quad (10.4)$$

This function maps the upper half E-plane onto a unit circular disc,  $|z| < 1$ . We also define, for fixed  $\lambda$ , the function

$$\varphi(z) = \frac{g(E)-g(i\lambda)}{2i\lambda g'(i\lambda)} \quad . \quad (10.5)$$

By construction  $g'(i\lambda)$  is never zero for  $\lambda > 0$ . Thus  $\varphi(z)$  is regular and univalent in the unit disc,  $|z| < 1$ , and its power series has the normalized form

$$\varphi(z) = z + a_2 z^2 + a_3 z^3 + \dots \quad . \quad (10.6)$$

Furthermore, one can easily check that  $\varphi(z)$  is real if and only if  $z$  is real,  $|z| < 1$ . For such univalent functions one can prove that the coefficients  $a_n$  in (10.6) satisfy the inequality

$$|a_n| \leq n \quad ; \quad n = 2, 3, 4, \dots \quad . \quad (10.7)$$

This puts upper bounds on all derivatives of  $g(E)$  at  $E = i\lambda$  which depend only on  $\lambda$  and  $g'(i\lambda)$ . Although it is unlikely that the bounds (10.7) are of direct practical use, they might be useful in some theoretical considerations.

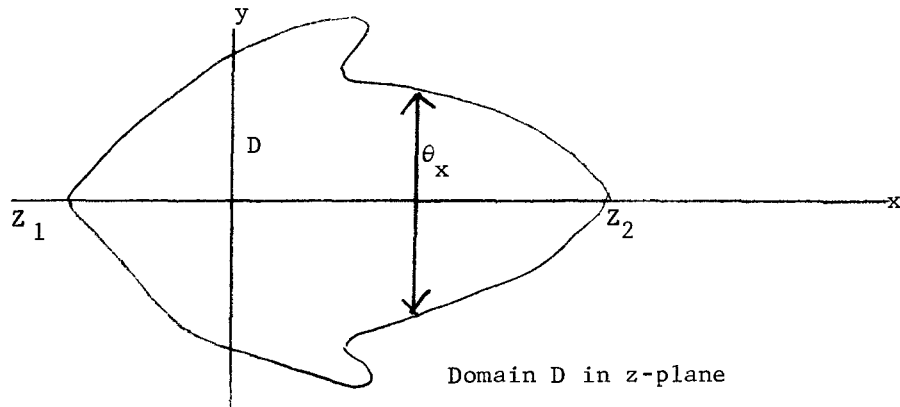
Another possibly more practical inequality follows from a theorem of Koebe. It gives us

$$|\varphi(e^{i\theta})| > \frac{1}{4} \quad , \quad 0 \leq \theta \leq 2\pi \quad . \quad (10.8)$$

#### B. Asymptotic Phase Theorems to $g(E)$

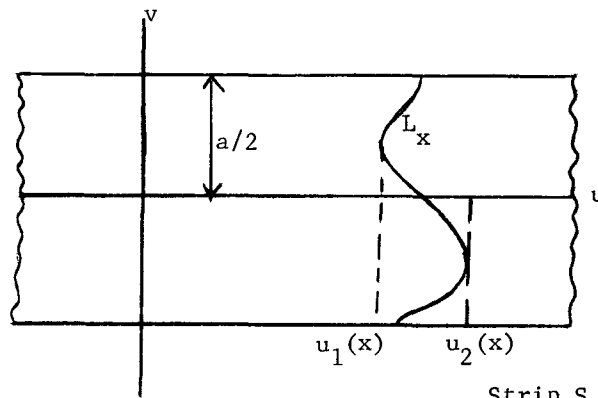
The fact that  $g(E)$  is univalent allows us to use much more powerful inequalities than that of Meiman given in the previous chapter. The main results of Ref. 25 follow from using a theorem due to Ahlfors. We start by stating that theorem.

We consider a simple domain  $D$  in the  $z$ -plane ( $z = x+iy$ ) which is simply connected and symmetric with respect to the  $x$ -axis. Let  $Z_1 = Y_1+iY_1$  and  $Z_2 = X_2+iY_2$  be the points on the boundary curve of  $D$  with the smallest and largest real part, respectively.



For any  $x$ ,  $X_1 < x < X_2$ , the vertical line  $\text{Re} z = x$  will have one or more intersections with  $D$ , each of which bisects  $D$  into two disconnected parts. Under our assumptions on  $D$ , there is one intersection which crosses the  $x$ -axis. This line segment we denote by  $\theta_x$  and its length by  $\theta(x)$  as shown above. The line segment  $\theta_x$  divides  $D$  into two disconnected parts in such a way that  $Z_1$  and  $Z_2$  belong to different parts. We require that  $\theta(x)$  is a continuous function of  $x$  for  $x_1 < x < x_2$  except at some isolated points.

Let  $w = u+iv = w(z)$  be a function which is regular and univalent in  $D$  and maps  $D$  conformally onto a strip  $S$  defined by  $|v| < \frac{1}{2}a$ ,  $a > 0$ , in such a way that  $u(Z_1) \rightarrow -\infty$  and  $u(Z_2) \rightarrow +\infty$



Strip S in  $w$ -plane

In this mapping the line segment  $\theta_x$  will be mapped onto a continuous curve  $L_x$  which connects the two boundary lines  $v = \pm \frac{1}{2}a$ . The largest and smallest values of  $u$  on  $L_x$  are denoted by  $u_2(x)$  and  $u_1(x)$  respectively, as shown above. The theorem of Ahlfors now states that

$$u_1(x_2) - u_2(x_1) \geq a \int_{x_1}^{x_2} \frac{dx}{\theta(x)} - 4a \quad (10.9)$$

holds for any pair  $x_2 > x_1$  such that

$$\int_{x_1}^{x_2} \frac{dx}{\theta(x)} > 2 \quad (10.10)$$

We now use the Ahlfors's theorem to prove the following results.

**Theorem 1:**

If  $g(E)$  for large real  $E$  satisfies

$$\frac{\text{Re} g(E)}{\text{Im} g(E)} \geq \tan \pi \alpha, \quad 0 < \alpha < \frac{1}{2}, \quad (10.11)$$

then  $g(E)$  has the lower bound for  $|E| > E_0$

$$|g(E)| \geq C \left(\frac{E}{E_0}\right)^{2\alpha}, \quad 0 < \alpha < \frac{1}{2}. \quad (10.12)$$

Proof:

We define  $z$  and  $w(z)$  by

$$\begin{aligned} z &= \ln\left(\frac{E}{C}\right) - i\pi/2, \quad C > 0, \\ w(z) &= \ln g(E) - i\pi/2. \end{aligned} \quad (10.13)$$

We apply Ahlfors's theorem to the mapping  $z \rightarrow w$ . The lines  $\text{Re}g/\text{Im}g = \pm \tan\pi\alpha$  correspond to the two straight lines in the  $w$  plane which are parallel to the  $u$ -axis ( $w = u+iv$ ) and separated by the distance  $a = 2\alpha\pi$ . We choose  $D$  to be the domain whose boundary curve consists of two vertical line segments,  $\text{Re}z = x_1 = \ln\left(\frac{E_2}{C}\right)$  and  $\text{Re}z = x_2 = \ln\left(\frac{E_1}{C}\right)$ , and two Jordan curves which are the inverse maps of the two parallel lines in the  $w$ -plane mentioned above, by the inverse transformation  $z = z(w)$ . It is obvious to check in this case that by definition

$$\theta(x) \leq \pi. \quad (10.14)$$

Thus from the Ahlfors's inequality we obtain

$$\begin{aligned} u_1(x_2) - u_2(x_1) &\geq 2\alpha\pi \left(\frac{x_2 - x_1}{\pi} - 4\right) \\ &= 2\alpha \ln \frac{E_2}{E_1} - 8\pi\alpha. \end{aligned} \quad (10.15)$$

From the definition of  $u_1(x_2)$  we know that

$$\ln |g(|E_2|e^{i\varphi})| \geq u_1(x_2), \quad \varepsilon \leq \varphi \leq \pi - \varepsilon. \quad (10.16)$$

If we choose  $\varphi = \pi/2$  we get

$$|g(i|E_2|)| \geq C \left(\frac{E_2}{E_1}\right)^{2\alpha}, \quad (10.17)$$

for  $E_2 \gg E_1$ . In Appendix C of Ref. 25 one shows that

$$|g(E)| > \frac{1}{(2)^{\frac{1}{2}}} |\text{Im}g(iE)|, \quad (10.18)$$

for real positive  $E$ . This with (10.17) completes the proof.

Theorem 2:

If  $g(E)$  satisfies

$$\frac{\text{Re}g(E)}{\text{Im}g(E)} \leq \tan\pi\alpha', \quad 0 < \alpha' < \frac{1}{2}, \quad (10.19)$$

for  $E > E_0$  then  $g(E)$  has the upper bound

$$|g(E)| \leq C \left(\frac{E}{E_0}\right)^{2\alpha'} \quad . \quad (10.20)$$

The proof of this theorem is given in Ref. 25 and is very similar to that of Theorem 1 except that one reverses the definitions of  $z$  and  $w(z)$ .

Several other theorems follow from the Ahlfors's inequality and the reader is referred to Ref. 25 for details. We close by mentioning one such result.

If for sufficiently large real  $E$  we have

$$\text{Re}g(E) \leq b, \quad b > 0, \quad (10.21)$$

where  $b$  is a positive constant, then  $g(E)$  has the following upper bound

$$|g(E)| \leq C \ln|E| \quad . \quad (10.22)$$

This essentially means that the total cross-section is bounded by a constant for large energies. Now if, for example,  $\text{Re}F(E)$  is negative for all  $E \geq E_0$  where  $E_0$  is some fixed large energy, then clearly (10.21) will be satisfied for all  $E > E_0$  with  $b = \text{Re}g(E_0)$ . Thus if the forward amplitude is repulsive at high energies as  $E \rightarrow \infty$  then the total cross section cannot go to infinity or more precisely,

$\int \sigma(E')/E' dE'$  does not diverge faster than  $\ln E$  as  $E \rightarrow \infty$ .

$\mu$

## REFERENCES

1. H. Lehmann, *Nuovo Cimento* 10, 578 (1958).
2. A. Martin, *Nuovo Cimento* 42, 930 (1966); *ibid.* 44, 1219 (1966).
3. J. Bros, H. Epstein and V. Glaser, *Nuovo Cimento* 31, 1265 (1964); and *Com. Math. Phys.* 1, 240 (1965).
4. K. Hepp, *Helv. Phys. Acta* 37, 639 (1964).
5. A. Jaffe, *Proceedings of the MIT Conference on Scattering* (1966).
6. M. Froissart, *Phys. Rev.* 123, 1053 (1961).
7. A. Martin, *Phys. Rev.* 129, 1432 (1963).
8. T. Kinoshita, J. Loeffel and A. Martin, *Phys. Rev.* 135, B1464 (1964).
9. Y.S. Jin and A. Martin, *Phys. Rev.* 135, B1375 (1964).
10. A. Martin, *Nuovo Cimento* 29, 993 (1963).
11. E. Leader, *Phys. Letters* 5, 75 (1963).
12. S.W. MacDowell and A. Martin, *Phys. Rev.* 135, B960 (1964).
13. Y.S. Jin and A. Martin, *Phys. Rev.* 135, B1369 (1964).
14. B. Simon, *Phys. Rev.* (to be published)(1969).
15. This argument is due to A. Martin and is given in a footnote in a paper by T. Kinoshita, *Phys. Rev.* 154, 1438 (1967).
16. I. Ya. Pomeranchuk, *Soviet Phys. JETP* 7, 499 (1958).
17. S. Weinberg, *Phys. Rev.* 124, 2049 (1961).
18. D. Amati, M. Fierz and V. Glaser, *Phys. Rev. Letters* 4, 89 (1960).
19. N.N. Meiman, *Soviet Phys. JETP* 16, 1609 (1963).
20. A. Martin, *Nuovo Cimento* 39, 704 (1965).
21. R.J. Eden, *Phys. Rev. Letters* 16, 39 (1966).
22. T. Kinoshita in *Perspectives in Modern Physics*, ed. R.E. Marshak, Interscience Publishers (New York, 1966), pp. 211-223.
23. N.N. Khuri and T. Kinoshita, *Phys. Rev.* 137, B720 (1965).
24. Y.S. Jin and S.W. MacDowell, *Phys. Rev.* 138, B1279 (1965).
25. N.N. Khuri and T. Kinoshita, *Phys. Rev.* 140, B706 (1965).

DYNAMICAL MODELS BASED ON CLASSICAL LIMITS

Lectures by: R. C. Arnold  
Argonne National Laboratory

Notes taken by: Robert Budny



The purpose of this lecture series will be to discuss attempts to explain high energy data using classical intuition augmented by Regge behavior.

### I. GENERAL FEATURES OF TWO BODY INTERACTIONS

Experiments show that, at high energies,  $\frac{d\sigma}{d\cos\theta}$  has a very sharp peak near  $\theta = 0^\circ$ , a smaller peak at  $\theta = 180^\circ$ , and is very low in between. These general features do not change as  $s$  varies. We will not consider the backward peak until later since the backward peak can be obtained by generalizing forward peak results. These features will have important implication for the models we will discuss.

Partial wave analysis of the amplitude gives

$$A(s,t) = \sum (2\ell+1) f_\ell(s) P_\ell(\cos\theta) \quad (1.1)$$

which can be normalized so  $\frac{d\sigma}{dt} = \frac{1}{4k^2} |A|^2$ . Unitarity at low energies gives

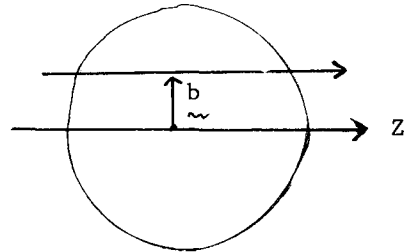
$$f_\ell(s) = \frac{e^{2i\delta_\ell(s)} - 1}{2ik}, \quad \text{where } \delta \text{ would be real.}$$

The observation that  $\frac{d\sigma}{dt}$  is very small between the forward and backward peaks indicates that many partial waves contribute to (1.1) so it is plausible to replace the sum over  $\ell$  with an integral. Near the forward direction and  $\ell$  large,  $P_\ell(\cos\theta) \approx J_0(\ell\theta)$ . Define  $b \equiv \frac{\ell}{k}$  = the impact parameter. Since  $(-t)^{\frac{1}{2}} \approx k\theta$ , (1.1) becomes

$$A = i \int_0^\infty b db J_0(b(-t)^{\frac{1}{2}}) f(s,b) \quad (1.2)$$

The integral can be extended to  $\ell = 0$  since low  $\ell$  waves do not appear important. If  $f(s,b)$  is approximately factorizable then the shape of the forward peak is independent of  $s$ , as is observed. In some cases the peak shrinks as  $s$  increases, but we will assume that this is not crucial.

Several aspects of (1.2) should be noted. The arguments used to motivate it from (1.1) are heuristic. However, (1.2) can be used as an exact representation of  $A$  in impact parameter space. In the case of spinning particles, (1.2) can be easily generalized by making  $b$  a 2 dimensional vector  $\perp$  to the incident momentum (see Fig. 1). Then an integral representation for  $J_0$  gives



Center-of-mass System coordinates

Fig. 1



$$A(s,t) = \int d^2 \underline{b} e^{i \underline{q} \cdot \underline{b}} F(s, \underline{b}) \quad (1.3)$$

which is the 2 dimensional Fourier transformation. For spinless particles,  $F$  depends only on  $s$  and  $|\underline{b}|$ . The representations (1.2) and (1.3) are very useful when  $s$  is large,  $t$  is small, and the radius of the interaction region large. In the resonance region where  $s$  is small, these representations could be used, but would be very complicated. When  $s$  is large,  $t$  is approximately the transverse momentum transferred and  $|\underline{q}|^2 \approx -t$ . The deBroglie wave packet spread is proportional to  $\frac{1}{k}$  so at high  $s$  the wave packet feels only a small part of the scatter at a time.  $b_{\max}$  is of the order of the  $\pi$  Compton wavelength. We might expect classical physics to be useful for constructing models when the wave packet size is much smaller than  $b_{\max}$ .

The problem now is to find  $f(s,b)$ . The concept of a potential is very useful in classical physics so let us try to use it to generate  $f(s,b)$ . One aspect of this concept which will be useful to us is the additivity of potentials. Sometimes the potential of a composite system is the sum of the potentials of each constituent, e.g., nuclear scattering or the quark model. We will use potentials which are instantaneous in time and depend on spatial parameters.

Suppose we are given a potential. How can we use it? 1) Schrödinger's equation is not relativistically invariant. Since we are interested in velocities close to  $c$ , we must be cautious. 2) Covariant equations lead to retardation difficulties. 3) The last possibility is to use the potential as an effective potential, i.e., like a single scattering term. If we know the outgoing and incoming wave function, we know the scattering matrix. The equation of motion is equivalent to a definition of the potential.

Consider one dimensional motion through a slowly varying potential<sup>1</sup>:

$$H\psi = i \frac{\partial}{\partial t} \psi = (P^2 + V)\psi, \quad P = -i \frac{\partial}{\partial x} \quad (1.4)$$

is Schrödinger's equation where  $2m = \hbar = 1$ . We expect the incoming wave to be modified by a phase change and absorption. The boundary condition is  $\psi \rightarrow e^{-i(kx - \omega t)}$  as  $x \rightarrow \infty$  so it is reasonable to try  $\psi(x,t) = e^{-iW(x,t)}$ . This gives

$$\frac{\partial W}{\partial t} = i \frac{\partial^2 W}{\partial x^2} + \left(\frac{\partial W}{\partial x}\right)^2 + V \quad (1.5)$$

The trial solution  $W = \alpha \int_{-\infty}^x dx' V(x') - kx + \omega t$  where  $\alpha, \omega$  are undetermined parameters gives

$$\omega = i\alpha \frac{dV}{dx} + (\alpha V(x) - k)^2 + V \quad (1.6)$$

We want to satisfy this for any  $V(x)$  so the choice  $\omega = k^2$  and  $\alpha = \frac{1}{2k}$  leaves

$$0 = \frac{i}{2k} \frac{dV}{dx} + \frac{1}{(2k)^2} V^2$$

where  $k \gg V$ ,  $\frac{dV}{dx}$  this is satisfied. This the eikonal approximation.

The eikonal wavefunction is

$$\psi = \exp \left[ -\frac{i}{2k} \int_{-\infty}^x dx' V(x') + i(kx - \omega t) \right] . \quad (1.7)$$

This is essentially the WKB approximation in one dimension. In three dimensions the eikonal wavefunction is given by

$$\psi(\underline{b}, \underline{x}) = \exp \left[ -\frac{i}{2k} \int_{-\infty}^{\underline{x}} dx' V(\underline{b}, x') + i(kx - \omega t) \right] \quad (1.8)$$

assuming that there is negligible transverse deflection of the incident particle, i.e., that  $\theta \approx 0$ .

The transition matrix element from state  $\underline{k}$  to state  $\underline{k}'$  is

$$T(\underline{k}', \underline{k}) = i \int d^3x V(x) \psi_{\underline{k}}^{\text{out}}(x) e^{i\underline{k}' \cdot \underline{x}} . \quad (1.9)$$

Choose a coordinate system with  $\underline{k}$  along the  $z$  axis. Define  $\underline{q} = (k_x' - k_x, k_y' - k_y)$ . Substitute (1.7) for  $\psi_{\underline{k}}^{\text{out}}(x)$  in (1.9) and compare with (1.3). Note  $k_z' \approx k_z$  so  $e^{i(k_z' - k_z)z} \approx 1$ . This gives

$$F(\underline{s}, \underline{b}) = \int_{-\infty}^{\infty} V(\underline{b}, z) dz \exp \left[ -\frac{i}{2k} \int_{-\infty}^z dz' V(\underline{b}, z') \right] . \quad (1.10)$$

(See Ref. 1). The  $s$  dependence is in  $V(\underline{b}, z)$ . A similar result can be obtained from the Bethe-Salpeter equation. The integral in (1.10) is of the form

$\int_a^b dx f'(z) e^{f(z)} = e^{f(b)} - e^{f(a)}$ . Thus

$$F(\underline{s}, \underline{b}) = 1 - \exp \left[ -\frac{i}{2k} \int_{-\infty}^{\infty} V(\underline{b}, z) dz \right] \equiv 1 - e^{i\chi(\underline{s}, \underline{b})} \quad (1.11)$$

with

$$\chi(\underline{s}, \underline{b}) = -\frac{i}{2k} \int_{-\infty}^{\infty} V(\underline{b}, z) dz . \quad (1.12)$$

Note that the assumption of a straight line trajectory is essential in getting (1.11).

Equations (1.11) and (1.12) constitute the eikonal approximation to the amplitude.

This is comparable to the partial wave expansion (1.1) with  $\chi(\underline{s}, \underline{b}) = 2\delta_{\underline{l}=\underline{k}\underline{b}}(\underline{s})$ ;

$$T_{\text{eikonal}} = \int d^2 \underline{b} e^{i \underline{q} \cdot \underline{b}} (1 - e^{i \chi}) \quad . \quad (1.13)$$

The essence of the eikonal approximation is that the phase shift is a homogeneous linear functional of the potential (Ref. 2).

We would like to describe the eikonal approximation without using the Schrödinger equation. Defining a "Born approximation" allows us to do this. If  $V$  is small then

$$T = T_{\text{Born}} = \int d^2 \underline{b} e^{i \underline{q} \cdot \underline{b}} (1 - e^{i \chi}) \quad (1.14)$$

which can be inverted, since  $\chi$  is small, to give

$$\chi = \int d^2 \underline{q} e^{i \underline{q} \cdot \underline{b}} T_{\text{Born}}(\underline{q}) \quad . \quad (1.15)$$

(see Ref. 2)

Equation (1.15) and  $F = 1 - e^{i \chi}$  can be used as a starting point for the eikonal approximation. Incidentally, these are true in the optical model. This allows us to use  $T_{\text{Born}}$  in the sense of a relativistic single scattering term at high energies. The eikonal approximation shows how to iterate such a term to get the complete amplitude.

We need a model for  $T_{\text{Born}}$  on the mass shell. Note that the connection of  $\chi$  with  $T_{\text{Born}}$  is trivial if we assume  $\chi$  small. We extend the small  $\chi$  functional form to large  $\chi$ . How do we know that calculating higher terms in  $\chi$  (multiple scattering corrections) gives reasonable results? The approach works in molecular and nuclear physics so let's be optimistic and try. The goal is to find a  $T_{\text{Born}}$  that will explain many features of data simply.

## II. SCATTERING BY COMPOSITE SYSTEMS<sup>3-6</sup>

Consider the scattering of an elementary particle by a composite system A. (Fig. 2) We will assume that there is an additive 2 body potential between the projectile and each constituent. We also assume no recoil or motion of the constituents during the collision. Then  $V_A(b, z) = \sum_j V_j(b - b_j, z - z_j)$  where the  $E$  dependence is suppressed. The additivity of the potential implies that the phase shifts are additive so

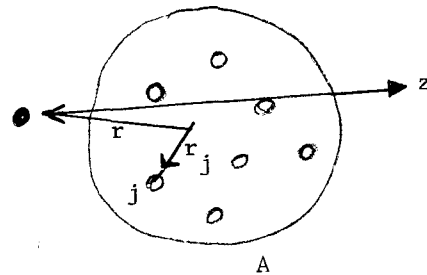


Fig. 2

$$\chi_A(\underline{b}) = \frac{i}{2k} \int_{-\infty}^{\infty} v_A(\underline{b}, z) dz = \sum_j \chi_j(\underline{b}-\underline{b}_j) \quad (2.1)$$

The potential concept was used to motivate the additivity of the phase shifts.

For a quantum description of target, use nuclear wave function

$$\begin{aligned} |\psi_1(r_1 \dots r_n)\rangle &= \text{initial state} \\ |\psi_2(r_1 \dots r_n)\rangle &= \text{final state} \end{aligned}$$

The transition amplitude is

$$T_{12} = \langle 2 | T(\underline{b}, \underline{b}_1 \dots \underline{b}_n) | 1 \rangle = \int \psi_2^*(r_1 \dots r_n) T(\underline{b}; \underline{b}_1 \dots \underline{b}_n) \psi_1(r_1 \dots r_n) d^3 r_1 \dots d^3 r_n \quad (2.2)$$

where  $\underline{r}_j = (\underline{b}_j, z_j)$ . For elastic scattering  $\psi_1 = \psi_2$  so (2.2) becomes

$$T_{11}(\underline{b}) = \int \rho(r_1 \dots r_n) T(\underline{b}; \underline{b}_1 \dots \underline{b}_n) d^3 r_1 \dots d^3 r_n \quad (2.3)$$

with  $\rho = |\psi|^2$ . The integration weighs each specific configuration with its probability.

In Glauber's theory of multiple scattering one defines "profile functions"

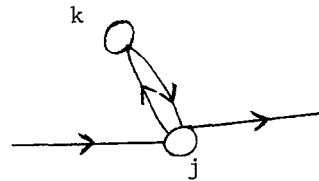
$$\Gamma_A \equiv 1 - e^{i\chi_A}, \quad \Gamma_j \equiv 1 - e^{i\chi_j(\underline{b}-\underline{b}_j)}$$

which implies

$$1 - \Gamma_A = \prod_j (1 - \Gamma_j) \quad \text{or} \quad \Gamma_A = \sum_j \Gamma_j - \sum_{\substack{i,j \\ (i \neq j)}} \Gamma_i \Gamma_j + \dots \quad (2.4)$$

with N summations. This is a multiple scattering series. The first term is linear in scattering from each constituent and is called the impulse term since it gives the impulse approximation. The second

term corresponds to two scatterings. Our approximation that the scattering is mainly forward means that the projectile is unlikely to be scattered twice by the same constituent as in Fig. 3.



As an example consider the elastic scattering of a  $\pi$  on deuterium.<sup>1</sup>

Fig. 3

$$T_D(b) = \int d^3r \left\{ \Gamma_p(b-b_1) + \Gamma_n(b-b_2) - \Gamma_p(b-b_1)\Gamma_n(b-b_2) \right\} \rho(r)$$

$$\underline{r} = (b_1, z) \quad |\psi|^2 = \rho \sim e^{-\alpha^2 r^2} = e^{-\alpha^2 (b_1^2 + z^2)}$$

$$\left(\frac{d\sigma}{dt}\right)_{p,n} \sim e^{t/4\beta^2} \quad (2.5)$$

assumed for scattering the  $\pi$  on free protons and neutrons implies that in the eikonal approximation  $\Gamma_{p,n} \sim ce^{-\beta^2 b^2}$ . The single scattering terms give

$$\int d^3r \rho(r) \Gamma(b-b_1) = ce^{-(\alpha^2 + \beta^2) b^2} \quad (2.6)$$

and the double scattering term gives

$$\int d^3r \rho(r) \Gamma(b-b_1) \Gamma(b+b_1) = c^2 e^{-(\alpha^2 + 2\beta^2) b^2} \quad (2.7)$$

The Fourier transform from impact parameter space to momentum transfer space gives

$$T(t) = ic \left\{ \exp \left[ \frac{t}{4(\alpha^2 + \beta^2)} \right] - c \exp \left[ \frac{t}{4(\alpha^2 + 2\beta^2)} \right] \right\} \quad (2.8)$$

$\frac{d\sigma}{dt}$  is proportional to the square of  $T(t)$  and has the features shown in Fig. 4. In general  $\frac{d\sigma}{dt}$  has  $N$  slopes when there are  $N$  constituents. As  $N \rightarrow \infty$  the curve becomes a Bessel function as in Fig. 5. This effect is observed in heavy nuclei.<sup>7-9</sup>

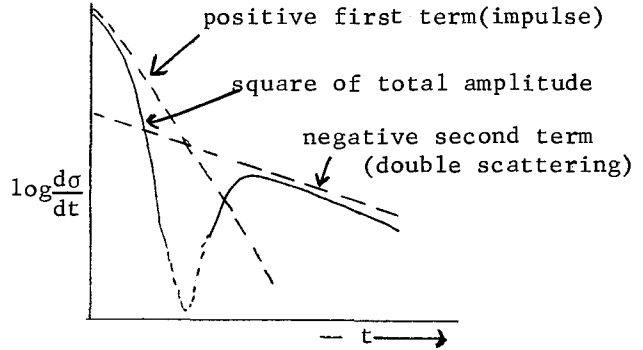


Fig. 4

Now we will relate the eikonal approximation to the droplet model<sup>10-12</sup> by making the number of constituents in our composite model  $N \rightarrow \infty$ . Assume all the constituents have the same wave function, for instance they could be in harmonic oscillator wave functions. Define  $S$  by  $T(b; b_1 \dots b_n) = 1 - S(b; b_1 \dots b_n)$ . Assuming the scattering is independent gives  $S = \prod_j S_j(b-b_j)$  where  $S_j(x) = 1 - \Gamma_j(x) = e^{iX_j(x)}$ . Calling  $\rho_j(r) = \phi_j^*(r)\phi_j(r)$ , using the factorization properties of  $\phi$  and  $S$ , and normalizing with  $\langle 2|1 \rangle = 1$

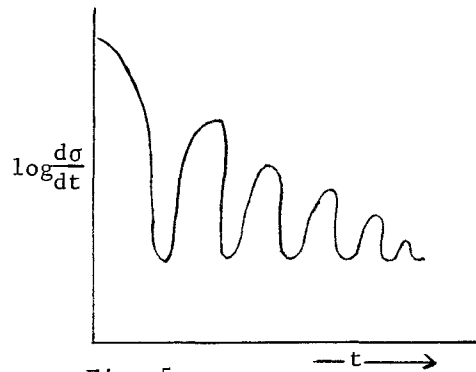


Fig. 5

in (2.2) gives

$$T(b) = 1 - \prod_{j=1}^n \int d^3 r_j \rho_j(r_j) e^{iX(b-b_j)} = 1 - [S_0(b)]^N \quad (2.9)$$

where

$$S_0(b) = \int d^3 r \rho(r) e^{iX(b-b_r)} = 1 - \Gamma_0(b) \quad (2.10)$$

$\Gamma_0(b)$  is the T matrix for one constituent. Then

$$T(b) = 1 - [1 - \Gamma_0(b)]^N \quad (2.11)$$

We want to get a simple result as  $N \rightarrow \infty$ . If we hold the cross section of the composite system constant, then the cross section of each constituent must decrease. A canonical assumption is

$$\Gamma_0(b) = \frac{1}{N} \gamma(b).$$

This gives

$$T(b) = 1 - \left[ 1 - \frac{\gamma(b)}{N} \right]^N \xrightarrow{N \rightarrow \infty} 1 - e^{-\gamma(b)} \quad (2.12)$$

Now consider the short range approximation. The term  $e^{iX(b-b_1)}$  in (2.10) acts as a delta function of  $b-b_r$ . Define

$$D(b) = \int_{-\infty}^{\infty} \rho(b, z) dz \quad (2.13)$$

Then  $\Gamma_0(b) = \frac{\gamma(0)}{N} D(b)$  gives

$$T(b) = 1 - e^{-\gamma(0)D(b)} \quad (2.13)$$

The number  $\gamma(0)$  is given by experiment.  $D(b)$  is independent of the projectile in this approximation. When the projectile is complex the same result holds. As an example, in optics  $\gamma(0)$  is the opacity and  $D(b)$  corresponds to the optical depth. Another example is  $\pi N$  scattering where  $D(b)$  has the shape given in Fig. 6.  $D(b)$  is the distribution of the proton with "R" representing its size. A third example is scattering from a nucleus.<sup>7-9</sup>  $D(b)$  is given by Fig. 7.

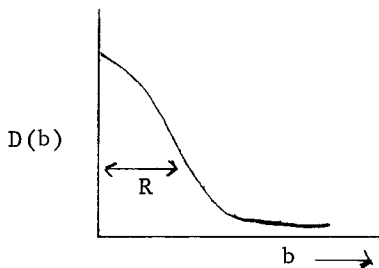


Fig. 6

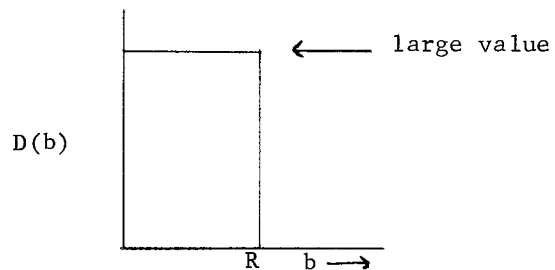


Fig. 7

$$1 - e^{-\gamma(0)D(b)} = \begin{cases} 1 & b < R \\ 0 & b > R \end{cases} \quad (2.14)$$

which gives (from (1.2) and (1.11)),

$$\begin{aligned} T(t) &= i \int_0^{\infty} b db J_0(b(-t)^{\frac{1}{2}}) [1 - e^{-\gamma(0)D(b)}] \\ &= i \int_0^R b db J_0(b(-t)^{\frac{1}{2}}) = \frac{iR^2 J_1(R(-t)^{\frac{1}{2}})}{R(-t)^{\frac{1}{2}}} \equiv iR^2 F(t) \end{aligned} \quad (2.15)$$

$F(t)$  is plotted in Fig. 8.  $T$  gives the diffraction pattern of black spheres. When  $\gamma$  is purely real it gives an imaginary  $T$ .  $\gamma$  can be made complex to give the correct phase for (say)  $\pi N$  scattering. Then (2.15) predicts  $T$  for  $\pi A$  scattering where  $N$  is a nucleon and  $A$  a nucleus. Fits to high energy  $\pi p$  and  $pp$  elastic scattering using as free parameters  $Re\gamma$  and  $Im\gamma$ , and assuming<sup>10,11</sup> that  $D$  is given by electromagnetic form factors, agree to about 10% when  $-t < 1 \text{ GeV}^2$ , as sketched in Fig. 9. In practice  $Im\gamma$  can be neglected. Note

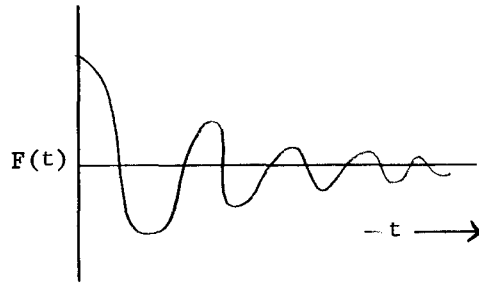


Fig. 8

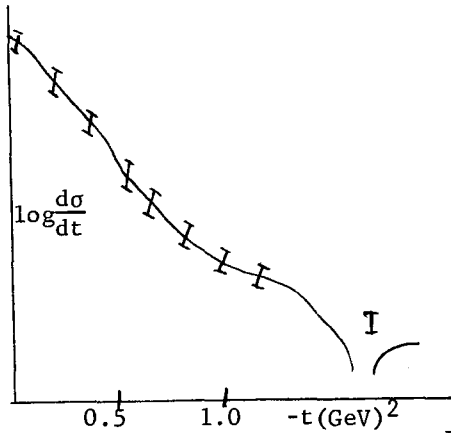


Fig. 9

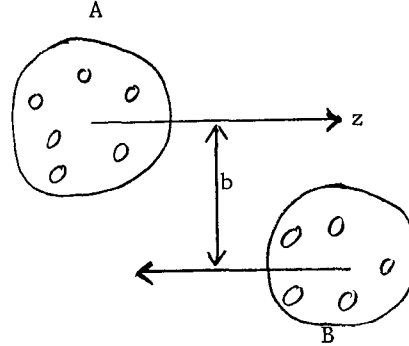


Fig. 10

that this model is inconsistent with moving Pomeron models since there is no shrinkage. The model gives  $\sigma_{\text{tot}} = 2\sigma_{\text{el}} = 2R^2$ , for the nuclear case (2.15).

Now we will generalize to the scattering of two composite systems A, B. See Fig. 10. The separation of the center of masses at collision is  $b$ .

$$T_{\alpha}(b_{\alpha}) = \int d^3 r_1 \dots d^3 r_N \langle B, 2 | T(b_{\alpha}; b_1 \dots b_N) | B, 1 \rangle, \quad (2.16)$$

where  $\alpha$  is a constituent in the projectile, A. This can be summed over  $\alpha$  to give

$$T_{AB}(b) = \int d^3 r_{1A}' \dots d^3 r_{N_A}' \langle A, 2 | \left[ 1 - \prod_{\alpha} (1 - T_{\alpha}(b-b_{\alpha}')) \right] | A, 1 \rangle . \quad (2.17)$$

For elastic scattering this becomes

$$T_{AB}^{el}(b) = 1 - \prod_{\alpha=1}^{N_A} \int d^3 r_{1A} \rho_A(r_1) e^{i\chi_B(b-b_{r_1})} \quad (2.18)$$

where  $i\chi_B \equiv i\chi_{(\text{constituent } +B \rightarrow \text{constituent } +B)} = -\alpha(0)D(b)$ . In the short range approximation as  $N_A, N_B \rightarrow \infty$  we find

$$T_{AB}^{el}(b) = 1 - \left[ \int d^3 r_{1A} \rho_A(r_1) e^{i\chi_B(b-b_{r_1})} \right]^{N_A} \rightarrow 1 - e^{i\chi_{AB}(b)} \quad (2.19)$$

with

$$\chi_{AB}(b) = i\gamma(0) \int d\underline{b}' D_A(\underline{b}' - \underline{b}) D_B(\underline{b}') . \quad (2.20)$$

This is a convolution of the distributions. When  $\gamma$  is constant this is the "coherent droplet model" of Chou and Yang.<sup>3</sup> The qualitative features of (2.18) and (2.19) hold even if  $N \neq \infty$ .  $D_A(b)$  and  $D_B(b)$  can be successfully (for  $\pi N$  and  $NN$  scattering) estimated by electromagnetic form factors. This approach can be applied to inelastic scattering with  $D_A(b)$  interpreted as an operator<sup>5</sup> that rearranges the distribution of  $A$ . What is needed are excitation form factors, e.g.,  $\gamma N \rightarrow N^*$ .

The qualitative features of a multiple scattering series can be seen using a Gaussian for  $\chi(b) = ice^{-b^2/2R^2}$  which can be justified from Regge theory (where  $R$  depends on  $s$ ), from statistical mechanics, or pragmatically. It gives

$$T(t) = iR^2 \left\{ ce^{tR^2/2} - \frac{c^2}{22!} e^{tR^2/4} + \dots - \frac{(-c)^n}{nn!} e^{tR^2/2n} + \dots \right\} . \quad (2.21)$$

When  $-t$  is small the series damps rapidly; however, for large  $-t$  higher order terms in the interaction strength  $c$  are important. The number of terms that are important is proportional to  $|t|$ . See Fig. 11. When  $-t$  is very large the saddle point from the method of least descent gives the envelope  $e^{-(R(-t)^{1/2})}$  for  $T$ . This is the Jaffe bound.

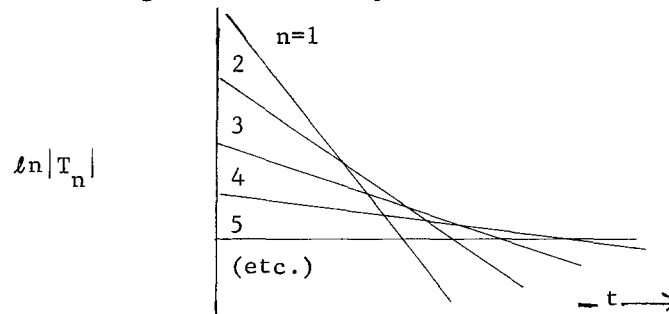


Fig. 11



### III. ABSORPTIVE FORMULA

We want to lead up to including Regge poles. Suppose  $V_{\text{effective}} = V_0 + V_1$  where  $V_1$  is weak and  $V_0$  has a simple or known form. For instance  $V_0$  could come from the Pomeron and  $V_1$  from the charge exchange or isospin dependent part. We have  $X(b) = X_0(b) + X_1(b)$  where  $X_1 \ll 1$  for all important  $b$ . In charge exchange this is satisfied when the energy is sufficiently high. Then

$$T(b) = 1 - e^{iX} \approx 1 - e^{iX_0(1+iX_1)} = (1 - e^{iX_0}) - ie^{iX_0} X_1 \quad (3.1)$$

Following (1.2) and (1.11), define

$$T_0(t) = i \int b db J_0(b(-t)^{\frac{1}{2}}) [1 - e^{iX_0(b)}] \quad (3.2)$$

$$T_1(t) = T - T_0 = \int b db J_0(b(-t)^{\frac{1}{2}}) e^{iX_0(b)} X_1(b) \quad (3.3)$$

Equations (3.2) and (3.3) are known as the absorption formula, also called the Sopkovich-Jackson-Gottfried absorption formula, or the distorted wave Born approximation because the factor  $e^{iX_0(b)}$  distorts the usual Born formula. If  $T_0(t)$  is known from the high energy limit of data, then we can invert  $T_0(b)$  to get  $e^{iX_0(b)}$ . The data on  $T_1(t)$  gives  $X_1(b)$  since  $T_1(t)$  is linear in  $X_1(b)$ .

As an illustration consider the black disk approximation in a nucleus. Figure 12 shows an example of what can occur in impact parameter space.  $T_1(t)$  has the lower partial waves absorbed by the  $e^{iX_0(b)}$  factor. Figure 13 shows what this gives in  $t$  space. The  $J_0$  and  $J_1$  contributions are out of phase. This phenomena is clearly seen in nuclei.

We could get  $X_1(b)$  from one particle exchange with amplitude  $\frac{g^2}{\mu^2 - t}$ . It is known that the absorption formulas describe modifications due to elastic scattering in the initial and final states. See Fig. 14. The formalism discussed above applied to inelastic processes like  $\pi^0 p \rightarrow \pi^+ n$ . We would like to extend it to processes like  $\pi^- p \rightarrow \omega n$  which is not really charge exchange unless we invoke SU(6) to equate the  $\pi$  and  $\omega$ . This is not totally satisfactory. Another

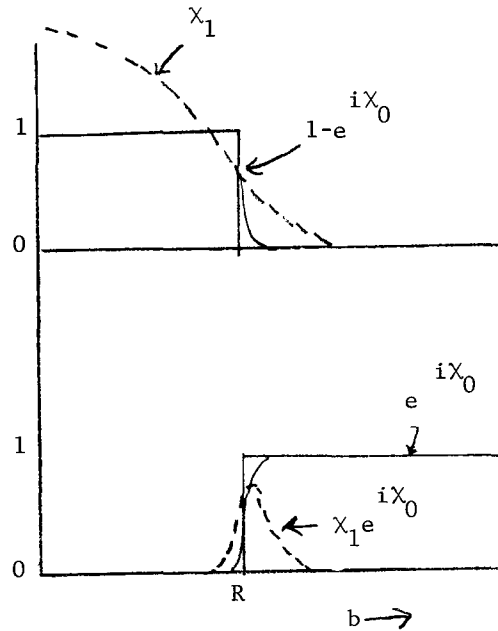


Fig. 12

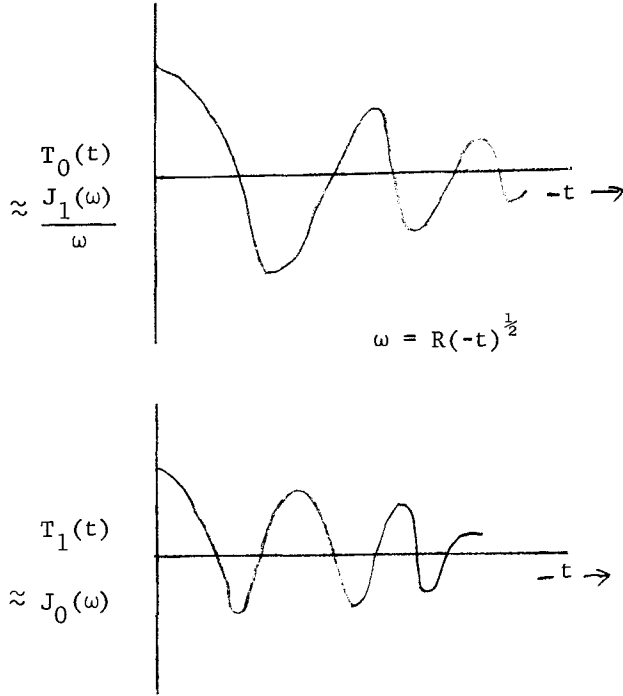


Fig. 13

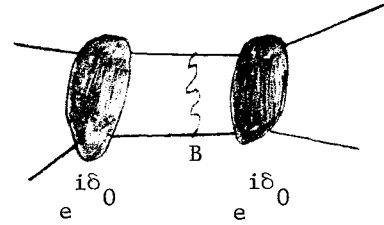


Fig. 14

justification of the application of the formalism to this reaction comes from studying the multichannel version of the problem.<sup>2</sup> Let channel 1 be  $\pi p$  and channel 2 be  $\omega n$ . Then we can associate different potentials for different channels.

$$\begin{aligned}
 T_{11}(\pi p \rightarrow \pi p) &: V_{11} \\
 T_{22}(\omega n \rightarrow \omega n) &: V_{22} \\
 T_{12}(\pi p \rightarrow \omega n) &: V_{12} .
 \end{aligned} \tag{3.4}$$

Then

$$T(t) = \begin{pmatrix} T_{11} & T_{12} \\ T_{21} & T_{22} \end{pmatrix} = i \int b db J_0(b(-t)^{\frac{1}{2}}) e^{\left\{ I - \exp[i\tilde{\chi}(b)] \right\}} \tag{3.5}$$

with  $\tilde{\chi} = \tilde{\chi}_0 + \tilde{\chi}_1$ ,  $\tilde{\chi}_0$  diagonal and  $\tilde{\chi}_1$  off diagonal,  $\ll I$ . If we ignore non-commutativity of  $e^{i\tilde{\chi}_0(b)}$  and  $i\tilde{\chi}_1(b)$ , we get

$$\tilde{T}_1(t) = \int b db J_0(b(-t)^{\frac{1}{2}}) e^{i\tilde{\chi}_0(b)} \tilde{\chi}_1(b) . \tag{3.6}$$

Usually it is assumed that  $V_{11} = V_{22}$  so  $\tilde{\chi}_0 = I\tilde{\chi}_0$  avoids the commutation problem.

#### IV. EFFECTIVE POTENTIAL AND OPTICAL MODEL

The formula

$$T(t) = i \int b db J_0(b(-t)^{\frac{1}{2}}) [1 - e^{i\chi(b)}] \quad (4.1)$$

was derived by considering the matrix element for the scattering of an elementary projectile by a composite target.

$$e^{i\chi} = \langle 0 | e^{i \sum_j \chi_j^{elem}} | 0 \rangle \quad (4.2)$$

We then assumed  $\chi_j^{elem}$  is independent of  $s$  and  $t$ , i.e.,  $g_i \delta(b-b_1)$ , and built up a theory of effective two body potentials for composite-composite scattering. The effective potential has a very simple constituent-constituent scattering "ancestor" even though it could appear very complicated.

So far the use of potentials was only for motivation. There are other methods of obtaining the eikonal formula. Later we will discuss a field theory with heavy vector meson exchange which gives the formula. Note that the potential description often resembles elastic unitarity so the Schrödinger equation is usually interpreted as keeping only elastic intermediate states. In composite theories rearrangements are important and are equivalent to inelasticity which in fact dominates. The nuclear optical potential in Glauber theory has much physical content in common with multiperipheral models. Unitarity gives

$$\text{Im}A = \sum \int |T_{pp \rightarrow n}|^2 d\Omega_n .$$

In the multiperipheral model  $T_{pp \rightarrow n}$  is the amplitude shown in Fig. 15. The sum over lots of intermediate states can give a Pomeron-like object, i.e.,  $A(s, t \approx 0) \sim is^{\alpha(t)}$  with  $\alpha(t) \approx 1 + \epsilon t$ . The scattering is dominated by inelastic intermediate states.

In alternate models like Huang's incoherent droplet model<sup>13</sup> hadrons are considered arrangement of bits. Another arrangement of  $p$  gives  $p+6\pi$ .  $N$  depends on kinetic energy so this model is a theory of interaction, not just the states of a  $p$  alone. During a collision the bits mix randomly. To determine the probability of a final state we just count the number of rearrangements giving the state. If something like this is true,

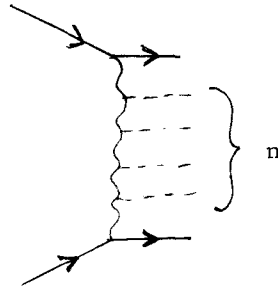


Fig. 15

then following Glauber,  $e^{iX}|0\rangle$  in (4.2) can be interpreted as a rearrangement of some of the constituents. Projecting this on  $\langle 0|$  gives the elastic matrix element, however, many inelastic intermediate states contribute.  $e^{iX}|0\rangle$  has a small overlap with  $\langle 0|$  for small impact parameters. In Fig. 15 the initial state has the role of  $\langle 0|$ . Both approaches in their simplest versions leave out the process in Fig. 16. Later we will look at this comparison again when discussing Regge cuts.

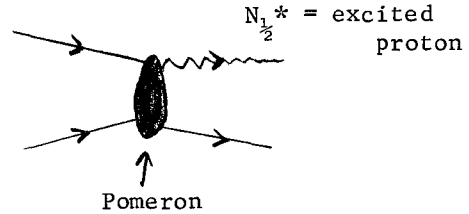


Fig. 16

Another way to study the potential is to add production processes to non-relativistic potentials.<sup>2</sup> This can be done with the multichannel considerations discussed previously. Denote 2-body channels by  $j$ . Then

$$(\nabla^2 + k^2)\psi_1 = \sum_j V_{1j}\psi_j \quad (4.3)$$

where the momenta are assumed to be the same in each channel. In Ref. 2 it is shown that we can find an effective potential that includes multichannel effects. In general it is nonlocal. The idea of the proof is to construct Green's function for the other channels  $2, \dots, n$  resulting in

$$V^{\text{eff}}(x', x) = \sum_{m,n} V_{1m}(x') G_{m \rightarrow n}(x', x) V_{n1}(x) + V_{11}(x) \delta(x' - x) \quad (4.4)$$

such that

$$(\nabla^2 + k^2)\psi_1 = \int V^{\text{eff}}(x', x) \psi_1(x') dx' \quad (4.5)$$

As the energy increases, we hope that (4.5) approaches  $V(x)$  effective-local  $\psi_1(x)$ .

Recently there has been much interest in field theoretic approaches to the eikonal model.<sup>14-20</sup> The goal is to derive  $X$  from a model field theory where  $S = \exp(iX)$  and  $X$  is the Born approximation. The most ambitious attempt is that of H. Cheng and T.T. Wu<sup>18</sup> in electromagnetism. Torgerson's approach<sup>14</sup> is to start with the interaction Lagrangian  $L_{\text{int}} = g\psi\gamma^\mu\psi V_\mu$  to couple spin  $\frac{1}{2}$  to neutral spin 1 particles. Elastic scattering of two fermions is then

$$\langle \text{final} | S | \text{initial} \rangle = \langle f | \text{Texp} \int d^4x L_{\text{int}} | i \rangle \quad (4.6)$$

which cannot be solved in general. We want the high  $s$  limit which supposedly is a classical limit so we neglect self energy diagrams (the fermion sees only its local region). Then the only diagrams remaining are those where each vector is emitted

and absorbed by a fermion. Glauber solved (4.6) within these assumptions in 1951, getting

$$\langle S \rangle = \langle \exp \left[ g^2 \int \Delta(x'-x) \right] \rangle \quad (4.7)$$

where  $\Delta$  is the Born term corresponding to one vector exchange. The assumptions imply that time ordering is not needed and that the emission and absorptions are independent.

### V. REGGE EXCHANGE

Consider a one particle exchange approximation to the amplitude,  $A \approx \frac{g^2}{\mu^2 - t}$  (See Fig. 17). In configuration space this corresponds to a Yukawa potential, i.e., in the s channel we see a potential. In the

t channel this looks like a resonance or bound state which shows a peak in the cross section at its mass. Since A does not depend on  $\cos\theta_t$  it is an s-wave resonance in the t channel. The Chew-Frautschi plots have many resonances. We want to include a whole family in a Born term like  $\frac{g^2}{\mu^2 - t}$ .

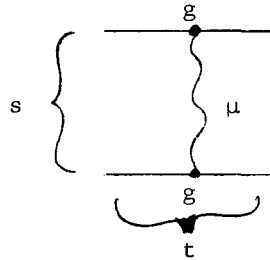


Fig. 17

To do this we use the Regge theory

formalism (ignoring signature, spin, and the possibility of cuts and fixed poles for now) to get  $\beta(t)s^{\alpha(t)}$  for the amplitude at large s and fixed t. This is the Born approximation to the potential due to the exchange of the family. If  $\beta(t)$  is slowly varying then we get  $e^{a+bt}$  for the amplitude where  $b = \tilde{b} \ln s$  and  $\tilde{b} = \text{constant}$ .

This approach gives selection rules on the particle quantum numbers. For instance, consider  $\pi^- p \rightarrow \pi^0 n$ . In the t channel the exchanged object must have isospin 1 so

$$\left. \frac{d\sigma}{dt} \right|_{t \approx 0} \sim \left. \frac{1}{s} \right|_s \left| \alpha(0) \right|^2 = \frac{2\alpha(0) - 2}{s} \quad (5.1)$$

The relevant trajectory is that of the  $\rho$  with  $\alpha(0) \approx \frac{1}{2}$ . Thus the effective spin of the exchanged object is  $\frac{1}{2}$ . This fits the data very well whereas one particle exchange does not.

If  $\alpha_p(0) = 1$  then the amount of shrinkage of  $\frac{d\sigma}{dt}$  as s increases indicates the slope of the P trajectory on the Chew-Frautschi plot. Sometimes there is shrinkage and sometimes there is none, suggesting that the trajectory may be flat. This is supported by the lack of evidence for mesons on such a trajectory. These facts suggest that the Pomeron is not a Regge pole and should be treated separately. We will look for a classical description of it.

## VI. HYBRID MODEL OR ABSORPTION MODEL<sup>21</sup>

In this model the Pomeron singularity is assumed to come from the droplet model and to be different from ordinary Regge poles. The potential is a sum of a droplet model term and Regge terms. The droplet model implies that the Pomeron is a fixed pole. If we assume that the droplet model holds literally at positive  $t$  then it violates analyticity and unitarity. This can be rectified by a cut which masks the Pomeron pole in the  $t > 0$  region of the Chew-Frautschi plot. We will not worry about this since we will apply the model only when  $t < 0$ . Note that we are not taking the radical Regge theory where all the singularities in the physical region of the  $J$  plane are simple moving poles. The Regge picture we will use has the following features: (not applied to elastic scattering)

- 1) No resonances in the  $t$  channel implies no forward peaks in the  $s$  channel (example, since no doubly charged meson resonances have been seen we expect no peaks in  $\pi^+ n \rightarrow \pi^- N^{++}$  which is true experimentally).
- 2) The energy dependence comes from  $\alpha(0)$ . This we find by extrapolation from positive  $m^2$ .
- 3) Shrinkage of the forward peak in charge exchange scattering.

Competing models such as the coherent droplet model do not give the above features since they do not have crossing and thus say nothing about the  $t$  channel. The hybrid model gives the above features.

As an example of a hybrid model calculation consider  $pp \rightarrow pp$  and neglect spin (which is a few percent correction). Suppose there is a Pomeron contribution to the amplitude  $A_P$  and a Regge pole contribution  $A_R$ . Assume that

$$A_P = iC[F_p(t)]^2 \quad (6.1)$$

where  $F_p$  is the electromagnetic form factor of the proton. Any non-magnetic form factor works. A useful fit is

$$F_p(t) \approx \left( \frac{\mu^2}{\mu^2 - t} \right)^2 \quad (6.2)$$

with  $\mu^2 \approx 0.7 \text{ GeV}^2$ .

(6.1) can be motivated by arguing that the interaction between bits is pointlike and the the distribution of bits is proportional to the electromagnetic form factors. We have normalized the amplitude to give

$$\frac{d\sigma}{dt} = |A(s,t)|^2. \quad (6.3)$$

We next assume exchange degeneracy so

$$A_R = \beta(t)S^{\alpha(t)-1} \quad (6.4)$$

which for  $[\omega+f_0, \rho+A_2]$  trajectories is real. For small  $t$

$$A_R \approx \gamma \exp(a+b_1 t) \quad (6.5)$$

$$\beta(t) \approx \gamma \exp(b_2 t), \quad b_1 = b_2 + \alpha' \ln s, \quad \gamma = \beta(0), \quad a = [\alpha(0) - 1] \ln s.$$

We neglect one particle exchange, such as  $\pi$  exchange which contributes a fraction of a millibarn when  $s$  is above 5 GeV. Equations (6.1), (6.2) and (6.5) give the eikonal

$$\begin{aligned} \chi(b) &= icb^3 K_3(\mu b) + \gamma s^{\alpha(0)-1} e^{-b^2/2R^2} \\ &= \chi_0(b) + \chi_1(b) \end{aligned} \quad (6.6)$$

where  $\chi_0$  is the Pomeron eikonal,  $\chi_1$  is the Regge eikonal,  $K_3$  is the third order Bessel function of imaginary argument,  $b$  is the impact parameter, and  $R^2 = 2b_1$ . Since  $\chi_0 \gg \chi_1$  we can substitute  $\chi_0$  and  $\chi_1$  in (3.2) and (3.3) getting

$$T_0 = i \int b db J_0(b(-t)^{\frac{1}{2}}) \left[ 1 - e^{-cb^3 K_3(\mu b)} \right] \quad (6.7)$$

$$T_1 = \int b db J_0(b(-t)^{\frac{1}{2}}) \gamma s^{\alpha(0)-1} e^{-b^2/2R^2} e^{i\chi_0(b)} \quad (6.8)$$

$e^{i\chi_0}$  can be approximated by  $[1 - ce^{-b^2/2R_0^2}]$ . From (6.7)  $|T_0|^2$  has the shape in Fig. 18 and  $T_1$  becomes to second order in  $b/R_0$

$$\begin{aligned} T_1 &\approx \gamma s^{\alpha(0)-1} \int b db J_0(b(-t)^{\frac{1}{2}}) e^{-b^2/2R^2} [1 - ce^{-b^2/2R_0^2}] \\ &\approx \gamma s^{\alpha(0)-1} \left\{ e^{\frac{R^2 t}{2-c}} \left( \frac{R_0^2}{R_0^2 + R^2} \right) e^{R^2 t/2} \right\} \end{aligned} \quad (6.9)$$

with  $R_2^{-2} = R_0^{-2} + R^{-2}$ .  $|T_1|^2$  also looks like Fig. 18 except the dips are displaced since the Pomeron and Regge pole contributions (6.1) and (6.4) are out of phase.  $|T|^2$  has the shape given in Fig. 19. As  $s$  increases the Regge pole vanishes and  $|T|^2 \rightarrow |T_0|^2$ , i.e., the dips get deeper. We shall later study the  $J$  plane singularities which lead to the two terms in (6.9)

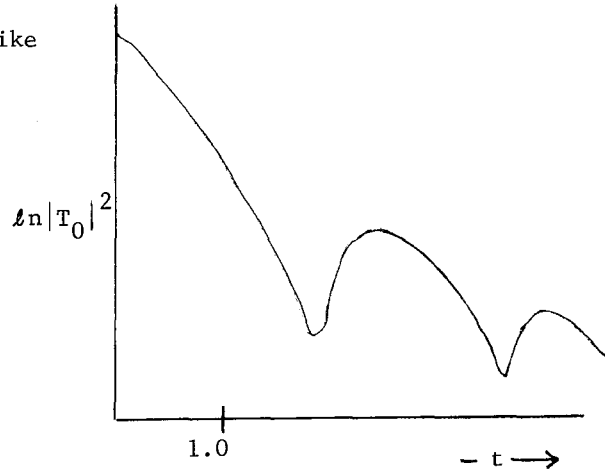


Fig. 18

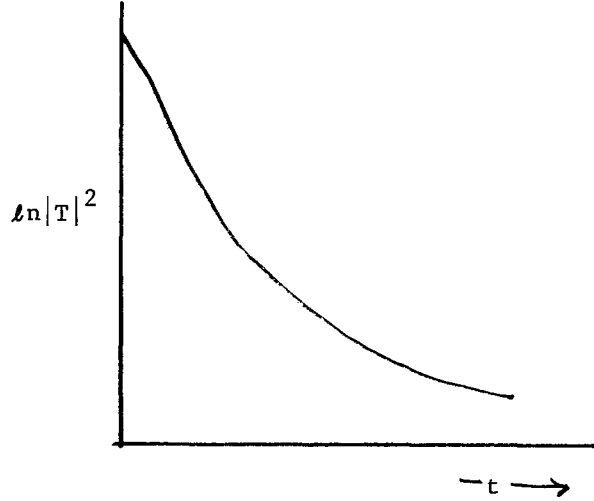


Fig. 19

### VII. COMPARISON OF MODELS

The hybrid model resulted from the assumption

$$A^{\text{Born}}(s, t) = A^{\text{droplet model}} + A^{\text{Regge pole}} \quad (7.1)$$

where  $A^{\text{droplet model}}$  is due to a fixed pole at  $\alpha = 1$ . The Frautschi and Margolis<sup>22-24</sup> model used (7.1) replacing the droplet term with a moving Pomeron term. Their Pomeron is assumed to have a trajectory  $\alpha(t) = 1 + \alpha' t$  and phase  $[1 + e^{-i\pi\alpha}] (\sin\pi\alpha)^{-1}$ , thus they get elastic shrinkage. It is easy to pass from one model to the other if  $\alpha' \approx 0$ .

Next we will compare predictions of various models for  $pp$ ,  $\bar{p}p$ ,  $pn$  scattering.  $\frac{d\sigma}{dt}$  for  $pp$  and  $\bar{p}p$  is given in Fig. 20. It is important to note that the curves cross over. The  $pp$  curve shrinks as  $s$  increases, the  $\bar{p}p$  forward peak expands, and the dip in the  $\bar{p}p$  curve becomes less pronounced. First consider what simple Regge theory implies about the cross-over. The Regge contribution to the elastic scattering is given by

$$pp = P + \omega + f_0 + \rho + A_2 \quad (7.3a)$$

$$\bar{p}p = P - \omega + f_0 - \rho + A_2 \quad (7.3b)$$

$$pn = P + \omega + f_0 - \rho - A_2 \quad (7.3c)$$

The sign change from (7.3a) to (7.3b) is due to odd signature vector poles. The sign change from (7.3a) to (7.3c) is due to  $I=1$  poles.

Assume the same trajectory function  $\alpha(t) = \frac{1}{2} + \alpha t$  for all but  $P$ . Empirically  $\sigma_{\text{tot}}(\bar{p}p) > \sigma_{\text{tot}}(pp) \approx \sigma_{\text{tot}}(pn) \approx \text{constant}$  for  $3 < s < 20 \text{ GeV}^2$ . The optical theorem



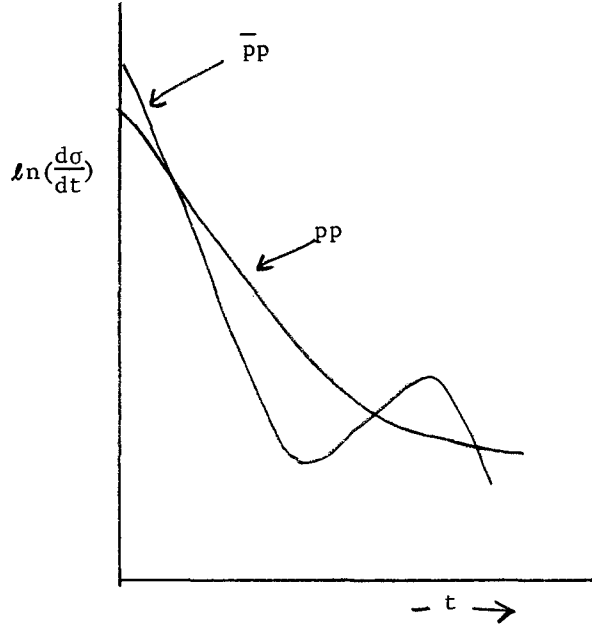


Fig. 20

then implies that  $\text{Im}(\rho+A_2) = \text{Im}(-\rho-A_2)$  independent of  $s$ . Since

$$\begin{aligned} \rho &= \frac{1-e^{-i\pi\alpha}}{\sin\pi\alpha} \beta_\rho(t) s^{\alpha(t)} \\ A_2 &= \frac{1+e^{-i\pi\alpha}}{\sin\pi\alpha} \beta_{A_2}(t) s^{\alpha(t)}, \end{aligned} \quad (7.4)$$

if  $\beta_\rho = \beta_{A_2}$  then, by (7.4),  $\text{Im}(\rho+A_2) = 0$ . If  $\beta_\omega = \beta_{f_0}$  also then there is cancellation of  $\text{Im}\omega$  with  $\text{Im}f_0$  leaving only  $\text{Im}P$  in  $\sigma_{\text{tot}}(pp)$  and  $\sigma_{\text{tot}}(pn)$ . We will assume complete exchange degeneracy  $\beta_\rho(t) = \beta_{A_2}(t)$ ,  $\beta_\omega(t) = \beta_{f_0}(t)$ . This is predicted by bootstrap schemes and finite energy sum rule.

$\beta_{A_2}(t)$  requires a zero at  $\alpha(t_0) = 0$  to cancel a pole in the physical region of  $\pi^- p \rightarrow \eta n$ . Exchange degeneracy implies that  $\beta_\rho(t_0) = 0$  so  $\frac{d\sigma}{dt}(\pi^- p \rightarrow \pi^0 n)$  should be 0 at  $t = t_0$ . This is not seen, but we can salvage exchange degeneracy by using cuts to fill in the dip at  $t=t_0$ . In general, to kill ghosts (as in  $A_2$ ) and to decouple spin flip amplitudes at nonsense wrong signature points we need zeroes of  $\beta$  at  $\alpha = 0, -1, -2, \dots$  corresponding to  $t = -0.5, -1.5, \dots$ .<sup>25-27</sup>

The cross-over effect in Fig. 20 is not due to nonsense zeroes and not due to large spin flip cancellation so it remains a mystery in the simple Regge model. The hybrid model gives it nicely since cancellation of the two terms in (6.9) for some  $t_0$  will give  $T_1 \approx 0$ . The P term in (7.3a and b) is large and imaginary whereas the

$\rho$ ,  $A_2$  terms are small. The  $f_0$  term has the same sign for  $pp$  and  $\bar{p}p$  scattering. The  $\omega$  term can explain the cross-over if its contribution (plus correction) is positive for  $t_0 < t < 0$  and negative for  $t < t_0$ .

In general from fits to polarization data we find that  $I=1$  exchange corresponds to helicity-flip and  $I=0$  corresponds to non-flip. The absorptive corrections to helicity-flip amplitudes are smaller than to helicity non-flip for small  $t$ .

The amplitude for the reaction  $\pi^- p \rightarrow \pi^0 n$  is predominantly helicity flip. The corrections go like  $t \ln s$ . The differential cross section and polarization are given by

$$\frac{d\sigma}{dt} = |G_+|^2 + |G_-|^2; \quad \mathcal{P} = \frac{2\text{Im}G_+^*G_-}{|G_+|^2 + |G_-|^2} \quad (7.5)$$

where  $G_-$  ( $G_+$ ) is the helicity (non) flip amplitude. If the phase of  $G_+$  and  $G_-$  are equal then  $\mathcal{P} = 0$ . This is the case if only one Regge pole contributes. The simple Regge model predicts that since only  $\rho$  is exchanged,  $\mathcal{P}$  should be 0. Experiments give  $\mathcal{P} \approx (15 \pm 5\%)$  for  $-t \in [0.1, 0.2] \text{ GeV}^2$ . In the hybrid model the phases of  $G_+$  and  $G_-$  are modified by absorptive corrections. When parameters are fitted to other reactions, the model gives Fig. 21. The unmeasured part of the polarization curve is very difficult to measure.

The polarization of the reaction  $\pi^+ p \rightarrow K^+ \Sigma^+$  is easier to measure since the decay of the  $\Sigma^+$  indicates its polarization.<sup>28</sup> The relevant trajectories are the  $K^*$ 's. If we assume exchange degeneracy and  $SU(3)$  symmetry we can use  $\rho$  and  $A_2$  parameters. The differential cross section and the calculated (M. Blackmon, private communication) and measured polarization are sketched in Fig. 22. (see next page) The break in  $\frac{d\sigma}{dt}$  occurs near the point where  $\mathcal{P}$  is maximum as can be seen from (7.5). Again exchange degeneracy without absorption corrections predicts zero polarization.

Now we will study the  $J$  plane singularities corresponding to the two terms in (6.9). Recall that the Sommerfeld-Watson transformation of the partial wave series  $\sum_l F_l(t) P_l(z_t)$  results in a background integral, a sum over Regge poles, and possibly a sum over cuts. The contour which initially enclosed the positive

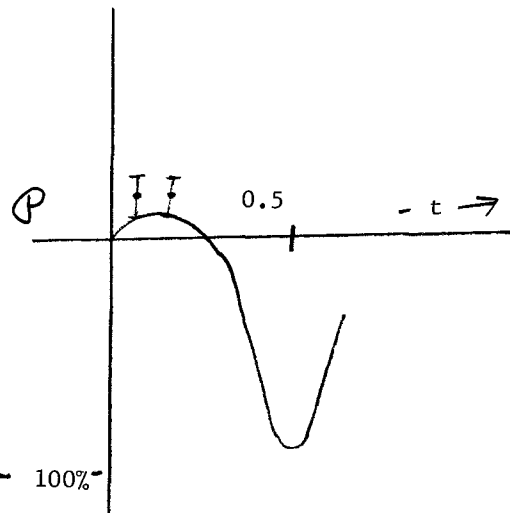


Fig. 21

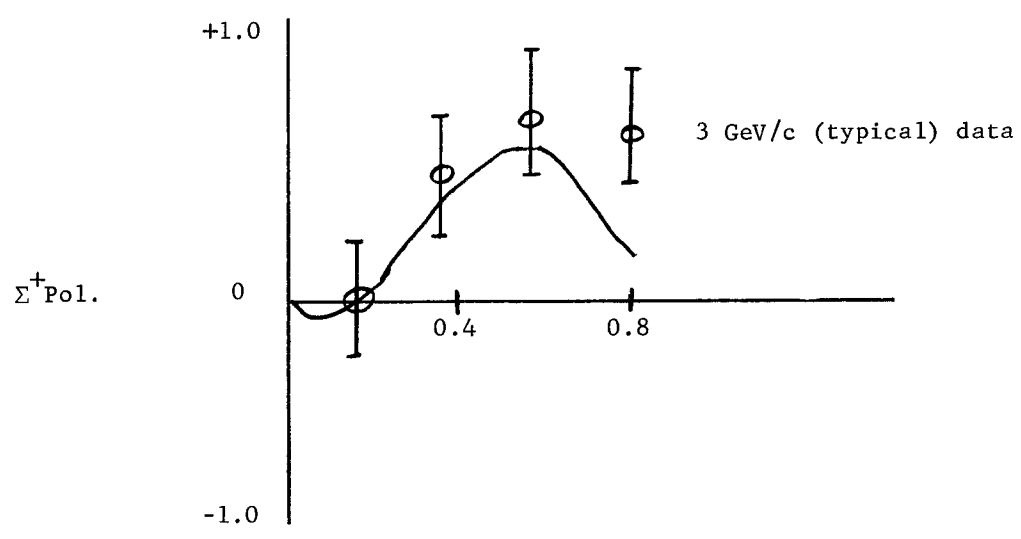
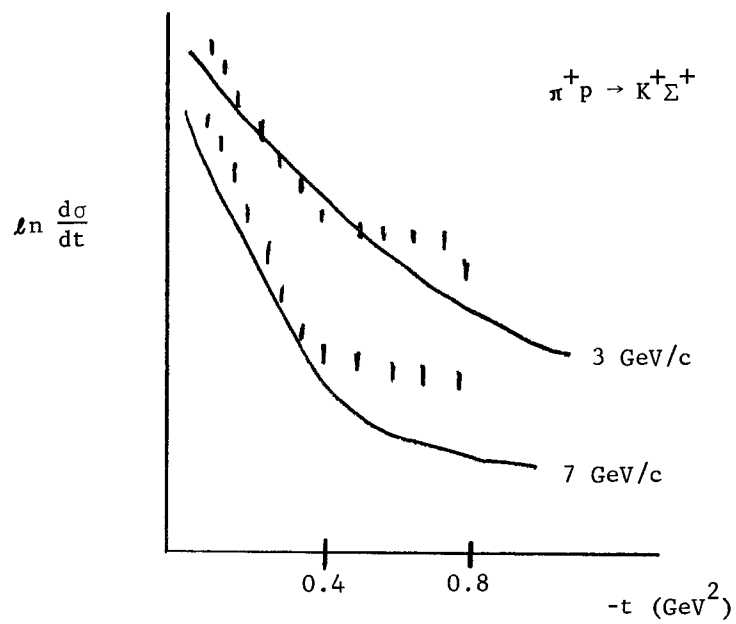


Fig. 22

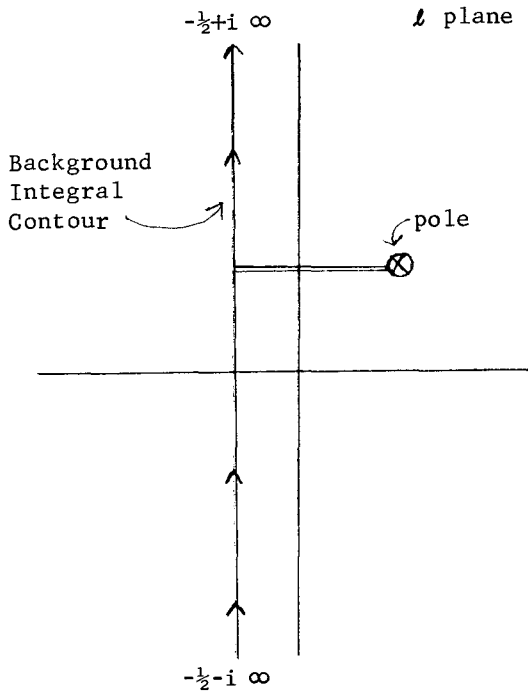


Fig. 23

integers has been opened as shown in Fig. 23. A simple pole at  $l = \alpha(t)$  has the asymptotic behavior in  $s$  with  $t$  fixed so  $\beta(t)s^{\alpha(t)}$ . A cut may be represented by a dense set of poles. Asymptotically this gives

$$\int_{-\infty}^{\alpha_c(t)} W(l,t) s^l dl \quad , \quad (7.6)$$

where  $\alpha_c(t)$  is the branch point and  $W(l,t)$  is the discontinuity across the cut which has been chosen to lie left of  $\alpha_c(t)$ . This can be approximated by  $\sum_n \beta_n(t) s^{\alpha_n(t)}$ . The region of the cut away from  $\alpha_c(t)$  does not effect the asymptotic behavior so only the discontinuity close to the end point matters. If the discontinuity is regular at the branch point, we may expand  $W$

$$\begin{aligned} W(l,t) &= W(\alpha_c(t)) + (l - \alpha_c(t)) \left( \frac{\partial W}{\partial l} \right)_{l=\alpha_c} + \dots \\ &= \beta_0(t) + (l - \alpha_c(t)) \beta_1(t) + \dots \end{aligned} \quad (7.7)$$

and substitute in (7.6). Using  $s^\alpha = e^{\alpha \ln s}$ , this gives

$$A = \int W(l,t) s^l dl = \beta_0(t) \frac{s^{\alpha_c(t)}}{\ln s} + \beta_1(t) \frac{s^{\alpha_c(t)}}{(\ln s)^2} + \dots \quad (7.8)$$

which is normalized so  $\frac{d\sigma}{dt} = \frac{1}{2} |A|^2$ . The series (7.8) converges too slowly for present experimental energies. However, if we knew the asymptotic behavior of the amplitude sufficiently well we could deduce the nature of the  $J$  plane singularities. The first term represents a constant discontinuity  $W$ . The other terms represent discontinuities that vanish at the branch point. If the Pomeron is a simple cut with constant discontinuity, then it produces a total cross section

$$\sigma_T = \frac{1}{s} \text{Im} A(s,0) = \frac{1}{s} \frac{s^{\alpha_c(0)}}{\ln s} \quad . \quad (7.9)$$

To compare with the hybrid model, consider the case  $T = T_0^{\text{Pomeron}} +$

$T_1$  charge exchange (CEX) at  $t=0$ . Then (6.9) gives

$$T_1^{\text{CEX}}(s,0) = \left( 1 - \frac{cR_0^2}{R_0^2 + R^2} \right) \beta(0) s^{\alpha(0)-1}. \quad (7.10)$$

The first term represents an ordinary Regge pole; however, since  $R^2 = 2(b_2 + \alpha' \ell ns)$  and  $R_0$  is independent of  $s$ , the second term, which is a correction term, has the asymptotic form  $\beta(0)(\ell ns)^{-1} s^{\alpha(0)-1}$  and thus represents a cut. [The normalizations in (6.9) and (7.8) differ by a factor of  $s$  so the branch point and Regge pole occur at  $\alpha(0)$ .] As  $s \rightarrow \infty$ ,  $R^2 \rightarrow \infty$ ,  $R_1^2 \rightarrow R_0^2 = \text{constant}$ . So for  $t \neq 0$ ,

$$A(s,t) \rightarrow - \frac{cR_0^2}{\alpha' \ell ns} e^{-tR_0^2/2} \beta(0) s^{\alpha(0)-1} \quad (7.11)$$

where  $|t \ell ns| \gg 1$  and  $|\ell ns| \gg 1$ . Since the power of  $s$  does not vary with  $t$  in this limit, the cut is fixed as shown in Fig. 24 for the case of the  $\rho$  trajectory.

In the Frautschi-Margolis model<sup>22-24</sup> with a moving Pomeron, the approximation  $e^{iX_0} \approx 1 - ce^{-b^2/2R_0^2}$  which was used to derive (6.9) must be replaced by a series of Gaussians, giving at large  $(-t)$

$$\sum \frac{(-c)^n}{n n!} e^{-tR_0^2/n} \rightarrow e^{-R_0^2(t)^{1/2}}, \quad (7.12)$$

with  $R_0^2 \propto \ell ns$ . The moving cuts accumulate to an effective line as shown in Fig. 25.

Most Regge theorists believe that there are cuts<sup>29-31</sup> in the  $J$  plane on the evidence from perturbation theory. The first such evidence came from Amati, Fubini and Stanghellini (AFS) who studied the unitarity diagrams in Fig. 26 and found that they give a cut whose discontinuity is  $\int A_n^* A_n$ . Mandelstam showed that when Fig. 26 is interpreted as a Feynman diagram, off-mass-shell contributions cancel the cut. He then found non-planar Feynman diagrams such as Fig. 27, which produced cuts at the same location as the AFS cuts. Unitarity cannot be used to give the discontinuity so the importance of the diagram is unknown. The absorptive model gives the cuts in the right position and gives the discontinuity with the correct sign relative to the pole. The correct sign is important since it produces the dip, the cross-over effect, and the polarization. Other models such as that of AFS give the wrong sign. This suggests that the cut is not due to two body unitarity. The multiperipheral model also gives the wrong sign unless absorption is added in the intermediate states<sup>32</sup> as illustrated in Fig. 28.

If the absorptive model is correct then it contains non-planar diagrams as in Fig. 27. For example, in deuteron-deuteron scattering the diagram in Fig. 29 gives a Regge cut according to Mandelstam's argument. It is also the second term in

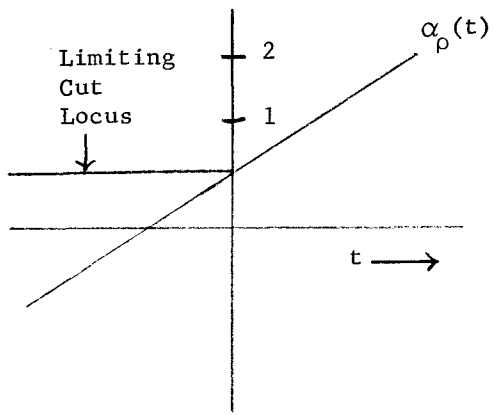


Fig. 24

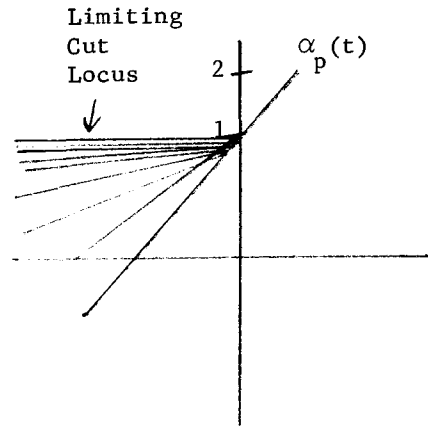


Fig. 25

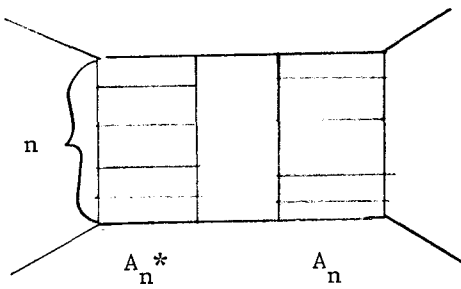


Fig. 26

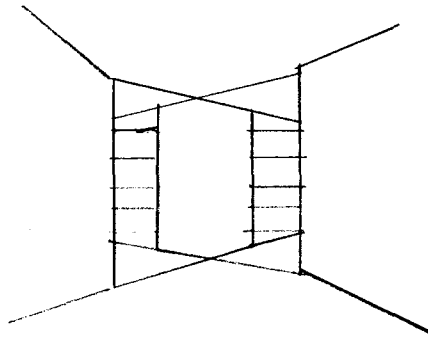


Fig. 27

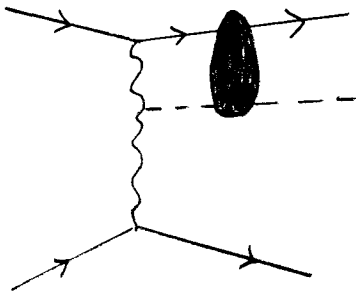


Fig. 28

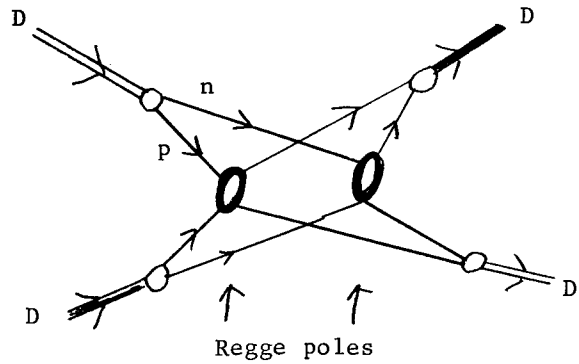


Fig. 29

the multiple scattering series.

Now we will examine in more detail the similarities and contrasts between the absorption model and unitarity models. We will see that (3.3) resembles elastic unitarity. Define  $\chi_1 = A_1^{\text{pole}}(s, b)$  and  $e^{i\chi_0} = 1 + iA_0(s, b)$ . Then (3.2) and (3.3) become

$$T_0(s, t) = \int b db J_0(b(-t)^{\frac{1}{2}}) A_0(s, b) \quad (7.13)$$

$$\begin{aligned} T_1(s, t) &= \int b db J_0(b(-t)^{\frac{1}{2}}) [1 + iA_0(s, b)] A_1^{\text{pole}}(s, b) \\ &\equiv A_1^{\text{pole}}(s, t) + A_1^c(s, t) \end{aligned} \quad (7.14)$$

where

$$A_1^{\text{pole}}(s, t) = \int b db J_0(b(-t)^{\frac{1}{2}}) A_1^{\text{pole}}(s, b) \quad (7.15)$$

and

$$A_1^c(s, t) = i \int b db J_0(b(-t)^{\frac{1}{2}}) A_0(s, b) A_1^{\text{pole}}(s, b) \quad (7.16)$$

is a correction term due to a cut. If the elastic contribution  $A_0$  is mostly positive imaginary, then  $A_1^c(s, t)$  has a minus sign relative to  $A_1^{\text{pole}}(s, t)$ .

The integral  $\int db$  was motivated by a discrete sum on  $l$ . In the  $s$  channel  $A_1^c$  has the expansion

$$A_1^c = i(\dots) \sum_l (2l+1) A_{0;l}(s) A_{1;l}^{\text{pole}}(s) P_l(z_s) \quad (7.17)$$

where

$$A_{0;l}(s) = \int dz' A_0(s, z') P_l(z') \quad (7.18)$$

and

$$A_{1;l}^{\text{pole}} = \int dz'' A_1^{\text{pole}}(s, z'') P_l(z'') \quad (7.19)$$

Then (7.16) is

$$A_1^c = i \int dz' dz'' A_0(s, z') A_1^{\text{pole}}(s, z'') \left[ \sum_{l=0}^{\infty} (2l+1) P_l(z) P_l(z') P_l(z'') \right] \quad (7.20)$$

The term in brackets is the Mandelstam kernel  $\theta(\Delta)/(\Delta)^{\frac{1}{2}}$  where

$\Delta = z^2 + z'^2 + z''^2 - z z z' - z z' z'' - z z z'' + 1$  and  $\theta$  is the step function. In  $t$  space (7.20)

becomes

$$A_1^c(s, t) = i \int dt' dt'' A_0(s, t') A_1^{\text{pole}}(s, t'') K(s, t; t'; t'') \quad (7.21)$$

which is the absorption or eikonal formula. The Mandelstam kernel  $K$  depends on  $s$

since the Jacobian transforming (7.20) to (7.21) does.

Now compare (7.21) with the results of two particle unitarity applied to the box diagram in Fig. 30. Let B be its amplitude

$$B(s) = \int \frac{\text{Im}B(s')}{s'-s} ds' \quad (7.22)$$

Two particle unitarity (AFS) gives the absorptive part of B,

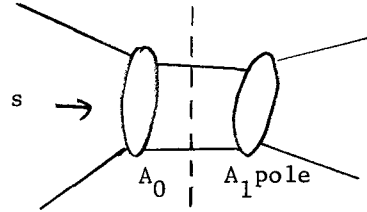


Fig. 30

$$\text{Abs}[B(s)] = \int dt' dt'' A_0^*(s, t') A_1(s, t'') K(s, t; t'; t'') \quad (7.23)$$

which looks similar to (7.21). K is the same, however (7.21) is the whole amplitude unlike  $\text{Abs}[B]$ . Also, (7.23) has a complex conjugation of an amplitude which is mostly imaginary so the sign is opposite.

In (7.23)  $A_1^{\text{pole}}$  is not necessarily a Regge pole. However, in such a case, suppose  $A_0 \sim s^{\alpha_0(t)-1}$  and  $A_1 \sim s^{\alpha_1(t)-1}$ . Now K has the property that as  $s \rightarrow \infty$ , it is significant only when  $(-t'')^{\frac{1}{2}} + (-t')^{\frac{1}{2}} \leq (-t)^{\frac{1}{2}}$ . Then

$$A^c(s, t) \rightarrow \int dt' dt'' s^{\alpha_0(t') + \alpha_1(t'') - 2} \quad (7.24)$$

For large s and small t this gives

$$A^c(s, 0) \sim \frac{s^{\alpha_c(0)-1}}{l \ln s} \quad (7.25)$$

where  $\alpha_c(0) = \alpha_0(0) + \alpha_1(0) - 1$ . The cut has the same position as the AFS model gave although the sign and magnitude are different. If we take  $t \neq 0$ , the slope of  $\alpha_c(t)$  can be found. For instance, if we start with  $\alpha_0 = \alpha_1 = \alpha_\rho$ , then we get  $\alpha_c' \equiv \alpha_\rho'/2$ . We can iterate choosing  $\alpha_0 = \alpha_{\rho\rho}$  and  $\alpha_1 = \alpha_\rho$ . The results are shown in Fig. 31. The cuts are not very interesting for  $t > 0$  since the pole contribution dominates. If the Pomeron and  $\rho$  are iterated then we get Fig. 32.

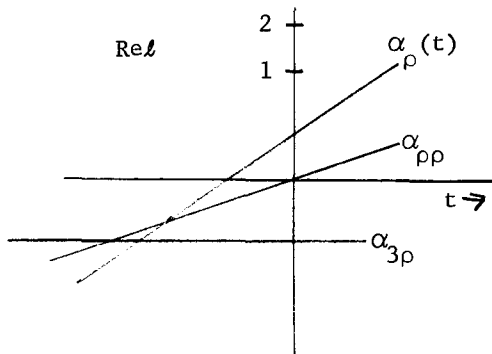


Fig. 31

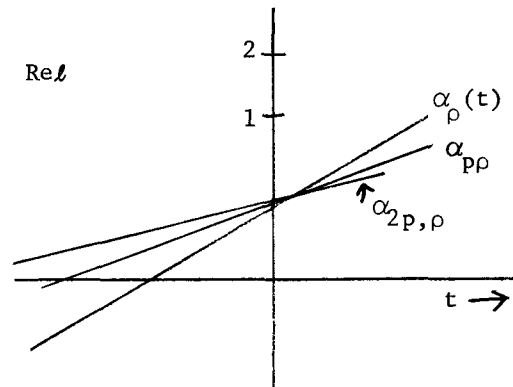


Fig. 32



To see how important the cuts are consider typical cross sections at  $E \sim 20$  GeV.

$$\begin{aligned} \sigma_{\text{total}} &\approx 25 \text{ mbarns} \\ \sigma_{\text{elastic}} &\approx 10 \text{ mbarns} \\ \sigma_{\text{charge exchange}} &\approx 100 \text{ } \mu\text{barns (single } \rho \text{ cut)} \\ \sigma_{\text{y-exchange}} &\approx 70 \text{ } \mu\text{barns} \\ \sigma_{\text{double charge exchange}} &\approx 1 \text{ } \mu\text{barns (double } \rho \text{ cut)}. \end{aligned}$$

The last is known to be small for some reactions but could be important for the diagram in Fig. 33.

We have seen that  $A_1^c(s,t)$  is related to Feynman diagrams in the shape of a box instead of unitarity diagrams such as Fig. 30. Mandelstam showed<sup>29</sup> that unless the intermediate particles are held on the mass shell, the Feynman diagram gives no cut. For some mysterious reason we need to throw away the contributions when the particles are off the mass shell. A heuristic justification for this is that if the intermediate particles are composite and loosely bound, then they can break

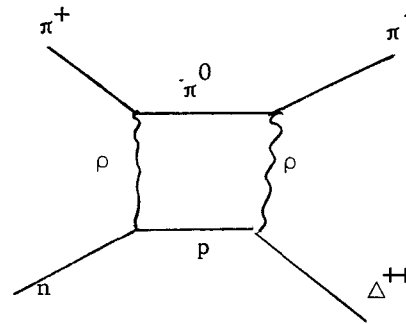
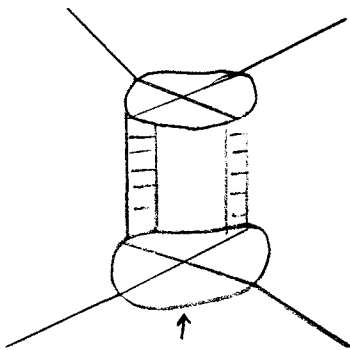


Fig. 33

up when they are off the mass shell. If we assume that the propagators oscillate wildly off the mass shell, then we need consider only mass shell contributions. Gribov and Migdal claim that the absorptive part of an amplitude such as in Fig. 26 is less than or equal to the sum over all orders of the non-planar Feynman diagrams in Fig. 34. If their argument can be strengthened then it will provide the justification.



(all crossed graphs)

Fig. 34

It was pointed out earlier that the hybrid model and multiperipheral model neglect Fig. 16. It was hoped that this correction is small. The correction to the cross section has been estimated at about 10%. Henyey *et. al.*<sup>33</sup> try to make the correction by multiplying  $A_1^c$  by  $\lambda$  with  $\lambda \geq 1$ .  $\lambda$  should be close to 1 since  $\lambda = 1$  gave reasonable results for the cross-over effect, polarization, and  $\frac{d\sigma}{dt}$ . If  $\lambda \gg 1$  then exchange degeneracy is intolerable and the location of dips in  $\frac{d\sigma}{dt}$  depend on  $s$ .

Henye et. al.<sup>33</sup> choose  $\lambda \approx 2$  and get secondary peaks in  $\frac{d\sigma}{dt}$  from multiple scattering. Data at higher  $s$  may decide which version of the absorptive model is better.

Another way of including absorption is to insert Regge poles in K matrix which is defined by  $T = B(1 - ipk)^{-1}$ .  $B$  is the Born approximation and has resonance poles. Poles and cuts are generated by this method; however, more art is needed to explain data.

### VIII. THEORIES OF PRODUCTION

A simple but unsuccessful model for production is the bremsstrahlung model which results from assuming that the particles are produced by the legs of elastic scattering amplitudes as illustrated in Fig. 35. The amplitude for the diagram is

$A_e(s, t) \frac{g}{s_1^{-m}}$  with  $A_{el}$  assumed to be the mass-shell amplitude, and  $g$  the (mass shell)  $\pi N$  coupling constant. This model works well in quantum electrodynamics (possibly because the photon's mass is strictly zero), but the results of this model are too large by at least a factor of ten for  $\pi N \rightarrow \pi\pi N$ .

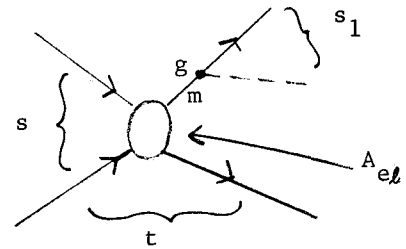


Fig. 35

The main reason for this failure is that the Compton wavelength of the emitted  $\pi$  is always smaller than or comparable to the interaction radius.

A more successful model is the "synchrotron radiation model" which is motivated by classical concepts of synchrotron radiation.<sup>34</sup> The power radiated in electrodynamics is proportional to  $(\frac{d}{dt}J)^2$ . We will consider  $pp \rightarrow pp\pi$  and assume that in the center of momentum system the protons have classical trajectories that are arcs of circles of radius  $\rho$  in the interaction region, which is a sphere of radius  $R$ . See Fig. 36. Such a circular trajectory would result if the interaction

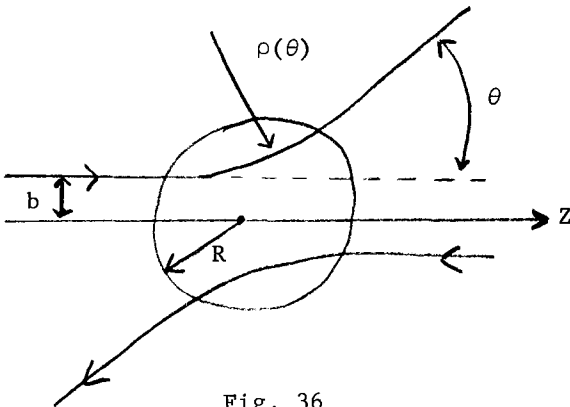


Fig. 36

region contained a uniform magnetic field.

The impact parameter  $b(\theta)$  is related to

$(\frac{d\sigma^{el}}{d\cos\theta})$ ,  $\rho$ , and  $R$  by the following argument.

The elastic cross section is given classically by  $d\sigma^{el} = 2\pi b db$ . Integrating, we get

$$\int_0^b 2\pi b' db' = \int_{\text{backward angle}}^{\cos\theta} \frac{d\sigma^{e\ell}}{d\cos\theta'} d\cos\theta' = \pi b^2(\theta) \quad . \quad (8.1)$$

When  $\cos\theta = 1$  we want:  $\pi b^2(0) = \pi R^2$  so  $b(0) = R$ . Geometry gives

$$\rho(\theta) = (R^2 - b^2)^{\frac{1}{2}} \cot\frac{\theta}{2} - b(\theta) \quad .$$

Next we assume the particle has a constant velocity so knowing  $\rho(\theta)$ , we know the trajectory  $\vec{r}(t)$ .

Next we postulate an appropriate classical current in the form of  $J(\vec{x}, t) = g\delta(\vec{x} - \vec{r}(t))$  assuming that it is a scalar. The LSZ formalism applied to the amplitude for the diagram in Fig. 37 gives

$$S(k) = \langle p_1' p_2' k; \text{out} | p_1 p_2; \text{in} \rangle \sim \int d^4x e^{ik \cdot x} \langle p_1' p_2'; \text{out} | J(x) | p_1 p_2; \text{in} \rangle \quad . \quad (8.3)$$

We are assuming that  $J$  is a c-number so it can be pulled out of the matrix element leaving

$$S(\vec{k}) \sim \langle p_1' p_2'; \text{out} | p_1 p_2; \text{in} \rangle \int d^3x e^{i\vec{k} \cdot \vec{x}} \int dt g \delta(\vec{x} - \vec{r}(t)) \quad (8.4)$$

where  $\langle | \rangle = A_{\text{elastic}}(p_1' p_2'; p_1 p_2) \delta^4(p_1 + p_2 - p_1' - p_2')$  is taken from data. If the interaction Lagrangian for mesons with nucleons is  $g_{\pi N} \bar{\psi} \gamma_5 \psi$ , then at large  $s$ ,  $-t$  with  $\psi$ 's localized in wave packets  $J$  is equivalent to  $g_{\pi N} \phi \delta(\vec{x} - \vec{r}(t))$  so we get  $g = g_{\pi N}$  in this region. Other assumptions are needed, for instance we can take for non-asymptotic  $t$  values the replacement

$$A_{\text{elastic}}(s, t) \rightarrow (A_{e\ell}(s, t_1) A_{e\ell}(s, t_2))^{\frac{1}{2}} \quad (8.5)$$

to give proper damping in  $t_1$  and  $t_2$ . Also we must symmetrize for the initial protons. Then we can substitute the trajectory  $\vec{r}(t)$  in (8.4) and get  $S(\vec{k})$ . Similar

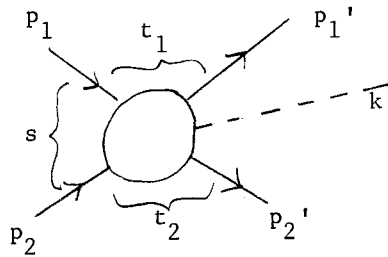


Fig. 37

arguments work for vector meson production. There are old data on  $pp \rightarrow p\pi\pi^+$ ,  $pp\pi^0$ ,  $pp\eta^0$ ,  $pp\omega^0$  at 12.5 GeV which agree fairly well with the model's predictions.<sup>34</sup>

The synchrotron radiation model works only for large angle production; for small angles we need to assume more quantum properties. We have considered a radiation eikonal model.<sup>35</sup> The main idea is to interpret the interaction

Lagrangian  $g\phi J$  as subtracting probability from elastic scattering. The assumptions are

- 1)  $J = g \frac{d}{dz} |\psi(b,z)|^2$  where  $\psi$  is given by (1.7) (one dimensional motion), and
- 2)  $V(b,z) \cong iA \exp[-\frac{b^2}{2R^2} - \frac{\gamma^2 z^2}{2R^2}]$  = the potential occurring in elastic scattering

where  $\gamma = E/M$  accounts for Lorentz contraction. The appropriate value of  $g$  can be obtained from Adler's self-consistency condition. The S matrix in (8.3) can be generalized to the case of  $n$  meson emission if the emissions are assumed to be independent:

$$S(k_1, \dots, k_n) = \int \langle p_1' p_2'; \text{out} | p_1 p_2; \text{in} \rangle \langle j_1(x_1) \rangle \dots \langle j_n(x_n) \rangle$$

$$= S_0 \prod_j S_1(k_j) \quad (8.6)$$

This can be summed to get

$$\sigma_n \sim \int d\Omega_n |S_n|^2 \cong \frac{(g^2 \Omega)^n}{n!} \Omega_n \cong \frac{(g^2 \Omega)^n}{n!} (\Omega)^n \quad (8.7)$$

where  $\Omega_n$  is a phase space factor. The total inelastic cross section is

$\sigma^{\text{inel}} = \sum_n \sigma_n \sim e^{g^2 \Omega}$ . The probability of producing  $n$  particles is

$$\frac{\sigma_n}{\sum_{n'} \sigma_{n'}} \sim \frac{(g^2 \Omega)^n}{n!} e^{-g^2 \Omega} \quad (8.8)$$

Maximizing gives  $\bar{n} \sim g^2 \Omega$  for a Poisson distribution. In Heckman's model,<sup>35</sup>

$$g^2 \Omega \cong \int \frac{d^3 k}{w} |J(k)|^2 \quad (8.9)$$

increases as  $\ln s$  at large  $s$ . This model can be used to calculate differential cross sections of  $pp \rightarrow \pi^+ + \text{anything}$  and  $pp \rightarrow p + \text{anything}$ . These are easy to measure with one armed spectrometers and the data have the general features at fixed  $s$  shown in Fig. 38. The prediction is in excellent agreement at small angles and starts to differ around angles of  $20^\circ$  in the center of momentum system.

Gundzik has worked on a scheme<sup>36</sup> to calculate  $pp \rightarrow pp$  using the concepts of the above models. In the unitarity diagram in Fig. 39,  $J$  is the source and sink of the intermediate pions. The phase of the emitted pions is important here. Also the similar diagram with two  $N^*$  in the intermediate state is important. Many parameters are needed in this model.

Another classical theory

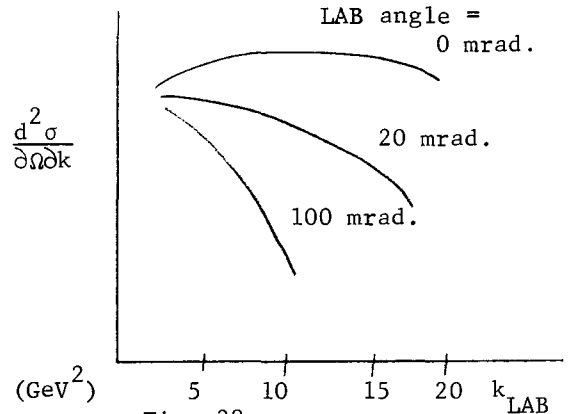


Fig. 38

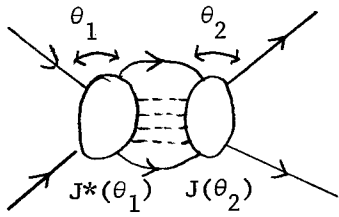


Fig. 39

of multiple production was constructed by Landau ten years ago. It is related to Huang's model since the hadrons are considered to be blobs of gas. When they collide they are assumed to form a symmetrical pill box containing shock waves. The shock wave generates entropy and the flux of entropy is identified with the amount of particles produced.<sup>37</sup> The sequence of events in a collision is illustrated in Fig. 40. The model predicts  $n \sim E_{lab}^{\frac{1}{2}}$ , which is not contradicted by available data.<sup>38</sup>

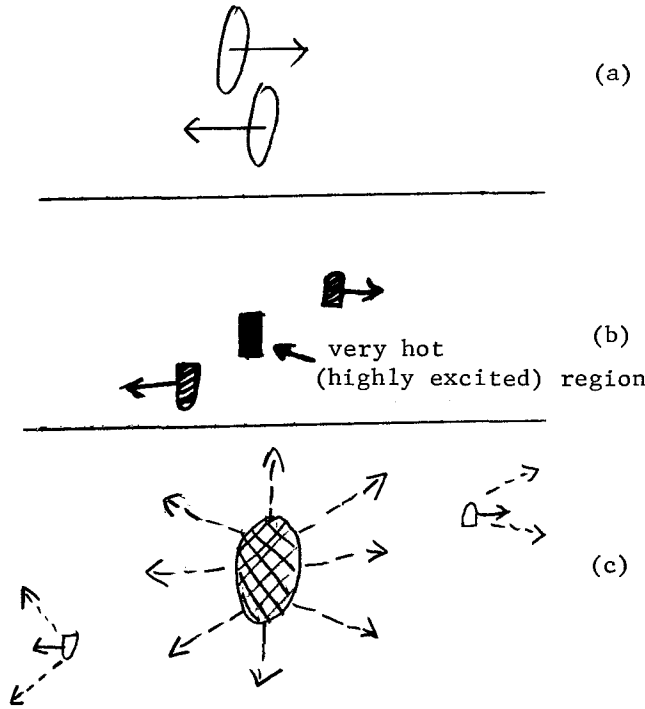


Fig. 40

The number emitted with angle  $\theta$  is

$$dn \sim ce^{-\frac{1}{2}((c')^{\frac{1}{2}} - (\eta)^{\frac{1}{2}})^2} d\eta \tag{8.10}$$

where  $c, c'$  are constants, depending on the initial state and  $\eta = \ln(\tan\theta)$ . The energy flux is given by

$$\omega(\theta) \sim e^{\frac{1}{3}(c''+\eta) - \frac{1}{3}(c''\eta)^{\frac{1}{2}}} \tag{8.11}$$

Hagedorn's fireball model is similar to the above model in the sense that both have a maximum temperature; however Hagedorn requires arbitrary parameters. Higher energy accelerators are needed to test these models.

In conclusion classically based models work better than diagrammatic models do for the above data. This might be expected since high  $s$  is expected to give classical limits. Of course, we may find surprises such as a breakdown of micro-causality; however the operational point of view says try until we find a problem.

### IX. DIELECTRIC SPHERES AND SHARP BOUNDARY MODELS

Consider the scattering of light, of wave number  $k$ , by a dielectric sphere of uniform index of refraction  $n$  and radius  $a$  in optics. Mie solved this fifty years ago. When  $(ka)$  gets large the solution becomes a sum of many Bessel functions. Nussenzweig<sup>39</sup> used the Sommerfeld-Watson transformation to study this problem. One finds a lot of fine structure as is illustrated in Fig. 41. The shape of  $\frac{d\sigma}{d\Omega}$  resembles that of hadron scattering. The peaks occur when  $\frac{db}{d\theta} = \infty$ . For instance, the backward peak can result from the rays in Fig. 42. The Sommerfeld-Watson transformation for the limit  $k \rightarrow \infty$  gives  $J$  plane singularities (Regge poles) on the locii in Fig. 43. The glory effect is due to poles on the curved section of the locii. The effect can sometimes be observed from an airplane flying over clouds. Sunlight scattered backward from water droplets of the right radius in the clouds can produce bright colored rings around the shadow of the plane. The color implies that the effect is due to a backward diffractive process from small droplets.

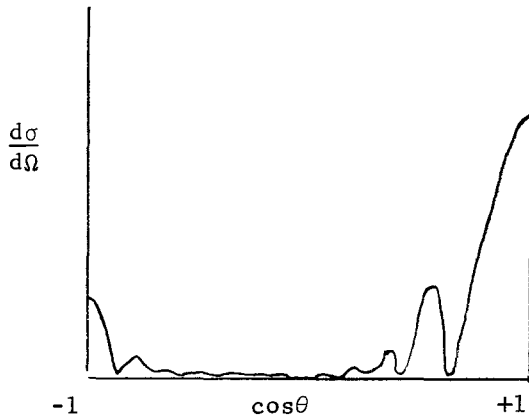


Fig. 41

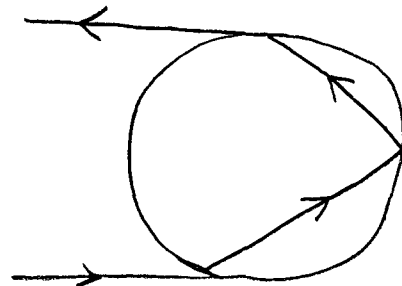


Fig. 42

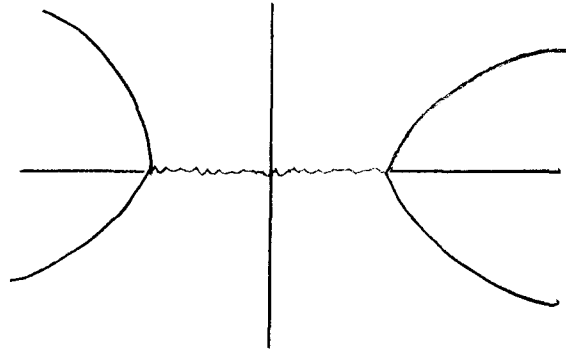


Fig. 43

A quick and dirty derivation of the glory effect from a sharp sphere<sup>40</sup> is the following: write the partial-wave expansion

$$f(\theta) = \frac{1}{2ik} \sum_l (2l+1) (e^{2i\delta_l} - 1) P_l(\cos\theta) \quad (9.1)$$

Since  $P_l(-z) = (-1)^l P_l(z)$ , (9.1) becomes

$$2ikf(\theta \simeq \pi) \sim \sum_{l=0,2,4} (2l+1) [e^{2i\delta_l} - e^{2i\delta_{l+1}}] P_l(-\cos\theta). \quad (9.2)$$

If we assume the  $e^{2i\delta_l}$  is a slowly varying function of  $l$  then the term in brackets can be approximated by  $\frac{\partial}{\partial l} e^{2i\delta_l}$  and (9.2) becomes

$$f(\theta \simeq \pi) = i \int b \, db J_0(b(-u)^{\frac{1}{2}}) \frac{\partial}{\partial b} [e^{2i\delta(b)} - 1] \quad (9.3)$$

Compare this with the forward amplitude

$$f(\theta \simeq 0) = ik \int b \, db J_0(b(-t)^{\frac{1}{2}}) [e^{2i\delta(b)} - 1] \quad (9.4)$$

Thus the backward peak is related to the forward peak. The prediction works roughly for the backward peaks of  $\pi^+ p$  and  $K^+ p$  but does not work for  $\pi^- p$  and  $K^- p$ . The  $s$  dependence of the peaks is predicted to be

$$\frac{d\sigma}{d\Omega}(\theta \simeq \pi) \simeq \frac{1}{s} \frac{d\sigma}{d\Omega}(\theta \simeq 0) \quad (9.5)$$

which is not strongly violated for such cases. (The assumption that  $e^{2i\delta_l}$  is slowly varying is not good in general.)

A more rigorous approach to the glory effect analogy for backward scattering

is to use the Regge pole expansion. If the Regge poles on the locii in Fig. 43 are assumed to occur at  $\alpha(s) = a+bs$  then the backward  $\pi p$  peak can be fit.<sup>41</sup> The backward peak in  $\pi C$  scattering has been studied in a model where the  $\pi$  is internally reflected.  $J_0(R(-u)^{\frac{1}{2}})$  fits the data.<sup>42</sup> M.C. Li has been working on similar applications.<sup>43</sup>

The sharpness of the edge of the dielectric sphere is very important in geometrical optics; however, for high  $s$  scattering of hadrons, the width of the edge becomes large. If the analogy holds, then the backward peak should go away.<sup>44</sup>

Suppose there is a discontinuity in  $n$  in hadrons, for instance, if they are droplets with a skin. Then excited states may be surface waves. For instance, in  $pp \rightarrow pN^*$  where  $N^*$  can be  $\frac{1}{2}^+(1480)$ ,  $3/2^-(1520)$ ,  $5/2^+(1690)$ ,  $7/2^-(2190)$ , etc., a simple surface-wave model explains the  $s$  and  $t$  dependence for the first two and fails for the second two.<sup>45</sup> The matrix element to excite  $Y_L^M$  surface wave can be approximated by<sup>45</sup>

$$T_L^M(\Delta) = \bar{c}_L Y_L^M(\frac{\pi}{2}, 0) \int_0^\infty b db J_M(\Delta b) H(b) \quad (9.6)$$

where  $H(b)$  is the distribution of matter in the interaction region (skin) and  $\Delta = (-t)^{\frac{1}{2}}$ . For a nearly-square well potential

$$H(b) \sim \frac{\partial}{\partial b} (1 - e^{iX(b)})$$

We can assume  $1 - e^{iX(b)}$  is a Gaussian in  $b$  and then sum the square of (9.6) over  $M$  to get the cross section. Perhaps this model is discovering systematics that will come out of someone's dynamics.

#### REFERENCES

1. R.J. Glauber, Lectures in Theoretical Physics, Vol. 1, p. 315 (Boulder Colorado Summer School)(1959). A recent review of optical potentials can be found in L.L. Foldy and J.D. Walecka, Ann. Phys. (N.Y.) 54, 447 (1969).
2. R.C. Arnold, Phys. Rev. 153, 1523 (1967). This contains relevant references up to 1966.
3. T.T. Chou and C.N. Yang, Phys. Rev. 170, 1591 (1968).
4. T.T. Chou and C.N. Yang, Rehovoth Conference (1967) p. 348.
5. T.T. Chou and C.N. Yang, Phys. Rev. 175, 1832 (1968).
6. T.T. Chou and C.N. Yang, Phys. Rev. Letters 20, 1213 (1968).
7. J.S. Trefil, Phys. Rev. 180, 1366 and 1379 (1969).
8. C. Wilkin, High Energy Scattering from Nuclei, Nuclear and Particle Physics, McGill University (1967) p. 439.



9. H. Feshbach, Semi-classical Approximation, 37th Course of Enrico Fermi School, (Varena) (1967).
10. T.T. Wu and C.N. Yang, Phys. Rev. 137, B708 (1965).
11. N. Byers and C.N. Yang, Phys. Rev. 142, 976 (1966).
12. H.M. Chan, Vienna Conference (review talk) (1966).
13. K. Huang, Phys. Rev. 156, 1555 (1967).
14. R. Torgerson, Phys. Rev. 143, 1194 (1966) (Field-Theoretic Eikonal work).
15. A.A. Logunov and A.N. Tavkhelidze, Nuovo Cimento 29, 380 (1963).
16. D.I. Blokhintsev, V.S. Barashenkov and B.M. Barbashov, English Transl: Soviet Physics Uspekhi 2, 505 (1969).
17. H.D.I. Abarbanel and C. Itzykson, Phys. Rev. Letters 23, 53 (1969).
18. H. Cheng and T.T. Wu, Phys. Rev. Letters 22, 666 (1969); 23, 351 (1969).
19. S.J. Chang and S. Ma, Phys. Rev. Letters 22, 1334 (1969).
20. M. Levy and J. Sucher, University of Maryland preprint 983 (1969).
21. C. Chiu and J. Finkelstein, Nuovo Cimento 57, 649 (1968).
22. S. Frautschi and B. Margolis, Nuovo Cimento, 56A, 1155 (1968).
23. S. Frautschi and B. Margolis, Nuovo Cimento 57A, 427 (1968).
24. S. Frautschi and B. Margolis, Nuovo Cimento 61A, 92 (1969).
25. C. Chiu and J. Finkelstein, Nuovo Cimento 57A, 92 (1968).
26. R.C. Arnold and M.L. Blackmon, Phys. Rev. 176, 2082 (1968).
27. M.L. Blackmon and G.R. Goldstein, Phys. Rev. 179, 1480 (1969).
28. S.M. Pruss, C.W. Akerlof, D.I. Meyer, S.P. Ying, J. Lales, R.A. Lundy, D.R. Rust, C.E.W. Ward and D.D. Jovanovitch, Phys. Rev. Letters 23, 189 (1969).
29. S. Mandelstam, Nuovo Cimento 30, 1127 and 1145 (1963).
30. J. Polkinghorne, J. Math. Phys. 6, 1960 (1965).
31. Ya. Azimov et. al., English Transl: Soviet Physics JETP 21, 1189 (1965).
32. L. Caneschi and A. Pignotti, Phys. Rev. Letters 22, 1219 (1969) and L. Caneschi, Phys. Rev. Letters 23, 254 (1969).
33. F. Henyey, G. Kane, J. Pumplin and M. Ross, Phys. Rev. Letters 21, 946 and 1782 (1968); Phys. Rev. 182, 1579 (1969).
34. R.C. Arnold and P. Heckman, Phys. Rev. 164, 1822 (1967).
35. P. Heckman, Ph.D. Thesis, University of Chicago; ANL-HEP
36. M.G. Gundzik, preprint ANL/HEP 6911 (Phys. Rev. to be published).
37. S. Fenster, talk in Argonne Symposium on Multiparticle Production, ANL/HEP 6909.
38. R. Murthy, ibid.
39. H.M. Nussenzweig, J. Math. Phys. 10, 82, 125 (1969).
40. R.C. Arnold, Argonne National Laboratory preprint (1968).
41. H.C. Bryant, SLAC-PUB-608, Stanford preprint (1969).
42. H.C. Bryant and N. Jarmie, Ann. Phys. (N.Y.) 47, 127 (1966).

43. M.C. Li, VPI preprint (1969).
44. E. Montroll and J.M. Greenberg, Phys. Rev. 86, 889 (1952). (They derived the precursor to the eikonal and backward scattering).
45. R.C. Arnold, Phys. Rev. 157, 1292 (1967).



FORMALISM AND PHENOMENOLOGY OF  
COMPLEX ANGULAR MOMENTUM

Lectures by:           Kerson Huang  
                          Massachusetts Institute of Technology

Notes taken by:       Frank E. Paige

Table of Contents

I. Regge Poles in Potential Scattering . . . . .	161
A. Regge Poles and Resonances . . . . .	161
B. Sommerfeld-Watson Transform . . . . .	164
C. Mandelstam Symmetry . . . . .	165
D. Exchange Potential and Signature . . . . .	167
II. Relevance of Regge Poles to Relativistic Scattering . . . . .	169
A. High Energy Scattering . . . . .	169
B. The Bootstrap Idea . . . . .	170
C. Chew-Frautschi Plot . . . . .	172
III. Relativistic Scattering of Spinless Particles . . . . .	173
A. Preliminaries . . . . .	173
B. Froissart-Gribov Continuation . . . . .	176
C. Regge Poles . . . . .	178
D. Reggeization . . . . .	180
E. Khuri Poles . . . . .	183
F. Factorizability of Regge Residues . . . . .	184
G. Complications Due to Spin and Intrinsic Quantum Numbers . . . . .	185
IV. Some Simple Physical Consequences . . . . .	190
A. Single Pole Dominance . . . . .	190
B. Total Cross Sections . . . . .	190
C. Diffraction Scattering . . . . .	192
D. The $\rho$ Trajectory . . . . .	196
E. The N and $\Delta$ Trajectories . . . . .	196
V. Regge Cuts . . . . .	199
A. Regge Cut from Two-Particle Unitarity . . . . .	199
B. Some Model Calculations . . . . .	201
C. Effect of Regge Cuts in Scattering . . . . .	202
VI. Towards Dynamics? . . . . .	205
A. Finite-Energy Sum Rules . . . . .	205
B. Duality . . . . .	208
C. Exchange Degeneracy . . . . .	209
D. Bootstrap of the $\rho$ Trajectory . . . . .	211
E. The Veneziano Model . . . . .	214
F. Veneziano Model for $\pi\pi$ Scattering . . . . .	219
VII. Spin . . . . .	222
A. Kinematics . . . . .	222
B. Helicity Amplitudes . . . . .	223
C. Kinematic Singularities and Constraints . . . . .	225
D. Example: $\pi\pi \rightarrow \pi\omega$ . . . . .	228
E. Conspiracy . . . . .	230
F. Reggeization of Helicity Amplitudes . . . . .	232
G. Sense and Nonsense . . . . .	239
VIII. Example: Pion-Nucleon Scattering . . . . .	241
A. Invariant Amplitudes . . . . .	241
B. Helicity Amplitudes . . . . .	242
C. Reggeization of Helicity Amplitudes . . . . .	245

## Introduction

In these lectures we discuss two-body hadronic scattering in the high-energy limit, under the hypothesis that it is dominated by Regge singularities, i.e., singularities in the finite parts of the complex angular momentum plane of the partial-wave amplitudes in the crossed channel. In particular we discuss the motivation of the hypothesis, the procedure for putting it into practical use, some of its experimental consequences, and possible glimpses into the dynamics of strong interactions. For general references the following books are recommended.

R.J. Eden, High Energy Collisions of Elementary Particles, (Cambridge, The University Press, (1967)).

E.J. Squires, Complex Angular Momentum and Particle Physics (W.A. Benjamin, New York (1964)).

P.D.B. Collins and E.J. Squires, Regge Poles in Particle Physics (Springer-Verlag, Berlin (1968)).

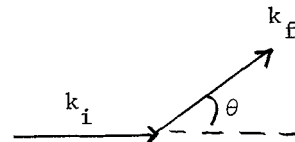
### I. Regge Poles in Potential Scattering

#### A. Regge Poles and Resonances:

As an introduction to the idea of Regge poles, we give a brief review of potential scattering, where they were first introduced as a new way to describe bound states and resonances.

Suppose a spinless non-relativistic particle is scattered by a central potential  $V(r)$ , with kinematics as shown in the accompanying sketch.

In units such that  $\hbar = 2m = 1$  let  $E$  be the energy of the particle and  $z$  be the cosine of the scattering angle:



$$\begin{aligned} E &= k^2 \\ k &= |\vec{k}_i| = |\vec{k}_f| \\ z &= \cos\theta = \vec{k}_i \cdot \vec{k}_f / k^2 \end{aligned} \quad (1.1)$$

The differential cross section is given by

$$\frac{d\sigma}{d\Omega} = |f(E, z)|^2 \quad (1.2)$$

where the scattering amplitude  $f(E, z)$  has the familiar partial-wave expansion

$$f(E, z) = \sum_{\ell=0}^{\infty} (2\ell+1) F_{\ell}(E) P_{\ell}(z) \quad , \quad (1.3)$$

where the partial-wave amplitude  $F_{\ell}(E)$  is determinable from the solution to the

radial equation

$$\frac{d^2 u_{\ell}}{dr^2} + E u_{\ell}(r) = \left[ V(r) + \frac{\ell(\ell+1)}{r^2} \right] u_{\ell}(r)$$

$$u_{\ell}(r) \rightarrow 0 \quad \text{as } r \rightarrow 0 \quad . \quad (1.4)$$

Asymptotically the solution is of the form

$$u_{\ell}(r) \rightarrow C \sin \left( kr - \frac{\pi\ell}{2} + \delta_{\ell}(E) \right) \quad . \quad (1.5)$$

The partial-wave amplitude is then given in terms of the phase shift  $\delta_{\ell}(E)$  by

$$F_{\ell}(E) = \frac{1}{2ik} [e^{2i\delta_{\ell}(E)} - 1] \quad . \quad (1.6)$$

It is a real analytic function of  $E$ , and it has a branch cut along the positive real  $E$  axis. There are no poles on the physical Riemann sheet except along the negative real axis, where they correspond to bound states of spin  $\ell$ . Complex poles can occur only in conjugate pairs on the second Riemann sheet. If they are close to the branch cut, the one just below the cut is near the physical region, and correspond to a resonance of spin  $\ell$ . Its conjugate partner is far from the physical region, and thus not directly "visible". (Except when the pair of poles are near  $E=0$ , but there threshold effects become important.)

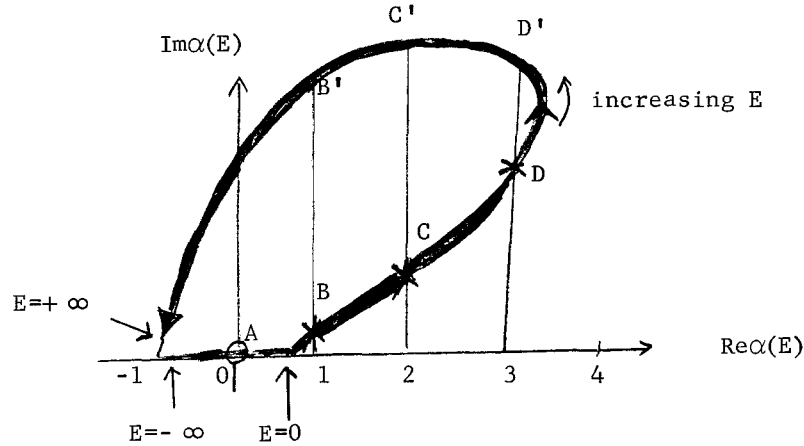
Regge shows that the same bound states and resonances show up as poles of  $F_{\ell}(E)$  in the complex  $\ell$ -plane, in the following way. First, from the radial equation for a superposition of Yukawa potentials, one can show that  $F_{\ell}(E)$  can be uniquely continued to complex  $\ell$ , thereby giving a function  $F(E, \ell)$ . It has the following properties:

1.  $F(E, \ell)$  is meromorphic for  $\text{Re} \ell > -\frac{1}{2}$ ,
2.  $F(E, \ell) \rightarrow 0$  as  $|\ell| \rightarrow \infty$ ,
3. The positions of the poles in  $\ell$  move with the energy  $E$ .

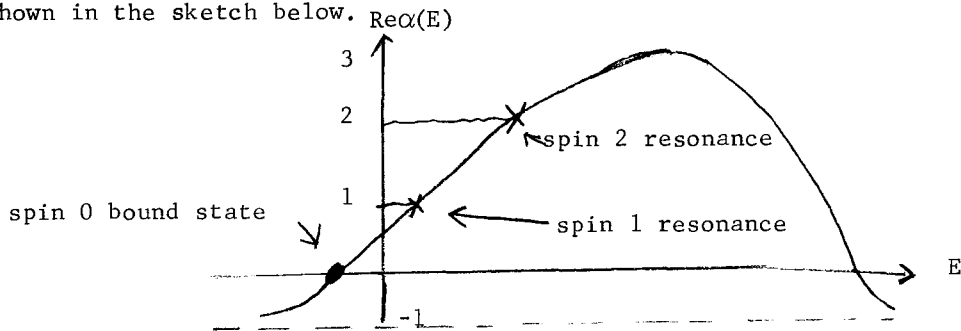
Such a moving pole is called a Regge pole, its locus  $\alpha(E)$  a Regge trajectory.

In the usual description, a resonance is identified with a pole of  $F(\ell, E)$  in  $E$ , at a positive integer value of  $\alpha(E)$ , which generally occurs at complex  $E$ . We now propose to keep  $E$  real and associate resonances with the behavior of  $\alpha(E)$  in the complex  $\alpha$  plane.

A typical locus of  $\alpha(E)$  in the complex angular momentum plane is shown in the sketch below.



The imaginary part  $\text{Im}\alpha(E)$  vanishes for  $E < 0$ . Whenever  $\text{Re}\alpha(E)$  passes through positive integer  $l$  with  $d[\text{Re}\alpha(E)]/dE > 0$ , a bound state or resonance of spin  $l$  occurs, provided  $\text{Im}\alpha(E)$  is small. In the sketch, for example, A is a bound state, and B, C, D are resonances. This family of bound states and resonances appear as recurrences of the same state. Other families can occur as well, and will be characterized by other trajectories. Each family is characterized by the principal quantum number (i.e. the number of nodes in the radial wave function). The points B', C', D' do not correspond to identifiable resonances, because the poles corresponding to them are far from the physical region. Actually, each trajectory  $\alpha(E)$  has a complex conjugate partner represented by its mirror image with respect to the  $\text{Re } \alpha$  axis. The mirror images of B, C, D and B', C', D' all lie too far from the physical region to be identifiable as resonances. Another way to exhibit the resonances is to plot  $\text{Re}\alpha(E)$  against  $E$ , as shown in the sketch below.



To see the correspondence between the new way and the old way of describing a resonance, let us examine  $F(E, l)$  near  $l = \alpha(E)$ :

$$F(E, l) \approx \frac{\beta(E)}{l - \alpha(E)} \quad (1.7)$$

Suppose that for some real value  $E = E_n$  we have  $\text{Re}\alpha(E_n) = n$ . Then in the neighborhood of  $E = E_n$  we can write

$$\text{Re}\alpha(E) \cong n + \alpha'(E - E_n), \quad \alpha' \equiv \frac{d\alpha}{dE} (E = E_n) \quad .$$



Hence

$$\begin{aligned}
 F(E, n) &\approx \frac{\beta(E_n)}{n - \alpha(E)} \\
 &\approx \frac{\beta(E_n)}{n - [n + \alpha'(E - E_n)] - i \operatorname{Im}\alpha(E_n)} \\
 &= -\frac{1}{\alpha'} \frac{\beta(E_n)}{E - E_n + i \frac{\operatorname{Im}\alpha}{\alpha'}}
 \end{aligned}
 \tag{1.8}$$

If  $\alpha' > 0$ , this is the familiar Breit-Wigner formula for a resonance with mass  $E_n$  and total width  $2 \frac{\operatorname{Im}\alpha(E_n)}{\alpha'}$ . If  $\alpha' < 0$ , there is still a pole on the second sheet, but it is not close to the physical region.

B. Sommerfeld-Watson Transform: To isolate the contribution of a Regge trajectory to the scattering amplitude, we write the partial-wave series in the form of a contour integral. Noting that  $1/\sin\pi\ell$  has poles at integer values of  $\ell$ , and

$$\operatorname{Res} \left[ \frac{\pi(-1)^\ell}{\sin\pi\ell} \right] = 1, \quad \ell=0, \pm 1, \pm 2, \dots$$

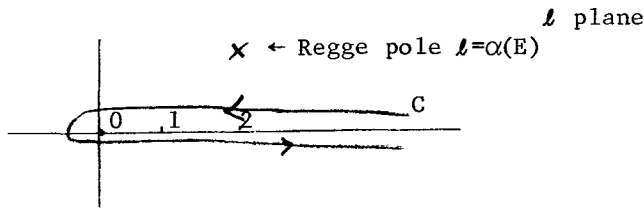
we have

$$f(E, z) = \sum_{\ell=0}^{\infty} (2\ell+1) P_\ell(z) F(E, \ell) = \frac{1}{2\pi i} \int_C d\ell \frac{\pi}{\sin\pi\ell} P_\ell(-z) F(E, \ell) \tag{1.9}$$

where we have used

$$P_\ell(-z) = (-1)^\ell P_\ell(z) \tag{1.10}$$

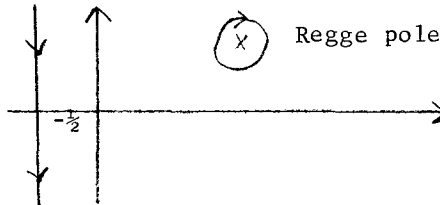
and where  $C$  is the contour shown in the accompanying sketch



For fixed  $|z| \leq 1$ ,

$$P_\ell(-z) \xrightarrow{|\ell| \rightarrow \infty} \frac{C}{(\ell)^{\frac{1}{2}}} e^{-\theta |\operatorname{Im}\ell|}, \quad (z = \cos\theta) \tag{1.11}$$

Since  $F(E, \ell) \rightarrow 0$  as  $|\ell| \rightarrow \infty$ , we can expand the contour, drop the piece at infinity, and pick up the Regge poles:



$$f(E, z) = \sum_{\alpha} \left[ - \frac{\pi(2\alpha+1)R(E)P_{\alpha}(-z)}{\sin\pi\alpha} \right] + \frac{1}{2i} \int_{-\frac{1}{2}+i\infty}^{-\frac{1}{2}-i\infty} d\ell \frac{P_{\ell}(-z)}{\sin\pi\ell} F(E, \ell) . \quad (1.12)$$

$\text{Re}\alpha > -\frac{1}{2}$

The term in brackets represents the contribution from a Regge trajectory  $\alpha(E)$ , which contains the effects of a whole family of bound states and resonances.

The original partial-wave expansion converges only for  $z$  lying in an ellipse with foci  $\pm 1$  (the Lehmann ellipse), but with (12) we can continue it outside of the ellipse. In particular (12) has a simple asymptotic form for  $|z| \rightarrow \infty$ . The region is of course unphysical for potential scattering; but for relativistic scattering it corresponds to high energy in the crossed channel. To obtain the asymptotic behavior we note

$$P_{\alpha}(z) \xrightarrow{|z| \rightarrow \infty} \frac{1}{(\pi)^{\frac{1}{2}}} \frac{\Gamma(\alpha + \frac{1}{2})}{\Gamma(\alpha + 1)} (2z)^{\alpha} \left[ 1 + O(z^{-2}) \right], \quad (\text{Re } \alpha > -\frac{1}{2}) . \quad (1.13)$$

Hence as  $|z| \rightarrow \infty$ ,

$$f(E, z) \sim \sum_{\text{Re}\alpha > -\frac{1}{2}} \left[ -(\pi)^{\frac{1}{2}} \frac{(2\alpha+1)}{\sin\pi\alpha} \frac{\Gamma(\alpha + \frac{1}{2})}{\Gamma(\alpha + 1)} (-2z)^{\alpha} \right] + O(z^{-\frac{1}{2}}), \quad (1.14)$$

where the term  $O(z^{-\frac{1}{2}})$  comes from the "background" integral in (12). If there are Regge poles with  $\text{Re}\alpha(E) > -\frac{1}{2}$ , then the highest one dominates the asymptotic behavior.

If there are no Regge poles with  $\text{Re}\alpha(E) > -\frac{1}{2}$ , then we learn nothing from (14). It won't help to push the background integral further to the left, even if that is possible. The reason is that  $P_{\alpha}(z) = P_{-\alpha-1}(z)$ , so that for  $\text{Re}\alpha < -\frac{1}{2}$  the asymptotic behavior of  $P_{\alpha}(-z)$  is

$$P_{\alpha}(z) \xrightarrow{|z| \rightarrow \infty} \frac{1}{(\pi)^{\frac{1}{2}}} \frac{\Gamma(-\alpha-\frac{1}{2})}{\Gamma(-\alpha)} (2z)^{-\alpha-1} [1+O(z^{-2})], \quad (\text{Re}\alpha < -\frac{1}{2}) \quad (1.15)$$

instead of (13), hence the background integral would still dominate over the pole contributions. Thus, we need to know something about the background integral in (12), and the Mandelstam symmetry comes to our aid.

C. Mandelstam Symmetry: The Mandelstam symmetry states

$$F(E, \ell) = F(E, -\ell-1) \text{ for } \ell = \text{half-integer.} \quad (1.16)$$

Note that the radial equation (4) is invariant under  $\ell \rightleftharpoons -\ell-1$ . If  $V(r) \rightarrow \infty$  faster than  $r^{-2}$  as  $r \rightarrow 0$ , so that it dominates over the centrifugal potential  $\ell(\ell+1)/r^2$ , then  $u_{\ell}(r)$  vanishes at  $r=0$  in a manner independent of  $\ell$ . In this case it is clear that the Mandelstam symmetry holds not only for half integers, but for all  $\ell$ . If, however, the centrifugal potential dominates over  $V(r)$  near  $r=0$ , then the two solutions to the radial equation have the respective behaviors

$$u_{\ell} \xrightarrow{r \rightarrow 0} \begin{cases} r^{\ell} \\ r^{-\ell-1} \end{cases} \quad (1.17)$$

For  $l > 0$  we must choose the first solution, while for  $l < 0$  we must choose the second solution. It turns out that the Mandelstam symmetry holds only for half-integer  $l$ .

We make use of the Mandelstam symmetry to do the Sommerfeld-Watson transform in a different way. First let us define

$$\mathcal{P}_l(z) = \begin{cases} P_l(z) & l = 0, 1, 2, \dots \\ 0 & l = -1, -2, \dots \end{cases} \quad (1.18)$$

This function can be continued to complex  $l$ :

$$\mathcal{P}_l(z) = -\frac{\tan \pi l}{\pi^{\frac{1}{2}}} Q_{-l-1}(z) = \frac{1}{(\pi)^{\frac{1}{2}}} \frac{\Gamma(l + \frac{1}{2})}{\Gamma(l + 1)} (2z)^l F\left(-\frac{l}{2}, \frac{1-l}{2}, \frac{1}{2} - l; \frac{1}{z^2}\right) \quad (1.19)$$

with asymptotic behavior

$$\mathcal{P}_l(z) \xrightarrow{|z| \rightarrow \infty} \frac{1}{(\pi)^{\frac{1}{2}}} \frac{\Gamma(l + \frac{1}{2})}{\Gamma(l + 1)} (2z)^l \left[ 1 + O(z^{-2}) \right], \quad (1.20)$$

which holds for all  $l$ . We note that  $\mathcal{P}_l(z)$  has simple poles at half-integer  $l$ , with residues given by

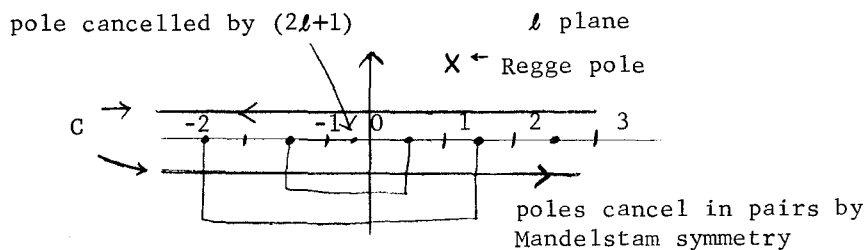
$$\text{Res } \mathcal{P}_l(z) = \frac{(-)^{l-\frac{1}{2}}}{\pi} Q_{-l-1}(z), \quad (l = \text{half-integer}) \quad (1.21)$$

$$\text{Res } \mathcal{P}_l(z) = -\text{Res } P_{-l-1}(z), \quad (l = \text{half-integer}) \quad (1.22)$$

The last equality comes from the well-known equality  $Q_l(z) = Q_{-l-1}(z)$  at half-integer  $l$ . We now write

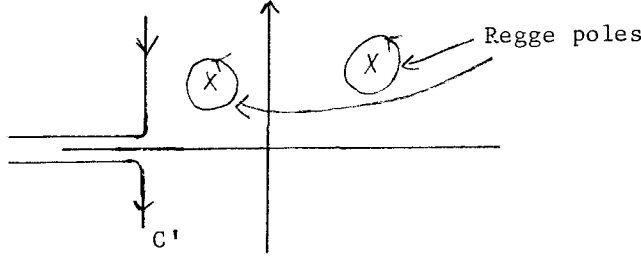
$$f(E, z) = \sum_{l=-\infty}^{\infty} (2l + 1) F_l(E) \mathcal{P}_l(z) = \frac{1}{z_1} \int_C \frac{dl}{\sin \pi l} (2l + 1) F(E, l) \mathcal{P}_l(z), \quad (1.23)$$

where the contour  $C$  is shown in the accompanying sketch.



The poles of  $\mathcal{P}_l(z)$  at half-integer  $l$  do not give spurious contributions to the integral because the one at  $l = \frac{1}{2}$  is cancelled by the factor  $(2l + 1)$ , and the other cancels in pairs by (16) and (22).

We now expand the contour and discard the contribution from infinity,



and obtain

$$f(E, z) = \sum_{\text{Re } \alpha > -L} \left[ \frac{-\pi \beta(2\alpha + 1)}{\sin \pi \alpha} P_{\alpha}(-z) \right] + \text{background integral.} \quad (1.24)$$

Hence

$$f(E, z) \underset{|z| \rightarrow \infty}{\sim} \sum_{\text{Re } \alpha > -L} \left[ -(\pi)^{\frac{1}{2}} \frac{\beta(2\alpha + 1)}{\sin \pi \alpha} \frac{\Gamma(\alpha + \frac{1}{2})}{\Gamma(\alpha + 1)} (-2z)^{\alpha} \right] + o(z^{-L}). \quad (1.25)$$

In this representation, the Regge poles always dominate the background integral.

D. Exchange Potential and Signature: Suppose we have an exchange potential

$$V(r) = V_1(r) + V_2(r)P \quad (1.26)$$

where

$$Pf(\vec{r}) = f(-\vec{r}) \quad (1.27)$$

Then the effect potential is different for even and odd partial waves, for the radial equation reads

$$\frac{d^2 u_{\ell}}{dr^2} + E u_{\ell} = \left[ \frac{\ell(\ell + 1)}{r^2} + V_1 + (-1)^{\ell} V_2 \right] u_{\ell}.$$

Since  $(-1)^{\ell}$  does not have a unique analytic continuation in  $\ell$ , we separately continue the two equations

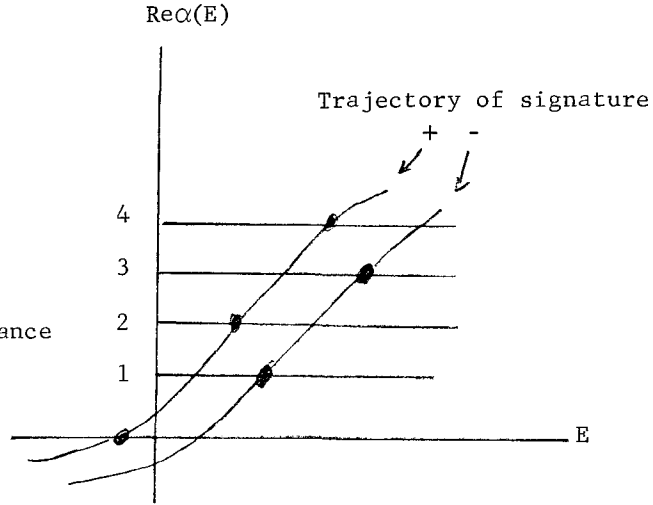
$$\frac{d^2 u_{\ell}^{\pm}}{dr^2} + E u_{\ell}^{\pm} = \left[ \frac{\ell(\ell + 1)}{r^2} + V_1 \pm V_2 \right] u_{\ell}^{\pm}$$

and obtain from them the two partial wave amplitudes  $F^{\pm}(E, \ell)$ . Clearly

$$\begin{aligned} F^{+}(E, \ell) &= F_{\ell}^{+}(E), (\ell \text{ even}) \\ F^{-}(E, \ell) &= F_{\ell}^{-}(E), (\ell \text{ odd.}) \end{aligned} \quad (1.28)$$

We refer to  $F^{\pm}(E, \ell)$  as partial-wave amplitudes of even (odd) signature. Regge poles occurring in  $F^{\pm}(E, \ell)$  will be characterized by signature. An even (odd) signed Regge pole produces a resonance only where it passes through an even (odd) integer

value. We illustrate this in the accompanying sketch. The two signatured trajectories become degenerate if either  $V_1=0$ , or  $V_2=0$ . Such a degeneracy is called exchange degeneracy.



● denotes a bound state or resonance

To carry out the Watson-Sommerfeld transform write

$$\begin{aligned}
 f(E, z) &= \sum_{l \text{ even}} (2l + 1) F^+(E, l) \mathcal{P}_l(z) + \sum_{l \text{ odd}} (2l + 1) F^-(E, l) \mathcal{P}_l(z) \\
 &= \frac{1}{2} \sum_{l = -\infty}^{\infty} (2l + 1) F^+(E, l) [\mathcal{P}_l(z) + \mathcal{P}_l(-z)] \\
 &\quad + \frac{1}{2} \sum_{l = -\infty}^{\infty} (2l + 1) F^-(E, l) [\mathcal{P}_l(z) - \mathcal{P}_l(-z)] \quad . \quad (1.29)
 \end{aligned}$$

Then, in a manner analogous to the earlier development, we obtain

$$\begin{aligned}
 &+ (E, z) \sum_{\alpha \text{ of } + \text{ signature}} \left\{ \frac{-\pi\beta(2d + 1)}{2 \sin\pi\alpha} [\mathcal{P}_\alpha(-z) + \mathcal{P}_\alpha(z)] \right\} \\
 &+ \sum_{\alpha \text{ of } - \text{ signature}} \left\{ - \frac{\pi\beta(2\alpha + 1)}{2 \sin\pi\alpha} [\mathcal{P}_\alpha(-z) - \mathcal{P}_\alpha(z)] \right\} \quad (1.30)
 \end{aligned}$$

+ (Background integrals).

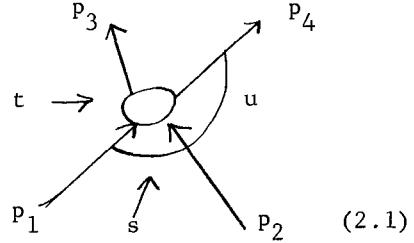
## II. Relevance of Regge Poles to Relativistic Scattering

We discuss some motivations for taking over the ideas of Regge poles from the realm of potential scattering, where it is proved, to the realm of relativistic scattering, where it is unproved. There is a practical and a theoretical motivation. The former rests on the hope that Regge poles will lead to a simple description of high energy scattering. The latter is based on the fact that the bootstrap hypothesis seems to find a concrete expression in terms of Regge poles.

### A. High-Energy Scattering

To illustrate the role of Regge poles in high-energy scattering, consider the elastic scattering of spinless particles of equal mass, represented schematically by the sketch shown, with

$$\begin{aligned} s &= (p_1 + p_2)^2 = 4(k^2 + m^2) \\ t &= (p_1 - p_3)^2 = -2k^2(1 - \cos\theta) \\ u &= (p_1 - p_4)^2 = -2k^2(1 + \cos\theta) \end{aligned}$$



where  $k$  and  $\theta$  are the center of mass three-momentum and scattering angle, respectively.

Let the scattering amplitude  $f(s, t)$  describe the  $s$ -channel reaction  $p_1 + p_2 \rightarrow p_3 + p_4$  for  $s > 4m^2$ ,  $t < 0$ . Then by crossing symmetry, the same function  $f(s, t)$  describes the  $t$ -channel reaction  $p_1 + \bar{p}_3 \rightarrow \bar{p}_2 + p_4$  when analytically continued to the region  $t > 4m^2$ ,  $s < 0$ . Similarly, if  $f(s, t)$  is analytically continued to the region  $u = 4m^2 - s - t > 4m^2$ ,  $s < 0$ ,  $t < 0$ , it describes the  $u$ -channel reaction  $p_1 + \bar{p}_4 \rightarrow \bar{p}_2 + p_3$ . Of course no such crossing symmetry exists in the case of potential scattering.

We now make a partial wave expansion in the  $s$ -channel:

$$f(s, t) = \sum_{\ell=0}^{\infty} (2\ell+1) F_{\ell}(s) P_{\ell}(z) \quad (2.2)$$

where

$$z = \cos\theta = 1 + \frac{t}{2k^2} \quad (2.3)$$

Suppose that we can continue  $F_{\ell}(s)$  into the complex  $\ell$  plane and carry out the Sommerfeld-Watson transform. Then, if the only singularities are simple poles, we will obtain as in potential scattering

$$f(s, t) \xrightarrow{(z) \rightarrow \infty} - \frac{\pi \beta(2\alpha+1)}{\sin\pi\alpha} P_{\alpha}(-z) \quad (2.4)$$

where  $\alpha(s)$  is the leading Regge pole in the  $s$ -channel. Using (2.3) and the asymptotic form of  $P_{\alpha}$ , we have

$$f(s,t) \xrightarrow[t \rightarrow \infty]{s \text{ fixed}} C(s)t^{\alpha(s)} , \quad (2.5)$$

which says that the energy dependence of high-energy t-channel scattering at fixed s is governed by the leading Regge pole in the s-channel. Similarly, for the s-channel reaction, forward scattering ( $\theta \rightarrow 0$ ) is governed by the leading t-channel Regge pole, and backward scattering ( $\theta \rightarrow \pi$ ) is governed by the leading u-channel Regge pole.

$$f(s,t) \xrightarrow[s \rightarrow \infty]{t \text{ fixed}} C(t)s^{\alpha(t)} \quad (2.6)$$

$$f(s,t) \xrightarrow[s \rightarrow \infty]{u \text{ fixed}} C(u)s^{\alpha(u)} . \quad (2.7)$$

We have not bothered to distinguish the trajectory  $\alpha$  in (2.5), (2.6), (2.7), but of course they need not be the same trajectory. The t-channel trajectory, for example, generates bound states resonances having the quantum numbers of the t-channel, and will be characterized by these quantum numbers. We assume that the trajectory function  $\alpha$  is independent of the external particles in the scattering process, and speak of "Regge pole exchange" in analogy with single-particle exchange. As we can see from (2.6) the salient feature of Regge pole exchange is that asymptotically the scattering amplitude is proportional to the  $\alpha^{\text{th}}$  power of the squared c.m. energy, where  $\alpha$  is the variable spin of the object exchanged in the crossed channel. As we change the momentum transfer t, the spin varies along the Regge trajectory. This furnishes a simple and physically attractive picture of high energy scattering.

#### B. The Bootstrap Idea

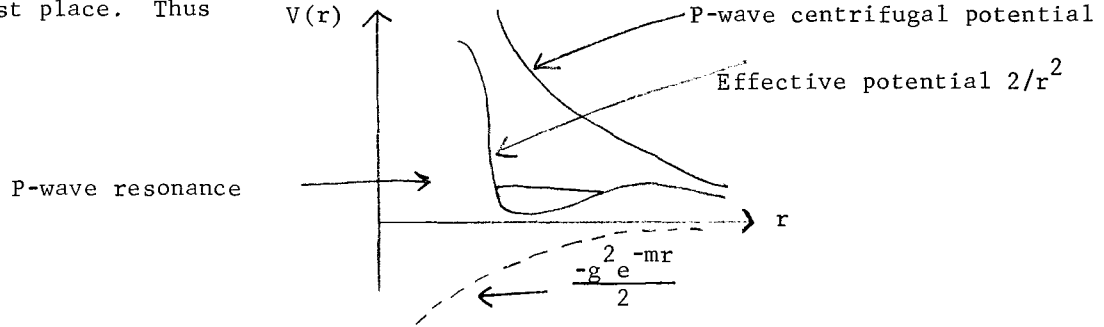
The bootstrap idea, first proposed by Chew and Mandelstam, is that among the hadrons there are no "elementary" particles, but that they are composite states of one another. It has been difficult to state this idea in a form that is both sufficiently practical and sufficiently precise, so that one may use it in an actual calculation. To appreciate the difficulty, let us look at some attempts at formulation.

A simple-minded example, which illustrates the idea, but which does not give a consistent scheme for calculation, is the following. Suppose we calculate  $\pi\text{-}\pi$  scattering by solving a non-relativistic Schrödinger equation with an attractive Yukawa potential

$$V(r) = -g^2 \frac{e^{-mr}}{r} , \quad (2.8)$$

which we regard as the adiabatic potential due to the exchange of a  $\rho$  meson of mass

m and coupling constant g. The P-wave phase shift,  $\delta_1(E;m,g)$  will then depend on the energy E of the  $\pi\pi$  system, as well as on the parameters m and g. If m and g are appropriately chosen the P-wave effective potential, as shown in the sketch below, can accommodate a resonance, whose position and width depend on m and g. The bootstrap requires that this resonance be the  $\rho$  meson that generated the potential in the first place. Thus



$\delta_1$  should pass through  $\pi/2$  at  $E = m$ , with a slope consistent with the decay width  $\Gamma$  for  $p \rightarrow \pi\pi$ :

$$\Gamma = g^2 C(\mu, m) \quad , \quad (2.9)$$

where C depends on the pion mass  $\mu$  and the  $\rho$  mass m in a known way. The relation between  $\Gamma$  and the phase shift may be obtained by noting

$$e^{i\delta_1} \sin \delta_1 = \frac{1}{\cot \delta_1 - i} \approx \frac{1}{\delta_1'(E_0)} \frac{1}{E - E_0 + [i/\delta_1'(E_0)]} \quad (2.10)$$

where  $\delta_1' = \partial \delta_1 / \partial E$ , and  $E_0$  is such that  $\delta_1(E_0) = \pi/2$ . Thus we require

$$\begin{aligned} \delta_1(m; m, g) &= \pi/2 \\ \delta_1'(m; m, g) &= \frac{2}{g^2 C(\mu, m)} \end{aligned} \quad (2.11)$$

from which  $m/\mu$  and g can be determined. This, however, is not a real example because the potential (2.8) is actually incorrect for spin 1 exchange, and there is no simple way to find a "correct" version. Also, pions don't obey the Schrödinger equation. A general way to state the bootstrap idea is that the requirements of analyticity, crossing symmetry, and unitarity, plus "boundary conditions" of some kind, should completely determine all scattering amplitudes, including the existence of particle poles, and their location and residues. To make this precise, one has to be more specific about the "boundary conditions". A suggestion that has underlined many practical calculations (the so-called N/D calculations) is to impose Levinson's theorem, taken over from potential scattering:

$$\delta_l(E=0) - \delta_l(E = \infty) = \pi N_l \quad (2.12)$$



where  $\delta_\ell(E)$  is the  $\ell^{\text{th}}$  wave phase shift, and  $N_\ell$  is the number of bound states (not resonances, but bound states), of spin  $\ell$ . When inelastic channels are open, one would replace  $\delta_\ell(E)$  by eigen-phase shifts. The idea expressed by (2.12) is that, since  $N_\ell=0$  when there is no interaction (i.e., when  $\delta_\ell \equiv 0$ ), there would be no "elementary" bound state. In mathematical examples\* in which (2.12) can be rigorously imposed, one does find that it determines the number of bound states and resonances that can occur, and places restrictions on their positions and coupling constants. But its general consequences has not been fully explored, owing to the difficulty in using it in a full relativistic scattering problem.

Instead of the Levinson theorem, it seems far simpler, and more satisfactory to take over from potential scattering the idea that all particles lie on Regge trajectories. The statement is precise, and is independent of a detailed formulation of the dynamical equations. It has the immediate experimental consequence that all known p hadrons should be classifiable according to Regge trajectories, which should also control the asymptotic behavior of scattering amplitudes.

### C. Chew-Frautschi Plot

We can immediately test the hypothesis that all hadrons lie on Regge trajectories by plotting the spin vs.  $(\text{mass})^2$  for known hadrons, resulting in what is known as Chew-Frautschi plots, as shown in the following figures. The trajectories that one might postulate from such a plot can be tested experimentally by analyzing high energy scattering data. A striking feature is that all known trajectories seem to be straight lines. The presence of the  $f^0$  at spin 2 on the  $\rho$  trajectory suggests that there is exchange degeneracy of the  $\rho$  and  $f$  trajectories.

---

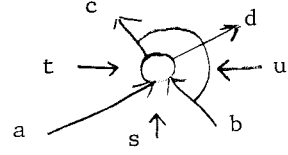
\* K. Huang and A.H. Mueller, Phys. Rev. 140, B365 (1965).

### III. Relativistic Scattering of Spinless Particles

#### A. Preliminaries

We consider the two body scattering process  $a+b \rightarrow c+d$ , and define as usual

$$\begin{aligned} s &= (p_a + p_b)^2 = ((p_{ab}^2 + m_a^2)^{\frac{1}{2}} + (p_{ab}^2 + m_b^2)^{\frac{1}{2}})^2 \\ t &= (p_a - p_c)^2 \\ u &= (p_b - p_c)^2 \end{aligned} \quad (3.1)$$



where  $p_{ab}$  is the magnitude of the three-momentum in the center of mass of  $a$  and  $b$ . These variables satisfy

$$s+t+u = \sum_{i=1}^4 m_i^2 \quad . \quad (3.2)$$

We write the S matrix for this process as

$$s = 1+iT \quad (3.3)$$

where

$$\langle cd|T|ab \rangle = (2\pi)^4 \delta^4(p_a + p_b - p_c - p_d) f(s,t) \quad (3.4)$$

where  $f(s,t)$  is Lorentz invariant, provided single-particle states are so normalized that the phase-space volume for one particle is invariant:

$$\int_{\text{one-particle states}} = \frac{1}{(2\pi)^3} \int \frac{d^3p}{E_p} \sum_{\alpha} \quad (3.5)$$

where  $\alpha$  indicates quantum numbers other than momentum. The differential cross section is

$$\frac{d\sigma}{d\Omega} = \frac{1}{4\pi^2 s} \frac{p_{cd}}{p_{ab}} |f(s,t)|^2 \quad (3.6)$$

Crossing symmetry states that  $f(s,t)$  describes different reactions in different domains of its arguments. The three reactions, or channels, are as follows:

$$\begin{aligned} \text{s-channel: } a+b &\rightarrow c+d, \text{ for } s > \max [(m_a + m_b)^2, (m_c + m_d)^2] \quad , \\ \text{t-channel: } a+\bar{c} &\rightarrow b+\bar{d}, \text{ for } t > \max [(m_a + m_c)^2, (m_b + m_d)^2] \quad , \\ \text{u-channel: } b+\bar{c} &\rightarrow \bar{a}+d, \text{ for } u > \max [(m_b + m_c)^2, (m_a + m_d)^2] \quad . \end{aligned} \quad (3.7)$$

We assume that  $f(s,t)$  can be analytically continued from one of these domains to another.

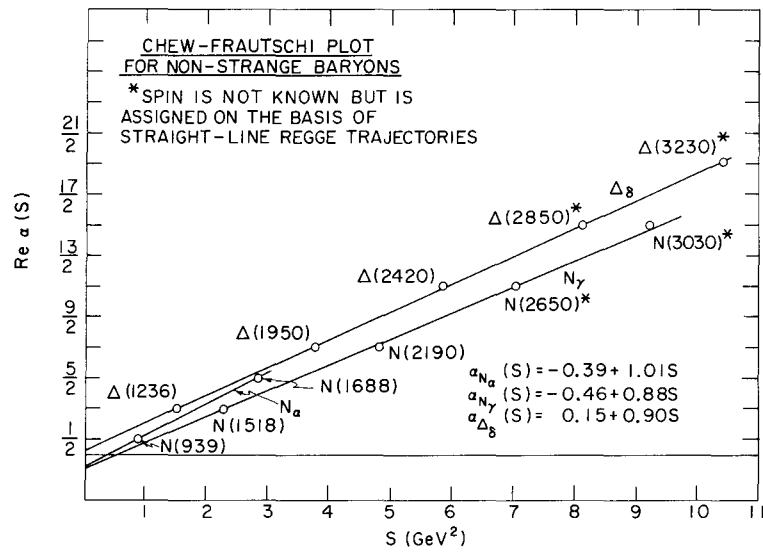
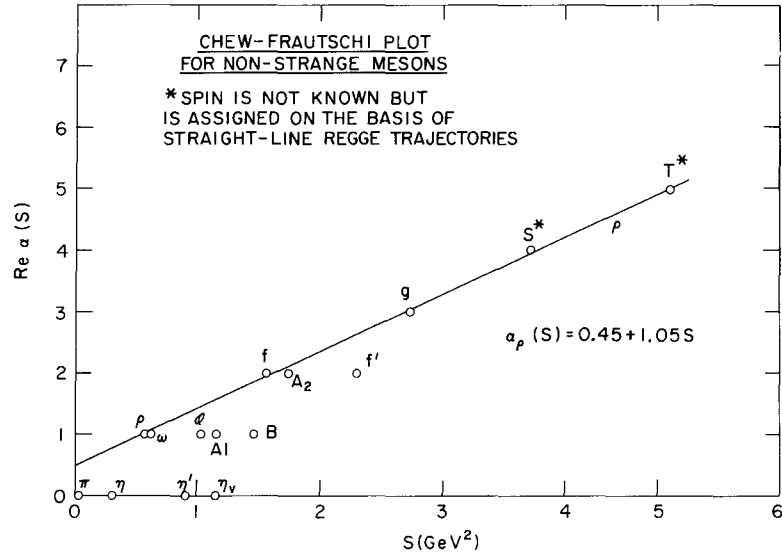
Unitarity states that  $S^\dagger S = 1$ , or

$$\frac{1}{2i}(T-T^\dagger) = \frac{1}{2}T^\dagger T \quad , \quad (3.8)$$

and time reversal invariance implies

$$\langle \alpha|T|\beta \rangle = \langle \beta|T|\alpha \rangle \quad . \quad (3.9)$$

Then, taking the matrix element of (3.8) we obtain



$$\text{Im}f_{ab \rightarrow cd}(s,t) = \frac{1}{2} \sum_n f_{cd \rightarrow n}^* (2\pi)^4 \delta^4(p_a - p_c - p_d) f_{ab \rightarrow n}. \quad (3.10)$$

The optical theorem reads

$$\text{Im}f_{ab \rightarrow ab}(s,0) = \frac{1}{2} k(s)^{\frac{1}{2}} \sigma_T(s) \quad (3.11)$$

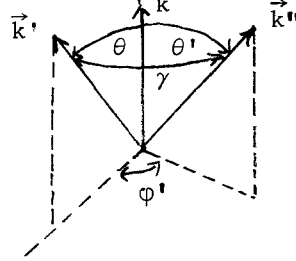
where  $\sigma_T(s)$  is the total cross section for  $a+b \rightarrow$  anything. By virtue of (3.10)  $f(s,t)$  has a series of branch cuts in  $s$ , with branch points at the various thresholds for  $ab \rightarrow n$ . The right hand side of (3.10) gives the discontinuities across the cuts. The discontinuity across the elastic cut is given by the elastic unitarity relation

$$\text{Im}f(s,t) = \frac{1}{8\pi^2} \frac{k}{(s)^{\frac{1}{2}}} \int d\Omega' f^*(s,t_1) f(s,t_2) \quad (3.12)$$

where, in the equal mass case,

$$\begin{aligned} t &= -2k^2(1-\cos\theta) \\ t_1 &= -2k^2(1-\cos\theta') \\ t_2 &= -2k^2(1-\cos\gamma) \\ \cos\gamma &= \cos\theta\cos\theta' + \sin\theta\sin\theta'\cos\phi' \end{aligned} \quad (3.13)$$

The geometrical relationship among the angles is shown below.



We can expand the two-body scattering amplitude  $f(s,t)$  in partial waves:

$$f(s,t) = \sum_{\ell=0}^{\infty} (2\ell+1) P_{\ell}(z_s) F_{\ell}(s). \quad (3.14)$$

If  $f$  is an elastic amplitude, then elastic unitarity takes the simple form

$$\text{Im}F_{\ell}(s) = \frac{1}{2\pi} \frac{k}{(s)^{\frac{1}{2}}} |F_{\ell}(s)|^2, \quad (3.15)$$

with the solution

$$F_{\ell}(s) = \frac{\pi(s)^{\frac{1}{2}}}{ik} (e^{2i\delta_{\ell}(s)} - 1), \quad \text{Im}\delta_{\ell}(s) \geq 0. \quad (3.16)$$

If the elastic threshold is the lowest threshold then  $\text{Im}\delta_{\ell}(s) = 0$ . Using the orthogonality of the Legendre polynomials, we can invert the partial wave expansion to obtain

$$F_{\ell}(s) = \frac{1}{2} \int_{-1}^{+1} dz P_{\ell}(z) f(s,t(z)), \quad (\ell=0,1,2,\dots) \quad (3.17)$$

### B. Froissart-Gribov Continuation

We wish to continue  $F_\ell(s)$  into the complex plane so that we may study its poles and other singularities there. In potential scattering this could be done by solving the Schrödinger equation for complex  $\ell$ . In relativistic scattering we must make use of dynamical assumptions. A guide to the analytic continuation is

**Carlson's Theorem:** Let  $f(z)$  be analytic for  $\text{Re} z \geq 0$ . Suppose  $f(z) = 0$  for  $z = 0, 1, 2, \dots$ , and that  $|f(z)| < \text{const} \times e^{\pi|z|}$  as  $|z| \rightarrow \infty$ . Then  $f(z) = 0$  for all  $\text{Re} z \geq 0$ .

Hence if we can find an analytic function  $F(E, \ell)$  which reduces to  $F_\ell(E)$  for  $\ell = 0, 1, 2, \dots$  and which grows less fast than  $e^{\pi|\ell|}$ , then we know that any other analytic continuation must grow at least as fast as  $e^{\pi|\ell|}$ . Since  $P_\ell(z)$  grows essentially like  $e^{\pi z|\ell|}$  for  $-1 < z < 1$ , and therefore does not possess a unique continuation, we have to examine the properties of  $f(s, t)$  to see whether  $F_\ell(s)$  has a unique continuation. We assume that  $f(s, t)$  satisfies an  $N$ -times subtracted dispersion relation at fixed  $s$ :

$$f(s, t) = \frac{t^N}{\pi} \int_{t_0}^{\infty} \frac{dt'}{t'^N} \frac{A_t(s, t')}{t' - t} + \frac{u^N}{\pi} \int_{u_0}^{\infty} \frac{du'}{u'^N} \frac{A_u(s, u')}{u' - u} + \sum_{i=0}^{N-1} a_i(s) t^i. \quad (3.18)$$

The first term gives rise to the analog of a potential, and the second term an exchange potential. Now both  $t$  and  $u$  are linear functions of  $z \equiv z_s$ , of the forms  $t = az + b$ ,  $u = -a'z + b'$ , where  $a > 0$ ,  $a' > 0$  in the  $s$ -channel physical region. Hence (3.18) may be rewritten in the  $s$ -channel physical region, as

$$f(s, z) = \frac{z^N}{\pi} \int_{z_1}^{\infty} \frac{dz'}{z'^N} \frac{D_1(s, z')}{z' - z} + (-1)^N \frac{z^N}{\pi} \int_{z_2}^{\infty} \frac{dz'}{z'^N} \frac{D_2(s, z')}{z' + z} + \sum_{i=0}^{N-1} c_i(s) z^i,$$

$$D_1(s, z) = A_t(s, t(z)), \quad D_2(s, z) = A_u(s, u(-z)), \quad z_1 \geq 1, \quad z_2 \geq 1. \quad (3.19)$$

For  $\ell = 0, 1, 2, \dots$ , (3.17) is certainly valid, and we can substitute (3.19) into it and interchange the order of integration to obtain

$$F_\ell(s) = \frac{1}{\pi} \int_{z_1}^{\infty} \frac{dz'}{z'^N} D_1(s, z') \frac{1}{2} \int_{-1}^{+1} dz \frac{z^N}{z' - z} P_\ell(z) + (-1)^N \frac{1}{\pi} \int_{z_2}^{\infty} \frac{dz'}{z'^N} D_2(s, z') \frac{1}{2} \int_{-1}^{+1} dz \frac{z^N}{z' + z} P_\ell(z) + \sum_{i=0}^{N-1} c_i(s) \frac{1}{2} \int_{-1}^{+1} dz z^i P_\ell(z). \quad (3.20)$$

Now

$$\begin{aligned}\frac{z^N}{z'-z} &= \frac{[(z-z')+z']^N}{z'-z} = -(z-z')^{N-1} - Nz'(z-z')^{N-2} - \dots + \frac{z'^N}{z'-z} \\ \frac{z^N}{z'+z} &= \frac{[(z+z')-z']^N}{z'+z} = +(z+z')^{N-1} - Nz'(z+z')^{N-2} + \dots + (-1)^N \frac{z'^N}{z'+z}.\end{aligned}\quad (3.21)$$

If  $\ell > N$ , then the polynomials do not contribute, and we obtain

$$F_\ell(s) = \frac{1}{\pi} \int_{z_1}^{\infty} dz' D_1(s, z') \frac{1}{2} \int_{-1}^{+1} dz \frac{P_\ell(z)}{z'-z} + \frac{1}{\pi} \int_{z_2}^{\infty} dz' D_2(s, z') \frac{1}{2} \int_{-1}^{+1} dz \frac{P_\ell(z)}{z'+z}.\quad (3.22)$$

Noting that

$$\frac{1}{2} \int_{-1}^{+1} dz \frac{P_\ell(z)}{z'-z} = Q_\ell(z')\quad (3.23)$$

we have

$$F_\ell(s) = \frac{1}{\pi} \int_{z_1}^{\infty} dz' D_1(s, z') Q_\ell(z') + \frac{1}{\pi} \int_{z_2}^{\infty} dz' D_2(s, z') Q_\ell(-z'),\quad (\ell=N, N+1, N+2, \dots).\quad (3.24)$$

Recall that for integer  $\ell$ ,

$$Q_\ell(-z) = (-1)^\ell Q_\ell(z)\quad (3.25)$$

so that

$$F_\ell(s) = \frac{1}{\pi} \int_{z_1}^{\infty} dz' D_1(s, z') Q_\ell(z') + (-1)^\ell \frac{1}{\pi} \int_{z_2}^{\infty} dz' D_2(s, z') Q_\ell(z')\quad (3.26)$$

As in potential scattering, we are therefore led to define the signatured partial wave amplitudes

$$F_\ell^\pm(s, \ell) = \frac{1}{\pi} \int_{z_1}^{\infty} dz D_1(s, z) Q_\ell(z) \pm \frac{1}{\pi} \int_{z_2}^{\infty} dz D_2(s, z) Q_\ell(z)\quad (3.27)$$

This is the Froissart-Gribov formula. As in potential scattering we have

$$F_\ell(s) = \begin{cases} F_\ell^+(s, \ell) & (\ell=0, 2, 4, \dots) \\ F_\ell^-(s, \ell) & (\ell=1, 3, 5, \dots) \end{cases}.\quad (3.28)$$

We must still show that (3.27) defines a unique continuation of  $F_\ell(s)$  to complex  $\ell$ . By hypothesis, the dispersion relation (3.19) requires only  $N$  subtractions. Hence the integrals in (3.27) converge at least for  $\text{Re } \ell \geq N$  and so define an analytic fraction there. Also, as  $|\ell| \rightarrow \infty$ ,  $Q_\ell(z) \sim C \ell^{-\frac{1}{2}} [z + (z^2 - 1)^{\frac{1}{2}}]^{-\ell - \frac{1}{2}}$ . Hence, since  $z_1 > 1$  and  $z_2 > 1$ ,  $F_\ell^\pm(s, \ell) \rightarrow 0$  as  $|\ell| \rightarrow \infty$  and so satisfies the hypotheses of Carlson's Theorem. It therefore gives a unique analytic continuation.

The Mandelstam symmetry

$$F^{\pm}(s, \ell) = F^{\pm}(s, -\ell-1) \quad (\ell = \text{half integer}) \quad (3.29)$$

is assumed to hold. It is formally true of (3.27), for  $Q_{\ell}$  has this property. However, the integrals do not converge as they stand and the assumption is that the analytic continuation still maintains this property.

Since  $Q_{\ell}(z)$  has simple poles at  $\ell = -1, -2, \dots$ ,  $F^{\pm}(s, \ell)$  would, in general, have fixed poles (i.e.,  $s$ -independent poles) at these values of  $\ell$ . These are inadmissible by the elastic unitarity relation (3.15). For, by similar arguments given above, (3.15) can be uniquely continued to complex  $\ell$  to read

$$\frac{1}{2i} \lim_{\epsilon \rightarrow 0} [F^{\pm}(\ell, s+i\epsilon) - F^{\pm}(\ell, s-i\epsilon)] = \frac{1}{2\pi} \frac{k}{(s)^{\frac{1}{2}}} F^{\pm}(\ell, s+i\epsilon) F^{\pm}(\ell, s-i\epsilon) \quad (3.30)$$

This cannot be satisfied if  $F^{\pm}(\ell, s)$  has real fixed poles in  $\ell$ .

To get rid of them, we require their residues to vanish, namely

$$\int_{z_1}^{\infty} dz D_1(s, z) P_{\ell}^i(z) = 0 \quad (\ell=0, 1, 2, \dots, i=1, 2) \quad (3.31)$$

### C. Regge Poles

We have seen that (3.27) defines an analytic function of  $\ell$  for  $\text{Re} \ell \geq N$ . For  $\text{Re} \ell < N$ , singularities may occur, the simplest being Regge poles. They arise from a failure of the integrals in (3.27) to converge at the upper limit. Suppose

$$D_i(s, z) \xrightarrow{z \rightarrow \infty} \tilde{\beta}_i(s) z^{\alpha(s)} \quad (i=1, 2) \quad (3.31)$$

We split the integrals into two parts, for example

$$\frac{1}{\pi} \int_{z_1}^{\infty} dz D_1(s, z) Q_{\ell}(z) = \frac{1}{\pi} \left( \int_{z_1}^Z + \int_Z^{\infty} \right) dz D_1(s, z) Q_{\ell}(z) \quad (3.32)$$

where  $Z$  is fixed but arbitrarily large. The first part, being a finite integral, defines an analytic function. The second part can be evaluated using (3.31) and the fact

$$Q_{\ell}(z) \xrightarrow{z \rightarrow \infty} C z^{-\ell-1}.$$

We then obtain

$$F^{\pm}(s, \ell) = \frac{\beta_1(s) \pm \beta_2(s)}{\ell - \alpha(s)} + [\text{Terms regular at } \ell = \alpha(s)] \quad (3.33)$$

Thus  $F^{\pm}(s, \ell)$  has a Regge pole at  $\ell = \alpha(s)$ , if  $\beta_1(s) \pm \beta_2(s) \neq 0$ .

To examine the singularities of  $\alpha(s)$  and  $\beta(s)$  we keep only the parts of (3.27)

that contribute to a Regge pole:

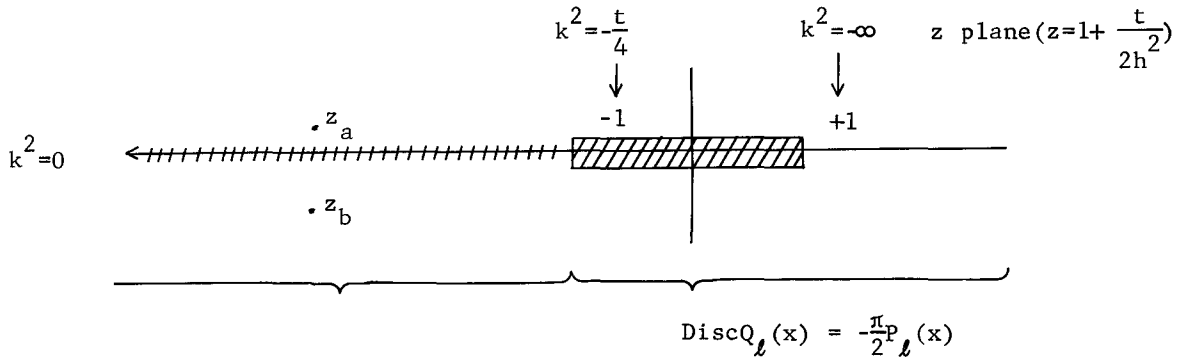
$$F_{\text{pole}}^{\pm}(s, \ell) = \frac{1}{\pi} \int_{\mathcal{C}} dz [D_1(s, z) \pm D_2(s, z)] Q_{\ell}(z) \quad (3.34)$$

This is valid in the s-channel physical region. To continue in s, we must first restore t and u as integration variables. We carry this out explicitly for the simple case of equal-mass scattering:

$$F_{\text{pole}}^{\pm}(s, \ell) = \frac{1}{2\pi k^2} \int_T^{\infty} dt [A_t(s, t) \pm A_u(s, t)] Q_{\ell}(1 - \frac{t}{2k^2}) \quad (3.35)$$

where T is positive and arbitrarily large. This can now be continued in s.

We first note that the function  $Q_{\ell}(z)$  has a cut from  $z = +1$  to  $z = -1$ , and one from  $z = -1$  to  $z = -\infty$ , with discontinuities as indicated in the sketch.



$$Q_{\ell}(z_a) = -e^{-i\pi\ell} Q_{\ell}(-z)$$

$$Q_{\ell}(z_b) = -e^{-\pi\ell} Q_{\ell}(-z)$$

$$(-z_a = -z_b = -z)$$

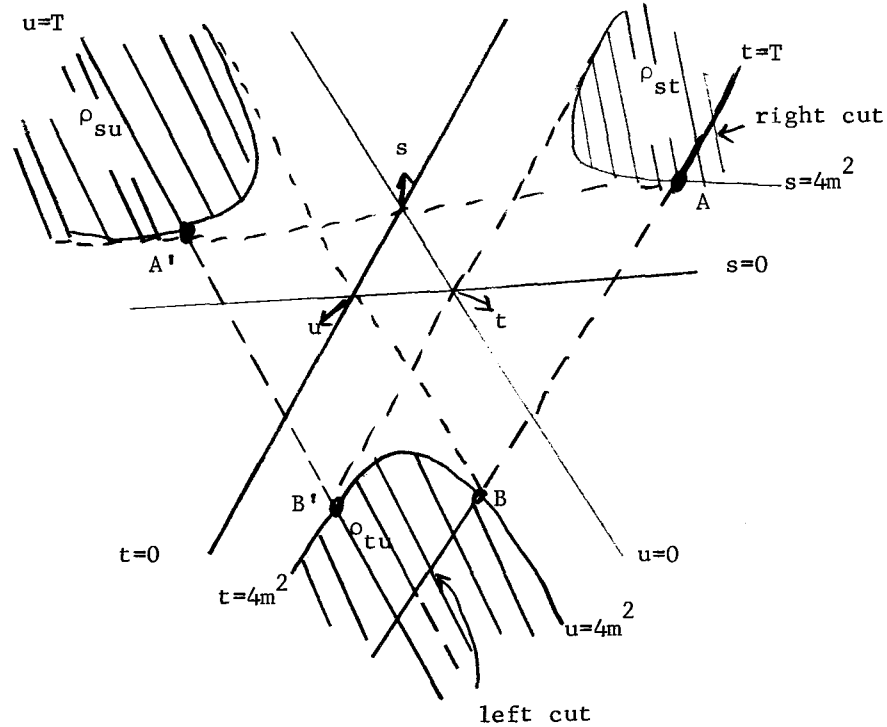
The cut from  $-1$  to  $-\infty$  gives rise to a s-cut in  $F_{\text{pole}}^{\pm}(s, \ell)$  from  $k^2 = 0$  to  $k^2 = -t/4$ . It is present only when  $\ell$  is non-integer. The combination  $(z-1)^{\ell} Q_{\ell}(z)$ , however, has no cut from  $-1$  to  $-\infty$ , even for non-integer  $\ell$ . Since  $k^2 = t/2(z-1)$ , we see that the combination  $F_{\text{pole}}^{\pm}(s, \ell)/k^{2\ell}$  has no cut from  $k^2 = 0$  to  $k^2 = -t/4$ . This means that for a Regge pole the reduced residue function

$$\bar{\beta}(s) = \beta(s)/k^{2\alpha(s)} \text{ (equal mass case)} \quad (3.36)$$

and the trajectory  $\alpha(s)$  can have only the cut from  $k^2 = -t/4$  to  $k^2 = -\infty$ , (coming from the cut of  $Q_{\ell}(z)$  from  $z = -1$  to  $z = +1$ ), plus other cuts coming from  $A_t + A_u$ . The former cut is, in fact, absent because  $t > T$ , and  $T \rightarrow \infty$ . The factor  $k^{2\ell}$  in (3.36) corresponds to the threshold condition  $\delta_{\ell}(k)_{k \rightarrow 0} \rightarrow k^{2\ell+1}$ , familiar from potential scattering.



We now examine singularities of  $F_{\text{pole}}^{\pm}$  due to those of  $A_{t-u}^{\pm}$ , which for fixed  $t$  has right and left hand cuts in  $s$ , and is real analytic. At fixed  $t$ , the  $s$ -cuts of  $A_t$  run from  $s_A(t)$  to  $\infty$ , and from  $s_B(t)$  to  $-\infty$ , as shown in the sketch below. Similarly the  $s$ -cuts of  $A_u$  run from  $s_{A'}(u)$  to  $\infty$ , and from  $s_{B'}(u)$  to  $-\infty$ . Since  $t$  is



integrated from  $T$  up, and  $T \rightarrow \infty$ , it is clear from the sketch that only the right cut remains in  $F_{\text{pole}}^{\pm}(s, \ell)$ , and it runs from  $4m^2$  to  $\infty$ . The left hand branch point recedes to  $-\infty$  because both  $B$  and  $B'$  recede to  $s = -\infty$  as  $T \rightarrow \infty$ . Therefore  $\alpha(s)$  and  $\bar{\beta}(s)$  can have a right cut, but no left cut. Since they are real analytic functions, they are real for  $s < 4m^2$ .

For the general mass case similar results are obtained. The reduced residue function is given by

$$\bar{\beta}(s) = \beta(s) / (p_{ab} p_{cd})^{\alpha(s)} \quad (3.37)$$

as a generalization of (3.36). Both  $\alpha(s)$  and  $\bar{\beta}(s)$  are real analytic functions, with possibly a right cut from the lowest  $s$ -channel threshold to  $\infty$ , but no left cut. Below threshold both  $\alpha(s)$  and  $\bar{\beta}(s)$  are real.

#### D. Reggeization

By Reggeization we mean the isolation of Regge pole contributions to the scattering amplitude. The way to do this is to perform the Sommerfeld-Watson transform. We write the partial wave expansion in the  $t$ -channel;

$$f(s, t) = \sum_{\ell=0}^{\infty} (2\ell+1) P_{\ell}(z_t) G_{\ell}(t) \quad (3.38)$$

where

$$z_t = \frac{t(s-u) + (m_d^2 - m_b^2)(m_c^2 - m_a^2)}{[(t - (m_c - m_a)^2)(t - (m_c + m_a)^2)(t - (m_b - m_d)^2)(t - (m_b + m_d)^2)]^{\frac{1}{2}}}$$

$$\xrightarrow{s \rightarrow \infty} \frac{s-u}{4p_{ac} p_{bd}} \quad (3.39)$$

We assume that the signatured amplitudes have only simple poles of the form

$$G^{\pm}(s, \ell) \sim \frac{\beta(s)}{\ell - \alpha(s)}$$

Then, repeating the steps of Sec. I-C, we find that as  $s \rightarrow \infty$

$$f(s, t) = \sum_{\alpha} R_{\alpha}(s, t) + (\text{background integral})$$

$$R_{\alpha}(s, t) \sim - \frac{\pi[2\alpha(t)+1]}{\sin\pi\alpha(t)} \beta(t)^{\frac{1}{2}} [\mathcal{P}_{\alpha}(-z_t) \pm \mathcal{P}_{\alpha}(z_t)] \quad (3.40)$$

where the  $\pm$  sign corresponds to signature =  $\pm 1$ . As a function of  $z_t$ , (3.38) converges in the Lehmann ellipse of the  $t$ -channel, which includes the  $t$ -channel physical region but not the  $s$ -channel physical region. We can now continue it to the  $s$ -channel physical region using (3.40). Before we do this, we must determine the phase of  $\mathcal{P}_{\alpha}(-z_t)$ , with the help of the relation

$$\mathcal{P}_{\alpha}(-z) = e^{\mp i\pi\alpha} \mathcal{P}_{\alpha}(z), \quad (\text{Im}z \geq 0) \quad (3.41)$$

In the physical region of the  $t$  channel,  $\text{Im}t > 0$  and  $s < 0$ . Hence,  $\text{Im}z_t > 0$ , so that

$$R_{\alpha}(s, t) \sim - \frac{\pi\beta(t)(2\alpha(t)+1)}{\sin\pi\alpha(t)} \frac{1}{2} (e^{-i\pi\alpha(t)} \pm 1) \mathcal{P}_{\alpha}(z_t) \quad (3.42)$$

and this can be continued to the  $s$ -channel physical region. The reason we must use (3.41) before the continuation is that the path of continuation passes through a branch point of  $\mathcal{P}_{\alpha}(z)$  in  $z$ , and the phase, if not determined beforehand, becomes ambiguous thereafter.

We now examine the singularities of  $R_{\alpha}(s, t)$  in  $t$ :

- 1)  $R_{\alpha}(s, t)$  has poles at the integers from the factor  $[\sin\pi\alpha(t)]^{-1}$ . We discuss

separately two types of poles:

(a) Those poles at  $\alpha=0,1,2,\dots$  correspond to physical particles of spin  $\alpha$ . Because of the signature factor, only the even or odd ones are actually present in  $R_\alpha$ . However, if  $\alpha(0) > 0$ , and the signature is positive, then  $\alpha=0$  corresponds to a particle of negative mass, a "ghost", which may be removed by assuming that  $\beta(t) \propto \alpha(t)$ . (There are other mechanisms to deal with this problem when the external particles have spin. See discussion later, in Sec. VII).

(b) Those poles at  $\alpha=-1,-2,-3,\dots$  correspond to unphysical, or "nonsense", values of singular momentum. They are automatically removed from  $R_\alpha$  because  $\mathcal{P}_\alpha(z)$  vanishes at these points. The signature factor then produces zeroes in  $R_\alpha(s,t)$  at nonsense wrong-signature values of  $\alpha$ , unless  $\beta(t)$  has poles at these values of  $\alpha$ . (See discussion later, in Sec. IV C).

2)  $R_\alpha(s,t)$  has poles at  $\alpha = \pm\frac{1}{2}, +3/2, \dots$ , arising from the poles of  $\mathcal{P}_\alpha(z)$ . The pole at  $\alpha=-\frac{1}{2}$  is cancelled by the factor  $(2\alpha+1)$ . For the others there are two possibilities.

(a) The residue of the pole may vanish.

(b) If the residue does not vanish, then the Mandelstam symmetry (3.29) requires that there be another trajectory at  $-\alpha-1$  with the same residue. The pole from this trajectory exactly cancels the original pole. This is known as a "compensating trajectory".

For negative values of  $\alpha$ , the compensating trajectory would lie above the original one. For this reason it is customary to assume that (a) is the correct choice and to take

$$\beta(t) \propto \frac{1}{\Gamma(\alpha(t)+\frac{3}{2})}$$

To obtain the required analyticity properties, the correct threshold behavior, and the absence of a ghost at  $\alpha(t) = 0$ , we write

$$\beta(t) = \frac{\alpha(t)}{\Gamma(\alpha(t)+\frac{3}{2})} \left( \frac{4p_{ac} p_{bd}}{s_0} \right)^{\alpha(t)} \gamma(t) \quad (3.43)$$

where  $s_0$  is an arbitrary scale factor. Then  $\gamma(t)$  is real analytic with no left hand cut. Recalling (1.20) and using the properties of the gamma function, we find that as  $s \rightarrow \infty$ ,

$$R_\alpha(s,t) \sim - \frac{\gamma(t)}{(\pi)^{\frac{1}{2}}} \Gamma(1-\alpha(t)) (e^{-i\pi\alpha(t)} \pm 1) \left( \frac{s}{s_0} \right)^{\alpha(t)} \quad (3.44)$$

This is the formula which is used in practical applications. Note that the threshold factor in (3. ) is cancelled by a similar factor in  $z_t$  [see (3.38)]. This is of course no accident, for  $R_\alpha(s,t)$  is expected on general grounds to be a real

analytic function of  $s$ . If the ghost-killing zero is not needed, and we do not put it in, then  $\Gamma(1-\alpha)$  in (3.44) is replaced by  $-\Gamma(-\alpha)$ .

### E. Khuri Poles

We have kept only the leading term in the asymptotic expression (3.44) for the contribution of a single Regge pole. Keeping the full asymptotic expansion of the hypergeometric function in the definition (1.19) of  $\mathcal{P}_\alpha(z_t)$ , we obtain

$$R_\alpha(s,t) = -\frac{\gamma(t)}{(\pi)^{\frac{1}{2}}} \Gamma(1-\alpha(t)) (e^{-i\pi\alpha(t)} \pm 1) \left(\frac{s}{s_0}\right)^{\alpha(t)} \left[ 1 + \sum_{n=1}^{\infty} d_n(t) \left(\frac{s}{s_0}\right)^{-n} \right] \quad (3.45)$$

The  $d_n(t)$  are just such that

$$R_\alpha(s,t) \rightarrow \text{const} \times \frac{P_\ell(z_t)}{\ell - \alpha(t)}, \quad \text{as } \alpha(t) \rightarrow \ell, \quad (3.46)$$

which is required for a resonance to have a definite spin. Thus (3.45) is significant if resonance positions are non-degenerate. If, however at the same energy there exist resonances of various spins, then the residue function in (3.46) could be an arbitrary polynomial in  $z_t$ , and the combination (3.45) is not particularly significant. Since we do not have full knowledge of all the resonances present, and since asymptotically only the leading term in (3.45) is significant, it would be advantageous to have an alternative expansion to the partial-wave expansion, such that the result of a Sommerfeld-Watson transformation would lead naturally to just one term in the infinite  $n$  sum in (3.45). Such an expansion is supplied by Khuri\*.

One can expand  $f(s,t)$  in a power series of  $s$  instead of in a series of Legendre polynomials in  $z_t$  in the form

$$f(s,t) = \sum_{n=0}^{\infty} c_n(t) s^n, \quad (3.47)$$

which converges in some circle in  $s$ . One then analytically continues  $c_n(t)$  in  $n$  to obtain  $c_n^\pm(t,n)$ , defined in the complex  $n$  plane (with signature introduced in the usual way). Assuming that  $c_n^\pm(t,n)$  has poles in  $n$  whose positions depend on  $t$ , (which might be called Khuri poles), one can pick up their contribution to (3.47) by doing the Sommerfeld-Watson transformation and obtain

$$f(s,t) = \sum_{\alpha} K_\alpha(s,t) + (\text{background integral})$$

$$K_\alpha(s,t) = -\frac{\gamma(t)}{(\pi)^{\frac{1}{2}}} \Gamma(1-\alpha(t)) (e^{-i\pi\alpha(t)} \pm 1) \left(\frac{s}{s_0}\right)^{\alpha(t)}$$

where  $\alpha(t)$  is the trajectory of a Khuri pole. Clearly, one Regge pole corresponds to an infinite family of Khuri poles, spaced successively by one unit. The leading

\* N.N. Khuri, Phys. Rev. 132, 914 (1963).

member of this family of Khuri poles coincides with the Regge pole. Conversely, one Khuri pole corresponds to an infinite family of Regge poles. As long as we do not have a dynamical theory, there is little to choose between the point of view of Regge poles and that of Khuri poles. In either case the requirements of analyticity and unitarity in all channels probably can only be satisfied with an infinite number of poles, Regge or Khuri. For formal considerations, however, Khuri poles are often convenient.

Instead of (3.47), we can, in fact, consider a power series in some other variable, for example in  $v = (s-u)/2s_0$ . Then we could arrive at (3.48) with  $K_\alpha(s,t)$  replaced by

$$K_\alpha(v,t) = - \frac{\gamma(t)}{(\pi)^{\frac{1}{2}}} \Gamma(1-\alpha(t)) (e^{-i\pi\alpha(t)} \pm 1) v^{\alpha(t)} \quad (3.48a)$$

which is convenient when it is important to take into account the symmetry of the scattering amplitude under  $s$ - $u$  interchange.

#### F. Factorizability of Regge Residues

The residue function  $\beta(s)$  of a Regge pole can be written as a product of two factors in a manner similar to coupling constants in field theory. This is a consequence of elastic unitarity, and we shall prove it for the case of the following set of  $s$ -channel reactions:

1.  $\pi+\pi \rightarrow \pi+\pi$  with partial wave amplitude  $F_1(s,\ell)$
2.  $\pi+\pi \rightarrow N+\bar{N}$  with partial wave amplitude  $F_2(s,\ell)$
3.  $N+\bar{N} \rightarrow N+\bar{N}$  with partial wave amplitude  $F_3(s,\ell)$  .

The spin of  $N$  is ignored for simplicity, and signature is understood. For  $4m_\pi^2 < s < 16m_\pi^2$  the  $2\pi$  state is the only intermediate state in the unitarity relation (3.10), for all three reactions. Therefore in that interval of  $s$ , the unitarity relations for the partial waves, continued in  $\ell$  are simple generalizations of (3.30):

$$\begin{aligned} \text{Im}F_1(s,\ell) &= \rho(s)F_1^*(s,\ell)F_1(s,\ell) \\ \text{Im}F_2(s,\ell) &= \rho(s)F_2^*(s,\ell)F_1(s,\ell) \\ \text{Im}F_3(s,\ell) &= \rho(s)F_2^*(s,\ell)F_2(s,\ell) \end{aligned} \quad (3.49)$$

where

$$\begin{aligned} \rho(s) &\equiv \frac{1}{4\pi} \left( \frac{s-4m_\pi^2}{s} \right)^{\frac{1}{2}} \\ \text{Im}F_n(s,\ell) &\equiv \frac{1}{2i} [F_n(s+i\epsilon,\ell) - F_n(s-i\epsilon,\ell)] \quad (n=1,2,3) \quad . \end{aligned} \quad (3.50)$$

Since all three reactions have the same quantum numbers, the same Regge pole  $\alpha(s)$  occurs in  $F_n(s,\ell)$ , ( $n=1,2,3$ ). Thus near  $\ell = \alpha(s+i\epsilon)$ ,

$$\begin{aligned}
F_n(s+i\epsilon, l) &\sim \frac{\beta_n(s+i\epsilon)}{l-\alpha(s+i\epsilon)} \\
F_n(s-i\epsilon, l) &\sim \frac{\beta_n(s-i\epsilon)}{\alpha(s+i\epsilon)-\alpha(s-i\epsilon)} \quad . \quad (3.51)
\end{aligned}$$

Substituting these into (3.49), multiplying through by  $l-\alpha(s+i\epsilon)$ , and taking the limit  $l-\alpha(s+i\epsilon) \rightarrow 0$ , we obtain

$$\begin{aligned}
\beta_1(s+i\epsilon) &= \frac{\rho(s)}{\text{Im}\alpha(s)} \beta_1(s-i\epsilon)\beta_1(s+i\epsilon) \\
\beta_2(s+i\epsilon) &= \frac{\rho(s)}{\text{Im}\alpha(s)} \beta_2(s-i\epsilon)\beta_1(s+i\epsilon) \\
\beta_3(s+i\epsilon) &= \frac{\rho(s)}{\text{Im}\alpha(s)} \beta_2(s-i\epsilon)\beta_2(s+i\epsilon) \quad . \quad (3.52)
\end{aligned}$$

Taking the quotient of the last two equations, we obtain

$$\beta_2(s+i\epsilon)^2 = \beta_1(s+i\epsilon)\beta_3(s+i\epsilon), \quad (4m_\pi^2 < s < 16m_\pi^2) \quad . \quad (3.53)$$

It is to be noted that our proof depends on the fact that there is no other state degenerate with the  $2\pi$  state. Similarly a generalization of the proof to take the spin of the nucleon into account works only because the pion has spin zero, and would not go through if there is spin degeneracy. If the  $2\pi$  state were degeneracy, the proof would have to be modified by considering new linear combinations of the degenerate states. Since (3.53) is analytic in  $s$ , we can continue it into the complex  $s$  plane. It therefore holds for all  $s$ . The reduced residue  $\gamma(s)$  defined in (3.43) also satisfies (3.53), because the factors in its definition trivially factorize. We can therefore write, as a solution to (3.53),

$$\begin{aligned}
\gamma_1(s) &= g_{\pi\pi}(s)g_{\pi\pi}(s) \\
\gamma_2(s) &= g_{\pi\pi}(s)g_{\text{NN}}(s) \\
\gamma_3(s) &= g_{\text{NN}}(s)g_{\text{NN}}(s) \quad . \quad (3.54)
\end{aligned}$$

The same proof can be used to show that the discontinuity function of a Regge cut has similar factorizability, for a Regge cut may be thought of as a continuous distribution of Regge poles.

#### G. Complication Due to Spin and Intrinsic Quantum Numbers

In order to apply the formulas we have derived to actual experiments, we have to understand, at least qualitatively, how our results are affected by the spin and intrinsic quantum numbers of the external particles. We now give a brief discussion of this. A detailed consideration of spin will be postponed till later.

If the particles have spin, we must specify their helicities  $\lambda_a$ ,  $\lambda_b$ ,  $\lambda_c$ , and  $\lambda_d$

as well as their momenta. We do this by using the helicity amplitudes  $f_{cd;ab}(s,t)$  of Jacob and Wick<sup>\*</sup>, where  $cd;ab$  is an abbreviation of  $\lambda_c, \lambda_d; \lambda_a, \lambda_b$ . The  $s$ - and  $t$ -channel amplitudes are no longer identical but are related by a crossing matrix. That is,

$$f_H^s(s,t) = \sum_{H'} \mathcal{M}_{HH'}(s,t) f_{H'}^t(s,t) \quad , \quad (3.55)$$

where  $H$  or  $H'$  denotes the relevant set of helicity indices. The crossing matrix  $\mathcal{M}_{HH'}$  has been calculated by Trueman and Wick<sup>\*\*</sup>. For our present purposes we only need to know that it is a real orthogonal matrix:

$$\mathcal{M}^T \mathcal{M} = 1 \quad . \quad (3.56)$$

The unpolarized differential cross section in the  $s$  channel is given by

$$\frac{d\sigma}{d\Omega} = \frac{1}{4\pi^2 s} \frac{k_f}{k_i} \frac{1}{(2J_a+1)(2J_b+1)} \sum_H |f_H^s(s,t)|^2 \quad , \quad (3.57)$$

where  $J_a$  and  $J_b$  are the incident spins. Because  $\mathcal{M}^T \mathcal{M} = 1$ , this is equivalent to

$$\frac{d\sigma}{d\Omega} = \frac{1}{4\pi^2 s} \frac{k_f}{k_i} \frac{1}{(2J_a+1)(2J_b+1)} \sum_H |f_H^t(s,t)|^2 \quad . \quad (3.58)$$

If  $f_H^s(s,t)$  describes elastic scattering,  $a+b \rightarrow a+b$ , then the optical theorem states

$$\text{Im} \langle f^s(s,0) \rangle = \frac{1}{2} k(s)^{\frac{1}{2}} \sigma_T(s) \quad (3.59)$$

where  $\sigma_T(s)$  is the total unpolarized cross section for  $a+b \rightarrow$  anything and  $\langle \rangle$  denotes the following helicity average:

$$\langle f^s(s,0) \rangle = \frac{1}{(2J_a+1)(2J_b+1)} \sum_{a,b} f_{ab;ab}^s(s,0) \quad . \quad (3.60)$$

It can be shown that

$$\langle f^s(s,0) \rangle = \frac{1}{(2J_a+1)(2J_b+1)} \sum_{a,b} f_{b,-b;a,-a}^t(s,0) \quad , \quad (3.61)$$

so that we can compute the  $s$ -channel total cross section directly in terms of  $t$ -channel Regge poles.

The helicity amplitudes are particularly appropriate for Regge pole analysis because they have simple partial wave expansions:

\* M. Jacob and G.C. Wick, Ann. Phys. (N.Y.) 7, 404 (1959).

\*\* T.L. Trueman and G.C. Wick, Ann. Phys. (N.Y.) 26, 322 (1964).

$$f_{cd,ab}^t(s,t) = \sum_J (2J+1) F_{cd,ab}^J(t) d_{\lambda\mu}^J(z_t)$$

$$\lambda = a-b, \quad \mu = c-d \quad z_t = \cos\theta_t \quad (3.62)$$

where  $d_{\lambda\mu}^J(z)$  is a rotation coefficient. If  $a=b=c=d=0$ , then (3.62) reduces to the partial wave expansion of the spinless case. Regge poles occur as  $J$ -poles of  $F_{cd,ab}^J$ , suitably continued into the  $J$  plane. The contribution of a single Khuri pole  $\alpha(t)$  to (3.62) has the same form as in the spinless case, except that the reduced residue now acquires helicity indices:

$$f_H^t(\text{pole}) = - \frac{\gamma_H(t)}{(\pi)^{\frac{1}{2}}} \Gamma(1-\alpha(t)) (e^{-i\pi\alpha(t)} \pm 1) \left(\frac{s}{s_0}\right)^{\alpha(t)}. \quad (3.63)$$

Actually the helicity amplitudes contain kinematic singularities and satisfy constraint equations that did not exist in the spinless case. This means that  $\gamma_H(t)$  have kinematic singularities, and that the  $\gamma_H(t)$  of different Regge poles may be related to one another at some value of  $t$ . The simplest of these constraints come from the requirement that in  $s$ -channel forward or backward scattering the total helicity be conserved. Through crossing this forces certain linear combinations of  $t$ -channel helicity amplitudes to vanish at these kinematic points.

We now turn to intrinsic quantum numbers, and use isospin as an example. If we do not work with scattering amplitudes of definite isospin, the no further complication arises. For example, consider the  $s$ -channel reaction  $\pi^- p \rightarrow \pi^- p$ , with the corresponding  $t$ -channel reaction  $\pi^- \pi^+ \rightarrow p\bar{p}$ . Crossing between the two channels is simply given by (3.55), in which  $f^s$  refers to  $\pi^- p \rightarrow \pi^- p$  and  $f^t$  refers to  $\pi^- \pi^+ \rightarrow p\bar{p}$ . If we decompose all scattering amplitudes into amplitudes with definite total isospin, however, then an isospin crossing matrix enters into the crossing relation. For example, let  $f_{H,I}^s$  denote the helicity amplitude for  $\pi^- p \rightarrow \pi^- p$  in the total isospin state  $I$ , and let  $f_{H',I'}^t$  denote the corresponding amplitude for  $\pi^- \pi^+ \rightarrow p\bar{p}$ . Then the crossing relation reads

$$f_{H,I}^s(s,t) = \sum_{H'I'} \mathcal{M}_{HH',II'}(s,t) C_{II'} f_{H',I'}^t(s,t), \quad (3.64)$$

where  $C_{II'}$  is the isospin crossing matrix. It is a constant matrix independent of  $s$  and  $t$ . We merely outline the procedure to derive it.

Suppressing helicity indices, and denoting a two-particle state by  $|p_1, I_1, m_1; p_2, I_2, m_2\rangle$ , where  $I$  is the particle isospin and  $m$  its  $z$ -component, crossing symmetry states

$$\begin{aligned} & \langle p_3, I_3, m_3; p_4, I_4, m_4 | T | p_1, I_1, m_1; p_2, I_2, m_2 \rangle \\ & = \langle -p_2, I_2, -m_2; p_4, I_4, m_4 | T | p_1, I_1, m_1; -p_3, I_3, -m_3 \rangle \end{aligned} \quad (3.65)$$



Now, both sides can be decomposed into linear combinations of amplitudes of definite total isospin and give a relation of the form

$$\sum_I a_{m_3 m_4, m_1, m_2}^I f_I^s = \sum_{I'} b_{-m_2, m_4; -m_1, -m_3}^{I'} f_{I'}^t \quad (3.66)$$

where a,b, are certain Clebsch-Gordan coefficients. We may now use the orthogonality relations of Clebsch-Gordan coefficients to solve (3.66), resulting in the crossing relation (3.64). The only delicate problem in the derivation is the choice of phases for the coefficients a and b. A clear and elementary discussion of this is given by Carruthers and Krisch.\* They have worked out isospin crossing matrices for many useful cases. For reference we cited some of these in Table I.

\* P. Carruthers and J. Krisch, Ann. Phys. (N.Y.) 33, 1 (1965).

Table I - I-spin Crossing Matrices

$$f_I^s(s,t) = \sum_{I'} C_{II'}^{st} f_{I'}^t(s,t)$$

---

	$I_s \backslash I_t$	0	1	2
s: $\pi\pi \rightarrow \pi\pi$	0	$\left(\frac{1}{3}\right)$	1	$\left(\frac{5}{3}\right)$
t: $\pi\pi \rightarrow \pi\pi$	1	$\left(\frac{1}{3}\right)$	$\left(\frac{1}{2}\right)$	$\left(-\frac{5}{6}\right)$
u: $\pi\pi \rightarrow \pi\pi$	2	$\left(\frac{1}{3}\right)$	$\left(-\frac{1}{2}\right)$	$\left(\frac{1}{6}\right)$

$$C^{st} = \begin{pmatrix} \frac{1}{3} & 1 & \frac{5}{3} \\ \frac{1}{3} & \frac{1}{2} & -\frac{5}{6} \\ \frac{1}{3} & -\frac{1}{2} & \frac{1}{6} \end{pmatrix}$$


---

	$I_s \backslash I_t$	0	1
s: $\pi N \rightarrow \pi N$	$\frac{1}{2}$	$\left(\frac{1}{(6)^{\frac{1}{2}}}\right)$	1
t: $\pi\pi \rightarrow \overline{NN}$	$\frac{3}{2}$	$\left(\frac{1}{(6)^{\frac{1}{2}}}\right)$	$\left(-\frac{1}{2}\right)$
u: $\pi N \rightarrow \pi N$			

$$C^{st} = \begin{pmatrix} \frac{1}{2} & \left(\frac{1}{(6)^{\frac{1}{2}}}\right) & 1 \\ \frac{3}{2} & \left(\frac{1}{(6)^{\frac{1}{2}}}\right) & -\frac{1}{2} \end{pmatrix}$$

	$I_s \backslash I_t$	$\frac{1}{2}$	$\frac{3}{2}$
same for	$\frac{1}{2}$	$\left(-\frac{1}{3}\right)$	$\left(\frac{4}{3}\right)$
s: $\pi K \rightarrow \pi K$ etc.	$\frac{3}{2}$	$\left(\frac{2}{3}\right)$	$\left(\frac{1}{3}\right)$

$$C^{sn} = \begin{pmatrix} \frac{1}{2} & \frac{3}{2} \\ \frac{1}{2} & \left(-\frac{1}{3}\right) & \left(\frac{4}{3}\right) \\ \frac{3}{2} & \left(\frac{2}{3}\right) & \left(\frac{1}{3}\right) \end{pmatrix}$$


---

	$I_s \backslash I_t$	$\frac{1}{2}$	$\frac{3}{2}$
s: $\overline{NN} \rightarrow \overline{NN}$	$\frac{1}{2}$	$\left(-\frac{1}{2}\right)$	$\left(-\frac{3}{2}\right)$
t: $\overline{NN} \rightarrow \overline{NN}$	$\frac{3}{2}$	$\left(-\frac{1}{2}\right)$	$\left(\frac{1}{2}\right)$
u: $\overline{NN} \rightarrow \overline{NN}$			

$$C^{st} = \begin{pmatrix} \frac{1}{2} & \frac{3}{2} \\ \frac{1}{2} & \left(-\frac{1}{2}\right) & \left(-\frac{3}{2}\right) \\ \frac{3}{2} & \left(-\frac{1}{2}\right) & \left(\frac{1}{2}\right) \end{pmatrix}$$

	$I_s \backslash I_t$	$\frac{1}{2}$	$\frac{3}{2}$
same for	$\frac{1}{2}$	$\left(-\frac{1}{2}\right)$	$\left(\frac{3}{2}\right)$
s: $KK \rightarrow KK$ etc.	$\frac{3}{2}$	$\left(\frac{1}{2}\right)$	$\left(\frac{1}{2}\right)$

$$C_{sn} = \begin{pmatrix} \frac{1}{2} & \frac{3}{2} \\ \frac{1}{2} & \left(-\frac{1}{2}\right) & \left(\frac{3}{2}\right) \\ \frac{3}{2} & \left(\frac{1}{2}\right) & \left(\frac{1}{2}\right) \end{pmatrix}$$


---

#### IV. Some Simple Physical Consequences

##### A. Single Pole Dominance

Suppose  $\alpha(t)$  is the leading Regge trajectory which can be exchanged in the t-channel. If there are no Regge cuts, it alone will dominate the s-channel scattering when s is sufficiently large. From (3.58) and (3.63) we obtain the asymptotic differential cross section:

$$\begin{aligned} \frac{d\sigma}{d\Omega} &= \frac{1}{4\pi^2} \frac{k_f}{s} \frac{k_i}{k_i} b(t) \Gamma^2(1-\alpha(t)) \left| \frac{e^{-i\pi\alpha(t)} \pm 1}{2} \right|^2 \left(\frac{s}{s_0}\right)^{2\alpha(t)}, \\ &= \frac{1}{4\pi^2} \frac{k_f}{s} \frac{k_i}{k_i} b(t) \Gamma^2(1-\alpha(t)) \left\{ \begin{array}{l} \cos^2 \frac{\pi\alpha(t)}{2} \\ \sin^2 \frac{\pi\alpha(t)}{2} \end{array} \right\} \left(\frac{s}{s_0}\right)^{2\alpha(t)}, \quad (\text{signature} = \pm 1), \quad (4.1) \end{aligned}$$

where

$$b(t) = \frac{1}{\pi} \frac{1}{(2J_a+1)(2J_b+1)} \sum_{a,b,c,d} \gamma_{cd;ab}^2(t). \quad (4.2)$$

Hence  $(k_i/k_f)(d\sigma/d\Omega)$  has a very simple asymptotic s-dependence:

$$\frac{k_i}{k_f} \frac{d\sigma}{d\Omega} = G(t) \left(\frac{s}{s_0}\right)^{2\alpha(t)-1}. \quad (4.3)$$

If we plot  $\ln\left(\frac{k_i}{k_f} \frac{d\sigma}{d\Omega}\right)$  vs.  $\ln\left(\frac{s}{s_0}\right)$  at fixed t, we should obtain a straight line whose slope is  $2\alpha(t)-1$ . This would enable us to determine the trajectory  $\alpha(t)$  for negative values of t by comparison with experiments. Most of the trajectories determined so far conform remarkably well to a straight line:

$$\alpha(t) = \alpha_0 + \alpha' t. \quad (4.4)$$

##### B. Total Cross Sections

By using the optical theorem (3.59) and the formulas (3.61) and (3.63), we can calculate the asymptotic total cross section in the s-channel in terms of the leading Regge pole  $\alpha(t)$  in the t-channel:

$$\sigma_T(s) \xrightarrow{s \rightarrow \infty} \frac{c_a c_b}{\Gamma(\alpha_0)} \left(\frac{s}{s_0}\right)^{\alpha_0-1}, \quad (4.5)$$

where  $\sigma_T$  is the total cross section for  $a+b \rightarrow$  anything, and  $\alpha_0 = \alpha(0)$ , and  $c_n$  ( $n=a,b$ ) is defined by

$$c_n = \frac{(4\pi^{\frac{1}{2}} s_0^{-1})^{\frac{1}{2}}}{(2J_n+1)} \sum_{\lambda} g_{\lambda, -\lambda}^{\bar{n}\bar{n}}(0), \quad (4.6)$$

where  $g_{\lambda\mu}^{\bar{n}\bar{n}}(t)$  is the coupling [in the sense of Eq. (3.54)] of the t-channel Regge pole to the  $\bar{n}\bar{n}$  system with helicities  $\lambda, \mu$ . Since the Froissart bound\* requires

\* See Khuri's lectures in this Summer School.

$\sigma_T < c(\ln s)^2$ , we see that no Regge trajectory can have an intercept  $\alpha_0$  greater than unity. If  $\alpha_0=1$  then according to (4.5)  $\sigma_T$  approaches a finite constant, otherwise it approaches zero by a power law.

It seems attractive to assume that there is a trajectory with  $\alpha_0=1$ , having the quantum numbers of the vacuum. It should have positive signature so that it does not create a zero-mass spin-one hadron. If such a trajectory exists, it would be exchanged in all elastic scatterings, and by (4.5) all total cross sections will approach constants as  $s \rightarrow \infty$ . Furthermore, the total cross sections for  $a+b$  and  $a+\bar{b}$  will be equal in that limit, because the trajectory will in both cases be coupled to  $a\bar{a}$  and  $b\bar{b}$  pairs, thus giving the same  $c_a c_b$ . These are just the conclusions of the Pomeranchuk theorem, and this trajectory is named the Pomeranchuk trajectory or the Pomeron and is denoted by  $\alpha_p(t)$ . However, experimental data so far have neither clearly confirmed nor ruled out the Pomeron. If it exists, then the factorized form of the coefficient in (4.5) predicts relations among asymptotic cross section, for example

$$\sigma_{\pi N}^2(\infty) = \sigma_{\pi\pi}(\infty)\sigma_{NN}(\infty) \quad . \quad (4.7)$$

Assuming that at  $p_{lab} = 30 \text{ GeV}/c$ , the total cross sections have essentially attained their asymptotic limit, as is consistent with the trends in the experimental data, one finds

$$\sigma_{\pi\pi}(\infty) = 16 \text{ mb.} \quad (4.8)$$

This number, of course, has not been measured experimentally.

While the Pomeron (assuming that it exists) gives the asymptotic constant cross section. The way this limit is approached depends on lower-lying Regge trajectories. Their effect on the total cross section is simple to calculate via the optical theorem, because the latter involves the amplitude linearly, so the contributions from different trajectories are simply additive. Consider, for example, pion-nucleon scattering. The  $s$  channel is  $\pi+N \rightarrow \pi+N$ , and the  $t$  channel is  $\pi+\pi \rightarrow N+\bar{N}$ . The quantum numbers of the  $t$  channel are  $P = +(-1)^J$ ,  $G = +1$ , and  $I = 0,1$ . The known trajectories with these quantum numbers are

$$\begin{aligned} I = 0: & \text{ } P, f^0 \quad (\text{signature} = +1) \\ I = 1: & \text{ } \rho \quad (\text{signature} = -1) \quad . \end{aligned} \quad (4.8)$$

Hence for large  $s$

$$\begin{aligned} f_0^\pm(s,t) &= K_p + K_f \\ f_1^t(s,t) &= K_\rho \end{aligned} \quad (4.9)$$

where  $K_p \equiv K_{\alpha_p}(s,t)$ , with  $K_\alpha(s,t)$  given by (3.48). Using the isospin crossing matrices of Table I, in Sec. III, we find

$$\begin{aligned}
f_{1/2}^s(s,t) &= \frac{1}{(6)^{\frac{1}{2}}} (K_P + K_f) + K_\rho \\
f_{3/2}^s(s,t) &= \frac{1}{(6)^{\frac{1}{2}}} (K_P + K_f) - \frac{1}{2} K_\rho
\end{aligned} \tag{4.10}$$

which leads to

$$\begin{aligned}
\sigma_{\pi^+ p} &= \frac{1}{(6)^{\frac{1}{2}}} \sigma_P + \frac{1}{(6)^{\frac{1}{2}}} - \frac{1}{2} \sigma_\rho \\
\sigma_{\pi^- p} &= \frac{1}{(6)^{\frac{1}{2}}} \sigma_P + \frac{1}{(6)^{\frac{1}{2}}} - \frac{1}{2} \sigma_\rho
\end{aligned} \tag{4.11}$$

Using the approximate value  $\alpha_\rho(0) \approx \alpha_{f_0}(0) \approx \frac{1}{2}$ , we have

$$\begin{aligned}
\sigma_{\pi^+ p}(s) &= \sigma_\infty + (c_f - c_\rho) s^{-\frac{1}{2}} \\
\sigma_{\pi^- p}(s) &= \sigma_\infty + (c_f + c_\rho) s^{-\frac{1}{2}},
\end{aligned} \tag{4.12}$$

where  $\sigma_\infty$ ,  $c_f$ ,  $c_\rho$  are constants. The constants  $c_f$  and  $c_\rho$  are proportional to residue functions evaluated at  $t=0$ . These residue functions must be positive when  $t$  as at the squared mass of a particle, but may change sign by the time we extrapolate to  $t=0$ . Assuming, however, that  $c_f$  and  $c_\rho$  are positive, we have

$$\sigma_{\pi^- p}(s) > \sigma_{\pi^+ p}(s) \tag{4.13}$$

which happen to be experimentally correct so far.

### C. Diffraction Scattering

In any elastic scattering, we expect the amplitude to be dominated by Pomeron exchange for small  $t$  and large  $s$  (i.e., high energy scattering near the forward direction):

$$f(s,t) = - \frac{1}{(\pi)^{\frac{1}{2}}} \gamma_P(t) \Gamma(1-\alpha_P(t)) \frac{e^{-i\pi\alpha_P(t)} \pm 1}{2} \left(\frac{s}{s_0}\right)^{\alpha_P(t)} \tag{4.14}$$

as  $t \rightarrow 0$ ,  $\alpha_P(t) \rightarrow 1$  by hypothesis. Then

$$\begin{aligned}
\Gamma(1-\alpha_P(t)) \frac{e^{-i\pi\alpha_P(t)} \pm 1}{2} &= \frac{\pi}{\sin\pi\alpha_P(t) \Gamma(\alpha_P(t))} e^{-i\frac{\pi}{2}\alpha_P(t)} \cos\frac{\pi}{2}\alpha_P(t) \\
&= \frac{\pi}{2 \sin\frac{\pi}{2}\alpha_P(t) \cos\frac{\pi}{2}\alpha_P(t) \Gamma(\alpha_P(t))} e^{-i\frac{\pi}{2}\alpha_P(t)} \cos\frac{\pi}{2}\alpha_P(t) \\
&\rightarrow -\frac{i\pi}{2} \quad \text{as } t \rightarrow 0.
\end{aligned}$$

Hence the amplitude is pure imaginary at  $t=0$ :

$$f(s,0) = i \frac{(\pi)^{\frac{1}{2}}}{2} \gamma_P(0) \left(\frac{s}{s_0}\right)^{\alpha_P(0)} . \quad (4.15)$$

This means that the ratio of the forward elastic cross section to the total cross section is as small as possible consistent with unitarity. That is to say, one may physically attribute the elastic scattering to the effect of all inelastic reactions. One calls this diffraction scattering because the same picture holds in the diffraction of light by a completely absorptive sphere. In that classical example, the incident light casts a shadow behind the sphere. The shadow is of course "caused" by the absorption (inelastic effects), but its existence requires that there be a definite amount of elastic scattering to cancel the incident wave behind the sphere.

Since the Pomeron has positive signature, the elastic cross section is

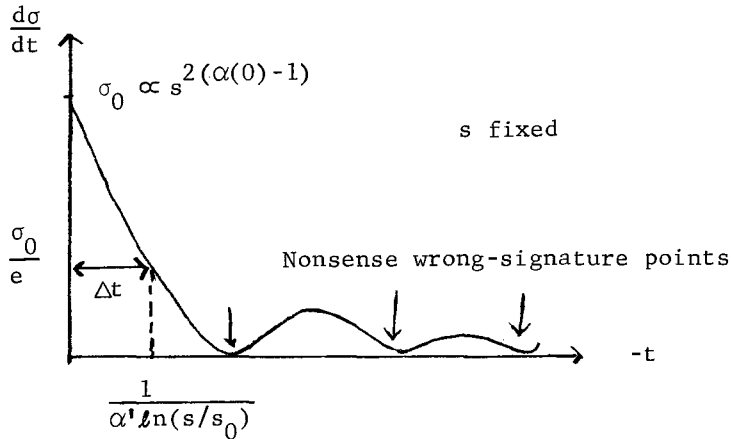
$$\frac{d\sigma}{d\Omega} = \frac{1}{4\pi^2 s} \gamma_P^2(t) \Gamma^2(1-\alpha_P(t)) \cos^2\left[\frac{\pi}{2}\alpha_P(t)\right] \left(\frac{s}{s_0}\right)^{2\alpha_P(t)} . \quad (4.16)$$

It is convenient to define

$$\frac{d\sigma}{dt} = \frac{\pi}{k^2} \frac{d\sigma}{d\Omega} \approx c(t) \left(\frac{s}{s_0}\right)^{2(\alpha_P(t)-1)}$$

$$c(t) = \pi \gamma_P^2(t) \Gamma^2(1-\alpha_P(t)) \cos^2\left[\frac{\pi}{2}\alpha_P(t)\right] . \quad (4.17)$$

A qualitative sketch of  $d\sigma/dt$  is given below.



This cross section exhibits certain characteristic features.  $2(\alpha_P(0)-1)$

1. The value of  $\sigma_0 = (d\sigma/dt)_{t=0}$  varies with  $s$  like  $\left(\frac{s}{s_0}\right)^{2(\alpha_P(0)-1)}$ , so that it is independent of  $s$  if  $\alpha_P(0)=1$ . The constancy of  $\sigma_0$  is indeed experimentally

observed in all elastic scatterings.

2. Suppose that the trajectory is linear in  $t$ ,

$$\alpha_p(t) = \alpha_0 + \alpha' t \quad , \quad (4.18)$$

then (4.16) becomes

$$\frac{d\sigma}{dt} = c(t) \left(\frac{s}{s_0}\right)^{2(\alpha_0-1)} e^{\alpha' t \ln \frac{s}{s_0}} \quad . \quad (4.19)$$

If  $c(t)$  varies slowly for small  $t$ , then the dominant  $t$  dependence comes from the exponential factor. Hence the cross section will show a forward peak with a characteristic width

$$\Delta t = \frac{1}{\alpha' \ln \frac{s}{s_0}} \quad (4.20)$$

which shrinks logarithmically with  $s$ . This shrinkage is observed in some but not all elastic scattering, possible because, in existing experiments, the energy is not sufficiently high, so that lower trajectories are still important.

3.  $d\sigma/dt$  vanishes at the nonsense wrong-signature points,  $\alpha_p(t) = -1, -3, -5, \dots$ , where the signature factor is zero, provided that  $\beta(t)$  has no poles there. This would produce dips in the cross section, similar to the diffraction minima outside of the central maximum in Fraunhofer diffraction. It was, however, pointed out by Jones and Teplitz\* and Mandelstam and Wang,\*\* that  $\beta(t)$  may have poles at precisely the nonsense-wrong signature points. The residues of these poles are proportional to certain integrals over the "third double spectral function"  $\rho_{tu}$ . Whether or not these poles actually exist is a dynamical question. We can only say that there is no general reason to expect a dip to occur except at nonsense wrong-signature points. If a dip does occur at such a point, then the type of pole mentioned above is either absent for some reason, or that its residue is small.

It is interesting to compare the characteristic features discussed above with that of the optical model of scattering, which includes the Fraunhofer diffraction of light. We start with the partial-wave expansion

$$\begin{aligned} f(s,t) &= \sum_{\ell=0}^{\infty} (2\ell+1) P_{\ell}(z) F_{\ell}(s) \\ &= \frac{\pi(s)}{ik} \sum_{\ell=0}^{\infty} (2\ell+1) P_{\ell}(z) (e^{2i\delta_{\ell}(s)} - 1) \quad . \quad (4.21) \end{aligned}$$

At high energies assume that many partial waves contribute, so that for small angle

\* C.E. Jones and V.L. Teplitz, Phys. Rev. 159, 1271 (1967).

\*\* S. Mandelstam and L.L. Wang, Phys. Rev. 160, 1490 (1967).

scattering we can use the approximation

$$P_{\ell}(\cos\theta) \xrightarrow[\substack{\ell \rightarrow \infty \\ \theta \rightarrow 0}]{} J_0(\ell\theta) = J_0(b(-t)^{\frac{1}{2}}),$$

$$b = \ell/k, \quad (4.22)$$

where  $b$  is the classical impact parameter. We further assume that absorption effects are important, so that  $\delta_{\ell}(s)$  is pure imaginary, and that it is only a function of  $b$ . Thus

$$f(s,t) \approx \frac{4\pi k^2}{i} \int_0^{\infty} db b J_0(b(-t)^{\frac{1}{2}}) \chi(b) \quad (4.23)$$

where

$$\chi(b) = e^{2i\delta_{\ell}(s)} - 1 \quad (4.24)$$

is real by assumption. The model is then specified by the choice of  $\chi(b)$ .

Suppose that the target is a black sphere with a sharp edge. Then all partial waves are completely absorbed if the impact parameter is less than the radius of the sphere, and completely unmodified otherwise. This corresponds to choosing

$$\chi(b) = \begin{cases} -\chi_0, & b < R \\ 0, & b > R \end{cases} \quad (4.25)$$

Then

$$f(s,t) = i4\pi k^2 \chi_0 \int_0^R db b J_0(\ell(-t)^{\frac{1}{2}})$$

$$= i4\pi k^2 \chi_0 \frac{R}{(-t)^{\frac{1}{2}}} J_1(R(-t)^{\frac{1}{2}}) \quad (4.26)$$

This gives a diffraction peak of half width  $\Delta t \sim 1/R^2$ , with diffraction minima occurring at the zeroes of  $J_1(R(-t)^{\frac{1}{2}})$ . The first zero is at  $R(-t)^{\frac{1}{2}} = 3.83$  which corresponds to a scattering angle

$$\theta = 1.22 \left( \frac{\lambda}{2R} \right), \quad (4.27)$$

a formula well-known to amateur telescope makers.

As a second example, let us consider an absorptive sphere with a fuzzy edge, represented by

$$\chi(b) = -\chi_0 e^{-b^2/R^2} \quad (4.28)$$

This leads to

$$f(s,t) = i4\pi k^2 \chi_0 \frac{R^2}{2} e^{\frac{1}{4}R^2 t} \quad (4.29)$$

and the cross section exhibits a diffraction peak of width  $\Delta t \sim 1/R^2$  but no



diffraction minima.

From these examples we gather that the width of the diffraction peak is related to the size of the target, while the depth of the diffraction minima is related to the sharpness of the edge of the target. If we compare this with Pomeron exchange, we see that the effective radius of a hadron as seen by another is

$$R \approx \left(4\alpha' \ln \frac{s}{s_0}\right)^{\frac{1}{2}} \quad (4.30)$$

which increases slowly with energy. We cannot say, however, that the presence of nonsense wrong-signature dips implies that hadrons have sharp edges, because this mechanism for dips is entirely different from that in the optical model. The scattering amplitude in the optical model is pure imaginary for all  $t$  - a consequence of the assumption that  $\chi(b)$  is real. In Pomeron exchange, however, the scattering amplitude is pure imaginary only at  $t=0$ . Away from  $t=0$  a real part comes in through the signature factor. It is precisely the interference between the real and imaginary parts that give rise to nonsense wrong-signature dips. If we must make a classical picture of a hadron according to the Regge picture, we would have to say that a hadron is a fuzzy black sphere surrounded by a real potential which exerts a direct and an exchange force.

#### D. The $\rho$ Trajectory

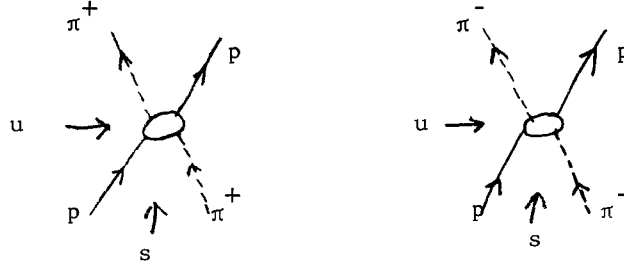
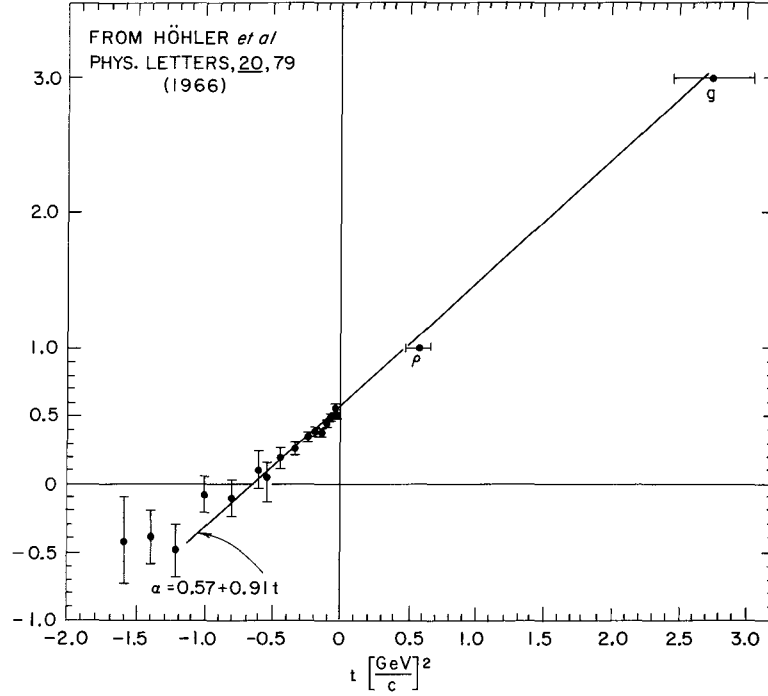
In the charge-exchange scattering  $\pi^- p \rightarrow \pi^0 n$ , the  $t$ -channel is  $\pi^0 \pi^+ \rightarrow n p$ , with quantum numbers  $I=1$ ,  $P=+(-)^J$ ,  $G=+1$ . The only known Regge trajectory with these quantum number is the  $\rho$ . Hence one may hope to extract its properties unambiguously from experiments, using the procedure described earlier. The result of such an analysis is shown in the accompanying figure, and we note that  $\alpha(t)$  is consistent with a straight line which extrapolates through the  $\rho$  and  $g$  mesons.

In the experimentally cross section, a marked dip is observed at  $t = -0.58\text{GeV}^2$ , which is consistent with the first nonsense wrong-signature point, where  $\alpha_\rho = 0$ .

The single pole model predicts that the spin-flip and the spin-nonflip amplitudes have the same phase, which comes entirely from the signature factor. Hence it predicts that the polarization is zero. Experimentally, however, the polarization is not zero. This indicates that perhaps a second Regge pole with the same quantum numbers is the  $\rho$ , or a cut is present.

#### E. The $N$ and $\Delta$ Trajectories

The  $N$  and  $\Delta$  trajectories may be studied in the backward scatterings  $\pi^+ p \rightarrow p \pi^+$  and  $\pi^- p \rightarrow p \pi^-$  (i.e., in the region of small  $u$  and large  $s$ ), as illustrated in the sketch below.



At large  $s$  and fixed  $u$ , both reactions are controlled by trajectories with baryon number  $B=+1$ . The  $u$  channel for  $\pi^- p \rightarrow p \pi^-$  is a pure  $I = 3/2$  state and so contains only the  $\Delta$  trajectory. The  $u$  channel for  $\pi^+ p \rightarrow p \pi^+$  is a mixture of  $I = 1/2$  and  $I = 3/2$  and so contains both the  $N$  and the  $\Delta$  trajectories. However, this cross section is much larger than that for  $\pi^- p \rightarrow p \pi^-$ , so we assume that the contribution of the  $I = 3/2$  state can be neglected, with the result that only  $N$  is exchanged. Thus the relevant amplitudes may be written

$$f_{\pi^+ p}^s(s, t) = -\pi \beta_N(u) (2\alpha_N(s)+1) \left(\frac{s}{s_0}\right)^{\alpha_N(u)} \frac{e^{-i\pi(\alpha_N(u)-\frac{1}{2})} + 1}{\sin\pi(\alpha_N(u)-\frac{1}{2})}$$

$$f_{\pi^- p}^s(s, t) = -\pi \beta_\Delta(u) (2\alpha_\Delta(u)+1) \left(\frac{s}{s_0}\right)^{\alpha_\Delta(u)} \frac{e^{-i\pi(\alpha_\Delta(u)-\frac{1}{2})} - 1}{\sin\pi(\alpha_\Delta(u)-\frac{1}{2})} \quad (4.31)$$

The salient feature of these formula is that, owing to the difference in signature of  $N$  and  $\Delta$ ,  $f_{\pi+p}^s$  has a dip at the nonsense wrong-signature point  $\alpha_N(u) = -\frac{1}{2}$ , whereas no dip is expected for  $f_{\pi-p}^s$  at  $\alpha_\Delta(u) = -\frac{1}{2}$  because that is not a nonsense wrong-signature point. This expectation is dramatically verified by experiments. Thus we see in both the cases of the  $\rho$  and the  $N$  trajectories that the poles of the residue function, which theoretically may occur at nonsense wrong-signature values, do not seem to be present.

If we adopt the point of view of Regge poles (rather than Khuri poles), then (4.31) merely represents the first term in the expansion of  $\mathcal{P}_\alpha(z_u)$  in powers of  $z_u$ . For equal mass scattering this is sufficient, for  $z_u \rightarrow \infty$  as  $s \rightarrow \infty$ . In the present case, however, the last property does not hold, for

$$z_u = \frac{u(s,t) - (m^2 - \mu^2)^2}{[u - (m+\mu)^2][u - (m-\mu)^2]} \approx \frac{u(s-t) - m^4}{(u - m^2)^2} \quad (4.32)$$

where  $m$  and  $\mu$  are respectively the nucleon and pion mass. In the exact backward direction  $\theta_s = \pi$  we have  $u \approx 2m^4/s$ , hence

$$z_u \xrightarrow{s \rightarrow \infty} 1 + O\left(\frac{1}{s}\right). \quad (\text{at } \theta_s = \pi) \quad (4.33)$$

Therefore we must keep all terms in the expansion of  $\mathcal{P}_\alpha(z_u)$ . This leads to a difficulty, namely when we re-expand the series in powers of  $s$ , the coefficients of all but the leading term diverge at  $\theta_s = \pi$ . Since this would violate analyticity, the non-leading powers must, in fact, be absent. This would call for the existence of an infinite family of Regge poles, spaced successively one unit beneath the leading one, with residue functions so arranged to effect the cancellation of all terms except the leading one. These new trajectories are called daughter trajectories. In this case, the leading pole plus the infinite family of daughters just precisely make up one Khuri pole. The interest of this theoretical problem lies in the fact that it illustrates a constraint placed on the existence of Regge poles by analyticity: You must take the whole family or none.

If we take the point of view of Khuri poles from the beginning, then this particular problem does not arise. However, when the trajectory of the nucleon Khuri pole passes through  $\frac{1}{2}$ , it calls for an infinite family of daughter Khuri poles to make up precisely one Regge pole, in order to make a nucleon of spin  $\frac{1}{2}$ . Thus it seems that a Regge pole or Khuri pole is generally accompanied by an infinite family. A more detailed study of daughter trajectories is given by Freedman and Wang.\*

---

\* D. Freedman and J.M. Wang. Phys. Rev. 153, 1596 (1967).

## V. REGGE CUTS

### A. Regge Cut from Two-Particle Unitarity

Although we have assumed until now that there are only poles in the  $l$  plane, elastic unitarity strongly suggests that there exist Regge cuts as well. To see this let us consider equal mass spin zero scattering, and consider a term in the unitarity relation corresponding to intermediate states containing two particles of the same mass as the external particles:

$$\text{Im}f(s,t) = \frac{1}{8\pi^2} \frac{k}{(s)^{\frac{1}{2}}} \int d\Omega' f_2^*(s,t_2) f_1(s,t_1) \quad (5.1)$$

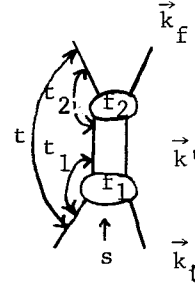
The kinematics is illustrated in the sketch, with

$$t = -|\vec{k}_f - \vec{k}_i|^2 = -2k^2(1 - \cos\theta)$$

$$t_1 = -|\vec{k}' - \vec{k}_i|^2 = -2k^2(1 - \cos\theta')$$

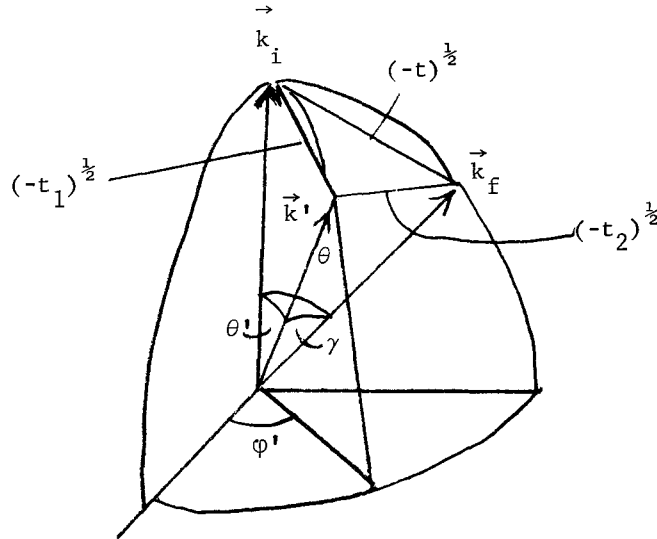
$$t_2 = -|\vec{k}_f - \vec{k}'|^2 = -2k^2(1 - \cos\gamma)$$

$$\cos\gamma = \cos\theta\cos\theta' + \sin\theta\sin\theta'\cos\phi' \quad (5.2)$$



A geometrical construction of  $t$ ,  $t_1$  and  $t_2$  is given in the sketch below, from which we see that

$$(-t_1)^{\frac{1}{2}} + (-t_2)^{\frac{1}{2}} \geq (-t)^{\frac{1}{2}} \quad (5.3)$$



The equality is actually never attainable, but as  $s \rightarrow \infty$  at fixed  $t$ , we have  $\theta \rightarrow 0$ , and the equality is almost fulfilled when  $\vec{k}_i, \vec{k}_f, \vec{k}'$  are coplanar:

$$(-t_1)^{\frac{1}{2}} + (-t_2)^{\frac{1}{2}} = (-t)^{\frac{1}{2}} + 0\left(\frac{1}{s}\right)$$

[for  $\theta = \theta' + \gamma$ ,  $s \rightarrow \infty$ ,  $t$  fixed (i.e.,  $\theta \rightarrow 0$ ) . (5.4)

We now let  $s$  become large and assume that  $f_1(s, t_1)$  and  $f_2(s, t_2)$  are each dominated by a single Regge pole:

$$\begin{aligned} f_1(s, t_1) &= A_1(t_1) s^{\alpha_1(t_1)} \\ f_2(s, t_2) &= A_2(t_2) s^{\alpha_2(t_2)} \end{aligned} \quad . \quad (5.5)$$

Hence

$$\begin{aligned} \text{Im}f(s, t) &= \frac{1}{8\pi^2} \frac{k}{(s)^{\frac{1}{2}}} \int_{-4k^2}^0 \frac{dt_1}{2k^2} \int_0^{2\pi} d\varphi' A_2^*(t_2) A_1(t_1) s^{\alpha_1(t_1) + \alpha_2(t_2)} \\ &\approx \frac{1}{8\pi^2} \int_{-\infty}^0 dt_1 \int_0^{2\pi} d\varphi' A_2^*(t_2) A_1(t_1) s^{\alpha_1(t_1) + \alpha_2(t_2) - 1} \end{aligned} \quad . \quad (5.6)$$

Let the maximum of the exponent of  $s$  be denoted by

$$\alpha_c(t) = \max[\alpha_1(t_1) + \alpha_2(t_2) - 1], \quad ((-t_1)^{\frac{1}{2}} + (-t_2)^{\frac{1}{2}} \geq (-t)^{\frac{1}{2}}). \quad (5.7)$$

We can then transform the integral to the form

$$\text{Im}f(s, t) = \int_{-\infty}^{\alpha_c(t)} d\ell D(\ell, t) s^\ell \quad (5.8)$$

where

$$D(\ell, t) = \frac{1}{8\pi^2} \int_{-\infty}^0 dt_1 \int_0^{2\pi} d\varphi' A_2^*(t_2) A_1(t_1) \delta(\ell - \alpha_1(t_1) - \alpha_2(t_2) + 1) \quad . \quad (5.9)$$

The right hand side of (5.8) looks like the contribution of a continuous line of Regge poles in the  $\ell$  plane starting at  $\alpha_c(t)$ . Hence there is a Regge cut from  $\ell = \alpha_c(t)$  to  $\ell = -\infty$ .

Assume that  $\alpha_1(t)$  and  $\alpha_2(t)$  are increasing functions of  $t$ , so that the maximum in (5.8) occurs at  $(-t_1)^{\frac{1}{2}} + (-t_2)^{\frac{1}{2}} = (-t)^{\frac{1}{2}}$ . Putting  $x = (-t_1)^{\frac{1}{2}}$ ,  $y = (-t_2)^{\frac{1}{2}}$ , the maximization condition reads

$$\delta\{\alpha_1(-x^2) + \alpha_2(-y^2) - 1 - \lambda(x+y)\} = 0 \quad (5.10)$$

where  $\lambda$  is a Lagrange multiplier. The solution is

$$\alpha_c(t) = \alpha_1(-x^2) + \alpha_2(-y^2) - 1 \quad (5.11)$$

where  $x, y$  are such that

$$\frac{d\alpha_1(-x^2)}{dx} = \frac{d\alpha_2(-y^2)}{dy} \quad . \quad (5.12)$$

For linear trajectories  $\alpha_i = \alpha_{0i} + \alpha_i' t$  ( $i=1,2$ ), the explicit solution is

$$\alpha_c(t) = \alpha_{01} + \alpha_{02}^{-1} + \frac{\alpha_1' \alpha_2'}{\alpha_1' + \alpha_2'} t \quad . \quad (5.13)$$

In particular, for  $\alpha_1(t) = \alpha_2(t) = \alpha_0 + \alpha' t$ , we obtain

$$\alpha_c(t) = (2\alpha_0 - 1) + \frac{1}{2} \alpha' t \quad . \quad (5.14)$$

This result was first derived in a slightly different way by Amati, Fubini and Stanghellini.\* The type of Regge cuts obtained here is usually referred to as an AFS cut.

Little is known about the discontinuity  $D(\ell, t)$  in (5. ) except that it must vanish at  $\ell = \alpha_c(t)$ .\*\* If we assume

$$D(\ell, t) \xrightarrow{\ell \rightarrow \alpha_c} c(t) (\alpha_c(t) - \ell)^a \quad , \quad (5.15)$$

where  $a > 0$ , then for large  $\ell ns$  we have

$$\text{Im}f(s, t) \xrightarrow{\ell ns \rightarrow \infty} c(t) s^{\alpha_c(t)} \int_0^{\infty} dx x^a e^{-x \ell ns} = \Gamma(a+1) c(t) \frac{s^{\alpha_c(t)}}{(\ell ns)^{a+1}} \quad . \quad (5.16)$$

Thus a Regge cut contribution differs from that of a Regge pole by a logarithmic factor. How high the energy should be in order that (5.16) be a good approximation depends on a more detailed knowledge of  $D(\ell, t)$ . Since  $\ell ns$  is a slowly varying function, (5.16) can hardly be distinguished from a Regge pole contribution over a limited range of  $s$ .

The argument we have given for the AFS cut is of course not rigorous, for the inelastic contributions to unitarity, which have been neglected, may alter our conclusion. These contributions consist of additive terms to the right side of (5.6), and they are positive at  $t=0$ . They may cancel the AFS cut, and replace it by a higher-lying Regge singularity. All we can say is that this seems implausible.

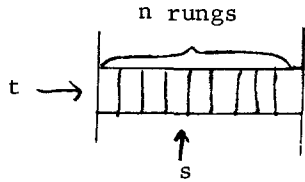
#### B. Some Model Calculations

The argument given earlier for the AFS cut is based only on elastic unitarity, and no appeal has been made to any detailed dynamical theory. We would like to give a brief qualitative description of some calculations based on Feynman diagrams. Any single Feynman diagram behaves asymptotically like  $s^p (\ell ns)^q$ , where  $p$  and  $q$  are fixed integers, and so does not exhibit Regge behavior. However, if we compute the leading asymptotic behavior of the  $n$ -rung ladder shown in the sketch and sum over  $n$ ,

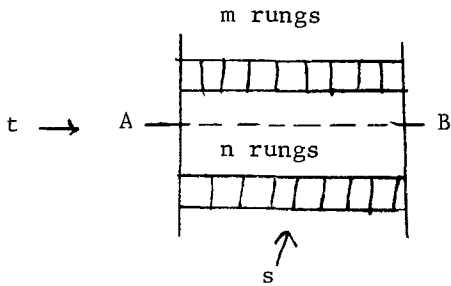
-----

\* D. Amati, S. Fubini and A. Stanghellini, Physics Letters 1, 29 (1962).

\*\* J. Bronzan and C.E. Jones, Phys. Rev. 160, 1494 (1967).



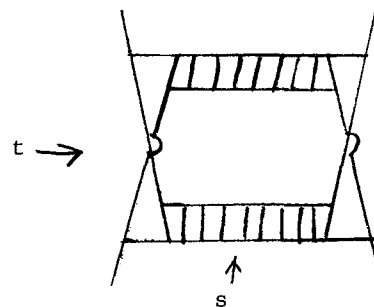
Feynman diagrams of the type shown in the sketch below; but they only made an



we do obtain asymptotic behavior of the form  $s^{\alpha(t)}$ . Therefore this sum of Feynman diagrams contains a Regge pole. The original Amati, Fubini and Stanghellini work was, in fact, based on a sum of approximate calculation. The exact sum of graphs can be written in the form of a dispersion integral, in which the absorptive parts are to be obtained by "cutting" the graph (i.e., replacing propagators by  $\delta$ -functions) in all possible ways and adding the contributions. The original AFS calculation retains only the two-particle absorptive part by cutting the graphs along

AB. This is not the same as two-particle unitarity, but the mathematics is similar and they obtained the cut whose branch point is given by (5. ).

Mandelstam\* has shown, however, that if one takes into account all of the multiparticle absorptive parts in the AFS calculation, the discontinuity of the AFS cut  $D(t, s)$  is identically zero for  $s$  on the physical sheet. He considers another class of Feynman diagrams, of the type shown in the sketch below, and shows that this does give rise to a Regge cut with the same branch point as the AFS cut. The essential difference between the new class of diagram and the old one is that the new class consists of non-planar graphs, representing an amplitude having a non-vanishing third double spectral function  $\rho_{tu}$ , whereas  $\rho_{tu} = 0$  for the AFS graphs. The lesson learned from these calculations seems to be that Regge cuts owe their existence to the third double spectral function. In this respect, they has a common root with the poles of Regge residues at nonsense wrong-signature points.



### C. Effect of Regge Cuts in Scattering

If we accept the existence of the Pomeron and that of AFS cuts, then the Pomeron would generate an infinite family of cuts, which would have an appreciable effect on elastic scattering as  $s \rightarrow \infty$ .

----- Let us first see how the Pomeron generates cuts, and for this purpose assume

\* S. Mandelstam, Nuovo Cimento 30, 1127 (1963).

that the Pomeron trajectory is linear:

$$\alpha_p(t) = 1 + \alpha' t \quad . \quad (5.17)$$

The AFS cut generated by the exchange of two Pomerons in the t-channel has branch points at

$$\alpha_2(t) = 1 + \frac{1}{2} \alpha' t \quad . \quad (5.18)$$

We can now take  $f_1(s, t_1)$  in (5.1) to be dominated by the PP cut and  $f_2(s, t_2)$  to be dominated by the Pomeron. Then we find a new AFS cut which may be looked upon as the effect of triple Pomeron exchange:

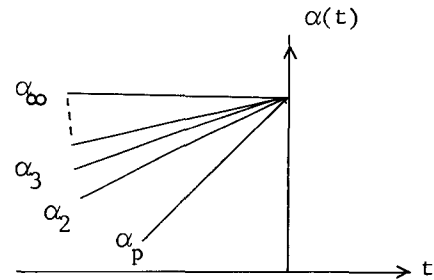
$$\alpha_3(t) = 1 + \frac{\alpha' (\frac{1}{2} \alpha' t)}{\alpha' + \frac{1}{2} \alpha'} = 1 + \frac{1}{3} \alpha' t \quad . \quad (5.19)$$

By repeating this argument, we find that the exchange of n Pomerons gives rise to an AFS cut with branch point at

$$\alpha_n(t) = 1 + \frac{1}{n} \alpha' t \quad . \quad (5.20)$$

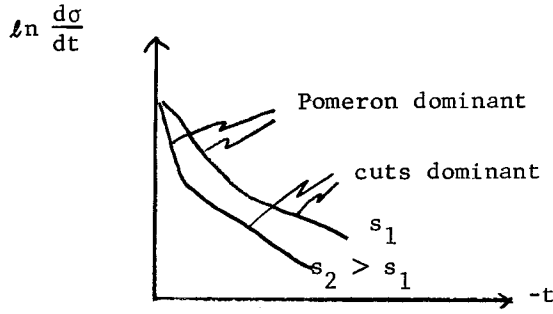
The trajectories of the family of cuts are shown in the sketch below.

How these cuts may affect high-energy scattering, of course, cannot be predicted before we have some dynamical information. Let us, however, make a reasonable guess. Let us assume that the coupling of the PP cut is much weaker than that of the Pomeron, and that the couplings of the higher cuts are progressively weaker still. Then at



small  $t$ , the separation of P-P and P becomes greater, and the P-P will take over. But by then the higher cuts also become well-separated, so that their total effect may be more important than that from any single one. Thus for a given large  $s$ , there is a small neighborhood of  $t=0$  in which the Pomeron dominates, and the cross section will have a diffraction peak which shrinks logarithmically with increasing  $s$ . Outside of this neighborhood, the PP cut and possible other higher cuts too, become important. The cross section then falls off less rapidly with  $-t$  in this region, since the slope of the cut trajectories are smaller. Furthermore, as  $s$  is increased, the separation between  $\alpha_p(t)$  and  $\alpha_{pp}(t)$  becomes greater, and so the neighborhood in which the Pomeron dominates shrinks with increasing  $s$ . Thus the cross section may have a qualitative behavior as illustrated in the sketch below.





We can make a crude calculation by assuming that the contribution of the  $n^{\text{th}}$  cut to the scattering amplitude has the form  $g^n s^n \alpha_n(t)$ , where  $g$  may have a weak dependence on  $s$ . Then the scattering amplitude can be written as

$$f(s,t) = \sum_{n=0}^{\infty} g^n s^{1+\frac{1}{n}\alpha' t} = s \sum_{n=0}^{\infty} \exp[n \ell n g + \frac{\alpha' t \ell n s}{n}] . \quad (5.21)$$

As  $s \rightarrow \infty$ , we convert the sum into an integral which we evaluate by the method of steepest descent:

$$f(s,t) \approx s \int_0^{\infty} dn \exp[n \ell n g + \frac{\alpha' t \ell n s}{n}] \approx s \exp[\bar{n} \ell n g + \frac{\alpha' t \ell n s}{\bar{n}}] \quad (5.22)$$

where  $\bar{n}$  is the value of  $n$  which maximizes the exponent:

$$\bar{n} = [\alpha' t \ell n s / \ell n g]^{\frac{1}{2}} . \quad (5.23)$$

Hence

$$\begin{aligned} f(s,t) &\approx s e^{-c(-t)^{\frac{1}{2}}} , \\ \frac{d\sigma}{dt} &\approx \frac{1}{\pi} e^{-2c(-t)^{\frac{1}{2}}} , \\ c &= 2[\alpha' \ell n s (-\ell n g)]^{\frac{1}{2}} . \end{aligned} \quad (5.24)$$

It is interesting that the  $t$  dependence is the fastest decrease allowed by the Cerrulus-Martin bound.\* If we assume that  $-(\ell n s)(\ell n g)$  is a constant, then at a fixed  $t$ , the cross section  $d\sigma/dt$  would fall with increasing  $s$  towards a limiting envelop. Experiments on pp scattering indicated that this might be so, but a more definite conclusion must await future experiments at higher energies.

\* F. Cerrulus and A. Martin, Physics Letters 8, 80 (1964). Also see Khuri's lectures in this Summer School.

## VI. TOWARDS DYNAMICS?

One of the motivations that we have mentioned for studying Regge poles is the hope that it helps to formulate the bootstrap hypothesis. We now discuss some important advances in this respect.

### A. Finite-Energy Sum Rules.

By combining analyticity and Regge asymptotic behavior, one can deduce an interesting sum rule that relates s-channel resonances to t-channel Regge poles. For this purpose note that Regge asymptotic behavior holds along any direction in the s-plane, if it holds at all. This is because  $\mathcal{P}_\alpha(z) \xrightarrow{z \rightarrow \infty} z^\alpha$  along any direction in the z-plane, hence the ratio of Regge to background terms is of the same order in any direction.

It is convenient to introduce

$$v = \frac{s-u}{2s_0} \tag{6.1}$$

where  $s_0$  is an arbitrary scale, and use  $v, t$  as independent variables. We decompose the scattering amplitude into terms symmetric and antisymmetric in  $v$ :

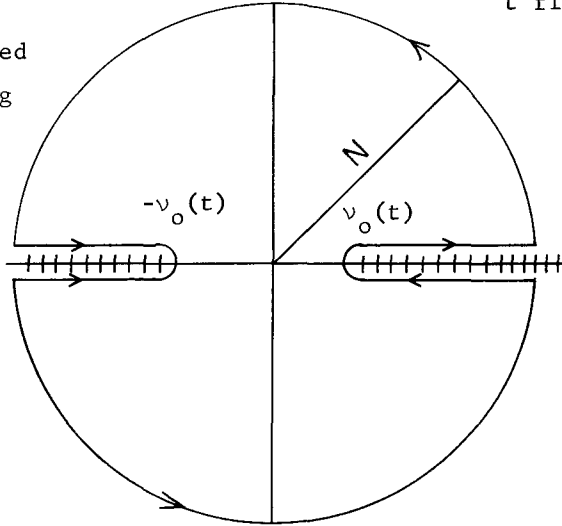
$$\begin{aligned} f(v, t) &= f^+(v, t) + f^-(v, t), \\ f^\pm(v, t) &= \pm f^\pm(-v, t). \end{aligned} \tag{6.2}$$

Clearly  $f^\pm(v, t)$  admits only t-channel Regge poles of signature  $\pm 1$ . In the complex  $v$  plane,  $f^\pm(v, t)$  has cuts along the real axis and no other singularity. If there are bound state poles, we include them as part of the cuts. The branch points of the cuts are functions of  $t$ , and for some  $t$  the right and left cuts may overlap. In that event we carry out our development for a value  $t$  for which they do not overlap and continue the results to the desired  $t$ . By Cauchy's theorem, then,

$$\frac{1}{2\pi i} \oint v^n f^\pm(v, t) = 0, \tag{6.3}$$

$v$  plane  
 $t$  fixed

where  $n$  is an integer, and the closed contour is shown in the accompanying sketch. Note the circle is of finite radius  $N$ . Since the contour has reflection symmetry with respect to  $v = 0$ , (6.3) is a trivial identity unless the integrand is an odd function of  $v$ . This means that (6.3) has content only for



$$n = \begin{cases} \text{even integer for } f^+(v,t) \\ \text{odd integer for } f^-(v,t), \end{cases} \quad (6.4)$$

and we shall only consider these values of  $n$ . Now separate the integral into an integral around the cuts plus that along the circle. Using the antisymmetry of  $v^n f^\pm(v,t)$ , we obtain

$$\frac{2}{\pi} \int_{v_0}^N dv v^n \text{Im} f^\pm(v,t) + \frac{1}{2\pi i} \int_C dv v^n f^\pm(v,t) = 0, \quad (6.5)$$

where  $C$  denotes a circle of radius  $N$ , excluding the two points on the real axis, and

$$\text{Im} f^\pm(v,t) = \frac{1}{2i} \lim_{\epsilon \rightarrow 0^+} [f^\pm(v + i\epsilon, t) - f^\pm(v - i\epsilon, t)]. \quad (6.6)$$

Regge asymptotic behavior states that for large  $v$

$$f^\pm(v,t) = \sum_{\substack{\alpha > L \\ \text{sgn} = \pm}} K_\alpha(v,t) + O(v^{-L}), \quad (6.7)$$

where  $K_\alpha(v,t)$  is given earlier in (3.48a). The integral of  $v^n K_\alpha$  over  $C$  is elementary:

$$\begin{aligned} \int_C dv v^n K_\alpha(v,t) &= A \int_C dv v^n [(-v)^\alpha \pm v^\alpha] \\ &= \pm 2A \int_C dv v^{n+\alpha} = \pm 2iA N^{\alpha+A+1} \int_{-\pi}^{\pi} d\theta e^{i(\alpha+n+1)\theta} \end{aligned}$$

$$= \pm 4iA \sin\pi(\alpha+n+1) N^{\alpha+n+1}/(\alpha+n+1) \quad (6.8)$$

where  $A = -\gamma\Gamma(1-\alpha)/(\pi)^{\frac{1}{2}}$ .

Therefore (6.5) becomes

$$\int_{\nu_0}^N d\nu \nu^n \text{Im}f^{\pm}(\nu, t) \pm \sum_{\substack{\alpha > -L \\ \text{sgn}=\pm 1}} \left[ + \frac{\gamma}{(\pi)^{\frac{1}{2}}} \frac{(-)^n}{\Gamma(\alpha)} \frac{N^{\alpha+n+1}}{\alpha+n+1} \right] + O(N^{-L}) = 0 \quad (6.9)$$

Neglecting  $O(N^{-L})$ , and writing the above explicitly for  $f^+$  and  $f^-$ , we have for sufficiently large  $N$ :

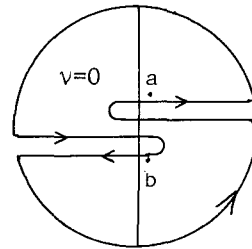
$$\int_{\nu_0}^N d\nu \nu^n \text{Im}f^+(\nu, t) \cong \sum_{\alpha, \text{sgn}=+1} \frac{\gamma N^{\alpha+n+1}}{(\pi)^{\frac{1}{2}} (\alpha+n+1) \Gamma(\alpha)}, (n \text{ odd}) \quad (6.10)$$

$$\int_{\nu_0}^N d\nu \nu^m \text{Im}f^-(\nu, t) \cong \sum_{\alpha, \text{sgn}=-1} \frac{\gamma N^{\alpha+m+1}}{(\pi)^{\frac{1}{2}} (\alpha+m+1) \Gamma(\alpha)} \cdot (m \text{ even})$$

These are the finite-energy sum rules (FESR) first derived by Dolen, Horn and Schmid\* by a slightly different method. They have given some actual numerical examples, which we shall not go into.

In the s-channel physical region,  $\nu_0(t)$  often becomes negative. The analytic continuation of (6.10) means that the original contour of integration actually looks like that shown in the sketch below.

We can, in fact, replace  $\nu_0$  by 0, if we understand  $\text{Im}f^{\pm}$  to be the discontinuity taken between points a and b shown in the sketch.



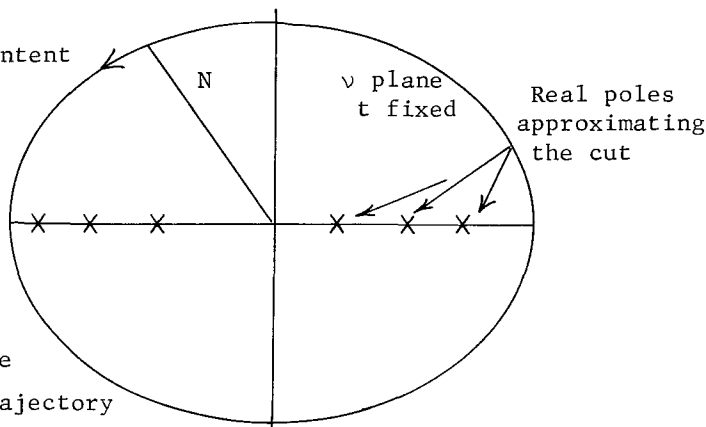
In these FESR, an integral of the amplitude extending over the s-channel low-energy region, which contains s-channel resonances, is approximately equated with the sum of t-channel Regge poles, which dominate the s-channel high-energy scattering. It therefore connects low-energy and high-energy phenomena, and connects exchanged particles (which produces a "potential") with resonances (which are "due" to the potential). Thus by combining analyticity with the Regge hypothesis, we begin to see some manifestations of the bootstrap.

\*-----  
\* R. Dolen, D. Horn, and C. Schmid, Phys. Rev. 166, 1768 (1968).

B. Duality.

To explore the dynamical implications of the FESR, we have to make simplifications in order to form an approximate picture of their real content. Suppose that in (6.10) the integrals on the left side can be separated in some manner into contributions from narrow resonances and a background. Harari<sup>\*</sup> conjectures that the background approximates the Pomeron contribution on the right side, while the narrow resonances add up approximately to the rest of the Regge poles. This division is of course ambiguous and cannot be made more precise until a dynamical theory emerges. We accept this conjecture, however, as a first approximation. That is, we approximate  $f^\pm$  on the left side by a sum of narrow resonances, and leave out the Pomeron on the right side, if it is there. Then in the  $\nu$  plane for  $f^\pm(\nu, t)$ , the right and left cuts are replaced by a series of poles that were originally on unphysical Riemann sheets, as indicated in the sketch below.

In this approximation the content of the FESR may be stated as follows: At a given  $t$  the sum of residues (generally  $t$ -dependent) of all the poles within a large circle of radius  $N$  is proportional to  $N^{\alpha+1}$  where  $\alpha = \alpha(t)$  is the leading non-Pomeron Regge trajectory



in the  $t$ -channel. The criterion for large  $N$  is that the leading trajectory dominates over the next one. Thus, although any one of the poles produces for large  $N$  a contribution  $\propto N^{-1}$ , the sum total of them gives  $N^{\alpha+1}$ . We say that the direct-channel resonances add up to a Regge pole in the crossed channel (which generates crossed-channel resonances). Conversely, a crossed-channel Regge pole already contains the contributions from all direct-channel resonances below a large energy  $N$ . This phenomenon is referred to as duality.

As defined above, duality is an immediate consequence of the FESR plus the narrow-resonance approximation. Of these, the FESR are on relative firm ground, both theoretically and experimentally. Thus a test of duality in this form is mainly a test of the narrow-resonance approximation. An interesting experimental test has been made by Schmid.<sup>†</sup> He calculated numerically the

-----  
<sup>\*</sup>H. Harari, Phys. Rev. Lett. 20, 1395 (1968). See also Harari's lectures in this summer school.

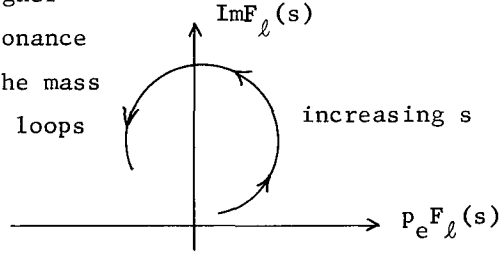
<sup>†</sup>C. Schmid, Phys. Rev. Lett. 20, 684 (1968).

partial wave projection of the amplitude for  $\pi N$  charge exchange scattering from  $\rho$ -trajectory exchange, which we write in a simplified way ignoring spin:

$$F_\ell(s) = \frac{1}{2} \int_{-1}^{+1} dz P_\ell(z) [-\gamma(t)\Gamma(1-\alpha(t))(e^{-i\pi\alpha(t)}-1)v^{\alpha(t)}], \quad (6.11)$$

where the parameters of the  $\rho$  trajectory are taken from fits to actual scattering data. He found that  $F_\ell(s)$  when plotted in the Argand diagram moves in a loop as a function of  $s$ , as shown in the sketch below.

Such loops are also made by a Breit-Wigner resonance of spin  $\ell$ . For a narrow resonance the top of the loop corresponding to the mass of the resonance. By interpreting the loops as resonances, Schmid found a semi-quantitative correspondence between his loops and the known direct channel resonances. Thus, although the Regge-exchange amplitude has no poles in  $s$ , its partial-mass projections mimics resonances. This is just what one would expect if one believes in duality. The mathematical reason why (6.12) gives rise to the loops is essentially the linearity of the  $\rho$  trajectory; namely, since  $\alpha(t) = \alpha_0 - 2\alpha'(1-z)k^2$ , the phase of the signature factor, which is solely responsible for the phase of  $F_\ell(s)$ , increases with  $s$ .



One might wonder whether the concept of duality is fundamental and can be stated as a general principle independent of the narrow-resonance approximation. We do not yet know the answer to this question. More likely, duality occupies a place similar to that of complementarity. Before quantum mechanics, complementarity cannot be precisely formulated, after quantum mechanics its precise formulation becomes uninteresting; but it served as a useful working principle that guided the way to quantum mechanics.

C. Exchange Degeneracy

The FESR (6.10) treats the even and odd parts of  $f(v,t)$  separately. To obtain a sum rule for  $f$  itself, multiply the first equation in (6.10) by  $N^m$ , the second by  $N^n$ , add the two equations and re-express  $f^\pm$  in terms of  $f$  by (6.2). We find in this manner

$$\begin{aligned} & \frac{1}{2} \int_{v_0}^N dv \operatorname{Im}[(v^n N^m + v^m N^n)f(v,t) + (v^n N^m - v^m N^n)f(-v,t)] \\ & \cong \sum_{\alpha} \frac{\gamma N^{\alpha+n+m+1}}{(\pi)^{\frac{1}{2}}(\alpha+n+m+1) \Gamma(\alpha)}, \quad \begin{pmatrix} n = \text{odd integer} \\ m = \text{even integer} \end{pmatrix}, \quad (6.12) \end{aligned}$$

where on the right side we sum over all trajectories  $\alpha > -L$ , of both signatures.

In the narrow-resonance approximation, we replace  $f(v,t)$  by a sum of zero-width resonance poles, and leave out the Pomeron contribution on the right side. Furthermore, we neglect the second term, which contains resonances in the u-channel, arguing that the factors  $v^{\frac{n,m}{N}} - v^{\frac{m,n}{N}}$  averages to something small, (i.e. of the same order as terms already neglected in the narrow-resonance approximation). Consider now a two-body system that has no s-channel resonances. Examples are  $pp$ ,  $\pi^+\pi^+$ ,  $pK^+$ . In our approximation the left side of (6.12) is zero. Therefore, the sum of Regge poles on the right side vanishes for all  $N$ . This means that if there is a Regge pole of a given signature, there must exist one of opposite signature, with the same trajectory function  $\alpha(t)$ , and equal and opposite residue function  $-\gamma(t)$ . It cannot have the same signature, for that would cancel the original Regge pole identically. This degeneracy between two Regge poles of opposite signature is called exchange degeneracy. It has the same physical meaning as in potential scattering.

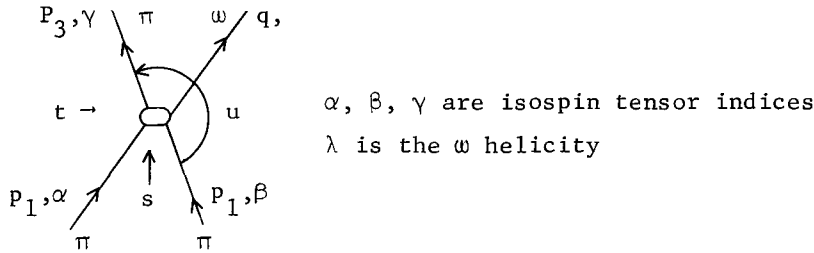
The requirement that exchange-degenerate trajectories have equal and opposite residue functions depends on one sign convention (3.48a), which has the signature factor in the form  $e^{-i\pi\alpha} \pm 1$ . If one redefines  $\gamma(t)$  to make the signature factor  $1 \pm e^{-i\pi\alpha}$ , then we would require equal residue functions. The exchange-degenerate trajectories must be such that when their contribution is added together, the term  $e^{-i\pi\alpha}$  is cancelled.

For  $\pi^+\pi^+$  scattering we know that the  $\rho$  trajectory is exchanged. Therefore a degenerate trajectory of opposite signature (i.e. positive) is called for. In the  $\pi^+\pi^-$  system in the t-channel, even signature means that the amplitude is symmetric under  $\pi^+\pi^-$  interchange, hence  $I = 0$  or  $I = 2$ . It cannot have  $I = 2$ , for in that case it would also couple to  $\pi^+\pi^+$ , contradicting the fact that there are no resonances in  $\pi^+\pi^+$ . Hence the exchange-degenerate partner of  $\rho$  has  $I = 0$ , and the only known trajectory with  $I = 0$ ,  $G = +1$ ,  $P = (-)^J$  is the  $f$  trajectory. Experimentally, the  $f$  meson lies remarkably close to the  $\rho$  trajectory, taken as the straight line passing through the  $\rho$  and  $g$  mesons.

In general, however, we should not be surprised if exchange degeneracy is only approximately realized in nature for its theoretical basis depends not only on the narrow-resonance approximation, but also on the neglect of the effects of u-channel resonances.

D. Bootstrap of the  $\rho$  Trajectory.

In a very interesting calculation, Ademollo et al.\* try to bootstrap the  $\rho$  trajectory using the FESR in the narrow-resonance approximation. They were able to do this only by introducing further assumptions. Let us see what they do in some detail, for the true significance of such schemes is not yet clear at the present time. They consider the reaction



$\pi \pi \rightarrow \pi \omega$ , for which the  $s, t, u$  channels are identical and have  $I = 1, G = +1, P = +(-1)^J$ . Hence in each channel only the  $\rho$  trajectory can contribute. This is a particularly happy choice because the Pomeron is not present, and we are spared the task of ejecting it forcefully.

Let the helicity amplitude be  $f_{\lambda, \alpha\beta\gamma}^s(s, t)$ . It must be antisymmetric in  $\alpha$  and  $\beta$  because  $I = 1$  in the  $s$  channel. Similarly, it is antisymmetric in  $\alpha$  and  $\gamma$  and in  $\beta$  and  $\gamma$ . Hence

$$f_{\lambda, \alpha\beta\gamma}^s(s, t) = \epsilon_{\alpha\beta\gamma} f_{\lambda}^s(s, t). \quad (6.13)$$

By Bose statistics,  $f_{\lambda}^s(s, t)$  is then antisymmetric in  $p_1$  and  $p_2, p_1$  and  $p_3$ . It is linear in the polarization vector  $\epsilon^{(\lambda)}$  of the  $\omega$ . Hence

$$f_{\lambda, \alpha\beta\gamma}^s = \epsilon_{\alpha\beta\gamma} \epsilon_{\mu\nu\sigma\tau} p_1^\mu p_2^\nu p_3^\sigma \epsilon^{(\lambda)\tau} A(s, t, u), \quad (6.14)$$

where the invariant amplitude is totally symmetric in  $s, t$ , and  $u$ , with

$$s + t + u = \Sigma = 3m_\pi^2 + m_\omega^2. \quad (6.15)$$

One can evaluate the coefficient of  $A(s, t, u)$  explicitly and show

$$\begin{aligned} f_{0, \alpha\beta\gamma}^s &= 0 \\ f_{+1, \alpha\beta\gamma}^s &= f_{-1, \alpha\beta\gamma}^s \\ &= \pm \frac{1}{2} \epsilon_{\alpha\beta\gamma} (stu - m_\pi^2(m_\omega^2 - m_\pi^2))^{\frac{1}{2}} A(s, t, u). \end{aligned} \quad (6.16)$$

Since  $f_{1, \alpha\beta\gamma}^s(s, t) \sim s^{\alpha(t)}$ , the asymptotic behavior for  $A$  is

\*-----  
M. Ademollo, H. R. Rubenstein, G. Veneziano, and M. A. Virasoro,  
Phys. Rev. 176, 1904 (1968).



$$A(s,t,u) \sim s^{\alpha(t)-1}. \quad (6.17)$$

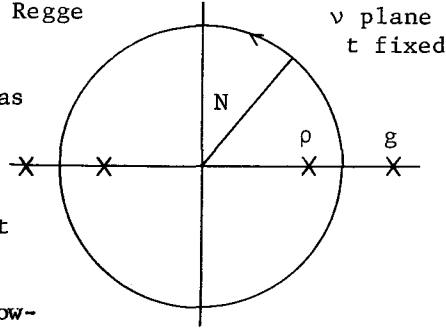
We again introduce the variable  $v = (s-u)/2s_0$  and write  $A(v,t)$  for the invariant amplitude. We consider the FESR from (6.10) with  $n=1$ :

$$\int_0^N dv v \operatorname{Im} A(v,t) = \frac{\bar{\gamma} N^{\alpha+1}}{(\pi)^{\frac{1}{2}}(\alpha+1)\Gamma(\alpha)} = \frac{\bar{\gamma} \alpha N^{\alpha+1}}{\Gamma(\alpha+2)} \quad (6.18)$$

where  $\bar{\gamma} = \gamma/(\pi)^{\frac{1}{2}}$ , and  $\alpha = \alpha(t)$  is the  $\rho$  trajectory.

Since we have omitted from the right hand side of (6.18) any lower-lying trajectories that may be present, it is valid only for sufficiently large  $N$ . Now Ademollo et al. make the additional assumption that for at least a limited range of  $t$ , (6.18) is valid even for  $N$  so small that in the interval  $0 < v < N$ ,  $A(v,t)$  has only one resonance, the  $\rho$  resonance. In terms of properties in the complex  $v$  plane, the assumption is that for at least a limit range of  $t$ , the contour integral of  $vA(v,t)$  over the circle shown in the sketch is well approximated by that of the leading Regge

pole contribution. There is no a priori justification for this assumption. It was introduced partly as an inspired guess, partly as a calculational convenience. But it turns out to be the condition that bootstraps the  $\rho$  with brilliant success.



Since this requires the FESR in the narrow-

resonance approximation to be satisfied in a non-asymptotic region of  $N$ , it may be called a condition of strong duality. We adopt this word as a shorthand for the assumption described and refrain from philosophizing. The input assumptions are that the  $\rho$  trajectory is linear and passes through 1 at  $t=m_\rho^2 \approx 0.5(\text{GeV}/c)^2$ :

$$\alpha(t) = \alpha_0 + \alpha' t, \quad \alpha(m_\rho^2) = 1 \quad (6.19)$$

This leaves only one unknown constant among  $\alpha_0$  and  $\alpha'$ . Now  $\alpha(t)$  makes  $t$ -channel resonances at  $\alpha = 1, 3, \dots$ , corresponding to  $t = m_\rho^2, m_\rho^2, \dots$ . By crossing symmetry, there are  $s$ -channel resonances at  $s = m_\rho^2, m_g^2, \dots$ , with corresponding  $v$  values at

$$v_\rho(t) = [(s-u)/2s_0]_{s=m_\rho^2} = (t-t_0)/2s_0$$

$$v_g(t) = v_\rho(t) + 2/\alpha's_0 \quad (6.20)$$

where

$$t_0 = m_\omega^2 + 3m_\pi^2 - 2m_\rho^2 = -0.53(\text{GeV}/c)^2. \quad (6.21)$$

Assuming strong duality, we cut off the integral in (6.18) at same point between the  $\rho$  and the  $g$  meson, i.e.,

$$v_\rho(t) < N < v_g(t). \quad (6.22)$$

To do the integral, we have to know the residue of the  $\rho$  pole at  $v = v_\rho(t)$ . This can be obtained from the input  $\rho$  trajectory through crossing symmetry, as follows. The  $\rho$  trajectory exchanged in the  $t$ -channel contributes to  $A(v,t)$  the Khuri term

$$K_\alpha(v,t) = \bar{\gamma} \Gamma(1-\alpha) (1-e^{-i\pi\alpha}) v^{\alpha-1}, \quad (6.23)$$

which has a pole at  $\alpha = 1$ :

$$K_\alpha(v,t) \xrightarrow{\alpha \rightarrow 1} \frac{2\bar{\gamma}}{1-\alpha} = -\frac{2\bar{\gamma}}{\alpha'} \frac{1}{t-m_0} . \quad (6.24)$$

Hence the residue is  $-2\bar{\gamma}/\alpha'$ . By crossing symmetry, the  $\rho$  pole in the  $s$ -channel must have the same residue. Hence

$$A(v,t) \xrightarrow{v \rightarrow v_\rho} -\frac{2\bar{\gamma}}{\alpha'} \frac{1}{s-m_0} = -\frac{2\bar{\gamma}}{\alpha' s_0} \frac{1}{v-v_\rho}, \quad (6.25)$$

which gives

$$\text{Im}A(v,t) = \frac{2\pi\bar{\gamma}}{\alpha' s_0} \delta(v-v_\rho) \quad (6.26)$$

in the range (6.22), in the narrow-resonance approximation. Substituting (6.26) into the FESR (6.18), we obtain

$$v_\rho(t) = \frac{\alpha' s_0 \alpha N^{\alpha+1}}{2\Gamma(\alpha+2)}. \quad (6.27)$$

Note that the residue function  $\bar{\gamma}(t)$  drops out.

We first note that  $v_\rho(t_0) = 0$ . Hence

$$\alpha(t_0) = 0, \quad (6.28)$$

and this completely determines the  $\rho$  trajectory, leading to

$$\alpha_0 = \frac{-t_0}{m_\rho^2 - t_0} = \frac{2m_\rho^2 - 3m_\pi^2 - m_\omega^2}{3m_\rho^2 - 3m_\pi^2 - m_\omega^2} \approx 0.5$$

$$\alpha' = \frac{1}{m_\rho^2 - t_0} = \frac{1}{3m_\rho^2 - 3m_\pi^2 - m_\omega^2} \approx 1(\text{GeV}/c)^2, \quad (6.29)$$

which are in remarkably good agreement with experiments. The condition (6.28) can be re-expressed in an amusing form by noting that  $\alpha_0 + \alpha' t_0 = \alpha(s) + \alpha(t) + \alpha(u) - 2$ . Hence, (6.28) is equivalent to the following condition for the  $\rho$  trajectory:

$$\alpha(s) + \alpha(t) + \alpha(u) = 2, \quad (6.30)$$

which is of course very well satisfied experimentally.

With  $\alpha(t)$  determined, it remains to be seen whether (6.27) can be satisfied for a range of  $t$ . Using (6.28), we can write  $v_\rho(t) = \alpha(t)/2\alpha' s_0$ , and substituting into (6.27) yields the condition

$$\frac{(\alpha' s_0)^2 N^{\alpha(t)+1}}{\Gamma(\alpha(t)+2)} = 1. \quad (6.31)$$

It is now noted that the following is a miraculously good approximation:

$$\frac{(1 + \frac{1}{2}\alpha)^{\alpha+1}}{\Gamma(\alpha+2)} \approx 1 \quad (-1 < \alpha < +1) \quad (6.32)$$

Therefore a solution of (6.31) for  $-1 < \alpha(t) < 1$  is

$$\begin{aligned} s_0 &= 1/\alpha' \\ N &= 1 + \frac{1}{2}\alpha(t) \end{aligned} \quad (6.33)$$

Thus the arbitrary scale  $s_0$  is now fixed. The cutoff  $N$  happens to fall exactly halfway between the  $\rho$  and the  $g$  meson, for using the  $\alpha(t)$  and  $s_0$  now determined, we find that

$$\frac{1}{2}[v_\rho(t) + v_g(t)] = 1 + \frac{1}{2}\alpha(t). \quad (6.34)$$

Ademollo et al. went on to investigate how they might extend the range of  $t$  in which the FESR is satisfied. It turns out that this involves pushing the cutoff  $N$  higher to include more resonances on the right-hand side, and at the same time including lower-lying trajectories on the right-hand side.

The most interesting aspect of this calculation is the fact that strong duality, which seems to be an ad hoc assumption, leads miraculously to some good results. We shall return to it in the Veneziano model, which is a crystallization of all the ideas we have discussed.

#### E. The Veneziano Model.

As we have seen, the FESR in the narrow-resonance approximation can be satisfied unexpectedly for a limited range of  $t$  by using a low cutoff as

the left-hand side and only one Regge pole as the right-hand side. To extend the range of  $t$ , the cutoff has to be increased, and more Regge poles have to be included. The Veneziano model is a simple formula that incorporates all these features. In short, it is a simple solution to the FESR in the narrow-resonance approximation.

Recalling what FESR means in the narrow-resonance approximation, we see that for the process  $\pi\pi \rightarrow \pi\omega$  a solution consists of finding an amplitude completely symmetric in  $s, t, u$ , having no cuts but only simple poles in  $s$ , and behaving like  $s^{\alpha(t)-1}$  as  $s \rightarrow \infty$ . Veneziano suggests the form

$$A(s, t, u) = +\gamma[V(s, t) + V(s, u) + V(t, u)] \quad (6.35)$$

where

$$V(s, t) = \frac{\Gamma(1-\alpha_s)\Gamma(1-\alpha_t)}{\Gamma(2-\alpha_s-\alpha_t)} = B(1-\alpha_s, 1-\alpha_t), \quad (6.36)$$

where  $\alpha_s \equiv \alpha(s)$ ,  $\alpha_t \equiv \alpha(t)$ , and where  $B(z, w)$  is the Beta function. Since  $\Gamma(z)$  is a meromorphic function with simple poles at  $z = 0, 1, 2, \dots$ ,  $V(s, t)$  has no cuts but has poles at  $\alpha(s) = 1, 2, 3, \dots$ . Because of the gamma functions in the denominator, there are no simultaneous poles in  $s$  and  $t$ .

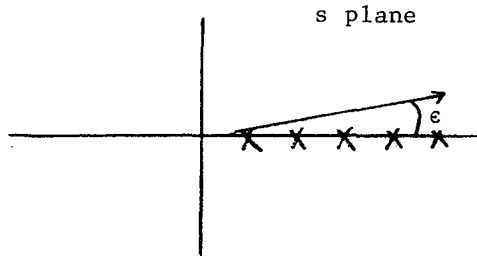
To compute the asymptotic behavior, we need the formula

$$\Gamma(a+bz) \xrightarrow{|z| \rightarrow \infty} (\pi)^{\frac{1}{2}} e^{-bz} (bz)^{a+bz-\frac{1}{2}}, \quad b > 0, |\arg z| \leq \pi - \epsilon. \quad (6.37)$$

We first rewrite (6.36) in the form

$$v(s, t) = \Gamma(1-\alpha_t) \frac{\Gamma(\alpha_s + \alpha_t - 1)}{\Gamma(\alpha_s)} \frac{\sin \pi \alpha_s}{\sin \pi (\alpha_s + \alpha_t - 1)} \quad (6.38)$$

The limit  $s \rightarrow \infty$  does not exist along the real axis because  $V(s, t)$  has an infinite number of poles there. To avoid this difficulty, which is inherent in the narrow-resonance approximation, we take the limit along a ray in the complex  $s$  planes at an arbitrarily small angle  $\epsilon$  with respect to the real axis.



Then

$$\begin{aligned} \sin \pi \alpha(s) &= \frac{1}{2i} [e^{i\pi\alpha_s} - e^{-i\pi\alpha_s}] \\ &\rightarrow -\frac{1}{2i} e^{-i\pi\alpha_s} [1 + O(e^{-2\pi\epsilon s})], \end{aligned} \quad (6.39)$$

and

$$\sin \pi(\alpha_s + \alpha_t - 1) \rightarrow -\frac{1}{2i} e^{-i\pi(\alpha_s + \alpha_t - 1)} [1 + O(e^{-2\pi\epsilon s})], \quad (6.40)$$

so that

$$V(s,t) \rightarrow \Gamma(1-\alpha_t) e^{-i\pi(\alpha_t - 1)} (\alpha's)^{\alpha_t - 1}. \quad (6.41)$$

Note that to get this result, the linearity of  $\alpha_s$  is crucial, at least asymptotically. For  $V(t,u)$  we can straightforwardly apply (6.37) to obtain

$$V(t,u) \rightarrow \Gamma(1-\alpha(t)) (\alpha's)^{\alpha(t)-1}. \quad (6.42)$$

Finally,

$$\begin{aligned} V(s,u) &= \frac{1}{\Gamma(1-2\alpha_o - \alpha'(\Sigma-t))} \frac{\Gamma(1-\alpha(u))}{\Gamma(\alpha(s))} \frac{\pi}{\sin \pi \alpha(s)} \\ &= O(e^{-\pi\epsilon s}) \end{aligned} \quad (6.43)$$

Hence

$$A(s,t,u) \xrightarrow{s \rightarrow \infty} -\gamma \Gamma(1-\alpha(t)) (e^{-i\pi\alpha(t)} - 1) (\alpha's)^{\alpha(t)-1}, \quad (6.44)$$

which is the proper Regge behavior. If we had used the complete asymptotic expansion for  $\Gamma(z)$ , we would have obtained in place of (6.44)

$$A(s,t,u) \xrightarrow{z \rightarrow \infty} -\gamma \Gamma(1-\alpha_t) (e^{-i\pi\alpha_t} - 1) (\alpha's)^{\alpha_t - 1} [1 + \sum_{n=1}^{\infty} c_n(t) s^{-n}].$$

Thus there are an infinite number of parallel "daughter" trajectories  $\alpha_n(t) = \alpha(t) - n$  ( $n = 1, 2, \dots$ ).

From the asymptotic behavior of the amplitude we would expect that at each mass there would be particles of all odd spins up to the leading trajectory. This is in fact the case. From (6.36) and the integral representation of the Beta function, we have

$$V(s,t) = \int_0^1 dx x^{-\alpha_s} (1-x)^{-\alpha_t}. \quad (6.45)$$

Using the binomial theorem, we obtain

$$\begin{aligned}
V(s,t) &= \sum_{n=0}^{\infty} (-1)^n \binom{-\alpha_t}{n} \int_0^1 dx x^{-\alpha_s + n} \\
&= \sum_{n=0}^{\infty} (-1)^n \binom{-\alpha_t}{n} \frac{1}{n+1-\alpha_s}
\end{aligned} \tag{6.47}$$

where

$$\begin{aligned}
(-1)^n \binom{-\alpha_t}{n} &= (-1)^n \frac{\Gamma(1-\alpha_t)}{n! \Gamma(1-\alpha_t-n)} \\
&= \frac{1}{n!} \alpha_t (\alpha_t + 1) (\alpha_t + 2) \dots (\alpha_t + n - 1) \\
&= \frac{1}{n!} R_n(\alpha_t).
\end{aligned} \tag{6.48}$$

$R_n(x)$  is called a Pochhammer polynomial of degree  $n$ . Hence

$$V(s,t) = \sum_{n=0}^{\infty} \frac{1}{n!} \frac{R_n(\alpha_t)}{n+1-\alpha_s}. \tag{6.49}$$

As  $\alpha_s \rightarrow n+1$ , therefore,

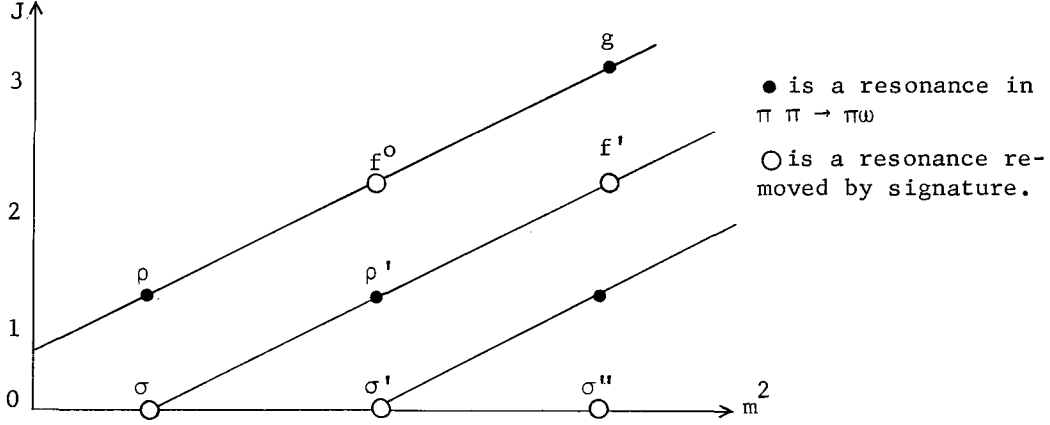
$$A(s,t,u) \rightarrow \gamma \frac{R_n(\alpha_t) + R_n(\alpha_u)}{n+1-\alpha_s}. \tag{6.50}$$

Since  $\alpha_t$  and  $\alpha_u$  are linear in  $t$ , the residue is a polynomial in  $t$  symmetric under  $t \leftrightarrow u$ . To find the spin of the resonances at  $\alpha_s = n+1$ , we have to express the residue in Legendre polynomials of  $z_s$ :

$$z_s = \frac{s(t-u)}{[s(s-4m_\pi^2)(s-(m_\omega-m_\pi)^2)(s-(m_\omega+m_\pi)^2)]^{\frac{1}{2}}}. \tag{6.51}$$

We note that this is linear in  $t$ , and odd under  $t \leftrightarrow u$ . Hence the residue is a polynomial in  $z_s$  containing only even powers. Since the  $\omega$  meson has spin one, this implies\* that at a mass  $m$  satisfying  $\alpha(m^2) = n+1$ , there are resonances of all odd spins up to  $n+1$ . Thus the Veneziano model requires that the mass spectrum forms a regular lattice on the Chew-Frantschi plot, as shown below.

\*-----  
 \* See Chapter 7 for partial-wave expansions.



It is clear that the Veneziano model satisfies the FESR because it has analyticity and Regge asymptotic behavior. With narrow resonance built in, it represents an elegant example of duality. However, while the FESR are satisfied, the trajectories are not completely determined. If one of the meson masses (say that of the  $\rho$  meson) is supposed to be given, we still have an arbitrary slope  $\alpha'$ . This again demonstrates, as in the previous calculation of Ademollo et al. that the FESR alone is not enough to bootstrap. In the previous case, the bootstrap comes from the ad hoc assumption of strong duality, which turns out to be equivalent to the requirement that not only even-spin mesons like the  $f^0$  be decoupled, but also all mesons (of whatever spin) at the same mass. For example, referring to the previous sketch, we would require that  $\rho'$  be decoupled also. From (6.50), we see that this would require

$$R_n(\alpha_t) + R_n(\alpha_u) \equiv 0 \quad (\text{for } n \text{ odd}), \quad (6.52)$$

By (6.48), this is equivalent to

$$\alpha_t(\alpha_t+1) \cdots (\alpha_t+n-1) \equiv -\alpha_u(\alpha_u+1) \cdots (\alpha_u+n-1), \quad (6.53)$$

(for  $n$  odd)

and is solved by setting  $\alpha_t = -(\alpha_u+n-1)$ . Noting that  $n+1 = \alpha_s$ , we obtain the condition

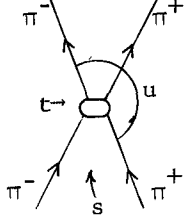
$$\alpha_s + \alpha_t + \alpha_u = 2, \quad (6.54)$$

which is the same as the consequence of strong duality in the earlier calculation of Ademollo et al., and which agrees well with experiments. In this model,

however, there seems to be no compelling reason to require it.\* For the present, therefore, strong duality remains a tantalizing idea not yet fully understood.

F. Veneziano Model for  $\pi$ - $\pi$  Scattering.

Lovelace<sup>†</sup> has made an interesting application of the Veneziano model to  $\pi$ - $\pi$  scattering. To take care of isospin complications, we first show that all 3 isospin amplitudes can be expressed in terms of a single symmetric function of  $s$  and  $t$ . Consider first  $\pi^+\pi^-$  scattering as illustrated in the sketch, and let



$$f_{\pi^+\pi^-}^S(s,t) = \varphi(s,t) \quad (6.55)$$

Since the  $t$ -channel also corresponds to  $\pi^+\pi^-$  scattering,

$$\varphi(s,t) = \varphi(t,s) \quad . \quad (6.56)$$

Since the  $u$ -channel corresponds to  $\pi^+\pi^+$  scattering,

$$f_{\pi^+\pi^+}^S(s,t) = \varphi(u,t) \quad . \quad (6.57)$$

Now decompose the  $\pi^+\pi^-$  amplitude into amplitudes  $f_I^S(s,t)$  of definite isospin  $I$  in the  $s$ -channel:

$$\varphi(s,t) = \frac{1}{6} f_2^S(s,t) + \frac{1}{2} f_1^S(s,t) + \frac{1}{3} f_0^S(s,t) \quad , \quad (6.58)$$

where  $f_2^S$  and  $f_0^S$  are even, and  $f_1^S$  is odd, under  $t \leftrightarrow u$ :

$$f_I^S(s,t) = (-1)^I f_I^S(s,u). \quad (6.59)$$

Thus

$$\varphi(s,u) = \frac{1}{6} f_2^S(s,t) - \frac{1}{2} f_1^S(s,t) + \frac{1}{3} f_0^S(s,t). \quad (6.60)$$

Subtracting (6.60) from (6.58), we obtain  $f_1^S(s,t) = \varphi(s,t) - \varphi(t,u)$ . We also know that  $\pi^+\pi^+$  is pure  $I = 2$ , hence by (6.57)  $f_2^S(s,t) = \varphi(u,t)$ . Substituting these results into (6.58), we find  $f_0^S(s,t)$ . The final results are:

$$\begin{aligned} f_0^S(s,t) &= \frac{3}{2} [\varphi(s,t) + \varphi(s,u)] - \frac{1}{2} \varphi(t,u) \quad , \\ f_1^S(s,t) &= \varphi(s,t) - \varphi(s,u) \quad , \\ f_2^S(s,t) &= \varphi(u,t) \quad . \end{aligned} \quad (6.61)$$

\*-----  
\* In the original paper of Veneziano, (6.54) was invoked to obtain signatured trajectories; but we have seen that signature emerges automatically without this condition.

† C. Lovelace, Phys. Letters, 28B, 264 (1968).



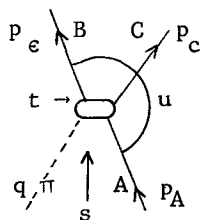
Therefore specifying  $\varphi(s,t)$  completely specifies  $\pi$ - $\pi$  scattering.

Lovelace constructed the Veneziano model for  $\pi$ - $\pi$  scattering by taking

$$\varphi(s,t) = -\gamma \frac{\Gamma(1-\alpha_s)\Gamma(1-\alpha_t)}{\Gamma(1-\alpha_s-\alpha_t)} \quad (6.62)$$

where  $\Gamma(1-\alpha_s-\alpha_t)$  rather than  $\Gamma(2-\alpha_s-\alpha_t)$  appears in the denominator because this amplitude should behave like  $s^{\alpha(t)}$  as  $s \rightarrow \infty$ . With this choice there are no resonances in the  $I = 2$  amplitude since  $\varphi(u,t)$  has no poles in  $s$ . There are resonances of both even and odd spin on  $\alpha_s$  in the  $I = 0$  amplitude, but only resonances of odd spin occur in the  $I = 1$  amplitude. The trajectory  $\alpha_s$  is identified as the exchange degenerate  $\rho$ - $f^0$  trajectory. This exchange degeneracy corresponds to the absence of  $I = 2$  resonances.

One of the most interesting aspects of this model is the prediction of a



zero in the amplitude coinciding with that required by the Adler self-consistent condition.

In general, in the reaction  $\pi A \rightarrow BC$ , where  $A B C$  are hadrons, the hypothesis of PCAC (partial conservation of axial vector current), plus some assumption about the absence of poles,

leads to the conclusion that the scattering amplitude must vanish as the four-momentum  $q$  of the pion approaches zero. This result is known as the Adler self-consistent condition. In terms of  $s,t,u$ , the zero is located at

$$\begin{aligned} s &= (p_A)^2 = m_A^2 \\ t &= (p_B)^2 = m_B^2 \\ u &= (p_A - p_B)^2 = m_C^2 \end{aligned} \quad (6.63)$$

which of course does not satisfy the constraint  $s+t+u = \Sigma m^2$ , because the pion is taken off the mass shell. For  $\pi$ - $\pi$  scattering (6.63) becomes

$$s=t=u = m_\pi^2 \quad (6.64)$$

Let us rewrite (6.62) in the form

$$\varphi(s,t) = -\gamma(1-\alpha_s-\alpha_t) B(1-\alpha_s, 1-\alpha_t) \quad (6.65)$$

At  $s=t=u = m_\pi^2$ , the Beta function cannot vanish, but the factor  $1-\alpha_s-\alpha_t$  vanishes if

$$\alpha(m_\pi^2) = \frac{1}{2}. \quad (6.66)$$

Combining this with  $\alpha(m_\rho^2) = 1$ , we find

$$\alpha_o = 0.483$$

$$\alpha' = 0.83$$

(6.67)

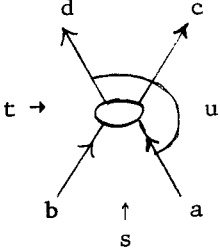
which is in excellent agreement with experiments.

## VII. SPIN

We now consider the full complications of spin. In particular we emphasize those features that owe their existence to spin, such as kinematic singularities, constraints, and sense-nonsense.

### A. Kinematics

For a general two-body process  $a+b \rightarrow c+d$  with arbitrary masses and spins, we specify single-particle states by their momenta and helicities. As usual let

$$\begin{aligned}
 s &= (p_a + p_b)^2 \\
 t &= (p_b - p_d)^2 \\
 u &= (p_a - p_d)^2
 \end{aligned}$$

(7.1)

which satisfy the relation

$$s + t + u = m_a^2 + m_b^2 + m_c^2 + m_d^2 \equiv \Sigma \quad . \quad (7.2)$$

The cosines of the center-of-mass scattering angles in the  $s$  and  $t$  channels are given by

$$\begin{aligned}
 z_s = \cos\theta_s &= \frac{s(2t+s-\Sigma) + (m_a^2 - m_b^2)(m_c^2 - m_d^2)}{\mathcal{L}_{ab} \mathcal{L}_{cd}} \quad , \\
 z_t = \cos\theta_t &= \frac{t(2s+t-\Sigma) + (m_d^2 - m_b^2)(m_c^2 - m_a^2)}{\mathcal{J}_{bd} \mathcal{J}_{ca}} \quad ,
 \end{aligned} \quad (7.3)$$

where

$$\begin{aligned}
 \mathcal{L}_{ab} &= \sqrt{[s - (m_a - m_b)^2] [s - (m_a + m_b)^2]} = \sqrt{4sp_{ab}^2} \quad , \\
 \mathcal{J}_{ca} &= \sqrt{[t - (m_c - m_a)^2] [t - (m_c + m_a)^2]} = \sqrt{4tp_{ca}^2} \quad ,
 \end{aligned} \quad (7.4)$$

where the square roots are positive for positive values of their arguments. The physical region corresponds to

$$\varphi(s, t) \geq 0 \quad , \quad (7.5)$$

where  $\varphi(s, t)$  is the Kibble function:

$$\begin{aligned}
 \varphi(s, t) &= stu - s(m_b^2 - m_d^2)(m_a^2 - m_c^2) - t(m_a^2 - m_b^2)(m_c^2 - m_d^2) \\
 &\quad - (m_a^2 m_d^2 - m_c^2 m_b^2)(m_a^2 + m_d^2 - m_c^2 - m_b^2) \quad .
 \end{aligned} \quad (7.6)$$

## B. Helicity Amplitudes

For the purpose of Regge analysis, it is particularly convenient to use the helicity amplitudes of Jacob and Wick,<sup>\*</sup> because they have simple partial-wave expansions. The helicity amplitude for s-channel scattering will be denoted by  $f_{cd,ab}^s(s,t)$ , where the subscripts denote both the particles and their helicities. For its definition and properties we refer to the original paper of Jacob and Wick. Our normalization is such that the differential cross section is given by

$$\frac{d\sigma}{d\Omega} = \frac{1}{4\pi^2} \frac{P_{cd}}{P_{ab}} |f_{cd;ab}^s(s,t)|^2 \quad (7.7)$$

Our amplitude is related to that of Jacob and Wick by

$$f_{cd;ab}^{JW}(s,t) = \sqrt{\frac{1}{4\pi^2} \frac{P_{cd}}{P_{ab}}} f_{cd;ab}^s(s,t) \quad (7.8)$$

The partial-wave expansion reads

$$f_{cd,ab}^s(s,t) = \sum_{J=\lambda_m}^{\infty} (2J+1) F_{cd;ab}^J(s) d_{\lambda_{\mu}}^J(z_s) \quad (7.9)$$

$$\lambda = a-b, \quad \mu = c-d, \quad \lambda_m = \max(\lambda, \mu)$$

where  $d_{\lambda_{\mu}}^J(z_s)$  are the usual rotation coefficients. The partial-wave amplitude

$F_{cd,ab}^J(s)$  is a matrix element taken between helicity states of definite total angular momentum  $J$  and  $z$  component  $M$ :

$$F_{cd;ab}^J(s) = \langle J, M; c, d | T(s) | J, M; a, b \rangle \quad (7.10)$$

These helicity states transform under spatial reflection  $P$  according to

$$P |J, M; a, b\rangle = \eta_a \eta_b (-)^{J-J_a-J_b} |J, M; -a, -b\rangle \quad (7.11)$$

where  $J_a, J_b$  are the spins of the particles  $a, b$ , and  $\eta_a, \eta_b$  their intrinsic parities.

---

\* M. Jacob and G.C. Wick, *Annals of Physics* 7, 404 (1959).

Thus parity conservation implies

$$F_{-c,-d;-a,-b}^J(s) = \eta_a \eta_b \eta_c \eta_d (-)^{J_c+J_d-J_a-J_b} F_{cd;ab}^J(s) \quad (7.12)$$

Time reversal invariance implies

$$F_{cd;ab}^J(s) = F_{ab;cd}^J(s) \quad (7.13)$$

Equations (7.12) and (7.13) serve to reduce the number of independent helicity amplitudes.

The crossing relation between the s and t channel helicity amplitudes is\*

$$f_{cd,ab}^s(s,t) = \sum_{C'A'D'b'} d_{A'a}^{J_a}(\chi_a) d_{b'b}^{J_b}(\chi_b) d_{c'c}^{J_c}(\chi_c) d_{D'd}^{J_d}(\chi_d) f_{c'A',D'b'}^t(s,t), \quad (7.14)$$

where

$$\begin{aligned} \cos\chi_a &= - \frac{(s+m_a^2-m_b^2)(t+m_a^2-m_c^2) - 2m_a^2(m_c^2-m_a^2+m_b^2-m_d^2)}{\mathcal{S}_{ab}\mathcal{T}_{ac}}, \\ \cos\chi_b &= \frac{(s+m_b^2-m_a^2)(t+m_b^2-m_d^2) - 2m_b^2(m_c^2-m_a^2+m_b^2-m_d^2)}{\mathcal{S}_{ab}\mathcal{T}_{bd}}, \\ \cos\chi_c &= \frac{(s+m_c^2-m_d^2)(t+m_c^2-m_a^2) - 2m_c^2(m_c^2-m_a^2+m_b^2-m_d^2)}{\mathcal{S}_{cd}\mathcal{T}_{ac}}, \\ \cos\chi_d &= - \frac{(s+m_d^2-m_c^2)(t+m_d^2-m_b^2) - 2m_d^2(m_c^2-m_a^2+m_b^2-m_d^2)}{\mathcal{S}_{cd}\mathcal{T}_{bd}}, \end{aligned} \quad (7.15)$$

and

$$\begin{aligned} \sin\chi_a &= \frac{2m_a\sqrt{\varphi(s,t)}}{\mathcal{S}_{ab}\mathcal{T}_{ac}}, \\ \sin\chi_b &= \frac{2m_b\sqrt{\varphi(s,t)}}{\mathcal{S}_{ab}\mathcal{T}_{bd}}, \\ \sin\chi_c &= \frac{2m_c\sqrt{\varphi(s,t)}}{\mathcal{S}_{cd}\mathcal{T}_{ac}}, \\ \sin\chi_d &= \frac{2m_d\sqrt{\varphi(s,t)}}{\mathcal{S}_{cd}\mathcal{T}_{bd}}. \end{aligned} \quad (7.16)$$

---

\* L. Trueman and G.C. Wick, Annals of Physics 26, 322 (1964).

We may write symbolically

$$f_H^S(s,t) = \sum_{H'} \mathcal{M}_{HH'}(s,t) f_{H'}^T(s,t) , \quad (7.17)$$

where  $\mathcal{M}$  is a real orthogonal matrix:  $\mathcal{M}^T \mathcal{M} = 1$ . It should be noted that (7.14) is not valid for an amplitude that differs from ours by a normalization factor that depends on  $s$  and  $t$ . In particular it is not valid for  $f^{JW}$  of (7.8).

The main advantages of helicity amplitudes are the following. (a) The number of independent amplitudes can be easily enumerated and written down for an arbitrary reaction. (b) By (7.11) it is easy to form helicity states of definite parity, and Regge trajectories couple to them independently. (c) It is straightforward to carry out the Sommerfeld-Watson transform on (7.9) to isolate Regge pole contributions.

Helicity amplitudes, however, have kinematic singularities and satisfy constraint equations at certain values of  $s$  and  $t$ . These are intrinsic in their definition and give rise to complicated structures in Regge residues that were not present in the spinless case.

Instead of helicity amplitudes one can describe the scattering process in terms of invariant amplitudes, which by definition is a set of independent amplitudes completely free of kinematic singularities and constraints. We shall not discuss them in general but merely illustrate them in specific examples. Although it can be proven that invariant amplitudes exist for an arbitrary reaction, there is yet no known method for their explicit construction in the general case. From our point of view the main disadvantage of invariant amplitudes is that the same Regge trajectory generally couples to more than one amplitude, so that Regge residues in different amplitudes cannot be independent.

### C. Kinematic Singularities and Constraints

According to Jacob and Wick, a general helicity state is defined as follows. First define the helicity state of a single particle at rest. Then define that for a moving particle by applying the boost operator of a Lorentz transformation. The helicity state for two particles is the product of two of the above, rotated in a standard way by the application of a total rotation operator. The helicity amplitudes are defined as T-matrix elements with respect to two-particle helicity states, and singularities and constraints generally arise from the fact that the boost and rotation operators become singular at certain kinematic points. These have nothing to do with the interactions of particles, and we call them kinematic singularities and constraints. An analysis from this point of view is

given by Trueman,<sup>\*</sup> who shows from general principles that kinematic singularities in  $s$  can occur only at one of the following places:

- (a) At  $\mathcal{S}_{ab} = 0$  or  $\mathcal{S}_{cd} = 0$ , namely  $s = (m_a + m_b)^2$  or  $s = (m_c + m_d)^2$ . The values corresponding to the + sign are thresholds, the others are called pseudothresholds.
- (b) Boundary of the physical region  $\varphi(s,t) = 0$ .
- (c) The point  $s = 0$ .

Kinematic constraints can occur only at pseudothresholds or at  $\varphi(s,t) = 0$ . Most important for our purpose, the kinematic singularities at (a) or (b) above can be factored out of the helicity amplitudes. Those at (c) can be factored out except for fermion-boson scattering in the general mass case, where there is a non-factorizable singularity of the type  $s^{\frac{1}{2}}$ . For this case, however, one can circumvent it by using  $W = s^{\frac{1}{2}}$  as independent variable.

Another approach, more elementary but less satisfactory from the point of view of general principles, is due to Wang.<sup>\*\*</sup> It makes use only of the crossing relation for helicity amplitudes and is a relatively straightforward constructive recipe in specific cases. We shall briefly describe this approach here.

Going back to the partial wave expansion

$$f_H^S(s,t) = \sum_{J=\lambda_m}^{\infty} (2J+1) F_H^J(s) d_{\lambda\mu}^J(z_s) \quad , \quad (7.18)$$

we see that the  $t$  dependence is contained in  $z_s$  in the rotation coefficient  $d_{\lambda\mu}^J(z_s)$ . Now

$$d_{\lambda\mu}^J(z) = D_{\lambda\mu}(z) e_{\lambda\mu}^J(z) \quad , \quad (7.19)$$

where

$$D_{\lambda\mu}(z) \equiv (1+z)^{\frac{1}{2}|\lambda+\mu|} (1-z)^{\frac{1}{2}|\lambda-\mu|} \quad , \quad (7.20)$$

and  $e_{\lambda\mu}^J(z)$  is a polynomial in  $z$ . (We use the notation of GGLMZ.<sup>\*\*\*</sup>) Since the factor  $D_{\lambda\mu}(z)$  is independent of  $J$ , it can be factored out of the sum in (7.18):

$$f_H^S(s,t) = D_{\lambda\mu}(z_s) \bar{f}_H^S(s,t) \quad , \quad (7.21)$$

\* T.L. Trueman, Phys. Rev. 173, 1684 (1968). Errata, Phys. Rev. 181, 2154 (1969).

\*\* L.L. Wang, Phys. Rev. 142, 1187 (1965).

\*\*\* M. Gell-Mann, M. Goldberger, F.E. Low, E. Marx, and F. Zachariasen, Phys. Rev. 133, B145 (1964).

where

$$\bar{f}_H^s(s,t) = \sum_{J=\lambda_m}^{\infty} (2J+1) F_H^J(s) e_{\lambda_\mu}^J(z_s) \quad . \quad (7.22)$$

The only  $t$ -singularities of  $\bar{f}_H^s(s,t)$  come from the possible divergences of the whole series. We presume that these are dynamical and not kinematic singularities. Similarly, if we put

$$f_H^t(s,t) = D_{\lambda_\mu}(z_s) \bar{f}_H^t(s,t) \quad , \quad (7.23)$$

then  $\bar{f}_H^t(s,t)$  has no  $s$ -kinematic singularities.

The new amplitudes  $\bar{f}^s$  and  $\bar{f}^t$ , however, are related through a crossing relation of the form

$$\bar{f}_H^s(s,t) = \sum_{H'} \mathcal{N}_{HH'}(s,t) \bar{f}_{H'}^t(s,t) \quad , \quad (7.24)$$

where the matrix  $\mathcal{N}$  can be deduced from the matrix  $\mathcal{M}$  in (7.17). Since  $\bar{f}^t(s,t)$  has no  $s$ -kinematic singularities by construction, all of the  $s$ -kinematic singularities of  $\bar{f}^s(s,t)$  must come from the known matrix  $\mathcal{N}(s,t)$ . Furthermore,  $\mathcal{N}(s,t)$  must cancel all of the  $t$ -kinematic singularities of  $\bar{f}^t(s,t)$ , because  $\bar{f}^s$  can have no such singularities. Thus by studying the matrix  $\mathcal{N}$  all the kinematic singularities in  $s$  and  $t$  can be recognized. In general this is an extremely tedious procedure, but one arrives at the same conclusion as mentioned before. In particular, we can factor out the  $s$ -kinematic singularities from each component of  $\bar{f}_H^s$ :

$$\bar{f}_H^s(s,t) = \mathcal{K}_H(s) \hat{f}_H^s(s,t) \quad (7.25)$$

where  $\hat{f}_H^s(s,t)$  is now free of all kinematic singularities,  $s$  or  $t$  (except for a  $s^{\frac{1}{2}}$  branch point for fermion-boson scattering in the general mass case).

Similarly we factor out all  $t$ -kinematic singularities from  $\bar{f}_H^t$ :

$$\bar{f}_H^t(s,t) = \mathcal{J}_H(t) \hat{f}_H^t(s,t) \quad (7.26)$$

where  $\hat{f}_H^t(s,t)$  is free of all kinematic singularities,  $s$  or  $t$ .

Substituting (7.25) and (7.26) into (7.24), we obtain a crossing relation of the form

$$\hat{f}_H^s(s,t) = \sum_{H'} \mathcal{L}_{HH'}(s,t) \hat{f}_{H'}^t(s,t) \quad (7.27)$$



where the matrix  $\mathcal{L}(s,t)$  generally has singularities in  $s$  and  $t$ , although  $\hat{f}_H^s$  cannot have these singularities. For values of  $s,t$  in the neighborhood of a singularity of  $\mathcal{L}(s,t)$ , let us write  $\mathcal{L}(s,t)$  as a matrix product between a matrix  $\mathcal{L}_1(s,t)$  containing the singularity, and a regular matrix  $\mathcal{L}_2(s,t)$  (of course  $\mathcal{L}_2$  may be simply the unit matrix):

$$\mathcal{L}(s,t) = \mathcal{L}_1(s,t) \mathcal{L}_2(s,t) \quad . \quad (7.28)$$

Then at the singularity, say  $s = s_0$ ,  $t = 0$ , we must have

$$\sum_{H'} [\mathcal{L}_2(s_0, t_0)]_{HH'} \hat{f}_H^t(s_0, t_0) = 0 \quad , \quad (7.29)$$

which is called a kinematic constraint.

The kinematic singularities and constraints discussed above lead to kinematic singularities and constraints in the  $t$ -channel partial-wave amplitudes  $G_H^J(t)$ . Since a Regge pole is a  $J$ -pole of the latter, with  $t$ -dependent residues, it follows that the Regge residues have known kinematic singularities and satisfy known constraints. In particular the constraints relate the residues of Regge poles of different quantum numbers at certain values of  $t$ .

D. Example:  $\pi\pi \rightarrow \pi\omega$

Earlier we have discussed the reaction  $\pi\pi \rightarrow \pi\omega$  in terms of an invariant amplitude (See Eq. (6.14)). Let us discuss it in terms of helicity amplitudes as an illustration.

There are three  $s$ -channel helicity amplitudes (See Eq. (6.13))  $f_\lambda^s(s,t)$ , where  $\lambda = 1, 0, -1$  is the helicity of  $\omega$ . The partial-wave expansion reads

$$f_\lambda^s(s,t) = \sum_{J=|\lambda|}^{\infty} (2J+1) F_\lambda^J(s) d_{0\lambda}^J(z_s) \quad , \quad (7.30)$$

where the partial-wave amplitude  $F_\lambda^J(s)$  is a matrix element between helicity states:

$$F_\lambda^J(s) = \langle \pi\omega; J, \lambda | T(s) | \pi\pi; J \rangle \quad . \quad (7.31)$$

Under the parity operation, the helicity states concerned transform as follows:

$$\begin{aligned} P | \pi\pi; J \rangle &= (-)^J | \pi\pi; J \rangle \\ P | \pi\omega; J, \lambda \rangle &= - (-)^J | \pi\omega; J, -\lambda \rangle \quad . \end{aligned} \quad (7.32)$$

The eigenstates of parity for the  $\pi\omega$  system are

$$|\pi\omega; J\pm\rangle = \frac{1}{\sqrt{2}} [ |\pi\omega; J, 1\rangle \mp |\pi\omega; J, -1\rangle ] \quad , \quad (7.33)$$

with

$$P|\pi\omega; J\pm\rangle = \pm (-)^J |\pi\omega; J\pm\rangle \quad . \quad (7.34)$$

By parity conservation the only non-vanishing matrix element between  $\pi\omega$  and  $\pi\pi$  states is

$$\langle\pi\omega; J+|T(s)|\pi\pi; J\rangle \equiv F^J(s) \quad , \quad (7.35)$$

in terms of which the partial-wave amplitudes are

$$F_1^J(s) = -F_{-1}^J(s) = \frac{1}{\sqrt{2}} F^J(s) \quad ,$$

$$F_0^J(s) = 0 \quad . \quad (7.36)$$

Therefore there are only two non-vanishing helicity amplitudes  $f_1^s(s,t)$  and  $f_{-1}^s(s,t)$ . Furthermore, owing to the fact that  $d_{\lambda\mu}^J(z) = (-)^{\lambda-\mu} d_{-\lambda, -\mu}^J(z)$ , they are equal to each other. Hence there is only one independent helicity amplitude  $f_1^s(s,t)$ . Since the reaction is the same for the s, t, and u channels,

$$f_1^s(s,t) = f_1^t(s,t) \quad (7.37)$$

up to a constant phase factor.

To factor out the kinematic singularities, we follow (7.21) and put

$$f_1^s(s,t) = (1-z_s^2)^{\frac{1}{2}} \bar{f}_1^s(s,t) \quad , \quad (7.38)$$

$$f_1^t(s,t) = (1-z_t^2)^{\frac{1}{2}} \bar{f}_1^t(s,t) \quad , \quad (7.39)$$

where  $\bar{f}_1^s(s,t)$  has no t-kinematic singularities, and  $\bar{f}_1^t(s,t)$  has no s-kinematic singularities. By (7.37), we have

$$(1-z_s^2)^{\frac{1}{2}} \bar{f}_1^s(s,t) = (1-z_t^2)^{\frac{1}{2}} \bar{f}_1^t(s,t) \quad . \quad (7.40)$$

Now we need to work out some kinematics:

$$z_s = (t-u)/4p_s q_s$$

$$z_t = (s-u)/4p_t q_t \quad , \quad (7.41)$$

where

$$p_s = \frac{1}{2}(s - 4m_\pi^2)^{\frac{1}{2}}$$

$$q_s = \{[s - (m_\omega + m_\pi)^2][s - (m_\omega - m_\pi)^2]/4s\}^{\frac{1}{2}} . \quad (7.42)$$

From these we find that

$$(1 - z_s^2)^{\frac{1}{2}} = \frac{1}{4p_s q_s} \left[ \frac{\varphi(s, t)}{s} \right]^{\frac{1}{2}}$$

$$(1 - z_t^2)^{\frac{1}{2}} = \frac{1}{4p_t q_t} \left[ \frac{\varphi(s, t)}{t} \right]^{\frac{1}{2}} , \quad (7.43)$$

where

$$\varphi(s, t) = stu - m_\pi^2(m_\omega^2 - m_\pi^2)^2 . \quad (7.44)$$

Substituting (7.43) into (7.40) we have

$$\frac{\bar{f}_1^s(s, t)}{4p_s q_s \sqrt{s}} = \frac{\bar{f}_1^t(s, t)}{4p_t q_t \sqrt{t}} . \quad (7.45)$$

Since  $\bar{f}_1^s$  has no  $t$ -kinematical singularity, and  $\bar{f}_1^t$  has no  $s$ -kinematical singularity, each side must be free of all kinematic singularities. That is

$$\frac{1}{4p_s q_s \sqrt{s}} \bar{f}_1^s(s, t) = A(s, t, u) \quad (7.46)$$

where  $A(s, t, u)$  is an invariant amplitude. Thus

$$f_1^s(s, t) = (1 - z_s^2)^{\frac{1}{2}} 4p_s q_s s^{\frac{1}{2}} A(s, t, u) = [\varphi(s, t)]^{\frac{1}{2}} A(s, t, u) , \quad (7.47)$$

which is identical with (6.16).

#### E. Conspiracy

As mentioned before, kinematic constraints on  $t$ -channel amplitudes can occur only at pseudothresholds, or on the boundary of the physical region. When the external masses are equal in pairs, the latter includes the point  $t = 0$ . A constraint occurring at this point is physically interesting, because it corresponds to forward scattering in the  $s$ -channel. Indeed, in many cases, such a constraint is a direct consequence of angular momentum conservation in the  $s$ -channel.

For concreteness, let us consider nucleon-nucleon scattering, for which there are  $2^4 = 16$  helicity amplitudes. Parity conservation and time-reversal invariance reduce the independent to 5, which we can choose to be  $f_{++;++}^s$ ,  $f_{+-;--}^s$ ,  $f_{+-;+-}^s$ ,  $f_{-+;-+}^s$ ,  $f_{++;+-}^s$ , where the subscripts  $\pm$  correspond to the helicity  $\pm\frac{1}{2}$  of a nucleon. Thus in  $f_{cd;ab}^s$ ,  $(a-b)$  and  $(c-d)$  are the components of the total angular momentum along the relative momentum for the initial and final state,

respectively. Conservation of angular momentum tells us that for forward scattering ( $t = 0$ ) we must have  $f_H^S(s,0) = 0$  if  $(a-b) \neq (c-d)$ . Therefore

$$f_{+-,-+}^S(s,0) = 0$$

$$f_{++,+}^S(s,0) = 0 \quad . \quad (7.48)$$

These also follow formally from (7.21) due to the fact that the corresponding  $D_{\lambda\mu}(z_s)$  vanish at  $t = 0$  ( $z_s = 1$ ). Using the crossing relation (7.14), we can convert these into linear relations imposed on  $f_H^t$ . When this is done in detail, we find that the second requirement of (7.48) is in fact satisfied identically, owing to parity conservation and the conservation of total spin, (the latter being a special feature of nucleon-nucleon scattering.) The first of (7.48) leads to a non-trivial constraint:

$$f_{++,++}^t + f_{+-,-+}^t - f_{++,-}^t - f_{+-,+}^t = 0, \quad (\text{at } t = 0). \quad (7.49)$$

Everything we have said so far applies equally well to backward scattering  $u = 0$ .

By the analyticity considerations outlined in our earlier discussion, we would of course arrive at the same constraint equation. However, we would also obtain other constraints at pseudothresholds, which cannot be deduced by such a simple physical argument.

If we assume that at high energies ( $s \rightarrow \infty$ ) the amplitudes occurring in (7.49) are dominated by  $t$ -channel Regge poles, then (7.49) relates the residues of various Regge poles at  $t = 0$ . The Regge poles are said to "conspire" if their individual residues do not vanish, and are said to "evade" otherwise.

The case of conspiracy is of special interest when one of the conspirators is the pion Regge pole. Because  $t = 0$  is so close to the physical pion pole  $t = 4\mu^2$ , a conspiring pion would give rise to an extremely sharp forward peak whose width is of order  $\mu^2$ . Such sharp peaks have been experimentally observed in forward  $np$  charge exchange scattering  $np \rightarrow pn$ , and in charged pion photoproduction  $\gamma p \rightarrow \pi^+ n$ . Although in principle this could be explained by pion conspiracy with another Regge pole (which would correspond to a scalar meson), actual calculations using the known  $\pi$ -N coupling constant  $g^2/4\pi = 15$  have failed to reproduce the numerical magnitudes of the forward peaks. It is possible that in these processes Regge cuts are important.\* So far, therefore, there is no clear evidence for conspiracy involving Regge poles only.

---

\* K. Huang and I.J. Muzinich, Phys. Rev. 164, 1726 (1967);  
D. Gordon and J. Froyland, Phys. Rev. 177, 2500 (1969).

## F. Reggeization of Helicity Amplitudes

We begin with the t-channel partial-wave expansion

$$f_{cd;ab}^t(s,t) = \sum_{J=\lambda}^{\infty} (2J+1) G_{cd;ab}^J(t) d_{\lambda\mu}^J(z_t) \quad (7.50)$$

$$\lambda \equiv a-b, \quad \mu \equiv c-d, \quad \lambda \geq \mu \geq 0, \quad J = \text{integer.}$$

The object is to calculate Regge pole contributions to this helicity amplitude. We restrict our discussions to integer J (and not half-integer) and assume that  $\lambda \geq \mu \geq 0$ . The case of half-integer J requires only trivial modifications and is discussed in GGLMZ. The restriction  $\lambda \geq \mu \geq 0$  represents no loss in generality, for all other cases can be reduced to this case by using properties of the rotation coefficients:

$$\begin{aligned} d_{\lambda\mu}^J(z) &= d_{-\mu, -\lambda}^J(z) = (-)^{\lambda-\mu} d_{\mu\lambda}^J(z) \\ d_{\lambda\mu}^J(z) &= (-)^{J+\lambda} d_{\lambda, -\mu}^J(-z) \quad . \end{aligned} \quad (7.51)$$

The discussion here follows closely that of GGLMZ, especially the Appendices of that paper. All the special functions used here conform to the notation of GGLMZ, which also contains useful tables for them. We put

$$f_{cd;ab}^t(s,t) = (1+z_t)^{\frac{1}{2}|\lambda+\mu|} (1-z_t)^{\frac{1}{2}|\lambda-\mu|} \bar{f}_{cd;ab}^t(s,t) \quad , \quad (7.52)$$

and recall from our earlier discussion that

$$\bar{f}_{cd;ab}^t(s,t) = \sum_{J=\lambda}^{\infty} (2J+1) G_{cd;ab}^J(t) e_{\lambda\mu}^J(z_t) \quad (7.53)$$

has no s-kinematic singularities. There are still t-kinematic singularities contained in  $G_{cd;ab}^J(t)$ . The functions  $e_{\lambda\mu}^J$  satisfy the properties (7.51).

In general,  $G_{cd;ab}^J(t)$  does not have definite parity, so trajectories of both parities will couple to it. To separate their contributions, we now introduce the parity-conserving helicity amplitudes. Using (7.11), we define helicity states of definite parity by

$$|J; a, b\rangle_{\pm} = \frac{1}{\sqrt{2}} \{ |J; a, b\rangle \pm \eta_a \eta_b (-1)^{J_a + J_b} |J; -a, -b\rangle \} \quad (7.54)$$

with

$$P|J; a, b\rangle_{\pm} = \pm (-1)^J |J; a, b\rangle_{\pm} \quad . \quad (7.55)$$

We define partial-wave amplitudes of definite parity by

$$G_{cd;ab}^{J,\pm}(t) = \pm \langle J;c,d | G^J(t) | J;a,b \rangle_{\pm} \quad , \quad (7.56)$$

which couples only to Regge poles of parity  $\pm(-)^J$ . The original partial-wave amplitudes are then given by

$$G_{cd;ab}^J(t) = \langle J;cd | G(t) | J;ab \rangle = \frac{1}{2} [G_{cd;ab}^{J+}(t) + G_{cd;ab}^{J-}(t)] \quad . \quad (7.57)$$

Next we define new linear combinations of the amplitudes  $\bar{f}$  that are more convenient for reggeization. The motivation is the following. We note that  $G^{J\pm}$  at most changes sign when we reverse the sign of all initial helicities, or all final helicities, or both. The coefficient  $e_{\lambda\mu}^J$ , however, does not have such a simple behavior (See Eq. (7.51)). Hence it is convenient to define new coefficients with simple behavior under helicity reversal and use them to define new helicity amplitudes. We define

$$e_{\lambda\mu}^{J\pm}(z) = \frac{1}{2} [e_{\lambda\mu}^J(z) \pm e_{\lambda,-\mu}^J(z)] \quad , \quad (7.58)$$

which at most changes sign when  $\mu \rightarrow -\mu$ . Then by (7.51)

$$e_{\lambda\mu}^{J\pm}(-z) = \pm (-)^{J+\lambda} e_{\lambda\mu}^{J\pm}(z) \quad . \quad (7.59)$$

The original coefficients are expressible as

$$e_{\lambda\mu}^J(z) = e_{\lambda\mu}^{J+}(z) + e_{\lambda\mu}^{J-}(z) \quad . \quad (7.60)$$

Now define new helicity amplitudes (the "good" amplitudes)

$$g_{cd;ab}^{\pm}(s,t) = \sum_{J=\lambda}^{\infty} (2J+1) [G_{cd;ab}^{J\pm}(t) e_{\lambda\mu}^{J+}(z_t) + G_{cd;ab}^{J\mp}(t) e_{\lambda\mu}^{J-}(z_t)] \quad . \quad (7.61)$$

Then (leaving helicity indices understood)

$$\bar{f}^t(s,t) = \frac{1}{2} [g^+(s,t) + g^-(s,t)] \quad . \quad (7.62)$$

Although  $g^{\pm}$  contains contributions from Regge poles of both parities,  $g^+$  is dominated by parity  $(-)^J$  and  $g^-$  by parity  $-(-)^J$  as  $z_t \rightarrow \infty$ . The reason is that  $e^{J+}$  dominates over  $e^{J-}$  asymptotically.

Before we can do the Watson-Sommerfeld transform on (7.61), we have to discuss how  $G^{J\pm}$  can be analytically continued into the J-plane. For this we have to invert (7.61) to obtain the analog of the Froissart-Gribov formula. Recall

first the orthonormality property

$$\int_{-1}^{+1} dz d_{\lambda\mu}^J(z) d_{\lambda\mu}^{J'}(z) = \frac{2}{2J+1} \delta_{JJ'} \quad . \quad (7.63)$$

Defining a new coefficient

$$c_{\lambda\mu}^J(z) = (1+z)^{\frac{1}{2}|\lambda+\mu|} (1-z)^{\frac{1}{2}|\lambda-\mu|} d_{\lambda\mu}^J(z) \quad , \quad (7.64)$$

we rewrite (7.63) in the form

$$\int_{-1}^{+1} dz e_{\lambda\mu}^J(z) c_{\lambda\mu}^{J'}(z) = \frac{2}{2J+1} \delta_{JJ'} \quad . \quad (7.65)$$

In analogy with (7.58) define

$$c_{\lambda\mu}^{J\pm}(z) = \frac{1}{2} [c_{\lambda\mu}^J(z) \pm c_{\lambda, -\mu}^J(z)] \quad (7.66)$$

with the property

$$c_{\lambda\mu}^{J\pm}(-z) = \pm (-)^{J+\lambda} c_{\lambda\mu}^{J\pm}(z) \quad . \quad (7.67)$$

Then we have the orthonormal relations

$$\begin{aligned} \int_{-1}^{+1} dz [e_{\lambda\mu}^{J+}(z) c_{\lambda\mu}^{J'++}(z) + e_{\lambda\mu}^{J-}(z) c_{\lambda\mu}^{J'-}(z)] &= \frac{2}{2J+1} \delta_{JJ'} \quad , \\ \int_{-1}^{+1} dz [e_{\lambda\mu}^{J+}(z) c_{\lambda\mu}^{J'-}(z) + e_{\lambda\mu}^{J-}(z) c_{\lambda\mu}^{J'++}(z)] &= 0 \quad . \end{aligned} \quad (7.68)$$

With the help of this, (7.61) can be inverted:

$$G^{J, \pm}(t) = \frac{1}{2} \int_{-1}^{+1} dz_t [c_{\lambda\mu}^{J+}(z_t) g^{\pm}(s, t) + c_{\lambda\mu}^{J-}(z_t) g^{\mp}(s, t)] \quad , \quad (7.69)$$

where helicity indices on  $G^{J\pm}$  and  $g^{\pm}$  are understood. Since  $g^{\pm}(s, t)$  has no  $s$ -kinematic singularities, it satisfies the dispersion relation

$$g^{\pm}(s, t) = \frac{1}{\pi} \int_{z_0}^{\infty} dz' \frac{A^{\pm}(t, z')}{z' - z_t} + \frac{1}{\pi} \int_{z_0}^{\infty} dz' \frac{B^{\pm}(t, z')}{z' + z_t} \quad , \quad (7.70)$$

where we have ignored possible subtractions, since they will not contribute to the final result, just as in the spinless case. Substituting (7.70) into (7.69) we obtain

$$\begin{aligned}
G^{\text{J}\pm}(t) &= \frac{1}{\pi} \int_{z_0}^{\infty} dz' A^{\pm}(t, z') \frac{1}{2} \int_{-1}^{+1} dz_t \frac{c^{\text{J}\pm}(z_t)}{z' - z_t} \\
&+ \frac{1}{\pi} \int_{z_0}^{\infty} dz' B^{\pm}(t, z') \frac{1}{2} \int_{-1}^{+1} dz_t \frac{c^{\text{J}\pm}(z_t)}{z' + z_t} \\
&+ \frac{1}{\pi} \int_{z_0}^{\infty} dz' A^{\mp}(t, z') \frac{1}{2} \int_{-1}^{+1} dz_t \frac{c^{\text{J}\mp}(z_t)}{z' - z_t} \\
&+ \frac{1}{\pi} \int_{z_0}^{\infty} dz' B^{\mp}(t, z') \frac{1}{2} \int_{-1}^{+1} dz_t \frac{c^{\text{J}\mp}(z_t)}{z' + z_t} . \tag{7.71}
\end{aligned}$$

Let

$$C_{\lambda\mu}^{\text{J}\pm}(z) = \frac{1}{2} \int_{-1}^{+1} dz' \frac{c^{\text{J}\pm}(z')}{z - z'} , \tag{7.72}$$

with the reflection property

$$C_{\lambda\mu}^{\text{J}\pm}(-z) = \pm (-)^{\text{J}+\lambda} C_{\lambda\mu}^{\text{J}\pm}(z) , \tag{7.73}$$

which follows from (7.67). Then

$$\begin{aligned}
G^{\text{J}\pm}(t) &= \frac{1}{\pi} \int_{z_0}^{\infty} dz' [A^{\pm}(t, z') C_{\lambda\mu}^{\text{J}\pm}(z') + A^{\mp}(t, z') C_{\lambda\mu}^{\text{J}\mp}(z')] \\
&+ \frac{1}{\pi} \int_{z_0}^{\infty} dz' [B^{\pm}(t, z') C_{\lambda\mu}^{\text{J}\pm}(-z') + B^{\mp}(t, z') C_{\lambda\mu}^{\text{J}\mp}(-z')] . \tag{7.74}
\end{aligned}$$

Using (7.73), we rewrite this as

$$\begin{aligned}
G^{\text{J}\pm}(t) &= \frac{1}{\pi} \int_{z_0}^{\infty} dz' [A^{\pm}(t, z') C_{\lambda\mu}^{\text{J}\pm}(z') + A^{\mp}(t, z') C_{\lambda\mu}^{\text{J}\mp}(z')] \\
&+ (-1)^{\text{J}+\lambda} \frac{1}{\pi} \int_{z_0}^{\infty} dz' [B^{\pm}(t, z') C_{\lambda\mu}^{\text{J}\pm}(z') - B^{\mp}(t, z') C_{\lambda\mu}^{\text{J}\mp}(z')] . \tag{7.75}
\end{aligned}$$

To continue this to complex  $J$ , we need to know some properties of  $C_{\lambda\mu}^{\text{J}\pm}$ .

The functions  $C_{\lambda\mu}^{\text{J}\pm}(z)$  are studied in GGLMZ and in greater detail in Andrews and Gunson.\* We need to know the following properties:

(i)  $C_{\lambda\mu}^{\text{J}\pm}(z)$  is a linear combination of Legendre functions of the second kind,  $Q_{\ell}(z)$ , with  $J-\lambda \leq \ell \leq J+\lambda$ .

---

\* Andrews and Gunson, J. Math. Phys. 5, 1391 (1964). They study a function  $e_J^{\lambda\mu}(z)$ , which is related to ours by  $C_{\lambda\mu}^{\text{J}}(z) = (-)^{\lambda-\mu} (1+z)^{\frac{1}{2}(\lambda+\mu)} (1-z)^{\frac{1}{2}(\lambda-\mu)} e_J^{\lambda\mu}(z)$  .



(ii)  $C_{\lambda\mu}^{J\pm}(z)$  has square root branch points in  $J$  for integer values of  $J$  satisfying  $-\lambda \leq J \leq -\mu-1$  or  $\mu \leq J \leq \lambda-1$ .

(iii)  $C_{\lambda\mu}^{J\pm}(z)$  has no other singularities in  $J$  except those coming from the Legendre functions  $Q_\ell(z)$ ,  $J-\lambda \leq \ell \leq J+\lambda$ . In particular the apparent poles at half-integer values of  $J$  in the explicit forms tabulated by GGLMZ are in fact absent: They cancel by virtue of the symmetry property  $Q_\ell(z) = Q_{-\ell-1}(z)$  at  $\ell = \text{half-integer}$ . The fixed  $J$ -poles coming from those of  $Q_\ell$  at  $\ell = -1, -2, \dots$  remain. They occur at  $J = \lambda-1, \lambda-2, \dots$

The analytic continuation of (7.75) to complex  $J$  proceeds in the same manner as the continuation in the spinless case. If the functions  $A^\pm, B^\pm$  in (7.75) are polynomial bounded, then each integral defines a unique continuation in  $J$  which is analytic for sufficiently large  $\text{Re } J$ . Since  $(-1)^{J+\lambda}$  does not have a unique analytic continuation, we introduce the signed amplitudes

$$\begin{aligned} \eta G^\pm(J, t) &= \frac{1}{\pi} \int_{z_0}^{\infty} dz' [A^\pm(t, z') C_{\lambda\mu}^{J+}(z') + A^\mp(t, z') C_{\lambda\mu}^{J-}(z')] \\ &+ \frac{\eta}{\pi} \int_{z_0}^{\infty} dz' [B^\pm(t, z') C_{\lambda\mu}^{J+}(z') - B^\mp(t, z') C_{\lambda\mu}^{J-}(z')] \quad , \quad (7.76) \end{aligned}$$

where  $\eta = \pm 1$ . This can now be continued to complex  $J$  and is the generalization of the Froissart-Gribov formula. It is related to  $G^{J\pm}$  for integer  $J$  by

$$G^{J\pm}(t) = \begin{cases} +G^\pm(J, t), & \text{for } J+\lambda \text{ even} \\ -G^\pm(J, t), & \text{for } J+\lambda \text{ odd} \end{cases} \quad . \quad (7.77)$$

We may call  $\eta$  the "apparent signature." It is the same as the signature if  $\lambda = \text{even integer}$  and is opposite of the signature if  $\lambda = \text{odd integer}$ . The functions  $C_{\lambda\mu}^{J\pm}$  have the property

$$C_{\lambda\mu}^{J\pm}(z) = C_{\lambda\mu}^{(-J-1)\pm}(z) \quad (J = \text{half-integer}) \quad . \quad (7.78)$$

Hence formally

$$\eta G^\pm(J, t) = \eta G^\pm(-J-1, t) \quad (J = \text{half-integer}) \quad , \quad (7.79)$$

which is the Mandelstam symmetry. To get rid of fixed  $J$ -poles coming from those in  $C_{\lambda\mu}^{J\pm}$ , we assume

$$\int_{-1}^{+1} dz P_J(z) \begin{cases} A^\pm(t, z) \\ B^\pm(t, z) \end{cases} = 0 \quad (J = \lambda-1, \lambda-2, \dots) \quad (7.80)$$

To carry out the Watson-Sommerfeld transform on (7.61), we first rewrite it as

$$\begin{aligned}
g_{\pm}^{\pm}(s, t) = & \frac{1}{2} \sum_{J=\lambda}^{\infty} (2J+1) \{ [{}_{+}G^{\pm}(J, t)] [e_{\lambda\mu}^{J+}(z_t) + e_{\lambda\mu}^{J+}(-z_t)] \\
& + [{}_{-}G^{\pm}(J, t)] [e_{\lambda\mu}^{J+}(z_t) - e_{\lambda\mu}^{J+}(-z_t)] \\
& + [{}_{+}G^{\mp}(J, t)] [e_{\lambda\mu}^{J-}(z_t) - e_{\lambda\mu}^{J-}(-z_t)] \\
& + [{}_{-}G^{\mp}(J, t)] [e_{\lambda\mu}^{J-}(z_t) + e_{\lambda\mu}^{J-}(-z_t)] \} . \quad (7.81)
\end{aligned}$$

To take advantage of the Mandelstam symmetry, we proceed as in the spinless case to replace  $e_{\lambda\mu}^{J\pm}(z)$  by a special continuation in  $J$ . The function  $e_{\lambda\mu}^{J\pm}(z)$  is a linear combination of Legendre polynomials and their derivatives. We define  $E_{\lambda\mu}^{J\pm}(z)$  as the function obtained from  $e_{\lambda\mu}^{J\pm}(z)$  by replacing all  $P_{\ell}(z)$  by  $\rho_{\ell}(z)$ . This function is discussed in more detail in GGLMZ. It has the following properties. For integer values of  $J$ , and  $\lambda \geq \mu \geq 0$ :

$$E_{\lambda\mu}^{(J+x)\pm}(z) \xrightarrow{x \rightarrow 0} \left\{ \begin{array}{ll} e_{\lambda\mu}^{J\pm}(z) & (J \geq \lambda) \quad (7.82a) \\ \sim 0(x^{\frac{1}{2}}) & (\mu \leq J \leq \lambda-1) \quad (7.82b) \\ \text{Finite number} & (-\mu \leq J \leq \mu-1) \quad (7.82c) \\ \sim 0(x^{\frac{1}{2}}) & (-\lambda \leq J \leq -\mu-1) \quad (7.82d) \\ \sim 0(x) & (J \leq -\lambda-1) \quad (7.82e) \end{array} \right.$$

At  $J = \text{half-integer}$ , it has  $J$ -poles with residues satisfying

$$\text{Res } E_{\lambda\mu}^{J\pm} = - \text{Res } E_{\lambda\mu}^{(-J-1)\pm} , \quad (J = \text{half-integer}) \quad (7.83)$$

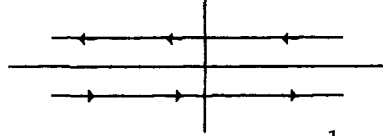
It also has square root branch points in  $J$ . In the partial-wave expansion these will always be cancelled by corresponding ones in  ${}_{\eta}G^{\pm}(J, t)$  arising from those of  $C_{\lambda\mu}^{J\pm}$ .

To simplify our discussion, we pretend for the moment that the range (7.82c) does not exist. This will be discussed separately in the next section on the problem of sense and nonsense.

If we ignore the range (7.82c), the discussion proceeds in parallel with that of the spinless case. We replace  $e_{\lambda\mu}^{J\pm}$  by  $E_{\lambda\mu}^{J\pm}$  in (7.81), extend the  $J$ -sum from  $-\infty$  to  $\infty$ , and replace it by a contour integral:

$$\begin{aligned}
g^{\pm}(s, t) = \frac{1}{2} \frac{1}{2\pi i} \int_C dJ \frac{\pi(2J+1)}{\sin\pi(J+\lambda)} \{ & [{}_{+}G^{\pm}(J, t)] [E_{\lambda\mu}^{J+}(z_t) + E_{\lambda\mu}^{J+}(-z_t)] \\
& - [{}_{-}G^{\pm}(J, t)] [E_{\lambda\mu}^{J+}(z_t) - E_{\lambda\mu}^{J+}(-z_t)] \\
& + [{}_{+}G^{\mp}(J, t)] [E_{\lambda\mu}^{J-}(z_t) - E_{\lambda\mu}^{J-}(-z_t)] \\
& - [{}_{-}G^{\mp}(J, t)] [E_{\lambda\mu}^{J-}(z_t) + E_{\lambda\mu}^{J-}(-z_t)] \} \quad , \quad (7.84)
\end{aligned}$$

where C is the contour shown below.



The factor  $(-1)^{J+\lambda}$  from the residue of  $[\sin\pi(J+\lambda)]^{-1}$  has been absorbed into the  $E_{\lambda\mu}^{J\pm}(z)$  functions by using (7.59). In addition to the poles of  $[\sin\pi(J+\lambda)]^{-1}$ , which reproduce the original sum, the integral also picks up the poles of  $E_{\lambda\mu}^{J\pm}(z)$  at the half-integers. The one at  $J = -\frac{1}{2}$  is cancelled by  $(2J+1)$ . By virtue of the Mandelstam symmetry (7.79) and the property (7.83), the rest cancel in pairs as in the spinless case.

A Regge pole of parity  $\pm (-)^J$ , apparent signature  $\eta$  [signature =  $\eta(-)^\lambda$ ] occurs in the form

$$\eta G_{cd;ab}^{\pm} \sim \frac{\beta_{cd;ab}(t)}{J-\alpha(t)} \quad . \quad (7.85)$$

Its contribution to  $g^{\pm}(s, t)$  is obtained by unfolding the contour in (7.84) in the same manner as in the spinless case. This is trivial to do for any particular Regge pole. It seems pointless to give a general formula, for we would merely drown in a sea of superscripts and subscripts.

The asymptotic behavior of  $g^{\pm}(s, t)$  for large  $z_t$  can be worked out in particular cases from the explicit formulas for  $E_{\lambda\mu}^{J\pm}$  tabulated in GGLMZ. In the asymptotic formulas, the true signature (instead of the apparent signature) always appears in the usual factor  $(e^{-i\pi\alpha} \pm 1)$ .

We give a list of factors that  $\beta_{cd;ab}(t)$  should contain:

- (1) Threshold factor  $[2p_{ab}p_{cd}/s_0]^{\alpha(t)}$ , where  $s_0$  is an arbitrary scale.
- (2) A factor  $[\Gamma(\alpha(t) - 3/2)]^{-1}$ , for the same reason as in the spinless case.
- (3) A factor coming from the J-branch points of  $C_{\lambda\mu}^{J\pm}$ ,

$$\prod_{n=\mu}^{\lambda-1} [\alpha(t)-n]^{\frac{1}{2}} \prod_{n=-\lambda}^{-\mu-1} [\alpha(t)-n]^{\frac{1}{2}} \quad ,$$

which will exactly cancel a corresponding factor in  $E_{\lambda\mu}^{\alpha\pm}$ .

- (4) A factor  $K_{cd;ab}(t)$  containing all the  $t$ -kinematic singularities of  $\bar{F}_{cd;ab}(t)$ .
- (5) A factor  $S(\alpha)$ , explained in the next section, having to do with "choosing sense."

In addition, at certain values of  $t$ , the residues of various Regge poles may satisfy kinematic constraints. Factorizability requires that  $\beta_{cd;ab}(t)$  have the form

$$\beta_{cd;ab}(t) = g_{cd}(t) g_{ab}(t) \quad . \quad (7.86)$$

#### G. Sense and Nonsense

The discussion of the Sommerfeld-Watson transform in the last section is incomplete, because we ignored the fact that  $E_{\lambda\mu}^{J\pm} \neq 0$  for integer  $J$ -values in the range  $-\mu \leq J \leq \mu-1$ . These terms are included in the representation (7.84), although they were not in the original partial-wave expansion (7.81) and should not be included. Actually there is a cancellation among these terms, and (7.84) is still correct; but this cancellation implies constraints on Regge poles that we have to take into account.

The cancellation occurs between the various terms in (7.84), made possible by certain symmetry properties of  $E_{\lambda\mu}^{J\pm}$  and  $C_{\lambda\mu}^{J\pm}$ , namely, for integer  $J$  in the range  $-\mu \leq J \leq \mu-1$ ,

$$E_{\lambda\mu}^{J\pm}(z) = E_{\lambda\mu}^{(-J-1)\mp}(z) \quad , \quad (7.87)$$

$$C_{\lambda\mu}^{J\pm}(z) = C_{\lambda\mu}^{(-J-1)\mp}(z) \quad . \quad (7.88)$$

The first can be proved by using the explicit formula Eq. (A9) of GGLMZ, and the second can be proved by induction by using the recursion formula, Eqs. (A13), (A14) of GGLMZ. The second relation leads via (7.76) and (7.80) to

$$\eta G_{\lambda\mu}^{\pm}(J,t) = -\eta G_{\lambda\mu}^{\mp}(-J-1,t) \quad (7.89)$$

for the same range of  $J$  values. Referring to (7.84) we note that the residues of  $(2J+1)/\sin\pi(J+\lambda)$  at  $J_0$  and  $-J_0-1$  are equal to each other. Hence the contributions from  $J = J_0$  and  $J = -J_0-1$  cancel in pairs: the first term in the curly bracket cancels the fourth, the second against the third. Therefore (7.84) is correct.

The equality (7.89) implies that if  $\eta G_{\lambda\mu}^{\pm}(J,t)$  has a pole at  $J = \alpha(t)$ , such that  $\alpha(t)$  is an integer with  $-\mu-1 < \alpha(t) < \mu$ , then  $-\eta G_{\lambda\mu}^{\mp}(-J-1,t)$  must have a pole

at  $J = -\alpha(t) - 1$ . That is, whenever  $t$  is such that a Regge trajectory  $\alpha(t)$  passes through integer value between  $-\mu - 1$  and  $\mu$ , there must be another trajectory passing through  $-\alpha(t) - 1$ , of the same residue but opposite parity and signature, unless the residue of  $\alpha(t)$  vanishes. Here, as in the discussion of the phenomenon associated with  $\alpha(t)$  passing through half-integer values, we have the alternatives of compensating trajectories vs. vanishing residues. In this case, however, the compensating trajectory has opposite parity and signature.

The integer  $J$ -values for  $J < \lambda$  are called nonsense values, a definition we have already introduced in the spinless case, where  $\lambda = 0$ . The range  $-\mu - 1 \leq J \leq \mu$  therefore contains nonsense values of  $J$ , since in our convention  $\lambda \geq \mu \geq 0$ . When a trajectory passes through these values, it is said to "choose sense" if its residue vanishes, and to "choose nonsense" otherwise. These represent different dynamical possibilities and one cannot decide in favor of either without a theory. The simpler of the two seems to be to choose sense, for that avoids introducing a compensating trajectory.

The factor  $S(\alpha)$  listed at the end of the last section is designed to make the residue vanish at the appropriate nonsense values of  $\alpha$ , if the trajectory chooses sense. If the trajectory chooses nonsense, then  $S(\alpha) = 1$ , and we must specifically include compensating trajectories in the analysis. Since  $S(\alpha)$  must not introduce singularities in  $\alpha$ , it is an entire function of  $\alpha$ , usually taken to be a polynomial.

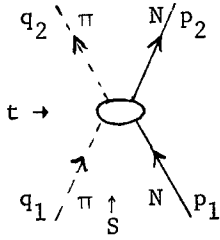
Nonsense values of  $\alpha$  also occur in the spinless case, of course. But there we were not faced with choosing sense or nonsense because the function  $P_\alpha$  does not have the peculiarity (7.82c), and consequently nonsense values of  $\alpha$  never give rise to a pole contribution to the Watson-Sommerfeld transform. An explicit example of sense and nonsense is given in GGLMZ, Appendix B.

### VIII. PION-NUCLEON SCATTERING

As a non-trivial example of reggeization with spin we shall consider pion-nucleon scattering in some detail. This example also gives us a chance to see the detailed relation between invariant and helicity amplitudes and the origin of the kinematic singularities and constraints.

#### A. Invariant Amplitudes

Let us consider  $\pi$ -N scattering in which the individual particles are in definite charge states. Analysis in terms of total I-spin states may be easily



obtained from what we do here and will not be discussed. Suppose we calculate the scattering amplitude by summing all Feynman graphs, then we would obtain a Feynman amplitude of the form

$$f = \bar{u}(p_2, s_2) T(p_2, q_2; p_1, q_1) u(p_1, s_1) \quad , \quad (8.1)$$

where  $u(p, s)$  is a Dirac spinor of momentum  $\vec{p}$  and z-component of spin  $s$ , and  $T$  is a  $4 \times 4$  matrix. We can write  $T$  as a linear combination of the 16 Dirac matrices\*

$$1, \gamma^\mu, \gamma^\mu \gamma^\nu, \gamma_5 \gamma^\mu, \gamma_5 \quad , \quad (8.2)$$

with coefficients constructed from the 3 available independent momenta

$$(p_1 + p_2)_\mu, (p_1 - p_2)_\mu, (q_1 + q_2)_\mu \quad , \quad (8.3)$$

in such a manner to insure that  $\bar{u}Tu$  is a Lorentz scalar. Thus terms proportional to  $\gamma_5 \gamma_\mu$  and  $\gamma_5$  are immediately ruled out, for they would require pseudovector and pseudoscalar coefficients, and none can be constructed from (8.3). Any invariant constructed from  $\gamma^\mu \gamma^\nu$  and (8.3) reduces to one constructed from 1 or  $\gamma^\mu$ , when the nucleons are on the mass shell. Under the same condition, the only independent invariant constructed from  $\gamma^\mu$  is  $\gamma \cdot (q_1 + q_2)$ . Thus the most general form is

$$T(p_2, q_2; p_1, q_1) = -A(s, t) + \frac{i}{2} \gamma \cdot (q_1 + q_2) B(s, t) \quad , \quad (8.4)$$

---

\* We use the convention in S. Gasiorowicz, Elementary Particle Physics, (John Wiley & Sons, New York, 1967), Chap. 2.

where A, B are functions having no singularities except the unitarity cuts and particle poles. By definition they have no kinematic singularities and no kinematic zeros and are called invariant amplitudes.

From the crossing property of Feynman graphs, the amplitude (8.1) also describes  $\pi\pi \rightarrow \bar{N}\bar{N}$  when we continue the  $q_2$  and  $p_2$  to the region where their components change sign. For the invariant amplitudes, this simply means that we continue the values of s,t from the s-channel physical region to the t-channel physical region.

### B. Helicity Amplitudes

The s-channel helicity amplitudes are

$$f_{\lambda_2,0;\lambda_1,0}^s(s,t) = \sum_{J=\frac{1}{2}}^{\infty} (2J+1) F_{\lambda_2,0;\lambda_1,0}^J(s) d_{\lambda_1\lambda_2}^J(z_s) \quad (8.5)$$

where  $\lambda_1$  and  $\lambda_2$  assume the values  $\pm\frac{1}{2}$ . We introduce a shorthand notation in which the amplitudes are labeled only by the signs of  $\lambda_2$  and  $\lambda_1$ ; for example,

$$f_{++}^s(s,t) = f_{+\frac{1}{2},0;+\frac{1}{2},0}^s(s,t) \quad . \quad (8.6)$$

Then by (7.11) parity conservation implies

$$\begin{aligned} F_{++}^J(s) &= F_{--}^J(s) \\ F_{+-}^J(s) &= F_{-+}^J(s) \quad . \end{aligned} \quad (8.7)$$

Using this and the properties (7.51) of the rotation coefficients, we find that there are only two independent helicity amplitudes, which we choose to be

$$\begin{aligned} f_1^s(s,t) &= f_{++}^s(s,t) = f_{--}^s(s,t) \\ f_2^s(s,t) &= f_{+-}^s(s,t) = -f_{-+}^s(s,t) \quad . \end{aligned} \quad (8.8)$$

Identical formulas hold for the t-channel amplitudes, if we change the superscripts from s to t.

The helicity amplitudes are in fact the amplitudes (8.1) with specific choices of the Dirac spinors:

$$\begin{aligned} f_{\lambda_2\lambda_1}^s(s,t) &= \bar{u}(p_2,\lambda_2) T(p_2,q_2;p_1,q_1) u(p_1,\lambda_1) \quad , \\ f_{\lambda_2\lambda_1}^t(s,t) &= \bar{u}(p_2,\lambda_2) T(p_2,-p_1;-q_2,q_1) v(-p_1,-\lambda_1) \quad , \end{aligned} \quad (8.9)$$

where  $u(p,\lambda)$  and  $v(p,\lambda)$  are respectively positive and negative energy spinors satisfying

$$\bar{u}(p,\lambda) u(p,\lambda) = -\bar{v}(p,\lambda) v(p,\lambda) = +1 \quad (8.10)$$

and

$$\begin{aligned} (\hat{p} \cdot \vec{\sigma}) u(p,\lambda) &= \lambda u(p,\lambda) \\ (\hat{p} \cdot \vec{\sigma}) v(p,\lambda) &= \lambda v(p,\lambda) \end{aligned} \quad (8.11)$$

To find the relation between helicity and invariant amplitudes we use (8.4) and find after a lengthy but straightforward calculation

$$\begin{aligned} f_1^s(s,t) &= -\sqrt{\frac{1+z}{2}} \frac{s}{s} \left[ A(s,t) + \frac{s-m^2-\mu^2}{2m} B(s,t) \right] , \\ f_2^s(s,t) &= -\sqrt{\frac{1-z}{2}} \frac{s}{s} \sqrt{\frac{m^2}{4s}} \left[ \frac{s+m^2-\mu^2}{m} A(s,t) + \frac{s-m^2+\mu^2}{m} B(s,t) \right] ; \end{aligned} \quad (8.12)$$

and

$$\begin{aligned} f_1^t(s,t) &= -\frac{1}{\sqrt{t-4m^2}} \left[ -\frac{(t-4m^2)}{2m} A(s,t) + \frac{s-u}{2} B(s,t) \right] , \\ f_2^t(s,t) &= -\frac{\sqrt{t} \sqrt{su-(m^2-\mu^2)^2}}{2m\sqrt{t-4m^2}} [B(s,t)] . \end{aligned} \quad (8.13)$$

Since A and B are by definition free of kinematic singularities, the kinematic singularities of the helicity amplitudes are hereby explicitly displayed. The following amplitudes are therefore free of all kinematic singularities:

$$\hat{f}_1^s = \left[ \frac{1}{2}(1+z_s) \right]^{-\frac{1}{2}} f_1^s , \quad \hat{f}_2^s = \left( \frac{s}{2} \right)^{\frac{1}{2}} \left[ \frac{1}{2}(1-z_s) \right]^{-\frac{1}{2}} f_2^s ; \quad (8.14)$$

$$\hat{f}_1^t = (t-4m^2)^{\frac{1}{2}} f_1^t , \quad \hat{f}_2^t = \frac{2m^2}{t^{\frac{1}{2}}} \left[ \frac{t-4m^2}{su-(m^2-\mu^2)^2} \right]^{\frac{1}{2}} f_2^t . \quad (8.15)$$

However, they are not completely independent. To see this we solve for A and B in terms of the set  $\hat{f}_1^s, \hat{f}_2^s$ , and alternatively the set  $\hat{f}_1^t, \hat{f}_2^t$ :

$$\begin{aligned} A(s,t) &= \frac{2m^2}{\beta^2} \left[ -(s-m^2+\mu^2) \hat{f}_1^s(s,t) + (s+m^2-\mu^2) \hat{f}_2^s(s,t) \right] , \\ B(s,t) &= \frac{4m^3}{\beta^2} \left[ \frac{s+m^2-\mu^2}{2m^2} \hat{f}_1^s(s,t) - \hat{f}_2^s(s,t) \right] , \end{aligned} \quad (8.16)$$

with

$$\beta^2 = [s - (m+\mu)^2] [s - (m-\mu)^2] . \quad (8.17)$$



Since  $A(s,t)$  and  $B(s,t)$  have no kinematic singularities, the square brackets must vanish at  $s = (m \pm \mu)^2$ . Similarly, in terms of the t-channel amplitudes

$$\begin{aligned} A(s,t) &= -\frac{2m^2}{t-4m^2} [\hat{f}_1^t(s,t) + \frac{s-u}{2m^2} \hat{f}_2^t(s,t)] \quad , \\ B(s,t) &= -\frac{1}{m} \hat{f}_2^t(s,t) \quad , \end{aligned} \quad (8.18)$$

so the square bracket must vanish at  $t = 4m^2$ . Note that no constraint is needed at  $t = 0$  and hence there is no conspiracy condition. What happens is that parity conservation in the t-channel automatically implies conservation of angular momentum in the forward direction in the s-channel.

The crossing relation for the helicity amplitudes is obtained by eliminating  $A(s,t)$  and  $B(s,t)$  between (8.16) and (8.18). Since the arguments of the square roots change signs during the continuation from the s-channel to the t-channel physical region, the calculation requires a careful consideration of phases. This is the whole point of the paper of Trueman and Wick. We take their result from (7.14):

$$f_{ab}^s(s,t) = \sum_{c=-\frac{1}{2}}^{+\frac{1}{2}} \sum_{d=-\frac{1}{2}}^{+\frac{1}{2}} d_{db}^{\frac{1}{2}}(\chi) d_{ca}^{\frac{1}{2}}(\pi-\chi) f_{cd}^t(s,t) \quad , \quad (8.19)$$

where

$$\begin{aligned} \cos\chi &= -\frac{(s+m^2-\mu^2)t}{\mathcal{S}\mathcal{J}} \\ \sin\chi &= \frac{2m\sqrt{\varphi(s,t)}}{\mathcal{J}} \\ \mathcal{S} &= [s - (m+\mu)^2] [s - (m-\mu)^2] \\ \mathcal{J} &= t(t-4m^2) \\ \varphi(s,t) &= stu - t(m^2-\mu^2)^2 \quad . \end{aligned} \quad (8.20)$$

The rotation coefficients are given in the following matrix

$$d^{\frac{1}{2}}(\chi) = \begin{bmatrix} \cos \frac{\chi}{2} & -\sin \frac{\chi}{2} \\ \sin \frac{\chi}{2} & \cos \frac{\chi}{2} \end{bmatrix} \quad . \quad (8.21)$$

Using this and (8.8), we obtain

$$\begin{bmatrix} f_1^s(s,t) \\ f_2^s(s,t) \end{bmatrix} = \begin{bmatrix} \sin\chi & -\cos\chi \\ \cos\chi & \sin\chi \end{bmatrix} \begin{bmatrix} f_1^t(s,t) \\ f_2^t(s,t) \end{bmatrix} . \quad (8.22)$$

C. Reggeization of Helicity Amplitudes

Let us now illustrate the procedure discussed in Section VII D by following it step by step for the present case. First we define

$$\begin{aligned} \bar{f}_1^t(s,t) &= \frac{1}{\sqrt{1+z_t}} f_1^t(s,t) \\ \bar{f}_2^t(s,t) &= \frac{1}{\sqrt{1-z_t}} f_2^t(s,t) . \end{aligned} \quad (8.23)$$

These amplitudes have no s-kinematic singularities and have the partial wave expansions

$$\begin{aligned} \bar{f}_2^t(s,t) &= \sum_{J=0}^{\infty} (2J+1) G_{++}^J(t) e_{00}^J(z_t) \\ \bar{f}_2^t(s,t) &= \sum_{J=1}^{\infty} (2J+1) G_{+-}^J(t) e_{01}^J(z_t) . \end{aligned} \quad (8.24)$$

Let  $|J, \lambda_1 \lambda_2\rangle$  be the  $\bar{N}\bar{N}$  state with angular momentum J and helicities  $\lambda_2, \lambda_1$ . Then

$$P|J; a, b\rangle = + (-1)^J |J; -a, -b\rangle . \quad (8.25)$$

The parity eigenstates are therefore

$$|J; a, b\rangle_{\pm} = \frac{1}{\sqrt{2}} [ |J; a, b\rangle \pm |J; -a, -b\rangle ] \quad (8.26)$$

with

$$P|J; a, b\rangle_{\pm} = \pm (-1)^J |J; a, b\rangle_{\pm} . \quad (8.27)$$

The parity-conserving partial wave amplitudes are

$$G_{ab}^{J\pm}(t) = \pm \langle J; a, b | G(t) | J; 0, 0 \rangle , \quad (8.28)$$

$|J, 00\rangle$  being the pion state. In terms of these we have

$$G_{ab}^J(t) = \frac{1}{2} [ G_{ab}^{J+}(t) + G_{ab}^{J-}(t) ] . \quad (8.29)$$

The states of  $\bar{N}N$  and the trajectories coupled to them are given below.

<u>Parity eigenstate</u>	<u>Abbreviation</u>	<u>Parity</u>	<u>G-parity</u>	<u>Trajectories</u>
$\frac{1}{\sqrt{2}}[ J,++\rangle +  J,--\rangle]$	$ J,0+\rangle$	$+(-1)^J$	+1	$P, \rho, f^0$
			-1	$\omega, A_2$
$\frac{1}{\sqrt{2}}[ J,++\rangle -  J,--\rangle]$	$ J,0-\rangle$	$-(-1)^J$	+1	$B$
			-1	$\pi$
$\frac{1}{\sqrt{2}}[ J,+-\rangle +  J,-+\rangle]$	$ J,1+\rangle$	$+(-1)^J$	+1	$P, \rho, f^0$
			-1	$\omega, A_2$
$\frac{1}{\sqrt{2}}[ J,+-\rangle -  J,-+\rangle]$	$ J,1-\rangle$	$-(-1)^J$	+1	—
			-1	$A_1$

Since the  $\pi\pi$  states all have  $P = +(-1)^J$  and  $G = +1$ , the only non-vanishing partial wave amplitudes are

$$G_{00}^{J+} \equiv \langle J, 0+ | G(t) | J, \pi\pi \rangle$$

$$G_{01}^{J+} \equiv \langle J, 1+ | G(t) | J, \pi\pi \rangle \quad . \quad (8.30)$$

Substituting this, via (8.29), into (8.24), we have the partial wave expansions

$$\bar{f}_1^t(s, t) = \frac{1}{2} \sum_{J=0}^{\infty} (2J+1) G_{00}^{J+}(t) e_{00}^J(z_t)$$

$$\bar{f}_2^t(s, t) = \frac{1}{2} \sum_{J=1}^{\infty} (2J+1) G_{01}^{J+}(t) e_{01}^J(z_t) \quad . \quad (8.31)$$

In the general discussion, we had further decomposed the above into the amplitudes  $g_{\pm}^{\pm}(s, t)$ . But for pion-nucleon scattering, only states with parity  $+(-1)^J$  couple and this is unnecessary. If we do it anyway, we find that

$$e_{00}^{J-}(z_t) = e_{01}^{J-}(z_t) = 0$$

$$e_{00}^{J+}(z_t) = e_{00}^J(z_t), \quad e_{01}^{J+}(z_t) = e_{01}^J(z_t) \quad , \quad (8.32)$$

and we are back to (8.31).

From the table in GGLMZ, we find

$$\begin{aligned} e_{00}^J(z_t) &= P_J(z_t) & c_{00}^J(z_t) &= P_J(z_t) \\ e_{01}^J(z_t) &= \frac{P_J'(z_t)}{\sqrt{J(J+1)}} & c_{01}^J(z_t) &= \frac{\sqrt{J(J+1)}}{2J+1} [P_{J-1}(z_t) - P_{J+1}(z_t)] \end{aligned} \quad (8.33)$$

Hence

$$\begin{aligned} E_{00}^J(z_t) &= \mathcal{P}_J(z_t) & C_{00}^J(z_t) &= Q_J(z_t) \\ E_{01}^J(z_t) &= \frac{\mathcal{P}_J'(z_t)}{\sqrt{J(J+1)}} & C_{01}^J(z_t) &= \frac{\sqrt{J(J+1)}}{2J+1} [Q_{J-1}(z_t) - Q_{J+1}(z_t)] \end{aligned} \quad (8.34)$$

Then from (7.79) we obtain

$$\begin{aligned} \bar{f}_1^t(s, t) &= \sum_{i=P, \rho, f^o} \frac{\pi \beta_{00}^i(t) (\alpha_i(t) + \frac{1}{2})}{\sin \pi \alpha_i(t)} [E_{00}^{\alpha_i(t)}(-z_t) + \eta_i E_{00}^{\alpha_i(t)}(z_t)] \\ \bar{f}_2^t(s, t) &= \sum_{i=P, \rho, f^o} \frac{\pi \beta_{01}^i(t) (\alpha_i(t) + \frac{1}{2})}{\sin \pi (\alpha_i(t) + 1)} [E_{00}^{\alpha_i(t)}(-z_t) - \eta_i E_{00}^{\alpha_i(t)}(z_t)] \end{aligned} \quad (8.35)$$

The signature  $\eta_i$  which appears here is the true signature.

We take the residue functions to be

$$\beta_{0\lambda}^i(t) = \frac{1}{\Gamma(\alpha_i(t) + \frac{3}{2})} \left( \frac{2^{p_{\text{min}} p_{\text{NN}}}}{s_i} \right)^{\alpha_i(t)} \gamma_{0\lambda}^i(t) \quad (8.36)$$

where  $s_i$  are arbitrary scales, the first factor provides the compensation required by the Mandelstam symmetry, and the second is the threshold factor. In  $\gamma_{00}^i(t)$ , we factor out the kinematic singularities of  $\bar{f}_1^t(s, t)$ :

$$\gamma_{00}^i(t) = \frac{1}{\sqrt{4\mu^2 - t}} \bar{\gamma}_{00}^i(t) \quad (8.37)$$

Factorization requires

$$\bar{\gamma}_{00}^i(t) \geq 0 \text{ for } t < 4\mu^2 \quad (8.38)$$

In  $\gamma_{01}^i(t)$ , we must factor out both the kinematic singularities of  $\bar{f}_1^t(s, t)$  and the branch points coming from  $C_{01}^J(z_t)$ :

$$\gamma_{01}^i(t) = \sqrt{t(4\mu^2 - t)} \sqrt{\alpha_i(t)(\alpha_i(t) + 1)} \bar{\gamma}_{01}^i(t) \quad (8.39)$$

Finally we obtain the s-channel amplitudes by using (8.35) and (8.22).



DYNAMICAL MODELS BASED ON UNITARITY AND ANALYTICITY

Lectures by:           W. R. Frazer  
                          University of California, La Jolla

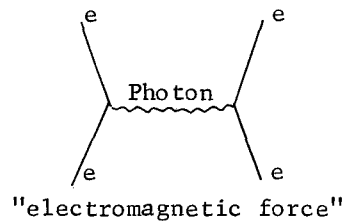
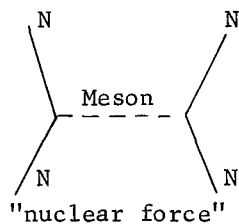
Notes taken by:       Harry J. Yesian



The organization of the material to be covered in these lectures will be the following.<sup>1,2</sup>

- (1) A review of some S-matrix properties including the analytic structure and the concept of polology.
- (2) Bootstrap theories including the N/D method and the  $\rho$ -meson bootstrap of Chew and Mandelstam.
- (3) Some specific models, including the Bethe-Salpeter equation and its implicit  $O(4)$  symmetry.
- (4) The multi-Regge Model in its simplest version.

We shall start today by going over some of the early attempts at formulating theories of strong-interaction dynamics. The starting point is with Yukawa, who postulated that the force between nucleons is mediated by the exchange of another particle with a finite mass. This is in analogy to the electromagnetic force which we know is mediated by the exchange of a photon between charged particles.

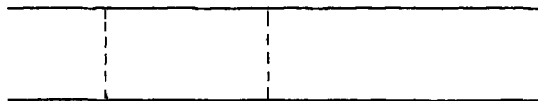


The basic approaches that one can then use are:

A. Translate the single meson exchange into a potential  $V \sim g^2 \frac{e^{-\mu r}}{r}$  and then try to solve the Schrödinger Equation. This leads to difficulties in the relativistic domain for a number of reasons.

B. Lagrangian Field Theory

- (1) Perturbation Theory. We know this fails because of the strength of the interaction. However, we can still use it as a guide to the singularity structure of the S-matrix.
- (2) Diagram Summing - a particular model which sums ladder diagrams is the Bethe-Salpeter equation in the ladder approximation.



Ladder diagram.



C. Abstracted Theories

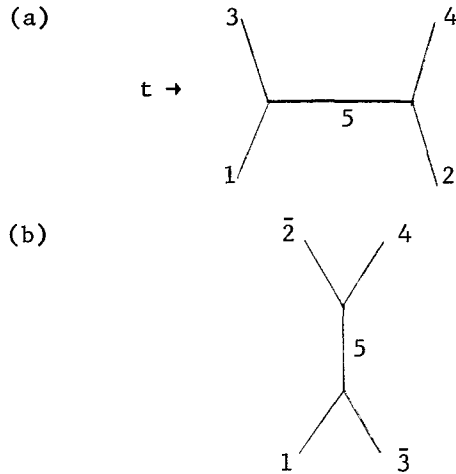
- (1) Axiomatic Field Theory. Not to be covered here.
- (2) S-Matrix Theory. Here one abstracts properties of the S-matrix from A or B above and uses them as "axioms" to develop a logically independent theory. The rest of this lecture will be concerned with this.

S-Matrix Properties

I will not attempt a logical, axiomatic approach in the manner pioneered by Stapp (see Ref. 2). My intention is only to review and motivate the assumptions behind S-matrix dynamics. These assumptions fall into two classes:

(1) Basic axioms: That is, axioms whose origin and status transcend the specific theories mentioned above.

(2) Abstractions: Included among these are the properties which are less well founded than those in (1) and which owe their origin to particular models. An example of this would be the idea that forces between strongly interacting particles are mediated by particle exchange. Closely connected with this would be crossing symmetry which is an abstraction from field theory. For example, consider the following two diagrams:



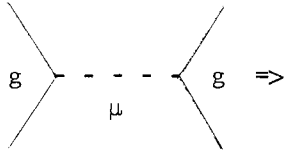
Neglecting complications due to spin, both diagrams (a) and (b) contribute a term

$$\frac{g_{135}g_{245}}{m_5^2 - t}$$

to the scattering amplitude for the respective processes. The statement that the coupling constants occurring in these two diagrams are the same is an example of the crossing property.

Now let's return to Yukawa's basic idea, alluded to above, that forces between hadrons (strongly-interacting particles) arise from hadron exchange. For example,

the first Born approximation in potential scattering tells us that there is a correlation between the mass of the exchanged particle,  $\mu$ , and the range of the interaction.



$$V(r) = g^2 \frac{e^{-\mu r}}{r}$$

Hence we see that the range of the interaction goes roughly like  $1/\mu$ . Now since the pion is the lightest mass hadron we know of, its role in strong-interaction dynamics will be special. We see that it is responsible for the longest range force. One way to isolate this long range force is to perform a modified phase shift analysis of nucleon-nucleon scattering data.<sup>3</sup> The highest partial waves are presumably affected only by pion exchange. Ignoring spin for the moment, one can divide the partial wave series into two pieces.

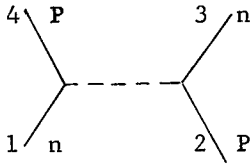
$$\begin{aligned} f(s, t) &= \sum_{\ell} (2\ell+1) f_{\ell}(s) P_{\ell}(\cos\theta) \\ &= \sum_{\ell < L_c} (2\ell+1) f_{\ell}(s) P_{\ell}(\cos\theta) + \sum_{\ell \geq L_c} (2\ell+1) f_{\ell}(s) P_{\ell}(\cos\theta) \end{aligned}$$

The second series can be replaced by the one-pion exchange contribution. Here we have chosen

$$L_c \approx kR, \quad R \approx \frac{1}{m_{\pi}}$$

where  $k$  is the center-of-mass momentum of one of the nucleons. In addition, since the one-pion exchange contribution has as parameters  $g^2$  and  $\mu^2$ , we can leave them as free parameters and make a determination of them from a  $\chi^2$  fit to the data. This was first done by Cziffra et al.<sup>3</sup> A later analysis by Signell<sup>4</sup> of different data gave better results, yielding values of 14 and 130 MeV for  $g^2$  and  $\mu$  respectively.

Another method of extracting the pion exchange contribution to nucleon-nucleon scattering was performed by Cziffra and Moravcsik.<sup>5</sup> In this instance, they dealt with backward n-p scattering (charge exchange) to isolate the  $I=1$  contribution in the crossed-channel.



If we define the Mandelstam invariants in the usual way

$$s = (P_1 + P_2)^2$$

$$t = (P_1 - P_3)^2$$

$$u = (P_1 - P_4)^2$$

the pion pole is at  $u = m_\pi^2$ . In the center-of-mass system  $u = -2k^2 \cdot (1 + \cos\theta)$ . Hence the location of the pion pole is at  $\cos\theta = -1 - \frac{m_\pi^2}{2k^2}$  in the  $\cos\theta$  plane. Since  $m_\pi^2$  is very small, we see that this pole is actually quite close to the physical region. The contribution of the pion to the unpolarized differential cross section is:

$$\frac{d\sigma}{d\Omega} = \frac{g^4}{s} \frac{(1+x)^2}{(x+x_0)^2}$$

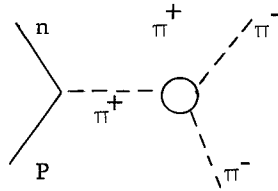
$$x = \cos\theta$$

$$x_0 = +1 + \frac{m_\pi^2}{2k^2}$$

To perform the extrapolation, one wants to extend the quantity  $(x+x_0)^2 \frac{d\sigma}{d\Omega}$  into the unphysical region where it is equal to  $\frac{g^4}{s} \left(\frac{m_\pi^2}{2k^2}\right)^2$  at the pion pole,  $u = m_\pi^2$ .

Despite the practical difficulties encountered in performing an extrapolation this method, as well as the modified phase shift analysis, give direct confirmation of Yukawa's hypothesis.

There are other more complicated reactions in which continuation away from unphysical regions has been useful. One such is the Chew-Low extrapolation which can be used to determine the nature of the  $\pi\pi$  interaction when one of the incoming pions is off the mass shell (see illustration below).



### Singularity Hunting:

Poles in the scattering amplitude come from the first Born approximation in potential scattering.

$$f_B^{(1)} = \frac{g^2}{\mu^2 - t}$$

The higher terms in the Born series for the scattering amplitude, say  $f_B^{(2)}$ , are given by<sup>6</sup>

$$f_B^{(2)} = \int_{4M^2}^{\infty} \frac{ds'}{\pi} \int_{4\mu^2}^{\infty} \frac{dt'}{\pi} \frac{\rho^{(2)}(s', t')}{(s'-s)(t'-t)}$$

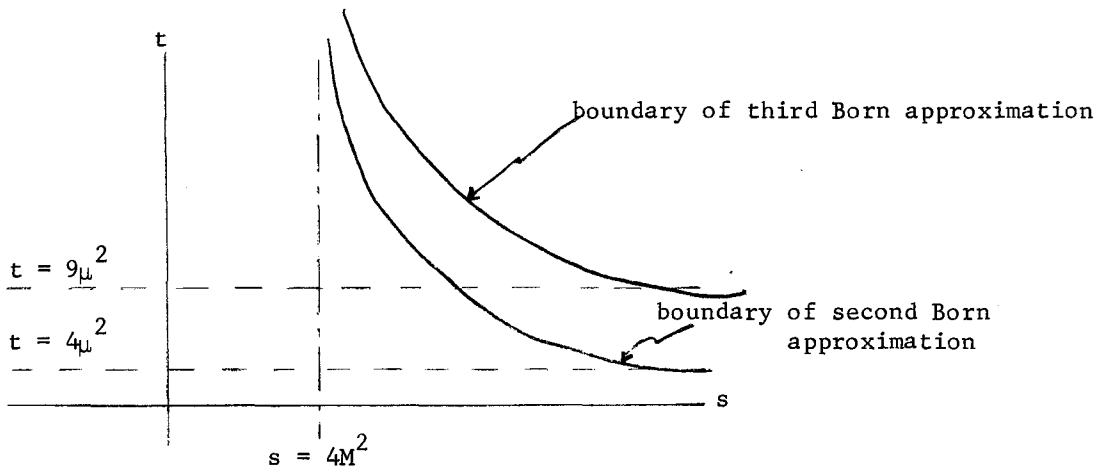
where

$$\rho^{(2)}(s', t') = \frac{\pi}{4} \frac{g^4 \theta(A)}{(2tA)^{\frac{1}{2}}}$$

and

$$A = \frac{1}{4} (S-4M^2)(t-4\mu^2) - \mu^4 .$$

A determines the boundary of the spectral function  $\rho(s, t)$ . For the process under consideration it is:



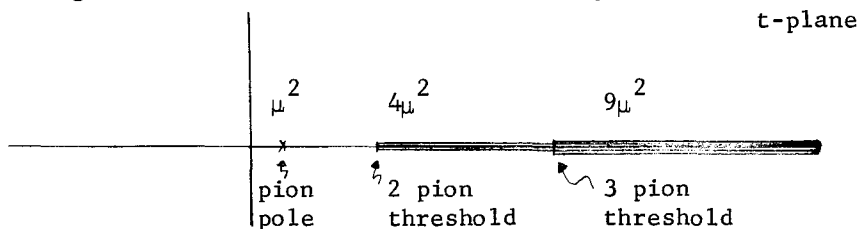
How does this compare with relativistic scattering? If one looks at the singularity structure of Feynman diagrams, one finds the same singularities as located in potential scattering.

The  $t$ -plane singularities arising from the Born series above are summarized by the representation

$$f(s, t) = \frac{g^2}{\mu^2 - t} + \int_{4\mu^2}^{\infty} \frac{dt'}{\pi} \frac{\sigma^{(2)}(s, t')}{t' - t} + \int_{(3\mu)^2}^{\infty} \frac{dt'}{\pi} \frac{\sigma^{(3)}(s, t')}{t' - t} + \dots$$

pion pole

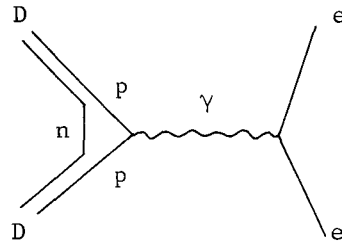
These singularities are shown in the following figure:



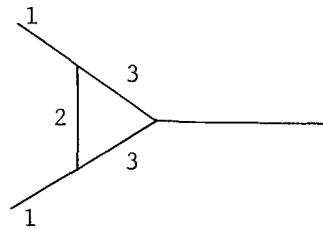
The branch points in the figure above are called normal threshold singularities.

Digression on Anomalous Thresholds:

Consider elastic electron-deuteron scattering. One diagram which contributes is the following.



On the basis of the normal thresholds discussed above, one might expect that the range of the force should be  $R \approx \frac{1}{2M_p}$ , or that the position of the nearest singularity is  $t \approx 4M_p^2$ . It turns out that if you calculate the threshold for the above Feynman diagram it is:  $t = 8M_p E_B$ . This is called an anomalous threshold. Here  $E_B$  is the binding energy of the deuteron. The problem is a more general one.<sup>7</sup> If you have a diagram of the following type:



and if  $M_1^2 > M_2^2 + M_3^2$ , then you will have an anomalous threshold. To understand the result in the case of electron-deuteron scattering, we know that the deuteron is a loosely bound system of a neutron and a proton. A rough estimate of the size of the deuteron and hence the range of the interaction can be read off from the deuteron wave function which goes like  $e^{-\alpha r}$ , where  $\alpha = (M_p E_b)^{\frac{1}{2}}$ . It is universally proportional to the square root of the binding energy. This is a very small number and hence the anomalous threshold is very close to the physical region.

#### FOOTNOTES AND REFERENCES

1. W.R. Frazer, "Elementary Particles."
2. Eden, Landshoff, Olive, and Polkinghorne, "The Analytic S-Matrix." Cambridge University Press.
3. P. Cziffra, M. MacGregor, M. Moravcsik, H. Stapp, Phys. Rev. 114, 880 (1959).
4. P. Signell, Phys. Rev. Letters 5, 474 (1960).
5. P. Cziffra, M. Moravcsik, Phys. Rev. 116, 226 (1959).
6. See for example, Goldberger and Watson, "Collision Theory," p. 599. We are assuming the kinematics of nucleon-nucleon scattering.
7. R. Karplus, C.M. Sommerfeld, E.H. Wichmann, Phys. Rev. 111, 1187 (1958).
8. R. Blankenbecler, M.L. Goldberger, N.N. Khuri, S. Treiman, Annals of Physics 10, 62 (1960).

Unitarity and Singularities:

What are the implications of unitarity for the singularity structure of the scattering amplitude? We begin by considering the partial wave expansion

$$f(s, t) = \sum_{\ell} (2\ell+1) f_{\ell}(s) P_{\ell}(\cos\theta)$$

for the elastic scattering amplitude. In what follows, we consider only the scattering of spinless particles. For the partial wave amplitudes, unitarity says: for  $s > s_{\text{threshold}}$

$$f_{\ell}(s) = \frac{e^{i\delta_{\ell}} \sin\delta_{\ell}}{k},$$

where  $\delta_{\ell}$  is real below the inelastic threshold. Alternatively, this can be expressed as

$$\text{Im}f_{\ell}(s) = k |f_{\ell}(s)|^2.$$

Now we postulate (or abstract from potential theory or field theory) that the partial wave amplitude is a real analytic function. This means that it is analytic in a region which includes part of the real axis, and that on part of the real axis, it is purely real. Such a function can then be shown to satisfy the Schwarz-Reflection principle

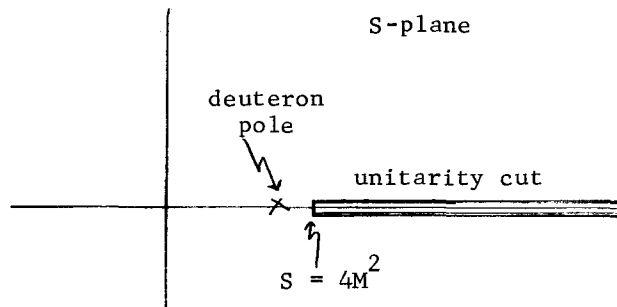
$$f_{\ell}(s^*) = f_{\ell}^*(s).$$

From this, we can calculate the discontinuity:

$$f_{\ell}(s+i\epsilon) - f_{\ell}(s-i\epsilon) = 2i \text{Im}f_{\ell}(s+i\epsilon).$$

From this we see that the partial wave amplitude has a cut beginning at the elastic threshold and extending to the right in the  $s$  plane along the real axis.

On the basis of scattering data, how can one infer the existence of bound states below threshold. For example, let us examine the  $^3S$ -wave n-p scattering amplitude  $f_0(s)$  which we know has the deuteron as a bound state



Ignoring for the time being inelastic contributions, we may write in the physical region  $s > s_T$

$$f_0(s) = \frac{e^{i\delta_0} \sin \delta_0}{k} = \frac{1}{k(\cot \delta_0 - i)} .$$

The statement of unitarity can be written in an alternative form as

$$\text{Im}\left(\frac{1}{f_0}\right) = -k .$$

Now we want to perform an extrapolation to the left of the branch point into the unphysical region. To do this we define a function

$$M(s) = \frac{1}{f_0(s)} + ik$$

where  $k$  is defined to have a cut in the  $s$  plane running to the right. Hence  $ik$  is a real analytic function to the left of its branch point. Now for  $s > s_T$  we have

$$\text{Im}M(s) = -k + k = 0$$

and for  $s < s_T$

$$\text{Im}M(s) = 0 + 0 = 0 .$$

Therefore  $M(s)$  is an analytic function in the vicinity of elastic threshold. For  $s$  in the physical region, it is

$$M = k \cot \delta_0 .$$

We can, therefore, make a power series expansion about  $s_T$  of the form

$$k \cot \delta_0 = -\frac{1}{a} + \frac{1}{2} r_0 k^2 + \dots .$$

Keeping only the first two terms, we may write

$$f_0(s) \approx \frac{1}{-\frac{1}{a} + \frac{1}{2} r_0 k^2 - ik} .$$

In the literature, this is known as the effective-range expansion. We may now take this formula and determine the parameters  $a$  and  $r_0$  from a fit to the scattering data in the region just above threshold. The experimental values are

$$\begin{aligned} a &= 3.82 \\ r_0 &= 1.20 \text{ (}\hbar/m\pi c\text{)} . \end{aligned}$$

Since the denominator of the partial wave amplitude is quadratic in  $k$ , the amplitude will have two poles. One of its poles falls very close to the deuteron pole. It represents a bound state of binding energy  $\epsilon = 2.21$  MeV, whereas the measured binding energy of the deuteron is  $E_B = 2.23$  MeV. The second pole lies farther away to the left on the real axis. As we shall see below, it falls in the region where our knowledge of the forces say there should be cuts. So we see that the simple "effective range" approximation does not reproduce these cuts, but gives a pole as an effective interaction.



When this same analysis is applied to the scattering in the singlet state, one finds that the pole far to the left of threshold still remains, while the analog of the deuteron pole, has moved onto the second sheet. It is known as a "virtual" bound state.

Now let us see what our knowledge of the forces implies about the singularity structure of partial wave amplitudes. We begin by considering the first Born approximation due to meson exchange. If we were talking about nucleon-nucleon scattering and were ignoring spin, this would simply be the one pion exchange contribution

$$f_B^{(1)}(s,t) = \frac{g^2}{\mu^2 - t} .$$

If we take the partial wave projection of this amplitude defined as:

$$f_B^{\ell}(s) = \frac{1}{2} \int_{-1}^1 dz P_{\ell}(z) f_B^{(1)}(s,z) .$$

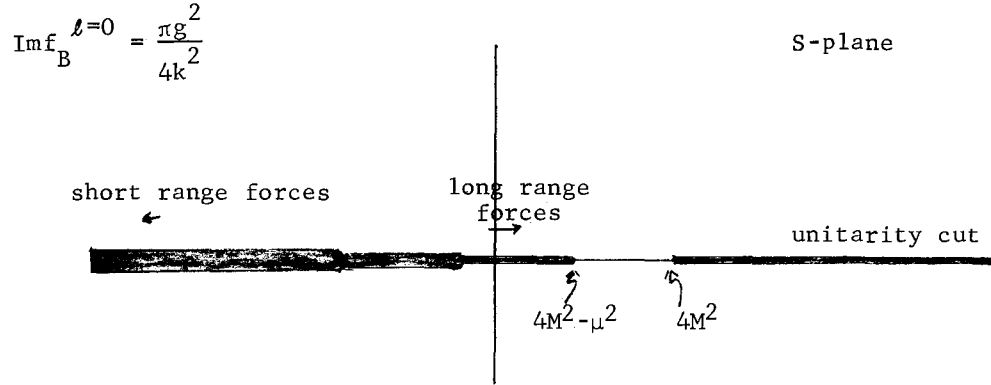
We find that this is equal to:

$$\frac{g^2}{4k^2} Q_{\ell} \left( 1 + \frac{\mu^2}{2k^2} \right)$$

where  $k^2$  is the magnitude of the center of mass momentum and  $Q_{\ell}(k)$  is the Legendre function of the second kind. In particular, for the S wave, we have

$$f_B^0(s) = \frac{g^2}{4k^2} \ln \left( \frac{\mu^2 + 4k^2}{\mu^2} \right) .$$

It is evident from this expression that we have a branch point in the S plane at  $s = 4M^2 - \mu^2$ . The other partial waves have a very similar singularity structure. We see that due to the smallness of the pion mass, that this branch point is actually quite close to the threshold branch point. The higher terms in the Born series corresponding to shorter range forces give correspondingly more distant singularities (branch cuts) to the left of elastic threshold. From the above form for the S-wave partial amplitude, the discontinuity across the left hand cut can be calculated to be



If we neglect inelastic scattering, unitarity tells us what the discontinuity across the right hand cut is. It says

$$\text{Im} \frac{1}{f^l(s)} = -k \quad s > s_{\text{threshold}}$$

It was hoped that a knowledge of the forces, plus elastic unitarity would be enough to determine the partial wave amplitude in the low-energy region. Although this has not usually turned out to be the case, let us examine the mechanics of this model before discussing its elaborations. We assume

$$\text{Im}f_l(s) = \sigma(s) \quad s < s_L$$

where  $s_L$  is the left-hand branch point, and where  $\sigma(s)$  is a known function. The N/D method, as this scheme is known, assumes that the partial wave amplitude can be written as a quotient

$$f_l(s) = \frac{N(s)}{D(s)}$$

where  $N(s)$  contains the left hand singularities and  $D(s)$  contains the unitarity cut. From the above three equations, we may write,

$$\begin{aligned} \text{Im}N(s) &= \sigma(s)D(s) & s < s_L \\ &= 0 & s > s_L \\ \text{Im}D(s) &= -kN(s) & s > s_T \\ &= 0 & s < s_T \end{aligned}$$

Hence we may write the following integral representations for  $N$  and  $D$ , provided the integrals converge.

$$N(s) = \frac{1}{\pi} \int_{-\infty}^{s_L} ds' \frac{\sigma(s')D(s')}{s'-s}$$

$$\frac{D(s)-D(s_0)}{s-s_0} = \frac{1}{\pi} \int_{s_T}^{\infty} \frac{ds' \text{Im}D(s')}{(s'-s)(s'-s_0)}$$

Here the integral representation for D has the form of a once-subtracted dispersion relation. We can fix the normalization of N and D by setting  $D(s_0) = 1$ . In general we could have an arbitrary number of subtractions in N and D. [CDD ambiguity] This is because the asymptotic behavior of  $f_{\ell}(s)$  says nothing about the asymptotic behavior of N or D separately. From the above equation for  $\text{Im}D(s)$ , we see that we can write this last integral representation in the following form.

$$D(s) = 1 - \frac{s-s_0}{\pi} \int_{s_T}^{\infty} \frac{ds' kN(s')}{(s'-s)(s'-s_0)}$$

We can now solve these equations by substituting for D in the N equation or vice versa. If we define

$$B(s) \equiv \frac{1}{\pi} \int_{-\infty}^{s_L} \frac{ds' \sigma(s')}{s'-s} \quad (\text{Born approximation to the partial wave amplitude})$$

we find

$$N(s) = B(s) - \frac{1}{\pi} \int_{-\infty}^{s_L} \frac{ds' \sigma(s')}{s'-s} \left[ \frac{s'-s_0}{\pi} \int_{s_t}^{\infty} \frac{ds'' k(s'')N(s'')}{(s''-s')(s''-s_0)} \right]$$

where  $k(s'') = (s''/4-M^2)^{\frac{1}{2}}$ . Performing a few manipulations, we find,

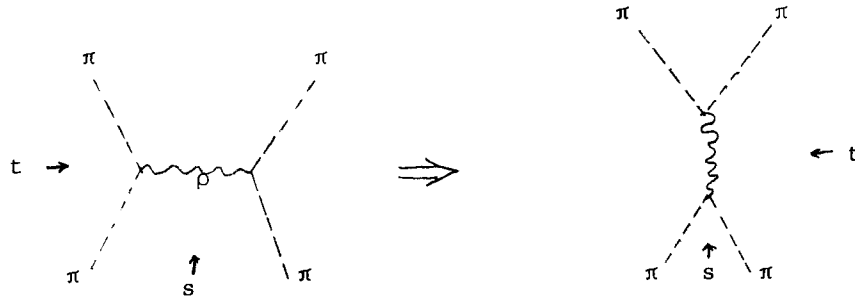
$$N(s) = B(s) + \frac{1}{\pi} \int_{s_T}^{\infty} ds'' K(s'', s) N(s'')$$

where the kernel K is

$$K(s'', s) = k(s'') \left[ \frac{(s''-s_0)B(s'') - (s-s_0)B(s)}{(s''-s)(s''-s_0)} \right]$$

Provided that  $\sigma(s)$  is sufficiently well behaved at infinity, the above equation for N is a non-singular Fredholm equation which can easily be solved on a computer. Once N(s) is determined, one can go back and substitute it into the integral representation and determine D(s). Then one can construct  $f_{\ell}(s) = N(s)/D(s)$ .

Now, let us take these ideas and try to apply them to a bootstrap scheme. An interesting possibility is the  $\pi\pi$  system which has the same quantum numbers in the s channel as in the t-channel. So for example, we may hope to understand the  $\rho$  meson as a resonance in the  $I=1, J=1$  partial wave as being produced primarily as a result of the exchange of the  $\rho$  meson in the t-channel. In terms of diagrams, this means:



One could try to adjust the input parameters such as the mass and coupling constant to obtain consistency with the width and position of the output resonance. However, in certain respects, this model comes to grief. Due to the fact that we are exchanging a particle of spin one in the t-channel, we are confronted with a problem of divergences. Using the Feynman rules to calculate the  $\rho$  meson exchange contribution to  $\pi\pi$  scattering we have

$$\begin{aligned}
 F(s,t) &= \frac{g^2 (P_1+P_3) \cdot (P_2+P_4)}{t-m_\rho^2} \\
 &= \frac{g^2}{t-m_\rho^2} \cdot (t-4\mu^2) \cdot \left(1 + \frac{2s}{(t-4\mu^2)}\right), \quad \begin{aligned} s &= (P_1+P_2)^2 \\ t &= (P_1-P_3)^2 \end{aligned} \\
 &= \frac{g^2}{t-m_\rho^2} \cdot (\text{threshold factor}) \cdot P_1(\cos\theta_t) \quad .
 \end{aligned}$$

The factor of  $s$  in  $\cos\theta_t$  ruins the convergence properties and the bootstrap scheme fails. In addition, we have ignored in this procedure the contribution of the shorter range forces and the inelastic intermediate state contributions to unitarity, which should affect the solution significantly.

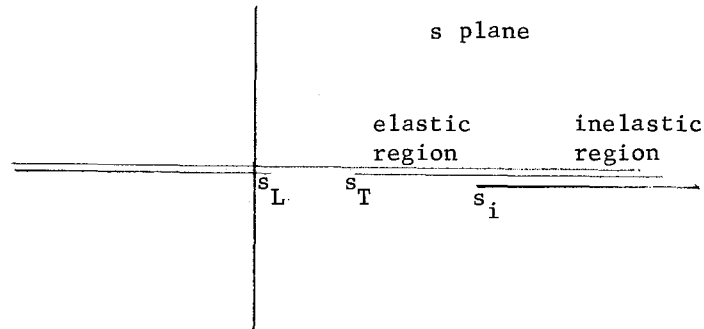
Another area where we may hope to gain some ground with this approach is in nucleon-nucleon scattering. Scotti and Wong<sup>9</sup> have fitted all the Nucleon-Nucleon scattering data up to 300 MeV (first inelastic threshold) in terms of masses and coupling constants of mesons exchanged. They included the  $\pi$ ,  $\eta$ ,  $\omega$ ,  $\phi$  and  $\rho$ .

Subsequently, Ball, Scotti and Wong took these same forces as input and performed an N/D calculation in the  $\bar{N}N$  channel. They were able to get bound states with all the above quantum numbers, although the masses didn't come out correctly.

#### REFERENCES

9. G.F. Chew and S. Mandelstam, Phys. Rev. 119, 467 (1960).
10. A. Scotti and D.Y. Wong, Phys. Rev. 138, B145 (1965).

Today we will begin by discussing briefly some elaborations of the N/D method in bootstrap schemes. Certainly one way that we can improve upon our earlier results is to consider the effects of the more distant singularities, such as inelastic thresholds.



So, for example, if we were considering  $\pi\pi$  scattering, we would like to take into account the  $\pi\pi$  intermediate state contributions to unitarity. It turns out to be not too difficult to deal with two body inelastic intermediate states in principle. So we may have a good handle on the problem if we were to approximate the  $\pi\pi$  intermediate state by grouping two of the final particles into a resonance configuration. Either as  $\rho N$  or  $\pi\Delta$ . One then considers the amplitude as a matrix. So for example we make the following generalization

$$T = ND^{-1} \quad \text{Forces}$$

$T_{11}$	$\pi\pi \rightarrow \pi\pi$	$\rho$ -exchange
$T_{12}$	$\pi\pi \rightarrow \rho\pi$	$\pi$ -exchange
$T_{22}$	$\rho\pi \rightarrow \rho\pi$	

and consider the coupled channel approach. One would, of course, consider different forces in each of the various channels. The unitarity condition for elastic scattering goes over into a very simple form here.

$$T^{-1}(s+i\epsilon) - T^{-1}(s-i\epsilon) = -k$$

where  $k$  is a matrix (diagonal) of center of mass momenta.

$$k = \begin{pmatrix} k_1 \theta(s-s_1) & 0 \\ 0 & k_2 \theta(s-s_2) \end{pmatrix} .$$

Here  $s_1$  and  $s_2$  are the thresholds for the two channels and  $k_i$  is the corresponding center of mass momenta. The matrix  $ND^{-1}$  method is then a straightforward generalization.

Another approach that attempts to consider the effect of inelastic processes is the following. In the inelastic region, we may still write

$$f_l = \frac{e^{2i\delta_l} - 1}{2ik} \quad \text{where } \delta_l = \delta_R + i\delta_I .$$

Now suppose  $\delta_I \neq 0$  and is a known function for  $s > s_I$ , then the solution to the problem can be written down immediately<sup>13</sup> as

$$\delta(s) = \frac{k(s)}{\pi} \int_{s_I}^{\infty} \frac{ds'}{k(s')} \frac{\delta_I(s')}{s' - s}$$

where for the moment we have ignored the left hand cut.<sup>14</sup> Unfortunately, this solution is not unique. If  $e^{2i\delta}$  is a solution to the problem, then so is

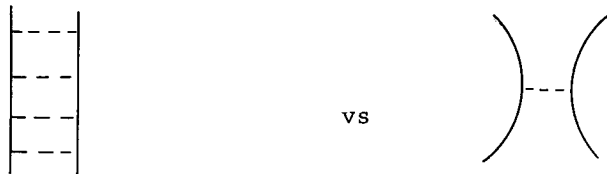
$$\frac{(k-\gamma)(k+\gamma^*)}{(k-\gamma^*)(k+\gamma)} \cdot e^{2i\delta} .$$

The extra multiplicative factor is designed not to destroy unitarity while it puts poles on the unphysical sheet. These are the analogs of the C.D.D. poles, and are necessary to fit the scattering phase shifts on occasion.<sup>15-16</sup>

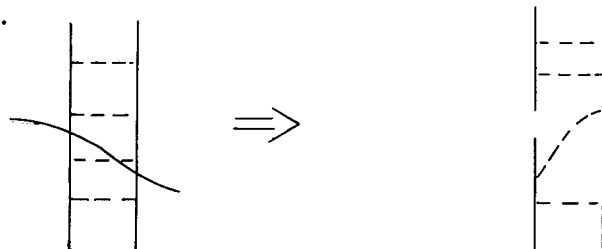
### Bethe-Salpeter Equation

Now we shall turn our attention to another dynamical model, the Bethe-Salpeter equation and analyze its implicit  $O(4)$  symmetry.<sup>17</sup> There are a number of reasons why we are interested in this model.

1) In its simplest version, the Bethe-Salpeter equation (hereafter B.S.) sums up ladder diagrams. This is in contrast to the N/D approach, which typically considers forces built out of single particle exchange only.



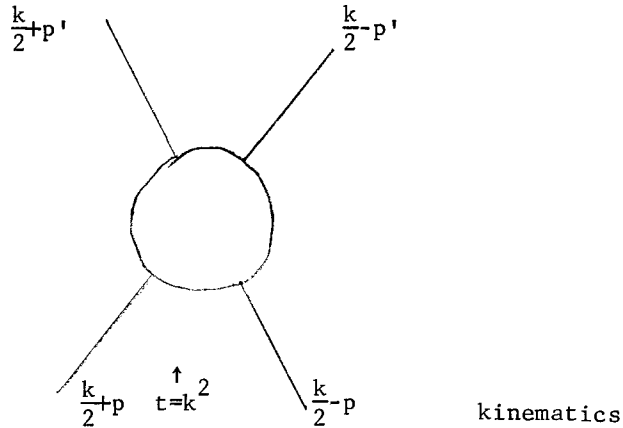
2) Some inelastic effects are included since you can break up the ladder in the following way.



3) At  $t=0$ , the Bethe-Salpeter equation exhibits  $O(4)$  symmetry. This point will be emphasized.

4) The equation is very similar to those of the Multiperipheral Model.

We will now analyze the B.S. equation at  $t=0$  and use the  $O(4)$  symmetry to reduce it to more tractable form.



The Feynman amplitude for the process depicted is  $M(p,p',k)$  and is a function of the invariants  $p \cdot p'$ ,  $p \cdot k$ ;  $p' \cdot k$ , etc. For the moment we are ignoring spin in the problem. In the center of mass system  $k$  takes the form

$$k = ((t)^{\frac{1}{2}}, 0, 0, 0) .$$

The fact that the elements of the ordinary rotation group  $O(3)$  leave the amplitude invariant leads to the ordinary partial wave expansion for the scattering amplitude. But at  $t = 0$

$$k = (0, 0, 0, 0)$$

and the amplitude should exhibit a higher symmetry.

This symmetry is  $O(3,1)$ .<sup>\*</sup> After performing a Wick rotation to transform ourselves to a Euclidean Metric, the symmetry becomes  $O(4)$  symmetry. We shall use this to diagonalize the B.S. equation for the case of equal mass particles, but this procedure can be extended to treat the unequal mass cases also.

The ordinary rotation group  $O(3)$  consists of 3 possible rotations.

- $R_1 \rightarrow$  rotation in 2-3 plane
- $R_2 \rightarrow$  " 1-3 plane
- $R_3 \rightarrow$  " 1-2 plane.

$O(4)$  consists of these plus 3 more elements ("boosts")

- $S_1$  rotation in 1-4 plane
- $S_2$  " 2-4 plane
- $S_3$  " 3-4 plane.

We can write down the elements as  $4 \times 4$  matrices and calculate the commutation relations of the generators.

$$R_i(\delta\theta) = 1 - iJ_i(\delta\theta)$$

$$S_i(\delta\theta) = 1 - iK_i(\delta\theta)$$

\* First considered by M. Toller and collaborators.



then:

$$\begin{aligned} [J_i, J_j] &= i\epsilon_{ijk} J_k \\ [J_i, K_j] &= i\epsilon_{ijk} K_k \\ [K_i, K_j] &= i\epsilon_{ijk} J_k \end{aligned}$$

If we form the linear combinations:

$$J_i^\pm = J_i \pm K_i$$

then

$$\begin{aligned} [J_i^\pm, J_j^\pm] &= i\epsilon_{ijk} J_k^\pm \\ [J_i^+, J_j^-] &= 0, \end{aligned}$$

that is they satisfy  $O(3)$  commutation relations.  $O(4)$  is isomorphic to  $SU(2) \otimes SU(2)$ .

Next we want to construct and label states according to eigenvalues of  $(J^+)^2$  and  $(J^-)^2$ . The eigenvalues are

$$\begin{aligned} (J^+)^2 &= j_1(j_1+1) \\ (J^-)^2 &= j_2(j_2+1) \end{aligned} \quad \text{states } |j_1 j_2 m_1 m_2\rangle .$$

We can construct states of physical angular momenta by using the vector addition rules

$$\vec{J} = \vec{J}^+ + \vec{J}^-$$

and combine states  $|j_1 j_2 m_1 m_2\rangle$  to construct states  $|j_1 j_2 JM\rangle$  by using appropriate Clebsch-Gordan coefficients in the usual way.<sup>18</sup>  $j_1$  and  $j_2$  do not have any direct physical meaning, whereas  $j$  does. We can also introduce the following convenient notation

$$\begin{aligned} n &= j_1 + j_2 = \text{Toller's } \lambda \\ M &= j_1 - j_2 \end{aligned}$$

so that according to the rules of vector addition, the physical angular momentum lies in the range

$$|M| \leq j \leq n .$$

The most general specification of an element of  $O(4)$  is

$$u(\varphi, \theta, \psi, \alpha, \beta, \gamma) = R_3(\varphi)R_2(\theta)S_3(\psi)R_3(\alpha)R_2(\beta)R_3(\gamma)$$

where the angles range over the following regions

$$0 \leq \beta, \psi, \theta \leq \pi \quad 0 \leq \alpha, \varphi, \gamma \leq 2\pi .$$

Then

$$u(\varphi, \theta, \psi, \alpha, \beta, \gamma | j_1 j_2 m_1 m_2 \rangle = \sum_{m_1' m_2'} \mathcal{D}_{m_1' m_2' m_1 m_2}^{j_1 j_2}(\varphi, \theta, \psi, \alpha, \beta, \gamma) | j_1 j_2 m_1' m_2' \rangle$$

where

$$\mathcal{D}_{m_1 m_2 m_1 m_2}^{j_1 j_2}(\varphi, \theta, \psi, \alpha, \beta, \gamma) = \sum_{m_1 m_2} \mathcal{D}_{m_1 m_1}^{j_1}(\varphi, \theta, \psi) \mathcal{D}_{m_1 m_1}^{j_1}(\alpha, \beta, \gamma) \\ \times \mathcal{D}_{m_2 m_2}^{j_2}(\varphi, \theta, -\psi) \mathcal{D}_{m_2 m_2}^{j_2}(\alpha, \beta, \gamma) .$$

Sandwiching u between states, we find,

$$\langle j_1 j_2 j', m' | \hat{u} | j_1 j_2 j, m \rangle = \sum_{m''} \mathcal{D}_{m' m''}^{j'}(\varphi, \theta, 0) d_{j', j m}^{j_1 j_2}(\psi) \mathcal{D}_{m'' m}^j(\alpha, \beta, \gamma)$$

where

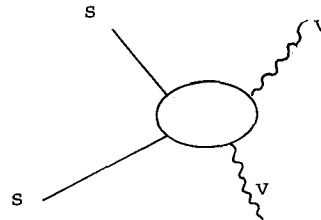
$$d_{j', j m}^{j_1 j_2} \delta_{m m'} = \langle j_1 j_2 j' m' | s_3(\psi) | j_1 j_2 j m \rangle \\ = \sum_{m_1 m_2} e^{-i(m_1 - m_2)\psi} c(j_1 j_2 j m_1 m_2 m) \cdot C(j_1 j_2 j' m_1 m_2 m) \times \delta_{m m'}$$

As an example

$$d_{j, 0, 0}^{(n, M=0)}(\psi) = N(n, j) (\sin \psi)^j C_{n-j}^{j+1}(\cos \psi)$$

where  $N(n, j)$  is a normalization factor.

Now let us take this machinery that we have built up and apply it to the scattering of scalar particles on vector particles



The helicity amplitude is defined in terms of the on-mass shell Feynman amplitude as follows: (we use the summation convention throughout)

$$T_{\lambda' \lambda}(s, t) = \epsilon_{\mu}^*(\lambda') M_{\mu\nu}(p, p', k) \epsilon_{\nu}(\lambda) .$$

The  $\epsilon$ 's are the polarization vectors for the vector particles. The amplitude  $M$  has the Lorentz-Invariance property

$$M_{\nu\mu}(p, p', k) = \Lambda_{\nu' \nu} M_{\nu' \mu'}(\Delta p, \Delta p', \Delta k) \Lambda_{\mu' \mu} .$$

In what follows we shall be working at  $k = 0$ . We go over to a convenient notation for performing the partial wave expansion in  $O(4)$

$$M_{\mu\nu}(p, p', k=0) = \langle \hat{p}', \mu | M(p, p') | \hat{p}, \nu \rangle$$

where  $p$  denotes the magnitude of  $p$  and  $\hat{p}$  specifies its orientation. Our states transform in the following way:

$$u(\Lambda) |\hat{p}\nu\rangle = \Lambda_{\nu',\nu} |\hat{\Delta p}, \nu'\rangle .$$

Passing from a cartesian index  $\mu$  to a pair of spherical tensor indices  $\Sigma\sigma$ , we have from above

$$u(\Lambda) |\hat{p}, \Sigma, \sigma\rangle = \mathcal{D}_{\Sigma', \sigma', \Sigma\sigma}^{\frac{1}{2}\frac{1}{2}}(\Lambda) |\hat{\Delta p}, \Sigma', \sigma'\rangle .$$

Now we want to construct the states which transform irreducibly, under  $O(4)$ . Recall how Jacob and Wick did this for  $O(3)$ . Consider

$$|jm\rangle = \int dR \mathcal{D}_{mm'}^{j*}(R) R |p, \theta, \varphi\rangle$$

where the integral is over the group volume. Then

$$\begin{aligned} R' |jm\rangle &= \int dR \mathcal{D}_{mm'}^{j*}(R) R' R |p, \theta, \varphi\rangle \\ &= \int_{R'R=S} d(R'R) \mathcal{D}_{mm'}^{j*}(R'^{-1} R'R) R'R |p\rangle \\ R'R &= S \end{aligned}$$

and using the group property, we have

$$\begin{aligned} R' |jm\rangle &= \int ds \mathcal{D}_{mm''}^{j*}(R'^{-1}) \mathcal{D}_{m''m'}^{j*}(S) S |p, \theta, \varphi\rangle \\ &= \mathcal{D}_{mm''}^{j*}(R'^{-1}) \int ds \mathcal{D}_{m''m'}^{j*}(S) S |p, \theta, \varphi\rangle . \end{aligned}$$

But since the  $\mathcal{D}$ 's are unitary, we have finally

$$R' |jm\rangle = \mathcal{D}_{m''m'}^j(R') |jm''\rangle ,$$

so that  $|jm\rangle$  does indeed transform as desired.

For  $O(4)$ , the state that transforms irreducibly is

$$\int d\Lambda \mathcal{D}_{jmj'm'}^{(n,M)*}(\Lambda) u(\Lambda) |\Sigma, \sigma, \bar{p}\rangle .$$

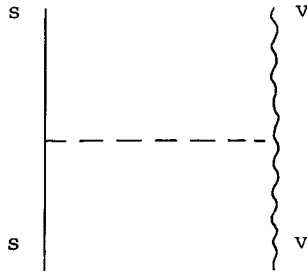
From this, we can find the following expansion coefficients,

$$\langle \hat{p}, \Sigma', \sigma' | nMj m \Sigma \rangle = N \sum_{\sigma} \mathcal{D}_{j, m, \Sigma, \sigma}^{(n,M)*}(\hat{p}) \mathcal{D}_{\Sigma', \sigma', \Sigma\sigma}^{\frac{1}{2}\frac{1}{2}}(\hat{p}) .$$

Now we can use this to diagonalize the B.S. equation

$$\begin{aligned} M_{\nu\mu}(p', p, k) &= B_{\nu\mu}(p', p, k) + \lambda \int d^4q M_{\nu\sigma}(p', q, k) \\ &\quad G_{\sigma\tau}(q, k) B_{\tau\mu}(q, p, k) . \end{aligned}$$

Here B is the kernel, which in the ladder approximation is simply

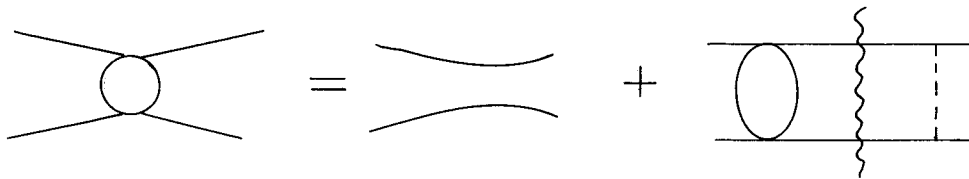


while G is the two particle propagator

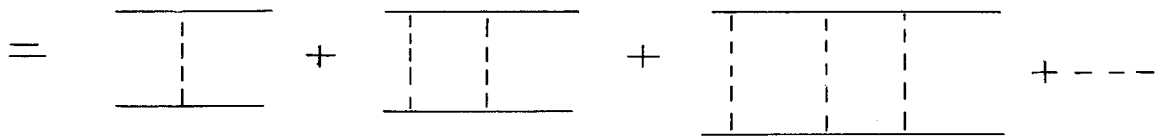
$$G_{\sigma\tau}(q,k) = \frac{1}{(k/2+q)^2 + m_s^2} \cdot \frac{\delta_{\sigma\tau} + (k/2-q)_\sigma (k/2-q)_\tau}{(k/2-q)^2 + m_v^2}$$

where we have used the standard Feynman rules with Euclidean metric.

Symbolically, the B.S. equation says



so that iterating the kernel through the integral generates the sum of all ladder diagrams



We first consider the B.S. equation for the scattering of spinless particles. By definition then,  $M=0$  and for forward scattering,  $K=0$ , we have:

$$\langle \hat{p}' | M(p', p) | \hat{p} \rangle = \langle \hat{p}' | B(p', p) | \hat{p} \rangle$$

$$\lambda \int d^4q \langle \hat{p}' | M(p, Q) | \hat{q} \rangle G(Q) \langle \hat{q} | B(Q, p) | \hat{p} \rangle$$

using the transformation coefficients:

$$\langle \hat{p} | n j m \rangle = N D_{j, m, 0, 0}^{(n, 0)}(\hat{p})$$

to protect our  $O(4)$  partial waves, and using the orthogonality property

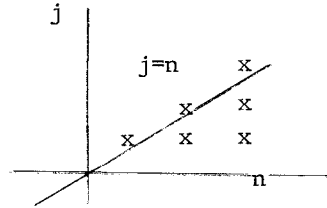
$$\int d\Omega_q \langle n' j' m' | q \rangle \langle q | n j m \rangle = \delta_{n, n'} \delta_{j j'} \delta_{m m'}$$

we obtain

$$M^n(p', p) = B^n(p', p) + \lambda \int Q^3 dQ M^n(p', Q) G(Q) B^n(Q, p) .$$

From this equation, we can infer the existence of daughter Regge poles. To do this, we assume that the solution of the equation can be analytically continued in the variable  $n$ . (This can indeed be proved in the ladder approximation). Poles in the  $n$ -plane, sometimes known as Toller poles, or Lorentz poles, manifest themselves as a sequence of Regge poles. To see this more clearly, the expression for the  $O(3)$  partial wave amplitude in terms of the  $O(4)$  partial wave amplitude is (where the coefficients  $\chi_{jn}$  are given in Ref.18)

$$T_j(t=0) = \sum_{n=j}^{\infty} \chi_{jn}^* M^n \chi_{jn}$$



where the terms in the sum represent the contribution of a horizontal array. The inverse formula, necessarily sums the vertical array,  $j = 0, \dots, n$ .

Making the transformation  $k = n-j$ , we have

$$T_j(t=0) = \sum_{k=0}^{\infty} \chi^* M^{k+j} \chi$$

where we have momentarily dropped the index on the transformation coefficients  $\chi$ .

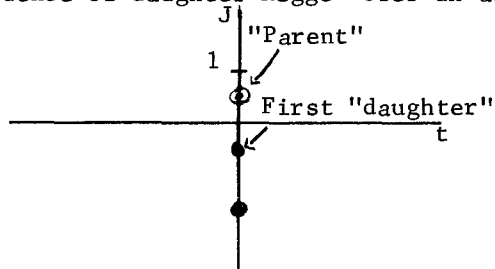
Now, suppose  $M^n$  has a Toller pole at  $n = n_0$ : e.g.,

$$M^n \sim \frac{1}{n-n_0} = \frac{1}{j+k-n_0}$$

then

$$T_j(t=0) = \sum_{k=0}^{\infty} \frac{\chi^* \chi}{j - (n_0 - k)}$$

Thus, a single Toller Pole generates a sequence of daughter Regge Poles in addition to the Parent Regge Pole at  $j = n_0$ .

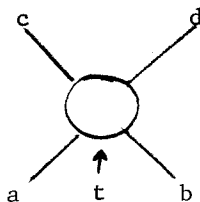


Chew Frautschi Plot.

For the equal mass case, the daughter trajectories are spaced by two units of angular momentum at  $t=0$ . Since we are working only at  $t=0$ , we can say nothing about whether the trajectories are parallel to one another. There exist elaborate arguments based on analyticity of the S-matrix which also imply the existence of daughter trajectories and give various relations between them.

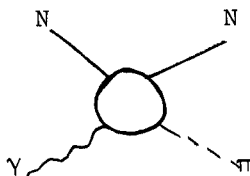
We can make an expansion of the B.S. equation about the point  $t=0$ , where we will obtain a breaking of the symmetry, and the equation is no longer diagonal. Such an expansion can lead to relations among the slopes of the Regge trajectories. In addition, the classification of Regge trajectories at  $t=0$  can be investigated within this framework. One restrictive feature of the model is that it gives only poles in the J plane, but no cuts. On the basis of such analysis, the pion has Toller quantum number  $M=1$  at  $t=0$ . But if the mass of the pion were zero, then  $J=0$ , at  $t=0$  so that the pion would have to have  $M=0$ . Experimentally, the pion seems to have  $M=1$ . To see this more clearly, let us examine the behavior of s-channel helicity amplitudes near

$t=0$ .



$$T_{\lambda_c \lambda_d \lambda_a \lambda_b}^s \propto (t)^{\frac{1}{2} \{ |M| - |\lambda_a - \lambda_b| + |M| - |\lambda_c - \lambda_d| \}}$$

where  $M$  is the Toller quantum number of the trajectory exchanged in the t-channel.



Now in  $\pi$  photoproduction on nucleons, the differential cross-section exhibits a forward spike near the forward direction with a width of  $\approx \mu^2$ . This motivates its explanation in terms of pion exchange. But for photoproduction  $|\lambda_a - \lambda_b| = 1$ . Hence, in order to restore the possibility of a forward peak, the pion must have  $M=1$ . A similar peak exists in the differential cross-section of backward n-p charge exchange scattering, where the interpretation in terms of an  $M=1$  pion is also strongly motivated.

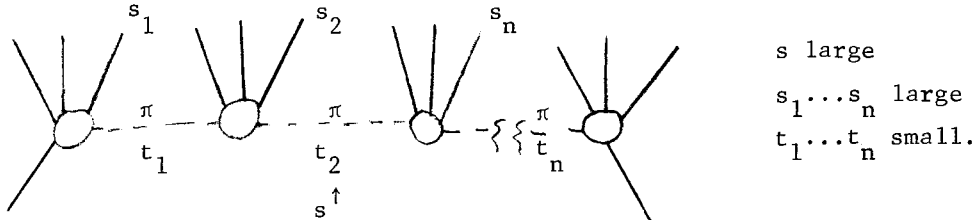
#### REFERENCES

11. J.D. Bjorken, Phys. Rev. Letters 4, 473 (1960).
12. J.S. Ball, W.R. Frazer and M. Nauenberg, Phys. Rev. 128, 478 (1962).
13. J.S. Ball and W.R. Frazer, Phys. Rev. Letters 7, 204 (1961).
14. M. Froissart, Nuovo Cimento 22, 191 (1961). In this paper, the method was generalized to take account of the left hand cuts.
15. G. Bart and R.L. Warnock, Phys. Rev. Letters 22, 1081 (1969).
16. See G. Frye and R.L. Warnock, Phys. Rev. 130, 478 (1963) for an alternative solution to the problem.
17. See, for example, G. Domokos and P. Suranyi, Nucl. Phys. 54, 529 (1964); D. Freedman and J.M. Wang, Phys. Rev. 153, 1596 (1957); *ibid* 160, 1560 (1967); W.R. Frazer, F.R. Halpern, H.M. Lipinski and D. Snider, Phys. Rev. 176, 2047 (1968); W.R. Frazer, H.M. Lipinski and D. Snider, Phys. Rev. 174, 1932 (1968).
18. V. Chung and D. Snider, Phys. Rev. 162, 1639 (1967). For the case of spin see H. Lipinski and D. Snider, Phys. Rev. 176, 2054 (1968).
- 18a. See, for example, J. Gunion and H. Lipinski, Phys. Rev.

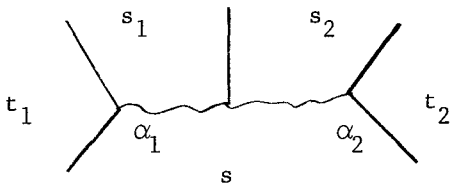
Multiperipheral Dynamics

The last dynamical model we shall consider is a recently-formulated bootstrap scheme which attempts to remedy one of the major weaknesses of earlier models, in that it attempts to take into account effects of inelastic processes explicitly. Such effects will play a major role in what follows.

One of the earliest attempts along these lines was formulated by Amati, Fubini, and Stanghellini,<sup>19</sup> who proposed that multipion exchange dominated high-energy, small-momentum-transfer inelastic scattering, in the following region of phase space



Recently attention has focussed on the Multi-Regge Pole Model, which has explained rather successfully much inelastic scattering data.<sup>20</sup>

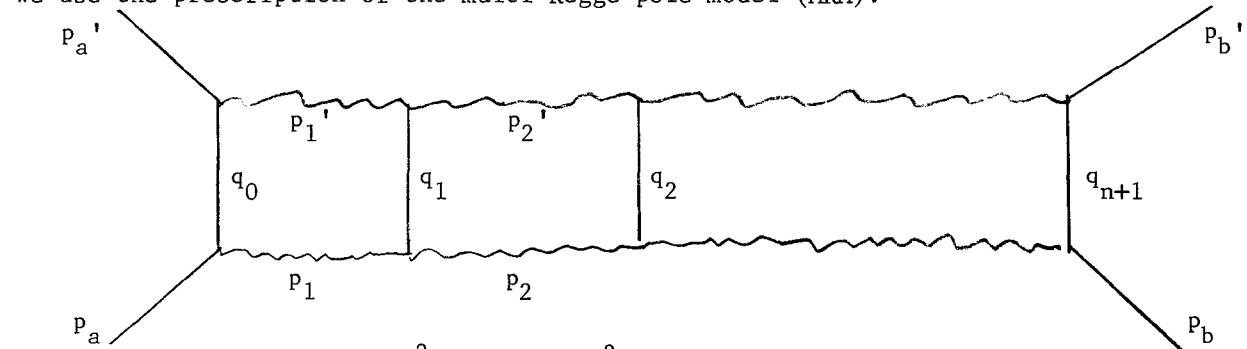


In spite of the fact that the multi-Regge region of phase space is small, we assume by invoking the concept of duality,<sup>21</sup> that on the average, it is an adequate representation of the scattering amplitude in the whole region of phase space.

Simplest Multi-Regge diagram.

The wiggly lines indicate Reggeons.

Consider the n-particle intermediate state contribution to the absorptive part of the elastic scattering amplitude for particles a and b. To parameterize this contribution we use the prescription of the multi-Regge pole model (MRM).<sup>22</sup>



Kinematics

$$s = (p_a + p_b)^2$$

$$s_1 = (p_1 + p_b)^2$$

$$s_2 = (p_2 + p_b)^2$$

$$s_3 = (p_3 + p_b)^2$$

$$t_1^- = p_1^2$$

$$t_1^+ = (p_1')^2$$

etc.

For the rungs of the diagram, we include only so called stable particles, for example  $\pi$  mesons, in order to avoid double counting. Duality says that the Regge pole



exchanges in our process account for, in an average way, resonant effects between particles on adjacent rungs.

Unitarity says that the absorptive part of the elastic scattering amplitude due to n-particles in the intermediate state is given in the MRM by:

$$A_n^{ab}(s,t) = \int d^4q_0 \dots d^4q_{n+1} \delta^4(\sum q_i - p_a - p_b) \delta^+(q_0^2 - \mu^2) \dots \delta^+(q_{n+1}^2 - \mu^2) \times$$

$$\begin{matrix} \alpha(t_1^+) + \alpha(t_1^-) \\ (S_{01}) \beta_a(t_1^-) \beta_a^*(t_1^+) \cdot \beta(t_1^-, t_2^-) \beta^*(t_1^+, t_2^+) \times \\ \alpha(t_2^+) + \alpha(t_2^-) \\ (S_{12}) \dots \dots \end{matrix}$$

where  $\beta_a$  represents the coupling of a Regge pole to the external particle a; and where  $\beta(t_1^+, t_2^+)$  represents the internal coupling of two reggeons in the multi-peripheral chain. In the above, we have left out the signature factor of the Regge trajectories. This will be put in correctly below. In addition, there can be many trajectories contributing so that each trajectory should have an index to identify it. The internal vertex functions could have dependence on vertex angles, but we shall ignore such dependence in our model.

The full absorptive part of the amplitude is gotten as;

$$A(s,t) = \sum_{n=0} A_n(s,t) \quad .$$

But since we don't want to form the sum explicitly, we must try and be clever. We try to write a recursive relation to get the  $n+1^{\text{th}}$  term from the  $n^{\text{th}}$  term. In order to do this we must undo an integration and define a new function  $B_n$  in the following way.

$$A_n(s,t) = \int d^4q_0 \delta^+(q_0^2 - \mu^2) \beta_a(t_1^-) \beta_a^*(t_1^+) B_n(p_a, p_a', q_0, p_b, p_b')$$

$B_n$  satisfies the following recursion relation.

$$B_n(p_a, p_a', q_0, p_b, p_b') = \int d^4q_1 \delta^+(q_1^2 - \mu^2) \beta(t_1^-, t_2^-) \beta^*(t_1^+, t_2^+) \alpha(t_1^+) + \alpha(t_1^-)$$

$$B_{n-1}(p_1', p_1, q_1, p_b', p_b) (S_{01})$$

Summing this equation from  $n=1$  to  $\infty$  and defining

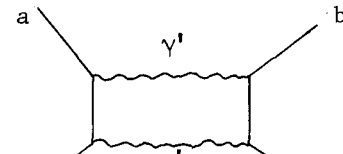
$$B = \sum_{n=0} B_n,$$

we obtain an integral equation for B

$$B^Y(p_a', p_a, q_0, p_b', p_b) = B_0^Y(p_a', p_a, q_0, p_b', p_b) + \int d^4q_1 \delta^+(q_1^2 - \mu^2) \cdot$$

$$(S_{01}) \alpha_{\gamma, \gamma}(t_1^+) + \alpha_{\gamma, \gamma}(t_1^-) \beta_{\gamma, \gamma}^*(t_1^+, t_2^+) \beta_{\gamma, \gamma}(t_1^-, t_2^-) B^\gamma(p_1', p_1, q_1, p_b, p_b')$$

where we have labelled the Regge trajectories explicitly. Here  $B_0$ , the inhomogeneous term, corresponds to the two particle intermediate state contribution.



$$B_0^{\gamma'} = \delta(s_1 - \mu^2) \beta_b^*(t_1^+) \beta_b(t_1^-) (s/s_1)^{\alpha_{\gamma'}(t_1^+) + \alpha_{\gamma'}(t_1^-)}$$

In order to conserve notation we introduce

$$\beta_{\gamma'\gamma}^*(t_1^+, t_2^+) \beta_{\gamma'\gamma}(t_1^-, t_2^-) = F_{\gamma'\gamma}(t_1^\pm, t_2^\pm)$$

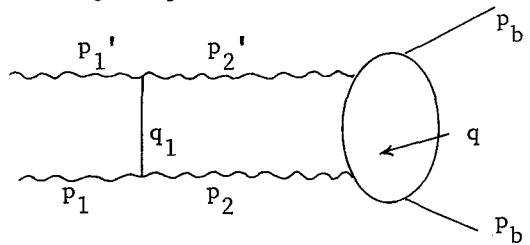
and to make the above integral equation more tractable, we make a change to Lorentz Invariant variables. That is, we want to change

$$\int d^4 q_1 \delta^+(q_1^2 - \mu^2) \implies \text{integral in terms of invariants.}$$

To do this, we perform a sequence of tricks

$$\int d^4 q_1 \delta^+(q_1^2 - \mu^2) = \int ds_2 \int d^4 q_1 \delta^4 q \delta^+(q_1^2 - \mu^2) \delta^4(q_1 + q - P) \delta(q^2 - s_2)$$

where  $p = p_1 + p_b$



The above integral when evaluated in the center of mass system  $\vec{P} = 0$ , gives

$$\int ds_2 \int \left( \begin{array}{c} \text{integral over 2} \\ \text{body phase space} \end{array} \right)$$

$$= \frac{|q_1|}{4(s_1)^{\frac{1}{2}}} \int ds_2 \int dt_2^+ dt_2^- \int d\Omega_{q_1} \delta(t_2^- - (q_1 - p_1)^2) \delta(t_2^+ - (q_1 - p_1')^2)$$

(Jacobian)

introducing the angular variables;

$$z = \hat{p}_1 \cdot \hat{p}_1'$$

$$z_1 = \hat{p}_1 \cdot \hat{q}_1$$

$$z_1' = \hat{p}_1' \cdot \hat{q}_1$$

we have by the standard addition formula

$$z_1' = z_1 + ((1-z_1^2)(1-z_1'^2))^{\frac{1}{2}} \cos\varphi$$

so that the integral over  $d\Omega_1$  reduces to an integral over  $d\varphi$  and  $dz_1$ . In addition, to simplify things, we take the asymptotic limit

$$s_1 \gg s_2, m_i^2$$

in which case we have:

$$\begin{aligned} z &= 1 + \frac{2t}{s_1} \\ z_1 &= 1 + \frac{2t_2^-}{s_1} \\ z_1' &= 1 + \frac{2t_2^+}{s_1} \end{aligned} .$$

The Jacobian of the transformation becomes, keeping terms of  $O(\frac{1}{s_1})$  only

$$J = \frac{2\theta(-\lambda)}{s_1 (-\lambda(t, t_2^+, t_2^-))^{\frac{1}{2}}} \quad \begin{aligned} \theta(x), x > 0 &= 1 \\ \theta(x), x < 0 &= 0 \end{aligned}$$

where  $\lambda$  is the triangle function

$$\lambda(a, b, c) = a^2 + b^2 + c^2 - 2ab - 2ac - 2cb .$$

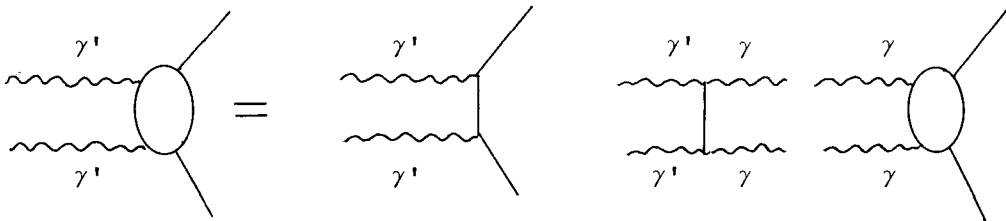
In this approximation, the multiperipheral integral equation becomes

$$\begin{aligned} B^{\gamma'}(s, s_1 t_1^{\pm}, t) &= B_0^{\gamma'}(s, s_1 t_1^{\pm}, t) + \sum_{\gamma} \int_0^1 \frac{ds_2}{s_1} \int \frac{dt_2^+ dt_2^-}{(-\lambda(t_2^{\pm}, t))^{\frac{1}{2}}} \cdot F_{\gamma', \gamma}(t_1^{\pm}, t_2^{\pm}) \\ &\quad (s_{01})^{\alpha_{\gamma', \gamma}(t_1^{\pm})} B^{\gamma}(s_1, s_2, t_2^{\pm}, t) \end{aligned}$$

where

$$\alpha_{\gamma, (t_1^{\pm})} = \alpha_{\gamma, (t_1^+)} + \alpha_{\gamma, (t_1^-)}$$

diagrammatically:



Now for high values of the subenergies  $s_{01}$ ,  $s$ , and  $s_1$ , we have the relation<sup>23</sup>

$$s = s_{01} s_1 \cdot f(\omega, t_s')$$

so that if we work in the limit that the Toller angle  $\omega$  is kept fixed, and absorb  $f$  into the vertex functions, we have

$$s_{01} \propto s/s_1 .$$

Previously we had

$$B_0^{\gamma'}(s, s_1, t_1^{\pm}, t) = \delta(s_1 - \mu^2) \beta_b(t_1^-) \beta_b^*(t_1^+) (s/s_1)^{\alpha_{\gamma, (t_1^+)} + \alpha_{\gamma, (t_1^-)}} .$$

We define  $y = s_2/s_1$  and factor the  $s$  dependence by defining<sup>24</sup>

$$B^{\gamma'}(s, s_1, t_1^{\pm}, t) = (s/s_1)^{\alpha_{\gamma, (t_1^+)} + \alpha_{\gamma, (t_1^-)}} B^{\gamma'}(s_1, t_1^{\pm}, t) .$$

The equation for  $b$  then becomes

$$b^{\gamma'}(s_1, t_1^{\pm}, t) = \delta(s_1 - \mu^2) F_{\gamma', b}(t_1^{\pm}, m^2) + \sum_{\gamma} \int_0^1 dy \int \frac{dt_2^{\pm}}{(-\lambda(t_2^{\pm}, t))^{\frac{1}{2}}} F_{\gamma', \gamma}(t_1^{\pm}, t_2^{\pm}) \cdot y^{-\alpha_{\gamma}(t_2^+)} (1-y)^{-\alpha_{\gamma}(t_2^-)} b^{\gamma}(s_2, t_2^{\pm}, t)$$

where

$$F_{\gamma', b}(t_1^{\pm}, m^2) = \beta_b^{*\gamma'}(t_1^+) \beta_b^{\gamma}(t_1^-)$$

We now perform a Mellin transformation on this amplitude  $b$  in order to extract its asymptotic behavior.

$$b^{\gamma'}(s_1, t_1^{\pm}, t) = \frac{1}{2\pi i} \int_{c-i\infty}^{c+i\infty} d (s_1/m^2)^j \mathcal{V}^{\gamma'}(j, t_1^{\pm}, t)$$

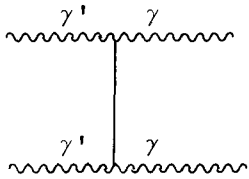
defines the Mellin transform amplitude  $\mathcal{V}$  where the contour  $c$  is taken to the right of all the singularities in the  $J$  plane of  $\mathcal{V}$ . The inverse of this transformation is given by

$$\mathcal{V}(j, t_1^{\pm}, t) = \frac{1}{m^2} \int_0^{\infty} ds_1 b(s_1, t_1^{\pm}, t) (s_1/m^2)^{-j-1}$$

The asymptotic behavior of the amplitude is governed by the singularities lying farthest to the right in the  $j$  plane. The Mellin transform of the integral equation becomes

$$\mathcal{V}^{\gamma'}(j, t_1^{\pm}, t) = F_{\gamma', b}(t_1^{\pm}, m^2) + \sum_{\gamma} \int \frac{dt_2^{\pm}}{(-\lambda(t_2^{\pm}, t))^{\frac{1}{2}}} \frac{F_{\gamma', \gamma}(t_1^{\pm}, t_2^{\pm}) \cdot \mathcal{V}^{\gamma}(j, t_2^{\pm}, t)}{J - [\alpha_{\gamma}(t_2^+) + \alpha_{\gamma}(t_2^-) - 1]}$$

Now in order to keep the model as simple as possible, we will assume that the internal vertex functions,  $F_{\gamma', \gamma}(t_1^{\pm}, t_2^{\pm})$ , factor



$$F_{\gamma', \gamma}(t_1^{\pm}, t_2^{\pm}) = \lambda^{\gamma' \gamma} g_{\gamma'}(t_1^{\pm}) g_{\gamma}(t_2^{\pm})$$

where  $\lambda^{\gamma' \gamma}$  is a matrix of coupling constants. In addition, we take

$$F_{\gamma', b}(t_1^{\pm}, m^2) = \lambda_b^{\gamma'} g_{\gamma'}(t_1^{\pm})$$

Then if we define the auxiliary function  $\beta$  as

$$g^{\gamma'}(j, t_1^{\pm}, t) = g^{\gamma'}(t_1^{\pm}) \beta_b^{\gamma'}(j, t) \quad ,$$

the equation for  $\beta$  becomes

$$\beta_b^{\gamma'}(j, t) = \lambda_b^{\gamma'} + \sum_{\gamma} \lambda^{\gamma' \gamma} \beta_b^{\gamma}(j, t) \rho^{\gamma}(j, t)$$

where

$$\rho^{\gamma}(j, t) = \int \frac{dt_2^{\pm}}{(-\lambda(t_2^{\pm}, t))^{\frac{1}{2}}} \frac{|g^{\gamma}(t_2^{\pm})|^2}{J - [\alpha_{\gamma}(t_2^+) + \alpha_{\gamma}(t_2^-) - 1]} \quad .$$

Now if we define the Mellin transform of the total absorptive part of the amplitude as:

$$A_{ab}(s, t) = \frac{1}{2\pi i} \int_{c-i\infty}^{c+i\infty} dj (s/m^2)^j a_{ab}(j, t)$$

then in terms of  $\beta$ , the Mellin transform of the absorptive part is

$$a_{ab}(j, t) = \sum_{\gamma'} \lambda_a^{\gamma'} \rho^{\gamma'}(j, t) \beta_b^{\gamma'}(j, t) \quad .$$

So that except for evaluating  $\rho(j, t)$ , the problem has been reduced to an algebraic one. Earlier, we had completely ignored the phase due to the signature in our equations. This gives the following form for  $\rho$

$$\rho^{\gamma}(j, t) = \int \frac{dt_2^{\pm}}{(-\lambda(t_2^{\pm}, t))^{\frac{1}{2}}} \frac{|g^{\gamma}(t_2^{\pm})|^2 \cos \frac{\pi}{2} (\alpha_{\gamma}(t_2^+) - \alpha_{\gamma}(t_2^-))}{J - (\alpha_{\gamma}(t_2^+) + \alpha_{\gamma}(t_2^-) - 1)} \quad .$$

On inspection we see that  $\rho(j, t)$  has a branch cut in the  $J$  plane. The position of the branch point is the same as the AFS branch point.<sup>19</sup> Now, let us take a simple model and actually calculate  $\rho$ . We will give the vertex functions exponential dependence in momentum transfer

$$g^{\gamma}(t_2^{\pm}) = e^{\frac{1}{2} k_{\gamma} t_2^{\pm}}$$

and take the trajectory functions to be linear

$$\alpha_{\gamma}(t) = a_{\gamma} + b_{\gamma} t \quad .$$

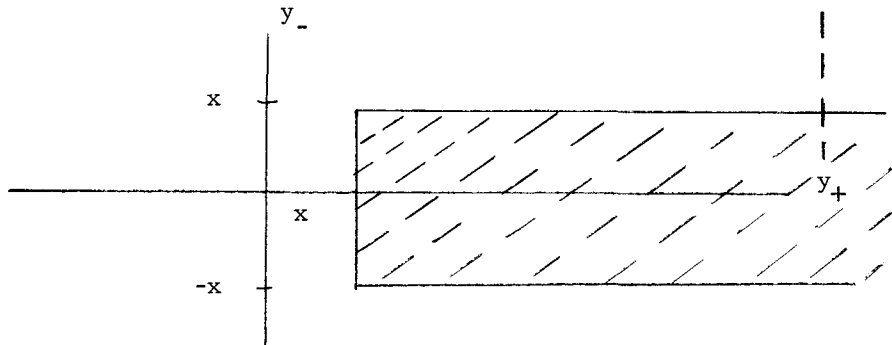
To simplify the integration, we make the change of variable

$$y_{\pm} = \frac{(-t_2^{\pm})^{\frac{1}{2}} \pm (-t_2^{\mp})^{\frac{1}{2}}}{2} ; \quad x = \frac{(-t)^{\frac{1}{2}}}{2}$$

after which the integral becomes

$$\rho^{\gamma}(j,t) = \frac{\int dy_+ dy_- (y_+^2 - y_-^2) e^{-2k_{\gamma}(y_+^2 + y_-^2)}}{\{(x^2 - y_-^2)(y_+^2 - x^2)\}^{\frac{1}{2}}} \cdot \frac{\cos(2\pi b_{\gamma} y_+ y_-)}{J-[2a_{\gamma} - 1 - 2b_{\gamma}(y_+^2 + y_-^2)]}$$

where the range of integration in the  $y_+ y_-$  plane is the shaded rectangle:



Making the substitution

$$\begin{aligned} y_+ &= r \cos \theta \\ y_- &= r \sin \theta \end{aligned} , \quad \text{the integral for } \rho \text{ becomes}$$

$$\rho^{\gamma}(j,t) = \frac{2 \int r dr d\theta \cos(2\theta) e^{-2k_{\gamma} r^2}}{\left\{ \left( \frac{x^2}{r^2} - \sin^2 \theta \right) \left( \cos^2 \theta - \frac{x^2}{r^2} \right) \right\}^{\frac{1}{2}}} \cdot \frac{\cos(\pi b_{\gamma} r^2 \sin 2\theta)}{J-[2a_{\gamma} - 1 - 2b_{\gamma} r^2]}$$

where the integral is broken up into two pieces

$$\begin{aligned} \text{(A)} \quad & x^2 \leq r^2 \leq 2x^2 & 0 \leq \theta \leq \cos^{-1} x/r \\ \text{(B)} \quad & 2x^2 \leq r^2 \leq \infty & 0 \leq \theta \leq \sin^{-1} x/r \end{aligned}$$

$$\begin{aligned} \rho^{\gamma}(j,t) &= \int_{x^2}^{2x^2} \frac{dr^2 e^{-2k_{\gamma} r^2}}{J-[2a_{\gamma} - 1 - 2b_{\gamma} r^2]} \cdot I_A(r^2) \\ &+ \int_{2x^2}^{\infty} \frac{dr^2 e^{-2k_{\gamma} r^2}}{J-[2a_{\gamma} - 1 - 2b_{\gamma} r^2]} \cdot I_B(r^2) \end{aligned}$$

where

$$I_A(r^2) = \int_0^{\cos^{-1}x/r} \frac{\cos 2\theta \cos(\pi b r^2 \sin 2\theta) d\theta}{\left\{ \left( \frac{x^2}{r^2} - \sin^2 \theta \right) \left( \cos^2 \theta - \frac{x^2}{r^2} \right) \right\}^{\frac{1}{2}}}$$

and

$$I_B(r^2) = \int_0^{\sin^{-1}x/r} \frac{\cos 2\theta \cos(\pi b r^2 \sin 2\theta) d\theta}{\left\{ \left( \frac{x^2}{r^2} - \sin^2 \theta \right) \left( \cos^2 \theta - \frac{x^2}{r^2} \right) \right\}^{\frac{1}{2}}}$$

Now if we make further the substitution

$$z = \frac{\sin 2\theta}{\frac{2x}{r} \left( 1 - x^2/r^2 \right)^{\frac{1}{2}}}, \quad \text{we find } I_A(r^2) = I_B(r^2)$$

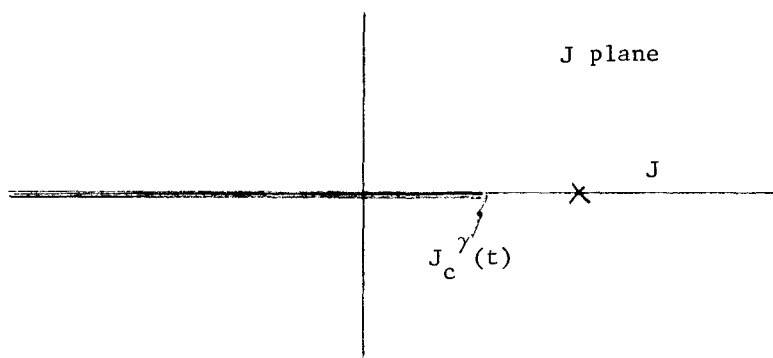
$$I_A(r^2) = J_0(2\pi b(r^2 - x^2)^{\frac{1}{2}} \cdot x) = I_B(r^2)$$

Making the replacement  $r^2 = r'^2 + x^2$ , the integral for  $\rho$  becomes (recalling that  $x^2 = -t/4$ )

$$\rho^\gamma(j, t) = 2k^\gamma e^{\frac{k}{2} t} \int_0^\infty \frac{dr'^2 e^{-2k^\gamma r'^2} J_0(\pi b r' (-t)^{\frac{1}{2}})}{J - (2\alpha_\gamma (-r'^2 + t/4) - 1)}$$

where  $\rho$  is normalized such that as  $J \rightarrow \infty$ ,  $\rho \sim \frac{1}{J}$ . From this expression, it is clear that  $\rho$  has a branch point in the  $J$  plane at  $J_c^\gamma(t) = 2\alpha_\gamma(t/4) - 1$ .

Now in order to perform the integral, we make the approximation that the region of  $J$  we are interested in is sufficiently well above the cut  $J^\gamma(t)$ , so that  $J \gg j^\gamma(t)$ .





In this limit we may take the denominator out of the integral for  $\rho$  and get

$$\rho^\gamma(j,t) \approx \frac{2k_\gamma e^{\frac{k_\gamma t}{2}}}{J - J^\gamma(t)} \int_0^\infty dr^2 e^{-2k_\gamma r^2} J_0(\pi b r (-t)^{\frac{1}{2}})$$

$$= \frac{e^{k_\gamma' t}}{J - J^{\gamma'}(t)} \quad \text{where} \quad k_\gamma' = \frac{k_\gamma}{2} + \frac{\pi^2 b^2}{8k_\gamma}$$

### One-Regge Pole Model

This is the simplest model in which the above equations can be analyzed. The trajectory labels  $\gamma$  can be dropped, and the equation for  $\beta_b(j,t)$  becomes

$$\beta_b(j,t) = \lambda_b + g^2 \beta_b(j,t) \rho(j,t)$$

$$\beta_b(j,t) = \frac{\lambda_b}{1 - g^2 \rho(j,t)}$$

where  $g^2$  is the internal coupling of the Regge pole in the multiperipheral chain. The equation for the Mellin transformed absorptive part is

$$a_{ab}(j,t) = \frac{\lambda_a \lambda_b \rho(j,t)}{1 - g^2 \rho(j,t)}$$

The Regge poles arise from the vanishing of the denominator. There will always be a Regge pole for real  $J$  to the right of the branch point. This is true regardless of the value of  $g^2$ , because  $\rho$  has a logarithmic singularity at the branch point. Now if  $g^2$  is sufficiently large so that the pole and the cut are well separated, we may substitute our approximate form for  $\rho$  and obtain

$$a_{ab}(j,t) = \frac{\lambda_a \lambda_b e^{k't}}{J - [2\alpha(t/4) - 1 + g^2 e^{k't}]}$$

We see that the position of the Regge pole is at:

$$\alpha_{out}(t) = 2\alpha_{in}(t/4) - 1 + g^2 e^{k't}$$

We can impose bootstrap consistency by demanding  $\alpha_{out}(t) = \alpha_{in}(t)$  in the linear approximation. This gives

$$a = 1 - g^2 \quad (\text{intercept})$$

$$b = 2g^2 k' \quad (\text{slope})$$

In addition, we can bootstrap the residue function by demanding equality of input and output residues

$$k' = k = \frac{k}{2} + \frac{\pi^2 b^2}{8k}$$

or

$$k = \frac{\pi b}{2}$$

this gives:

$$b = 2g^2 k = 2g^2 \frac{2\pi b}{2} \quad \text{or} \quad g^2 = \frac{1}{\pi}$$

$$a = 1 - g^2 = 1 - \frac{1}{\pi} \cong 0.68.$$

The iterated solution for the trajectory function gives

$$\alpha(t) = 1 - g^2 + g^2 \sum_{n=0}^{\infty} 2^n \left[ e^{\frac{kt}{4^n}} - 1 \right].$$

These results are not unreasonable for a high ranking meson trajectory such as the  $\rho$ -meson, but they simply cannot account for the Pomeranchuk singularity. For one thing, the intercept of the trajectory is not high enough. This is because the  $g^2$  predicted by the known multiplicities of secondaries

$$\bar{n} = g^2 \log(s/m^2)$$

which is given by this model is  $g^2 \approx 1. \sim 1.5$ . Hence  $a$  which is given by

$$a = 1 - g^2 \quad \text{is too small.}$$

So the one pole model is too simple to account for the highest lying vacuum singularity. We must go to at least a two-input pole model. The input is to be a meson trajectory and the Pomeranchuk trajectory. The results of the model are that the slope of the output Pomeranchuk pole is  $\approx 1.5$  times the "normal" meson trajectory slope.

A particularly simple limit of the 2 pole model is when the coupling of the Pomeranchuk to the meson in the multiperipheral chain can be ignored. In their limit, the Mellin transformed absorptive part of the elastic amplitude for particles  $a$  and  $b$  is given by

$$a_{ab}(j,t) = \text{Pole} + \text{Cut.}$$

Here, the pole term represents the inelastic part of the total cross-section, while the cut term comes from double Pomeranchuk exchange and represents the elastic part of the total cross-section. (see Ref. 24)

#### REFERENCES

19. D. Amati, S. Fubini and A. Stanghellini, Nuovo Cimento 26, 896 (1962).
20. For a review of the status of the model, see the review talk by Czyzewski, Proceedings of the Vienna Conference, 1968.
21. G.F. Chew and A. Pignotti, Phys. Rev. Letters 20, 1078 (1968).
22. G.F. Chew, M.L. Goldberger and F.E. Low, Phys. Rev. Letters 22, 208 (1969).
23. See N. Bali, G.F. Chew and A. Pignotti, Phys. Rev. 163, 1572 (1967), Eq. (C.5). Also, Phys. Rev. Letters 19, 614 (1967) Eq. (3).
24. For additional references see G.F. Chew and W. Frazer, UCRL Report 18681; W. Frazer and C. Mehta, Phys. Rev. Letters 23, 258 (1969).

MULTIPERIPHERAL DYNAMICS

Lectures by: Geoffrey F. Chew  
University of California, Berkeley

Notes taken by: David K. Campbell



In these lectures the central, unifying theme will be the "bootstrap" concept. Specifically, we shall discuss the relations among the many different models partially embodying this idea, with particular emphasis on the multiperipheral model. We shall approach the problem within the framework of S-matrix theory, and I shall assume some familiarity with the techniques used in that theory and a rudimentary knowledge of the analytic structure of the S-matrix. <sup>(1)</sup>

The fundamental content of the bootstrap idea is self-consistency: that is, <sup>(2)</sup> "nature is as it is because this is the only possible nature consistent with itself." The philosophical implications of such an hypothesis and its relation to "normal" scientific theories--as well as most of the material in today's lecture--are discussed in detail in reference (2).

We will attempt to construct a partial bootstrap limited to the hadrons and based on the assumption that the hadrons by themselves are "self-consistent", in some sense all being composites of one another. In developing the theory, we will allow no arbitrary hadronic parameters--like for instance, the masses and coupling constants of elementary particles in a local field theory --- but we will require a set of "arbitrary" postulates as constraints on the S-matrix. In effect we hope that by constraining the S-matrix to satisfy certain constraints we will enable the partial hadronic bootstrap to succeed even though a theory consistent with the full bootstrap philosophy would have to include and account for electromagnetic, weak, and gravitational interactions as well. The relevance of the constraints in limiting the theory to hadronic interactions will become clear when we enumerate them.

First, let me motivate the ideas of "compositeness" and "self-consistency." We can recognize three distinct roles taken by particles in strong interactions. The hadrons may appear as:

- 1) constituent particles in a composite, for instance, as the neutron and proton in a deuteron;
- 2) carriers of the strong forces, like the pion in the Yukawa model; and finally as
- 3) the composites themselves.

Demanding "self-consistency" of these different roles in a particular hadron system can lead immediately to a crude bootstrap; in  $\pi\pi$  scattering, one can imagine requiring that the forces caused by exchange of the  $\rho$  pole (in the t-channel) are sufficient to produce the  $\rho$  resonance (in the s-channel). But it is clear that this picture, couched in a non-relativistic language, is insufficient to describe strong interactions, for which relativistic effects are essential. Indeed, to describe the  $\pi$  as a bound state of, say  $\bar{N}N$ , requires assuming a binding energy equal to many times the rest mass of the composite particle.

Thus we must consider a relativistic theory. The extreme difficulties inherent

in relativistic quantum field theories suggest that these may be inappropriate for describing the bootstrap. We will instead use the S-matrix description of strong interactions. Here one asserts that in measuring the probability for scattering an initial configuration of momenta into a final configuration, one is measuring quantities related to S-matrix elements. By establishing or postulating fundamental properties of the S-matrix, one is able to correlate different measurements.

What, then, are the fundamental properties of the S-matrix? To limit the theory to the strong interactions and to embody the idea of compositeness we require the S-matrix to satisfy four constraints.

1) Space-time constraints: We assume Poincare invariance of the S-matrix which together with the Fourier transform relation between macroscopic space-time and momentum leads to the conservation laws in momentum space. We also require the cluster decomposition property, which asserts that events widely separated in space-time are independent.

2) First degree analyticity: The S-matrix elements are analytic functions of momenta with only those singularities related to the causal aspects of space-time and to unitarity. We assume as well that the same function, continued analytically, describes the scattering amplitude in all reactions related by the interchange of ingoing particles with outgoing antiparticles; this is crossing.

3) Unitarity: This asserts  $SS^+ = 1$ , combining the quantum idea of superposition of states with the conservation of probability.

4) Second degree analyticity: By this constraint we mean that "all poles are Regge poles," that is, that there exist no elementary particles corresponding to Kroenecker delta singularities in angular momentum. This is also known as "nuclear democracy" or "Regge boundary condition."

Our bootstrap hypothesis is that these postulates determine the hadronic S-matrix uniquely.

Before we begin to examine this hypothesis, let us consider two questions. How do these postulates achieve our goal of limiting the theory to hadrons so that we can reasonably expect a successful bootstrap involving hadrons alone? Given these postulates about the S-matrix, how do we develop a calculational procedure?

The answer to the first question is (superficially at least) clear. The assumption of Poincare invariance implies that we are neglecting general relativistic effects. Further, analyticity of the first kind in the presence of unitarity is incompatible with the existence of mass zero particles and thus---assuming that descriptions of electromagnetic, weak and gravitational forces involving zero mass photons, neutrinos and gravitons respectively are correct---we are excluding these interactions from our theory. Hence these postulates may allow a partial bootstrap of the hadrons separately.

The second question is more difficult because there is no definite starting point for making calculations. Essentially, given approximate knowledge of the S-matrix in a small region, we can, by applying the constraints, extend and continue this knowledge to surrounding regions. However, the complexity of the theory precludes just writing down the answer. So we will construct models satisfying some of the postulates in a restricted domain and then "continue" the results to relate different regions of the S-matrix. The major emphasis of the lectures will be on discussing simple models which allow us to correlate different parts of the S-matrix within the bootstrap framework.

#### REFERENCES

1. (a) R.J. Eden, P.V. Landshoff, D.I. Olive and J.C. Polkinghorne, The Analytic S-Matrix, Cambridge University Press (1966); (b) G.F. Chew, The Analytic S-Matrix W.A. Benjamin and Co., New York (1966); (c) G.F. Chew, Review article in "Old and New Problems in Elementary Particle Physics" (Bernardini Festschrift).
2. G.F. Chew, Science 161, 762 (1968).



Today's lecture will serve primarily as a brief review of the terminology and concepts of S-Matrix theory.<sup>(1)</sup>

I will assert, rather than prove, most of the needed properties of the S-matrix, in order to avoid deep forays into an unfamiliar formalism. The first properties are unquestioned, although in some cases the direct logical relation to the fundamental postulates has not been completely established. Let us begin with a definition. We will call a channel any collection of particles which can constitute an initial or a final state. Communicating channels are channels which share the same conserved quantum numbers so that S-matrix elements among them do not vanish identically.

### I. Cluster Decomposition:

We will discuss this postulate in order to introduce and illustrate a useful diagrammatic technique. Recall that this hypothesis stated that widely separated events were independent. This implies that if we consider particles at all times far apart, there will be no interaction. We can illustrate this principle with the aid of simple diagrams in which a line corresponds to the motion of a real physical particle and "bubbles" correspond to interactions among particles.

Consider a real physical scattering process in a three particle channel. We could represent this general scattering as in Fig. 1 (term 0). By the cluster decomposition hypothesis, there will exist configurations such that the particles are so widely separated that no deflection of momentum takes place: that is, such that the particles do not interact at all. This is indicated schematically in Fig. 1 by term (1). We can equally well imagine interactions involving just two particles (term 2) or all three particles (term 3).

Each "connected" portion of one of these diagrams contains as a factor a delta function of the sum of the interacting particle momenta: term (1), for instance, contains the product of three  $\delta$ -functions corresponding to the requirement that all three particles move undeflected. The total S-matrix, of course, will contain a  $\delta$ -function corresponding to overall momentum conservation. That part of the S-matrix corresponding to all particles interacting (after factoring off the  $\delta$ -function) is called the "connected part." Thus term (3) in Fig. 1 represents the connected part of the three particle to three particle S-matrix element.

### II. Analytic Structure of the S-matrix:

We can use the diagrammatic approach developed above to indicate how studies of the singularities of the S-matrix proceed. In the first instance, we will restrict ourselves to those values of the external momenta which are allowed physically. But the requirement of

analyticity allows continuation of the S-matrix elements to domains outside the "physical region." We will discuss this later.

Consider first the correspondence between poles in the S-matrix and particles. One of the ways in which the scattering of three particles can take place is by the physical double scattering process, as shown in Fig. 2. It can be shown that the possibility of this double scattering occurring implies the existence of a pole of the form

$$\frac{\lambda}{(p_1+p_2-p_4)^2 - m^2}$$

in the connected part. Further, the residue of the pole is factorable into factors depending on the two bubbles((A) and (B)) independently.

Another singularity can be shown to arise from the more complicated physical triple scattering illustrated in Fig. 2(b). It was first emphasized by Coleman and Norton that the requirement that diagram 2(b) describe a physically possible triple scattering implies that the space-time displacements satisfy  $\tau_{AB} + \tau_{BC} = \tau_{AC}$ . These give a condition on the external momentum which allows one to calculate the location of this singularity.

In general, any "diagram" involving a real scattering process will correspond to a singularity of the S-matrix. The canonical techniques for locating these are called the "Landau rules". Note that the more complicated singularities will normally be branch points (on the real axis). Consider a special example of a physical region singularity: the normal threshold, shown in Fig. 2(c). This physical situation arises if these particles come out with no relative momentum so that they can interact again. Thus the singularity occurs at zero relative kinetic energy and hence at

$$(p_1+p_2+p_3)^2 = (\sum_{i=1} m_i)^2.$$

To be certain that the significance of the diagrams is clear, I should emphasize that they are not field theoretic or Feynman diagrams but are graphical representations of real processes which correspond to singularities in the S-matrix. The S-matrix is not a sum of these diagrams; they merely give the location of the singularities. If we know the discontinuities across the singularities they represent (unitarity helps here) and if we know the asymptotic behavior of the amplitude (second degree analyticity helps here), then we can write dispersion relations for the S-matrix element.

Suppose we now wish to extend our study of singularities to the "unphysical region" of the external momenta. We must clearly have a prescription for continuing

analytically past the Landau branch points discussed above. The "+ iε prescription" says that to remain on the Riemann sheet on which the physical scattering amplitude is the boundary value of the analytic S-matrix element, we must follow "paths" as shown in Fig. 3. With this prescription we can continue beyond the lowest physical threshold to the "unphysical region." One extremely important singularity in the unphysical region is the single particle singularity in the two particle connected part. Since we are at present considering stable particles, we know that the singularity corresponding to the formation and "decay" of the single particle intermediate shown in Fig. 4 must be in the unphysical region. Continuing analytically to  $s = m^2$  demonstrates - as we would anticipate - that there is a pole in the S-matrix corresponding to this single particle "intermediate" state. Further, factorization still holds. The Landau rules, because they are analytic, will still describe the positions of the general singularities outside the physical region.

### III. Crossing:

Although we asserted this as a part of the fundamental postulate of analyticity, crossing can be "proved" considering a diagram such as shown in Fig. 5. By varying  $p_0$  from  $p_0 > m$  to  $p_0 < -m$  while staying on the pole at  $p^2 = m^2$ , one can continue from the process illustrated in Fig. 5(a) to that of Fig. 5(b) where the scattering order is reversed. The particle then will have the antiparticle quantum numbers of the particle  $m$ . By factorization we conclude that  $\bar{B}$ , the amplitude  $B$  with particle  $m$  "crossed," is the analytic continuation of  $B$ .

### IV. Hermitian analyticity:

We will present an intuitive heuristic argument for the property, first given by Stapp.<sup>(3)</sup> Roughly speaking, before an interaction the particles can be represented by an incoming wave,  $e^{-ikr}$ , whereas afterwards they may be considered to be an outgoing wave,  $e^{+ikr}$ . So the transformation  $k \rightarrow -k$  should take  $S$  to  $S^{-1}$  which equals  $S^+$  by unitarity. Now  $k \propto (s-s_t)^{\frac{1}{2}}$  where  $s_t$  is threshold of  $s$ . Thus, the path of continuation shown in Fig. 6, which takes  $k \rightarrow -k$ , will take  $S$  to  $S^+$ . Note that if there are many branch points (thresholds), the continuation must go around the lowest threshold.

### V. The Cutkosky Discontinuity Formula:<sup>(4)</sup>

Consider the consequences of unitarity and cluster decomposition for the S-matrix element shown in Fig. 7(a).  $S^+S = 1$  gives us the diagrammatic equation shown in Fig. 7(b), which corresponds to the equation

$$M_{ba}(s_+) - M_{ba}^+(s_+) = ic \int_n d\phi_n M_{bn}^+(s_+) M_{na}(s_+)$$

where  $n$  denotes a physical intermediate channel,  $s_+ \equiv s+i\epsilon$ , and

$$d\phi_n = \prod_{k \in n} d\phi_k = \prod_{k \in n} d^4 p_k \delta^+(p_k^2 - m_k^2)$$

is the phase space element.

By hermitian analyticity

$$M_{ba}^+(s_+) = M_{ba}(s_-), \text{ where } s_- \equiv s - i\epsilon,$$

and thus

$$M_{ba}(s_+) - M_{ba}(s_-) = ic \int d\phi_n M_{bn}(s_-) M_{na}(s_+).$$

This formula can then be continued analytically. Analogous formulae can be derived for the discontinuity associated with any Landau singularity.

We come now to a second set of properties related to poles associated with unstable particles. Here we will, in general, not attempt to indicate how these follow from the basic postulates. We know that poles corresponding to stable particles lie on the real axis below the physical region. Further, we assert that on the first or physical Riemann sheet (recall that Landau singularities are in general branch points) there are no complex poles; this can be proved in axiomatic field theories, for instance.

#### VI. Resonances and Unstable Particles:

Resonances, being short-lived unstable particles, also correspond to poles - but poles on the second Riemann sheet. These poles are near the physical region, lying just below the real axis. Of course, Hermitian analyticity (think of it as  $f^*(z^*) = f(z)$ ) requires that these resonances have partners, but the partners are not on the same Riemann sheet and can readily be seen to be far from the physical region. As an example, consider a threshold causing an  $n$ -sheeted structure to arise. In general, Hermitian analyticity holds only on the physical sheet - obviously the function can not be real below threshold on all sheets. So if we wish to continue the equation  $f^*(z^*) = f(z)$  we must do so along complex conjugate paths originating on the physical sheet. Hence the "partner" of a resonance (lying on the second Riemann sheet) will be a pole on the  $(n)^{\text{th}}$  Riemann sheet, which is far removed from the physical  $(+i\epsilon)$  limit (Fig. 8).

We may extend the diagrammatic technique to include unstable particles by considering resonance poles in many-particle channel amplitudes and using factorization. Thus, the connected part of a  $2 \rightarrow 2$  amplitude involving an unstable particle can be defined by the procedure illustrated in Fig. 9.

#### (A) Virtual (or anti-bound) states:

If a pole lies on the second Riemann sheet, just below a branch point, it is

called a virtual state; the physical manifestation of this pole - sometimes also called a "threshold enhancement," is in a sense "half" a resonance. An example of such a virtual state is the  $^1S$  anti-bound state of the nucleon-nucleon system, which lies just below threshold in NN scattering. We may note, parenthetically, that unless the discontinuity across a branch point is large there will not be a large local variation of the amplitude. But unitarity shows that

$$\text{disc } F \simeq |f|^2$$

so that unless  $f$  is large in the vicinity, as in the case of "threshold enhancement" - a branch point may not make its presence visible. (See Fig. 10)

#### Complex Normal Thresholds

Once we have noted the existence of complex resonance poles, we can see that resonances - perhaps together with stable particles - can combine to create complex normal thresholds on unphysical sheets. (See Fig. 11). To illustrate this, consider  $\pi N$  scattering. Among the singularities therein will be a branch cut on an unphysical sheet corresponding to  $\Delta\pi$  branch point. Drummond<sup>(5)</sup> has shown that the discontinuity formula for complex normal thresholds is analogous to that for normal thresholds.

#### Wooly Cusps:

By analogy to the normal threshold case, we expect it is possible that there are resonance poles in "virtual" positions with respect to complex normal thresholds. The effect of such poles in the physical region is called a "wooly cusp."<sup>(6)</sup>

#### REFERENCES

- 1) a. H. Stapp, Space-time Properties in the Physical Region, UCRL Report (BNL # 62-265).  
 b. H. Stapp, Macroscopic Causality and the Physical Region, UCRL Report  
 c. H. Stapp, Two Lectures in S-Matrix Theory, UCRL Report 18729.  
 d. Jagolnitzer, Analyticity in S-Matrix Theory, UCRL Report (BNL 69-248).
- 2) S. Coleman and R.E. Norton, Nuovo Cimento 38, 438 (1965).
- 3) D. Olive, Nuovo Cimento 26, 73 (1962).
- 4) R.E. Cutkosky, J. Math. Phys. 1, 429 (1960)
- 5) I.T. Drummond, Phys. Rev. 140, B482 (1965)
- 6) M. Nauenberg and A. Pais, Phys. Rev. 126, 260 (1962)

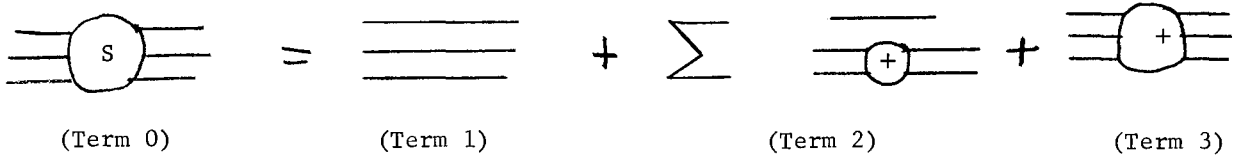


FIG. 1 The Schematic Cluster Decomposition of the  $3 \rightarrow 3$  Scattering Amplitude

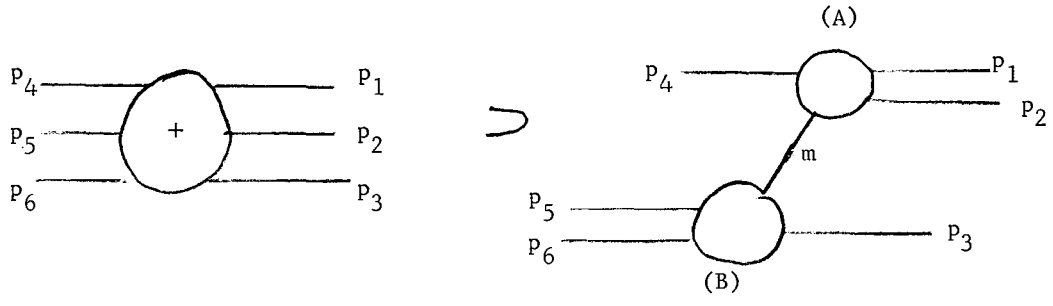


FIG. 2(a) A Physical Double Scattering Process in the Connected Part of the  $3 \rightarrow 3$  Scattering Amplitude

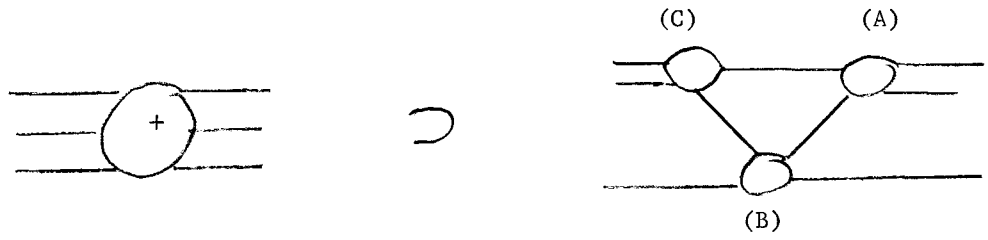


FIG. 2(b) A Physical Triple Scattering Process in the Connected Part of the  $3 \rightarrow 3$  Scattering Amplitude

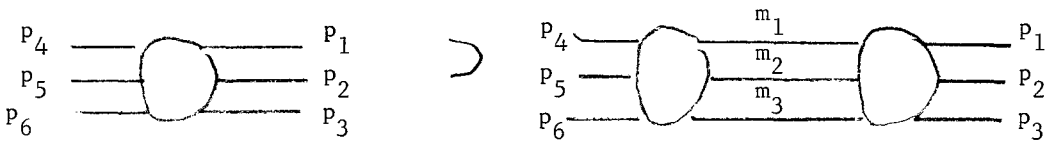


FIG. 2(c) The 3 Particle "Normal Threshold" in the Connected Part of the  $3 \rightarrow 3$  Scattering Amplitude

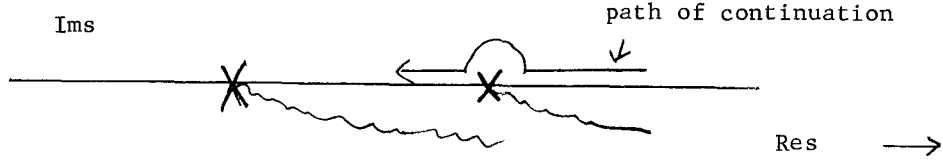


FIG. 3 The Path of Analytic Continuation around a Threshold

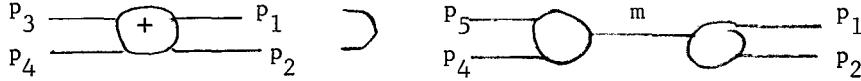


FIG. 4(a) A Single Particle Intermediate State Pole in the Unphysical Region of the 2 → 2 Connected Part

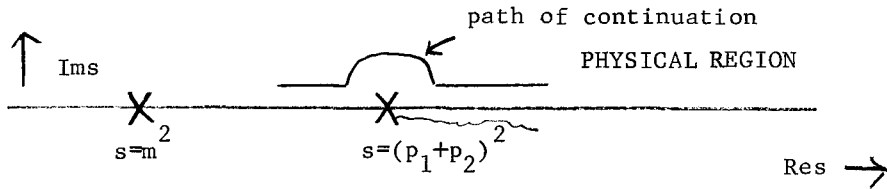


FIG. 4(b) The Path of Analytic Continuation out of the Physical Region

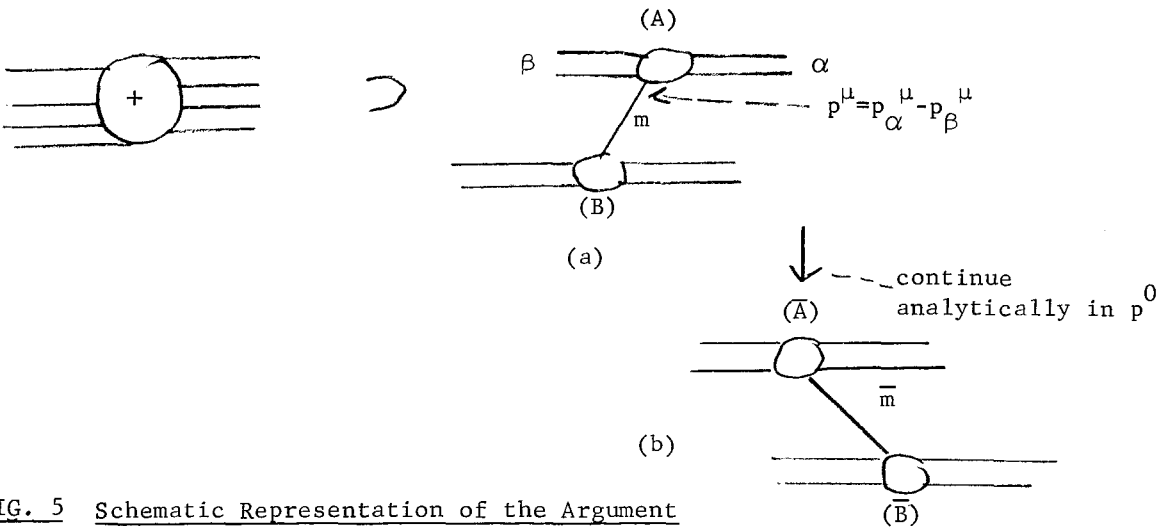


FIG. 5 Schematic Representation of the Argument for Crossing in S-Matrix Theory

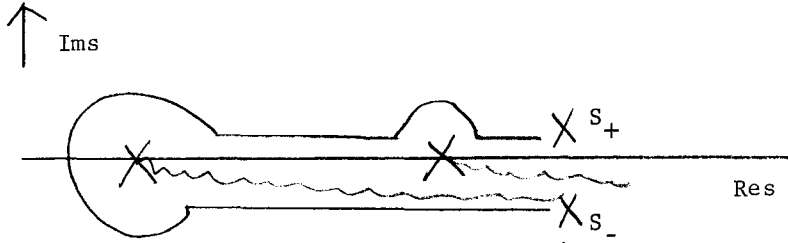


FIG. 6 The Path of Analytic Continuation Relating  $S^\dagger$  to  $S$  and Illustrating Hermitian Analyticity

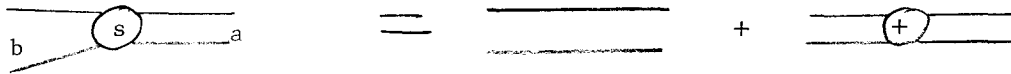


FIG. 7(a) The Schematic Cluster Decomposition of the  $2 \rightarrow 2$  Scattering Amplitude

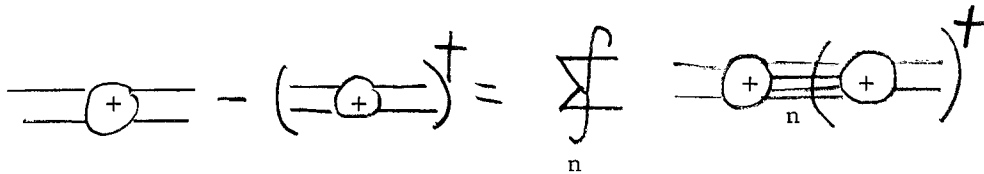


FIG. 7(b) The Schematic Unitarity Equation for the Connected Part of the  $2 \rightarrow 2$  Scattering Amplitude

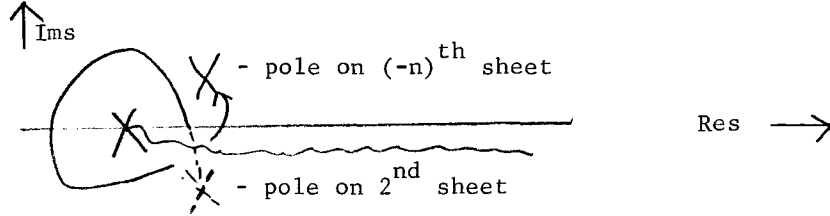


FIG. 8 Resonance "partners" Lying on Different Riemann Sheets

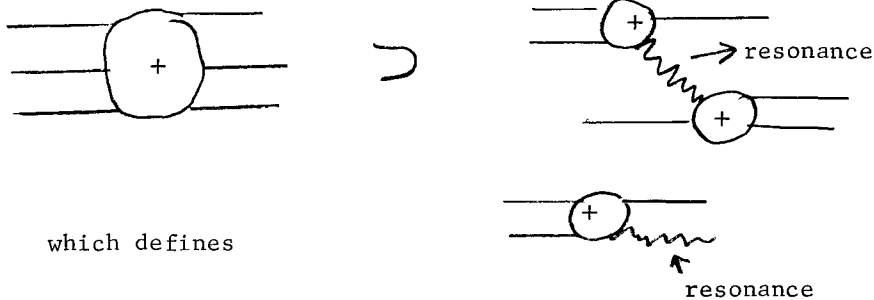


FIG. 9 The Method of Defining Amplitudes Involving Resonances as External Particles



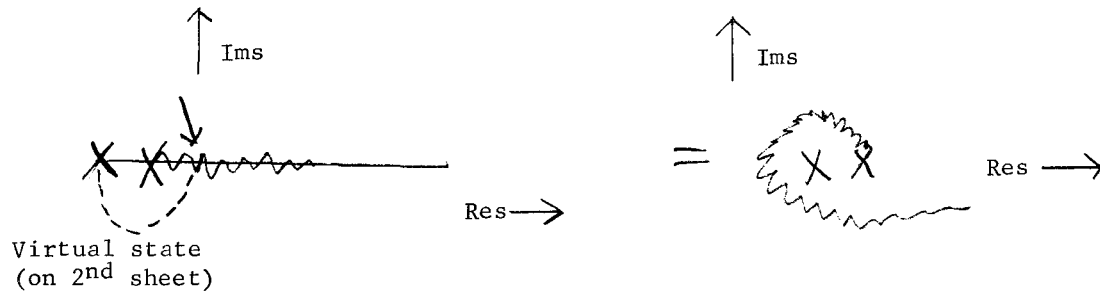


FIG. 10 A Virtual State or Threshold Enhancement

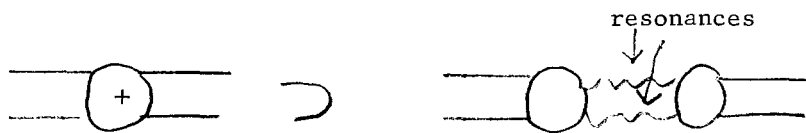


FIG. 11 Resonance Normal Thresholds in the Connected Part of the 2 → 2 Scattering Amplitude

To continue with the discussion of general properties of the analytic S-matrix, I will illustrate how unitarity - with very little else - may be applied directly to explain certain physical phenomena.

I. Partial Wave Discontinuity Formula:

Recall the general discontinuity formula

$$M_{ba}(s_+) - M_{ba}(s_-) = ic \int d\phi_n M_{bn}(s_-) M_{na}(s_+).$$

This equation can be simplified immensely, if we consider the special case where

- 1) a, b and n are two body channels (with arbitrary masses, however);
- and 2) only the effects of a single intermediate inelastic channel  $\hat{n}$  are included.

Taking into account only the channel  $\hat{n}$  implies that, instead of encircling all the branch points to obtain the full discontinuity, the path of continuation encircles just the threshold for  $\hat{n}$ . (Fig. 1). Then the discontinuity equation becomes (assuming spinless particles)

$$M_{ba}(s) - M_{ba}(s_n) = ic \int d^4p_1 d^4p_2 \delta^+(p_1^2 - m_1^2) \times \delta^+(p_2^2 - m_2^2) M_{bn}(s) M_{na}(s_n)$$

The two body phase space integral can be done completely using partial wave projections. Let  $A_{ba}^{\ell}(s)$  be the partial wave projection of the amplitude  $M_{ba}(s)$ . Defining the reduced amplitude  $B_{ba}^{\ell}$  by  $A_{ba}^{\ell} = (q_a q_b)^{\ell} B_{ba}^{\ell}$ , where  $q_i$  is the center of mass momentum in the  $i^{\text{th}}$  channel, we find

$$B_{ba}^{\ell}(s) - B_{ba}^{\ell}(s_n) = 2i\rho_n^{\ell}(s) B_{bn}^{\ell}(s_n) B_{na}^{\ell}(s) \quad (1)$$

Here  $\rho_n^{\ell} = \frac{2q_n^{2\ell+1}}{(s)^{\frac{1}{2}}}$ ; note that the definition of  $\rho$  determines the normalization of the partial waves. Further, we note that by  $B_{ba}^{\ell}(s_n)$  we mean that function which is the analytic continuation of  $B_{ba}^{\ell}(s)$  onto the next Riemann sheet (in a counter-clockwise sense) with respect to the branch point  $\hat{n}$ .

We notice immediately from this equation that:

- 1) in the partial wave amplitudes poles will be shared among communicating channels;
- 2) poles can not occur at exactly the same value of  $s$  on both sheets as, if they could, we would have a single pole on the left hand side equaling a double pole on the right-hand side;
- but 3) if the residue of the pole on the first sheet is small, so that the discontinuity - which is proportional to this residue - is also small, then there can exist a pole on the second sheet slightly displaced from the  $s$ -value of the

original pole. For the displacement to go to zero, the residues must also vanish; thus the branch point disappears as the poles coalesce. This is necessary for consistency with 2).

As an example, take the  $\pi N$  system. The first few physical thresholds are shown in Fig. 2. The  $\Delta(1236)$  resonance, although strongly coupled to the  $\pi N$  channel, is weakly coupled to  $2\pi N$ . From Eq. (1) we then expect that the  $2\pi N$  branch cut will have a small discontinuity across it. Hence continuing around the cut on a path as shown in Fig. 2, will reveal a pole,  $\tilde{\Delta}$ , on the next sheet, with its location only slightly displaced from that of the  $\Delta$ .

These weak branch points occur rather frequently and in many cases one is justified in ignoring them. The success of "zero-width" models - which completely ignore cut effects - substantiates this. Note that in general discussion of cuts in any variable, energy or angular momentum, is of little physical significance unless the discontinuities across the cuts are specified - say perhaps from a model.

Now consider the special case in which channel  $n =$  channel  $a$ . Then Eq. (1) can be solved explicitly for  $B_{ba}^{\ell}(s_a)$  to give

$$B_{ba}^{\ell}(s_a) = \frac{B_{ba}^{\ell}(s)}{1 + 2i\rho_a^{\ell}(s)B_{aa}^{\ell}(s)} .$$

This, as we shall see, leads us to expect poles for low  $\ell$  to congregate near thresholds; the threshold enhancement effect. Suppose that, for some reason, the amplitude  $B_{aa}(s)$  is large near threshold. If its partial wave projection  $B_{aa}^{\ell}(s)$  is also large, since  $\rho_a^{\ell}(s)$  can have any phase (in complex directions) near threshold, there will exist some direction away from threshold in which

$$2i\rho_a^{\ell}(s)B_{aa}^{\ell}(s)$$

is real and negatively increasing. When this quantity reaches the value -1, there will be a pole in  $B_{bn}^{\ell}(s_a)$ . From the form of  $\rho^{\ell}$  we see that the lowest partial waves - because for them  $\rho^{\ell}$  grows most rapidly away from threshold - are most favorable for these zeroes.

What effects could cause  $B_{aa}$  to be large near threshold? A typical cause is the existence of a nearby pole in the crossed variable. Consider  $NN$  scattering as an illustration (Fig. 3). Here the pion pole in the  $t$ -channel (and  $u$ -channel) (see Fig. 3(a) and (b)) renders the amplitude large in the physical region near threshold (Fig. 3(c)), assuming the pion coupling to the  $\bar{N}N$  system is not extremely small. Hence by unitarity, as expressed in Eq. (1), we anticipate poles near threshold in the  $s$ -channel. These are found in the deuteron and the  ${}^1_0S_0$  virtual state.

Further examples of this can readily be found; in general the smallness of the pion mass allows the systematic production of singularities near thresholds. For definiteness, I will give two more examples. Consider the elastic two body scattering,  $a \rightarrow a$ , where  $a$  is a two body channel with masses  $m_1$  and  $m_2$ .

Solving the kinematics shows that the  $s$  channel threshold values of the Mandelstam variables are

$$\begin{aligned} s_T &= (m_1 + m_2)^2 \\ t_T &= 0 \end{aligned}$$

and

$$u_T = (m_1 - m_2)^2.$$

Cross-channel poles near threshold will thus be poles near  $t=0$  or near  $u = (m_1 - m_2)^2$ . For  $N, \Delta$  scattering, as Fig. 4(a) illustrates, there is a pion pole in the  $u$  channel. Since the value  $u = m_\pi^2$  is near the threshold value  $u_T = (m_\Delta - m_N)^2$ , we expect threshold enhancement to occur. Yet another example is backward  $\pi N$  scattering, in which the diagram of Fig. 4(b) can contribute. Here the crossed channel pole occurs at  $u = m_N^2$ , whereas the threshold is at  $u_T = (M_N - m_\pi)^2$ . Again "threshold enhancement" predicts a pole near threshold in the  $s$ -channel. However, here our caution is relevant that the partial wave projection of the amplitude must be large. One finds that the projection on the  $S$ -wave ( $l=0$ ) in the  $s$ -channel is small so that an  $l=0$  resonance is not formed. In the  $I=3/2$   $P$ -wave, however, there is a large projection, and we find the  $\Delta$  in the vicinity of the threshold.

The study of threshold effects is particularly important in classical nuclear physics. Here all the bound states and resonances lie near threshold and can be discussed as threshold effects. The smallness of the pion mass, which allows the approximate isolation of these threshold states from other singularities of the  $S$ -matrix, is necessary for the validity of classical nuclear physics. This brings us directly to our next topic.

#### Small parameters in $S$ -matrix theory:

We have seen that, in some sense, the smallness of the pion mass allows us to separate classical nuclear physics from high energy physics. In general in hadron dynamics, we latch on to small parameters whenever possible.<sup>1</sup> The above discussion on isolating threshold effects is one example of how a small parameter may enable us to simplify our considerations. Other types of small parameters are the widths of resonances, which are typically on the order of 100 MeV. In the limit that these widths go to zero one can construct a theory in which unitarity is ignored (all branch point effects  $\rightarrow 0$ ) and the  $S$ -matrix contains only poles; this is the Veneziano model. In this model the Regge trajectory functions are all linear and the amplitude can be scaled arbitrarily. To understand the scale of the

amplitude and to permit resonances to have widths one must include the effects of unitarity. We anticipate that models based on small parameters and ignoring (or violating) certain of the fundamental postulates of the theory will apply only to a limited part of the S-matrix. Such models, however, may have the advantage of being mathematically "clean". The simplicity of the "zero width" model is manifest. Although the discussion of threshold effects may have seemed complicated, a model<sup>2</sup> considering only threshold effects has a simple potential theory limit as  $m_\pi/M_N \rightarrow 0$ .

### III. The Multiperipheral Model

Early in the discussions of production experiments, it was discovered that the peripheral model, which considers singularity diagrams of the form of Fig. 5 - in which the process  $NN \rightarrow NN+2\pi$  is considered - provided a good fit to the data.<sup>3</sup> The smallness of the pion mass separates its pole from the higher singularities (Fig. 6) and motivates the assertion that at least for small values of  $t < 0$  the amplitude for  $NN \rightarrow NN+2\pi$  may be expressible in the form

$$M_{NN \rightarrow NN+2\pi}^i \approx \frac{M_{N\pi \rightarrow N\pi}^i(p_x, q; k_{x_1}, k_{x_2}) M_{N\pi \rightarrow N\pi}^i(p_{y_1}, q; k_{y_1}, k_{y_2})}{t - m_\pi^2}$$

where the  $M^i$ 's are "off-mass shell" amplitudes and the momenta are defined in Fig. 5.

Amati, Bertocchi, Fubini and Stanghellini, and Tonin<sup>3</sup> considered an extension of the model to arbitrary production processes. The resulting multiperipheral model is of great importance, for it explains simultaneously production processes and the Regge behavior of  $2 \rightarrow 2$  elastic amplitudes. ABFST showed that maximizing the number of pion poles for a given multiplicity leads one to the unique set of singularity diagrams in Fig. 7.

From their original model they predicted:

- 1) that the total cross section would have Regge asymptotic behavior,  $s^{\alpha(t)}$ , with the power  $\alpha(t)$  determined by the eigenvalues of a Fredholm kernel;
- 2) that the transverse momenta of produced particles would approach a limiting distribution independent of energy and independent of the number of "links" in the chain; and
- 3) that the average multiplicity would increase as  $\ln s/s_0$ .

Each of these predictions is in agreement with - or at least not in conflict with - experiment.

The important features which we wish to abstract from this model are two. Any model which possesses them can loosely be called multiperipheral. First, the amplitude for the production of  $n+2k$  particles is obtained from that for  $n$  just by adding more links to the chain; thus, in some sense there is factorization. Second, the region of small  $t_i$  is dominant.

Before we proceed to incorporate these features in a specific model, I want to introduce a recently-developed set of variables useful to describe the kinematics of complicated production processes; these "Toller variables" will thus be the subject of our next lecture.

#### REFERENCES

1. G.F. Chew, Phys. Rev. Letters 22, 364 (1969).
2. (a) J.M. Charap and S.P. Fubini, Nuovo Cimento 14, 540 (1959); (b) Nuovo Cimento 15, 73 (1969); (c) A. Martin and Gy. Targonski, Nuovo Cimento 20, 1182 (1961).
3. (a) D. Amati, S. Fubini and A. Stanghellini, Nuovo Cimento 26, 896 (1962); (b) L. Bertocchi, S. Fubini and M. Tonin, Nuovo Cimento 25, 626 (1962).

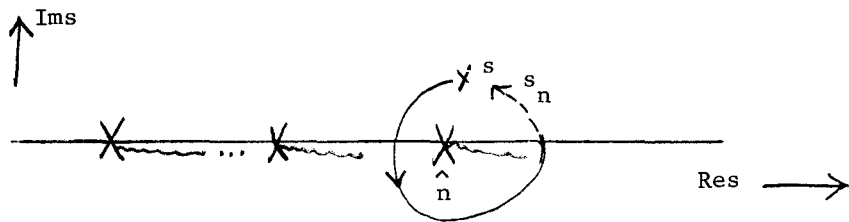


FIG. 1. Continuation around the  $\hat{n}$  Threshold

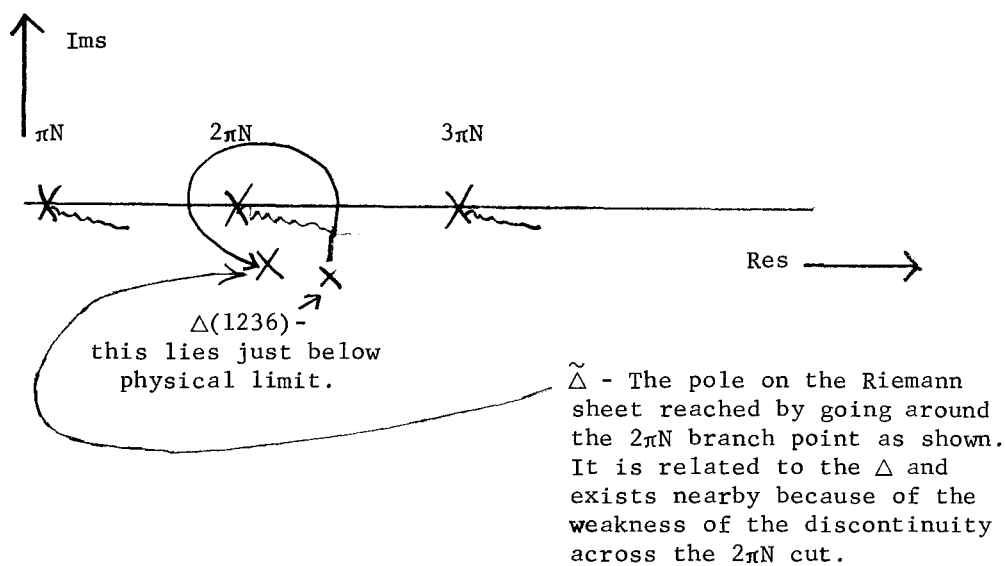
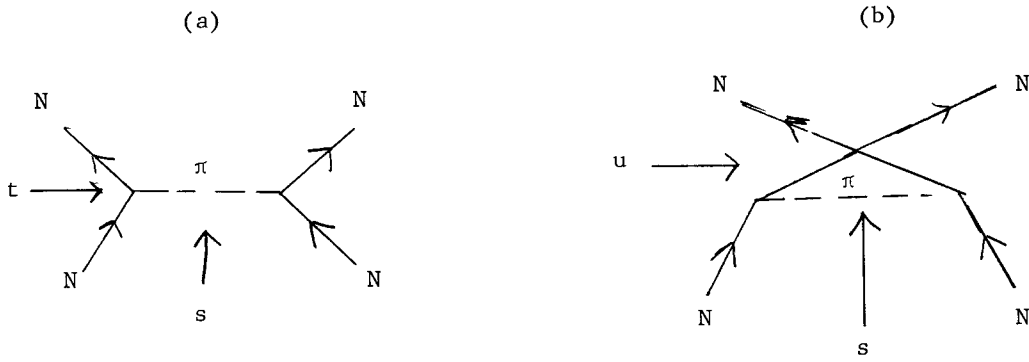
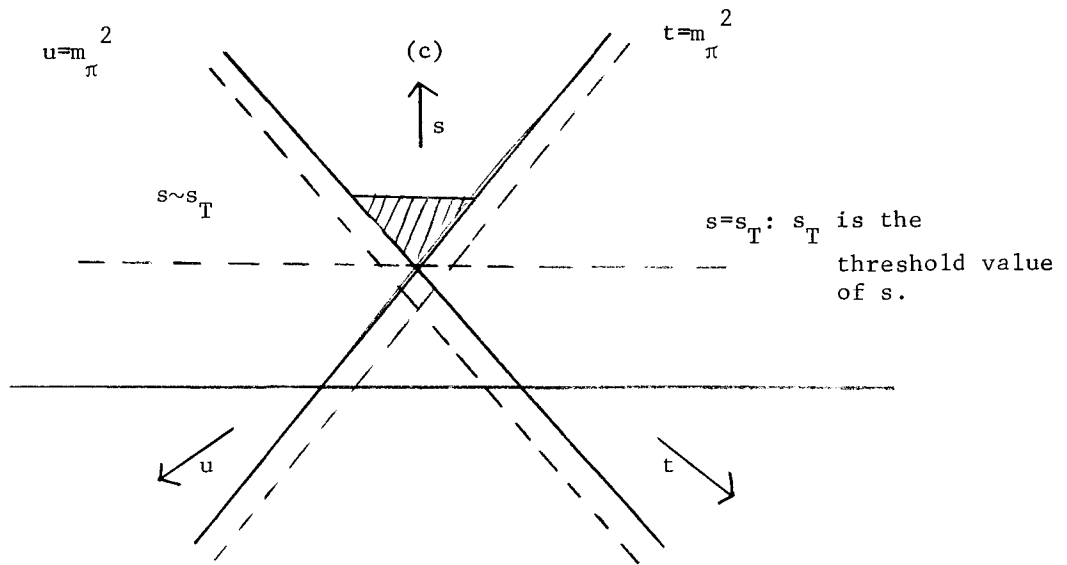


FIG. 2. The  $\pi N$  System Singularity Structure



**FIG 3.** Pion Poles in NN Scattering



**Fig. 3c.** The Mandelstam Plot for NN Scattering



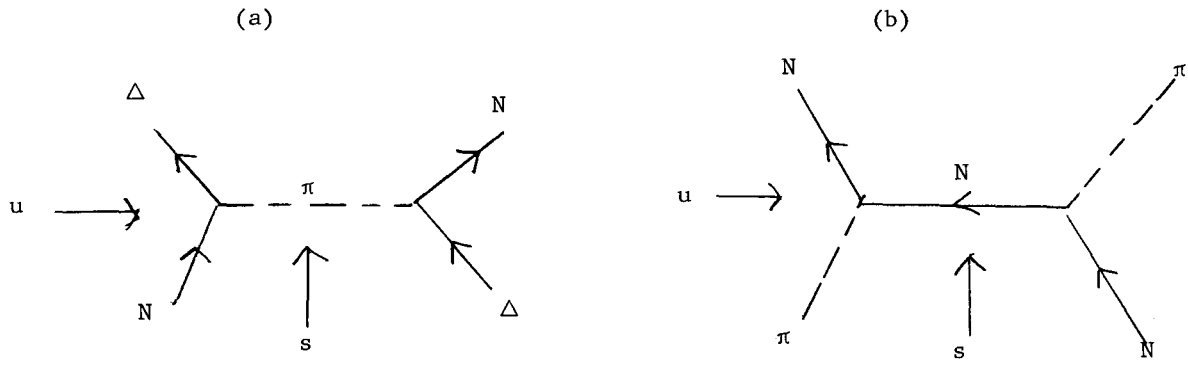


Fig. 4a. The Pion Pole in  $N\Delta$  Scattering  
 Fig. 4b. The Nucleon Pole in  $\pi N$  Scattering

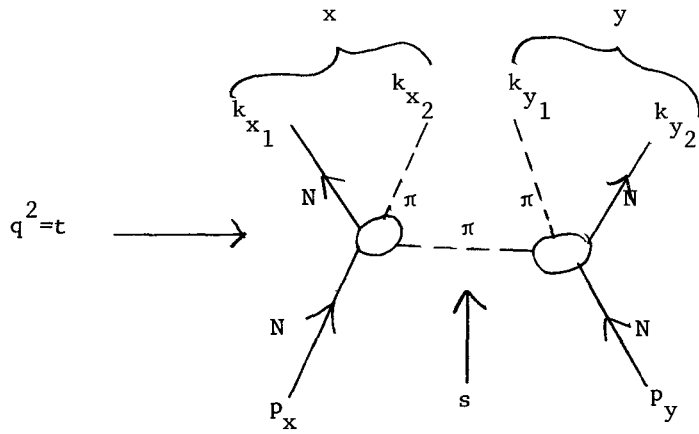


Fig. 5. The Peripheral Model for  $NN \rightarrow NN+2\pi$

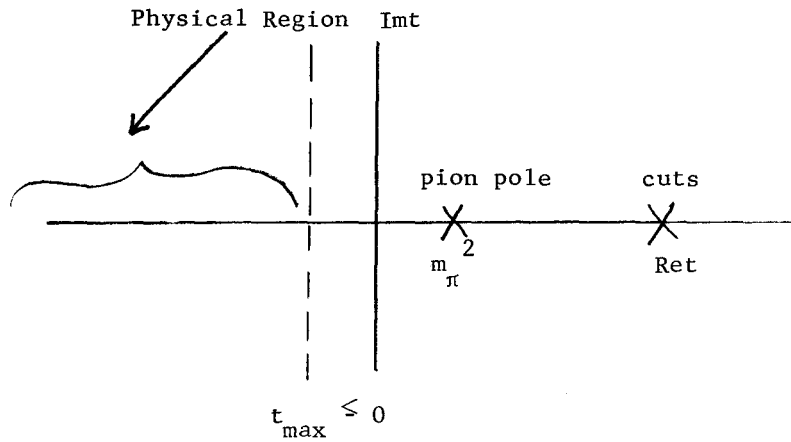


Fig. 6. The Nearness of the Pion Pole to the Physical Region

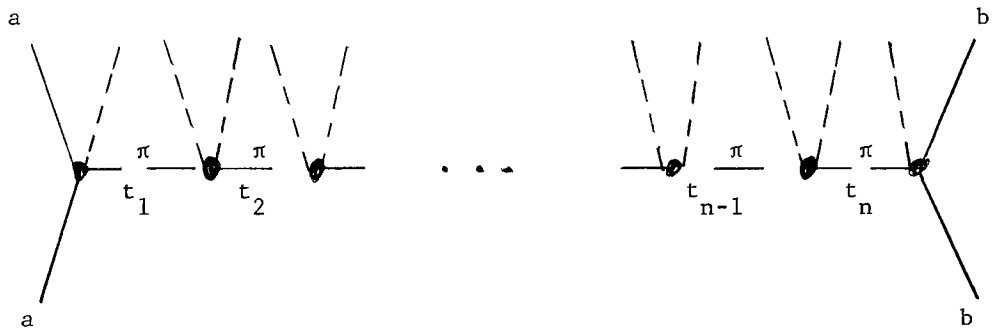


Fig. 7. The Multiperipheral Model for  $ab \rightarrow ab+2n\pi$

#### IV. Toller Variables

A fundamental advance in the kinematics of many particle-connected parts follows from group theoretic techniques developed by Toller.<sup>1</sup> Instead of describing each particle in the connected part shown in Fig. 1 by three components of momentum and a spin projection (or helicity), the Toller approach associates a 6 parameter Lorentz transformation with the particle. Let us agree on an arbitrary reference frame, say, the lab frame for definiteness; the Lorentz transformation,  $b_i$ , associated with the  $i^{\text{th}}$  particle relates this fixed frame to a particular rest frame of particle  $i$ : we will call this rest frame  $[i]$ .<sup>2</sup> The full amplitude for the process in Fig. 1 is thus written as a function of the  $n+4$  Lorentz transformations  $M = M(b_{\alpha}, b_{\beta}, b_0, \dots, b_{n+1})$ .

In general we need 3 parameters to relate the fixed reference frame to a rest frame of particle ( $i$ ); these will replace the three variables associated with momentum. Once the transformation to a rest frame has been accomplished, the 3 remaining parameters will be those of a rotation and will account for the spin degree of freedom. Two of them will simply specify the  $z$ -axis, along which the spin is projected, and the third will describe the dependence of the amplitude on rotations about this  $z$ -axis. Hence this third variable,  $\phi$ , is related to the spin projection quantum number  $m$  via

$$M(\dots\phi\dots) = \sum_m g_m(\dots) e^{im\phi} .$$

It may appear that this description is highly redundant. In place of four variables for each particle, 3 continuous ones for momenta and 1 discrete one for helicity, there are the 6 parameters of the Lorentz transformation. But we've seen already that two of these 6 parameters only define the direction with respect to which the spin is measured, so that there are really only 4 degrees of freedom for each particle. What is superfluous in the description is that whereas the spin projection  $m$  takes on only a finite number of discrete values, we are using a continuous variable to describe this degree of freedom. But the symmetry between the description of spin and that of momentum - or rather, the lack of asymmetry - in this formalism more than compensates for this redundancy.

Next consider a modification of this technique in more detail. In Fig. 2, which is meant as a schematic momentum flow diagram, we define momentum transfers  $Q_i$ , ( $Q_i^2 = t_i$ ). Our goal eventually will be to write the amplitude as a function of group theoretic variables related to these momentum transfers as well as of other group theoretic variables; as will become clear, this set of variables is chosen because of its convenience for  $n$  particle amplitude in general and for the multi-peripheral (Reggeised or not) model in particular.

From Fig. 2 we have immediately that

$$Q_i = -p_\alpha + \sum_{j=0}^{i-1} p_j$$

and

$$P_i = Q_{i+1} - Q_i .$$

If  $m_0 \geq m_\alpha$  or, in general, if  $(p_0 + p_1 + \dots + p_{i_0})^2 \geq p_\alpha^2$ , then every  $Q_i$ , or every  $Q_i$  for  $i > i_0$ , is spacelike. Since we wish to consider production of arbitrary numbers of particles, a typical  $Q_i$  will clearly be spacelike. Hence we shall consider a simple case in which all  $Q_i$  are such that

$$Q_i^2 = t_i < 0 .$$

To proceed we define various frames of reference and study transformation between them; in Fig. 3(a) the different frames are indicated by crosses on the lines representing momenta.

1) The frame [i] is a rest frame for the  $i^{\text{th}}$  particle, so that in it  $p_i = (m_i, 0)$ . Hence in this frame

$$Q_i = Q_{i+1} \equiv \lambda_i$$

so that

$$Q_i = (Q_i^0, \lambda_i) \text{ and } Q_{i+1} = (Q_{i+1}^0, \lambda_i) .$$

Further, we choose [i] to be the particular rest frame in which  $\lambda$  lies along the  $\hat{z}$  direction; specifying this rest frame corresponds to using the two "redundant" parameters to define the direction along which spin is measured. Therefore in [i] we may write

$$Q_i = (Q_i^0, 0, 0, \lambda_i), \quad Q_i^2 - \lambda_i^2 = t_i$$

and

$$Q_{i+1} = (Q_{i+1}^0, 0, 0, \lambda_i), \quad Q_{i+1}^2 - \lambda_i^2 = t_{i+1} .$$

2) The expression [i,r] is shorthand for "the right-hand frame for  $Q_i$ ", denoting a frame where

$$Q_i = (0, 0, 0, (-t_i)^{\frac{1}{2}}) ,$$

which is reached from the frame [i] by a pure z boost. The frame [i+1,l] is one in which

$$Q_{i+1} = (0, 0, 0, (-t_{i+1})^{\frac{1}{2}}) ,$$

also being reached from [i] by a pure z boost. Clearly these frames are related by a pure z boost to each other. These three boosts are labelled as illustrated schematically in Fig. 3(b). To solve for them explicitly we use the group property

$$B_i = B_i^1 B_i^2$$

or, in terms of parameters,

$$\cosh q_i = \cosh(q_i^1 + q_i^2).$$

Directly from the forms of  $Q_i$  and  $Q_{i+1}$  we have

$$\cosh q_i^1 = \frac{\lambda_i}{(-t_i)^{\frac{1}{2}}}$$

$$\cosh q_i^2 = \frac{\lambda_i}{(-t_{i+1})^{\frac{1}{2}}}$$

so that

$$\cosh q_i = \frac{\lambda_i^2}{(-t_i)^{\frac{1}{2}}(-t_{i+1})^{\frac{1}{2}}} - \frac{Q_i^0 Q_{i+1}^0}{(-t_i)^{\frac{1}{2}}(-t_{i+1})^{\frac{1}{2}}}$$

Using  $Q_{i+1}^0 = m + Q_i^0$ , we obtain immediately

$$\cosh q_i = \frac{m^2 - t_i - t_{i+1}}{2(-t_i)^{\frac{1}{2}}(-t_{i+1})^{\frac{1}{2}}}$$

The Boost  $B_i(q_i)$  is called a VERTEX BOOST as it relates  $[i,r]$  to  $[i+1,l]$  and thus transforms "across" the  $i^{\text{th}}$  vertex.

3) Now for each  $Q_i$  there exist two frames:  $[i,r]$  and  $[i,l]$ . In both of these  $Q_i$  is of the form

$$Q_i = (0,0,0,(-t_i)^{\frac{1}{2}}).$$

Hence these frames must be related by a transformation leaving this form invariant; but this is by definition true for any elements of the little group of  $Q_i$ . For this case (spacelike  $Q_i$ ), the little group is  $O(2,1)$ ; let  $g_i$  represent an element of this (3 parameter) group with parameters  $(\hat{\mu}_i, \xi_i, \nu_i)$ . Here  $\mu_i$  and  $\nu_i$  are rotations about the  $\hat{z}$ -axis and  $\xi_i$  is a boost in the  $x$  direction.

4) The ends of the chain require special attention. In the  $[0]$  frame  $-p_\alpha = Q_1$  and both are in the  $\hat{z}$  direction: that is,

$$p_\alpha = (p_\alpha^0, 0, 0, \lambda_0)$$

and

$$Q_1 = (Q_1^0, 0, 0, -\lambda_0).$$

We may thus define a  $z$ -boost which takes us to a particular (rest)frame  $[\alpha,r]$  in which

$$p_\alpha = (m, 0, 0, 0).$$

The transformation between  $[\alpha,r]$  and the rest frame originally attached to  $p_\alpha$  is an element of the little group for  $p_\alpha$ , which is  $O(3)$ . Call this  $p_\alpha[\alpha] \equiv [\alpha,l]$

transformation  $r_\alpha$ . Note in addition that exactly as in Sec. 2) above we can show that  $[1, \ell]$  is reached from  $[\alpha, r]$  by a boost along the  $\hat{z}$ -direction. There we find that the parameter of the boost,  $q_0$ , is given by

$$\sinh q_0 = \frac{m_0^2 - t_1 - m_\alpha^2}{2m_\alpha(-t_1)^{\frac{1}{2}}} .$$

We can readily use the Lorentz transformations between these various frames to construct any of the transformations,  $b_i$ , between the particle rest frames  $[i]$  and the arbitrary reference frame. If we know the transformation between the frame  $[i, r]$  and the arbitrary frame, the boost  $B_i^1$  (where  $B_i^1$  is as defined in 2) will take us from  $[i, r]$  to  $[i]$ . Then by transforming along the chain one finds

$$a_i = b_{\alpha} r_{\alpha} B_0(q_0) g_1 B_1(q_1) g_2 \cdots B_{i-1}(q_{i-1}) g_i$$

where the order of applying the transformation is from left to right, and  $B_i(q_i)$  is a vertex boost in the  $z$  direction with parameter  $q_i$ .

Thus an alternative set of variables to describe the amplitude is  $r_\alpha, r_\beta, g_1, \dots, g_{n+1}, q_0, q_1, \dots, q_{n+1}$ ; here we have incorporated Lorentz invariance by removing the dependence on the arbitrary reference frame in throwing away  $b_\alpha$ . Finally we note that since  $q_0, q_{n+1}$  are determined by  $t_1, \dots, t_{n+1}$ , we may take as our complete set of variables

$$M = M(r_\alpha, g_1, \dots, g_{n+1}, r_\beta, t_1, \dots, t_{n+1}) .$$

Conservation of momentum has been satisfied implicitly by shifting attention from the outgoing particles to the  $Q_i$ . That this is true can be shown by counting the number of degrees of freedom in our variables and comparing this with the known total number. To specify completely the kinematics of a process involving  $N$  particles with spin one needs  $3N-10$  variables to describe momenta and  $N$  "helicity" degrees of freedom. With  $N = n+4$ , we find a total of  $4n+6$ . Now there are  $n+1$   $g_i$ 's with three parameters each and  $n+1$   $t_i$ 's; in addition there are  $r_\alpha$  and  $r_\beta$ , which correspond to the two helicity degrees of freedom of the external particles. [Recall that for each of  $r_\alpha$  and  $r_\beta$  two of the parameters are used to define the direction of spin projection.] Thus again the total is  $4n+6$ .

One great advantage of this final set of variables is that they are not mutually constrained; the  $t_i$ 's can take on any value from 0 to  $-\infty$  and the  $g_i$ 's can be any elements of  $O(3,1)$ .

Examples: Consider two examples of the usefulness of these variables.

1) The Multi-Regge Hypothesis: Given  $M$  as a function of the  $g_i$ , we can expand its dependence on any of the  $g_i =$  say  $g_{i_0}$  - in terms of the irreducible representations of  $O(2,1)$ . Schematically,

$$M(\dots g_{i_0} \dots) = \int dj M \dots^j(\dots) D \dots^j(g_{i_0}) ,$$

where  $j$  is a continuous index and is the analogue of angular momentum in  $O(3)$ . If the function  $M^j$  contains poles in the complex  $j$  plane near which

$$M^j \simeq \frac{R}{j - \alpha_{i_0}(t_1)}$$

then it can be shown that the right-most pole in  $j$  will control the asymptotic behavior of the amplitude as  $\xi_{i_0} \rightarrow \infty$ . But from the asymptotic form of  $D^j(q_i)$  we obtain

$$M_{\xi_{i_0} \rightarrow \infty} \simeq G_1(r_\alpha, g_1, \dots, g_{i-1}, \mu_i, t_1, \dots, t_i) (\cosh \xi_{i_0})^{\alpha_{i_0}(t_{i_0})} \\ \times G_2(v_i, g_{i+1}, \dots, g_{n+1}, t_i, \dots, t_{n+1}) .$$

Since the two particle subenergy,  $s_{i_0}$ , defined by  $s_{i_0} = (p_{i_0-1} + p_{i_0})^2$ , is related to  $\cosh \xi_{i_0}$  by

$$s_{i_0} = t_{i_0-1} + t_{i_0+1} + 2(-t_{i_0+1})^{\frac{1}{2}}(-t_{i_0-1})^{\frac{1}{2}} \cosh \xi_{i_0} ,$$

this expression gives Regge asymptotic behavior in the sub-energy  $s_{i_0}$ . This is indicated graphically in Fig. 4(a). If we postulate that this behavior holds as all of the two particle sub-energies,  $s_i$ , go to infinity (all  $t_i$  and all  $\mu_i, v_i$  fixed) (and thus each  $\xi_i \rightarrow \infty$ ), we have the multi-Regge hypothesis

$$M_{\xi_1, \dots, \xi_n \rightarrow \infty} \simeq \beta_1(t_1, v_\alpha, \mu_1) s_1^{\alpha_1(t_1)} f_{12}(t_1, t_2, v_1, \mu_2) s_2^{\alpha_2(t_2)} \dots s_{n+1}^{\alpha_{n+1}(t_{n+1})} \beta_{n+1}(t_{n+1}, v_{n+1}, \mu_\beta)$$

as illustrated in Fig. 4(b).

2) The General Reggeon Connected Part: Toller has further generalized this work to include any "tree graph" (no closed loops) momentum flow diagram. (Fig. 5a) This technique enables one to give meaning to a general "Reggeon connected part" (see Fig. 5(b)) by factoring off the "Reggeon connected part" from a higher amplitude in a specified asymptotic limit. This approach is conceptually similar to that introduced to define connected parts for unstable particles.

#### The Multi-Peripheral Model (MPM):

The two central hypotheses of any multi-peripheral model were mentioned last time:

- 1) that there exists some "reason" for the amplitude to "want to stay in a region where the  $t_i$ 's are small."
- and 2) once an ordering of the produced particles is chosen such that hypothesis

(1) is satisfied, the amplitude "factorizes" in the sense that

$$M_{n+l} \cong K M_n \quad ,$$

where K is a factor depending only on a finite number of variables for particles "adjacent" to those labelled  $n+l, n+l-1, \dots, n$  (see Fig. 6).

This factorization property can be realized either with ordinary particle ( $\pi$ ) poles or with Regge poles. To resolve the question of which model is more realistic we turn to experiment. It turns out that the average value of the two particle sub-energies,  $s_i$ , does not increase with  $s$ ; thus we expect that the multi-Regge hypothesis will not be applicable directly.

To see that  $s_i$  does not increase with energy we note that kinematical considerations imply<sup>3</sup>

$$\left(\frac{s}{s_0}\right) \sim \left(\frac{s_1}{s_0}\right) \left(\frac{s_2}{s_0}\right) \dots \left(\frac{s_u}{s_0}\right) F(t_i, \dots)$$

where

$$s = (p_\alpha + p_\beta)^2$$

is the overall invariant energy and  $s_0$  is a suitable scale factor. If the multiplicity is  $n$ , then the average subenergy  $\bar{s}_i$  roughly satisfies

$$\left(\frac{\bar{s}_i}{s_0}\right)^n \approx \left(\frac{s}{s_0}\right) \quad \text{and thus} \quad \left(\frac{\bar{s}_i}{s_0}\right) = \left(\frac{s}{s_0}\right)^{1/n} \quad .$$

But experimentally (and from some theoretical arguments) we find that the average multiplicity  $\bar{n}$  grows like

$$\bar{n} \approx \epsilon \ell n \left(\frac{s}{s_0}\right) \quad .$$

Hence

$$\left(\frac{\bar{s}_i}{s_0}\right) \approx \left(\frac{s}{s_0}\right)^{\frac{1}{\epsilon \ell n s / s_0}} \approx e^{\frac{1}{\epsilon}}$$

which does not grow with  $s$ .

Of course, the concept of duality suggests that extrapolation of the high energy limit of the multi-Regge model to low energies might still give a good approximation to the average behavior. Since the mean subenergy  $s_i^{\frac{1}{2}}$  is less than 1 GeV, however, one would be asking more from duality than may be reasonable. So in the model that we'll discuss next time, we will assume that multi-pion exchange, rather than multi-Regge exchange, is the relevant multi-peripheral mechanism.

#### REFERENCES

1. M. Toller, Nuovo Cimento 52A, 341 (1969).
2. G.F. Chew and C. DeTar, Phys. Rev. 180, 1577 (1969).
3. N. Bali, G.F. Chew and A. Pignotti, Phys. Rev. Letters 19, 614 (1967).



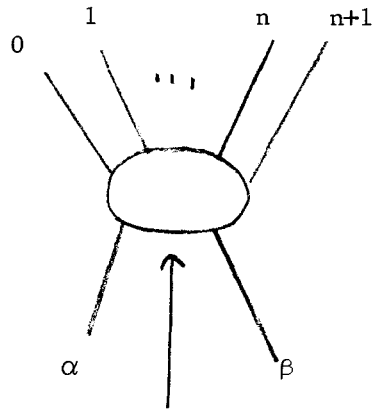


FIG. 1. The  $2 \rightarrow n+2$  connected part.

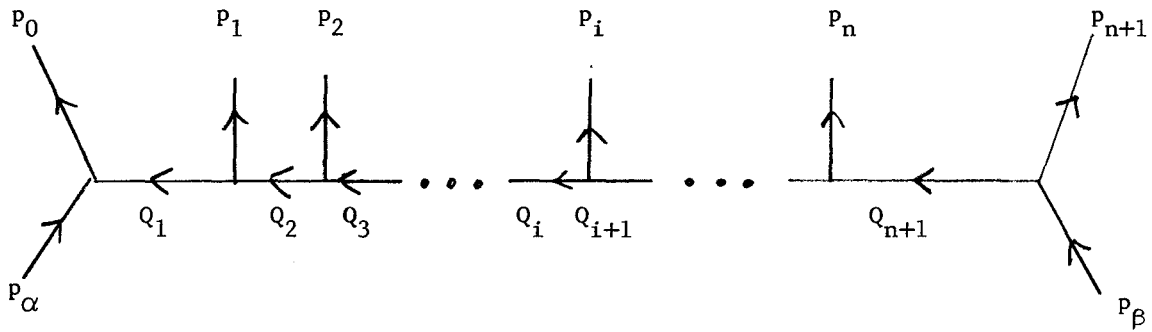


FIG. 2. Schematic Momentum Flow Diagram

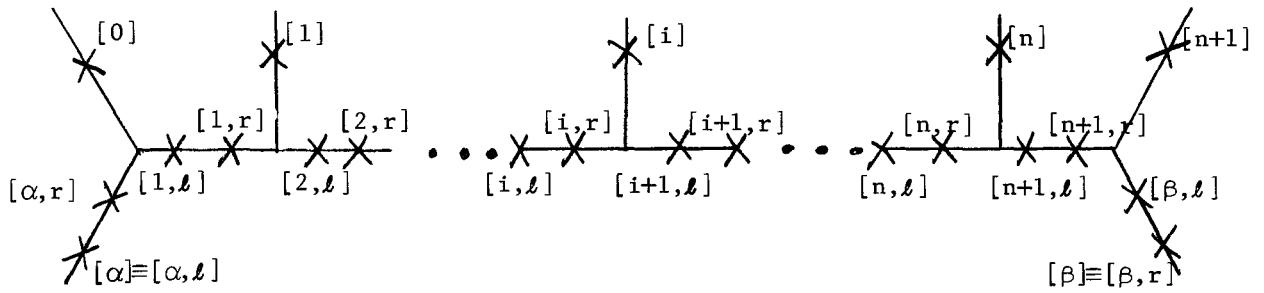


FIG 3a. Definitions of Lorentz Frames

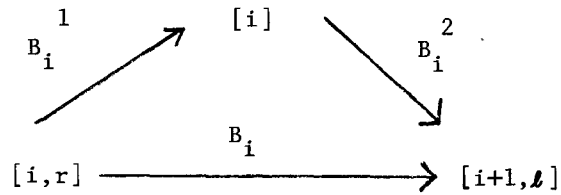


FIG. 3b. Relations among the Vertex Boosts

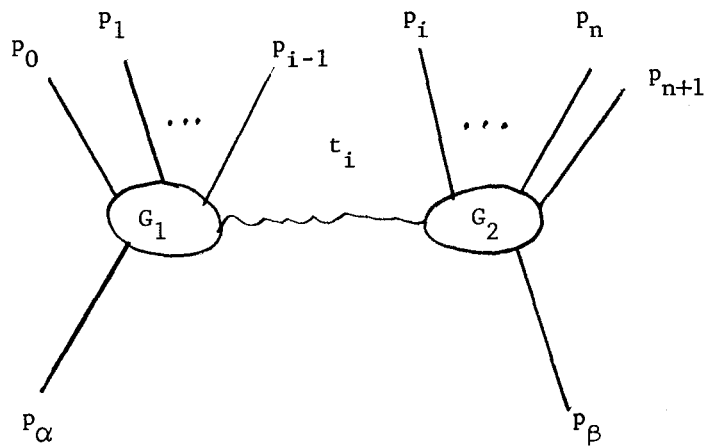


FIG. 4a. A Single Reggeon Exchange Limit

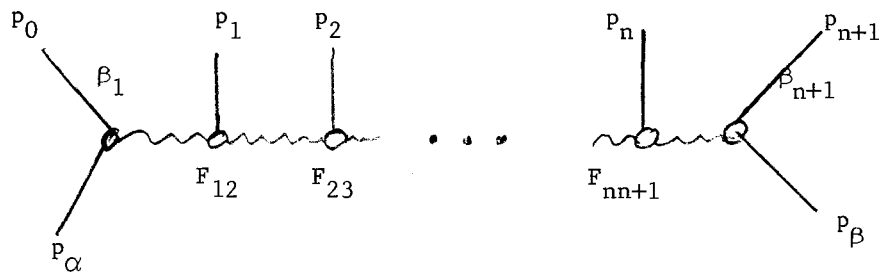


FIG. 4b The Multi-Reggeon Exchange Limit

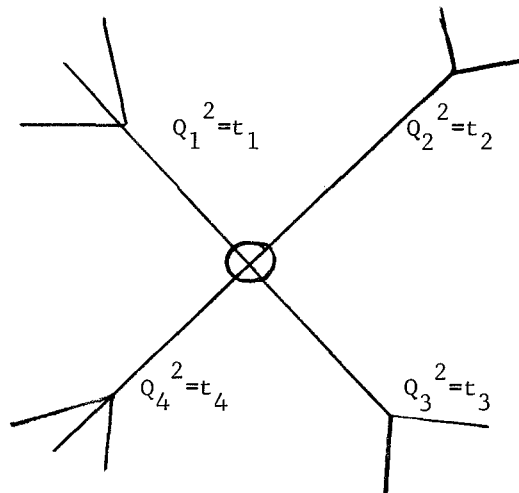


FIG. 5a. A 4 "limb" tree graph

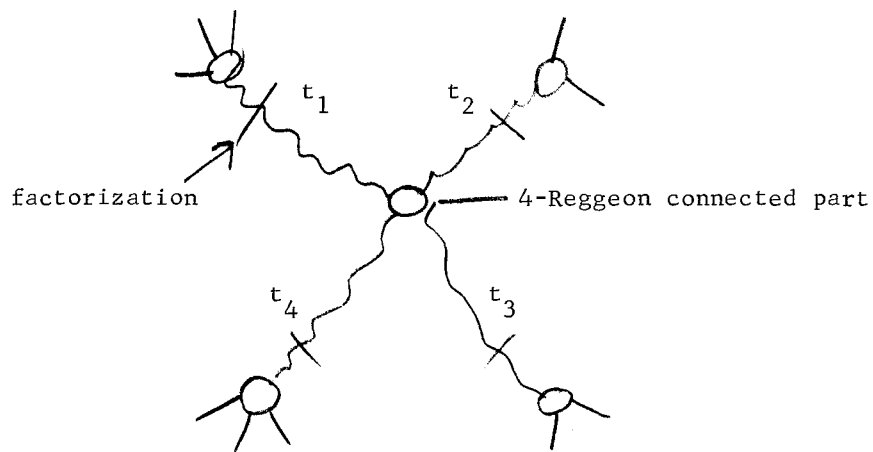


FIG. 5b. The 4 Reggeon Connected Part

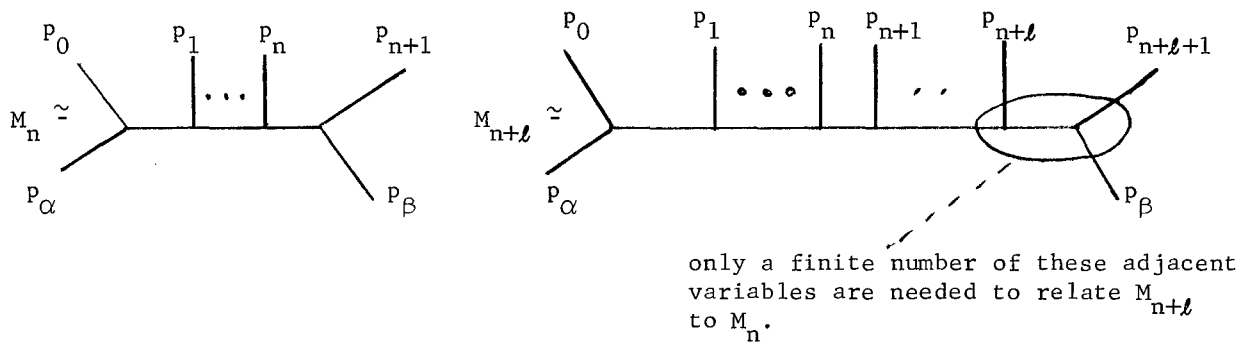


FIG. 6. Factorization along the Multi-Peripheral Chain

Before I plunge into the details of the multiperipheral model of hadron dynamics, which will be the central part of the next several lectures, I should outline our intentions and approaches. We will aim to construct a model for the imaginary part of the elastic amplitude for the process  $\alpha\beta \rightarrow \alpha\beta$ . We will proceed by using the multiperipheral model to describe the inelastic processes  $\alpha\beta \rightarrow \alpha'\beta'+n$ , where  $n$  indicates an  $n$ -particle state and then by applying unitarity in the form

$$\text{Im}M_{\alpha\beta \rightarrow \alpha\beta}^{el} = \sum d\Phi_n M_{\alpha\beta \rightarrow \alpha'\beta'+n}^* M_{\alpha\beta \rightarrow \alpha'\beta'+n}$$

More particularly, on the basis of experimental evidence, we will restrict the intermediate states  $\alpha'\beta'+n$  to be  $\alpha'\beta'+(n)\pi$ ; we will then maximize the number of "pion poles" in the multiperipheral chain to obtain the old model of ABFST. Finally we will derive an explicit integral equation for a quantity -  $B(a,t)$  - related to the total imaginary part,  $\text{Im}M_{\alpha\beta}^{el}$ .

Limiting our considerations to forward scattering, so that the invariant momentum transfer,  $\tau$ , equals zero, we are evidently dealing with the total cross-section (from the optical theorem). In addition, since the scattering is elastic, at  $\tau=0$  the four-vector momentum transfer also vanishes - that is,

$$t \equiv k^2,$$

and

$$k^\mu = (k_0, \vec{k}) ,$$

then for elastic scattering  $\tau = 0$  implies  $k^\mu = (0,0,0,0)$ . Thus the little group of  $k$  is the full Lorentz group,  $O(3,1)$ , and we can expand the amplitude in terms of the representations of the Lorentz group. Since the integral equation for  $B(a,t)$  also has this symmetry at  $\tau=0$ , we will diagonalize it with respect to  $O(3,1)$ . This will lead to Fredholm<sub>1</sub> integral equations for the expansion coefficients  $B^\lambda(t)$ ; here  $\lambda$  is the continuous parameter (partially) labelling the irreducible representatives of  $O(3,1)$ . Singularities occurring for particular values of this parameter - Toller poles and cuts - will correspond to families of Regge poles and cuts. From our specific pion-dominated multiperipheral model, we hope to generate both the Pomernanchuk and rho trajectories; in the forward scattering limit we will learn only about their intercepts at  $t=0$ , which should be given by poles at  $\lambda \simeq 1$  and  $\lambda \simeq \frac{1}{2}$ , respectively.

For the first part of the exercise, in which we derive and diagonalize the equation for  $B^\lambda(t)$ , we will ignore isospin for simplicity. When we turn in detail to the specific model which is to generate the P and  $\rho$  trajectories, we will, of course, include this slight complication.

2

To motivate the "multiperipheral model with pion-pole dominance" we appeal to

two experimental observations:

1) the most frequently produced secondary particles in highly inelastic processes are pions;

2) if the produced particles are ordered according to longitudinal momenta the mean invariant momentum transfers,  $t_i$ , are small: thus the amplitudes are large only in the region where pion poles are nearby.

Now G-parity forbids the coupling of an odd number of pions, so the multiperipheral chain with only pions as secondaries, having the maximum number of pion links, is as shown in Fig. 1. Assuming factorization at the pion poles we may write

$$M_{\alpha\beta \rightarrow \alpha'\beta'+n\pi} = f_{\alpha}^{(m^2, t_1, t_2, g_1)} d(g_2, t_2) \\ \times \dots f_{i}^{(t_i, t_{i+1}, t_{i+2}, g_{i+1})} \dots d(g_n, t_n) \\ f_{\beta}^{(t_n, t_{n+1}, m_{\beta}^2, g_{n+1})}$$

where

$$d(g, t) = \frac{h(t)}{t - m_{\pi}^2} \quad \text{with } h(m_{\pi}^2) = 1 .$$

To proceed we must be able to express the unitarity integral in terms of the Toller variables. Consider the  $n$  pion contribution to unitarity, which is given by

$$\text{Im} M_{\alpha\beta \rightarrow \alpha\beta}^{(n)}(b_{\alpha}, b_{\beta}) = \int d\Phi^{(n)} M_{\alpha\beta \rightarrow \alpha'\beta'+n}^{*(n)} M_{\alpha\beta \rightarrow \alpha'\beta'+n}^{(n)}$$

and corresponds to the diagram of Fig. 2. The normal differential phase space for the intermediate state  $\alpha'\beta'+n$  is

$$d\Phi^{(n)} = \sum_{\text{spins}} d^4 p_{\alpha'} d^4 p_1 \dots d^4 p_n d^4 p_{\beta'} \delta^+(p_{\alpha}^2 - m_{\alpha'}^2) \dots \\ \delta^+(p_{\beta'}^2 - m_{\beta'}^2) \delta^{(4)} \left( \sum_{i=1}^n p_i + p_{\alpha'} + p_{\beta'} - p_{\alpha} - p_{\beta} \right) .$$

Of course, for pions the spin sum can be ignored. In terms of Toller variables this becomes <sup>3</sup>

$$d\Phi^{(n)} = \frac{1}{(2\pi)^{3(n+2)}} \frac{1}{2^{2n+3}} \sinh q_1 \dots \sinh q_{n+1} \cosh q_{\beta}$$

$$\begin{aligned}
& \times dt_1 \dots dt_{n+1} d^3 g_2 \dots d^3 g_{n+1} d^3 r_\beta \\
& \times d\mu_1 \delta \left( \sinh q_0 - \frac{(-t_1)^{\frac{1}{2}}}{2m_\alpha} \right)^3
\end{aligned}$$

where

$$d^3 g = d\mu d(\cosh \xi) d\nu$$

and

$$d^3 r = d\psi d\cos\theta d\phi$$

In the group theoretic variables the sum over helicities for the  $i^{\text{th}}$  particle has been absorbed into the  $d\mu_{i+1}$  part of the  $d^3 g_{i+1}$ . Further,  $q_0$  is to be regarded as a function of  $t_1, \dots, t_{n+1}$ ,  $g_2, \dots, g_{n+1}$ , and  $r_b$ , and for fixed  $b_a$  and  $b_b$ , is determined uniquely by the constraint.

$$b_\alpha^{-1} b_\beta = r_a q_0 g_1 q_1 g_2 \dots g_{n+1} q_{n+1} r_b \quad 3$$

This same constraint also determines uniquely  $r_a$  and  $g_1$  in terms of the integration variables for fixed  $b_\alpha^{-1} b_\beta$ . Thus a quick check shows that, if we include the sums over spins and the corresponding integrals over  $\mu_i$ , both forms have  $4n+4$  independent integration variables.

Defining

$$D(t) = |d(t)|^2, \quad \text{where} \quad d(t) = \frac{h(t)}{t - m_\alpha^2},$$

and

$$F(t_i, t_{i+1}, t_{i+2}, g_{i+1}) = |f|^2,$$

we find that

$$\begin{aligned}
& \text{ImM}_{\alpha\beta}^{(n)} \rightarrow \alpha\beta = \frac{1}{(2\pi)^{3(n+2)}} \frac{1}{2^{2n+3}} \frac{1}{m_\alpha m_\beta} \\
& \times \int \sinh q_1 \dots \sinh q_{n+1} \cosh q_\beta dt_1 \dots dt_{n+1} \\
& \times d\mu_1 d^3 g_2 \dots d^3 g_{n+1} d^3 r_\beta \delta \left( \sinh q_0 - \frac{(-t_1)^{\frac{1}{2}}}{2m_\alpha} \right) \\
& \times F_\alpha(m_\alpha^2, t_1, t_2, g_1) D(g_2, t_2) \dots F(t_i, t_{i+1}, t_{i+2}, g_{i+1}) \dots \\
& D(g_n, t_n) F_\beta(m_\beta^2, t_n, t_{n+1}, g_{n+1}) \quad .
\end{aligned}$$

To generate a tractable integral equation that, in essence, sums the series over  $n$ , we resort to the trick of defining a sort of incomplete imaginary part by undoing the integration over  $d^3 r_\beta$  to give

$$B^{(n)}(b_\alpha^{-1} a_{n+2}, t_{n+2}) =$$

$$\text{const } (x) \int \delta(\sinh q_0 - \frac{(-t_1)^{\frac{1}{2}}}{2m_\alpha}) \sinh q_1 \dots \sinh q_{n+1}$$

$$dt_1 \dots dt_{n+1} d^3 g_2 \dots d^3 g_{n+1} F_\alpha(m_\alpha^2, t_1, t_2, g_1) D(g_2, t_2)$$

$$\dots F(t_n, t_{n+1}, t_{n+2}, g_{n+1}).$$

$B^{(n)}$  can be represented diagrammatically as in Fig. (3a). There  $a_{n+2}$  is the Lorentz transformation connecting frame  $[n+2, \mu]$  to the arbitrary standard frame.

Some insight into  $B^{(n)}$  may be gained if I illustrate its relation to  $I^{(n)}$  in the simple case where  $\beta$  is a pion state. In this instance we find that we need only continue  $t_{n+2}$  to  $m_\pi^2$  and integrate over  $d^3 r_\beta$  to get  $I^{(n)}$  from  $B^{(n)}$ : that is,

$$I^{(n)}(b_\alpha^{-1} b_\beta) = \int B^{(n)}(b_\alpha^{-1} r_\beta^{-1} b_\beta, m_\beta^2) d^3 r_\beta.$$

As the diagram of Fig 3(b) might suggest, we can establish a recursion relation among the  $B^{(n)}$ . It is

$$B^{(n)}(a, t) = \frac{1}{(2\pi)^6} \frac{1}{2^4} \int d^3 g'' d^3 g' dt'' dt' \sinh q''$$

$$\sinh q' D(g'', t'') F(t'', t', t, g') B^{(n-2)}(a'', t'').$$

Summing over  $n$  generates the Neumann series for the integral equation

$$B(a, t) = B^0(a, t) + \int d^3 g'' d^3 g' dt'' dt' k(g', g'', t'', t, t')$$

$$B(a'', t'').$$

where

$$k = \frac{1}{(2\pi)^6} \frac{1}{2^4} \sinh q' \sinh q'' D(g'', t'') F(g', t'', t', t).$$



and where

$$a = a''g''q''g'q' \quad .$$

Notice that the integration variable  $t'$  appears only in  $K$  - in fact only in  $F$  - so that we may redefine  $K$  to include the integration over  $t'$  if we wish. As we anticipated, the equation is invariant under simultaneous Lorentz transformation of  $a$  and  $a''$ . This corresponds to the extended symmetry of the full amplitude at  $\tau=0$ , where the little group of  $k^\mu$  becomes  $O(3,1)$ . We may thus usefully expand the equation in terms of representations of the full Lorentz group by defining

$$B(a,t) = \int B^{\lambda M} \dots(t) D^{\lambda M} \dots(a) d\lambda \quad .$$

It should be mentioned here that  $\lambda$  is a continuous and  $M$  is a discrete label for the representations of  $O(3,1)$ , - or, almost equivalently of  $SL(2,c)$ . We will not be concerned with the other indices, nor will we discuss the important technical question of the completeness of the  $D^{\lambda M}$ .<sup>4</sup> These questions can be resolved, and the result is an equation of the form

$$B^{\lambda M}(t) = B_0^{\lambda M}(t) + \int_{-\infty}^0 dt'' B^{\lambda M}(t'') K^{\lambda M}(t'', t)$$

where we have redefined  $K$  to include the integral over  $t'$ .

Provided that the kernel  $K$  falls off rapidly as  $t'' \rightarrow -\infty$ ,<sup>2</sup> this is a normal Fredholm equation and can be treated by the standard methods. However, putting  $h(t) = 1$  to give  $d(t) = \frac{1}{t - m_\pi}$  does not lead to a sufficiently rapid vanishing of  $K$ .

Thus we will require - and this is experimentally moderately well justified - that  $h(t)$  provide a cut-off of some sort for  $K$ . Recall the crucial fact that  $t$  in this equation is not the overall momentum transfer in the process  $\alpha\beta \rightarrow \alpha\beta$ ; this variable,  $\tau$ , was set equal to zero long ago. We've seen that  $t$  is the variable which, for  $\beta=\pi$ , if continued to  $m_\pi^2$ , relates  $B$  to the total absorptive part  $\text{Im}M$ .

From the theory of Fredholm equations we know that:

$$(1) \quad B^{\lambda M}(t) = \frac{N^{\lambda M}(t)}{D^{\lambda M}}$$

where  $D^{\lambda M}$  is the Fredholm determinant;

(2) if the inhomogeneous term,  $B_0^{\lambda M}$  and the kernel,  $K^{\lambda M}$  are analytic in  $\lambda$  then the only singularities of  $B^{\lambda M}$  not in  $K$  or  $B_0$  are given by zeroes of  $D^{\lambda M}$ .

Note that these poles in  $\lambda$  correspond to solutions of the homogeneous equation, and their location depends only on the kernel  $K^{\lambda, I}(t'', t)$  and not on the inhomogeneous term. These are the Toller poles and give rise to families of ordinary Regge poles.

The singularity which lies farthest right in the complex  $\lambda$  plane, at, say,  $\lambda_R$ , is the one which controls the asymptotic behavior of the complete imaginary part,

$$\text{Im} M_{\alpha\beta} \rightarrow \alpha\beta (s, \tau=0) \propto \lim_{s \rightarrow \infty} s^{\lambda_R}.$$

If we did not restrict our consideration to forward scattering, we would find that the little group of  $k$ , where  $k^2 = \tau$ , is  $O(2,1)$ ; expanding the amplitude in terms of this little group leads to ordinary Regge poles.

To study this Fredholm equation in more detail we need to establish the specific form of the kernel. At this stage we will incorporate isospin and make several additional assumptions necessary to relate  $K$  to known or measurable quantities.

First, we will assume the pion has  $M=0$ , so that the  $M$  label can in effect be dropped from all our equations. Our motivation for this assumption is that, since  $M$  represents the lowest value of the angular momentum contained in the decomposition of a representation of  $O(3,1)$  into eigen-representations of angular momentum, an  $M=1$  classification is incompatible with a zero mass pion; this follows because for a zero mass pion at the point  $t=0$  the Regge trajectory of the pion must pass through  $j=0$ . As the smallness of the pion mass has been crucial to many of our previous considerations, we feel that consistency with the zero mass limit is desirable. Incidentally, the success of the assumption that extrapolations to  $m_\pi=0$  are "smooth" in many current algebra calculations also suggest this classification.

Second, we must assume something about the quantities

$$F(t_i, t_{i+1}, t_{i+2}, g_{i+1}) = |f(t_i, t_{i+1}, t_{i+2}, g_{i+1})|^2.$$

As inspection of Fig. 4 shows

$$F(m_\pi^2, t_{i+1}, m_\pi^2, g_{i+1}) = \frac{d\sigma_{\pi\pi}^{el}}{dt_{i+1}}$$

Thus if we redefine the kernel  $k$  to include the integral over  $t_{i+1}$  and if we make the approximation that for the limited region of values of  $t_i$  and  $t_{i+2}$  in which the multiperipheral amplitude is large

$$F(t_i, t_{i+1}, t_{i+2}, g_{i+1}) \simeq \frac{d\sigma_{\pi\pi}^{el}}{dt_{i+1}},$$

we may express the kernel in terms of the three elastic cross-sections of definite isospin. Since we want to discuss the kernel in terms of definite  $t$ -channel isospin (see Fig. 4), we must introduce the crossing matrix  $\beta_{II}$ , to relate the  $s$ - and  $t$ -channel isospins. We will discuss later the nature and magnitude of the errors introduced by assuming

$$F = \frac{d\sigma_{\pi\pi}^{el}}{dt}$$

even when the "pion-like" lines are off the pion mass shell.

Third, to make explicit the rapid fall-off at large  $t$  required for a Fredholm equation, we assume that in

$$d(t) = \frac{h(t)}{t - \frac{m^2}{\pi}} ,$$

where  $h(t)$  is as shown in Fig. 5

Incorporating these assumptions into our previous equations, we find for the kernel the equation

$$K^{\lambda, I}(t'', t) = \int_{\frac{4m^2}{\pi}}^{\infty} ds \frac{e^{-(\lambda+1)\eta(s, t'', t)}}{\lambda+1} \frac{h(t'')h(t)}{(t'' - \frac{m^2}{\pi})(t - \frac{m^2}{\pi})} C^I(s)$$

where we've symmetrized the kernel between  $t''$  and  $t$  and where

$$\cosh \eta = \frac{s - t - t''}{2(-t)^{\frac{1}{2}}(-t'')^{\frac{1}{2}}}$$

and

$$C^I(s) = \frac{1}{16\pi^3} \left[ s(s - 4\frac{m^2}{\pi}) \right]^{\frac{1}{2}} \sum_{I'} \beta_{II'} \sigma_{I'}^{el}(s)$$

with

$$\beta_{II'} = \begin{pmatrix} \frac{1}{3} & 1 & \frac{5}{3} \\ \frac{1}{3} & \frac{1}{2} & -\frac{5}{6} \\ \frac{1}{3} & -\frac{1}{2} & \frac{1}{6} \end{pmatrix}$$

To analyze this equation for  $K^{\lambda, I}$  we must know something about the behavior of the  $C^I(s)$ . The three elastic cross-sections of definite isospin have the behavior shown in Fig. 6. From the form of the crossing matrix,  $\beta_{II'}$ , we are led to expect the behavior shown in Fig. 7 for the three functions

$$\frac{C^I(s)}{\left[ s(s - 4\frac{m^2}{\pi}) \right]^{\frac{1}{2}}} .$$

Now, ignoring isospin momentarily, Regge behavior predicts for the asymptotic behavior in  $s$  of the elastic cross-section

$$\sigma^{el} \cong \frac{1}{32\pi} \int_{-4k^2}^0 \frac{dt}{2k^2} \frac{1}{s} |\beta(t)|^2 s^{2\alpha(t)} .$$

Assuming linear trajectories, this gives

$$\sigma^{e1} \simeq \frac{1}{32\pi} s^{2[\alpha(0)-1]} \int_{-4k^2}^0 |\beta(t)|^2 e^{2\alpha't} \ell ns .$$

With reasonable assumptions on  $\beta(t)$ , this yields a leading behavior of the form

$$\sigma^{e1} \propto \frac{s^{2[\alpha(0)-1]}}{\ell ns}$$

Thus we expect that the asymptotic behavior of  $C^I(s)$  will be roughly

$$C^I(s) \underset{s \rightarrow \infty}{\simeq} [s \sigma^{e1}] \simeq C^I \frac{(s/s_0)^{\beta_I}}{\ell ns/s_0} ,$$

where  $\beta_I$  will be discussed below.

To include isospin, as we must in order to calculate  $C^I(s)$ , we must be somewhat careful. We wish to calculate the asymptotic behavior of the expression shown diagrammatically in Fig. 4 for definite values of isospin in the t-channel. This leading behavior arises from exchanging the highest allowed Regge trajectory in each amplitude of Fig. 4; this corresponds to a Regge cut behavior. Amati, Fubini and Stanghellini<sup>5</sup> have shown that if trajectories  $\alpha_1(t)$  and  $\alpha_2(t)$  are exchanged in the two amplitudes, then the resulting cut gives a leading asymptotic behavior with exponent  $\alpha_1(0) + \alpha_2(0) - 1$ . For the three values of isospin we find:

- 1)  $I=0$ . The leading trajectory allowed to both amplitudes is the Pomernanchuk,

so

$$\beta_0 = 2\alpha_p(0) - 1 \simeq 1$$

and

$$C^0(s) \sim \frac{\text{const}}{\ell ns} s$$

2)  $I=1$ . We can exchange a P and a  $\rho$  or two  $\rho$ . The former clearly provides the leading behavior and thus

$$\beta_1 = \alpha_p(0) + \alpha_\rho(0) - 1 \simeq \frac{1}{2} ,$$

so

$$C^1(s) \sim \frac{\text{const}}{\ell ns} s^{\frac{1}{2}}$$

- 3)  $I=2$ . Here only two  $\rho$ 's are allowed so

$$\beta_2 = 2\alpha_\rho(0) - 1 \simeq 0$$

and so

$$C^2(s) \sim \frac{\text{const}}{\ell ns} .$$

Before we continue in the next lecture with our detailed study of the kernel, I would like to mention briefly the relation of this multi-pion pole model to the multi-Regge model discussed by, among others, Chew, Pignotti and Frazer.<sup>6</sup> In the multi-Regge model what we've taken as the  $\pi\pi$  amplitude is replaced by a Reggeized amplitude for all values of  $s$ . While this is anticipated to be correct for large values of  $s$ , if we attempt to use the Regge form for low values of  $s$  in the  $I=0$  amplitude, for instance, we clearly cannot hope to approximate the behavior in the resonance region by the PP contribution alone. But if we incorporate a  $\rho\rho$  contribution, we may find that the sum of the PP and  $\rho\rho$  contribution can roughly approximate the resonance region (Fig. 8). Thus the multi-Regge model with at least two input trajectories may be similar to the model we've been discussing.

#### REFERENCES

1. W.V. Lovitt, Linear Integral Equations, (McGraw-Hill), New York, N.Y. (1924).
2. G.F. Chew, T.W. Rogers and D.R. Snider, Multiperipheral Dynamics with Pion-Pole Dominance, UCRL Report (to appear).
3. G.F. Chew and C. DeTar, Phys. Rev. 180, 1577 (1969).
4. A.H. Mueller and I.J. Muzinich, Diagonalization of the Integral Equation for Multiperipheral Dynamics at Vanishing Values of the Momentum Transfer, Ann. Phys. (N.Y.) (to be published) BNL 13728.
5. D. Amati, S. Fubini and A. Stanghellini, Nuovo Cimento 26, 896 (1962)
6. G.F. Chew and A. Pignotti, Phys. Rev. 176, 2112 (1968); G.F. Chew and W.R. Frazer, Phys. Rev. 181, 1914 (1969).

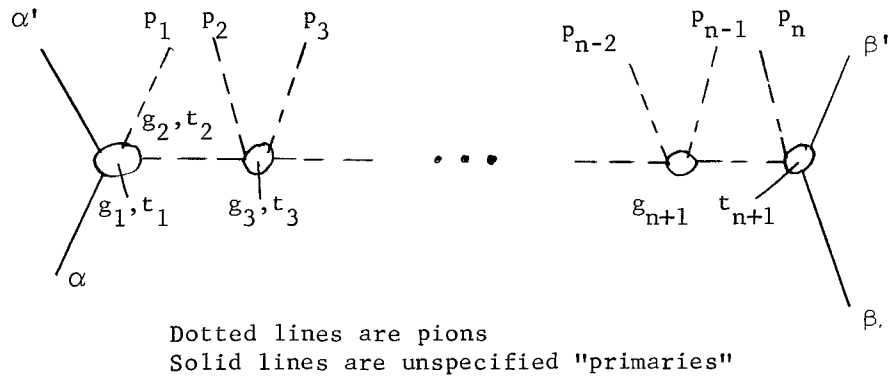


**FIG. 1.** The Pion-Dominated Multiperipheral Chain

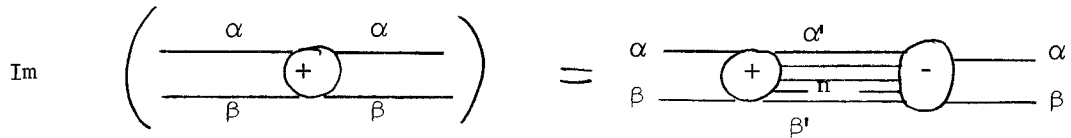


**FIG. 2.** The  $\alpha'\beta'+n\pi$  Contribution to Unitarity in  $\alpha\beta \rightarrow \alpha\beta$

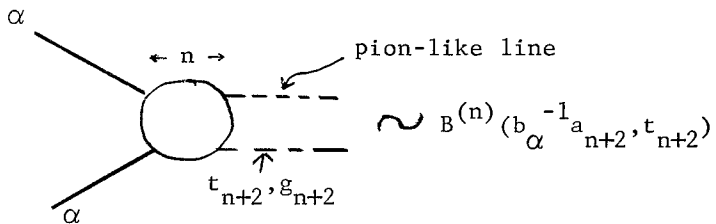


**FIG. 3(a)** Schematic Representation of the Incomplete Imaginary Part  $B^{(n)}$

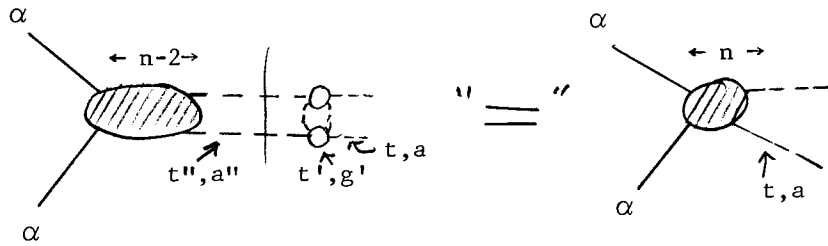


FIG. 3(b). Schematic Representation of the Recursion Relation Between  $B^{(n-2)}$  and  $B^{(n)}$

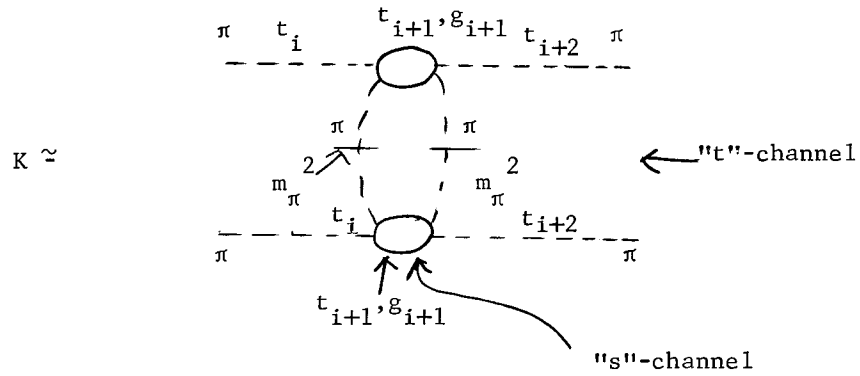


FIG. 4. Schematic Representation of the Fredholm Kernel

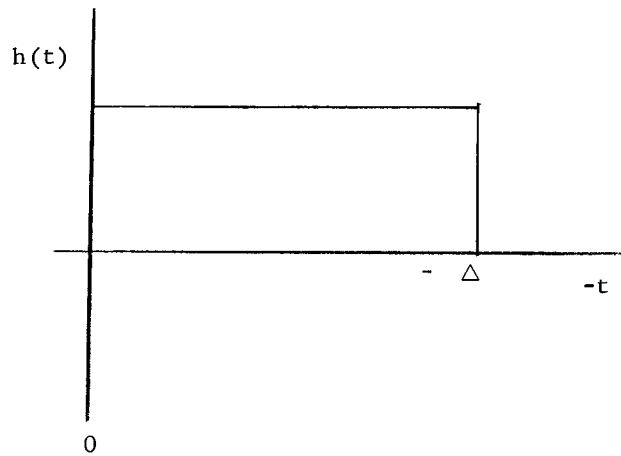


FIG. 5. The Function  $h(t)$

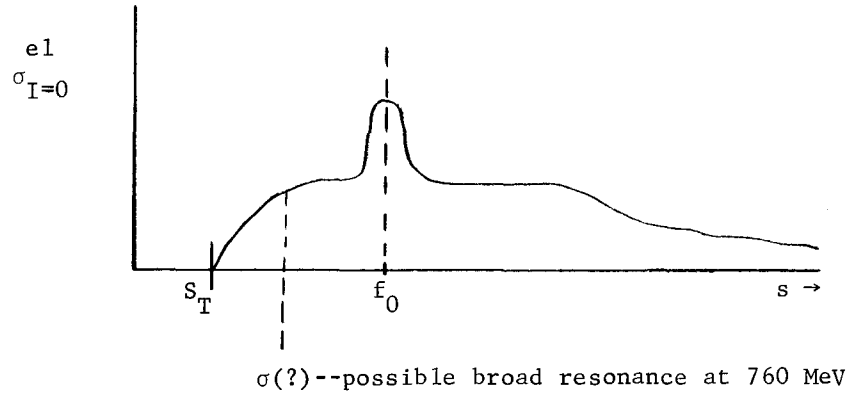


FIG. 6(a)

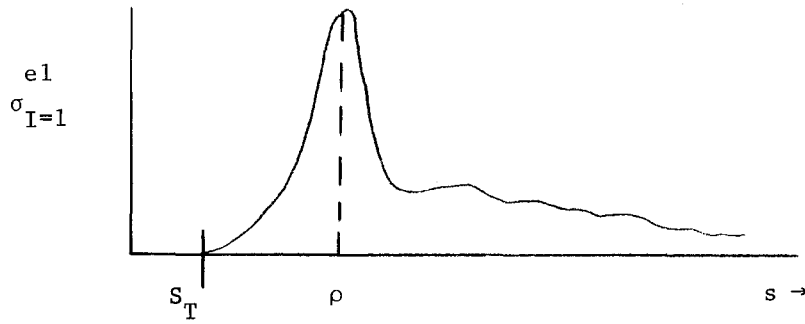


FIG. 6(b)

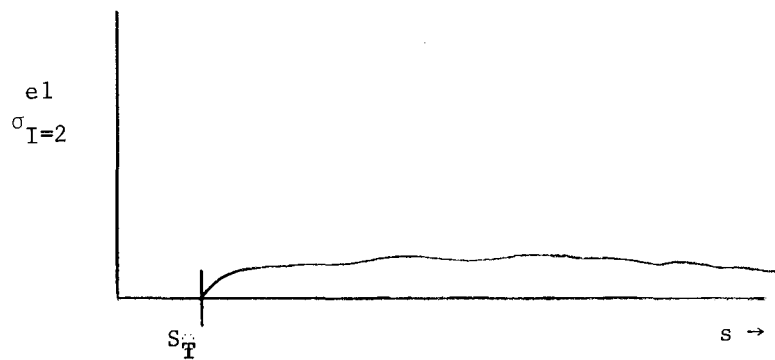


FIG. 6(c)

FIGS. 6 The Three Elastic  $\pi\pi$  Cross Sections for  $I = 0,1,2$



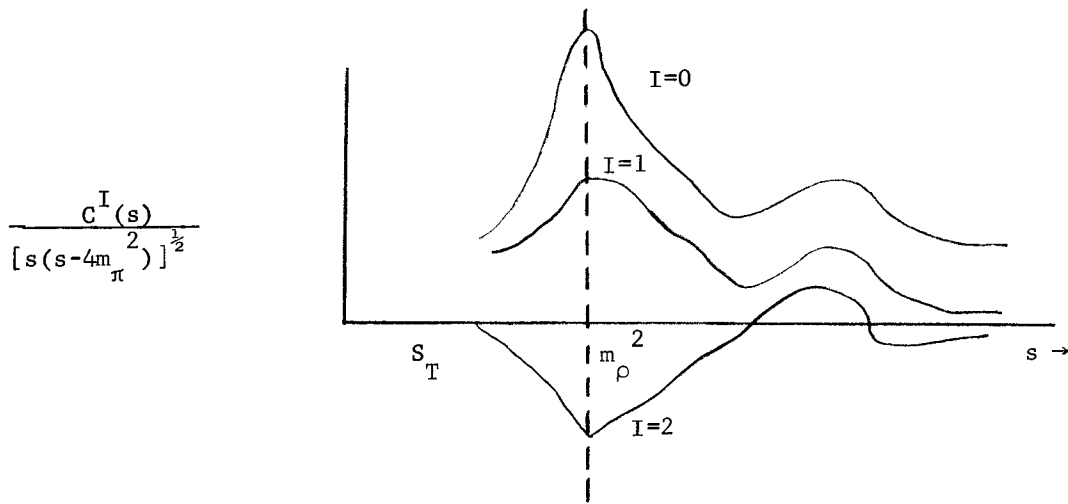


FIG. 7 The Three Quantities  $\frac{C^I(s)}{[s(s-4m_\pi^2)]^{\frac{1}{2}}}$

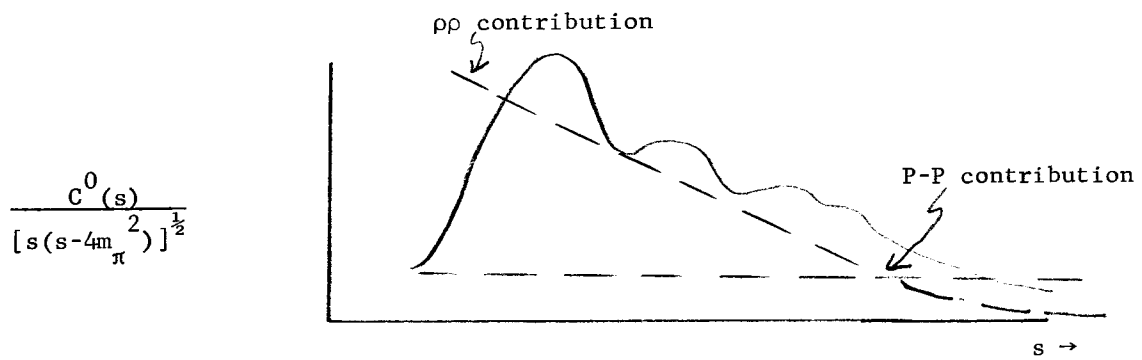


FIG. 8. A Possible Two Regge Trajectory Fit to  $\frac{C^0(s)}{[s(s-4m_\pi^2)]^{\frac{1}{2}}}$ .

From the equations we established last time for  $B^{\lambda, I}(t)$  and  $K^{\lambda, I}(t)$  we can, if we assume something about the behavior of  $\sigma_I^{e1}(s)$ , readily determine numerically the rightmost singularity in the complex  $\lambda$  plane. However, we can gain more insight into the problem by solving it analytically in the "first Fredholm approximation". This yields the result that the poles in  $\lambda$  can be found by solving for  $\lambda$  the equation

$$\begin{aligned} 0 &= D^I(\lambda) \approx 1 - \text{Tr} K^{\lambda, I}(t', t) \\ &= 1 - \int_{-\infty}^0 dt \frac{h^2(t)}{(t - m_{\pi}^2)^2} \int_{\frac{4m_{\pi}^2}{2}}^{\infty} ds \frac{e^{-(\lambda+1)\eta(s, t)}}{\lambda+1} C^I(s) \end{aligned}$$

where  $\cosh \eta(s, t) = 1 - \frac{s}{2t}$ . For the approximation to be valid we need one of two conditions.

1) The kernel must be factorisable in  $t$  and  $t'$ . Since

$$K^{\lambda, I}(t', t) = \int_{\frac{4m_{\pi}^2}{2}}^{\infty} ds \frac{e^{-(\lambda+1)\eta(s, t', t)}}{\lambda+1} C^I(s) \frac{h(t')h(t)}{(t' - m_{\pi}^2)(t - m_{\pi}^2)}$$

where  $\cosh \eta = \frac{s-t-t'}{s(-t)^{\frac{1}{2}}(-t')^{\frac{1}{2}}}$ , this factorisation will not hold unless  $s \gg t, t'$ .

This condition will be satisfied in the multi-Regge model, which has already used an expression valid only at asymptotic  $s$ . But we have seen the importance of the low-energy resonance contributions, so we don't want to make the assumption that  $s \gg t, t'$ .

2) The leading eigenvalue must be widely separated from the rest of the spectrum and the approximation must be used only in the neighborhood of the leading eigenvalue. As numerical calculations indicate that this condition holds, we may use the approximation.

Let us first take a very rough look at the analytic structure of  $D^I(\lambda)$  in  $\lambda$ . Singularities in  $\lambda$  coming from divergences of the integrals will probably arise from the upper limit of the  $s$  integration because of the cut-off in  $t$  assured by the  $h(t)$ . As  $s/|t|$  approaches infinity,

$$e^{\eta} \approx \frac{s}{|t|} = \frac{s}{-t}$$

and hence, using the asymptotic form of  $C^I(s)$ ,

$$C^I(s) = (s/s_0)^{\beta_I},$$

we see that the integral in the equation for  $D^I(\lambda)$  will exist and be analytic in  $\lambda$  for  $\text{Re} \lambda > \beta_I$ . In fact, as Fig. 1 illustrates, the situation is in some sense a

mirror image of that in the energy plane, as  $D^I(\lambda)$  is real analytic for  $\text{Re}\lambda > \beta_I$ . Further, if the kernel is positive definite, as is true for  $I=0$  and  $I=1$  but not for  $I=2$ , then the integral becomes logarithmically positive-infinite as  $\lambda$  approaches  $\beta_I$ . Since the integral falls to zero exponentially as  $\lambda \rightarrow \infty$ , at some value  $\hat{\lambda}^I$   $\beta_I < \hat{\lambda}^I < \infty$ , we expect  $D^I(\hat{\lambda}^I) = 0$ , corresponding to a (Toller) pole in  $B^{\lambda^I}(t)$ . In fact, to anticipate the results somewhat, we expect  $\hat{\lambda}^0 \approx 1$  (the Pomanchuk trajectory intercept) and  $\hat{\lambda}^1 \approx \frac{1}{2}$  (the rho trajectory intercept), so that since  $\beta_0 \approx 1$  and  $\beta_1 \approx \frac{1}{2}$ , for both  $I=0$  and  $I=1$  the poles should lie only slightly to the right of the cuts which start at  $\lambda = \beta_I$ .

Before beginning a more detailed study of the integral, we can make a simplification by noting that as  $t \rightarrow 0$ ,  $e^\eta \approx s/-t$ , and thus

$$e^{-(\lambda+1)\eta} \approx (-t/s)^{\lambda+1} .$$

Hence for  $\lambda > 0$  the  $t$  integration gets little contribution from the region near  $t=0$ , and we may approximate

$$\left( \frac{1}{t-m} \right)^2 \approx \left( \frac{1}{t} \right)^2 .$$

This enables us to perform the  $t$  integration by changing variables to  $\cosh\eta$ ,

$$dx \equiv d(\cosh\eta) = \frac{s}{2} \frac{dt}{t^2} , \text{ at fixed } s ,$$

and obtaining

$$\int_{-\infty}^0 \frac{dt}{t^2} e^{-(\lambda+1)\eta(s,t)} = \frac{2}{s} \frac{1}{\lambda(\lambda+2)} .$$

We will discuss these approximate poles in  $\lambda$  later.

If we look now at the integral over  $s$ , it becomes

$$\frac{1}{\lambda(\lambda+1)(\lambda+2)} \int_{\frac{4m}{\pi}}^{\infty} \frac{ds}{s} C^I(s)$$

which diverges, for  $I=0$  and  $I=1$ , by inspection of the asymptotic form of  $C^I(s)$ .

What's gone wrong? Our trouble stems from the combined high  $s$  and high  $t$  regions and can be resolved by recalling that we should have included the  $t$  cut-off; this is necessary both to assure that the equation be Fredholm and to agree with experiment which shows that the amplitudes vanish very rapidly at high values of  $|t|$ .

So let's backtrack a bit and be more careful. First, insert a cut-off in  $t$  at  $|t| = \Delta$ , as discussed in the last lecture. Then, breaking the integral over  $s$  into two parts, corresponding to integrals over the low and high energy regions respectively, we have

$$D^I(\lambda) \cong 1 - \frac{1}{\lambda+1} \int_{-\Delta}^0 \frac{dt}{t^2} \int_{\frac{4m^2}{\pi}}^{s_{\max}} e^{-(\lambda+1)\eta(s,t)} C^I(s) \\ - \frac{1}{\lambda+1} \int_{-\Delta}^0 \frac{dt}{t^2} \int_{s_{\max}}^{\infty} e^{-(\lambda+1)\eta(s,t)} C^I(s) \quad .$$

To guide the analysis of these integrals let me indicate what we expect qualitatively. Empirically, the average meson pair subenergy  $\bar{s}$  is  $\lesssim 1$  GeV. Thus in determining the value of  $\hat{\lambda}^I$  for which  $D(\hat{\lambda}^I) = 0$  we expect that the low-energy, resonance-dominated term will provide the dominant contribution. We will first study the high energy term and show that this is in fact a small contribution. Then we will discuss the low energy integral in detail.

In concentrating on the "high energy" term,  $I_{\text{h.e.}}^I$ , we may make the following approximations:

1) we suppose that  $s_{\max}$  is large enough so that

$$C^I(s) \cong \frac{C^I(s/s_0)^{\beta_I}}{\ln(s/s_0)} \quad \text{for } s \geq s_{\max} \quad ; \quad \text{and}$$

2) we assume that for all  $t$  such that  $|t| < \Delta$ ,  $t/s$  is sufficiently small for  $s > s_{\max}$  so that

$$e^{-(\lambda+1)\eta(s,t)} \cong (-s/t)^{-(\lambda+1)} \quad .$$

Thus

$$I_{\text{h.e.}}^I \cong \frac{C^I}{\lambda+1} \int_{-\Delta}^0 \frac{dt}{t^2} \int_{s_{\max}}^{\infty} ds \frac{s^{-(\lambda+1)} (s/s_0)^{\beta_I}}{\ln(s/s_0)} \quad .$$

Doing the  $t$  integration gives

$$I_{\text{n.e.}}^I \cong \frac{C^I}{\lambda+1} \frac{\Delta^\lambda}{\lambda} \int_{s_{\max}}^{\infty} ds \frac{s^{-(\lambda+1)} (s/s_0)^{\beta_I}}{\ln(s/s_0)} \quad .$$

Now we want to know how this behaves as  $\lambda \rightarrow \beta_I$ , since at least for  $I=0$  and  $I=1$  we expect the leading poles to be close to the  $\beta_I$ . Writing

$$I_{h.e.}^I \cong \frac{C^I}{\lambda+1} \frac{(\Delta/s_0)^\lambda}{\lambda} \int_{\ln(s_{\max}/s_0)}^{\infty} \frac{d(\ln s/s_0)}{\ln(s/s_0)} \exp[-(\lambda-\beta_I)\ln s/s_0]$$

we find, for  $(\lambda-\beta_I)\ln(\frac{s_{\max}}{s_0}) \ll 1$ ,

$$I_{h.e.}^I \approx \frac{C^I}{\lambda+1} \frac{(\Delta/s_0)^\lambda}{\lambda} \ln \left[ \frac{1}{(\lambda-\beta_I)\ln(\frac{s_{\max}}{s_0})} \right]$$

Note that, for the  $I=0$  case, there is an important subtlety which we must clarify. If the Pomeranchuk were a Regge pole with  $\alpha_P(0) = 1$  exactly, then the P-P Regge cut would occur at  $2\alpha_P(0)-1 = 1$  as well. Thus we would have  $\hat{\lambda}^0 = 1 = \beta_0$ , and the above derivation would give a divergent result for the high energy integral. It is, therefore, essential for the Pomeranchuk to lie slightly below 1, say at  $\alpha_P(0) = 1-a$ , so that  $\beta_0$  lies below the pole, at  $2\alpha_P(0)-1 = 1-2a$ .<sup>1</sup> This result is in agreement with an analysis by Finkelstein and Kajantie<sup>2</sup> in which they showed, under certain assumptions, that  $\alpha_P(0)$  must be strictly less than 1 in order to maintain unitarity. We can even estimate roughly how much below 1 the intercept of the Pomeranchuk trajectory must lie by using the experimental knowledge that at  $\hat{\lambda}^0$  the high energy contribution is "small". Choosing explicit numbers for the parameters,

$$\begin{aligned} \Delta &\lesssim s_0 = 1 \text{ GeV}^2, \\ s_{\max} &= 20 \text{ GeV}^2, \\ \sigma_{\pi\pi}(s) &\cong 2\text{mb for } s > s_{\max} \end{aligned}$$

and thus  $C^0 \approx 0.1$ . Taking  $a = 0.05$  in  $\hat{\lambda}^0 \equiv \alpha_P(0) = 1-a$  and  $\beta_0 = 1-2a$ , gives

$$I_{h.e.}^0 = \frac{0.1}{2} \left(\frac{\Delta}{s_0}\right) \ln \left( \frac{1}{(0.05)\ln 20} \right) \ll 1,$$

and indeed  $I_{h.e.}^0$  must provide the major contribution to the vanishing of  $D^0(\hat{\lambda}^0)$ . To check the assertion the  $I_{h.e.}^I$  is small for  $I=1$  as well we note simply that  $\hat{\lambda}^1 \equiv \alpha_\rho(0)$  and  $\beta_1 = \alpha_P(0) + \alpha_\rho(0) - 1$  so that  $\hat{\lambda}^1 - \beta_1 = a$  and the same order of magnitude estimate of  $I_{h.e.}^I$  results.

Consider next the low energy integral, to see whether the model in fact predicts  $D^I(\hat{\lambda}^I) = 0$  for  $\hat{\lambda}^0 \approx 1$  and  $\hat{\lambda}^1 \approx 1/2$ . We have

$$I_{1.e.}^I \cong \frac{1}{\lambda+1} \int_{-\Delta}^0 dt \frac{1}{t^2} \int_{\frac{4m_\pi^2}{2}}^{s_{\max}} ds e^{-(\lambda+1)\eta} C^I(s) .$$

Here we see that the  $t$ -cutoff at  $\Delta$  is not necessary to prevent the integral from diverging. Further, we can establish that the important region in the  $t$  integration is  $t \approx s$ . Thus there will be little contribution from high values of  $t$ ; this allows us to take  $\Delta$  to infinity and to do the  $t$  integral analytically to get

$$I_{1.e.}^I(\lambda) = \frac{1}{\lambda+1} \int_{\frac{4m_\pi^2}{2}}^{s_{\max}} \frac{ds}{s} C^I(s) \frac{2}{\lambda(\lambda+2)} .$$

Knowledge of the elastic cross-sections in this resonance region will immediately allow us to do the  $s$  integral numerically. First, though, consider the  $\lambda$  dependence. We know this can't be correct as  $\lambda \rightarrow \infty$ , for the integral should go to zero exponentially; our approximations are at fault here. But what about the poles in  $\lambda$  at 0, -1, and 2?

- 1) The pole at  $\lambda = -1$  is easily explained. It comes essentially from treating the pion as an elementary particle in the multiperipheral chain so that  $\alpha_\pi^I(t) = 0$  for all  $t$ . Then the contribution of the diagram shown in Fig. 2 is expected to be  $2\alpha_\pi(0) - 1 \approx -1$ , and hence we can expect a pole at  $\lambda = -1$ .
- 2) The pole at  $\lambda=0$  is associated with the neglect of the pion mass in the approximation

$$\frac{1}{(t-m_\pi^2)^2} \rightarrow \frac{1}{t^2} .$$

In the limit  $m_\pi \rightarrow 0$  there would exist a pole at  $\lambda=0$ ; for the small physical  $m_\pi$  there is a large peak in  $I_{1.e.}^I$  at  $\lambda = 0$ . An interesting observation is that this gives a singularity in the same place as if we singled out the  $\rho$  trajectory in the  $\pi\pi$  amplitudes (see Fig. 3) since  $2\alpha_\rho(0)-1 \approx 0$ . Thus the small pion mass is reproducing the behavior of the  $\rho$ ; this is a point which we don't really understand.

Now let us return to a rough evaluation of the low energy integral. As we are primarily interested in values of  $\lambda$  near  $\frac{1}{2}$  or 1, the singularity at  $\lambda=0$  is most important. Collecting all the other factors in  $I_{1.e.}^I$  into a "residue" at the pole  $\lambda=0$  and assuming that the  $\rho$  dominates the resonance contribution we get

$$D^I(\lambda) \approx 1 - \frac{R}{\lambda} \beta_{I1} \quad ,$$

where

$$\beta_{I1} = \begin{pmatrix} I=0 & 1 \\ I=1 & \frac{1}{2} \\ I=2 & -\frac{1}{2} \end{pmatrix} .$$

If we find that  $R \approx 1$  - this ideally should follow simply from the value of the integral over  $s$  - we see that

$$1) \quad \hat{\lambda}^0 \approx 1 = \alpha_p(0) \quad , \quad \text{and}$$

$$2) \quad \hat{\lambda}^1 \approx \frac{1}{2} = \alpha_\rho(0) \quad .$$

$$\text{We also find} \quad \hat{\lambda}^2 \approx -\frac{1}{2} \quad ,$$

but we are not really justified in identifying this immediately with a trajectory intercept, because of the crudity of our approximation.

In the next lecture I will discuss what the actual value of the resonance integral is; although we will find qualitative agreement with our above conclusions, the quantitative result is not correct.

#### REFERENCES

1. G.F. Chew and A. Pignotti, Phys. Rev. 176, 2112 (1968).
2. J. Finkelstein and K. Kajantie, Physics Letters 26B, 305 (1968).

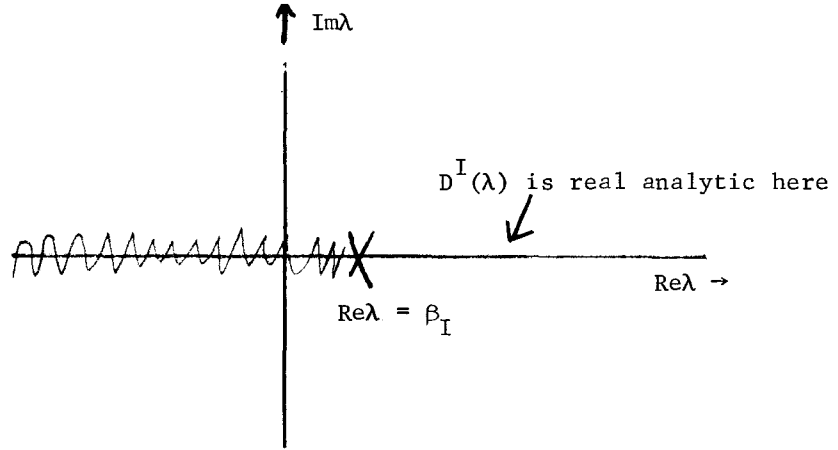


FIG. 1 Rough Analytic Structure of  $D^I(\lambda)$

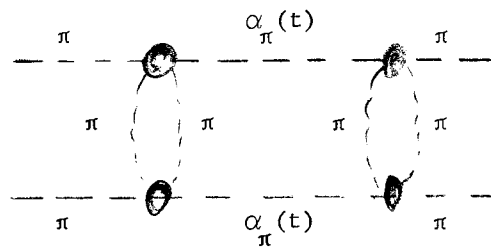


FIG. 2. A Reggeized Pion in the Multi-Peripheral Chain

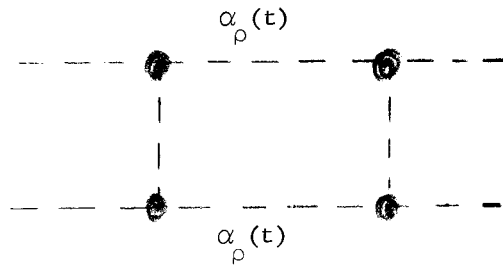


FIG. 3. Rho Regge Trajectories Dominating the  $\pi\pi$  Amplitudes



I ended the last lecture with a hint that, although the qualitative results regarding relative locations of the P and  $\rho$  trajectory intercepts were encouraging for the simple pion multiperipheral model, the quantitative aspects were less satisfactory. I'd like to go into greater detail on this difficulty now. First, what do we mean by "quantitatively less satisfactory"? Recall that to produce a Toiler pole at  $\hat{\lambda}^I$  we required  $D^I(\hat{\lambda}^I) = 0$ . Further, we argued that in

$$D^I = 1 - I_{h.e.} \cdot I_{l.e.}^I,$$

the low energy or resonance term would provide the dominant contribution necessary to produce the zero in D. Thus we require, for  $I=0$ ,

$$D^0(\hat{\lambda}^0) \cong 1 - \frac{2}{\hat{\lambda}^0(\hat{\lambda}^0+1)(\hat{\lambda}^0+2)} \int_{4m_\pi}^{s_{\max}} \frac{ds C^0(s)}{s} \cong 0$$

and for  $I=1$ ,

$$D^1(\hat{\lambda}^1) \cong 1 - \frac{2}{\hat{\lambda}^1(\hat{\lambda}^1+1)(\hat{\lambda}^1+2)} \int_{4m_\pi}^{s_{\max}} \frac{ds C^1(s)}{s} \cong 0.$$

To produce the observed P ( $\hat{\lambda}^0 \approx 1$ ) and the observed  $\rho$  ( $\hat{\lambda}^1 = \frac{1}{2}$ ) intercepts, we require  $D^0(1) \approx 0$  and  $D^1(\frac{1}{2}) \approx 0$ , which implies

$$1 = \frac{1}{3} \int_{4m_\pi}^{s_{\max}} \frac{ds C^0(s)}{s}$$

$$1 = \frac{16}{15} \int_{4m_\pi}^{s_{\max}} \frac{ds C^1(s)}{s}.$$

In both cases we find the integrands are about a factor of three too small; strictly speaking, this would mean that neither the P nor the  $\rho$  has the experimentally observed intercept in this model and might seem quite disturbing. However, there are arguments suggesting that, at least in this simple version of the model, one should not worry about this disagreement.

First, in asserting that

$$F(t_i, t_{i+1}, t_{i+2}, g_{i+1}) \cong \frac{d\sigma^{el}}{dt_{i+1}}$$

to simplify the model, we completely neglected off-mass shell effects: that is, effects produced when  $t_i$  and  $t_{i+2}$  take values other than  $t_i = m_\pi^2 = t_{i+2}$ . There is a standard prescription which suggests that, since the P-wave  $\rho$  resonance dominates the low energy  $\pi\pi$  amplitude, in continuing the amplitude off the mass shell one should include a factor of the center of mass momentum to the first power. (see Fig. 1)

Since we are dealing with the modulus of the amplitude squared, we should include a factor of the center of mass momenta,  $q$ , squared. From Fig. 1 we have for arbitrary  $t$

$$q_{\text{off}}^2 = \frac{s}{4} - t \text{ and for } t = m_\pi^2, q_{\text{on}}^2 = \frac{s}{4} - m_\pi^2,$$

where  $q_{\text{off}}^2$  and  $q_{\text{on}}^2$  indicate the off mass shell and on mass shell momenta respectively.

Taking  $s = m_\rho^2$  as a typical example, we get the ratio, neglecting  $m_\pi^2$ ,

$$\frac{q_{\text{off}}^2}{q_{\text{on}}^2} \approx 1 - \frac{4t}{m_\rho^2}.$$

With  $\bar{t} = -0.2$  and  $m_\rho^2 = 0.6$ , this ratio becomes approximately 2 which indicates that the inclusion of off mass shell effects might produce a substantial increase in the value of the low energy integral.

Second, any contributions from higher mass meson states will also tend to increase the integral over  $C^I(s)$ . Thus including the effects of produced and exchanged K mesons by introducing the SU(3) meson octet of  $\pi$ -K instead of the SU(2) meson triplet of pions is one possible and potentially useful generalisation of the present model; later, we will come back to the octet model for a brief, qualitative survey.

Let us now briefly consider the relation of  $\lambda$  branch points and poles in the multiperipheral model. In the expression

$$B^{\lambda, I}(t) = \frac{N^I(\lambda, t)}{D^I(\lambda)}$$

we can also approximate  $N^I(\lambda, t)$  by a Fredholm expansion. To lowest order, corresponding to our approximation for  $D^I(\lambda)$ ,

$$\begin{aligned} D^I(\lambda) &= \mathbf{1} - \text{Tr } K^{\lambda, I}(t', t) \\ &\approx \mathbf{1} - \frac{\tilde{R}^I}{\lambda} - \epsilon_I \left( \frac{\Delta}{s_0} \right) \ln \left[ \frac{1}{(\lambda - \beta_I) \ln(s_{\text{max}}/s_0)} \right] \end{aligned}$$

we find

$$N^I(\lambda, t) = B_0^{\lambda, I}(t).$$

Thus the analytic structure of  $N^I(\lambda, t)$  in this approximation is that of  $B_0^{\lambda, I}(t)$ . In

our moder  $B_0^{\lambda, I}(t)$  has similar analytic structure in  $\lambda$  to the kernel,  $K^{\lambda, I}(t', t)$ , and thus we expect  $N^I(\lambda, t)$  in general to have Regge cuts but no Regge poles. There is, however, one subtle point which arises and disappears almost before we can mention it. If we have included non-elementary pions - that is, pions for which  $\alpha'(t) \neq 0$  -  $N^I(\alpha, t)$  would have a branch point at  $\lambda = -1$ . But since we've put in an elementary pion,

$$N^I(\lambda, t) \underset{\lambda \rightarrow -1}{\simeq} \frac{R}{\lambda+1} .$$

This, in fact, just cancels the pole at  $\lambda = -1$  in  $D^I(\lambda)$ , so that there is neither pole nor zero in  $B^{\lambda, I}(t)$  at  $\lambda = -1$ .

Since the cases of interest are for  $I=0$  and  $I=1$ , let me now restrict the considerations to these values of isospin. Then the analytic structure of  $B^{\lambda, I}(t)$  is roughly as shown in Fig. 2, with a pole at  $\hat{\lambda}^I$  coming from the zero of  $D^I(\lambda)$  and a branch cut beginning at  $\lambda = \beta_I$  also from  $D^I(\lambda)$ . Recall that the logarithmic term producing the cut in  $D^I(\lambda)$  and thus in  $B^{\lambda, I}(t)$  is of the form

$$\Sigma_I \left( \frac{\Delta}{s_0} \right) \ln \left[ \frac{1}{(\lambda - \beta_I) \ln(s_{\max}/s_0)} \right]$$

where  $\Sigma_I$  is a small constant. Thus unless  $\lambda - \beta_I = a \rightarrow 0$ , the branch point will be weak. Consider first the situation when  $a \neq 0$ . Then the branch point is weak, and, by the arguments I discussed several lectures ago, there is also a pole on the second Riemann sheet reached by going through the cut. (see Fig. 2). This second pole participates in a very interesting effect relevant to what happens when, in non-forward scattering,  $\hat{\lambda}^I(\tau) \rightarrow \beta_I(\tau)$ , where  $\tau$  is the overall momentum transfer. Consider the case for  $I=0$ . Here we find

$$\beta_0 = \alpha_p(\tau/4) - 1$$

where  $\hat{\lambda}^0(\tau)$

$$\hat{\lambda}^0(\tau) = \alpha_p(\tau).$$

If we assume that  $\alpha_p(\tau) = \alpha_p(0) + \alpha_p'(0) \cdot \tau$ ,  $\alpha_p'(0) > 0$ , then at some value  $\tau = \tau_0 < 0$  the cut will overtake the pole. But this seems impossible, once according to our previous analysis the leading pole is always to the right of the branch point. What transpires is that, as  $a \rightarrow 0$ , the discontinuity across the cut becomes large and the pole on the second Riemann sheet moves farther away from the pole on the first sheet. Further, the residue of the first sheet pole approaches zero as  $a \rightarrow 0$ , and, in essence, the second pole moving as illustrated in Fig. 3a, "takes over". In terms of a conventional single sheet description, we never see the second pole; we see a peak in the discontinuity across the cut (Fig. 3b).

We may note parenthetically that, had we simply ignored the cut, we would

have obtained similar physical results. This illustrates once more the principle that a weak singularity is essentially no singularity; to make almost any physically meaningful deduction from analytic structure arguments one must know the discontinuities across, as well as the location of, the singularities.

Conclusions from the Pion-Dominated Multiperipheral Model:

- 1) The characteristics of trajectories and residues are determined by the resonances - that is, in some sense by the trajectories themselves. Here we've not been able to exploit this connection directly, since we've taken the cross section in the resonance region as an empirical input. The most direct hope for a bootstrap the simple multi-Regge model, fails because the two particle subenergies are not large enough. Attempts to use "duality" to extend the Regge expression to the resonance region are fraught with difficulties we've already mentioned; but even so, inputting two Regge poles may lead to an acceptable model. Eventually, applying self-consistency in some quantitatively more accurate model may lead to a good bootstrap of the trajectories. This is in contrast to the Veneziano model in which one can arbitrarily change the scale of trajectory parameters.
- 2) The Pomeranchuk trajectory is qualitatively like the rho trajectory; within the context of this model, there seems no way to single out the Pomeranchuk from all other Regge trajectories.

This is in conflict with the numerical results of the older Regge phenomenological fits, which suggest a very "flat" P, and with the spirit of some of the recent duality models, which treat the P differently from all other trajectories. With regard to the first point, a recent fit by Dikmen<sup>1</sup> is relevant. In  $\pi N$  scattering there is no shrinkage of the forward peak. The standard explanation attributes this to the "flatness" of the P trajectory,  $\alpha_P'(t) \approx 0$ . But Dikmen discovered that plotting the direct channel resonance contributions in the near forward direction gave a sharply peaked distribution as shown in Fig. 4. Further, this resonance contribution goes to zero as  $S \rightarrow \infty$ , so that, if the Pomeranchuk trajectory were flat, the peak would expand. Hence the width of the P contribution must shrink if the total forward peak width remains constant. Dikmen finds that the data are consistent with  $\alpha_P'(t) \approx 0.7 \text{ GeV}^{-1}$  for  $t$  near zero.

In view of the duality hypothesis one might question Dikmen's technique, namely, if the Pomeranchuk is similar to all other trajectories, is it consistent to add it to a sum of resonances? The answer is that it may be consistent with Regge pole-resonance duality if the Pomeranchuk corresponds to weakly coupled exotic resonances. Then adding the P to a sum of non-exotic resonances would not be double counting. Note that our general discussion of unitarity as a discontinuity formula leads us to expect poles in all reaction amplitudes, exotic or not. If sufficiently far from the physical region, exotic resonances could

easily appear as a rather flat background. SU(3)

SU(3) Generalisations of the Meson-Dominated Multiperipheral Model.

We've mentioned previously that one way to increase the kernel strength in the multiperipheral model to produce output Regge poles at the correct positions is to increase the number of distinguishable low-mass particles which can be produced and exchanged in the multiperipheral chain. One obvious way to do this is to introduce, instead of the SU(2) triplet of pions, the SU(3)  $\pi$ -K octet. Let us look briefly at this possibility.

The analogues of the three isospin amplitudes obtained from the decomposition

$$1 \otimes 1 = 2 \oplus 1 \oplus 0$$

are the six SU(3) amplitudes in the decomposition of the Kronecker product of two octets,

$$8 \otimes 8 = 1 \oplus 8_S \oplus 8_A \oplus 10 \oplus \overline{10} \oplus 27.$$

Here  $8_S$  and  $8_A$  stand for the symmetric and antisymmetric octets respectively. The crossing matrix, from which we can make many quick deductions, can be written<sup>2</sup>

	1	$8_S$	$8_A$	10	$\overline{10}$	27	(s-channel)
1	$\frac{1}{8}$	1	1	$\frac{5}{4}$	$\frac{5}{4}$	$\frac{27}{8}$	
$8_S$	$\frac{1}{8}$	$-\frac{3}{10}$	$\frac{1}{2}$	$-\frac{1}{2}$	$-\frac{1}{2}$	$\frac{27}{40}$	
$8_A$	$\frac{1}{8}$	$\frac{1}{2}$	$\frac{1}{2}$	0	0	$-\frac{9}{8}$	
10	$\frac{1}{8}$	$-\frac{2}{5}$	0	$\frac{1}{4}$	$\frac{1}{4}$	$-\frac{9}{40}$	
$\overline{10}$	$\frac{1}{8}$	$-\frac{2}{5}$	0	$\frac{1}{4}$	$\frac{1}{4}$	$-\frac{9}{40}$	
27	$\frac{1}{8}$	$\frac{1}{5}$	$-\frac{1}{3}$	$-\frac{1}{12}$	$-\frac{1}{12}$	$\frac{7}{40}$	

(t-channel)

From the first row we see immediately that the singlet trajectory in the t-channel - that is, the Pomernanchuk - will again have the highest intercept. This follows because the contributions are from elastic cross sections which are positive definite. Which trajectory will come next? Taking a hint from experiment, we assume that, since there are no observed resonances in the 10,  $\overline{10}$ , or 27 channels, the main contributions will come from 1,  $8_A$ , and  $8_S$ . Comparing the second and third rows shows that  $8_S$  and  $8_A$  trajectories receive equal contributions from the singlet and  $8_A$  resonances but that whereas the  $8_A$  trajectory receives a positive contribution from the  $8_S$  resonances the  $8_S$  trajectory receives a negative contribution from the  $8_S$  resonances. To make the argument more concrete, recall that Bose statistics require that the  $8_S$  states have even orbital angular momentum,  $l$ , and that  $8_A$  states have odd  $l$ .

Since the  $\pi$ -K octet is spinless, this means that the  $8_S$  corresponds to an octet of even spin resonances [ $f^0, A_2$ , etc] and the  $8_A$  to an octet of odd spin resonances [ $\rho, K^*, \omega$ ]. Thus our arguments have shown that the  $\rho$  trajectory should come out above the  $f^0$  trajectory; however, since the  $\rho$  resonance is stronger than the  $f^0$ , this splitting of the trajectories need not be large. Hence the hypothesis of exchange degeneracy of the  $f^0$ - $\rho$  trajectories may still be approximately correct.

Finally, we note that 10 and  $\overline{10}$  receive no contribution from the large  $\rho$  resonance and 27 receives a negative contribution. Thus it is probable that the leading trajectories for these channels will be well below the others.

Qualitatively this agrees well with observation. However, for two reasons, it is not clear that this model is more acceptable than the SU(2) pion model. First, SU(3) symmetry is badly broken in the sense that  $m_\pi \ll m_K$ . Second, in single peripheral exchanges the pion fits experimental results well, but the kaon does not.

At this stage, I think we've carried the multiperipheral model as far as we can at present. In the next lectures, I plan to turn to some very interesting recent work on the "strip" model to show how some of the ambiguities in the multiperipheral model can be avoided and how a numerically quite successful bootstrap can be obtained.

#### REFERENCES

1. F. Ned Dikmen, Phys. Rev. Letters 22, 622 (1969).
2. D.E. Neville, Phys. Rev. 132, 844 (1963).

LECTURE 7

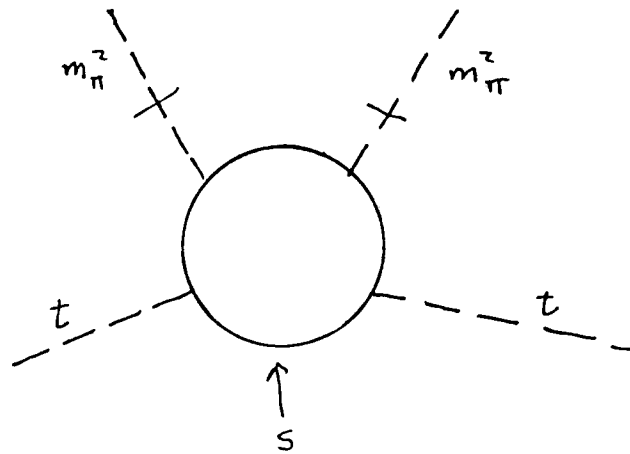


FIGURE 1

The  $\pi$ - $\pi$  Scattering Amplitude with two Pions on the Mass Shell

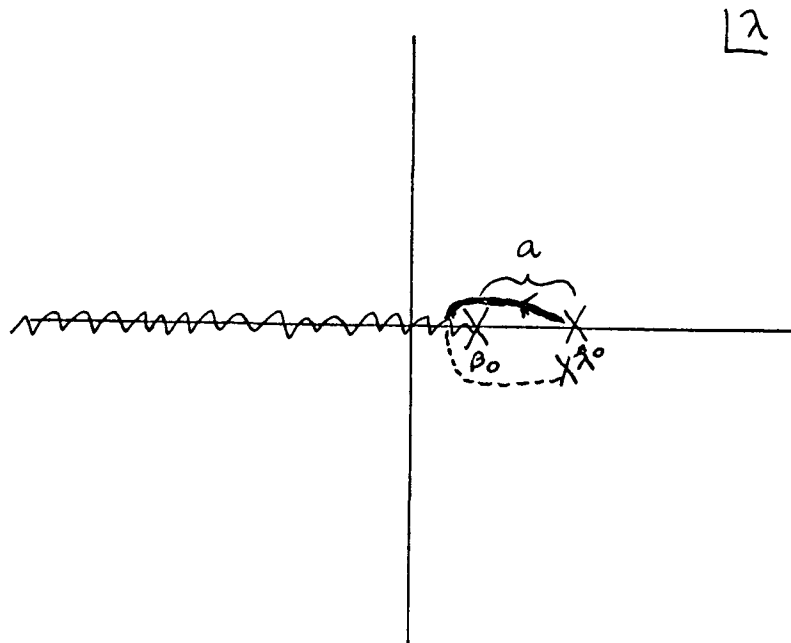


FIGURE 2

The Analytic Structure of  $B^{\lambda, 0}(t)$

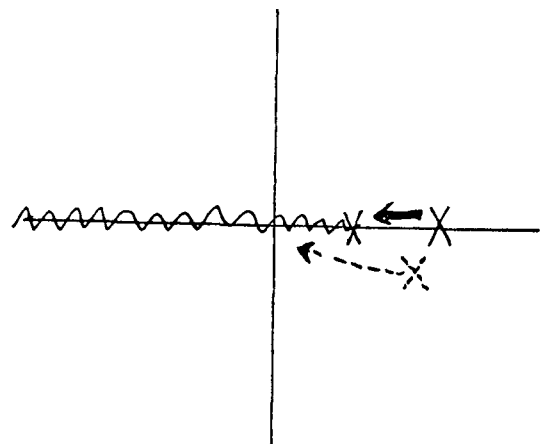


FIGURE 3 (a)

The Movement of First and Second Sheet Poles as  $\lambda - \beta \rightarrow 0$

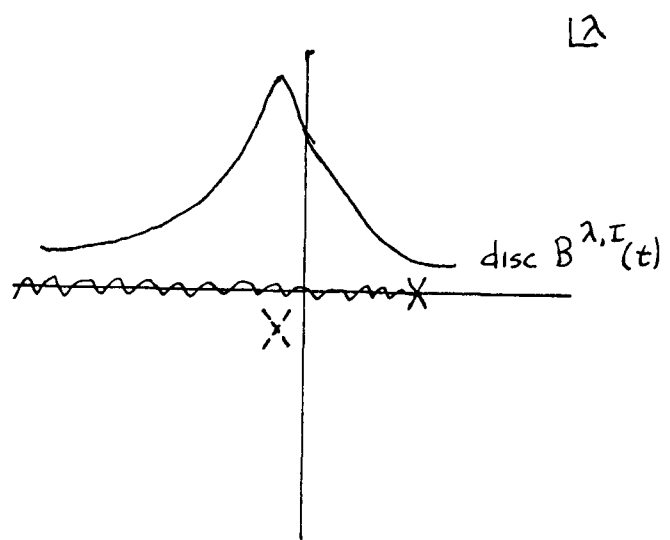


FIGURE 3 (b)

The Large Discontinuity in  $B^{\lambda, I}(t)$  Caused by the Second Sheet Pole



In the next two lectures I shall discuss, as a final example of specific approximations to the S-matrix, the "strip model" of the four-particle connected part. There exist several different, but related, versions of this model<sup>(1-4)</sup>; they share a common set of similar initial hypotheses but differ in the methods used to calculate the functions involved.

#### BASIC PROPERTIES OF THE STRIP MODEL:

What is the common denominator of these strip models?<sup>5</sup>

To discuss this question, let me begin by recalling two salient features of two-body scattering:

- (1) in the s-physical region there are frequently strong peaks in the low-energy cross sections associated with resonances in s; these peaks die out above  $S \approx 2 \text{ GeV}^2$  indicating that the couplings of such resonances to the two-body channels become smaller at high energies;
- (2) when there are direct channel resonances, the cross channel reactions show forward or backward peaks, which persist to asymptotic energies; apart from these peaks, the high energy cross sections are very small.

Thus, if we draw a plot of the Mandelstam invariant s, t, and u (see Figure 1a), we see that the amplitude is large only in the shaded parts of the physical region -- that is, the parts in which at least one of the three Mandelstam invariants is small. If we make the hypothesis that the amplitude (See Ref. (1) for arguments supporting this), continued out of the physical region, remains large only in a region of width roughly comparable to that in which it is large inside the physical region, we obtain the three "strips" as shown in Figure 1b; here the "s-strip" is associated with small values of s and all values of t and u. This division of the Mandelstam plot into "strips" suggests a model which divides the amplitude into three parts by writing

$$M(s,t,u) = M^s(s,t,u) + M^t(s,t,u) + M^u(s,t,u) \quad (1)$$

where  $M^s$  is associated with the s-strip and similarly for  $M^t$  and  $M^u$ . Since within the s-strip the values of s are always less than some  $s_1$ , we expect that with  $M^s$  will be associated the low energy resonances in the s-channel. Further, since -- again within the s-strip -- the channels to which the resonances couple strongly are the two-particle thresholds in the s-channel, it is natural to incorporate these thresholds into  $M^s$ . Of course, identical considerations apply to  $M^t$  and  $M^u$  in the t and u channels respectively. Finally, we note from Figure 1 that the asymptotic behaviour in the s-channel is contained in  $M^t$  and  $M^u$ ; as at

high energies the multiparticle thresholds become important, it is reasonable to assign all the multiparticles s-channel thresholds to  $M^t$  and  $M^u$ .

In the s-channel, we may think of the decomposition of equation (1) as being of the form

$$M = M^s + V^s$$

where  $V^s$  is some "potential" acting in the s reaction. Our hope is to formulate a set of dynamical equations so that, given  $V^s$  as an input, we may calculate  $M^s$ . In this connection it is important to note that  $V^s$  both contains the low-lying resonances in the crossed variables and controls the asymptotic behaviour in the s-channel. Thus we might hope to parameterize  $V^s$  either by a few resonances in t and u or by a sum of Regge pole contributions; in fact, we shall see that both these parameterizations have been employed in the literature.<sup>6</sup> Note that if we can establish a procedure for calculating  $M^s$  given  $V^s = M^t$  and  $M^u$ , we can also obtain from it  $M^t$  given  $M^s + M^u$  and  $M^u$  given  $M^s + M^t$ . A self-consistent solution to the dynamics would thus represent a bootstrap.

To summarize this section, let me state succinctly the basic assumptions of the strip model. The amplitude may be written in the form

$$M = M^s + M^t + M^u .$$

Each of the terms is assumed to have Mandelstam analyticity,<sup>2</sup> that is, to satisfy a double dispersion relation similar to

$$M(s,t) = \frac{1}{2} \iint_{\pi}^{\infty} \frac{\rho(s',t')}{(s'-s)(t'-t)} ds' dt'$$

where we've ignored other double spectral terms for simplicity.

In addition,  $M^s$

- (1) contains the s-channel low-lying resonances and two-particle thresholds;
- (2) contains multiparticle thresholds in t and u;
- (3) approaches a limiting behaviour as  $s \rightarrow \infty$  such that  $M^s/V^s \rightarrow 0$  (since  $V^s = M^t + M^u$  is assumed to control the asymptotic behaviour);
- (4) is such that, as  $t \rightarrow \infty$  at fixed (small)  $|s|$ ,

$$M^s \simeq \beta(s) t^{\alpha(s)} .$$

This fourth property, the Regge asymptotic condition, is not always included as input into the model. The original strip model,<sup>(1)</sup> for instance, generates -- rather than assumes -- Regge behaviour in its dynamical equations.

### THEORETICAL IMPLICATIONS OF STRIP MODEL ASSUMPTIONS:

Before we attempt to formulate explicit dynamical equations, let me consider some of the immediate theoretical consequences of the "strip approximation" to the amplitude. To discuss this point and to simplify the later mathematical manipulations, I will henceforth consider the specific case of  $\pi$ - $\pi$  scattering as a single channel problem. Thus, the only two-body threshold in  $M^s$  will be the  $\pi$ - $\pi$  channel, and the multiparticle s-channel thresholds in  $M^t$  and  $M^u$  will begin with the  $4\pi$  branch point at  $16 m_\pi^2$ . Further, we may enjoy the advantages of no spin complications and equal mass kinematics. As we shall see, G-parity considerations and the existence of a well-established resonance (the  $\rho$ ) also make this a particularly favourable case. One clear disadvantage is that the  $\pi$ - $\pi$  interaction has not yet been directly measured. However, we shall suppose that it has the general features mentioned above and found in, say,  $\pi N$  scattering. In the following, I will suppress the isospin indices, as they are not essential to our purposes.

For the moment let me neglect the u-channel contribution for clarity. The amplitude may then be written

$$M = M^s + M^t ,$$

and our decomposition implies that there are no individual terms in the amplitude containing both s and t two-body thresholds. Similarly, there are no individual terms containing inelastic thresholds in both s and t. Using the singularity diagram we introduced earlier, we may illustrate this situation graphically; namely, the diagrams shown in Figures 2a and 2b are included in the strip approximation, but those shown in 2c and 2d are not. Note here the importance of the G-parity considerations in  $\pi$ - $\pi$  scattering. The diagram shown in Figure 2c cannot occur in  $\pi$ - $\pi$  scattering because G-parity forbids the  $3\pi$  couplings. If such a diagram were allowed, then the boundary of the true double spectral function,  $\rho(s,t)$ , would be as in Figure 3a, whereas the boundary of the strip approximation double spectral function would be as in Figure 3b. Since the model we have outlined would then fail to get even the boundary of  $\rho(s,t)$  correct, it would be very unsatisfactory. However, as G-parity considerations do apply, both the actual double spectral function and the strip approximation double spectral function have the boundary shown in Figure 3c.

Let us delve into these points in more explicit detail. If we introduce the notation  $M_s$  to denote the s-discontinuity of the amplitude, then the decomposition

$$M = M^s + M^t$$

implies that  $M_s^s$  is the full elastic discontinuity in the s-channel and that  $M_s^t$  is the full inelastic discontinuity in the s-channel; that is,

$$M_s^s \equiv M_{s-el}$$

$$M_s^t \equiv M_{s-inel}$$

and

$$M_t^t \equiv M_{t-el}$$

$$M_s^t \equiv M_{t-inel} \quad .$$

Using Mandelstam analyticity, we may write

$$M_{s-el} = \frac{1}{\pi} \int \frac{\rho_{s-el}}{(t'-t)} dt' \quad (2)$$

and

$$M_{s-inel} = \frac{1}{\pi} \int \frac{\rho_{s-inel}}{(t'-t)} dt' \quad . \quad (3)$$

Thus taking the t-discontinuity of (2),  $M_{s-el,t} \equiv M_{st}^s = \rho_{s-el}$  and, by analogy,

$$M_{t-el,s} \equiv M_{ts}^t = \rho_{t-el} \quad .$$

But taking the t-discontinuity of (3) gives

$$\rho_{s-inel}(s,t) = M_{s-inel,t} \equiv M_{st}^t = M_{ts}^t \equiv \rho_{t-el}(t,s) \quad . \quad (4)$$

Thus the essential approximation of the strip model consists in putting the inelastic part of the double spectral function equal to the (reflection of the) elastic part of the cross channel double spectral function. For the case of  $\pi\pi$  scattering, equation (4) is exact in the shaded region of Figure 3(c), that is, for the t-strip,

$$\frac{4s m_\pi^2}{(s-16m_\pi^2)} \leq t \leq \frac{16s m_\pi^2}{(s-16m_\pi^2)} \left[ 1 + \frac{8s m_\pi^2}{(s-16m_\pi^2)(s-4m_\pi^2)} \right]$$

and similarly for the s-strip. Outside this region, equation (4) is only an approximation, but inelastic effects are seen to play a central role in the model.

The strip model incorporates maximal analyticity of the first kind, including crossing, and also maximal analyticity of the second kind. A major remaining restriction is unitarity. In its most general form, unitarity is unmanageable. But we see that within the strip-model the entire amplitude is constructed from elastic double spectral functions, and these may be computed on the basis of unitarity by a technique due to Mandelstam.<sup>(2)</sup> The result "satisfies" unitarity to the extent that the inelastic discontinuity is adequately described by the above approximation.

THE MANDELSTAM ITERATION:

To begin the discussion let me introduce the so-called "signature decomposition"<sup>3</sup> of the amplitude in the s-channel, which divides M into two functions  $M^\pm$ , each having a branch cut in the  $\cos\theta_s \equiv z_s$  plane only for  $z_s > 1$ . In this context we consider the amplitude as a function of  $z_s$  rather than t because of the simpler symmetry properties in  $z_s$  than in t. We write

$$M = M^R + M^L$$

where  $M^R$  contains the cut beginning at  $z_s = 1 + 2 \frac{m_\pi^2}{q^2}$  and  $M^L$  the cut at  $z_s = -(1 + 2 \frac{m_\pi^2}{q^2})$  -- see Figure 4. This division is trivially possible simply by writing two dispersion integrals over the two (separated) cuts. Defining

$$M^\pm = [M^R(s, z_s) \pm M^L(s, -z_s)]$$

we find that

$$M(s, z_s) = \frac{1}{2}[M^+(s, z_s) + M^+(s, -z_s)] + \frac{1}{2}[M^-(s, z_s) - M^-(s, -z_s)] .$$

Thus the total decomposition of the amplitude is

$$M^\pm = M^{s\pm} + V^{s\pm}$$

where each individual term -- for example,  $V^{s+}$  -- has only a right-hand cut. The crucial point is that the two-particle unitarity integration maintains the  $\pm$  labelling -- that is,

$$\text{Im } M^\pm \propto \int d\Omega_{e1} (M^\pm)^* M^\pm .$$

This can be proved, for instance, by expanding the amplitude in partial waves. From this point, I will drop the (+) notation, but it is understood that in writing M we mean  $M^+$  or  $M^-$ .

The assumptions of analyticity allow us to write dispersion relations in  $t$  for both  $V^S$  and  $M^S$  separately,

$$V^S(s, t) = \frac{1}{\pi} \int_{\frac{4m_\pi^2}{2}}^{\infty} \frac{dt' V_t^S(t', s)}{(t' - t)} \quad (5)$$

and

$$M^S(s, t) = \frac{1}{\pi} \int_{\frac{16m_\pi^2}{2}}^{\infty} \frac{dt' M_t^S(t', s)}{(t' - t)} \quad (6)$$

A significant point here is that since  $M^S$  does not contain the  $\pi$ - $\pi$  threshold in the  $t$ -channel, its  $t$ -discontinuity begins at  $16m_\pi^2$ . Because  $M^S$  is defined to contain the entire 2-particle  $s$ -cut and no inelastic  $s$ -cuts, we have

$$\frac{1}{2i} [M^S(s+i\epsilon, z_s) - M^S(s-i\epsilon, z_s)] = \frac{q}{32\pi^2 \sqrt{s}} \int d\Omega' M(s-i\epsilon, z_s'') M(s+i\epsilon, z_s') \quad , \quad (7)$$

where  $4(q^2 + m^2) = s$  ,

$$z_s'' = z_s z_s' + \cos\phi' \sqrt{1-z_s^2} \sqrt{1-z_s'^2} \quad ,$$

and  $d\Omega' = d(\cos\theta') d\phi'$  .

If we define

$$\rho^S(s, t) = \frac{1}{2i} [M_t^S(s+i\epsilon, t) - M_t^S(s-i\epsilon, t)] \quad (8)$$

then  $\rho^S$  is the elastic double spectral function in the  $s$ -channel. Evidently,

$$M_t^S = \frac{1}{\pi} \int_{s_0(t)}^{\infty} \frac{ds' \rho^S(s', t)}{s' - s} \quad (9)$$

where  $s_0(t) = \frac{4(4m_\pi^2)}{t - 16m_\pi^2} + 4m_\pi^2$  is the boundary of  $\rho^S(s, t)$ .

Substituting from equations (5) and (6) into equation (7) and using equation (8) we obtain

$$\frac{1}{\pi} \int_{t_0(s)}^{\infty} \frac{\rho^s(s, t') dt'}{(t' - t)} \equiv \frac{1}{2i} [M(s + i\epsilon, z_s) - M(s - i\epsilon, z_s)] =$$

$$= \frac{q}{32\pi^2 \sqrt{s}} \int d\Omega' \left[ \frac{1}{\pi} \int_{4m^2}^{\infty} \frac{dt_1 M_t^*(s, t_1)}{t_1 + 2q^2(1 - z_s')} \right] \left[ \frac{1}{\pi} \int_{4m^2}^{\infty} \frac{dt_2 M_t(s, t_2)}{t_2 + 2q^2(1 - z_s'')} \right] \quad (10)$$

where  $t_0(s) = 16m^2 + \frac{4(16m^2)}{s - 4m^2}$ .

Doing the (non-trivial) angular integrations over  $d\Omega'^{(2)}$  we obtain

$$\frac{1}{\pi} \int_{t_0(s)}^{\infty} \frac{dt' \rho^s(s, t')}{(t' - t)} = \frac{1}{16\pi^2 q \sqrt{s}} \int_{4m^2}^{\infty} \int_{4m^2}^{\infty} \frac{dt_1 dt_2 M_t^*(s, t_1) M_t(s, t_2)}{K^{\frac{1}{2}}(t_1, t_2, t; q^2)}$$

$$\times \ln \frac{t - t_1 - t_2 - \frac{t_1 t_2}{2q^2} + \sqrt{K}}{t - t_1 - t_2 - \frac{t_1 t_2}{2q^2} - \sqrt{K}} \quad (11)$$

Here  $K(t, t_1, t_2; q^2) = t^2 + t_1^2 + t_2^2 - 2t_1 t_2 - 2t t_1 - 2t t_2 - \frac{t_1 t_2 t}{q^2}$ .

In the s-channel physical region,  $t < 0$  for all values of  $t_1$  and  $t_2$  in the region of integration, so  $K > 0$  and the integrand is non-singular. We can obtain an explicit equation for  $\rho^s(s, t)$  by taking the t-discontinuity of both sides of equation (11). Since evaluating the discontinuity of the right-hand side requires a rather subtle argument, let me outline the calculation briefly. Viewed as a function of  $t$  for positive real  $t_1$  and  $t_2$ ,  $K(t, t_1, t_2; q^2)$  is as shown in Figure 5. Its zeros are at

$$t_{\pm} = t_1 + t_2 + \frac{t_1 t_2}{2q^2} \pm 2 \left[ t_1 t_2 \left( 1 + \frac{t_1}{4q^2} \right) \left( 1 + \frac{t_2}{4q^2} \right) \right]^{\frac{1}{2}},$$

both of which are greater than zero and thus at unphysical values of  $t$  in the s-channel. If we continue equation (10) as a function of  $t$  from  $t < 0$  into the region  $t > 0$ , the first potential singularity we will encounter occurs at  $t_-$ .

However, encircling this point in the  $t$ -plane shows that the possible singularity arising from  $K^{-\frac{1}{2}} \rightarrow -K^{-\frac{1}{2}}$  is cancelled by a minus sign coming from the inversion of the argument of the logarithm, which is evaluated on its principal

branch. Above  $t_-$ , since  $K < 0$ , the logarithm acquires an imaginary part which changes in such a way that near  $t_+$  one finds

$$\ln x = \ln x + 2\pi i$$

thus at  $t = t_+$  the cancellation of the potential singularity from  $K^{-\frac{1}{2}}$  cannot occur, and we find

$$\rho^s(s, t) = \frac{1}{8\pi^2 q \sqrt{s}} \int_{\frac{4m^2}{\pi}}^{K=0} \int dt_1 dt_2 \frac{M_t^*(s, t_1) M_t(s, t_2)}{K^{\frac{1}{2}}(t, t_1, t_2; q^2)} \quad (12)$$

where the region of integration is shown in Figure 6. Within this region of integration it is always true that  $K \geq 0$  and that

$$t \geq t_{\pm} = t_1 + t_2 + \frac{t_1 t_2}{q} + 2 \left[ t_1 t_2 \left( 1 + \frac{t_1}{4q} \right) \left( 1 + \frac{t_2}{4q} \right) \right]^{\frac{1}{2}}$$

so that

$$t \geq (\sqrt{t_1} + \sqrt{t_2})^2 \quad (13)$$

for all  $s$ .

This final inequality is extremely important, for it allows an iterative solution for the amplitude  $M^s$  to be constructed, given  $V^s$ . To see this recall that from equation (9) we may write

$$M_t^s = \frac{1}{\pi} \int_{s_0(t)}^{\infty} \frac{ds' \rho^s(s', t)}{s' - s} + V_t^s \quad (14)$$

In this equation the first term is zero below  $t = 16m_{\pi}^2$  but the second is non-zero above  $t = 4m_{\pi}^2$ . Hence the full  $t$ -discontinuity of the amplitude between  $t = 4m_{\pi}^2$  and  $t = 16m_{\pi}^2$  comes from the "potential" term, which we assume is known. Above  $t = 16m_{\pi}^2$  we must add to this known discontinuity the one calculated from the dispersion integral over  $\rho^s(s, t)$ . Equation (13) and the form of the region of integration in equation (12) guarantee that knowing  $M_t^s$  up to  $t = \tilde{t}$  implies that we may calculate, from equation (12),

$$\rho^s(s, t) \text{ up to } t = (\sqrt{\tilde{t}} + \sqrt{4m_{\pi}^2})^2 .$$

Since we are given  $M_t^s (= V_t^s)$  up to  $t = 16m_{\pi}^2$ , we may calculate  $\rho^s$  up to  $36m_{\pi}^2$ , from which we may generate  $\rho^s$  up to  $64m_{\pi}^2$ . Thus the dynamics of the strip model is contained in equations (12) and (14), which are solved by the Mandelstam



iteration technique.<sup>(2)</sup> In the next lecture I shall mention briefly the results of this procedure, but spend more time discussing the difficulties, related to convergence problems for the integrals, which affect the model.

Let me close with a brief digression on the relationship of the strip model to the multiperipheral model we studied earlier. Although this connection is somewhat tenuous and not mathematically precise, it does illustrate that similar physical approximations and assumptions are being used.

Recall that in the MPM we approximated inelastic unitarity by a sum of terms of the form

$$\text{Im}_{\text{inel}} M = \sum_{n>2} \int M_n^* M_n d\Omega_n$$

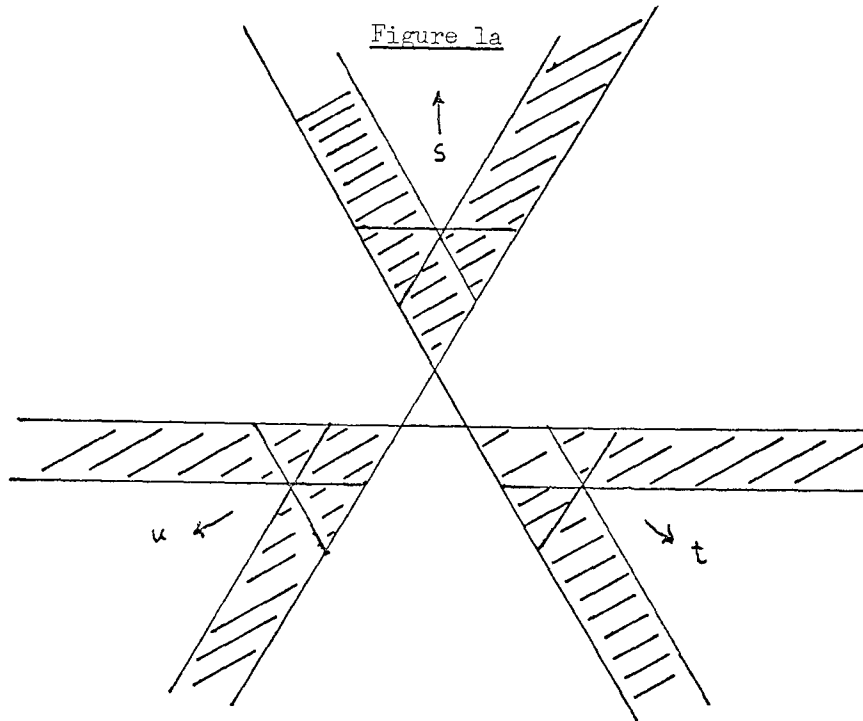
where  $M_n$  corresponded to the multiperipheral amplitude for a  $2 \rightarrow n$  production process. (See Figures 7 and 8 and note that we are ignoring G-parity.) We see immediately that, in Figure 8, if we "cut" the singularity diagram with a line in the t-sense, we always have a two-particle state. In taking the sum over all n, we are of course summing over all k in Figure 8 so that we are approximating the full amplitudes shown in Figure 9. But this looks remarkably similar to our strip model approximation that  $\rho^{s\text{-inel}} = \rho^{t\text{-el}}$ .

Note the crucial difference that in the strip model diagram of Figure 10 the t-lines are on mass shell  $\delta$ -functions whereas in Figure 9 they represent poles.

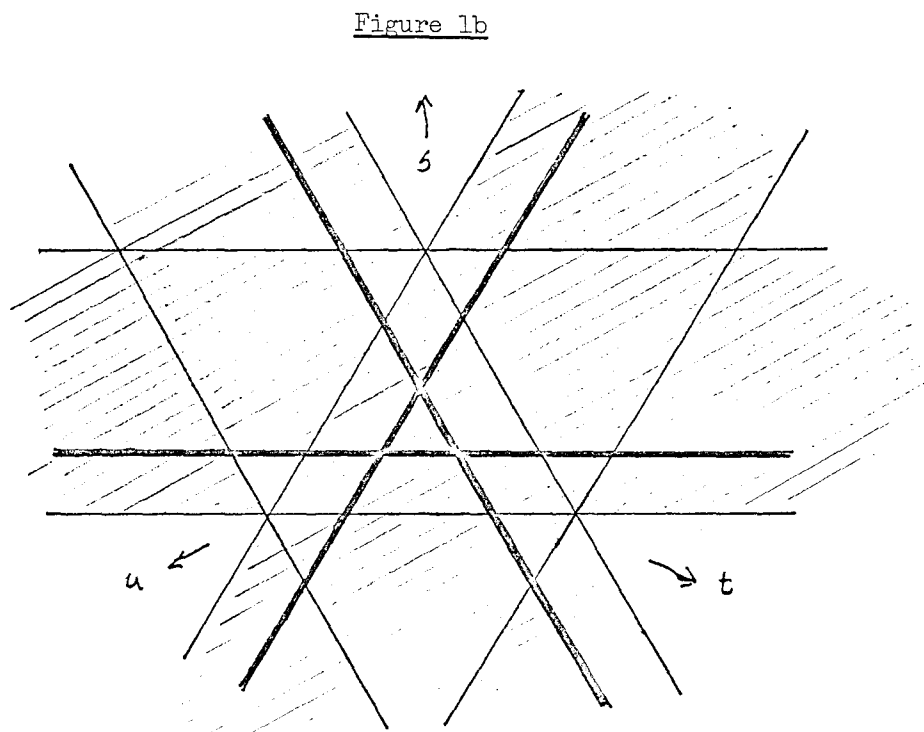
Conversely, by analogy with potential theory, we may think of the Mandelstam iteration as reconstructing<sup>(8)</sup> the Born series, as indicated in Figure 11 for the t-channel being the direct channel. Here the t-channel always contains two-particle states, and taking the t-channel discontinuity ( $= \text{Im}_{t\text{-el}} M$ ) gives, roughly speaking, the same correspondence as deduced above between the two models.

#### REFERENCES

1. G.F. Chew and S. Frautschi, Phys. Rev. 123, 1478 (1961).
2. S. Mandelstam, Phys. Rev. 112, 1344 (1958).
3. G.F. Chew and C.E. Jones, Phys. Rev. 135, B208 (1964).
4. P.D.B. Collins and R. Johnson, Phys. Rev. 177, 2472 (1968); 182, 1755 (1969).
5. For a general discussion of these models see:  
(a) G.F. Chew, The Analytic S-Matrix, W.A. Benjamin, New York (1966); (b) P.D.B. Collins and E.J. Squires, Regge Poles in Particle Physics, Springer Tracts in Modern Physics, Vol. 45, Springer-Verlag, Berlin (1968), Chap. VI, Sections 6 and 7.
6. (a) B.M. Brandsen, Nuovo Cimento 30, 207 (1963); (b) N.F. Bali, G.F. Chew and S-Y. Chu, Phys. Rev. 150, 1352 (1966). These references parametrize the potential by low energy t-channel resonances. References 3 and 4 use Regge poles.
7. The notation  $V_t^s(t',s)$  is introduced to agree with that of Ref. 6(b).
8. R. Blankenbecler, M.L. Goldberger, N.N. Khuri and S.B. Treiman, Ann. Phys. (N.Y.) 10, 62 (1960).

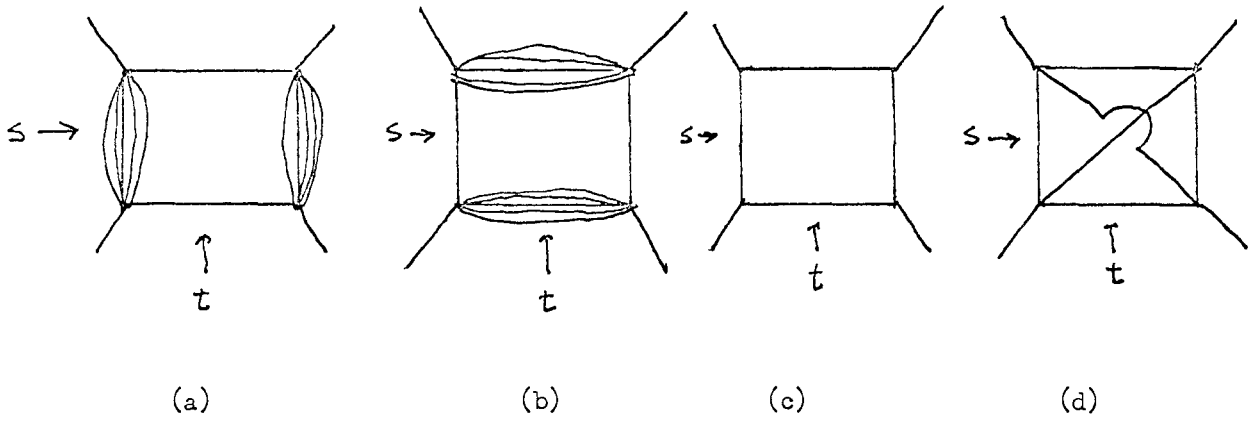


The parts of the physical region in which the  $2 \rightarrow 2$  amplitude is large



THE THREE STRIPS IN THE MANDELSTAM PLOT

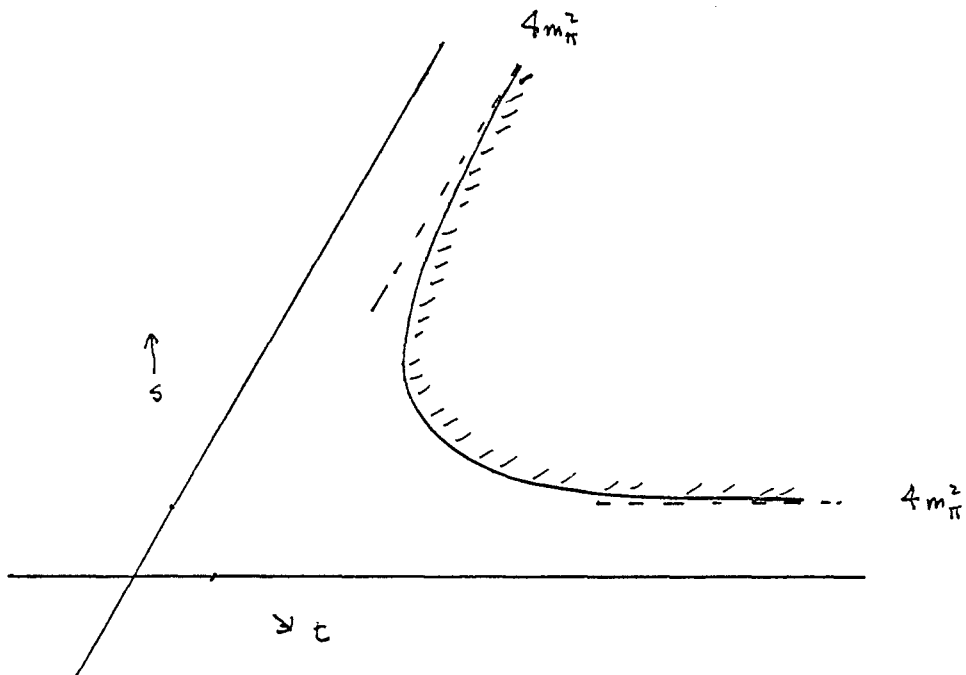
Figure 2



SINGULARITY DIAGRAMS INCLUDED  
IN STRIP APPROXIMATION

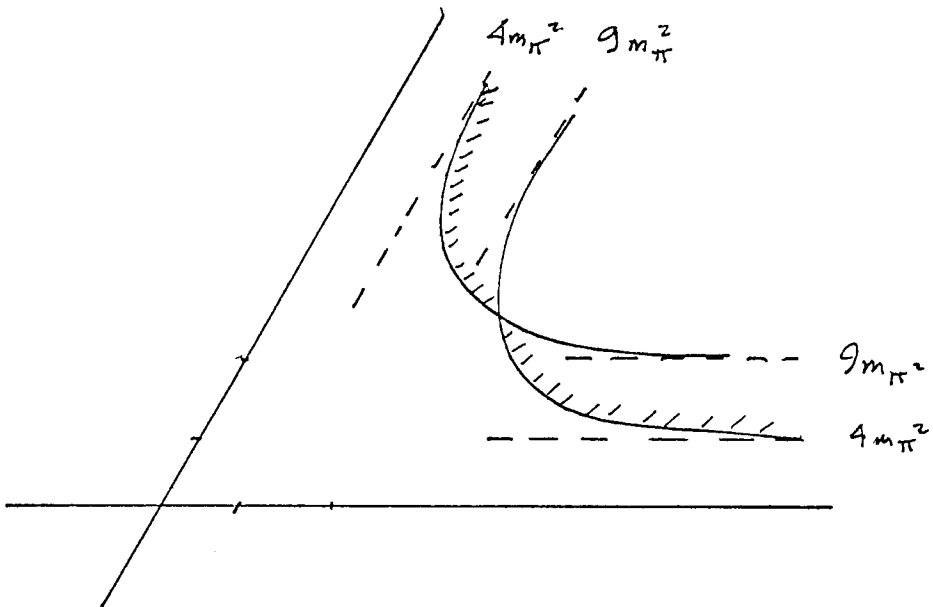
SINGULARITY DIAGRAMS NOT INCLUDED  
IN STRIP APPROXIMATION

Figure 3a



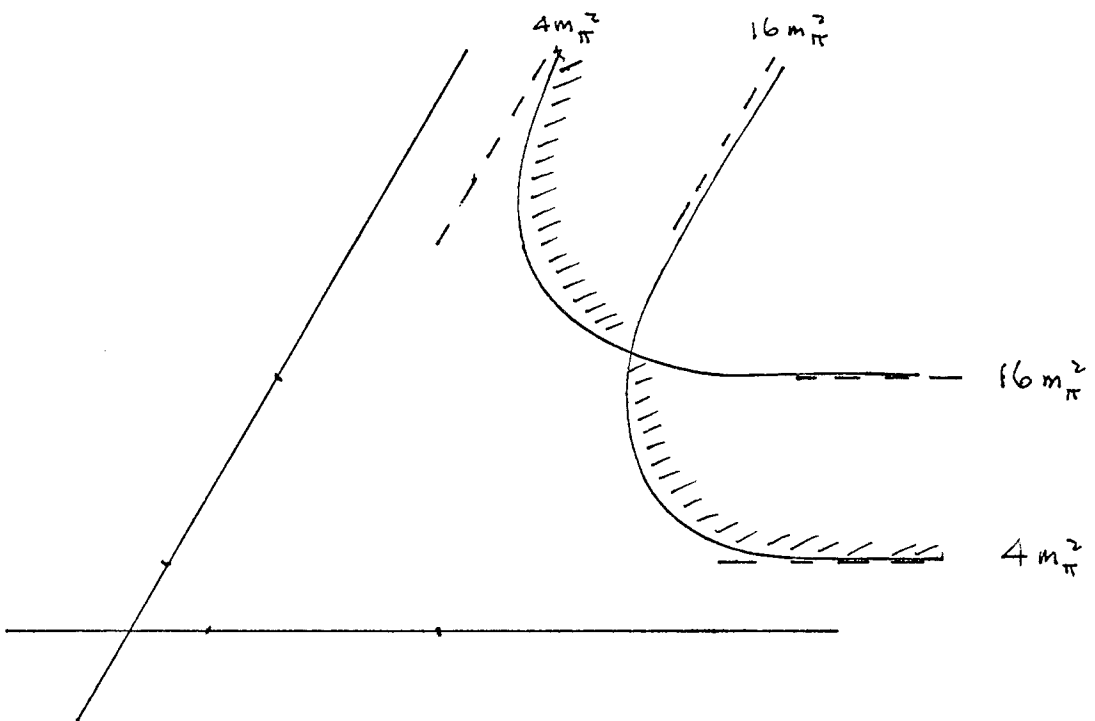
BOUNDARY OF TRUE  $\rho(s,t)$  FOR  $\pi-\pi$  SCATTERING WITHOUT  $G$ -PARITY

Figure 3b



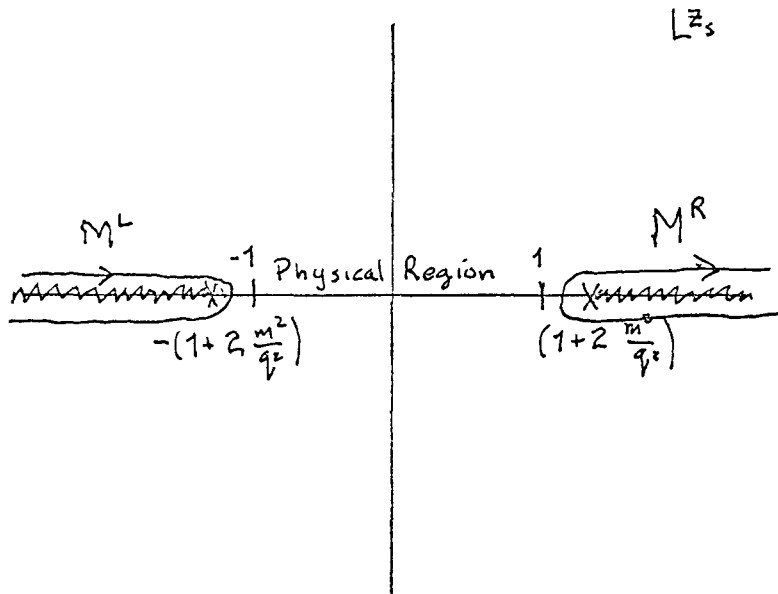
BOUNDARY OF STRIP APPROXIMATION  $\rho(s,t)$  FOR  $\pi$ - $\pi$  SCATTERING WITHOUT  $G$ -PARITY

Figure 3c



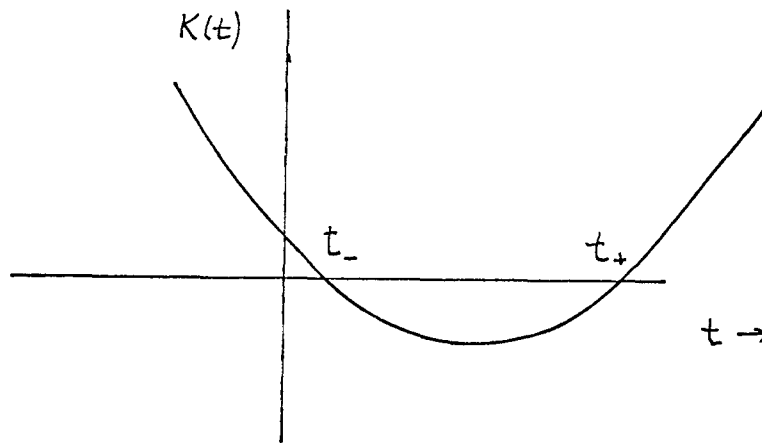
BOUNDARY OF  $\rho(s,t)$  FOR  $\pi$ - $\pi$  SCATTERING WITH  $G$ -PARITY

Figure 4

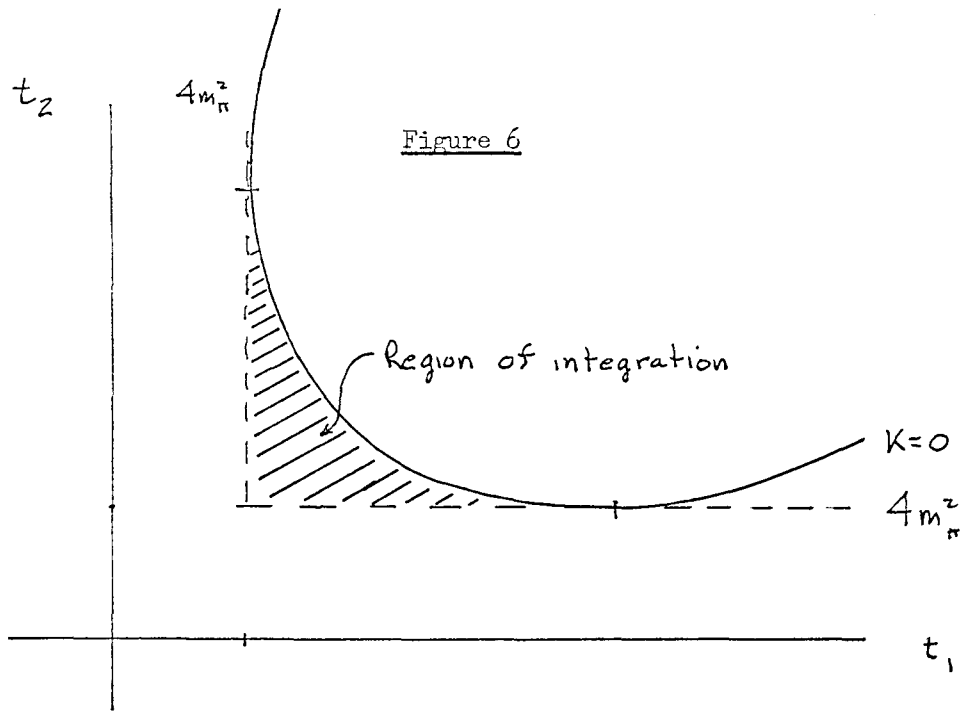


THE DEFINITION OF  $M^L$  AND  $M^R$  BY DISPERSION INTEGRALS

Figure 5

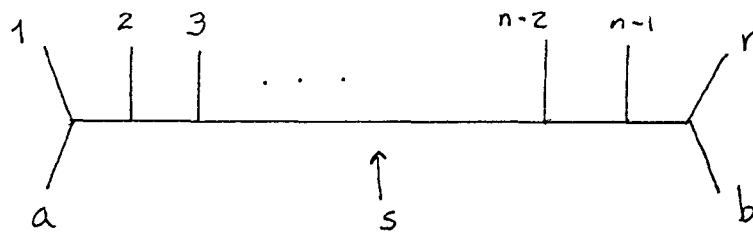


$K(t, t_1, t_2; q^2)$  PLOTTED AGAINST  $t$  AT FIXED  $t_1, t_2, q^2 > 0$



REGION OF INTEGRATION FOR EQUATION (10)

Figure 7



THE MULTIPERIPHERAL MODEL FOR A  $2 \rightarrow n$  PRODUCTION PROCESS

Figure 8

$$\text{Im}_{s\text{-inel}} M = \sum_{\substack{k > 1 \\ (n > 2)}} \int d\mathcal{R}_n$$

THE APPROXIMATION TO INELASTIC UNITARITY IN THE MULTIPERIPHERAL MODEL

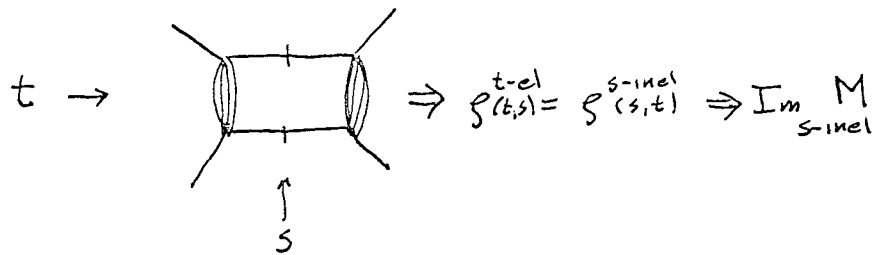
Figure 9

$$\text{Im}_{s\text{-inel}} M =$$

FULL AMPLITUDES  $A_1$  AND  $A_2$  (MINUS POLE TERMS) IN THE APPROXIMATE INELASTIC UNITARITY EQUATION

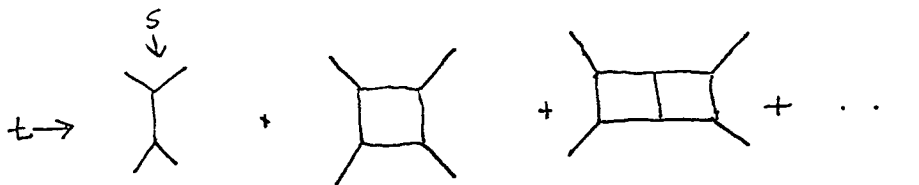


Figure 10



ELASTIC UNITARITY IN THE  $t$ -CHANNEL GIVES, IN STRIP MODEL, INELASTIC UNITARITY IN  $s$ -CHANNEL

Figure 11



THE MANDELSTAM ITERATION RECONSTRUCTING THE BORN SERIES

CONVERGENCE DIFFICULTIES AND REGGE ASYMPTOTIC BEHAVIOUR:

In the last lecture I mentioned that "convergence" difficulties plague the original strip model in the form we've discussed so far. As these problems must be resolved before any useful results can be obtained, let me deal with them directly, before going on to summarize the outcome of this approach.

Recall that our fundamental equations were

$$\rho^S(s,t) = \frac{1}{8\pi^2 q\sqrt{s}} \int_{-2}^{K=0} \int_{-2}^2 \frac{dt_1 dt_2 M_t^*(t_1, s) M_t(t_2, s)}{K^2(t, t_1, t_2; q^2)} \quad (1)$$

and

$$M_t(t, s) = \frac{1}{\pi} \int_{s_0(t)}^{\infty} \frac{ds' \rho^S(s', t)}{(s'-s)} + V_t^S(t, s) \quad (2)$$

From these we could calculate the amplitude via  $M + M^S + V^S$  and

$$M^S = \frac{1}{\pi} \int_{-2}^{\infty} \frac{M_t^S(t', s) dt'}{16m^2 (t'-t)} \quad (3)$$

But in writing equation (3) in the form shown, we've assumed that  $M_t^S$  vanishes as  $t \rightarrow \infty$  so that the integral converges. In general, this will not be the case. In particular, if  $M^S(s, t)$  has an s-channel pole, then the integral cannot converge. This follows in the simple case of one S-wave resonance by noting that, if

$$M^S = \frac{g^2}{s-m} + \tilde{M}^S \quad (4)$$

then  $M_t^S = \tilde{M}_t^S$ , where  $\tilde{M}^S$  does not contain the s-channel pole. Thus if both (3) and (4) are to hold, the  $t'$  integral must diverge and the subtraction term necessary to define the integral in the standard sense can then be identified with the resonance parameters.

Assuming that, in the general case,  $M_t^S$  does not vanish as  $t \rightarrow \infty$ , how do we evaluate the integral in equation (3)? Let me discuss two approaches.

The most direct way to gain convergence is, as I've indicated, to introduce subtractions in the  $t'$  integration. In the so-called "S-wave dominant" model for the  $\pi$ - $\pi$  interaction, Chew and Mandelstam<sup>(1)</sup> introduced one subtraction by writing

$$M(s, t) = f_0(s) + \frac{t}{\pi} \int_0^{\infty} \frac{dt'}{(t'-t)t'} M_t^S(t', s).$$

Here the function  $f_0(s)$  is a constant with respect to  $t$ : hence the name "S-wave dominant" model. Even after imposing unitarity, via the N/D technique, the subtraction term still contains one free parameter,  $\lambda$ , if one does not require that the S-wave amplitude coincide with the continuation of the Froissart-Gribov amplitude to the point  $\ell = 0$ . This freedom, at the time the model was proposed, was considered desirable, for  $\lambda$  could correspond to the fundamental coupling constant in the  $\phi^4$  Lagrangian field theory of the  $\pi$ - $\pi$  interaction. But although Atkinson<sup>(2)</sup> has proved rigorously that consistent solutions satisfying crossing and unitarity exist to the reciprocal equations we wrote down for  $M_t^S$  and  $\rho^S(s,t)$ , when one introduces a subtraction in equation (3), the solutions (which had already been obtained numerically before Atkinson's proof) are rather uninteresting. The  $\rho$  resonance, for example, does not appear. This leads us to seek another way, other than the simple subtractions, by which to define the integral in equation (3) when the discontinuity does not vanish as  $t \rightarrow \infty$ .

The alternative approach we have called "second-degree analyticity" and was suggested by Chew and Frautschi,<sup>(3)</sup> who, motivated by Regge's work on potential theory, postulated that all physical angular momentum values be connected by the Froissart-Gribov interpolation. The asymptotic form of the amplitude and its  $t$  discontinuity are then unambiguously connected. For example, if the leading  $J$  singularity is a simple pole at  $J = \alpha(s)$ ,

$$M_t^S(s,t) \xrightarrow{t \rightarrow \infty} \frac{r(s) P_{\alpha(s)}(-Z_s)}{\sin \pi \alpha(s)} \approx \frac{\tilde{\beta}(s) t^{\alpha(s)}}{\sin \pi \alpha(s)} \quad (5)$$

and

$$M_t^S(t,s) \xrightarrow{t \rightarrow \infty} r(s) P_{\alpha(s)}(Z_s) \approx \beta(s) t^{\alpha(s)} \quad (6)$$

Note that  $M^S$  contains  $s$  poles while  $M_t^S$  does not. Nevertheless, according to second-degree analyticity, the amplitude is completely determined by its discontinuities. If we can find a region of  $s$  in which  $\alpha(s) < 0$  so that the integral in equation (3) converges, we can define the expression for all values of  $\alpha(s)$  by analytic continuation. Both in potential theory and in the ladder diagram models of perturbation theory, the behavior of the real part of the Regge trajectory, as shown in Figure 1, guarantees that such a region exists.

The crucial point is that, although one might still say that "subtractions" are needed when one continues into the region where  $\alpha(s) > 0$ , these subtractions are completely determined if the discontinuity -- and thus  $\alpha(s)$  by equation (6) -- is known. Hence there are no fundamental constants corresponding to elementary particles or their couplings in this approach.

In practice we do not need to make an explicit continuation to determine  $M^S$  given  $M_t^S$ . Rather, since we know that the asymptotic form of the discontinuity is given by (6), we can subtract from  $M_t^S$  the leading Regge terms. To identify the Regge functions  $\alpha(s)$  and  $\beta(s)$  we can use the Mandelstam iteration -- subject to a cut-off requirement that I'll mention in a moment -- to calculate  $M_t^S$  out to large  $t$  and, by comparing our results with the form implied by (6), deduce  $\alpha(s)$  and  $\beta(s)$ . We'll discuss this method in more detail in the next section. We may then write an expression involving a convergent integral plus Regge terms for  $M^S$ . Although this expression will be formally similar to that obtained by making subtractions at infinity, let me emphasize once more that now there are no arbitrary subtraction constants in the equations.

We have so far resolved the first convergence problem. Our solution was to invoke the "Regge boundary condition," or, as we've sometimes called it, maximal analyticity of the second kind. There remains a second difficulty, which can only loosely be called a "convergence" problem. It is that, in general, our calculational procedure involving the Mandelstam iteration provides no guarantee that  $M^S(s,t)$  becomes small compared to  $V^S$  outside the  $s$ -strip. This requirement is crucial for the consistency of the model, as  $V^S$  is assumed to dominate at asymptotic values of  $s$ . In fact we can show that our iteration scheme is such that, if the "potential,"  $V^S$ , contains as input elementary particle poles of spin greater than one or Regge poles for which  $\alpha(s) > 1$  for any  $s > 0$ , then  $M_t^S(t,s)$  will grow explosively with increasing  $s$ . To see this, recall that in equations (1) and (2) the relevant regions of the invariants in which to evaluate  $\rho^S(s,t)$  and  $M_t^S(t,s)$  are  $s$  and  $t$  both greater than 0. Suppose that for some region of  $t > 0$ ,  $V_t^S \approx s^{\alpha(t)}$  with  $\alpha(t) > 1$ . Then equation (1) implies  $\rho^S(s,t)$  will receive a contribution -- just by putting  $t_1 = t_2$  in the integral -- of the form

$$\rho^S(s,t) = s^{2\alpha(t_1)-1}$$

for  $t \geq 4t_1$ . Equation (2) then implies that  $M_t^S(t,s)$  will have the same behaviour, and thus a second iteration gives

$$\rho^S(s,t) = s^{4\alpha(t_1)-3}$$

for  $t \geq 16t_1$ . Similarly, the  $n^{\text{th}}$  iteration gives

$$\rho^S(s,t) = s^{2^n \alpha(t_1) - 2^n + 1}$$

for  $t \geq 4^n t_1$ . For  $\alpha(t_1) > 1$ , this leads to an increasing asymptotic behavior for  $M^S(s, t)$  in  $s$  as  $t$  increases. <sup>(4)</sup>

When analyzed in detail the above phenomenon corresponds to the development of Regge cuts, resulting from the iteration of Regge poles. With linear pole trajectories the leading cut always lies below the leading pole for positive  $t$  (it turns out that  $\alpha_c(t) = 2\alpha(t/4) - 1$ ), and so at large  $s$  the function  $M^S$  remains small compared to  $V^S$ . However, it is computationally difficult to handle indefinitely-rising powers in the strip model, and, at present, in the literature this difficulty has been circumvented by inserting a high  $s$  cut-off of some sort. In the next section, I'll mention two forms of the cut-off and discuss the results finally obtained from the cut-off, convergent equations.

#### RESULTS FROM THE STRIP MODEL WITH A NON-REGGE POTENTIAL:

At least two explicit strip model numerical calculations using non-Regge potentials have been published. <sup>(5)</sup> In reference (5a) the necessary cut-off in  $s$  was obtained by letting the potential,  $V^S(s, t)$ , approach zero rapidly above some critical value,  $s_1$ . This is in conflict with our assumption that  $V^S(s, t) \approx \beta(t) s^{\alpha(t)}$  as  $s \rightarrow \infty$ , but since the calculations of reference (5a) are concerned with the limit  $t \rightarrow \infty$ , in which  $M^S$  is expected to dominate, this conflict may not be serious. In reference (5b) use is made of a simpler, and in view of our assumptions, perhaps more justifiable cut-off. Equation (1) is re-written in the form

$$\rho^S(s, t) = \frac{g(s)}{8\pi^2 q\sqrt{s}} \int \int_{4m^2}^{K=0} \frac{M_t^* M_t dt_1 dt_2}{K^{\frac{1}{2}}(t, t_1, t_2; q^2)}$$

where  $g(s)$  goes rapidly to zero above  $s = s_1$ , the edge of the unphysical strip.

In both cases the input to the model is the potential  $V^S$ , parameterized in terms of one or more elementary particle poles. The equations of the Mandelstam iteration are then used to calculate  $M^S$  to high values of  $t$ , for which we expect  $M_t^S \approx \beta(s) t^{\alpha(s)}$ . From this equation we see that  $\alpha(s)$  and  $\beta(s)$  may be calculated from

$$\begin{aligned} \ln |M_t^S(t, s)| &= \ln \beta(s) + \operatorname{Re} \alpha(s) \ln t \\ \arg [M_t^S(t, s)] &= \arg \beta(s) + \operatorname{Im} \alpha(s) \ln t \quad . \end{aligned} \quad (7)$$

I should note that in both potential theory <sup>(6)</sup> and the cut-off relativistic theory <sup>(5b)</sup> it has been shown that the Mandelstam iteration does in fact lead to Regge asymptotic behavior; thus, in particular, equation (7) can be applied.

In practice an approximately determinable asymptotic power,  $\alpha(s)$ , can be recognized after only three Mandelstam iterations.<sup>(7)</sup>

The general shape of the output trajectories is as shown in Figure 2. Note that in the strip model we expect trajectories to "turn over" at large positive values of their arguments. Assuming that  $\alpha(s)$  satisfies a dispersion relation

$$\alpha(s) = \alpha(\infty) + \frac{1}{\pi} \int_{-\infty}^{\infty} \frac{\text{Im } \alpha(s') ds'}{(s' - s)} \quad ,$$

this behaviour follows immediately from the fact that  $\text{Im } \alpha(s) \rightarrow 0$  outside the strip.<sup>(8)</sup>

Since both calculations employed elementary particles as input and got Regge poles as output, they were not attempting to find self-consistent, bootstrapping solutions. However, in both cases the elementary  $\rho$  pole was included in the input potential and an output Regge trajectory, with isospin = 1, could be made to satisfy

$$\alpha^{I=1} \left( m_{\rho}^2 \right) = 1$$

for reasonable values of the input and cut-off parameters. The width of this " $\rho$ " meson, however, was much too large. In addition, the slope of the  $\rho$  trajectory was too small. A second trajectory, one with  $I = 0$  and the quantum numbers of the vacuum -- therefore a candidate for the Pomeranchuk trajectory -- was also generated. Its properties were similar to those of the  $\rho$  trajectory and thus only partly satisfactory.

#### THE "NEW" STRIP APPROXIMATION:

From the point of view of the bootstrap philosophy, the calculations we've just outlined are somewhat unsatisfactory. Rather than utilizing the full crossing symmetry of the  $\pi$ - $\pi$  system, the previous models have used elementary particle poles as input to generate output Regge poles. An almost equivalent statement is that the original strip model calculations have not made full use of the fourth fundamental postulate of S-matrix theory, that of maximal analyticity of the second kind.

To remedy this defect Chew and Jones<sup>(9)</sup> proposed the "new" strip model. Taking over bodily the physical arguments about the strips of the Mandelstam plot being the important regions in which the amplitude is large, they noted that, since Regge poles both contain low energy direct channel resonances and control asymptotic behaviour in the crossed channel, within the strip region a sum of

Regge poles could perhaps provide a good approximation to the amplitude. Since the strip structure is maintained, the decomposition of the amplitude is still

$$M = M^S + M^t + M^u \quad ,$$

where all three terms now have Regge forms. Hence the new strip approximation to the amplitude may be written, including signature, as

$$\begin{aligned} M(s,t,u) = & \sum_i (R_i^S(s,t) + \xi_i R_i^S(s,u)) + \sum_j (R_j^t(t,s) + \xi_j R_j^t(t,u)) \\ & + \sum_k (R_k^u(u,s) + \xi_k R_k^u(u,t)) \quad , \end{aligned} \quad (8)$$

where the sums over  $i$ ,  $j$ , and  $k$  are over the leading Regge trajectories and  $\xi_i$  is the signature factor of the  $i^{\text{th}}$  trajectory. Here  $R_i^S(s,t)$  is a specific function, whose form we shall discuss later, which contains an  $s$ -channel Regge pole. The Regge trajectories involved are then to be determined self-consistently from the dynamical equations.

One cornerstone of the original strip model which we must be careful to include in the "new" model is maximal analyticity of the first kind. This requirement can be invoked by insisting that each individual Regge term satisfy the Mandelstam representation. What does our new model suggest about the double spectral functions? Now an  $s$ -channel Regge pole term would be expected to provide a significant contribution to the double spectral function only outside the  $t$ -channel resonance region -- that is for  $t > t_1$ , with  $t_1 \approx 3 \text{ GeV}^2$ . For such values of  $t$ , the actual boundary curve of the double spectral function is approximately the line  $s = s_0$ . Applying identical considerations in the  $t$ -channel -- and limiting ourselves for the moment to  $\rho_{st}(s,t)$  -- we find that we should try to construct a Regge term with a non-zero double spectral function in the shaded region of Figure 3. The upper limit of the  $s$ -strip,  $s_1$ , again marks the edge of the region in which two-particle thresholds and low-lying resonances are dominant.

Clearly, one obvious defect of this approximation is that the "corners" of the double spectral functions have been neglected. Arguments have been proposed<sup>(9c)</sup> that these regions are unimportant, but, as we shall later see, this omission is connected with the fundamental difficulty in the new strip model.

An explicit expression for a Regge term satisfying all the above considerations is<sup>(9b)</sup>

$$R_i^S(s, t) = \frac{1}{2} [2\alpha_i(s) + 1] \gamma_i(s) (-q_s^2)^{\alpha_i(s)} \times \left\{ \frac{-\pi}{\sin \pi \alpha_i(s)} P_{\alpha_i(s)} \left( 1 + \frac{t}{2q_s^2} \right) + \int_{-1 - \frac{t_1}{2q_s^2}}^1 \frac{P_{\alpha_i(s)}(Z')}{Z' + 1 + \left( \frac{t}{2q_s^2} \right)} \right\} . \quad (9)$$

Note that this contains both s-channel resonance poles, via the Regge pole, and s-channel two-particle thresholds, via the trajectory and residue functions  $\alpha(s)$  and  $\gamma(s)$ . Further, its double spectral function has the boundary shown in Figure 4; recall that the upper limit,  $s_1$ , must be imposed by the dynamical equations.

To formulate dynamical equations for the model we invoke two-particle unitarity. Although one could proceed as in the original strip model with the Mandelstam iteration technique, historically the N/D method was chosen. The motivation for this choice is that the N/D equations provide a simpler scheme for numerical calculations. The Mandelstam iteration procedure, since it involves functions of two variables and since  $K^{-\frac{1}{2}}$  is infinite on the integration boundary, requires high numerical accuracy.

The N/D technique involves the partial wave projection of  $M(s, t)$  in, say, the s-channel. Let me call this projection  $B_1(s)$ . Let us then define

$$B_1^P(s) = B_1(s) - \frac{1}{\pi} \int_{s_0}^{s_1} \frac{\text{Im } B_1(s')}{(s' - s)} ds'$$

and note that  $B_\ell^P(s)$  contains no s poles and correspondingly is holomorphic in  $\ell$  for  $\text{Re } \ell \geq 0$ . As  $s \rightarrow \infty$ ,  $B_1(s) \rightarrow B_1^P(s)$ ; in fact,  $s_1$  is the point above which  $B_1(s) \simeq B_1^P(s)$ . Note the (inexact<sup>(9b)</sup>) analogy to the original strip model's decomposition

$$M = M^S + V^S ,$$

where  $M \rightarrow V^S$  as  $s \rightarrow \infty$ .

If we now write  $B_1 = N_1/D_1$  and demand that  $N_1$  contain all the singularities of  $B_1^P$ , then  $D_1$  will have only the "strip" cut from  $s_0$  to  $s_1$ . Imposing two-particle unitarity,

$$\text{Im } B_1(s) = \rho_\ell(s) B_1^*(s) B_1(s) ,$$

on  $D_1$  in this region implies



$$\text{Im } D_1(s) = -\rho_\ell(s) N_1(s) \quad ,$$

and, with second-degree analyticity, leads eventually to an integral equation for  $N_1(s)$ ,

$$N_1(s) = B_1^P(s) + \frac{1}{\pi} \int_{s_0}^{s_1} \frac{ds' [B_\ell^P(s') - B_\ell^P(s)]}{(s'-s)} \rho_\ell(s') N_\ell(s') \quad . \quad (10)$$

The method of solution is to parameterize the input Regge functions,  $\alpha(t)$  and  $\gamma(t)$ , in an appropriate manner, to calculate  $B_1^P(s)$ , and then to solve equation (10) numerically.

Unfortunately, the solutions obtained in this manner are far from satisfactory.<sup>(10)</sup> If one inputs only a  $\rho$  meson trajectory, both a  $\rho$  and a P emerge. Further, the output  $\rho$  trajectory,  $\alpha_\rho(s)$ , does not pass through 1 for  $s > 0$ . Including both  $\rho$  and P as inputs leads to even worse results. If the P is added in a straightforward manner, the  $\rho$  ends up as a ghost state on the physical sheet.

To discover the source of the difficulties mentioned above, Collins went back to potential theory. Here the input of the two Regge poles,  $\rho$  and P, corresponds to the superposition of two potentials, one attractive and one repulsive, as shown in Figure 5. If in this potential theory model Collins took the left-hand cut in  $B_\ell$  to be just the cut of the potential, which in fact corresponds to the Born approximation, then ghost states similar to ghost " $\rho$ " mentioned previously could arise. Of course, such states do not exist in the full solution to the Schrödinger equation and arise simply because of the inadequacy of the approximation. Now the Mandelstam iteration we've outlined previously yields in the limit of an infinite number of iterations the exact solution to the Schrödinger equation.<sup>(11)</sup> Thus, Collins argued, in the relativistic problem perhaps by iterating the Regge "potential" through the Mandelstam equations several times, thereby obtaining the correct boundary for the double spectral function, one might be able to overcome the inadequacies of the model. This is the procedure followed in the Collins-Johnson version of the strip model, to which I now turn.

#### COLLINS-JOHNSON MODEL:

Collins and Johnson's method for implementing the strip model begins by adopting the approximation to the amplitude given in equation (8), but written in the form, for the s-channel,

$$M = M^S + V^S \quad .$$

Then, using the Mandelstam iteration with  $V^s$  as input, they calculate the corner of the s-channel elastic double spectral function from the true boundary to  $t = t_1$  (see Figure 6). Above  $t_1$ , of course, the Regge form of the amplitude is already assumed to give the double spectral function to sufficient accuracy. Crossing and the knowledge of  $\rho^{s-el}(s,t)$  enable them to evaluate the corners of  $\rho^{t-el}$  and  $\rho$  as well. Note that, in the spirit of the original model, we could include an approximation to inelastic effects by setting

$$\rho^{t-el}(s,t) = \rho^{s-inel}(s,t) \quad .$$

In fact, Collins and Johnson do use this approximation to incorporate inelastic effects, by a technique developed by Frye and Warnock,<sup>(13)</sup> on the far right-hand cut of the N/D equations. In the next step, the contributions of the original potential and the corner of the double spectral function (region X of Figure 6) to the (left-hand cut of the) partial wave,  $B_1(s)$ , are calculated. The result is then fed into the Frye-Warnock N/D equations, and these equations are solved numerically.

The explicit numerical calculations involved inputting the  $\rho$  and P trajectories and residues, suitably parameterized,<sup>(12,14)</sup> and matching input to output parameters. The trajectories and residues are shown in Figure 7. Collins and Johnson in this way were able to "bootstrap" the  $\rho$  with parameters,  $\alpha_\rho(0) \approx .55$ ,  $\Gamma_\rho = 143$  MeV, the first time that such parameters have been obtained from a bootstrap model.

Let me summarize the results of the Collins-Johnson strip model; I feel they are both successful and promising.

- (1) There is weak dependence on the strip width parameter,  $s_1$ . This removes any arbitrary parameters from the model.
- (2) The trajectories are roughly linear with unit slope for  $|t| < 1 \text{ GeV}^2$ . Recall that on the scale of Figure 7,  $1 \text{ GeV}^2 = 50 \frac{m_\pi^2}{\pi}$ . We've already explained why the strip model is expected to give trajectories that turn over, so even this small range of linearity is gratifying.
- (3) The trajectory intercepts can be self-consistent in the ranges

$$\begin{aligned} &.3 \lesssim \alpha_\rho(0) \lesssim .7 \\ \text{and} &.9 \lesssim \alpha_P(0) \lesssim 1.2. \end{aligned}$$

As the calculations were not done to infinity, the Froissart bound limit  $\alpha_P(0) \leq 1$  does not directly apply. Note that, as in the multiperipheral model,  $\alpha_P(0) - \alpha_\rho(0) \approx .5$ .

- (4) The  $P'(f^0)$  trajectory was not generated.

- (5) A self-consistent solution was obtained with  $\Gamma_{\rho}^{\text{input}} = \Gamma_{\rho}^{\text{output}} = 143 \text{ MeV}$ .
- (6)  $\sigma_{\text{Total}}^{\pi\pi} = 26 \text{ mb}$ . The expected result, using factorization and  $\pi\text{N}$  and  $\text{NN}$  data, is roughly 15 mb. The diffraction peak in  $d\sigma/dt$  is too broad by about a factor of two.
- (7) The low energy S-wave "looks good" in the sense that it is small. This is an important result, never before obtained from a bootstrap model without arbitrary parameters. This smallness is usually "explained" through PCAC and the Adler condition, which requires that at the unphysical, off-mass shell point,  $s = t = u = m_{\pi}^2$ , the amplitude should vanish. The Collins-Johnson result suggests that the physical content of PCAC is already contained in our bootstrap conditions.

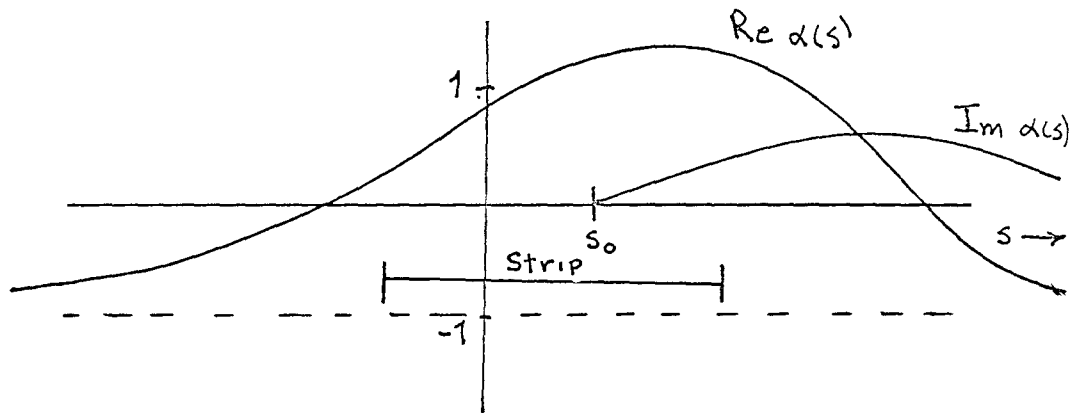
This summary of results concludes my comments on the strip model and marks the end of our detailed analysis of approximations to the S-matrix. In the final lecture I'll compare the various models we've discussed to see how much success the hadron bootstrap program can claim.

#### REFERENCES

1. G.F. Chew and S. Mandelstam, Phys. Rev. 119, 467 (1960).
2. D. Atkinson, "A Proof of the Existence of Functions that Satisfy Exactly Both Crossing and Unitarity, III. Subtractions," ICTP/68/29.  
Atkinson introduces a cut-off function similar to that in reference (5b) into the equation for  $\rho^S(s,t)$ .
3. G.F. Chew and S.C. Frautschi, Phys. Rev. 123, 1478 (1961).
4. G.F. Chew, S.C. Frautschi, and S. Mandelstam, Phys. Rev. 126, 1202 (1962).
5. (a) B.H. Brandsen, P.G. Burke, J.W. Moffat, R.G. Moorhouse, and D. Morgan, Nuovo Cimento 30, 207 (1963).  
(b) N.F. Bali, G.F. Chew, and S-Y. Chu, Phys. Rev. 150, 1352 (1966).
6. S. Mandelstam, Annals of Physics 21, 302 (1963).
7. P.G. Burke and C. Tate, Proceedings of the International Conference on High Energy Physics, CERN, p. 507 (1962).
8. N.F. Bali, Phys. Rev. 150, 1358 (1966).
9. (a) G.F. Chew, Phys. Rev. 129, 2363 (1963).  
(b) G.F. Chew and C.E. Jones, Phys. Rev. 135, B208 (1964).  
(c) C.E. Jones, Phys. Rev. 135, B214 (1964).
10. (a) P.D.B. Collins and V.L. Teplitz, Phys. Rev. 140, B663 (1965).
11. R. Blankenbecler, M.L. Goldberger, N.N. Khuri, and S.B. Treiman, Ann. Phys. (N.Y.) 10, 62 (1960).
12. P.D.B. Collins and R.C. Johnson, Phys. Rev. 177, 2472 (1969); Phys. Rev. 182, 1755 (1969).
13. G. Frye and R.L. Warnock, Phys. Rev. 130, 478 (1963).
14. A. Ahmadzadeh and I.A. Sakmar, Physics Letters 5, 145 (1963).
15. P.D.B. Collins and E.J. Squires, Regge Poles in Particle Physics, Julius Springer Verlag (Berlin), 1968.

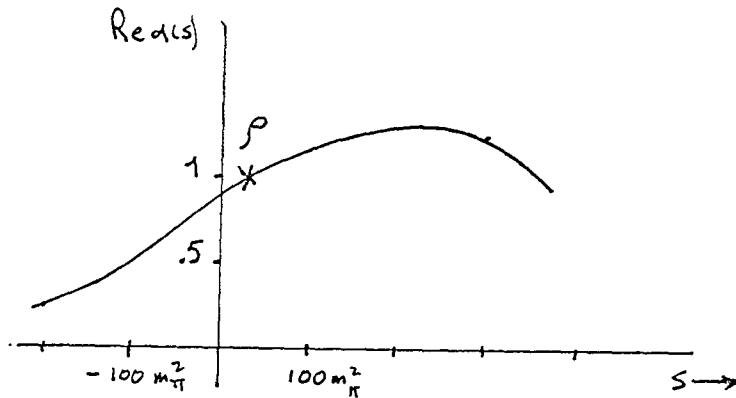
LECTURE 9

FIGURE 1



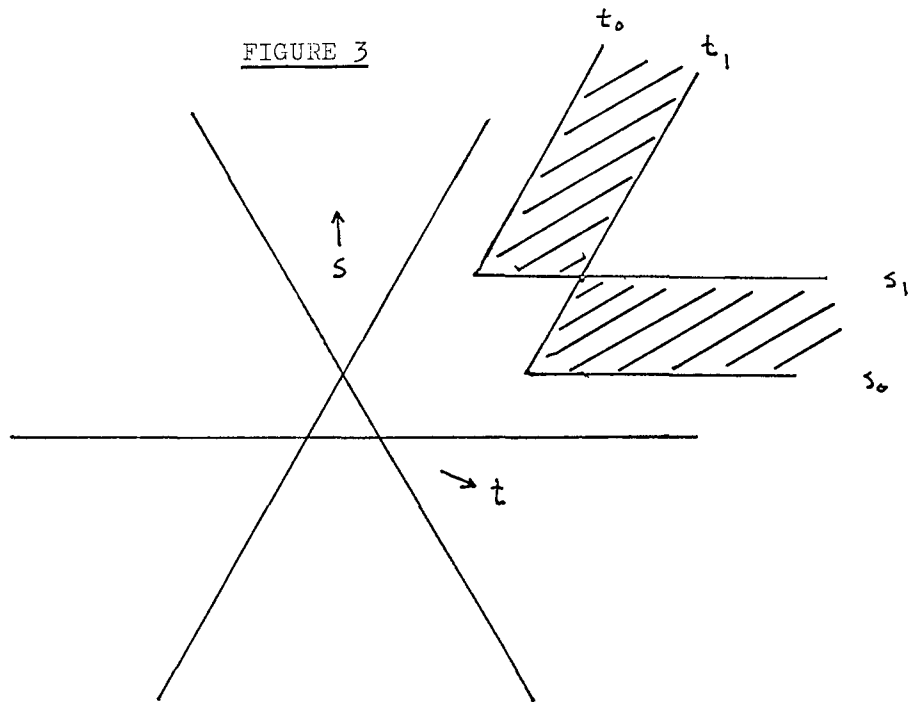
The behavior of a Regge trajectory in potential theory or in perturbation theory

FIGURE 2



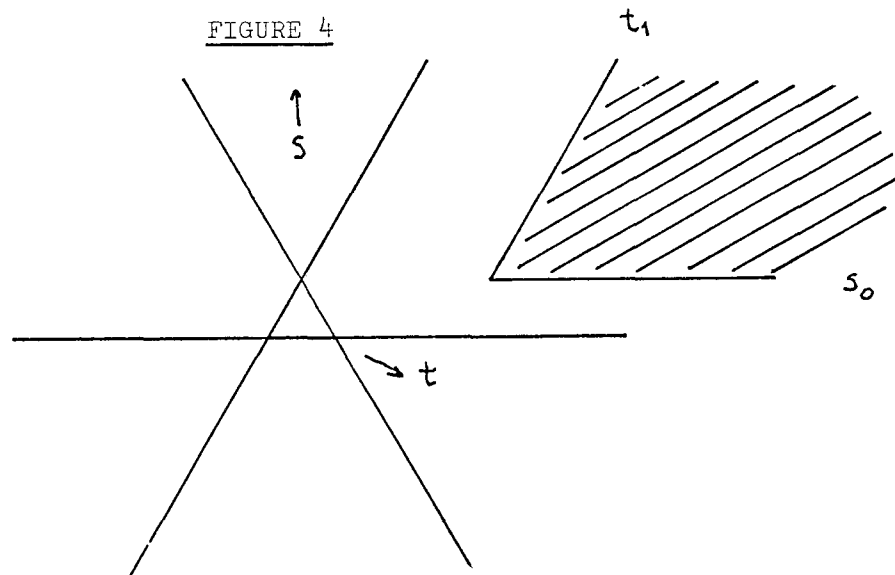
The  $I = 1$  trajectory in the original strip model calculation of reference (8)

FIGURE 3



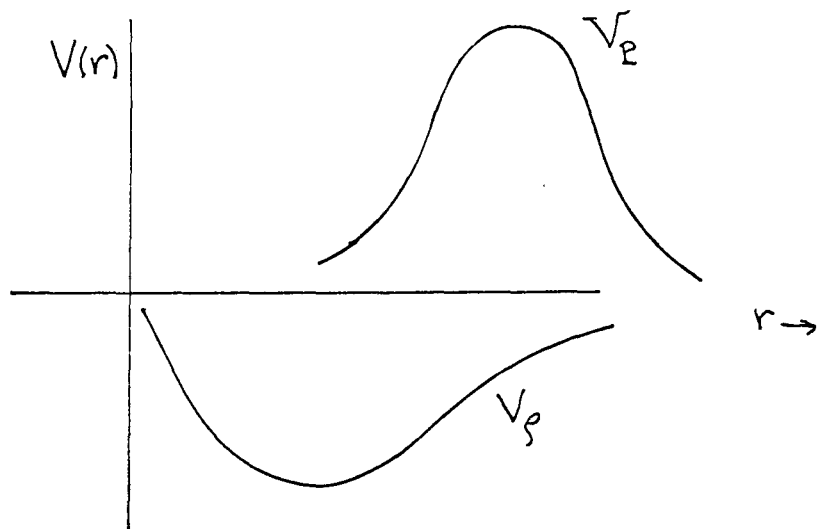
The region in which the Regge terms dominate the double spectral function  $\rho(s,t)$

FIGURE 4



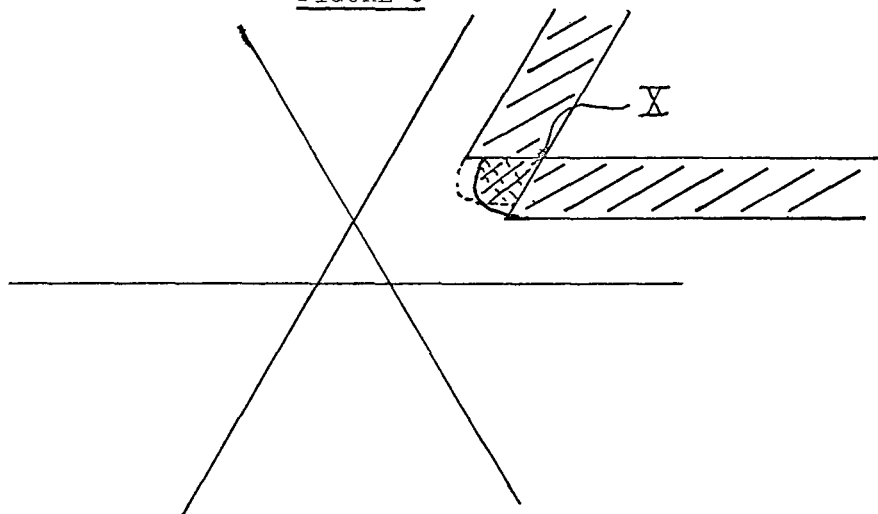
The support of the double spectral function of  $R_i^S(s,t)$   
(Shaded region)

FIGURE 5



The potential theory analogue of P and  $\rho$  Regge pole input to the strip model

FIGURE 6



The Regge-dominated strips and the "corner" regions of  $\rho^S(s,t)$  calculated in the unitarized strip model

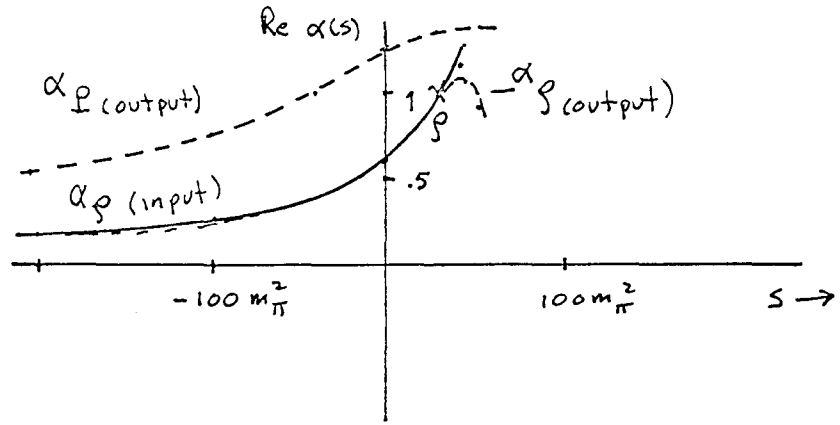


FIGURE 7

Regge trajectories in the unitarized strip model



In this final hour I'd like to stand back from the details of the models we've been discussing to recapitulate the essence of my lectures and to speculate on future developments.

We've seen that the complexity of the S-matrix postulates has forced resort to models that attempt to satisfy only some of the basic principles while explicitly ignoring others. Two different models emphasizing different fundamental hypotheses are "complementary" in that where one succeeds partially the other fails badly. One of our long-term goals must be to try to establish overlapping domains of validity for different models; in this manner we can hope to understand interrelations among different parts of this S-matrix.

Most of our approximate solutions have been based on, motivated by, or justified by the existence of small parameters. Since they have been central to our discussion let me now summarize these small parameters and the models to which they lead.

1) Widths of Resonances:

The width of a typical  $B=0$  resonance, say  $\Gamma_\rho \approx 125$  MeV, is sufficiently small, relative to most hadronic masses, to allow a meaningful "zero-width" model -- the Veneziano Model -- to be constructed. Saturating the amplitude with nothing but zero width resonances means neglecting branch points and unitarity in general. Empirically, this technique seems most successful in interactions having baryon number,  $B$ , equal to zero - that is, in purely mesonic processes. With  $B=1$  there are already difficulties; in  $\pi N$  scattering, for instance, the important  $\Delta(1236)$  resonance has not successfully been described. As the baryon number increases, the importance of threshold effects multiplies. A model which ignores unitarity cannot possibly be valid in the domain of large baryon number.

2) Coupling of Pomeranchuk Trajectory:

A small parameter which we have briefly mentioned is the value of cross sections at very high energy. This can be translated into the statement that the "coupling constant,  $g_p^2$  - more properly, the Regge residue - of the Pomeranchuk trajectory is small.<sup>1</sup> Such a weak coupling allows one to construct models which, as a first approximation, neglect the Pomeranchuk. Incorporating duality suggests that this implies the neglect of exotic resonances, leading naturally to a quark-type model. Mandelstam<sup>2</sup> has discussed such models in the tree graph approximation and obtained a mathematically consistent solution for  $SU(n)$ , although ghost states -- negative residues at resonance poles, implying negative resonance widths -- are a major problem.

3) Pion Amplitudes near Threshold:

The smallness of a scattering amplitude containing pions (and no direct channel pole graphs) near threshold follows simply in a field theoretic framework from the assumption of PCAC but is awkward to discuss within the "on-mass-shell" S-matrix

formalism. Thus the results of Collins and Johnson on the smallness of the  $\pi\pi$  S-wave amplitude near threshold are encouraging, as no PCAC assumption was used as input into their model.

#### 4) The Pion Mass:

In three separate models we've discovered that the smallness of the pion mass justifies important approximations. Since we've concentrated our attention on these models in the previous lectures, I'll just mention them briefly here. They are: a) the potential theory model which we used to understand threshold states; b) the multiperipheral model; and c) the strip model.

From this summary, what may we conclude about the interrelations among the many models? In particular, can we see any trace of the overlapping domains of validity we hope to establish?

First, recall the relation of the strip model to the multiperipheral model; this we discussed in detail in the last lecture. By including more of the fundamental postulates, the strip model is able to resolve an ambiguity inherent in our specific version of the multiperipheral model. In its capacity to predict the narrow width the strip model provides motivation for the Veneziano model.

Another connection, less obvious and more speculative, may exist between the strip model and the Veneziano model. Since both seem capable of describing the  $\rho$  resonance in the  $\pi\pi$  system, perhaps we could improve the output from the strip model by inserting as input the form of Regge residue function suggested by the Veneziano model - that is, put

$$\gamma(t) \propto \Gamma[1-\alpha_\rho(t)] \quad .$$

The resulting Regge trajectory and residue function may have wider regions of validity than those obtained without this additional constraint.

We've already mentioned a third interrelation among the small parameters: namely, the strip model result and the smallness of the S wave  $\pi\pi$  scattering amplitude, which corresponds to a consequence of PCAC.

Finally, we consider a possible constraint on internal symmetry from multiperipheral or strip models. If one inputs into the strip model a meson singlet state with no internal quantum numbers - corresponding to a U(1) symmetry - one finds that the force resulting is not sufficient to allow the bootstrap condition to be satisfied.<sup>4</sup> On the other hand, if one postulates the existence of too many equivalent low-lying states, then the force may increase as much as to violate the Froissart bound. Thus self-consistency may provide a restriction on the multiplicity of low-lying states; but this multiplicity of states of similar mass and spin is what we normally regard as "internal symmetry". Thus in some sense we may be able

to understand the "n" in SU(n). That bootstrap theories may lead to unitary "symmetries" has, by the way, been known for some time. Cutkosky<sup>3</sup> showed in 1963 that if one considers vertices as in Fig. 1 and demands that each particle be described as a bound state of the other two, one is led to unitary symmetries as possible solutions of the consistency conditions.

One might feel that the partial success of the SU(3)xSU(3) current-current form of the weak interactions would require, in order to "explain" SU(3), that weak interactions be included in bootstrap. My view is that we have not begun to understand the weak interactions. Conserved currents are a concept borrowed from the electromagnetic interaction; although there is success in first-order phenomenology, if taken seriously in higher orders, the local current hypothesis for weak interactions leads to horrendous difficulties. In short, I think the speculation that SU(3) may be explicable in terms of the strong interactions alone is reasonable.

For nearly ten years the principles underlying the hadron bootstrap have been unchanged. It is natural in a theory based on broad, general hypotheses that progress is slow. But until we find

- 1) a violation of the underlying principles; or
- 2) a model which satisfies all the postulates but which clearly does not correspond to the physical world; or
- 3) a proof of non-uniqueness of the solution,

the concept compels attention.

#### REFERENCES

1. D. Wong, Phys. Rev. 181, 1900 (1969).
2. S. Mandelstam, "A Relativistic Quark Model Based on the Veneziano Representation I. Meson Trajectories", University of California preprint 3/69; Phys. Rev. (to be published).
3. R.E. Cutkosky, Phys. Rev. 131, 1888 (1963).
4. P.D.B. Collins, Phys. Rev. 131, B696 (1965); P.D.B. Collins and V. Teplitz, Phys. Rev. 140, B663 (1965).

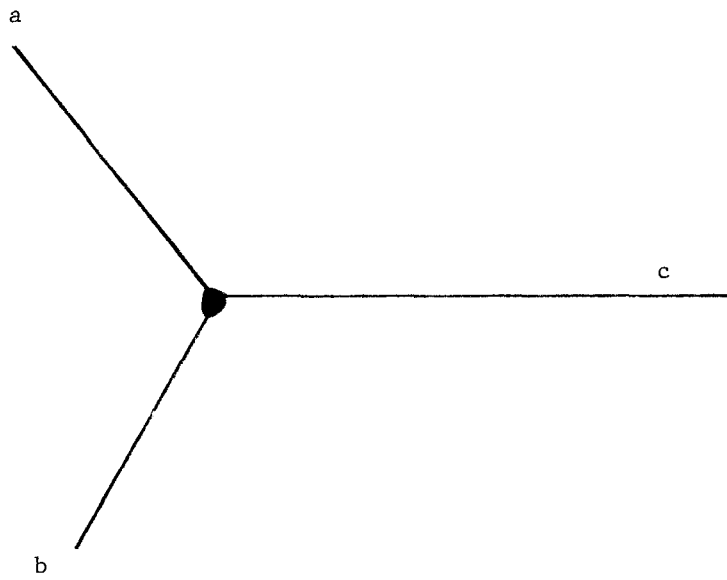


Fig. 1 A Three Particle Vertex



RECENT DEVELOPMENTS  
DUALITY AND HADRON DYNAMICS

Lectures by: H. Harari



## I. INTRODUCTION

The concept of duality is probably the most important new development in strong interaction dynamics in the last few years. Today, we can hardly imagine a discussion of hadronic processes without mentioning ideas such as finite energy sum results, resonance dominance, global duality and local duality, the connection between the Pomanchuk singularity and the non-resonant background, exchange degeneracy, the absence of exotic exchanges, duality diagrams and the Veneziano formula. The purpose of these notes is to review, step by step, the historical and logical developments of the various aspects of duality. In every step of this development we will try to emphasize the assumptions needed in order to proceed, the consequences of these assumptions, the experimental justification for making such assumptions, and the experimental status of the predictions which follow from these assumptions.

The rapid development of this subject has led to a certain amount of confusion in the literature. It is very often stated that some aspect of duality is consistent or inconsistent with experiment on the basis of a certain prediction, while the prediction itself can really be obtained from a weaker set of assumptions (which does not necessarily coincide with the particular aspect of duality under discussion). A typical example is the frequently made statement that the apparent absence of a  $\rho'$  meson at 1250 MeV provides evidence against the Veneziano formula. We must remember, however, that the existence of the  $\rho'$  is already predicted by the assumption of local duality which is only one of the many ingredients which go into the construction of the Veneziano formula. The absence of the  $\rho'$ -meson is therefore evidence against strict local duality. The Veneziano formula is to be blamed, only to the extent that it utilizes local duality as one of its ingredients. Another example which is much more crucial is the failure of various predictions of the exchange degeneracy hypothesis. In many of these predictions, the failure can be traced to a failure of Regge pole theory (to be distinguished from a theory including cuts). If Regge pole theory fails and if cuts are necessary, we should modify everything in the formulation of duality, beginning with the original form of the finite energy sum rule. Only after such proper modifications are inserted into the formulation of the sum rules of the duality scheme, and of the exchange degeneracy hypothesis, we will be able to test this hypothesis within the framework of duality and decide whether or not it is experimentally valid. In view of these and many other similar cases, we shall try to clarify some of the confusion which has propagated through the literature on this subject, and we shall put the blame for each success or failure on the appropriate theoretical considerations which lead to the tested prediction. In our discussion we follow a chart (Fig. 1) which indicates the theoretical sequence of assumptions which have led to the development of the



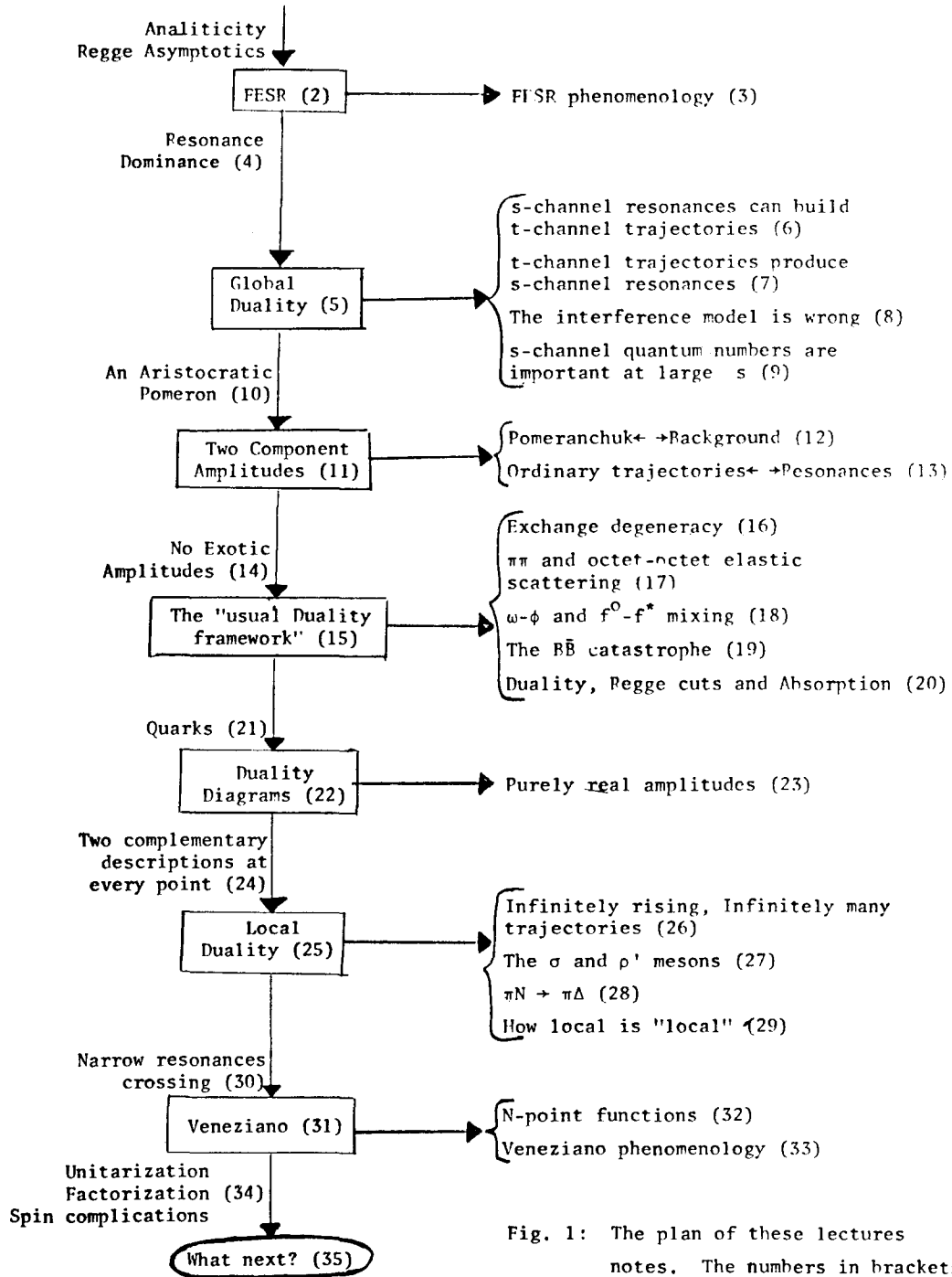


Fig. 1: The plan of these lectures notes. The numbers in brackets denote the section numbers.

various ideas, beginning with finite energy sum rule and ending with the extensions of the Veneziano formula. This chart shows the new assumptions which are needed in every stage as well as the experimental and theoretical consequences which result from these assumptions. We shall discuss every one of these items both from the theoretical point of view and from the experimental point of view, mention the experimental status of the various ideas involved and propose new experimental tests wherever possible. Since this is supposed to be a general review of the subject, we will avoid minor technical details such as discussion of various ghost killing mechanisms, details of Regge cut contributions, choice of cutoff values in the sum rules, higher moment sum rules, and many other interesting technical questions which are related to duality in one way or the other. We shall mainly concentrate on the basic concept of duality.

## II. FINITE ENERGY SUM RULES (FESR)

Finite energy sum rules<sup>1,2</sup> are historically and logically the simple mathematical tool that has led to the idea of duality<sup>2</sup> in hadron physics. The sum rules themselves are merely a clever mathematical representation of the assumptions that are used in deriving them, namely: Analyticity and asymptotic Regge behavior. Without further dynamical assumptions (such as resonance dominance) the sum rules do not and cannot yield any new physics beyond the ideas used in the derivation. In particular, without such additional assumptions, the finite energy sum rules (FESR) do not necessarily lead even to duality itself.

The familiar derivation of the FESR involves the assumption that a scattering amplitude  $f(\nu, t)$  obeys, for  $\nu > N$ , a Reggeistic expansion:

$$f(\nu, t) = \sum_i \beta_i(t) \frac{1 \pm e^{-i\pi\alpha_i(t)}}{\sin\pi\alpha_i(t)} \nu^{\alpha_i(t)} .$$

Here,  $\nu$  is the laboratory energy of the incident particle,  $t$  is the invariant momentum,  $\alpha_i(t)$  and  $\beta_i(t)$  are the trajectory and residue function of the  $t$ -channel Regge poles, respectively. Using the usual analyticity requirements and crossing properties which are needed for writing ordinary fixed- $t$  dispersion relations, sum rules of the following typical form can be derived<sup>1,2</sup>:

$$\int_0^N \text{Im}f(\nu, t) d\nu = \sum_i \beta_i(t) \frac{\alpha_i(t)+1}{\alpha_i(t)+1} .$$

Similar sum rules can be written for the real part of  $f(\nu, t)$ , for various combinations of the real and imaginary parts, for higher moments  $[\nu^n \text{Im}f(\nu, t)]$ , etc.

We have no good reason to doubt the validity of the analyticity assumptions

needed for deriving the finite energy sum rules. However, we do have very good reasons to doubt the validity of Regge pole theory. There are many phenomenological indications that contributions of Regge cuts are extremely important in many cases.<sup>3</sup> We do not see any reason or justification to neglect them in writing the asymptotic behavior of the amplitude which appears in the FESR. This point which is often ignored, is extremely important, since many of the questionable predictions of various duality assumptions seem to contradict experiments precisely in those cases where Regge pole theory is in trouble. It is not clear at all whether these failures are failures of duality or whether they are failures of Regge pole theory. If the latter is the case, it is conceivable that the duality assumption will become consistent with experiment, once Regge cuts are properly included in the formulation. We shall return to the subject of Regge cuts frequently in this review (particularly in Sec. 20) but let us emphasize immediately that a clear formulation of the various aspects of duality which includes the effects of Regge cuts is badly needed. To our knowledge, such a formulation does not yet exist. It is completely trivial to add some logarithmic cut terms on the right hand side of the FESR but this is not sufficient for providing us with a complete duality theory including Regge cuts. We have to understand much better the contribution of Regge cuts to various specific partial waves in the s-channel and the possible connection between Regge cuts and the absorption model before we can claim to understand the role played by cuts in the duality scheme.

For the time being, however, let us follow the usual route of ignoring cuts and discuss the physical content of the finite energy sum rules.

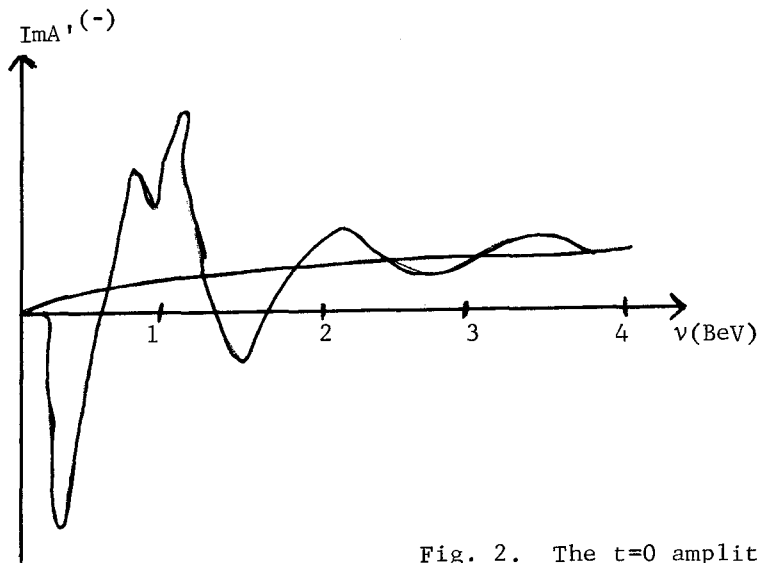


Fig. 2. The  $t=0$  amplitude for  $\pi^- p \rightarrow \pi^0 n$

This is perhaps best illustrated by Fig. 2, in which the physical amplitude for  $\pi N$

charge exchange at  $t=0$  is shown together with a low energy extrapolation of its high energy Regge parametrization.<sup>2</sup> The two amplitudes approach each other as the energy  $\nu$  grows and the areas under the two curves have to be equal according to the FESR. The extrapolated Regge amplitude represents some kind of an average of the true physical amplitude over the interval  $(0..N)$ .

So far we have given an explicit form only to the high energy part of the amplitude. We did not assume anything for the low energy part of the amplitude, which appears on the left hand side of the FESR. Figure 2 therefore tells us that the extrapolated Regge pole contribution is balanced by whatever terms which appear in the low energy side of the relation. Depending on whether or not we make further theoretical assumptions for the low energy part of the amplitude, we can use the finite energy sum rule either for pure phenomenological studies or for dynamical calculations.

### III. FINITE ENERGY SUM RULE PHENOMENOLOGY

The basic content of the FESR is a relation between the low energy part of an amplitude and its high energy part. The left hand side of the FESR is given by the physical amplitude at low energies. The right hand side of the FESR involves the parameters of the dominant Regge trajectories which can in principle, be completely determined by the physical amplitude at high energies. The FESR enables the low energy data to impose constraints on the parameters appearing in the high energy Regge description. Conversely, the high energy data, through its Regge parametrization, can impose constraints on whatever low energy parametrization one may wish to use. Theoretically, it is conceivable that extremely accurate low energy data for a certain physical amplitude may lead to a better determination of its high energy Regge parameters than some poor quality high energy data for the same amplitude. We know, of course, that infinitely accurate data at a given region would be sufficient to determine the entire physical amplitude in other regions by a unique analytic continuation. The finite energy sum rules essentially provide us with an approximate, non-unique way of doing a similar thing in the realistic case of data with finite experimental errors. Many applications of this idea have been proposed by various authors<sup>4</sup> and, in some cases, have indeed improved our understanding of the high energy amplitudes.

### IV. FINITE ENERGY SUM RULE AND HADRON DYNAMICS - RESONANCE DOMINANCE

The dynamical use of FESR appears when we assume that the dominant phenomena on its left hand side are described by the s-channel exchange of the same set of Regge trajectories which appear on the right hand side of the FESR. This leads immediately to a bootstrap scheme which uses as input analyticity, Regge behavior and additional dynamical assumptions such as resonance dominance, and which yields

as output sets of equations among hadronic masses and coupling constants (or trajectories and residue functions). It is the resonance dominance assumption which converts the FESR from a mathematical tool to a profound statement about strong interaction dynamics. For example, in Fig. 2, if we assume that the actual physical amplitude is completely dominated by resonances and that the high energy amplitude is completely dominated by Regge poles we learn that the extrapolated contribution of the Regge poles balances the total contribution of the resonances alone, and it is precisely such a relation which we find useful for studying the spectrum of hadrons.

At this point we must add that the resonance dominance assumption in its localized sense (i.e., a resonance contribution dominates its immediate energy neighborhood) is reasonable only for the imaginary part of the amplitude. A resonance creates a clear bump in the energy dependence of the imaginary part of its partial wave amplitude. At the resonance position (at least for a simple Breit-Wigner resonance) the real part of the amplitude vanishes (Fig. 3).

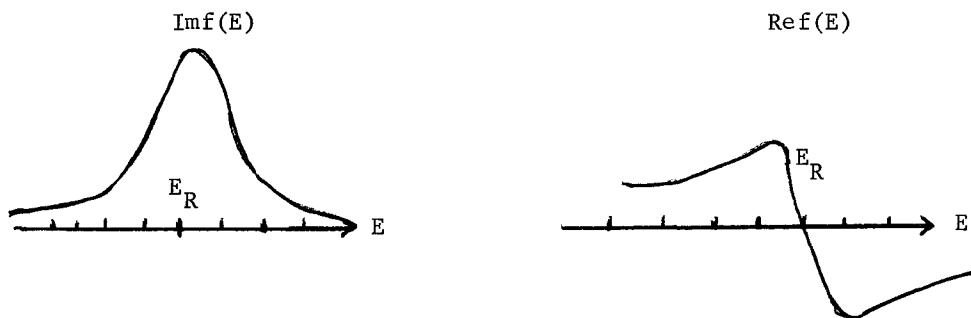


Fig. 3. The imaginary part and the real part of an ordinary Breit-Wigner resonance

It would therefore be ridiculous to assume that resonances dominate the real part of the amplitude around the resonance energy. We could compute the resonance contribution to the real part by inserting its contribution to the imaginary part into a dispersion relation. We could then find that the real part of the amplitude gets contributions from very distant resonances. In the following section we shall, therefore, utilize the resonance dominance assumptions only for the imaginary part of the amplitude.<sup>5</sup>

## V. GLOBAL DUALITY

As long as the low energy resonances dominate the left hand side of the FESR, we find ourselves with the following situation: A sum of t-channel Regge poles balances a sum of s-channel resonances. In other words, the dominant poles which are exchanged in the t-channel determine the s-channel singularities and vice versa. This notion contradicts the traditional approach according to which the s-channel

resonances should be added to the t-channel exchanges in the description of hadronic scattering amplitudes. What we now say is that the s-channel resonances by themselves should be sufficient to determine the complete amplitude. At the same time, the t-channel Regge poles by themselves should also be sufficient for determining the amplitude. We have two complete complementary descriptions of the same physical situation. Any of these descriptions is complete by itself and need not be supplemented by contributions from the other description. This is the fundamental idea of duality. We refer to it as Global Duality if the equality between the sum of t-channel resonances and the sum of t-channel Regge poles is true only in an average sense (over a region, say, from 0 to N). It is conceivable that in some cases the equality between these two descriptions can be true in a smaller region such as in the region of a specific resonance or over a range of a few MeV. In such a case we may talk about local duality. We shall return to the idea of local duality in Secs. 24-29 and for the time being concentrate on global duality.

The usefulness of global duality depends in a crucial way on the simplicity of the two complementary descriptions of the scattering amplitude which are being considered here. In some cases the s-channel description may be very simple, but the t-channel picture is totally useless and complicated. (This is the case, e.g., for  $\pi N$  scattering at  $(s)^{\frac{1}{2}} = 1.24$  BeV). In some other cases the t-channel picture may be simple and attractive, while the s-channel picture involves an enormous number of resonances and is, again, useless and complicated. (This would presumably happen for  $\pi^- p \rightarrow \pi^0 n$  at 20 BeV). In some other cases, both pictures may be complicated and the duality idea will be of no use at all. It is possible, however, that in some situation both the s-channel picture and the t-channel picture are fairly simple. In these cases the equality between the sum of s-channel resonances and the sum of t-channel trajectories becomes a sufficiently simple equation and the solution of such an equation may give us meaningful, interesting results. In order to test the idea of duality and to find its immediate dynamical consequences, we will therefore have to concentrate on cases in which the two complementary descriptions are both simple.

But before we turn to the applications, we should convince ourselves that it is indeed possible for a few s-channel resonances to produce the main characteristics of one or a few t-channel trajectories and that, on the other hand, it is possible for a t-channel Regge trajectory to exhibit some of the characteristics of a small number of s-channel resonances.

#### VI. CAN A FEW RESONANCES PRODUCE THE CHARACTERISTICS OF A t-CHANNEL TRAJECTORY?

Three of the most common characteristic properties of a t-channel exchange (whether a Regge pole, a cut, or any other simple peripheral exchange) are the

following:

- a) An angular distribution with a forward peak and a rapid variation as a function of  $t$ .
- b) A possible dip structure which is fixed in  $t$  for all energy values.
- c) A smooth energy dependence for a fixed value of  $t$ .

It is not difficult to see how a number of  $s$ -channel resonances can add up in such a way as to produce a sharp forward peak with a rapid variation in  $t$ . This will happen, for instance, when a number of resonances with different spins exist at the same energy. If the contributions of these resonances to the physical scattering amplitude add with a positive relative sign in the forward direction, the combined effect at  $t=0$  will be a sharp forward peak, while at larger  $t$ -values, cancellations between the contributions of the different resonances will take place and the numerical value of the amplitude will be much smaller. This phenomenon is, of course, well known but it is not often appreciated how striking the angular distribution produced by a small number of resonances can be. An interesting example is shown in Fig. 4. We consider the  $\pi$ - $\pi$  elastic scattering amplitude at a c.m. energy of approximately 1900 MeV and assume that at this energy the amplitude is completely given by five  $s$ -channel resonances with spins 4, 3, 2, 1 and 0. The relative importance of these resonances in the particular example shown in Fig. 4 is taken<sup>6</sup> from the prescription of the Veneziano formula, but this is totally irrelevant for our discussion here. What is relevant is the observation that five resonances with relatively low spins can produce such an impressive forward peak with such a strong  $t$ -variation at small angles. Any uninformed observer who would see this figure without knowing what was plotted here would undoubtedly claim that this is a typical curve representing a strong peripheral exchange contribution. His conclusion would not be necessarily wrong! In fact, it could be perfectly consistent with the statement that we have here five  $s$ -channel resonances. There is no necessary contradiction between the two points of view and it is clear that a relatively small number of resonances can reproduce angular distributions which would normally be considered as typical peripheral distributions.

A slightly more complicated problem is the question of producing dips in the angular distribution at fixed values of  $t$  for all energies, a property which is common to many simple  $t$ -channel exchanges. An arbitrary collection of  $s$ -channel resonances will not have such a property. The positions of the dips in the angular distribution of an  $s$ -channel resonance are, of course, dictated by the spin of the resonance (which determines which Legendre polynomial dominates the amplitude at that particle energy) and by the energy of the resonance. A very strict relation between the energies of the various  $s$ -channel resonances and their spin values has to exist in order to force all the prominent  $s$ -channel resonances to produce dips at

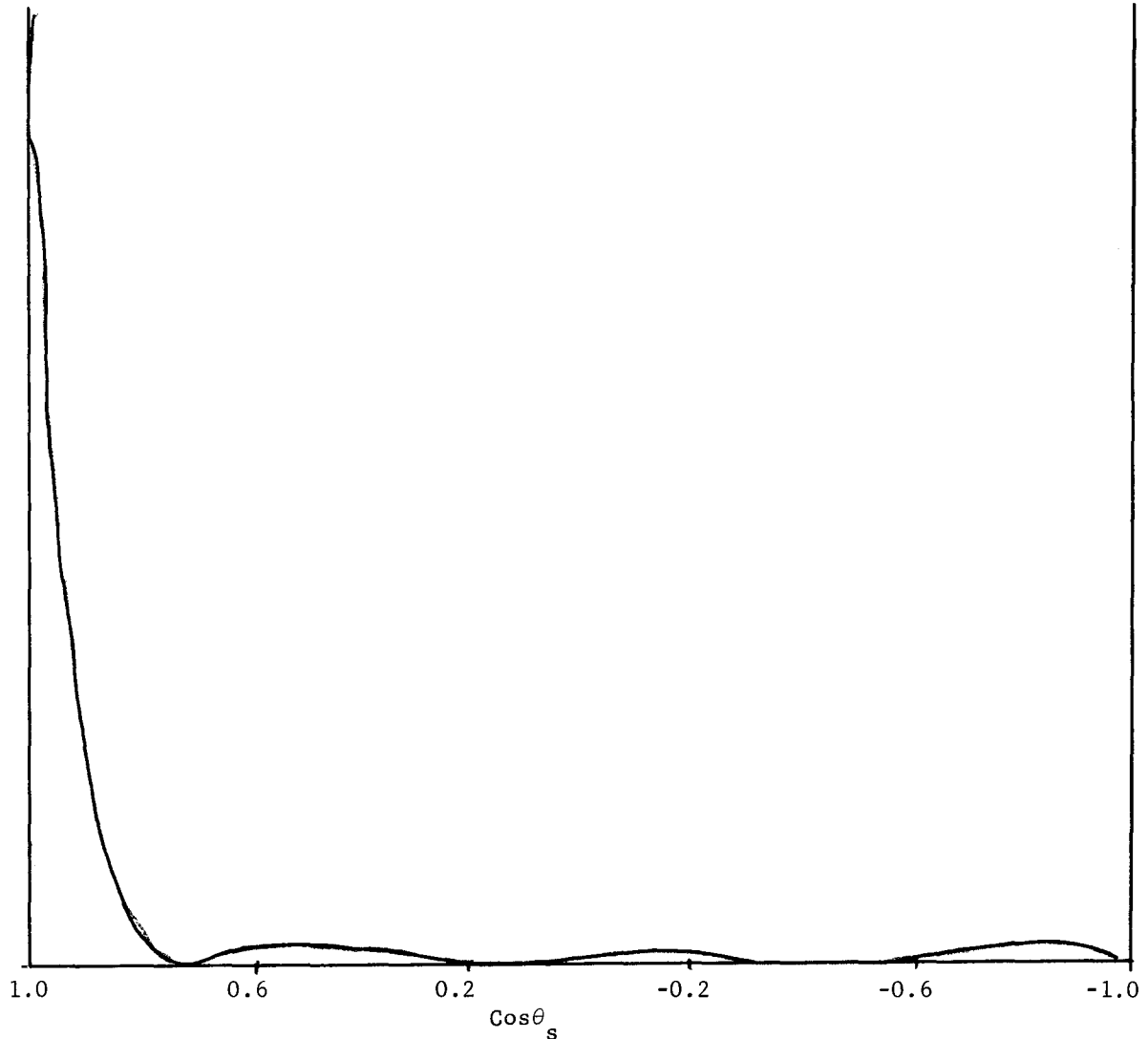


Fig. 4. Angular distribution of  $\pi\pi$  elastic scattering assuming  $J=4,3,2,1$  and  $0$  resonances (from Ref. 6).

the same  $t$ -values. Before discussing the general condition which is necessary for such a situation, let us return to our example of  $\pi\text{-}\pi$  elastic scattering and study the dip structure of the first few prominent resonances.

At the mass of the  $\rho$  meson the  $\pi\text{-}\pi$  amplitude is probably dominated by the first Legendre polynomial  $P_1(\cos\theta)$ . The amplitude will therefore vanish at the point  $\theta = 90^\circ$ . This corresponds, at the mass of the  $\rho$  meson, to a value of  $t = -0.25 \text{ BeV}^2$  (Fig. 5a). If we further assume that at the mass of the  $f^0$  meson (1250 MeV) the dominant feature in the amplitude is the second Legendre polynomial we find that the first zero in the angular distribution of  $\pi\text{-}\pi$  elastic scattering



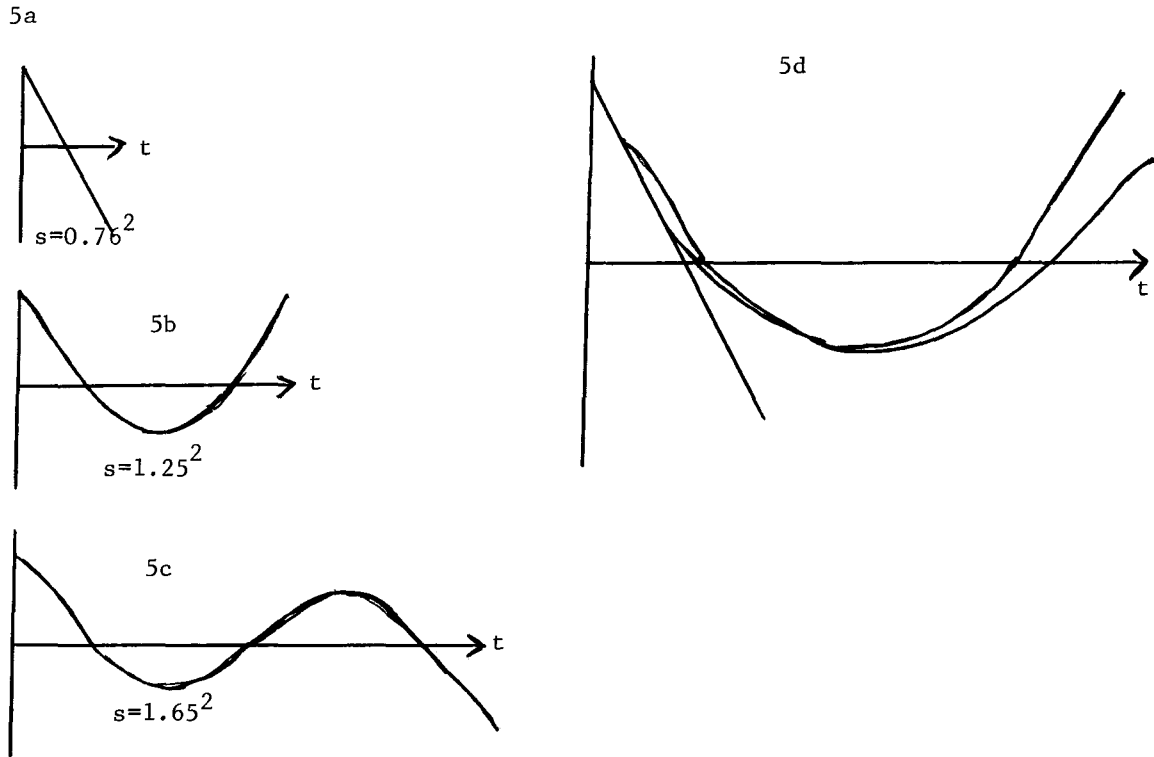


Fig. 5.  $t$  dependence of  $\pi\pi$  scattering at the  $\rho$ ,  $f^0$  and  $g$  meson masses (5a,5b,5c) superimposed on the same  $t$ -distribution (5d).

at this energy is produced at  $t = -0.31 \text{ BeV}^2$  (Fig. 5b). At a center of mass energy of 1650 MeV,  $\pi$ - $\pi$  elastic scattering is presumably dominated by the  $g$  meson with a spin-parity  $3^-$ . We find that the first zero in the angular distribution of the  $\pi$ - $\pi$  amplitude at this energy occurs at  $t = -0.29 \text{ BeV}^2$  (Fig. 5c). The remarkable coincidence between the first zeros in the amplitudes of the three prominent  $\pi$ - $\pi$  resonances (Fig. 5d) indicates how, in general, different  $s$ -channel resonances may produce dips in angular distributions at the same values of  $t$ . It happens in the following way: As we go to higher and higher energies the angular distributions cover wider and wider ranges in  $t$ . If the zeros would be at the same values of the angle  $\theta$ , they would correspond to larger and larger absolute values of  $t$  as the energy grows. If, however, as the energy grows, we have prominent resonances of larger and larger spins, we have contributions of higher Legendre polynomials and the first zero in the angular distribution occurs at smaller and smaller values of  $\theta$ . There is a competition between the widening of the range in  $t$  and the approach

of the first zero in  $\theta$  towards the forward direction. If the two effects precisely cancel each other, we will observe the phenomenon of having the first zero in the angular distribution at a fixed value of  $t$  for all energies. This is precisely what happens in our example of the  $\rho$ ,  $f$ , and  $g$  mesons and this is also what happens (in a slightly more complicated situation) in  $\pi N$  elastic scattering.<sup>2</sup> The asymptotic relation between the spin of the resonance and its mass, which guarantees a fixed value of  $t$  for the first zero in the angular distribution is  $J \sim (s)^{\frac{1}{2}}$ .

This relation also determines the most peripheral partial wave which is allowed to contribute to the scattering if the radius of interaction is fixed. We can see this in the following simple way. For an impact parameter  $R$ , the angular momentum in the c.m. frame is  $l \sim kR$ , where  $k$  is the c.m. momentum. If we assume a fixed radius of interaction,  $R$ , the largest angular momentum allowed to contribute at a given center of mass momentum  $k$  will be proportional to  $k$ , and, therefore, proportional to  $(s)^{\frac{1}{2}}$ . We therefore conclude that if the prominent resonances in the  $s$ -channel are always the peripheral resonances ( $l \sim (s)^{\frac{1}{2}}$ ) it is guaranteed that the first zero in the angular distribution of every one of these resonances will appear at the same  $t$ -value at all energies, thus producing our second characteristic property of a peripheral  $t$ -channel exchange.

The third property of  $t$ -channel exchanges, namely, the smooth energy dependence for fixed values of  $t$  can be reproduced by  $s$ -channel resonances only if a fairly large number of resonances compensate each other at various energies so as to produce bumps in the energy dependence of specific partial wave amplitudes which correspond to valleys between bumps in the energy dependence of other partial wave amplitudes. In such a way (Fig. 6) a number of  $s$ -channel resonances can produce structure in the energy dependence of the partial wave amplitudes but no structure

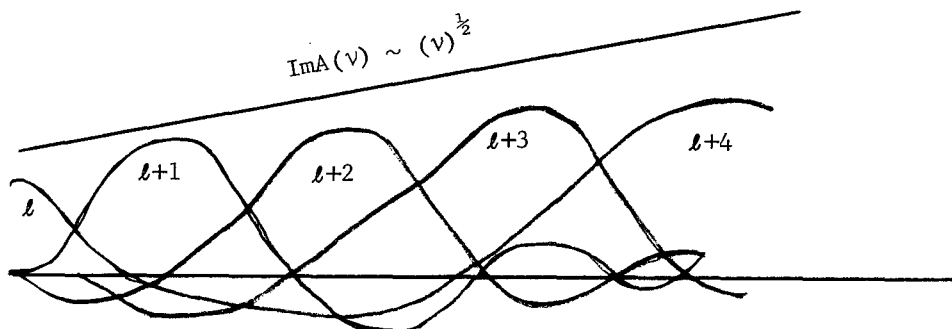


Fig. 6.

whatsoever in the energy dependence of the total physical scattering amplitudes. It is clear that here more than in the previous two characteristic properties, a detailed compensation among the s-channel resonances is important, and indeed this property (smooth energy dependence) is normally not obeyed by small numbers of s-channel resonances. In particular, in  $\pi$ - $\pi$  scattering in the region of the  $\rho$ ,  $f$ , and  $g$  mesons the energy dependence is not yet smooth although the two other properties are already obeyed. At higher energies, however, as the number of resonances presumably increases rapidly, the smooth energy behavior materializes as a result of the statistical cancellations of the many resonances.

We have thus demonstrated that, given enough constraints (which are not too unreasonable!) between s-channel resonances, a fairly small number of them can reproduce many of the characteristic features of peripheral t-channel exchanges and therefore provide us with a description of scattering amplitudes which is complementary to the description provided by the exchange of Regge poles.

#### VII. CAN A t-CHANNEL TRAJECTORY REPRODUCE THE PROPERTIES OF s-CHANNEL RESONANCE?

An s-channel resonance is characterized by a bump in the energy dependence of a specific partial wave amplitude. It can also be characterized by a circle in the Argand diagram for the phase shift of the same partial wave. In order to understand how Regge poles in the t-channel reproduce the same physical amplitude as the one described by s-channel resonances we have to study whether the projections of the t-channel trajectories on the s-channel partial wave amplitudes is capable of producing such peaks in the energy dependence.<sup>7</sup> In order to do so, let us again consider  $\pi$ - $\pi$  elastic scattering and assume (for no good reason at all) that the entire scattering amplitude at all values of  $\nu$  and  $t$  is given by the expression  $f(\nu, t) = e^{i\pi\alpha(t)}$ . Figure 7 shows<sup>8</sup> the angular dependence of the real and the imaginary parts of this amplitude at different center of mass energy  $E^*$ . The amplitude is independent of  $\nu$  but the range of  $t$ -values available at any given energy, depends on the value of  $\nu$ . The amplitude shows oscillations both in the real and in the imaginary part as a function of  $t$  or  $\theta$ . In order to study the behavior of specific partial wave amplitudes, we have to perform the partial wave expansion of our amplitude. Let us first consider the S-wave part ( $l = 0$ ). The real and imaginary parts of the S-wave partial wave amplitude can be obtained by integrating the real and imaginary part of the amplitude from  $\theta = 0$  to  $180^\circ$  at every given energy. Such an integration will produce oscillations which are caused by the variation in the maximal allowed value of  $|t|$ . The outcome of such a calculation is shown in Fig. 7b. We obtained a spiralling phase shift which creates clear circles in the Argand diagram with a radius which is decreasing with energy. It is clear that as a function of energy, the imaginary part of the S-wave amplitude will

show peaks at various energy values and such peaks will be interpreted as S-wave resonances in the s-channel. A similar situation occurs when we project the P-wave component of the same amplitude and we find the situation demonstrated in Fig. 8.

All of these arguments only demonstrate that our fictitious amplitude  $e^{i\pi\alpha(t)}$  possesses typical resonance properties in the s-channel. It is not difficult, however, to convince ourselves that if we add one to our amplitude, or if we divide it by a smooth function of  $t$  ( $t < 0$ ), such as  $\sin\pi\alpha(t)$ , we will not change this property of the amplitude. In other words, the signature factor of the Regge pole exchange amplitude guarantees that its projection on s-channel partial waves will produce "s-channel resonances", namely bumps in the energy dependence of specific partial wave amplitudes. The entire Regge amplitude which is, of course, much more complicated than the signature factor alone, normally retains this property, although the number of resonances, their position, elasticities and their various regularities may change as a result of the details of the other factors appearing in the Regge formula.

We can therefore conclude that, on one hand, the t-channel trajectories are capable of producing the most obvious properties of s-channel resonances and on the other hand it is perfectly conceivable that a small number of such s-channel resonances can reproduce the typical characteristics of a peripheral exchange. While this does not prove that the duality idea is experimentally valid, it does indicate that it is theoretically self-consistent and that it does not contradict any fundamental notion such as the concept of a resonance or the concept of a peripheral exchange. Whether experiments obey the predictions of this restrictive scheme we will see in the next sections.

#### VIII. DUALITY AND THE INTERFERENCE MODEL

The most crucial consequence of our assumptions so far (namely: analyticity, Regge pole dominance in the t-channel and resonance dominance in the s-channel) is the statement that s-channel resonances should not be added to t-channel exchanges<sup>2)</sup> in constructing a hadronic scattering amplitude.

This contradicts the basic idea of the interference model<sup>9</sup> which proposes to do precisely what duality forbids us to do: to add s-channel resonances and t-channel trajectories. The first experimental test of duality is, therefore, to study whether or not the interference model can be ruled out by experiment. In other words - to discover whether the addition of resonances and t-channel poles really leads to double counting. Very strong arguments against the interference model have already been proposed in the original work of Dolen, Horn and Schmid<sup>2</sup> and in several other papers.<sup>10</sup> In our opinion the best argument against the interference model can, in fact, be found in the recent attempts<sup>11</sup> to resurrect the model. It

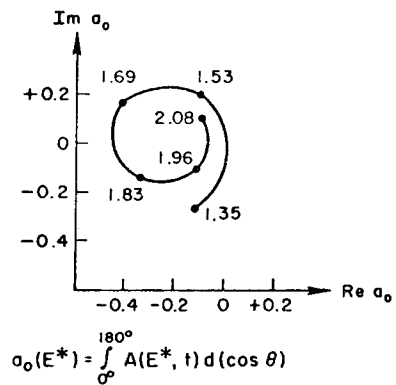
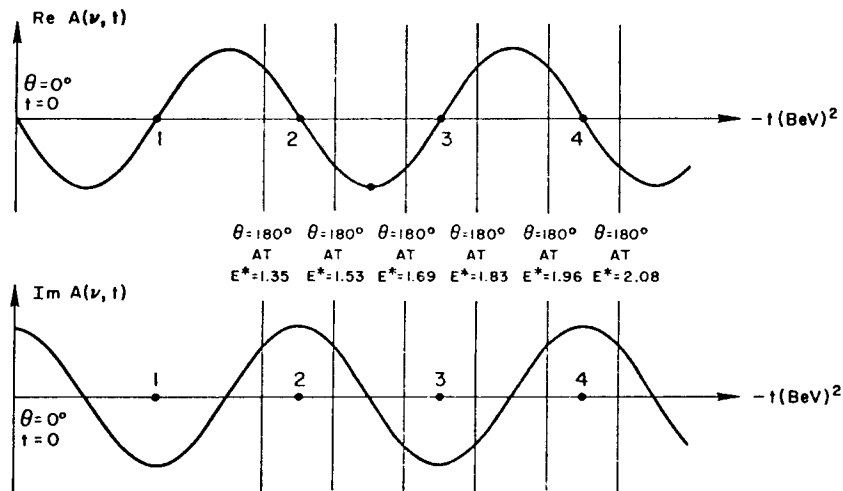


**Figure 7:**  $\text{Re } A(\nu, t)$  and  $\text{Im } A(\nu, t)$  plotted against  $t$ .  $A(\nu, t) = e^{i\pi\alpha(t)}$ ;  $\alpha(t) = 0.5 + t$ . The  $\theta = 180^\circ$   $t$ -values at various c.m. energies  $E^*$  are marked, assuming that the process under discussion is elastic  $\pi - \pi$  scattering. The S-wave projection of  $A(\nu, t)$  is plotted below as a function of  $E^*$  in an Argand plot.

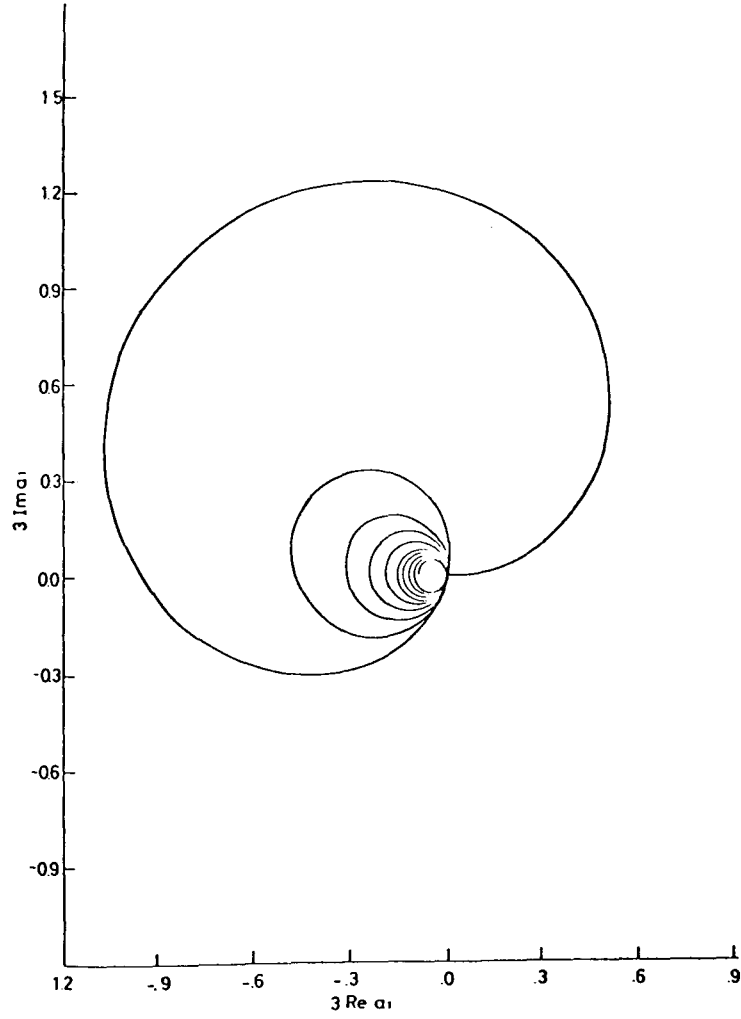


Figure 8: The P-wave Argand plot of  $A(\nu, t) = e^{i\pi\alpha(t)}$ . The figure is taken from Chiu and Kotanski, reference .8.

is indeed true that these attempts have led to magnificent fits to the physical amplitudes of processes such as  $\pi N \rightarrow \pi N$ .<sup>11</sup> But a brief glance at the artificial assumptions and the awkward resonance properties required by these fits should be sufficient to convince us that they have very little to do with a reasonable physical description of a strong interaction scattering amplitude. A typical example is provided by Fig. 9 in which we see how a scattering amplitude which practically vanishes is said by the proponents of the interference model to be a sum of two quantities, equal in magnitude and opposite in sign, representing the contributions of an s-channel resonance and a t-channel trajectory. Let us emphasize here that on purely mathematical grounds it is dubious whether the interference

---

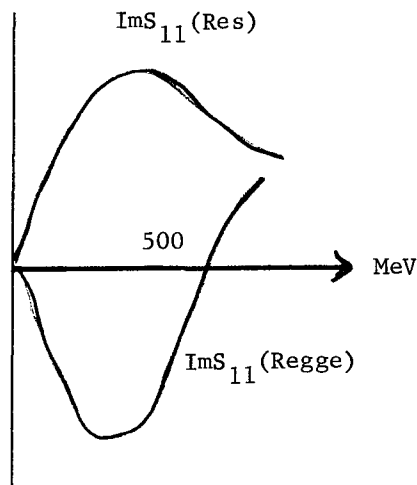


Fig. 9. An example of an interference model "explanation" of the  $S_{11}$   $\pi N$  amplitude. A "new" 1440 MeV  $S_{11}$  resonance is invented in order to compensate a Reggeistic contribution and to give a total physical amplitude which practically vanishes (from Ref. 11).

---

model or any other such flexible model (or for that matter, duality) can ever be rigorously ruled out. But we are not interested here in mathematics. We are trying to find a meaningful description of hadronic processes. Any description which involves resonances corresponding to dips rather than peaks in the energy dependence of an amplitude, or which invokes non-existent resonances which cancel non-existent Regge poles in order to produce a vanishing physical amplitude, certainly does not qualify as a simple physical picture.

#### IX. S-CHANNEL QUANTUM NUMBERS ARE IMPORTANT AT LARGE s-VALUES

According to the traditional picture of hadronic reactions, s-channel resonances dominate low energy amplitude and have nothing to do with high energy amplitudes, while peripheral exchanges in the t-channel dominate high energy amplitudes and are irrelevant to low energy amplitudes. Such a situation would indicate that small angle, high energy phenomena in a given scattering process are not dependent in any crucial way on the internal quantum numbers of the reaction in the

s-channel. Thus, a typical exchange model would not distinguish between processes such as elastic  $K^+p$  and  $K^-p$  scattering. In both cases the same exchanges are allowed in the t-channel (Fig. 1), while the s-channel quantum numbers (which are different) are said to be irrelevant to high energy, small angle scattering.

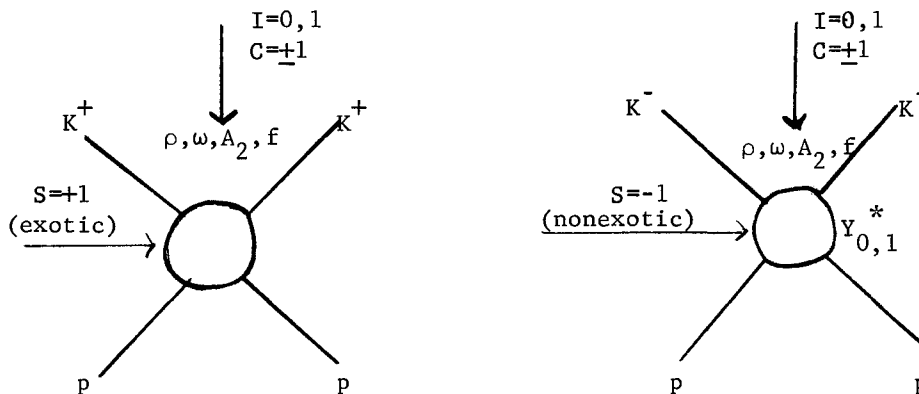


Fig. 10.  $K^+p \rightarrow K^+p$  and  $K^-p \rightarrow K^-p$  have the same t-channel quantum numbers but totally different s-channel properties.

Duality, however, relates the t-channel exchanges to the s-channel resonances and therefore demands that the s-channel quantum numbers which control the s-channel resonances, will also be important in describing high energy, small angle, phenomena. In particular, if we have two processes in which in one case no s-channel resonances exist while in the other case many s-channel resonances exist, we should find traces of this empirical fact even in the high energy domain, in spite of the fact that in such energies the effects of resonances are not directly observed. Consequently, processes such as  $K^+p$  and  $K^-p$  elastic scattering should show different characteristics well above the region of the prominent s-channel resonances. Simple regularities which will show that s-channel quantum numbers are indeed important for describing high energy, small angle, phenomena will provide us with supporting evidence for the idea of duality. They would not be possible in a simple interference model, for example, because in such a model the resonances are added to the dominant t-channel features and do not dictate any specific behavior to the t-channel exchanges.

There are, at least, two very clear systematic phenomena which indicate that s-channel internal quantum numbers are very important for high energy scattering. We believe that one of them is fairly well understood, while the other can be only vaguely understood in terms of qualitative statements and it does not have, so far,



any explicit quantitative description.

The first observation is shown in Fig. 11 where all the known total hadronic cross sections are plotted versus energy. There are 10 known total cross sections in the range between 2 and 20 BeV. Four of them show very little or no energy dependence.  $K^+p$  and  $K^+n$  total cross sections are, for example, constant (within 1 mb) from two to 20 BeV.  $pp$  and  $pn$  total cross sections are also approximately

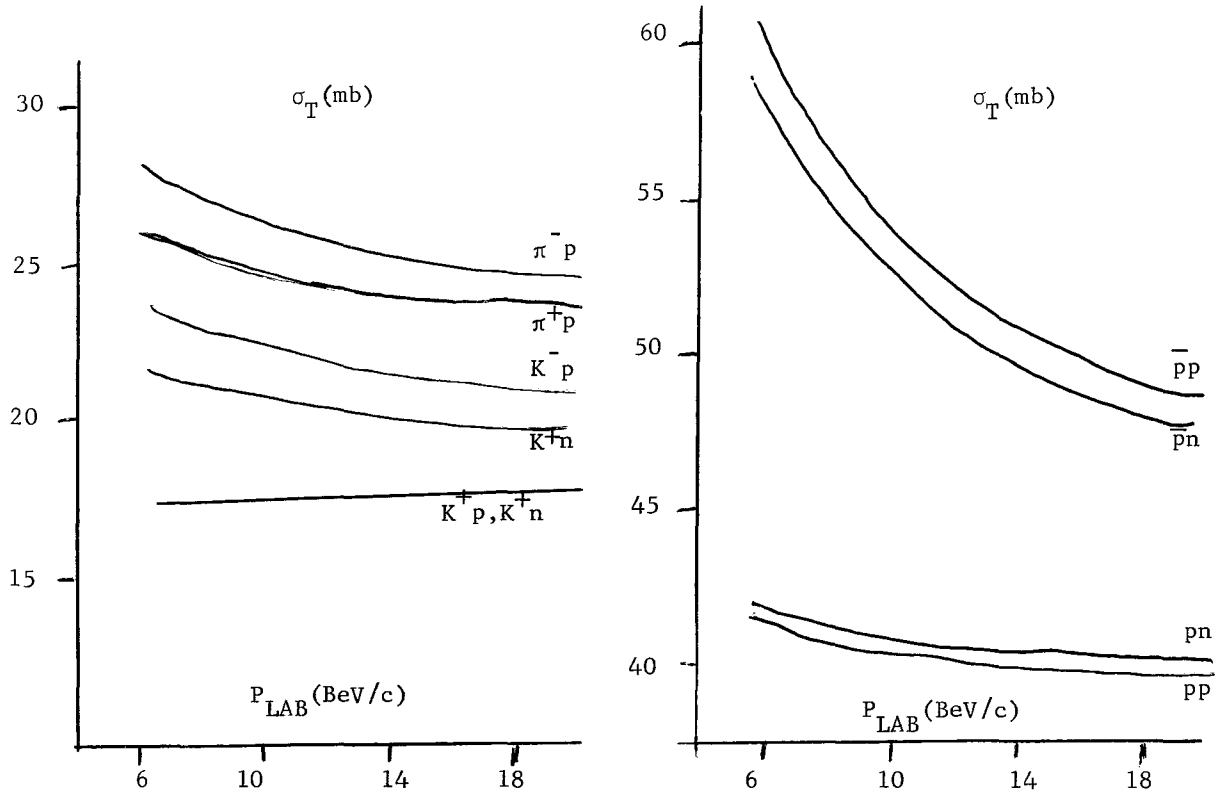


Fig. 11 Smooth curves approximating total hadronic cross sections

constant in this energy range. (They certainly vary much less than  $\bar{p}p$  and  $\bar{p}n$ ). All other six total cross sections are not constant. They decrease towards an asymptotic value which is probably constant. The clear energy dependence of these six processes is correlated in a striking way with the fact that these six processes are the ones in which many s-channel resonances are found. On the other hand, the four processes with constant total cross sections are precisely the ones having exotic s-channel quantum numbers for which no known s-channel resonances exist. This cannot be an accident. It is a very clear indication that the s-channel quantum numbers, through the s-channel resonances, do have something to say about high energy phenomena. The complete explanation for this<sup>12</sup> will be given in

Secs. XI and XII, after we shall discuss the particular role played by the Pomernanchuk singularity within the duality framework, but the correlation speaks for itself even on pure empirical grounds.

Another systematic set of experimental results which indicate a strong correlation between the internal quantum numbers in the s-channel and small angle, high energy, scattering is shown in Fig. 12. The angular distribution for high energy elastic scattering for several initial states is shown. Again, we find that the various processes can be clearly divided into two groups. Processes such as  $pp$  and  $K^+p$  elastic scattering show an angular distribution without any clear dip structure. On the other hand, processes such as  $\pi^+p$ ,  $\pi^-p$ ,  $\bar{p}p$  and  $K^-p$  elastic scattering show a dip structure with dips somewhere around  $t = -0.6 \text{ BeV}^2$ . The correlation is, again, based on the fact that processes with exotic s-channel quantum numbers do not have dips in the angular distribution while processes with non-exotic s-channel quantum numbers and hence with many s-channel resonances, do show dips in their angular distribution. A simple explanation of this correlation would be, of course, to claim that the dips are entirely due to the contributions of s-channel resonances and are therefore absent in processes which do not allow any such resonances. This statement, while "explaining" this striking regularity, does not really provide us with a quantitative way of describing it. In fact, it turns out that a simple Regge pole model which includes the restrictions on the Regge pole parameters implied by duality and the absence of exotic s-channel resonances, is inconsistent with this experimental observation. If we want to reconcile the presence of dips in non-exotic elastic processes and their absence in exotic elastic processes, with a simple exchange model we have to include either Regge cuts or absorption effects. How to do this precisely is not yet clear and this is obviously one of the most interesting open problems.

Quite independent of the fact that we cannot present here a quantitative explanation of this regularity, let us emphasize again that its mere existence is another piece of supporting evidence for the idea of duality. It would be extremely difficult to explain the one-to-one correspondance between exotic and non-exotic s-channel quantum numbers on one hand and the absence and presence of dips in angular distributions at high energies on the other hand without taking into account the influence of s-channel resonances on high energy, small angle scattering. Such an influence is built into the duality idea and is completely foreign to models such as interference model. We may therefore claim that the prediction of duality that s-channel quantum numbers are important and crucial for describing small angle high energy scattering is verified at least by two independent remarkable sets of regularities of the experimental data.

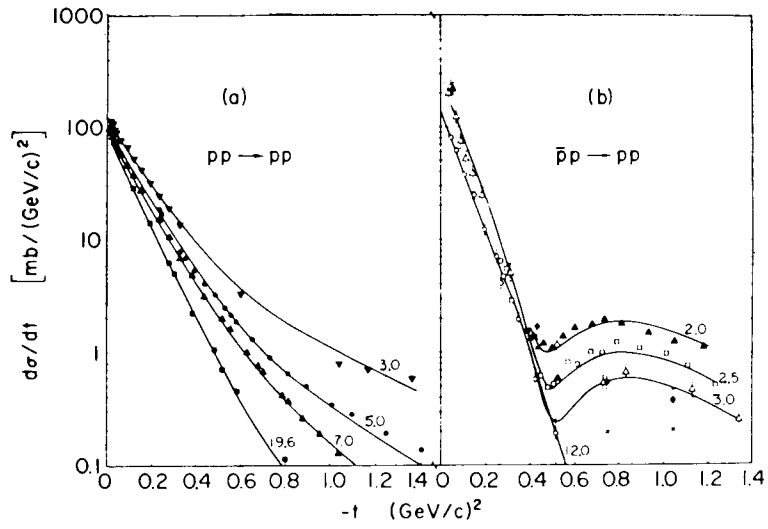


Figure 12: Angular distributions for elastic reactions. Exotic channels do not show dips in angular distribution while non-exotic channels have dips (D.R.O. Morrison, Lund Conference review).

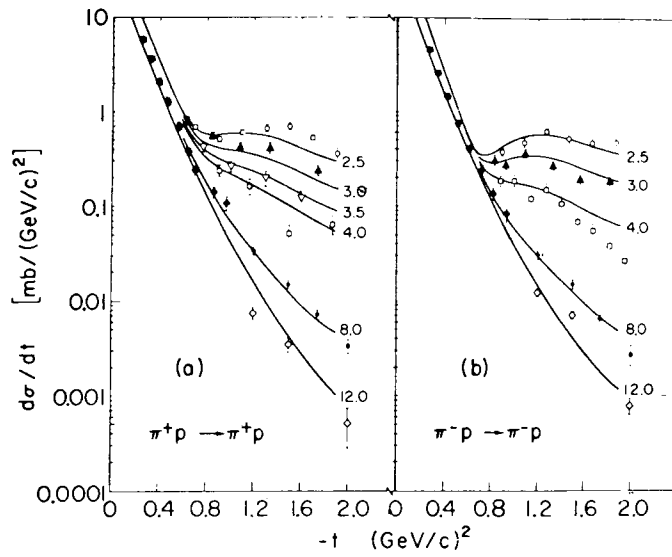


Figure 12. (Continued).

$K^+p$  ELASTIC SCATTERING

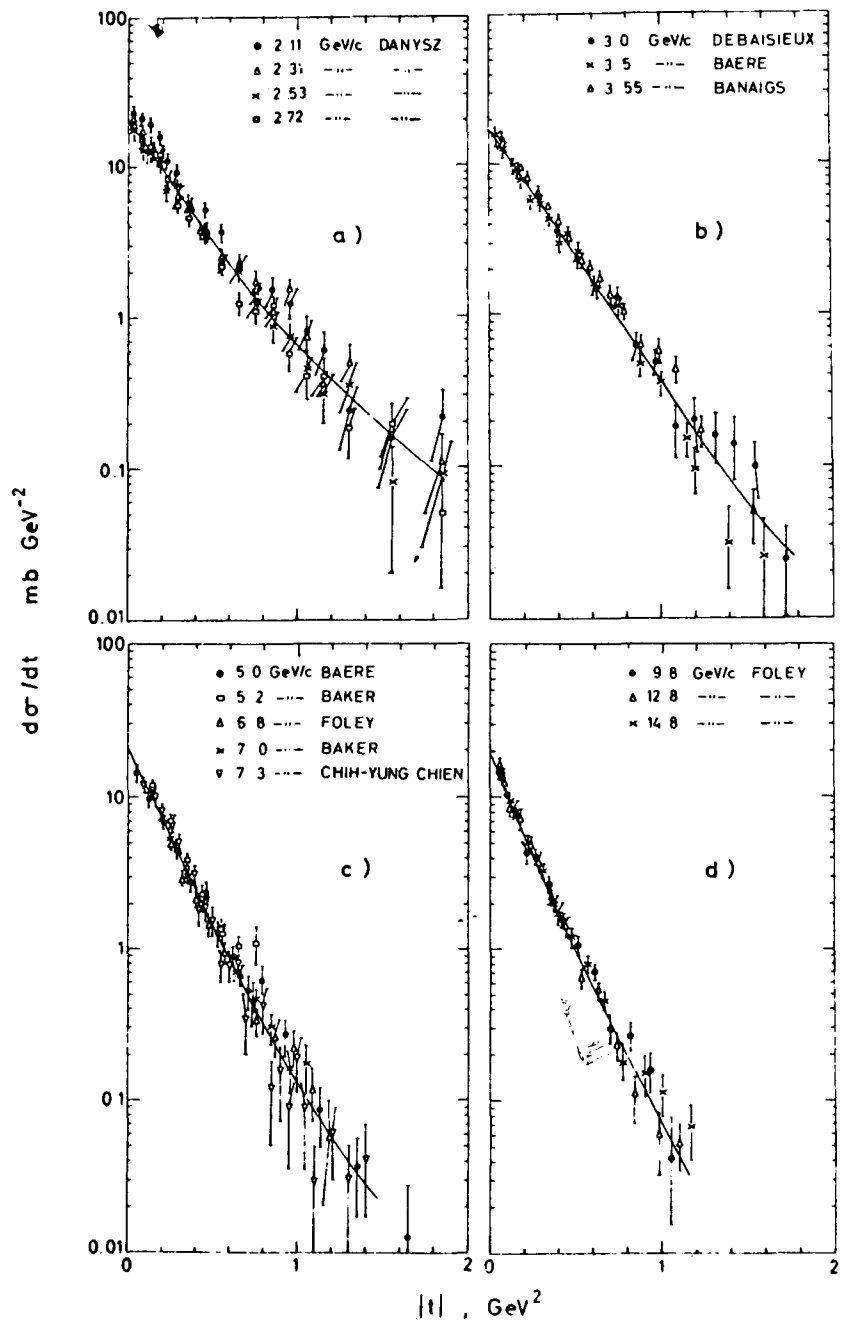


Figure 12. (continued).

$K^-p$  ELASTIC SCATTERING

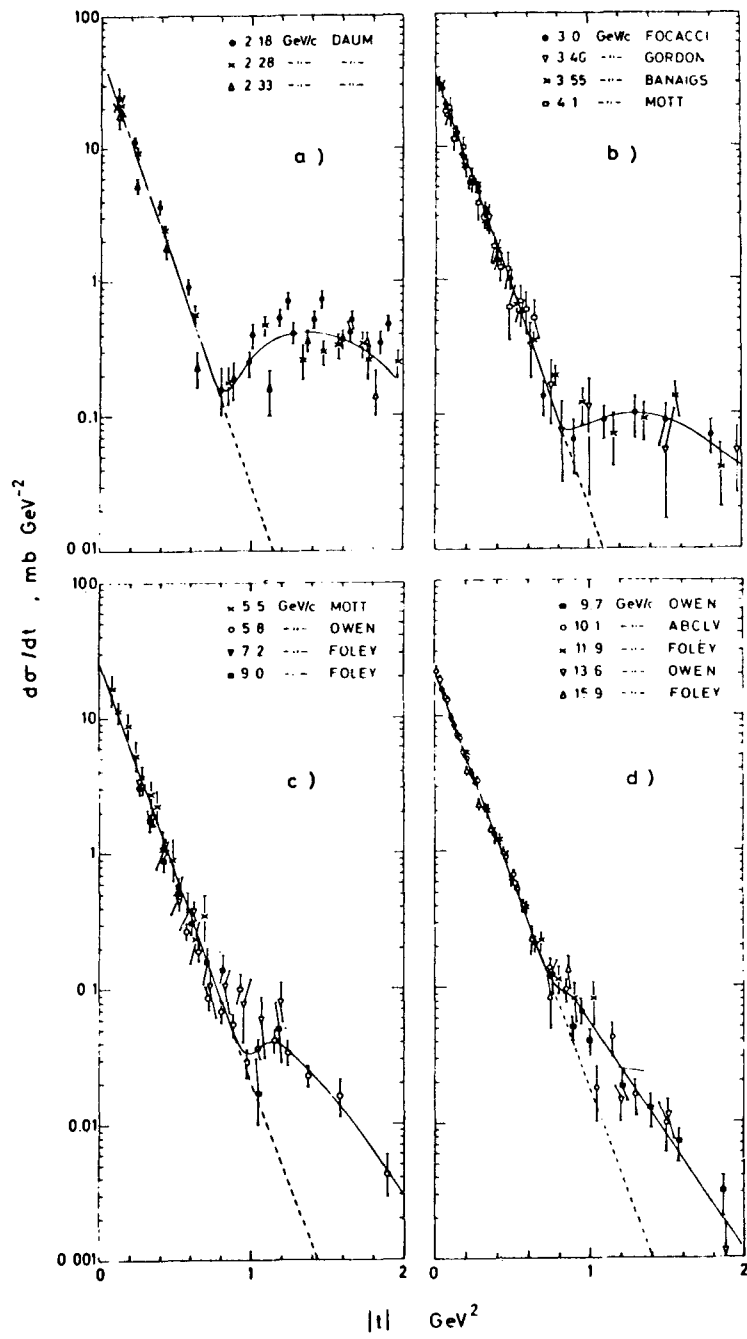


Figure 12. (Continued)

## X. AN ARISTOCRATIC POMERANCHUK SINGULARITY

So far we have assumed that the t-channel Regge poles are balanced in the sense of duality by the s-channel resonances and that from the s-channel point of view the amplitude is completely dominated by resonances. At this point we must make an extremely important exception.<sup>12,13</sup> In order to realize the necessity of making such an exception, let us consider again a process with exotic s-channel quantum numbers, such as  $K^+p$  elastic scattering (Fig. 1). In this process no s-channel resonances exist, but the Pomernanchuk singularity contributes in the t-channel as much as it contributes in  $K^-p$  elastic scattering. Consequently, the Pomernanchuk singularity cannot be related to the contribution of s-channel resonances, since it contributes equally to two processes, one of which has no s-channel resonances while the other has a large number of such resonances. We therefore have to assume that the Pomernanchuk singularity in the t-channel should be viewed from the s-channel point of view as a non-resonating background rather than as a quantity dominated by resonances.

Another way of stating our motivation for proposing such a conjecture can be the following: The Pomernanchuk trajectory contributes only to the  $I=0$  t-channel amplitude. The crossing matrix tells us that an  $I=0$  t-channel amplitude has equal projections on all s-channel isotopic spins. Therefore, in order for the Pomernanchuk to be related to any kind of s-channel structure, such a structure should be completely independent of the isotopic spin in the s-channel. This is clearly not a characteristic property of a resonance or of a simple sum of resonances. In that respect the Pomernanchuk is completely different from other t-channel trajectories in such a way that the overall projection on a specific s-channel isotopic spin vanishes. The Pomernanchuk trajectory, however, is higher than all other trajectories and, for sufficiently large energies, can never be cancelled by any other t-channel contribution. It must therefore stand by itself and be reflected as an isospin independent contribution in the s-channel. Such a contribution could easily be some kind of a background but could hardly be associated with resonance structure in the s-channel. We shall therefore modify our original resonance dominance assumption of Sec. IV, to include one term which is not dominated by resonances and which does not even have contributions of resonances. This term will be the Pomernanchuk singularity (from the t-channel point of view) or a non-resonant background (from the s-channel point of view). The rest of the scattering amplitudes will be assumed, as before, to be completely described either by t-channel Regge poles (other than the Pomeron) or by s-channel resonances with no background.

## XI. TWO COMPONENT AMPLITUDES

After making the resonance dominance assumption for all amplitudes other

than those contributed by the Pomeranchuk and after making the specific exception of the Pomeranchuk singularity, we now have a general description of hadronic amplitudes in terms of two additive components.

The first component can be viewed from the s-channel point of view as non-resonating background and from the t-channel point of view as the Pomeranchuk contribution. In terms of simple optical models this part of the amplitude will be considered the contribution of the total absorption by some kind of a black disc. The contributions to such a term will probably come from all partial waves within the allowed radius of interaction, namely, from all c.m. angular momenta  $l \lesssim kR$ . We shall see later, that the same term, from the point of view of the quark model, will be described as a combination of quark-quark and quark-antiquark elastic scattering contributions without annihilations and creations of quark-antiquark pairs.

The second part of our two component amplitude includes what may be described as many s-channel resonances without any substantial background, or a number of t-channel Regge poles (and possibly cuts). In terms of a simple optical picture we would presumably propose that this part of the amplitude is dominated by the peripheral partial waves (defined by the approximate relation  $l \sim kR$ ). Those partial waves will then be dominated by peripheral s-channel resonances or, by combined contributions of t-channel poles and cuts. Again, we shall see later, that from the quark model point of view, this part of the amplitude is given by the annihilation of one pair of a quark and an antiquark accompanied by the creation of another such pair.

The separation of the hadronic amplitudes into two such parts is of great interest. It leads immediately to many experimental predictions. The most striking predictions are those which utilize the possibility that one of the two parts of the amplitude is absent. For example, processes in which no s-channel resonances exist are predicted to have only a Pomeranchuk contribution in the t-channel, with all other trajectories cancelling each other in the imaginary parts of the amplitude.<sup>12</sup> This is indeed the case experimentally for  $K^+p$ ,  $K^+n$ ,  $pp$ , and  $pn$  scattering. Another clear prediction of the separation of the hadronic amplitudes is the prediction that in cases where the Pomeranchuk cannot contribute, namely in processes involving the exchange of charge, strangeness, or any other non-vanishing quantum number, the entire amplitude has to be given by resonances and the total contribution of the non-resonant background should be very small or negligible.

Notice, however, that the separation of the amplitude into its two parts is linear, namely, the two parts are additive and they can be kept separate from each other only in a set of linear dynamical relations such as the finite energy sum rules. Non linear relations such as the unitarity relations do not a priori leave

the two parts of the amplitude disconnected. In fact, it is very interesting to try and find a relation between the two parts of the amplitude or between the s-channel resonances and the Pomeranchuk singularity using the unitarity relation. Several attempts in this direction have not led to satisfactory results. However this question is still open and it deserves much attention.

## XII. THE POMERANCHUK SINGULARITY AND NON-RESONANCE BACKGROUND

In order to study the experimental validity of the conjecture stated in the previous two sections we have to verify two major points. First, we have to show that the Pomeranchuk singularity in the t-channel is built (in the sense of finite energy sum rules) by the non-resonant background alone without any resonance contributions. Second (and this is a separate problem) we have to show that the other trajectories, the so called ordinary trajectories, are built (again, in the sense of FESR) only from s-channel resonances without any substantial background contributions. The best evidence that the Pomeranchuk contribution is built from background alone can be obtained by studying the example that we have mentioned already, namely, the total cross section for  $K^+p$  and  $K^-p$  scattering. Figure 13 shows the experimental data for these two cross sections plotted versus  $\nu$ , the laboratory energy of the incident K meson.  $\nu > m_K$  is the region for physical scattering in the  $K^-p$  channel and  $\nu < -m_K$  is the physical region for  $K^+p$  scattering. The Pomeranchuk contribution which is constant in  $\nu$  and symmetric under the transformation  $\nu \rightarrow -\nu$  is clearly seen in the figure. It is essentially represented by the entire total cross section for  $K^+p$  scattering and by a constant portion (indicated in the figure) of the total cross section for  $K^-p$  scattering. One important point which is seen in the figure is that the total cross section for  $K^-p$  scattering is always larger or equal than the constant Pomeranchuk portion and it decreases towards the constant. This means that in every energy the total cross section can be viewed as a sum of two terms, one of which is the constant Pomeranchuk term which is presumably related to background in the s-channel, and the other term is the resonance contribution which has to be positive definite in an elastic process (and the total cross section is proportional to the forward imaginary elastic amplitude). We can therefore conclude from the figure that in  $K^+p$  scattering the Pomeranchuk term is entirely built from non-resonance background while in  $K^-p$  scattering, while we cannot prove it, it is perfectly reasonable to assume that the constant Pomeranchuk term does not include any resonance contributions.

Note that we also predict<sup>12</sup> here that all total cross sections must decrease to their constant asymptotic value, a fact which is verified experimentally and which had not been explained before (Fig. 11).

Another way of testing the same hypothesis is to consider a process for



which we have a phase shift analysis at low energies (such as  $\pi N$  elastic scattering) and to separate the resonance contribution from the background term. We may then use FESR to compute the contribution of the Pomernanchuk trajectory by inserting only the background into the left hand side of the FESR. We can also compute the contribution of the  $\rho$  and  $P'$  trajectories (which are presumably the dominant "ordinary" trajectories contributing to  $\pi N$  scattering) by inserting the resonant contribution in the left hand side of the FESR. If by doing so, we find approximately the correct properties of the  $P$ ,  $P'$  and  $\rho$  trajectories, we may assume that at least in this process we have a separation of the amplitude to two components with a one-to-one correspondence between the background and the Pomeron and between the resonances and the ordinary Regge trajectories. A detailed analysis along these lines which was carried out<sup>14</sup> has led to very encouraging conclusions. Figure 14 shows a comparison<sup>14</sup> between the full physical amplitude for  $\pi N$  scattering at low energies and an amplitude which is constructed theoretically by adding the s-channel resonances found in the phase-shift analysis to the extrapolated contribution of the Pomernanchuk trajectory. Only if the Pomernanchuk contribution is well approximated by the non-resonant background, should such a theoretical model fit the data. The reasonable agreement between the model and the data indicates that, to a good approximation, this is indeed the case.

Among the many other pieces of evidence<sup>14</sup> in favor of this hypothesis, let us mention only one additional interesting case. The process  $\gamma p \rightarrow \rho^0 p$  is presumably dominated by Pomernanchuk exchange at high energies. In this process clear indications are observed for the  $\Delta(1920)$  resonance. This resonance presumably sits on some background (Fig. 15). If we assume that the background under the resonances is given by the extrapolated Pomernanchuk contribution we find that the resonance accounts for approximately  $5 \mu b$  of the total cross section for this process, at a c.m. energy of 1920 MeV. This would lead us to a prediction for the strength of the same resonance in the process  $\gamma n \rightarrow \rho^0 \bar{p}$  in which the Pomernanchuk singularity cannot be exchanged in the t-channel. In such a process, according to our conjecture, the entire cross section will be dominated by resonances and, in particular, at a c.m. energy of 1920 MeV the cross section will be dominated by the  $\Delta(1920)$ . The cross section for  $\gamma n \rightarrow \rho^0 \bar{p}$  at this energy should therefore be approximately  $2.5 \mu b$  (there is a factor two between the  $\Delta$  contributions in the two processes because of isospin coefficients). If, however, a substantial part of the Pomernanchuk contribution to  $\gamma p \rightarrow \rho^0 p$  is contributed by the resonances (and in particular by the  $\Delta(1920)$ ), the contribution of the 1920 MeV resonance to this process should be larger than  $5 \mu b$ . In that case the cross-section for  $\gamma n \rightarrow \rho^0 \bar{p}$  should be larger. This provides us with an interesting experimental test for this hypothesis. A recent bubble chamber experiment at DESY has provided for the first time cross-

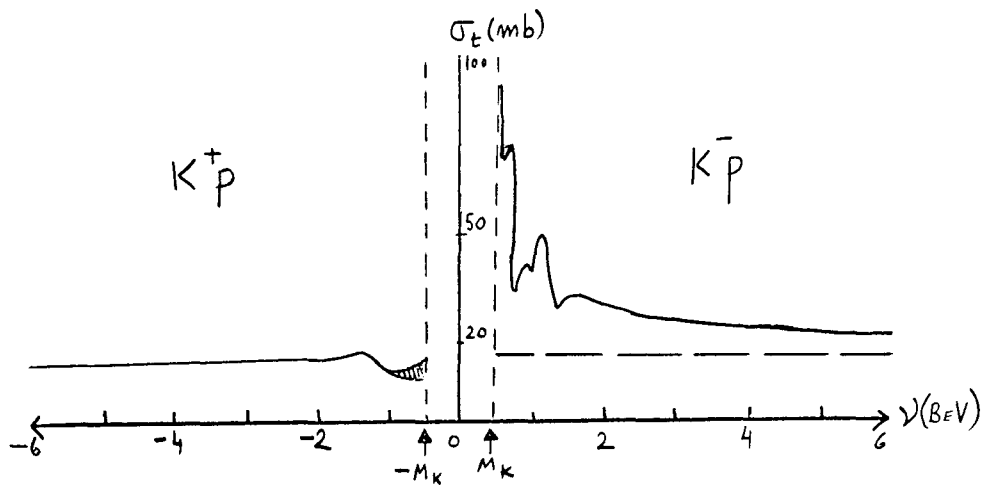


Figure 13.  $K^+p$  and  $K^-p$  total cross-sections (J.D. Jackson, Lund review talk).

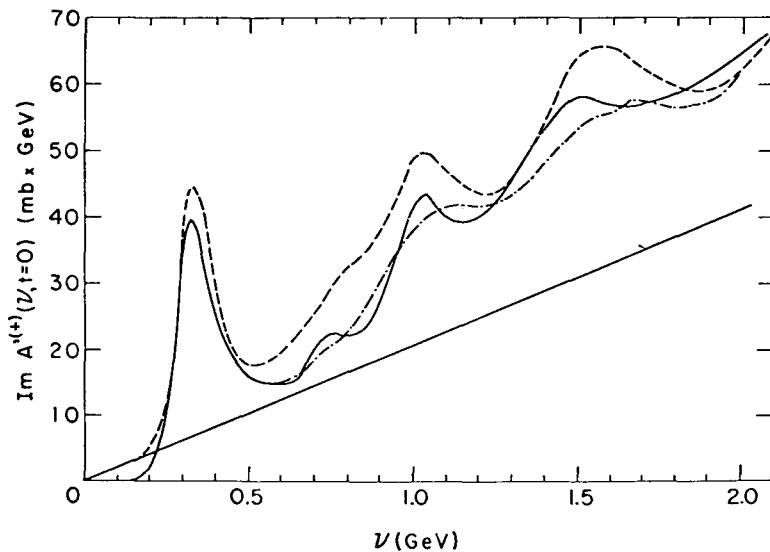


Figure 14: Solid line - data (from  $\sigma_t(\pi N)$ ); dashed-dotted line - reconstructed data from CFBN  
 phase shifts: dashed line - resonances + Pomeron (from reference 14).

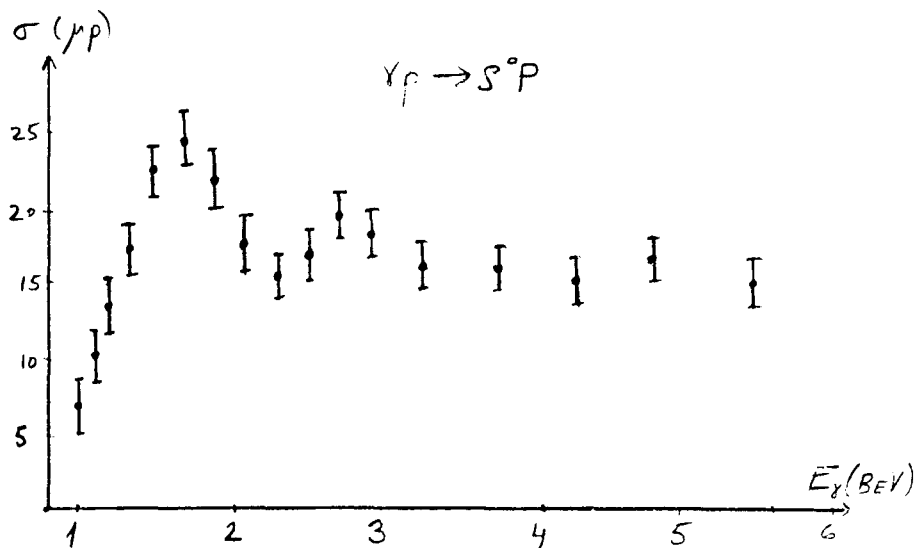


Figure 15:  $\sigma(\gamma p + \rho^0 p)$ . The  $\Delta(1920)$  is clearly seen (F. Pipkin, Review talk at the SLAC Conference, 1967).

section for the  $\rho^-$  photoproduction process and the results are in good agreement with the assumption that the background under the 1920 resonance in  $\gamma p \rightarrow \rho^0 p$  is fully accounted for by the extrapolated Pomeranchuk contribution.

This and many other arguments<sup>14</sup> that we shall not reproduce here convince us that the possibility that the Pomeranchuk contribution is built by the s-channel background is at least consistent with experiment and probably true in general.

### XIII. s-CHANNEL RESONANCES AND t-CHANNEL "ORDINARY" TRAJECTORY

We shall now study the second part of our conjecture, namely: the "ordinary" trajectories in the t-channel are built in the sense of FESR only from s-channel resonances, without any substantial background contributions. In order to do so, we have to consider processes in which the Pomeranchuk contribution is absent and see whether or not the entire amplitude for such processes is given by s-channel resonances. The only place where this could be done in a convincing way is, of course, to study an amplitude which is well known experimentally in a physical region in which we have good reasons to believe that we have already identified all the existing s-channel resonances. Processes in which only part of the resonances are identified will not do because we cannot be sure that the part of the amplitude which we would consider as "non-resonant" does not include additional resonances.  $\pi N$  scattering is, therefore, again, the only place where we can study our hypothesis in detail. In order to do this, it is very useful to recalculate<sup>14</sup> the  $\pi N$  phase shifts of the usual s-channel partial waves but to use definite t-channel isotopic spins. It is trivial to re-combine the  $I_s = 1/2$  and  $I_s = 3/2$  s-channel components of a given s-channel partial wave amplitude and to construct the  $I_t = 0$  and  $I_t = 1$  components of the same partial wave amplitude. Doing so we find ourselves with s-channel partial wave amplitude having definite t-channel isotopic spins. The amplitudes with  $I=1$  in the t-channel do not allow the Pomeranchuk to contribute and, therefore, according to our conjecture, should be completely dominated by s-channel resonances. The amplitudes with  $I=0$  in the t-channel should indicate the existence of the very same resonances but should also show a clear component coming from the Pomeranchuk singularity, namely, a clear indication of a purely imaginary rising background. In Fig. 16 we show the Argand diagrams for the partial wave amplitudes constructed in this way.<sup>14</sup> We see that for  $I_t = 1$  the amplitudes describe fairly clear circles without any strong indications of background. For  $I_t = 0$  similar circles appear but they are clearly superimposed on a rising imaginary background and the general feature observed is some kind of a spiralling curve which moves upwards in the diagram. We therefore see that most of the  $I_t = 1$  amplitudes are indeed controlled by resonances alone, while the  $I_t = 0$  amplitudes definitely have a large non-resonance contribution. The same

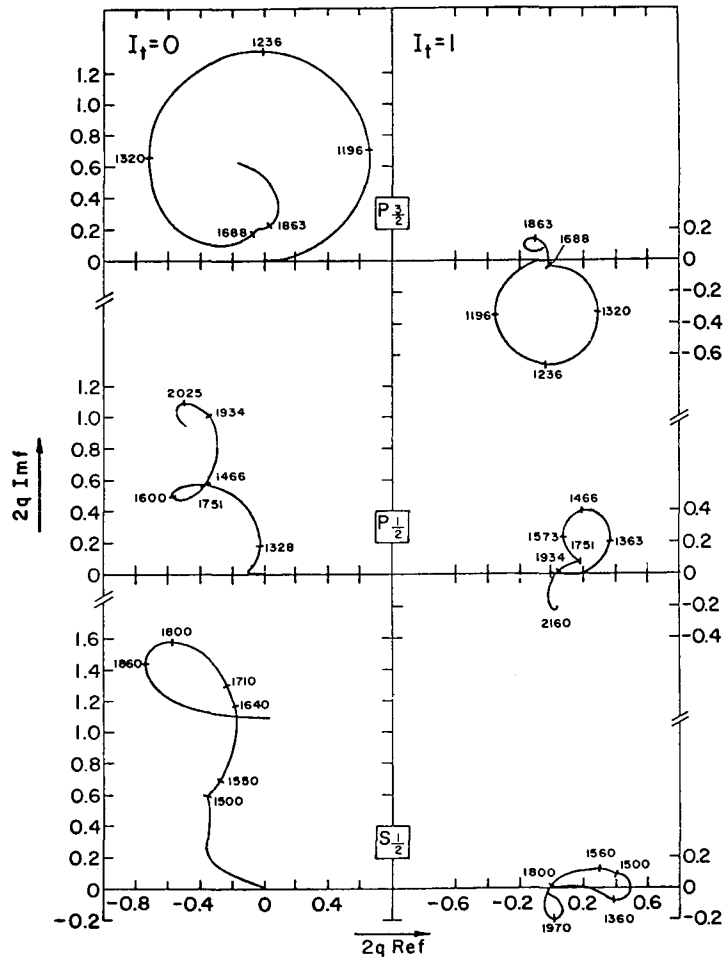


Fig. 16 (Reference 14).

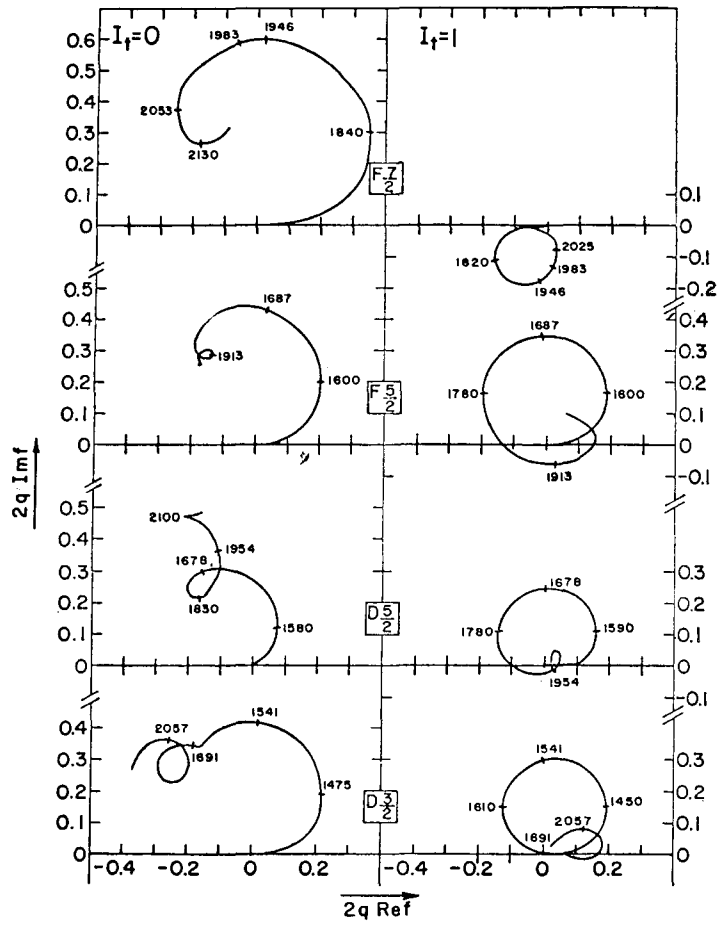


Fig. 16 (cont'd)

conclusion can be displayed in a more striking way if we plot the imaginary parts of the same s-channel partial wave amplitudes with definite t-channel isotopic spins as a function of energy. Resonances should be observed as bumps in the imaginary part. Figure 17 shows<sup>14</sup> that for  $I_t = 1$  amplitudes the resonances are very clearly observed and there is no background to speak of; for  $I_t = 0$ , however, the same resonances are again superimposed on a rising imaginary background, presumably coming from the Pomeranchuk contribution. We consider the  $I_t = 1$  curves in Figs. 16 and 17 as extremely strong evidence for the hypothesis that the non-Pomeranchuk term in hadronic amplitudes is indeed strongly dominated by s-channel resonances and we propose that this is actually a general property of such amplitudes. Unfortunately, no other process has a sufficiently good phase shift analysis and it is very hard to reach definite final conclusions on the basis of one success. It would be extremely interesting to see whether future better phase shifts for  $K^+p$  and  $K^-p$  scattering, as well as for photoproduction processes will confirm our conclusions. A recent attempt<sup>15</sup> to reproduce this analysis for photoproduction of single  $\pi$  mesons has indicated encouraging results but the quality of the phase shift analysis for such processes is such that we cannot claim this to be a definite success.

#### XIV. THE ABSENCE OF EXOTIC AMPLITUDES

So far we have not used the absence of exotic amplitudes as a fundamental principle within the duality framework. We have used this in studying some of our examples such as the often quoted case of  $K^+p$  scattering, but we have never made this a condition for the existence or the truthfulness of duality. Duality may very well be true, independent of the existence or absence of exotic amplitudes. However, we have emphasized that duality becomes useful particularly in those cases in which both the s-channel and the t-channel description of the process are very simple. We know that at high energy the t-channel description is almost always simple. When can we expect the s-channel description to be also simple at high energy? One clear example is the case when the s-channel description says that due to the absence of resonances, the imaginary part of the amplitude has to vanish. This is certainly a simple description!

A similar situation occurs at low energies. The s-channel picture at very low energies is almost always simple. When could we expect the t-channel picture at low energies to be simple? Presumably only when the t-channel picture indicates that no exchanges are allowed in the t-channel! Our experience is such that whenever some exchanges are allowed, the t-channel features at low energies and the s-channel features at high energies are so complicated that we cannot really use them in an efficient way. It is precisely this observation which gives such an

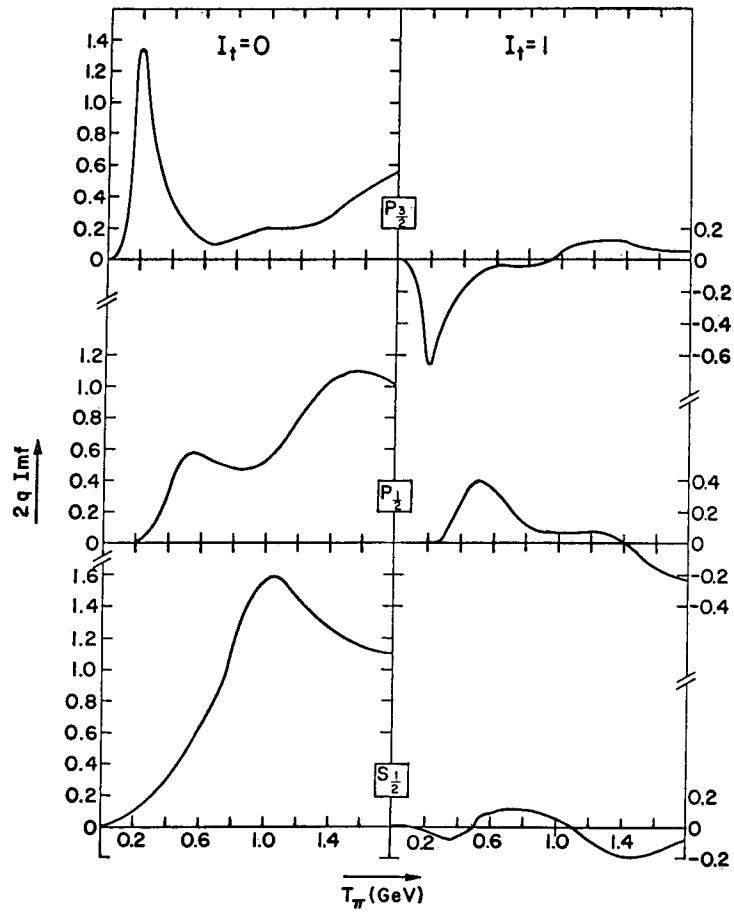


Fig. 17 (from Reference 14).

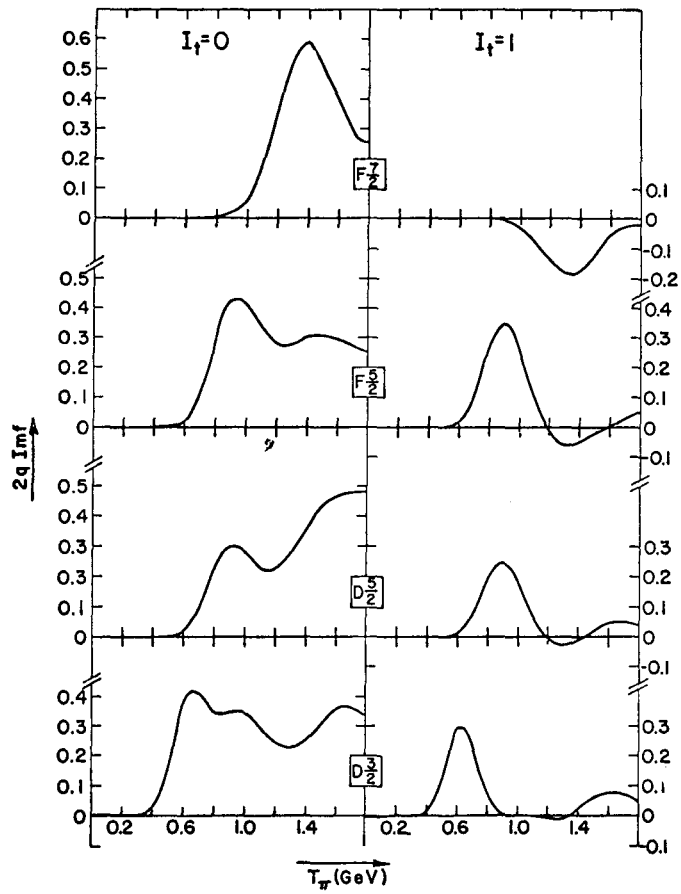


Fig.17 (cont'd)



enormous importance to the question of absence of exotic amplitudes with respect to the duality idea. It is the absence of such amplitudes which provides us with many many cases in which both the s- and the t-channel pictures are simple over relatively large energy regions. Most of the interesting predictions of duality are obtained in cases where exotic amplitudes could exist and are assumed not to exist. It is therefore of crucial importance to study from a purely experimental point of view the validity of the statement that in the s- as well as in the t- and u-channels no exotic quantum numbers are ever exchanged.

Let us start with the s-channel. In the s-channel we have assumed that (except for the Pomeranchuk contributions) only resonances contribute to the imaginary part of the amplitude. This means that in order to show that s-channel amplitudes with exotic quantum numbers vanish, it will be sufficient to show that no exotic resonances exist (the Pomeranchuk contribution in the t-channel definitely has projections on exotic s-channel quantum numbers but in any event we remove the entire Pomeranchuk contributions before starting any duality bootstrap calculation. When we refer to the absence of exotic amplitudes we really mean absence of exotic amplitudes outside the Pomeranchuk contribution). So far there is no strong evidence for any exotic resonance except for the possible  $K^+ p$  and  $K^+ n$  resonances around 2 BeV. Without getting involved in the discussion concerning the existence of these resonances, let us immediately remark that even if these resonances exist, their contributions are so small compared with other effects, or with the size of ordinary non-exotic resonances, that they can certainly be neglected within the approximations of our general considerations here. In the context of duality, it is therefore totally irrelevant whether or not small, quantitatively unimportant, exotic resonances exist. Thus, in processes such as  $K^+ n \rightarrow K^0 p$ ,  $Kp \rightarrow K\Delta$ ,  $pp \rightarrow p\Delta$ ,  $pn \rightarrow np$ , etc., the imaginary part of the entire amplitude will have to vanish.<sup>12</sup>

The question of exotic amplitudes in the t-channel or u-channel is more involved. Even if no exotic resonances exist we could easily have exotic amplitudes due to double exchanges. The simplest example is, of course, the possibility of exchanging two  $\pi$  mesons in the t-channel in an I=2 state. Many other combinations of two mesons, meson-baryon, etc. could easily produce similar effects. The assumption that no exotic quantum numbers are exchanged in the t- or u-channel is therefore much stronger than the assumption of the absence of exotic resonances. It includes one more idea, in the same way that the assumption of no exotic amplitudes in the s-channel includes both the absence of exotic resonances and the resonance dominance idea. The extra ingredient needed for forbidding t- and u-channel exotic exchanges is to state that the exchange of two poles or two particles (both of which are other than the Pomeranchon) is forbidden. Note that the cuts produced by exchanging an ordinary pole and a Pomeranchon will always have the

internal quantum numbers of the ordinary pole and therefore, since the ordinary pole is presumably non-exotic, so would be the cuts which it produces by joining the Pomeranchon. Such cuts are known to be important but they are not exotic.

There are at least two simple ways to study experimentally whether or not exotic exchanges in the t- and u-channel are important. The usual way in which this is done is simply to study processes in which only exotic quantum numbers can be exchanged. Typical examples are  $\pi^- p \rightarrow \pi^+ \Delta^-$ ,  $K^- p \rightarrow p K^-$ ,  $\pi^- p \rightarrow K^+ Y^{*-}$ , etc. In every one of these processes, and the many other examples which can be constructed in a similar way, either the t-channel or the u-channel involves the exchange of exotic quantum numbers. The absence of exotic exchanges would therefore predict that we shall not have the usual strong peripheral peak in the angular distribution at small t or at small u. The experimental data show indeed that such peaks are absent, but in many cases the upper limit is only of the order of a few percent. For example, in  $\bar{p} p \rightarrow \bar{\Sigma}^- \Sigma^-$  a tiny (exotic) forward peak of the order of 5% of the forward peak of  $\bar{p} p \rightarrow \bar{\Sigma}^+ \Sigma^+$  was found.<sup>16</sup> That means that the square of the exotic  $\bar{p} p \rightarrow \Sigma \Sigma$  amplitudes is not larger than a few percent of the square of a typical non-exotic amplitude. The exotic amplitude itself could however, be as large as 20 or 30 percent of the non-exotic amplitude!

It is therefore extremely important to study interference between exotic and non-exotic amplitudes, and this brings us to the second way in which we can experimentally investigate the presence of exotic amplitudes. We have to look for sets of processes which allow both exotic and non-exotic quantum numbers in the t-channel and study the various isotopic spin amplitudes which are exchanged. A typical example would be to consider  $K^- p \rightarrow \pi^- \Sigma^+$  and  $K^- p \rightarrow \pi^0 \Sigma^0$ . These two processes allow the exchange of a  $K^*$  meson in the t-channel. Both have non-exotic quantum numbers in the t-channel. Quite independent of the particular exchange mechanisms that we assume, we can easily see that the t-channel isotopic spin can be 1/2 or 3/2. We will therefore have two independent complex isotopic spin amplitudes to describe these processes, and we have no definite predictions from isospin conservation alone. If, however, the amplitude with  $I = 3/2$ , which is exotic, has to vanish, we remain only with one isospin amplitude in the t-channel and that means that the two processes have to be proportional to each other by a well defined Clebsch-Gordan coefficient. We predict that the ratio between the two cross sections for these processes is 4:1. An experimental determination of this ratio will enable us to see whether indeed the exotic amplitude is absent. Any deviation from this 4:1 ratio will indicate an interference between exotic and non-exotic exchanges. Unfortunately the data on  $K^- p \rightarrow \pi^0 \Sigma^0$  are still fairly poor and it is impossible to decide whether or not we do have exotic exchanges in this particular example.

Strangely enough the only evidence for interference between exotic exchanges

and non-exotic exchanges comes from photoproduction experiments at SLAC. The two reactions studied there are  $\gamma N \rightarrow \pi \Delta$  and  $\gamma N \rightarrow K \Sigma$ . If we assume that t-channel I = 2 exchanges in  $\gamma N \rightarrow \pi \Delta$  are forbidden we predict a 3:1 ratio between  $\gamma p \rightarrow \pi^- \Delta^{++}$  and  $\gamma n \rightarrow \pi^- \Delta^+$ , and the same ratio between the cross sections for  $\gamma n \rightarrow \pi^+ \Delta^-$  and  $\gamma p \rightarrow \pi^+ \Delta^0$ . Similarly, the absence of I = 3/2 exchanges in  $\gamma N \rightarrow K \Sigma$  predicts a 2:1 ratio between  $\frac{d\sigma}{dt} (\gamma p \rightarrow K^+ \Sigma^0)$  and  $\frac{d\sigma}{dt} (\gamma n \rightarrow K^+ \Sigma^-)$ . The experiments show in these cases clear deviations from the predicted ratios.<sup>17</sup> Figures 18 and 19 show the data. The deviations indicate an interference term between exotic and non-exotic amplitude of the order of about 20% of the entire amplitude. This is perfectly consistent with the statement that the purely exotic processes are of the order of a few percent (say, 5%) of typical similar non-exotic processes. If we take the SLAC data seriously, we have to conclude that the assumption that no exotic quantum numbers are allowed is correct only within 20%. It is extremely crucial to perform many more experiments along these lines to see whether indeed the interference between exotic and non-exotic contributions is so large. A 20% deviation could affect in a definite way many of our duality calculations and considerations, since so many interesting predictions of the duality scheme depend on the absence of exotic exchanges.

#### XV. THE "USUAL DUALITY FRAMEWORK"

We have so far made the following set of assumptions:

- 1) Finite energy sum rules (i.e., analyticity and Regge asymptotics).
- 2) Resonance dominate the left hand side of the FESR.
- 3) A special role is played by the Pomeranchuk singularity.
- 4) No exotic amplitudes exist.

This set of assumptions is the framework to which we normally refer when we talk about "duality". When the word "duality" is mentioned without specifying any specific set of assumptions, most often we refer to the four assumptions outlined above. It is this collection of assumptions which enable us to perform a large number of bootstrap calculations and to deduce many interesting results and connections between masses and coupling constants of Regge trajectories and hadronic states. The next few sections will be devoted to studying the consequences of these assumptions. We will particularly emphasize the various bootstrap results, the most interesting of which is perhaps the general requirement of exchange degeneracy. Note that the assumptions described so far do not include local duality, duality diagrams, or any version of the Veneziano formula. Any one of these would involve additional assumptions and will be discussed later in these notes.

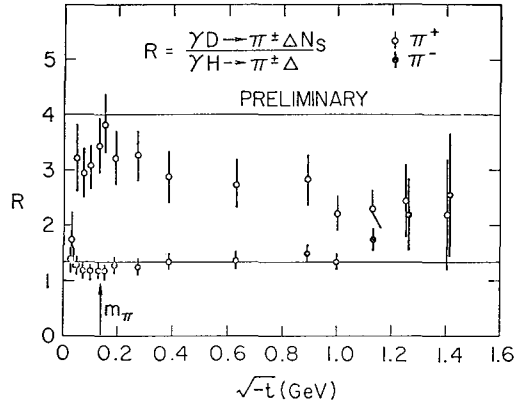


Figure 18: Evidence for exotic t-channel amplitudes in  $\gamma N \rightarrow \pi \Delta$ . The lines show the ratios predicted if no exotic exchanges are allowed (Reference 17).

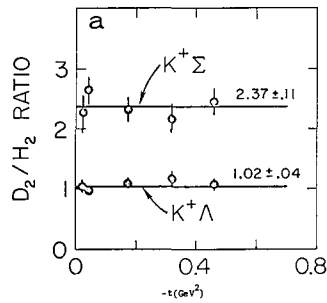


Figure 19: Evidence for exotic exchanges in  $\gamma N \rightarrow K \Sigma$ . The predicted  $D_2/H_2$  ratio is 3, if no exotic amplitudes are allowed. The  $\gamma N \rightarrow K \Lambda$  data shows that the deuteron effects are small since isospin alone predicts a  $D_2/H_2$  ratio of 1 (Reference 17).

## XVI. EXCHANGE DEGENERACY

The idea of exchange degeneracy between trajectories of opposite signature had been proposed<sup>18</sup> long before duality was invented. Duality, however, provides us with a logical way of predicting exchange degeneracy. There is a very close connection between the absence of exotic amplitudes in one channel and the degeneracy between exchanged trajectories in another channel according to the duality hypothesis. This can be seen in a very simple qualitative way by the following argument. Suppose that we have a specific process with exotic quantum numbers in a given channel. The imaginary part of the amplitude in that channel has to vanish. The same imaginary part of the same amplitude, according to duality, should be described in terms of exchanges of trajectories in the crossed channel of the same process. In the crossed channel, however, the quantum numbers will not be exotic, in general. The total contribution in the crossed channel to our amplitude will vanish if and only if at least two trajectories will contribute and cancel each other. Such a cancellation can occur at all energies, if and only if the two trajectories have the same value of  $\alpha(t)$  and are therefore degenerate.

From the point of view of one channel the amplitude will vanish because it has exotic quantum numbers; from the point of view of the other channel it will vanish because two non-exotic trajectories cancel each other. Note that the cancellation between the trajectories requires two independent conditions:

- (i) A degeneracy of the trajectory functions.
- (ii) A relation between the residue functions.

The first condition by itself is sometimes called "weak" exchange degeneracy.

A typical example would be to consider  $\pi^+\pi^+$  elastic scattering at high energies. Since  $\pi^+\pi^+$  have  $I = 2$  we conclude that the imaginary part of this elastic amplitude has to vanish (except for the Pomeranchuk contribution). The same process in the t-channel may have contributions from the Pomeranchuk (which is removed from the calculation), from the P' trajectory and from the  $\rho$  trajectory. In order for the imaginary part of the  $\pi^+\pi^+$  elastic amplitudes to vanish, the t-channel contributions of the P' and  $\rho$  trajectories have to cancel each other at all energies. This means that we have two relations among the parameters of these trajectories:

$$\alpha_{\rho}(t) = \alpha_{P'}(t)$$

$$\beta_{\rho}^{\pi\pi \rightarrow \pi\pi}(t) = \beta_{P'}^{\pi\pi \rightarrow \pi\pi}(t) \quad .$$

Similar relations can be derived by considering other processes. The  $\omega$  and  $A_2$  trajectories as well as various other trajectories can be related in this

way. In order to test these relations we have to study two different problems. For  $t > 0$  we have to investigate the observed hadronic spectra and find whether indeed the Regge trajectories of the appropriate particles really coincide. For  $t < 0$ , we have to consider specific reactions in which the relevant trajectories can be exchanged and compare with experiments relations which follow from the exchange degeneracy predictions.

Let us first study  $t > 0$ . The  $\rho$ ,  $\omega$ ,  $f^0$  and  $A_2$  trajectories are presumably approximately degenerate. A similar relation holds for the  $\phi$  and the  $f^*$  trajectories (Fig. 20). The baryon resonances do not show such clear patterns of exchange degeneracy. However, several  $Y^*$  trajectories do coincide and obey some of the exchange degeneracy predictions. The best example is perhaps the degeneracy between  $\Lambda(1115)$  and the  $Y_0^*(1520)$  trajectories. Other exchange degeneracy relations are observed for  $Y_1^*$  trajectories. In general it is probably fair to state that for the leading meson trajectories exchange degeneracy holds extremely well for  $t > 0$  while for baryons it is, at best, an approximate relation.

In order to test exchange degeneracy for negative  $t$ -values we can simply study various reactions which isolate specific trajectories in the  $t$ -channel, utilize these reactions to study the particular parameters of the trajectories and compare the trajectories functions which are found by such an analysis. For example, an analysis of  $\pi^- p \rightarrow \pi^0 n$  can determine the parameters of the  $\rho$  trajectory; an analysis of  $\pi^- p \rightarrow \eta n$  enables us to determine the parameters of the  $A_2$  trajectory. A comparison of the results of the calculations can show whether or not the  $\rho$  and  $A_2$  trajectories are degenerate. This method is, however, not very reliable because it depends on many assumptions made in the analysis. It depends, for example, on the absence or presence of secondary trajectories and/or their relative importance; it depends on assumptions concerning ghost-killing mechanisms and other details regarding the parametrization of the residue functions of the involved trajectories, etc. A much more direct way of studying exchange degeneracy for  $t < 0$  could be the following. A positive signature trajectory has a signature factor for the form  $1 + e^{i\pi\alpha(t)}$ . A negative signature trajectory has a signature factor of the form  $1 - e^{i\pi\alpha(t)}$ . In Fig. 21 the two signature factors are shown on an Argand diagram. It is very easy to see that the angle between the signature factor and the real axis (which determine the phase of the amplitude) depends on  $\alpha$ . It is very important, however, to note that if the  $\alpha$  values of the two opposite signature trajectories are the same, the angle between the two signature factors on the diagram will always be  $90^\circ$  independent of the particular value of  $\alpha$ , as long as it remains the same! This leads us to a very interesting prediction: There cannot be any interference between two opposite signature trajectories which are exchange degenerate. Note that this strong prediction follows only from the degeneracy

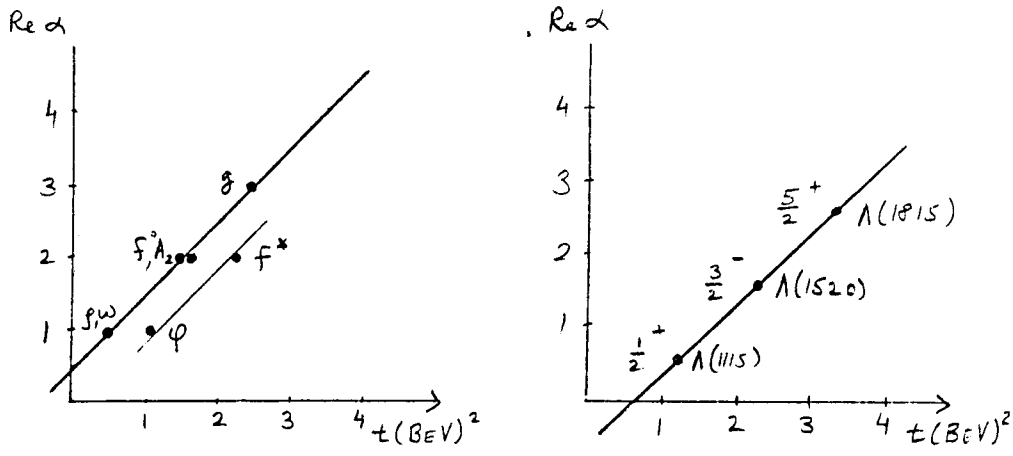


Figure 20: Examples of exchange degenerate trajectories.

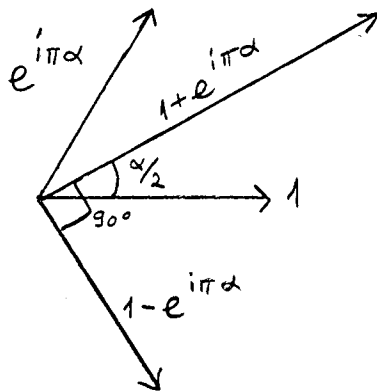


Figure 21: The relative phase between opposite signature trajectories of the same  $\alpha$ -value is  $90^\circ$ . No interference is allowed.

of the trajectories ("weak" exchange degeneracy) and does not depend on the relation among the residue functions which is also predicted by duality and the absence of exotic states. Testing exchange degeneracy by studying the absence or presence of interference between two opposite signature trajectories is therefore a very clean direct test of exchange degeneracy, but it really tests only part of the prediction. The other part, namely, the relation between the residue function is not tested in this way.

The simplest way of testing whether or not there is interference between opposite signature trajectories is to consider pairs of processes which are related to each other by a transformation from the s-channel to the u-channel. As an example let us consider the two processes  $K^- p \rightarrow \pi^- \Sigma^+$  and  $\pi^+ p \rightarrow K^+ \Sigma^+$ . In these two processes the dominant exchanges in the t-channel are presumably the  $K^*$  and  $K^{**}$  trajectories. These are a vector and a tensor trajectory which are supposedly exchange degenerate if the duality idea and the absence of exotic states are true ( $K^*-K^{**}$  degeneracy can be derived, e.g., by considering  $K^+ \pi^+ \rightarrow \pi^+ K^+$ ). The contribution of every one of these trajectories to the two processes is identical in magnitude. However, the tensor trajectory which has an even signature will also contribute with the same sign to the two amplitudes, while the vector trajectory, having a negative signature, will change sign between the two processes. The total cross-section for the two processes will therefore involve the square of the contributions of the tensor and vector trajectories and an interference term between the two trajectories with opposite signs for the two processes. The difference between the two cross sections will therefore be given by the interference term. We have seen however, that if the  $K^*$  and  $K^{**}$  are exchange degenerate there will not be any interference term, independent of the particular t-value that we study. We therefore predict that  $\frac{d\sigma}{dt}$  for the two processes will be identical at forward angles, for sufficiently high energies (sufficiently high energies are defined here as energies for which secondary trajectories are negligible, since there could be interference terms between the leading trajectories and the secondary trajectories even if the secondary trajectories come in exchange degenerate pairs).

Similar predictions can be derived for pairs of processes such as  $K^- p \rightarrow \bar{K}^0 n$  and  $K^0 p \rightarrow K^+ n$ . It is easy to find many other examples following the same line of analysis. Figure 22 shows a comparison with experiment of the predictions for  $Kp \rightarrow \pi\Sigma$  and  $\pi p \rightarrow K\Sigma$ . This is taken from the work of Gilman.<sup>19</sup> Figure 23 shows a comparison with experiment of exchange degeneracy predictions for  $KN$  and  $\bar{K}N$  charge exchange taken from the work of Cline et al.<sup>20</sup> Figures 24-26 show comparison with experiment of exchange degeneracy predictions taken from the work of Lai and Louie.<sup>21</sup>

In all of these cases, it is very clear that the success of the exchange degeneracy predictions is at best limited. Deviations of factors of two are frequent



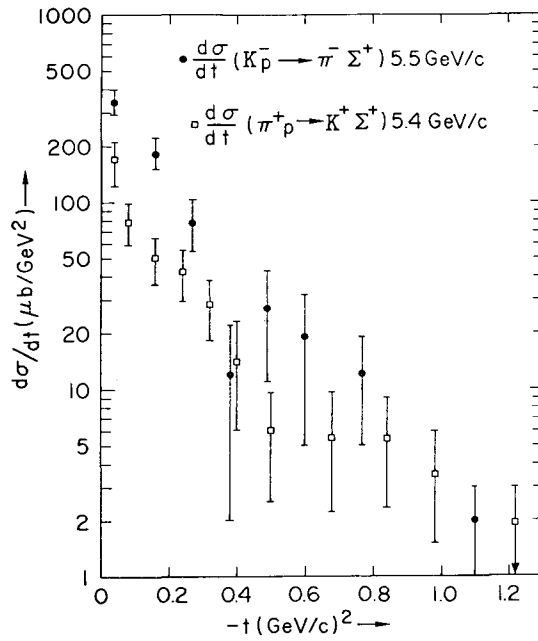


Fig. 22

Exchange degeneracy predicts equal cross sections for the two processes (from Reference 19).

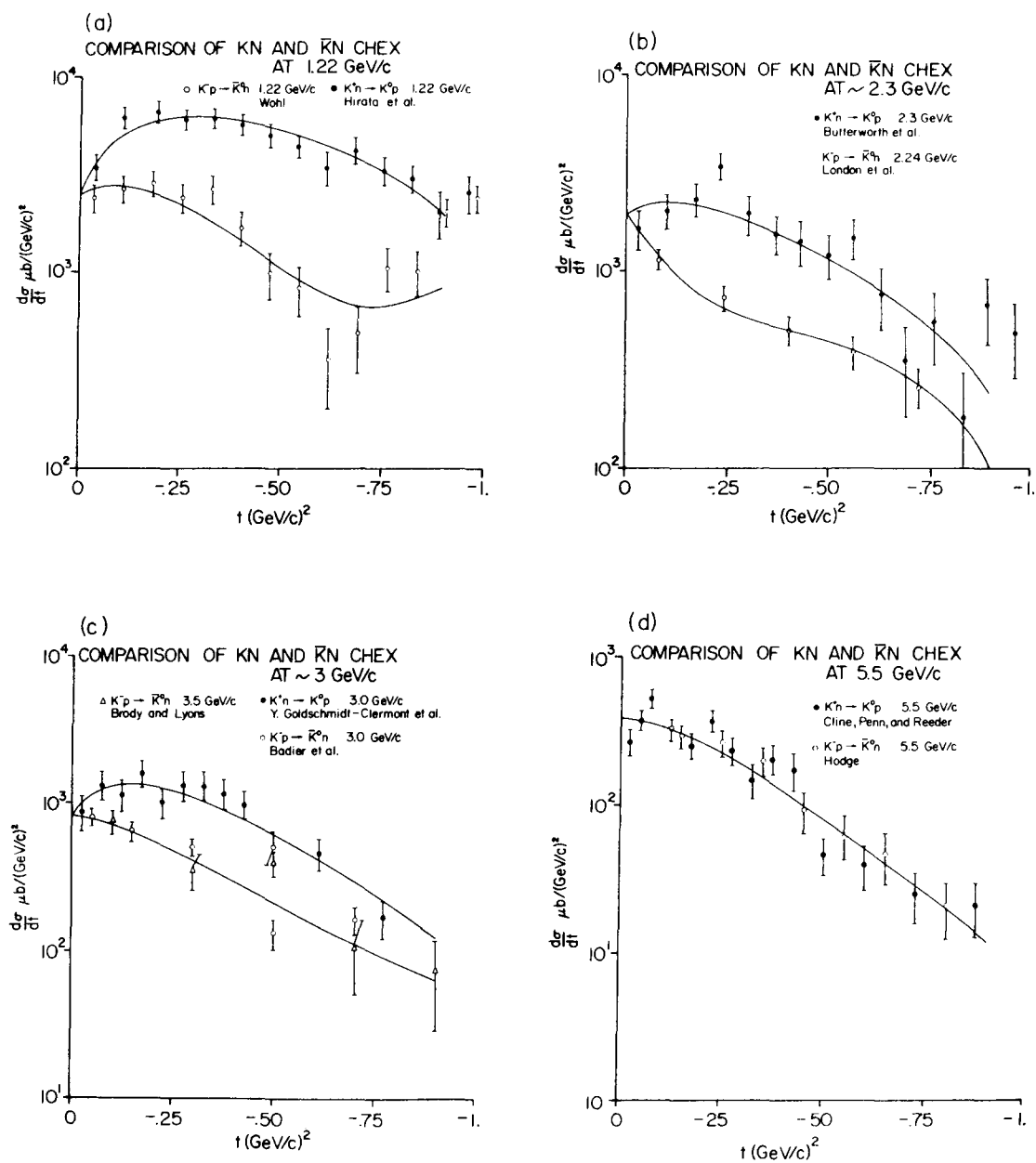


Fig. 23

The two cross sections for  $K^+n \rightarrow K^0p$  and  $K^+p \rightarrow \bar{K}^0n$  should be equal, if exchange degeneracy holds (reference 21).

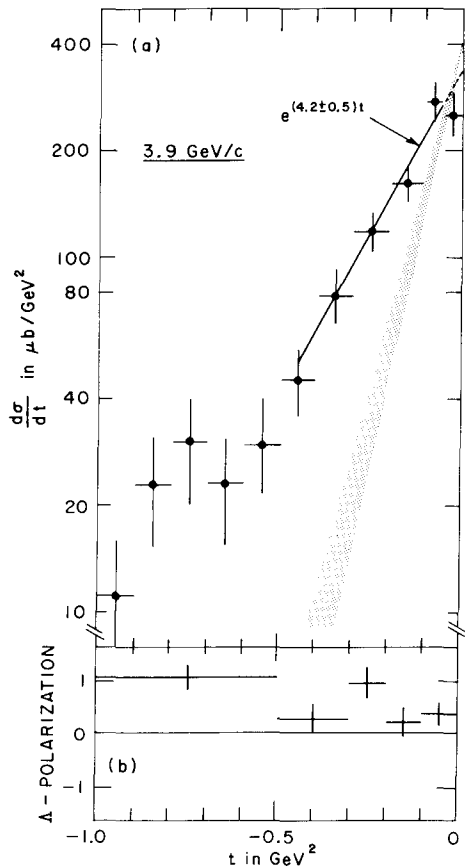


Fig. 24

Angular distribution for  $K^-n \rightarrow \Lambda \pi^-$  and  $\pi^-p \rightarrow K^0 \Lambda$ . The slope is different (and should be the same from exchange degeneracy, Reference 21).

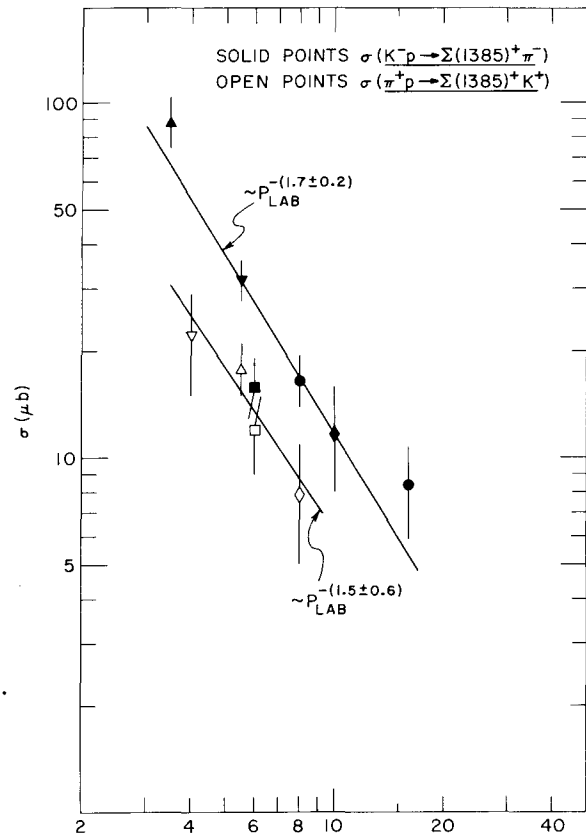


Fig. 26

The two cross sections are predicted to be the same by exchange degeneracy (reference 21).

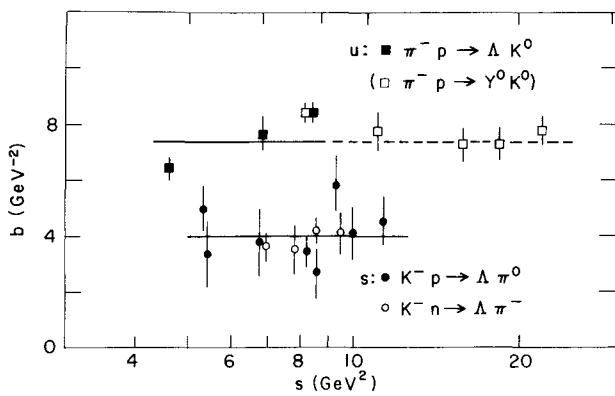


Fig. 25

Energy dependence of the slope of the  $t$ -dependence of  $\frac{d\sigma}{dt}$ . It should be the same for  $\pi N \rightarrow K \Lambda$  and  $\bar{K} N \rightarrow \pi \Lambda$  (Reference 21).

and we certainly cannot claim that this is an exact property of high energy amplitudes. The question arises whether this failure should be interpreted as a failure of duality. We do not know of any definite answer to this question. We suspect, however, that at least part of the failure is to be blamed on the use of Regge pole theory without adding contributions of Regge cuts or some kind of absorption corrections. The reason is that, quite independent of duality or exotic amplitudes, we do know that the masses of the  $K^*$  and  $K^{**}$  resonances and the slopes of their trajectories are such that the trajectories must be approximately exchange degenerate. Since our predictions do not depend on relations between residue functions, all we are testing here is really the dominance of these two trajectories in the t-channel and an approximate equality between their trajectory functions. It is these properties which lead us to inconsistency with experiment. It is true that these properties are predicted by the absence of exotic states and duality but it is also true that we would believe these properties even if we have never heard about duality or exotic amplitudes. The failure of the exchange degeneracy predictions at this level indicate, we feel, that the contributions of the Regge cuts are very important in these energies. This should come as no surprise since there is a very solid amount of evidence for the extreme importance of Regge cuts in many other high energy reactions. An optimist who believes in duality could point out that the only place in which these exchange degeneracy predictions work among the examples that we have presented here is the case of  $K^+n$  scattering. In this case the amplitude is actually exotic in the s-channel and we know from other data ( $K^+p$  and  $K^+n$  total cross sections) that the imaginary part of the exotic s-channel amplitude indeed vanishes. This means that the  $\rho$  and  $A_2$  trajectories in the t-channel really cancel each other in the imaginary part in these particular amplitudes. The failures come in processes in which the s-channel is not exotic and the exchange degeneracy assumption is obtained only by using other processes which do have exotic amplitudes and by applying factorization to results obtained from these processes. Factorization is, of course, a specific strong property of Regge poles which is not shared by Regge cuts and, in fact, the apparent violation of the factorization property provides us with some of the strongest reasons to believe that Regge cuts are important in many cases.<sup>22</sup> One could therefore claim that we should really test exchange degeneracy in the way discussed here, only for cases in which the s-channel is indeed exotic and only there should we expect the contributions of opposite signature t-channel trajectories to cancel each other.

Such a point of view could be considered as optimistic, as it maintains that duality is basically correct, while our phenomenology is not good enough. It is also very pessimistic since it restricts tremendously the predictive power of the entire scheme. Once factorization is ruled out as a reliable tool (and it may

very well be that we have to rule it out in view of the many failures of Regge pole theory) we are left with predictions only for processes which are exotic in a certain channel and reactions such as  $Kp \rightarrow \pi\Lambda$  or  $Kp \rightarrow \pi\Sigma$  remain without any predictions. We may recover many of the predictions for these reactions by replacing the factorization assumption by SU(3) assumptions. But SU(3) is also known to be only an approximate symmetry, and it is often broken for high energy reactions. Failures in such cases could then be blamed on SU(3) by a religious supporter of duality.

To summarize the question of validity of exchange degeneracy we can say that we are really facing here an interesting puzzle. Exchange degeneracy is clearly a meaningful concept since it is so successful for mesons in the positive t-region and since it gives so many interesting consistency conditions in duality bootstrap calculation such as the ones that we shall discuss in the next few sections. On the other hand exchange degeneracy for Regge poles, ignoring any contributions from Regge cuts, does lead to a substantial number of inconsistencies with experiment, such as the ones displayed in Figs. 22-26. It should be very interesting to find out whether one can incorporate Regge cuts into the exchange degeneracy idea in such a way as to maintain the positive features of this approach while resolving the difficulties outlined above.

#### XVII. THE DUALITY BOOTSTRAP: MESON-MESON SCATTERING

As a simple example to the duality bootstrap, let us again consider the case of  $\pi\pi$  elastic scattering. In this case we have three s-channel isotopic spin amplitudes:  $I_s = 0,1,2$ . In the t-channel we also have three independent isotopic spin amplitudes:  $I_t = 0,1,2$  (Fig. 27). At any given point in the s,t plane all  $\pi\pi \rightarrow \pi\pi$  processes can be completely described either in terms of the three s-channel isospin amplitudes or in terms of the three t-channel isospin amplitudes. The transformation between the three s-channel amplitudes and the three t-channel amplitudes is, of course, given by the isotopic spin crossing matrix. If we now assume that no exotic amplitudes are allowed, we find that one of the three t-channel amplitudes ( $I_t=2$ ) has to vanish. Furthermore, the imaginary part of the exotic  $I_s=2$  amplitude in the s-channel will also vanish (except for the Pomeron contribution, which again remains outside the scope of the discussion). The two vanishing amplitudes in the two different channels are, of course, different amplitudes. The vanishing of either of them imposes a constraint on the amplitudes in the other channel. For example, the vanishing of the  $I_t=2$  amplitude tells us that the particular combination of the three s-channel amplitudes which correspond to  $I=2$  in the t-channel has to vanish. We find ourselves therefore with three s-channel amplitudes satisfying two equations: The first one is trivial - it says that the imaginary part of the  $I_s=2$  in the t-channel also vanishes. This means that the  $I=0$

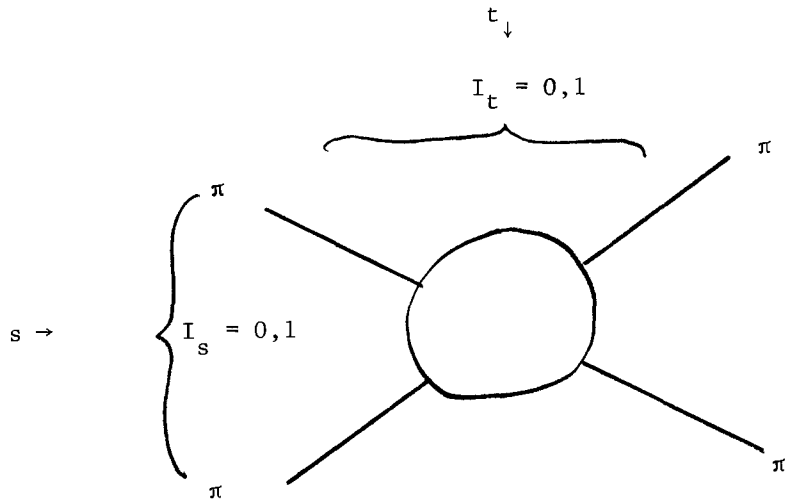


Fig. 27.  $\pi\pi$  scattering

and  $I=1$  amplitudes in the  $s$ -channel are related to each other. To summarize, we start with three independent amplitudes which we can choose to be either the three  $s$ -channel isospin eigenstates or the three  $t$ -channel isospin eigenstates. We have two independent homogeneous equations among these three amplitudes and we therefore remain with one and only one solution which is unique up to multiplicative factor.

This result is extremely strong. It says that the various charge modes of the process  $\pi\pi \rightarrow \pi\pi$  (elastic, charge exchange, and double charge exchange) can all be described, at a given point in the  $s$ - $t$  plane, in terms of one and only one number which completely determines all the various amplitudes at this particular point. This result indicates that we have here a degree of symmetry which is much higher than ordinary isotopic spin symmetry, and it gives us a relation between the amplitudes which, at this level, is still quite independent of the particular assumptions that we make about the exchange mechanisms. We have assumed that no exotic amplitudes are allowed and that duality is obeyed but, so far, we assumed nothing about the specific trajectories or cuts or any other peripheral mechanism responsible for high energy  $\pi\pi$  scattering. If we now supplement our result by the statement that the dominant exchanged trajectories, in addition to the Pomeron, are the  $\rho$  and  $P'$  trajectories, our result will teach us that the  $\rho$  and the  $P'$  are exchange degenerate as we have already discussed in the previous section. But quite independent of that, we see that we have obtained the strong result that all amplitudes for  $\pi\pi \rightarrow \pi\pi$  are given in terms of one constant which determines the overall magnitude of the scattering amplitude.

We can generalize the previous discussion of  $\pi\pi$  scattering to the general

case of scatterings of two mesons belonging to the SU(3) octet of pseudoscalar mesons going into two other mesons belonging to the same octet. We therefore have here a process of the type  $8 + 8 \rightarrow 8 + 8$ . Let us first assume complete SU(3) invariance. In that case we shall have five independent SU(3) amplitudes in the s-channel, corresponding to the SU(3)  $\underline{1}$ ,  $\underline{8}_D$ ,  $\underline{8}_F$ ,  $\underline{10+\overline{10}}$ , and  $\underline{27}$  representations. The  $\underline{10}$  and  $\overline{10}$  amplitudes are related to each other, and the  $\underline{8}_D$  and  $\underline{8}_F$  amplitudes do not have a cross term because of the charge conjugation properties of the pseudoscalar mesons. The general meson-meson scattering amplitude can, therefore, be described in terms of 5 independent complex SU(3)-invariant amplitudes at every given point of s and t. From the t-channel point of view, we also have five independent amplitudes corresponding again to the  $\underline{1}$ ,  $\underline{8}_D$ ,  $\underline{8}_F$ ,  $\underline{10+\overline{10}}$ , and  $\underline{27}$  representations (Fig. 28), and, again, the five t-channel amplitudes can be expressed in terms of the five s-channel amplitudes by the usual SU(3) crossing matrix.

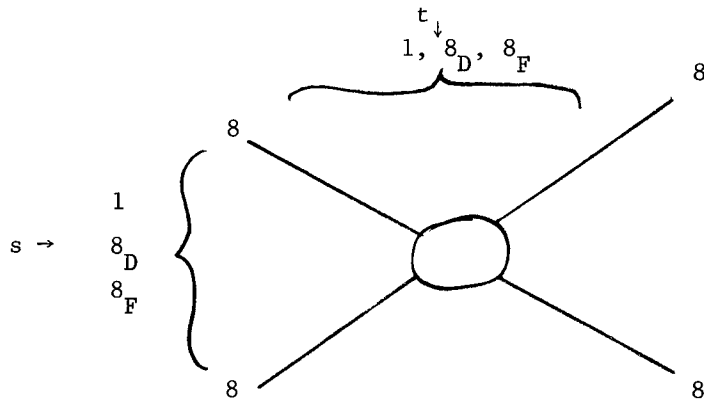


Fig. 28: Octet-octet scattering

We now assume that no exotic amplitudes are allowed. This forbids the exchange of the  $\underline{27}$  and  $\underline{10}$  amplitudes in the t-channel, and it leads us to two linear relations among the five s-channel amplitudes, namely, the particular combinations of s-channel amplitudes corresponding to the  $\underline{27}$  and to the  $\underline{10+\overline{10}}$  in the t-channel have to vanish. In addition to these two requirements, however, we have two other constraints. The imaginary parts of the  $\underline{27}$  and  $\underline{10}$  amplitudes in the s-channel should also vanish because of the assumed absence of exotic states in the s-channel (again, the Pomeron term is removed). Altogether we therefore have four independent constraints among our five amplitudes. These four constraints are the vanishing of the  $\underline{27}$  and  $\underline{10}$  amplitudes in the s-channel and the vanishing of the  $\underline{27}$  and  $\underline{10}$  amplitudes in the t-channel. With four homogeneous constraints among five amplitudes, we again remain with one and only one solution for the entire system of processes. This means that the entire list of processes of the form  $8+8 \rightarrow 8+8$ ,

when all external mesons are members of the pseudoscalar octet, can be described, for a given point in the  $s$ - $t$  plane, in terms of one quantity representing the overall magnitude of the process. That means that processes such as  $\pi K \rightarrow \pi K$ ,  $K\eta \rightarrow K\eta$ ,  $\pi\pi \rightarrow \overline{K}K$ , etc. are all related to each other in terms of one parameter.

This is an extremely strong result and it leads to some fascinating conclusions. It tells us that we must have an exchange of octets as well as a singlet in the  $s$ - and  $t$ -channel. The singlet is quite independent of the Pomeranchuk singularity which has been removed from the calculations at the very beginning! Had we assumed, for example, that the singlet channel also vanishes and only octet exchanges are allowed, we would immediately run into an inconsistency, namely, we would find that the only available solution is the one in which all amplitudes identically vanish. We are, therefore, forced to have a singlet in addition to the two octets. The singlet has to be degenerate with the two octets in its energy dependence if it has to cancel them for every value of  $s$  and  $t$ . We therefore conclude that, at least in this case, we must have degenerate nonets of tensor mesons exchanged in the set of processes  $8+8 \rightarrow 8+8$ . Similar considerations for other sets of  $SU(3)$  invariant processes lead us to the conclusion that we also need degenerate nonets of vector mesons.

This prediction is remarkable not only because it is experimentally true but also because this is the first time that the requirement that the vector and tensor mesons will appear in nonets follows for a model which has nothing to do (or at least does not seem to have anything to do) with the quark model. So far, the only motivation, other than empirical observation, for the existence of nonets has been the quark model, and here our simple set of assumptions of duality and the absence of exotics, forces us into degenerate nonets for these types of particles. This result is interesting in many respects. First of all, it is an extremely strong relation obtained from reasonable and (seemingly) not so strong assumptions. Second, it is not inconsistent with experiment in its gross features in the sense that to the extent that we may believe in  $SU(3)$  invariance, it is conceivable that we do have indeed an octet of vector mesons and a nonet of tensors which are really exchanged in pseudoscalar-pseudoscalar scattering (the singlet vector mesons cannot couple in an  $SU(3)$  invariant theory to two pseudoscalar mesons). But the most interesting aspect is perhaps the fact that this is our first encounter with a duality prediction which follows from the absence of exotic states and which resembles very strongly quark model predictions. In the next few sections we will return to many additional results of this nature, and we shall again and again observe this mystery of the amazing consistency between duality and the absence of exotics on one hand, and the entire framework of the quark model on the other hand.



XVIII. THE DUALITY BOOTSTRAP:  $\omega$ - $\phi$  and  $f^0$ - $f^*$  MIXING

We shall not study a refinement of the previous discussion which was proposed by Chiu and Finkelstein.<sup>23</sup> They have studied the same set of processes, namely, pseudoscalar-pseudoscalar scattering in an SU(3) limit but allowed the exchange trajectories to be split in mass. More explicitly, they allowed the  $\omega$  and  $\phi$  trajectories and the  $f^0$  and  $f^*$  trajectories to be non-degenerate, as they are in nature. In this way they force a splitting of the nonets (or to be more precise, a splitting between the two isotopic spin singlets of each nonet) but they do not a priori specify the octet-singlet mixing angle responsible for this splitting. They then propose the following set of considerations: From  $\pi^+\pi^+ \rightarrow \pi^+\pi^+$  it follows that the  $\rho$  trajectory has to be cancelled by a tensor trajectory. The tensor trajectory can be either the  $f^0$  or the  $f^*$  trajectory, but not both since they are not degenerate with each other. Let us choose the  $f^0$  and define  $f^0$  as the trajectory degenerate with the  $\rho$ . That immediately tells us that the  $f^*$  trajectory does not couple to the  $\pi\pi$  system, since otherwise we would need another  $\rho$  trajectory degenerate with the  $f^*$ , in order to cancel its contribution to  $\pi^+\pi^+$  elastic scattering. So, the first predictions are that  $\rho$  and  $f^0$  are exchange degenerate, their coupling to the pion are the same, and the  $f^*$  does not couple to pions. We now proceed to discuss  $K^+\pi^+$  elastic scattering. This is again an exotic amplitude in the s-channel. Its imaginary part presumably vanishes except for the Pomeranchuk term. The t-channel exchanges which are allowed are again  $\rho$  and  $f^0$  and the only new information that we gather is that the  $\rho KK$  and  $f^0 KK$  couplings are equal. Let us now proceed to discuss  $K^+K^+$  and  $K^+K^0$  elastic scattering. These processes are again exotic in the s-channel and again t-channel cancellations are needed. The t-channel trajectories which are allowed are  $\rho$ ,  $f^0$ ,  $\omega$ ,  $A_2$ ,  $\phi$ ,  $f^*$ . The type of exchange degeneracy requirement that we get from these reactions is that pairs  $\rho$ - $A_2$ ,  $\omega$ - $f^0$  and  $\phi$ - $f$  are exchange degenerate. Since we have already determined before that  $\rho$  and  $f^0$  are degenerate, the four trajectories  $\rho$ ,  $\omega$ ,  $A_2$  and  $f^0$  have to have the same coupling to the  $KK$  system. In particular, the  $\rho KK$  coupling is equal to  $\omega KK$ . SU(3), however, claims that the  $\rho KK$  coupling is related to the  $\omega_8 KK$  coupling, since  $\rho$  and  $\omega_8$  are in the same octet and the coupling is unique (of the F type). The physical  $\omega$  can be written as  $\omega = \omega_8 \cos\theta + \omega_1 \sin\theta$ .  $\omega_1$  does not couple to two K-mesons since two K-mesons in a pure P wave must be in an antisymmetric SU(3) representation while  $\omega_1$  is in the SU(3) singlet which is symmetric with respect to the interchange of the two octets. The coupling of the physical  $\omega$  to  $\bar{K}K$  must therefore go through its  $\omega_8$  component. This leads us to a determination of the octet-singlet mixing angle. The mixing angle which is found,<sup>23</sup> amazingly enough, is  $\cos^2\theta = 1/3$ , the canonical quark model mixing angle.

This result of Chiu and Finkelstein is even more striking than our previous

statement about the necessity of having nonets of vector and tensor mesons. This is a clear triumph of the idea of duality plus absence of exotic exchanges and the removal of the Pomeron, a triumph which is shared only by the quark model, in the sense that these are the only two models which give the correct  $\omega$ - $\phi$  mixing angle. Incidentally, the  $f^0$ - $f^*$  mixing angle can be obtained in a similar way. Notice that the input assumptions do involve, in a sense, some quark model considerations, since the quark model is the only model which predicts the absence of exotic states. The output is very clearly of the type of predictions that the quark model gives. However, in the derivation and throughout the various arguments used, neither the work quark, nor any implicit quark arguments were used. This again hints that there is some very peculiar and strange consistency between the idea of duality and the absence of exotic amplitudes on one hand and the quark model on the other.

An even more peculiar consistency in this context was discovered by Schwimmer.<sup>24</sup> So far we have forbidden the existence of exotic amplitudes, where "exotic" meant anything that cannot be constructed from three quarks or from a quark and an antiquark, from the point of view of internal quantum numbers. But there is another type of exotic states which are forbidden in the quark model, and which are not found in nature. These are mesons with natural parity, namely,  $P = (-1)^J$ , and negative value of CP. Such mesons cannot be constructed from a quark and an antiquark. Schwimmer has assumed that no such mesons exist and derived the following interesting result. Let us consider  $\pi\eta$  elastic scattering. In the s-channel  $\pi\eta$  can produce only  $C = +1$  resonances. The parity and angular momentum of  $\pi\eta$  resonances, in general, can be  $0^+$ ,  $1^-$ ,  $2^+$ ,  $3^-$ ... . Since  $C = +1$  and since all of these mesons must be of natural parity, the assumption of no exotic states leads us to the statement that all  $\pi\eta$  resonances must be of positive parity and even partial wave. That means that the forward and backward peaks in high energy  $\pi\eta$  elastic scattering will be of the same size (we again ignore completely the Pomeron contribution in the t-channel which would correspond to a background in the s-channel and which may have contributions to odd CP, natural parity partial waves). If the forward and backward peaks in elastic  $\pi\eta$  scattering are the same, the strength of the trajectories exchanged in the forward and backward directions must be the same and their  $\alpha$  values must be the same. In the forward direction, however, the leading trajectory is the  $f^0$  trajectory. In the backward direction it is the  $A_2$  trajectory. We therefore immediately conclude that the  $A_2$  and  $f^0$  trajectories are exchange degenerate and their couplings to  $\pi$ 's and  $\eta$ 's are related. Furthermore, by studying other processes such as  $\pi\eta \rightarrow \pi\chi$  and  $\pi\chi \rightarrow \pi\chi$ , Schwimmer has shown that the  $f$ - $f^*$  mixing angle must be the canonical quark model mixing angle and by studying other sets of processes such as  $\pi\eta \rightarrow \rho\omega$  he found the same result for the vector meson nonet. This result is even more puzzling

than the previous one. We again started with an assumption (no exotic amplitudes) which can be taken either from experiment or from the quark model, we supplemented it by duality and we ended up with a result which is a typical statement of the quark model. The mystery is, however, greater here because the input assumptions are related to the spin and charge conjugation property of the mesons in the quark model while the output results relate to the internal symmetry properties. This is different than the previous case in which both the input and the output were related to the internal quantum number properties of states in the quark model! We quote these results as well as the results mentioned in the previous section as indications that at least the algebraic structure of the quark model is somehow buried in a very interesting and subtle way within the entire framework of duality.

#### XIV. THE DUALITY BOOTSTRAP: THE BARYON-ANTIBARYON CATASTROPHE

Since we are discussing various examples of bootstrap calculations using duality and the absence of exotic amplitudes, we should also mention the only case in which this scheme clearly fails. This is the case of baryon-antibaryon elastic scattering. It was first pointed out by Rosner<sup>25</sup> that, if we assume (i) no exotic amplitudes are allowed; (ii) the Pomernachuk singularity is removed according to our cooking recipe; (iii) duality; and if, furthermore, we make the same assumptions for meson-meson, meson-baryon, baryon-baryon and baryon-antibaryon elastic scattering the overall consistency requirement of all of these assumptions for all of these processes leads to a disastrous result for baryon-antibaryon scattering. The result is that, except for the Pomeranchuk contribution, all baryon-antibaryon total cross sections have to vanish. This is, of course, totally unreasonable and clearly in contradiction with experiment. Several prospects have been suggested in order to resolve the difficulty. One of them, due to Rosner,<sup>25</sup> says that exotic mesons made out of two quarks and two antiquarks indeed exist, but they couple only to the baryon-antibaryon system and not to the meson-meson system and therefore they avoided being detected so far. While we cannot rule out such a possibility we must admit that it is a totally unsatisfactory excuse. Even if such mesons exist, it would be very peculiar to observe that this framework was so consistent, so restrictive (but not too restrictive) and so similar to the quark model in so many processes and all of a sudden it fails in this particular example. Another proposal for curing the baryon-antibaryon difficulty is due to Lipkin.<sup>26</sup> He suggested that, in terms of the quark model, the concept of an s-channel resonance in meson-meson and meson-baryon scattering is simply the annihilation of one of quark and antiquark pair: In baryon-antibaryon scattering, and only in this case, the annihilation of one pair of quark and antiquark does not lead to an s-channel mesonic resonance. It leads to, at least, two meson resonances in the s-channel.

Lipkin therefore proposes that the words "resonance dominance" in our previous set of assumptions should be replaced by the words "the dominance of quark-antiquark annihilations" and therefore everything would remain the same for meson-meson and meson-baryon scattering while in baryon-antibaryon scattering two meson intermediate states or annihilations of baryon-antibaryon into two mesons would also be considered under the same heading as the single quark-antiquark annihilations and would correspond to t-channel Regge exchanges rather than to the Pomeron terms. This proposal also does not resolve the difficulty because it would have to explain what happens in processes of the type  $B\bar{B} \rightarrow MM$ . This process does not lead to any difficulty since it is simply the crossed channel process for meson-baryon elastic scattering, and if we assume that baryon-antibaryon goes to two mesons should be considered as a non-background contribution even if it does not proceed through s-channel resonances, we will have to abandon all the successes in the meson-baryon case (and via factorization even in the meson-meson case). We therefore feel that the difficulty in baryon-antibaryon scattering is not resolved yet, and we believe that it is the main difficulty of the model. Furthermore, it is conceivable that this failure is trying to teach us something. It is very difficult to believe that all the beautiful self-consistency of all the other processes is spurious and the baryon-antibaryon case is really the case which tells us that we are dealing here with an unreasonable scheme. We prefer the opposite point of view, namely, that there is here a beautiful self-consistent scheme of assumptions, results and predictions, both in the sense that it does not lead to any contradictions and in the sense that it is consistent in such a mysterious way with the quark model. The baryon-antibaryon case is an exception not because it contradicts everything else but because we are probably handling it in a wrong way and we are probably avoiding some crucial property of this particular process which is different from the other processes. Unfortunately, no one has come up yet with a convincing way of resolving this. We shall come back to this difficulty as well as to some of the previous successes outlined in the previous sections when we discuss duality in Sec. XXII.

## XX. DUALITY, REGGE CUTS AND ABSORPTION

In spite of the fact that we have formulated the duality idea in terms of a model involving Regge poles only, we have mentioned many times the necessity of introducing important contributions of Regge cuts into the calculation of high energy hadronic scattering amplitudes. The necessity of including such contributions is implied by a large number of phenomenological studies of hadronic reactions. Quite independent of the entire question of validity of duality, we have already emphasized in these notes that it would be totally unreasonable to ignore this

necessity in discussing duality both from the theoretical point of view and from the practical point of view. From the theoretical point of view we have to know how to include the cut contributions in the general considerations, beginning with the cut contributions to the right hand side of the FESR and ending with the question whether the Regge cuts correspond to resonances in the s-channel or to background in the s-channel. From the practical point of view, the question is even more crucial. We have faced a large number of inconsistencies between various predictions of the general duality scheme and experiment, such as some of the exchange degeneracy predictions and such as the baryon-antibaryon catastrophe. We have emphasized that in many of these cases, the phenomenology of these same reactions that are studied here within the framework of duality is not clear at all. Furthermore, we have shown that the application of various duality predictions to some of the involved reactions includes the assumption of factorization, an assumption which is special to Regge poles and is not obeyed by Regge cuts.

Apart from the assumption of factorization, Regge cuts, for practical purposes, are not so different from Regge poles, in the sense that in many cases the contribution of a Regge cut can be parametrized in terms of a so called "effective pole" which reproduces most of the properties of the cut contribution. It is clear that such an effective pole cannot reproduce all the properties of the cut, but through a limited energy region, and for most practical purposes, such an approach could be valid and in fact could even be a reasonable way of applying Regge cut phenomenology to the data, in view of the large number of parameters which are necessary in including Regge cuts in a more appropriate way. Let us remember, however, that such effective Regge poles (which are really imitations of Regge cuts and do not correspond to any physical particle) have no reason to obey the factorization assumption, and therefore whenever we discuss high energy hadronic processes in terms of Regge cuts or in terms of "effective Regge poles" we cannot and should not use factorization and we should not be concerned about failures of our theory which follows from an extensive use of the factorization assumption.

All of these remarks are valid only in a negative way. They reduce the number of cases to which we can apply meaningful predictions of duality and they provide us with an excuse for some of the failures of the model. In order to include Regge cuts properly within the duality framework, we must, however, understand better the physical meaning of such cuts and incorporate them in the general analysis of the processes. One interesting approach which tries to provide us with the simple physical meaning to the contribution of the Regge cuts is the approach of the absorption model. The classical absorption model of the early 1960's is well known to be totally inadequate. However, this model had two basic ingredients. It starts with a Born term (a single particle exchange amplitude

calculated by perturbation theory) and then continues by applying the absorption corrections to this Born term. The basic physical idea of the absorption model is that the partial waves which are important in any given inelastic process are the most peripheral partial waves which are allowed within the radius of the interaction. This idea is quite independent of the first step that used to be included in the absorption model, namely, the calculation of the Born term. When the old absorption model failed it was never clearly indicated whether it failed because the Born term is a totally inadequate starting point or whether the second step, the absorption step, is an unreliable physical principle. We suspect that it is the first possibility which occurs, namely, the Born term is a totally unreliable and unjustified starting point, while the idea of absorption may have some justification in high energy inelastic processes. We feel that in order to study the validity of the idea of absorption, we must look for predictions which are independent of the first step of the analysis, namely, predictions which can be compared with experiment and which would be valid regardless of what is the original approximation that we use. We will not go into a detailed analysis of this question here, since our main topic here is not the absorption model. Let us only remark that such predictions can be found and in spite of the fact that they are mostly of a qualitative nature (such as predictions on whether or not dips will occur in specific cases) some success has been obtained with these predictions. For the purposes of unifying the absorption model and the Regge cut picture on one hand and the duality idea on the other hand, it will be sufficient if we establish here some general principles for the contribution of Regge cuts, consistent with the absorption model, and then try to incorporate these principles into the duality framework.

The main principle that we assume here is very simple. We demand that in any given inelastic process the strong contributions come from the most peripheral s-channel partial waves within the radius of interaction, namely, from partial waves obeying the relation  $l \sim kR$ . We shall further assume that from the t-channel point of view we have a complicated combination of Regge poles and Regge cuts which is arranged in such a way that its projection on the s-channel partial waves will obey our previous requirement, namely, the Regge pole contributions and the Regge cut contributions will be such that the total projection on low partial waves in the s-channel will be small and the main strength of the process will come from the most peripheral partial waves. We therefore have here an s-channel picture and a t-channel picture which are very qualitative and not very specific but still give us some information.

To this picture we shall now add the requirement that the s-channel partial waves are dominated by resonances. That means that, since the most important contributions come from the peripheral s-channel partial waves, the most

important contributions come from the peripheral resonances. Another way of saying this is that we are using our previous resonance dominance of Sec. IV, but adding to it the requirement that the strongest coupling in any given inelastic process will be that of those resonances obeying the relation  $l \sim kR$ . This is our s-channel picture. From the t-channel point of view, we claim that the same peripheral resonance contributions are described by the combination of Regge poles and Regge cuts that we have mentioned before.

This picture immediately leads to one result which is very interesting and which we have already mentioned in our discussion in Sec. VI. In Sec. VI we have seen that s-channel resonances can construct contributions which will have a dip structure in the angular distribution of fixed values of  $t$  for all energies, provided that these s-channel resonances obey the relation  $l \sim kR$ . Now that we have added a dynamical assumption motivated by the absorption model which states that the prominent and important resonances indeed belong to such partial waves, we automatically have a combination of s-channel resonances which is guaranteed to provide us with  $t$ -distributions which have a certain fixed feature at fixed values of  $t$  at all energies! This is a typical property that we would like the combination of our t-channel exchanges to have, and it is interesting that this property is guaranteed by our dynamical absorption assumption.

We now have a simple picture in which the resonance dominance concept of Sec. IV is restricted to resonance dominance in the peripheral s-channel partial waves with no important resonances (or any other contributions) in low partial waves. The "ordinary t-channel trajectories" now include both t-channel Regge poles and t-channel Regge cuts in such a way that they are consistent with the s-channel description. Almost every single argument and assumption that we have made in our theoretical considerations, so far, can be left unchanged by our way of including cuts. In particular, the Pomeranchuk contribution is still of a specific nature and is still the only one related to the background; the ordinary trajectories which now include the cut contributions are built by resonances; the amplitude is still built in terms of two additive components; the assumption of no exotic amplitudes can remain valid, provided that the important cuts are cuts which are obtained by the repeated exchange of a non-exotic pole and a Pomeranchon (but the absorption model, of course, requires that these are indeed the prominent cuts); exchange degeneracy remains a prediction of the theory in a slightly modified way. For  $t < 0$  values the degeneracy is between the poles as well as the cuts, or, to be more precise, the degeneracy or the cancellations should occur somehow between the combined pole-cut contribution of one set of quantum numbers and the combined pole-cut contribution of another set. Instead of saying that the  $\rho$  trajectory and the  $P'$  trajectory are degenerate for  $t < 0$  we shall say that the energy

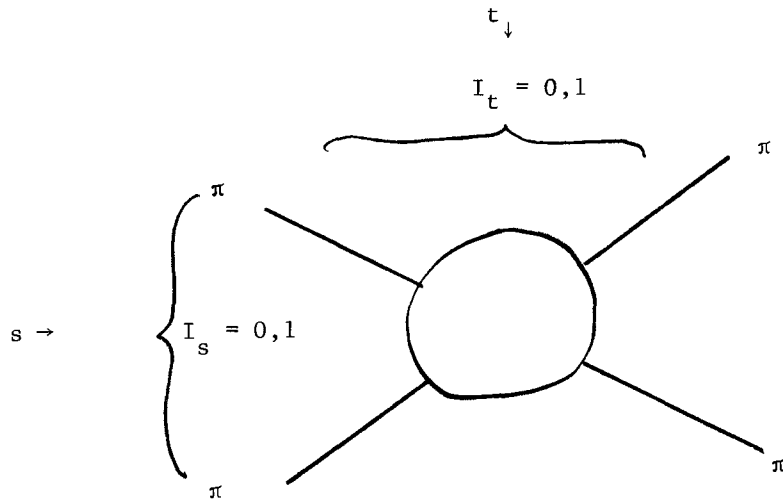


Fig. 27.  $\pi\pi$  scattering

and  $I=1$  amplitudes in the  $s$ -channel are related to each other. To summarize, we start with three independent amplitudes which we can choose to be either the three  $s$ -channel isospin eigenstates or the three  $t$ -channel isospin eigenstates. We have two independent homogeneous equations among these three amplitudes and we therefore remain with one and only one solution which is unique up to multiplicative factor.

This result is extremely strong. It says that the various charge modes of the process  $\pi\pi \rightarrow \pi\pi$  (elastic, charge exchange, and double charge exchange) can all be described, at a given point in the  $s$ - $t$  plane, in terms of one and only one number which completely determines all the various amplitudes at this particular point. This result indicates that we have here a degree of symmetry which is much higher than ordinary isotopic spin symmetry, and it gives us a relation between the amplitudes which, at this level, is still quite independent of the particular assumptions that we make about the exchange mechanisms. We have assumed that no exotic amplitudes are allowed and that duality is obeyed but, so far, we assumed nothing about the specific trajectories or cuts or any other peripheral mechanism responsible for high energy  $\pi\pi$  scattering. If we now supplement our result by the statement that the dominant exchanged trajectories, in addition to the Pomeron, are the  $\rho$  and  $P'$  trajectories, our result will teach us that the  $\rho$  and the  $P'$  are exchange degenerate as we have already discussed in the previous section. But quite independent of that, we see that we have obtained the strong result that all amplitudes for  $\pi\pi \rightarrow \pi\pi$  are given in terms of one constant which determines the overall magnitude of the scattering amplitude.

We can generalize the previous discussion of  $\pi\pi$  scattering to the general



case of scatterings of two mesons belonging to the SU(3) octet of pseudoscalar mesons going into two other mesons belonging to the same octet. We therefore have here a process of the type  $8 + 8 \rightarrow 8 + 8$ . Let us first assume complete SU(3) invariance. In that case we shall have five independent SU(3) amplitudes in the s-channel, corresponding to the SU(3)  $\underline{1}$ ,  $\underline{8}_D$ ,  $\underline{8}_F$ ,  $\underline{10+\overline{10}}$ , and  $\underline{27}$  representations. The  $\underline{10}$  and  $\overline{10}$  amplitudes are related to each other, and the  $\underline{8}_D$  and  $\underline{8}_F$  amplitudes do not have a cross term because of the charge conjugation properties of the pseudoscalar mesons. The general meson-meson scattering amplitude can, therefore, be described in terms of 5 independent complex SU(3)-invariant amplitudes at every given point of s and t. From the t-channel point of view, we also have five independent amplitudes corresponding again to the  $\underline{1}$ ,  $\underline{8}_D$ ,  $\underline{8}_F$ ,  $\underline{10+\overline{10}}$ , and  $\underline{27}$  representations (Fig. 28), and, again, the five t-channel amplitudes can be expressed in terms of the five s-channel amplitudes by the usual SU(3) crossing matrix.

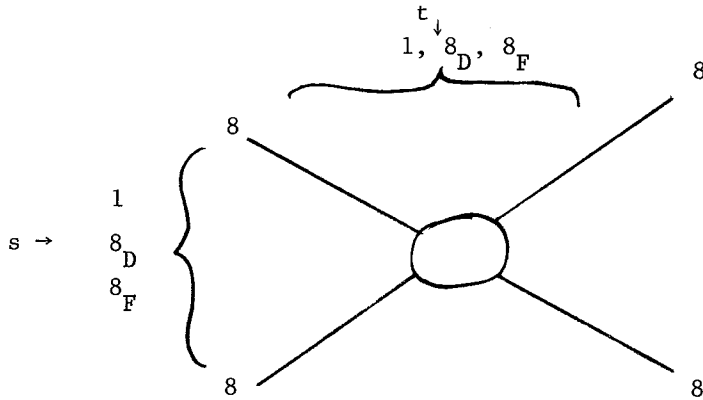


**Fig. 28:** Octet-octet scattering

We now assume that no exotic amplitudes are allowed. This forbids the exchange of the  $\underline{27}$  and  $\underline{10}$  amplitudes in the t-channel, and it leads us to two linear relations among the five s-channel amplitudes, namely, the particular combinations of s-channel amplitudes corresponding to the  $\underline{27}$  and to the  $\underline{10+\overline{10}}$  in the t-channel have to vanish. In addition to these two requirements, however, we have two other constraints. The imaginary parts of the  $\underline{27}$  and  $\underline{10}$  amplitudes in the s-channel should also vanish because of the assumed absence of exotic states in the s-channel (again, the Pomeron term is removed). Altogether we therefore have four independent constraints among our five amplitudes. These four constraints are the vanishing of the  $\underline{27}$  and  $\underline{10}$  amplitudes in the s-channel and the vanishing of the  $\underline{27}$  and  $\underline{10}$  amplitudes in the t-channel. With four homogeneous constraints among five amplitudes, we again remain with one and only one solution for the entire system of processes. This means that the entire list of processes of the form  $8+8 \rightarrow 8+8$ ,

when all external mesons are members of the pseudoscalar octet, can be described, for a given point in the  $s$ - $t$  plane, in terms of one quantity representing the overall magnitude of the process. That means that processes such as  $\pi K \rightarrow \pi K$ ,  $K\eta \rightarrow K\eta$ ,  $\pi\pi \rightarrow \overline{K}K$ , etc. are all related to each other in terms of one parameter.

This is an extremely strong result and it leads to some fascinating conclusions. It tells us that we must have an exchange of octets as well as a singlet in the  $s$ - and  $t$ -channel. The singlet is quite independent of the Pomeranchuk singularity which has been removed from the calculations at the very beginning! Had we assumed, for example, that the singlet channel also vanishes and only octet exchanges are allowed, we would immediately run into an inconsistency, namely, we would find that the only available solution is the one in which all amplitudes identically vanish. We are, therefore, forced to have a singlet in addition to the two octets. The singlet has to be degenerate with the two octets in its energy dependence if it has to cancel them for every value of  $s$  and  $t$ . We therefore conclude that, at least in this case, we must have degenerate nonets of tensor mesons exchanged in the set of processes  $8+8 \rightarrow 8+8$ . Similar considerations for other sets of  $SU(3)$  invariant processes lead us to the conclusion that we also need degenerate nonets of vector mesons.

This prediction is remarkable not only because it is experimentally true but also because this is the first time that the requirement that the vector and tensor mesons will appear in nonets follows for a model which has nothing to do (or at least does not seem to have anything to do) with the quark model. So far, the only motivation, other than empirical observation, for the existence of nonets has been the quark model, and here our simple set of assumptions of duality and the absence of exotics, forces us into degenerate nonets for these types of particles. This result is interesting in many respects. First of all, it is an extremely strong relation obtained from reasonable and (seemingly) not so strong assumptions. Second, it is not inconsistent with experiment in its gross features in the sense that to the extent that we may believe in  $SU(3)$  invariance, it is conceivable that we do have indeed an octet of vector mesons and a nonet of tensors which are really exchanged in pseudoscalar-pseudoscalar scattering (the singlet vector mesons cannot couple in an  $SU(3)$  invariant theory to two pseudoscalar mesons). But the most interesting aspect is perhaps the fact that this is our first encounter with a duality prediction which follows from the absence of exotic states and which resembles very strongly quark model predictions. In the next few sections we will return to many additional results of this nature, and we shall again and again observe this mystery of the amazing consistency between duality and the absence of exotics on one hand, and the entire framework of the quark model on the other hand.

XVIII. THE DUALITY BOOTSTRAP:  $\omega$ - $\phi$  and  $f^0$ - $f^*$  MIXING

We shall not study a refinement of the previous discussion which was proposed by Chiu and Finkelstein.<sup>23</sup> They have studied the same set of processes, namely, pseudoscalar-pseudoscalar scattering in an SU(3) limit but allowed the exchange trajectories to be split in mass. More explicitly, they allowed the  $\omega$  and  $\phi$  trajectories and the  $f^0$  and  $f^*$  trajectories to be non-degenerate, as they are in nature. In this way they force a splitting of the nonets (or to be more precise, a splitting between the two isotopic spin singlets of each nonet) but they do not a priori specify the octet-singlet mixing angle responsible for this splitting. They then propose the following set of considerations: From  $\pi^+\pi^+ \rightarrow \pi^+\pi^+$  it follows that the  $\rho$  trajectory has to be cancelled by a tensor trajectory. The tensor trajectory can be either the  $f^0$  or the  $f^*$  trajectory, but not both since they are not degenerate with each other. Let us choose the  $f^0$  and define  $f^0$  as the trajectory degenerate with the  $\rho$ . That immediately tells us that the  $f^*$  trajectory does not couple to the  $\pi\pi$  system, since otherwise we would need another  $\rho$  trajectory degenerate with the  $f^*$ , in order to cancel its contribution to  $\pi^+\pi^+$  elastic scattering. So, the first predictions are that  $\rho$  and  $f^0$  are exchange degenerate, their coupling to the pion are the same, and the  $f^*$  does not couple to pions. We now proceed to discuss  $K^+\pi^+$  elastic scattering. This is again an exotic amplitude in the s-channel. Its imaginary part presumably vanishes except for the Pomeranchuk term. The t-channel exchanges which are allowed are again  $\rho$  and  $f^0$  and the only new information that we gather is that the  $\rho KK$  and  $f^0 KK$  couplings are equal. Let us now proceed to discuss  $K^+K^+$  and  $K^+K^0$  elastic scattering. These processes are again exotic in the s-channel and again t-channel cancellations are needed. The t-channel trajectories which are allowed are  $\rho$ ,  $f^0$ ,  $\omega$ ,  $A_2$ ,  $\phi$ ,  $f^*$ . The type of exchange degeneracy requirement that we get from these reactions is that pairs  $\rho$ - $A_2$ ,  $\omega$ - $f^0$  and  $\phi$ - $f^*$  are exchange degenerate. Since we have already determined before that  $\rho$  and  $f^0$  are degenerate, the four trajectories  $\rho$ ,  $\omega$ ,  $A_2$  and  $f^0$  have to have the same coupling to the  $KK$  system. In particular, the  $\rho KK$  coupling is equal to  $\omega KK$ . SU(3), however, claims that the  $\rho KK$  coupling is related to the  $\omega_8 KK$  coupling, since  $\rho$  and  $\omega_8$  are in the same octet and the coupling is unique (of the F type). The physical  $\omega$  can be written as  $\omega = \omega_8 \cos\theta + \omega_1 \sin\theta$ .  $\omega_1$  does not couple to two K-mesons since two K-mesons in a pure P wave must be in an antisymmetric SU(3) representation while  $\omega_1$  is in the SU(3) singlet which is symmetric with respect to the interchange of the two octets. The coupling of the physical  $\omega$  to  $\bar{K}K$  must therefore go through its  $\omega_8$  component. This leads us to a determination of the octet-singlet mixing angle. The mixing angle which is found,<sup>23</sup> amazingly enough, is  $\cos^2\theta = 1/3$ , the canonical quark model mixing angle.

This result of Chiu and Finkelstein is even more striking than our previous

statement about the necessity of having nonets of vector and tensor mesons. This is a clear triumph of the idea of duality plus absence of exotic exchanges and the removal of the Pomeron, a triumph which is shared only by the quark model, in the sense that these are the only two models which give the correct  $\omega$ - $\phi$  mixing angle. Incidentally, the  $f^0$ - $f^*$  mixing angle can be obtained in a similar way. Notice that the input assumptions do involve, in a sense, some quark model considerations, since the quark model is the only model which predicts the absence of exotic states. The output is very clearly of the type of predictions that the quark model gives. However, in the derivation and throughout the various arguments used, neither the work quark, nor any implicit quark arguments were used. This again hints that there is some very peculiar and strange consistency between the idea of duality and the absence of exotic amplitudes on one hand and the quark model on the other.

An even more peculiar consistency in this context was discovered by Schwimmer.<sup>24</sup> So far we have forbidden the existence of exotic amplitudes, where "exotic" meant anything that cannot be constructed from three quarks or from a quark and an antiquark, from the point of view of internal quantum numbers. But there is another type of exotic states which are forbidden in the quark model, and which are not found in nature. These are mesons with natural parity, namely,  $P = (-1)^J$ , and negative value of CP. Such mesons cannot be constructed from a quark and an antiquark. Schwimmer has assumed that no such mesons exist and derived the following interesting result. Let us consider  $\pi\eta$  elastic scattering. In the s-channel  $\pi\eta$  can produce only  $C = +1$  resonances. The parity and angular momentum of  $\pi\eta$  resonances, in general, can be  $0^+$ ,  $1^-$ ,  $2^+$ ,  $3^-$ ... . Since  $C = +1$  and since all of these mesons must be of natural parity, the assumption of no exotic states leads us to the statement that all  $\pi\eta$  resonances must be of positive parity and even partial wave. That means that the forward and backward peaks in high energy  $\pi\eta$  elastic scattering will be of the same size (we again ignore completely the Pomernchuk contribution in the t-channel which would correspond to a background in the s-channel and which may have contributions to odd CP, natural parity partial waves). If the forward and backward peaks in elastic  $\pi\eta$  scattering are the same, the strength of the trajectories exchanged in the forward and backward directions must be the same and their  $\alpha$  values must be the same. In the forward direction, however, the leading trajectory is the  $f^0$  trajectory. In the backward direction it is the  $A_2$  trajectory. We therefore immediately conclude that the  $A_2$  and  $f^0$  trajectories are exchange degenerate and their couplings to  $\pi$ 's and  $\eta$ 's are related. Furthermore, by studying other processes such as  $\pi\eta \rightarrow \pi\chi$  and  $\pi\chi \rightarrow \pi\chi$ , Schwimmer has shown that the  $f$ - $f^*$  mixing angle must be the canonical quark model mixing angle and by studying other sets of processes such as  $\pi\eta \rightarrow \rho\omega$  he found the same result for the vector meson nonet. This result is even more puzzling

than the previous one. We again started with an assumption (no exotic amplitudes) which can be taken either from experiment or from the quark model, we supplemented it by duality and we ended up with a result which is a typical statement of the quark model. The mystery is, however, greater here because the input assumptions are related to the spin and charge conjugation property of the mesons in the quark model while the output results relate to the internal symmetry properties. This is different than the previous case in which both the input and the output were related to the internal quantum number properties of states in the quark model! We quote these results as well as the results mentioned in the previous section as indications that at least the algebraic structure of the quark model is somehow buried in a very interesting and subtle way within the entire framework of duality.

#### XIV. THE DUALITY BOOTSTRAP: THE BARYON-ANTIBARYON CATASTROPHE

Since we are discussing various examples of bootstrap calculations using duality and the absence of exotic amplitudes, we should also mention the only case in which this scheme clearly fails. This is the case of baryon-antibaryon elastic scattering. It was first pointed out by Rosner<sup>25</sup> that, if we assume (i) no exotic amplitudes are allowed; (ii) the Pomernachuk singularity is removed according to our cooking recipe; (iii) duality; and if, furthermore, we make the same assumptions for meson-meson, meson-baryon, baryon-baryon and baryon-antibaryon elastic scattering the overall consistency requirement of all of these assumptions for all of these processes leads to a disastrous result for baryon-antibaryon scattering. The result is that, except for the Pomeranchuk contribution, all baryon-antibaryon total cross sections have to vanish. This is, of course, totally unreasonable and clearly in contradiction with experiment. Several prospects have been suggested in order to resolve the difficulty. One of them, due to Rosner,<sup>25</sup> says that exotic mesons made out of two quarks and two antiquarks indeed exist, but they couple only to the baryon-antibaryon system and not to the meson-meson system and therefore they avoided being detected so far. While we cannot rule out such a possibility we must admit that it is a totally unsatisfactory excuse. Even if such mesons exist, it would be very peculiar to observe that this framework was so consistent, so restrictive (but not too restrictive) and so similar to the quark model in so many processes and all of a sudden it fails in this particular example. Another proposal for curing the baryon-antibaryon difficulty is due to Lipkin.<sup>26</sup> He suggested that, in terms of the quark model, the concept of an s-channel resonance in meson-meson and meson-baryon scattering is simply the annihilation of one of quark and antiquark pair: In baryon-antibaryon scattering, and only in this case, the annihilation of one pair of quark and antiquark does not lead to an s-channel mesonic resonance. It leads to, at least, two meson resonances in the s-channel.

Lipkin therefore proposes that the words "resonance dominance" in our previous set of assumptions should be replaced by the words "the dominance of quark-antiquark annihilations" and therefore everything would remain the same for meson-meson and meson-baryon scattering while in baryon-antibaryon scattering two meson intermediate states or annihilations of baryon-antibaryon into two mesons would also be considered under the same heading as the single quark-antiquark annihilations and would correspond to t-channel Regge exchanges rather than to the Pomeron terms. This proposal also does not resolve the difficulty because it would have to explain what happens in processes of the type  $B\bar{B} \rightarrow MM$ . This process does not lead to any difficulty since it is simply the crossed channel process for meson-baryon elastic scattering, and if we assume that baryon-antibaryon goes to two mesons should be considered as a non-background contribution even if it does not proceed through s-channel resonances, we will have to abandon all the successes in the meson-baryon case (and via factorization even in the meson-meson case). We therefore feel that the difficulty in baryon-antibaryon scattering is not resolved yet, and we believe that it is the main difficulty of the model. Furthermore, it is conceivable that this failure is trying to teach us something. It is very difficult to believe that all the beautiful self-consistency of all the other processes is spurious and the baryon-antibaryon case is really the case which tells us that we are dealing here with an unreasonable scheme. We prefer the opposite point of view, namely, that there is here a beautiful self-consistent scheme of assumptions, results and predictions, both in the sense that it does not lead to any contradictions and in the sense that it is consistent in such a mysterious way with the quark model. The baryon-antibaryon case is an exception not because it contradicts everything else but because we are probably handling it in a wrong way and we are probably avoiding some crucial property of this particular process which is different from the other processes. Unfortunately, no one has come up yet with a convincing way of resolving this. We shall come back to this difficulty as well as to some of the previous successes outlined in the previous sections when we discuss duality in Sec. XXII.

## XX. DUALITY, REGGE CUTS AND ABSORPTION

In spite of the fact that we have formulated the duality idea in terms of a model involving Regge poles only, we have mentioned many times the necessity of introducing important contributions of Regge cuts into the calculation of high energy hadronic scattering amplitudes. The necessity of including such contributions is implied by a large number of phenomenological studies of hadronic reactions. Quite independent of the entire question of validity of duality, we have already emphasized in these notes that it would be totally unreasonable to ignore this

necessity in discussing duality both from the theoretical point of view and from the practical point of view. From the theoretical point of view we have to know how to include the cut contributions in the general considerations, beginning with the cut contributions to the right hand side of the FESR and ending with the question whether the Regge cuts correspond to resonances in the s-channel or to background in the s-channel. From the practical point of view, the question is even more crucial. We have faced a large number of inconsistencies between various predictions of the general duality scheme and experiment, such as some of the exchange degeneracy predictions and such as the baryon-antibaryon catastrophe. We have emphasized that in many of these cases, the phenomenology of these same reactions that are studied here within the framework of duality is not clear at all. Furthermore, we have shown that the application of various duality predictions to some of the involved reactions includes the assumption of factorization, an assumption which is special to Regge poles and is not obeyed by Regge cuts.

Apart from the assumption of factorization, Regge cuts, for practical purposes, are not so different from Regge poles, in the sense that in many cases the contribution of a Regge cut can be parametrized in terms of a so called "effective pole" which reproduces most of the properties of the cut contribution. It is clear that such an effective pole cannot reproduce all the properties of the cut, but through a limited energy region, and for most practical purposes, such an approach could be valid and in fact could even be a reasonable way of applying Regge cut phenomenology to the data, in view of the large number of parameters which are necessary in including Regge cuts in a more appropriate way. Let us remember, however, that such effective Regge poles (which are really imitations of Regge cuts and do not correspond to any physical particle) have no reason to obey the factorization assumption, and therefore whenever we discuss high energy hadronic processes in terms of Regge cuts or in terms of "effective Regge poles" we cannot and should not use factorization and we should not be concerned about failures of our theory which follows from an extensive use of the factorization assumption.

All of these remarks are valid only in a negative way. They reduce the number of cases to which we can apply meaningful predictions of duality and they provide us with an excuse for some of the failures of the model. In order to include Regge cuts properly within the duality framework, we must, however, understand better the physical meaning of such cuts and incorporate them in the general analysis of the processes. One interesting approach which tries to provide us with the simple physical meaning to the contribution of the Regge cuts is the approach of the absorption model. The classical absorption model of the early 1960's is well known to be totally inadequate. However, this model had two basic ingredients. It starts with a Born term (a single particle exchange amplitude

calculated by perturbation theory) and then continues by applying the absorption corrections to this Born term. The basic physical idea of the absorption model is that the partial waves which are important in any given inelastic process are the most peripheral partial waves which are allowed within the radius of the interaction. This idea is quite independent of the first step that used to be included in the absorption model, namely, the calculation of the Born term. When the old absorption model failed it was never clearly indicated whether it failed because the Born term is a totally inadequate starting point or whether the second step, the absorption step, is an unreliable physical principle. We suspect that it is the first possibility which occurs, namely, the Born term is a totally unreliable and unjustified starting point, while the idea of absorption may have some justification in high energy inelastic processes. We feel that in order to study the validity of the idea of absorption, we must look for predictions which are independent of the first step of the analysis, namely, predictions which can be compared with experiment and which would be valid regardless of what is the original approximation that we use. We will not go into a detailed analysis of this question here, since our main topic here is not the absorption model. Let us only remark that such predictions can be found and in spite of the fact that they are mostly of a qualitative nature (such as predictions on whether or not dips will occur in specific cases) some success has been obtained with these predictions. For the purposes of unifying the absorption model and the Regge cut picture on one hand and the duality idea on the other hand, it will be sufficient if we establish here some general principles for the contribution of Regge cuts, consistent with the absorption model, and then try to incorporate these principles into the duality framework.

The main principle that we assume here is very simple. We demand that in any given inelastic process the strong contributions come from the most peripheral s-channel partial waves within the radius of interaction, namely, from partial waves obeying the relation  $l \sim kR$ . We shall further assume that from the t-channel point of view we have a complicated combination of Regge poles and Regge cuts which is arranged in such a way that its projection on the s-channel partial waves will obey our previous requirement, namely, the Regge pole contributions and the Regge cut contributions will be such that the total projection on low partial waves in the s-channel will be small and the main strength of the process will come from the most peripheral partial waves. We therefore have here an s-channel picture and a t-channel picture which are very qualitative and not very specific but still give us some information.

To this picture we shall now add the requirement that the s-channel partial waves are dominated by resonances. That means that, since the most important contributions come from the peripheral s-channel partial waves, the most



important contributions come from the peripheral resonances. Another way of saying this is that we are using our previous resonance dominance of Sec. IV, but adding to it the requirement that the strongest coupling in any given inelastic process will be that of those resonances obeying the relation  $l \sim kR$ . This is our s-channel picture. From the t-channel point of view, we claim that the same peripheral resonance contributions are described by the combination of Regge poles and Regge cuts that we have mentioned before.

This picture immediately leads to one result which is very interesting and which we have already mentioned in our discussion in Sec. VI. In Sec. VI we have seen that s-channel resonances can construct contributions which will have a dip structure in the angular distribution of fixed values of  $t$  for all energies, provided that these s-channel resonances obey the relation  $l \sim kR$ . Now that we have added a dynamical assumption motivated by the absorption model which states that the prominent and important resonances indeed belong to such partial waves, we automatically have a combination of s-channel resonances which is guaranteed to provide us with t-distributions which have a certain fixed feature at fixed values of  $t$  at all energies! This is a typical property that we would like the combination of our t-channel exchanges to have, and it is interesting that this property is guaranteed by our dynamical absorption assumption.

We now have a simple picture in which the resonance dominance concept of Sec. IV is restricted to resonance dominance in the peripheral s-channel partial waves with no important resonances (or any other contributions) in low partial waves. The "ordinary t-channel trajectories" now include both t-channel Regge poles and t-channel Regge cuts in such a way that they are consistent with the s-channel description. Almost every single argument and assumption that we have made in our theoretical considerations, so far, can be left unchanged by our way of including cuts. In particular, the Pomeranchuk contribution is still of a specific nature and is still the only one related to the background; the ordinary trajectories which now include the cut contributions are built by resonances; the amplitude is still built in terms of two additive components; the assumption of no exotic amplitudes can remain valid, provided that the important cuts are cuts which are obtained by the repeated exchange of a non-exotic pole and a Pomeranchon (but the absorption model, of course, requires that these are indeed the prominent cuts); exchange degeneracy remains a prediction of the theory in a slightly modified way. For  $t < 0$  values the degeneracy is between the poles as well as the cuts, or, to be more precise, the degeneracy or the cancellations should occur somehow between the combined pole-cut contribution of one set of quantum numbers and the combined pole-cut contribution of another set. Instead of saying that the  $\rho$  trajectory and the  $P'$  trajectory are degenerate for  $t < 0$  we shall say that the energy

dependence and the strength of the  $\rho$ -pole and the  $\rho$ -P' cut is equal to those of the P' pole and the P'-P cut. These predictions will maintain exchange degeneracy of poles for positive t, will maintain the degeneracy of poles for negative t, but will not lead to the simple predictions of exchange degeneracy that we studied in Sec. XVI because the signature factors are not so simple any more, the factorization property is not obeyed and many of the restrictive properties of Regge poles are not assumed any more. We are losing here a great deal of predictive power but also a great number of inconsistencies with experiment. Whether that should make us happy or not is a question of taste. If we really wanted to look for excuses, we could even blame the catastrophe of the baryon-antibaryon system on the presence of Regge cuts and the failure of factorization. We believe, however, that this failure is more fundamental as we shall see when we discuss the duality diagrams and we suspect that we cannot get away with such a simple excuse.

We realize that we have not presented here (and neither did anyone else, so far) a complete theory incorporating the Regge cuts within the framework of duality. We want to remark, however, that such a theory is badly needed and that it is not necessarily inconsistent with duality. We should be particularly satisfied with the coincidence between our conditions of Sec. VI on the relation between the spin and the energy of resonances which produced fixed properties in t and the requirement of the absorption model. Needless to say, the solution of this problem of Regge cuts should come first on the phenomenological level by studying many phenomenology problems and only later it could be understood within the framework of duality.

## XXI. DUALITY AND QUARKS

One of the most fascinating aspects of duality is the intimate relation between the duality bootstrap and the quark model. In some of the previous sections and in particular in Secs. XVII and XVIII, we have seen that duality relates in a very peculiar way completely different results which are normally derived from the quark model. From a more fundamental point of view, the relation between duality and the quark model sounds very peculiar. Duality is a bootstrap scheme and as such, does not distinguish between the elementarity property of the different hadronic states. Complete hadronic democracy according to the bootstrap idea is perfectly consistent with duality. On the other hand, the quark model is, of course, based on a completely different idea, namely, on the idea that all the observed hadrons are constructed from some more fundamental building blocks. The possibility that such a model of fundamental building blocks is consistent in the mathematical sense with a typical workable bootstrap theory, is by itself surprising and it certainly does not have any precedence in any other case in the history of

strong interaction dynamics.

In order to study the connection between duality and the quark model, we should distinguish between two different levels of discussion. From the mathematical point of view, it is absolutely clear that the quark model is related to duality. The examples of Secs. XVII and XVIII illustrate this, but even without them the important role played by the assumption of non-exotic amplitudes within the duality framework is by itself a guarantee that the quark model is mathematically relevant here. The first question that we have to formulate and answer is, therefore: is the quark model capable of producing simple mathematical tools or a simple mathematical scheme which will enable us to discuss duality (including the assumption of no exotic amplitudes) in a convenient way, such that many of the algebraic predictions can be derived easily in terms of this quark terminology?

The second level of analysis which is much more physical and more fundamental is, of course, the possibility of constructing a duality theory for a case in which physical concrete quarks exist in nature. In such a case we will have to explain all of the concepts discussed above, such as s-channel resonances, t-channel poles, t-channel cuts, the Pomeranchuk contribution, the exotic amplitude etc., in terms of operations among the quarks themselves and in terms of quark-quark and quark-antiquark scattering amplitudes. In such a case we will have to study whether or not the existence of the duality properties imply something for the particular dynamics that the quarks obey. This question is much more speculative of course, because we do not know if the quarks exist, but it is also much more fundamental and is of much greater importance than the simple possibility of constructing a mathematical quark theory of duality.

## XXII. DUALITY DIAGRAMS

The mathematical connection between the quark model and the ideas of duality and the absence of exotic amplitudes is best illustrated in terms of the duality diagrams.<sup>27,28</sup> These diagrams specify the particular quark properties of the hadronic scattering amplitudes which has to be obeyed in order to guarantee that duality, resonance dominance, and the absence of exotic amplitudes will be valid. In order to construct a duality diagram, we imagine that a meson is described in terms of two quark lines running in opposite directions while a baryon is described in terms of three quark lines running in the same direction. The process  $M+M \rightarrow M+M$  (where M is any non-exotic meson) is described by the diagram of Fig. 29a. We see that the two incoming mesons combine in such a way that the quark of one meson and the antiquark of the other meson annihilate each other while the remaining quark-antiquark pair produce a non-exotic mesonic state in the s-channel. At the same time, if we consider the process from the t-channel point

of view, we see that a non-exotic meson (i.e., a quark-antiquark pair) is exchanged in the t-channel. This particular way of connecting the quark lines is the only way which will guarantee that both the s-channel and the t-channel do not have any exotic quantum numbers. In a similar way Fig. 29b shows the duality diagram for the processes  $M+B \rightarrow M+B$  (where M, B are any non-exotic meson and baryon respectively). Here, we see that the s-channel intermediate state is a three-quark state, namely, a non-exotic baryonic system, while the t-channel intermediate state is a quark-antiquark state, namely, a non-exotic meson. These two conditions can be guaranteed only by the particular way of drawing the diagram shown in Fig. 29b. Any other diagram with the same external lines but with internal lines crossing each other, for example, will not obey the requirement of non-exotic amplitudes in all channels. This is shown in Fig. 29c, where meson-baryon scattering is described in terms of a diagram with one pair of quark lines crossing each other. In this case, we see that the s-channel includes states of four quarks and one antiquark; such states are exotic according to our terminology and we do not want them to contribute.

Meson-baryon scattering at small backward angles can be described in terms of the diagram of Fig. 29d. In that case we see that a non-exotic baryon is the s-channel intermediate state, and a similar non-exotic baryonic state is exchanged in the u-channel.

The basic rules of drawing the diagrams are very simple. We demand that (i) all external and internal mesons are pure quark-antiquark states, (ii) all external and internal baryons are three quark states, (iii) every quark line retains its identity. In addition, we demand that (iv) the two ends of any given quark line must belong to different external particles. With this set of requirements we can easily see that meson-meson scattering meson-baryon scattering and baryon-antibaryon annihilation into two mesons can be easily described in terms of diagrams which satisfy all of these rules. (There will, of course, be specific processes within these general families of reactions which will not correspond to legal diagrams, but at least some processes of every one of these general families can be described by duality diagrams).

The case of baryon-antibaryon scattering is the only case that cannot be described in terms of a legal duality diagram. This is shown in Fig. 29e. Both the s-channel and the t-channel in baryon-antibaryon elastic scattering are mesonic channels. If we would take both channels to be described by non-exotic mesons, we would allow only one pair of quark lines to be transmitted in every channel. The total number of internal lines would therefore be four, two in the s-channel and two in the t-channel. The total number of external ends of lines in baryon-antibaryon elastic scattering is, of course, 12 and we therefore have six quark lines altogether. However, only four of them are allowed to belong to

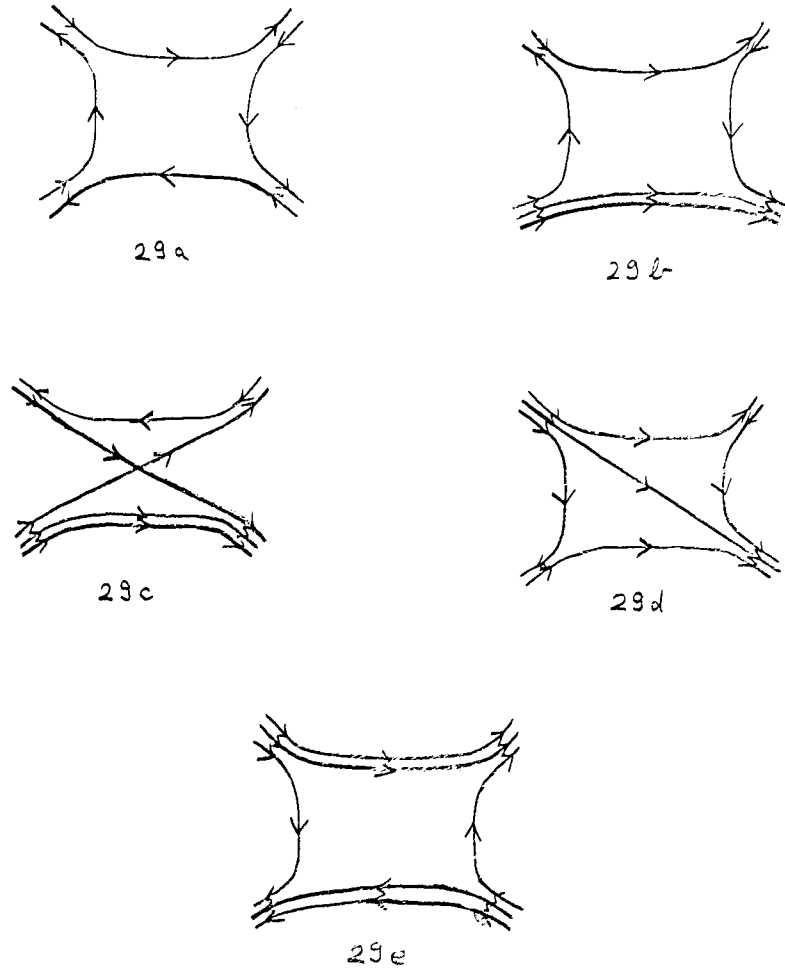


Figure 29: Duality Diagrams.

- (a)  $M+M \rightarrow M+M$ ; (b) legal diagram for  $M+B \rightarrow M+B$ ; (c) illegal diagram for  $M+B \rightarrow M+B$ ; (d)  $M+B \rightarrow B+M$ ; (e)  $\bar{B}+B \rightarrow \bar{B}+B$ .

s-channel or t-channel intermediate states! It is obvious that under these conditions we cannot draw a legal duality diagram and therefore we expect that baryon-antibaryon scattering can obey our general set of requirements (including the absence of exotic amplitudes) only in a trivial way, namely, only by vanishing. This is consistent with the observation<sup>25</sup> mentioned in Sec. XIX concerning the baryon-antibaryon catastrophe, and in this case we can see from the duality diagrams in a very simple way why the baryon-antibaryon elastic amplitude is predicted to vanish by the absence of exotic states and duality.

We already see that the duality diagrams are a useful tool for deciding which processes are forbidden and which are allowed according to our set of requirements. Just by drawing the simple diagrams we have noticed that meson-meson and meson-baryon scattering allow at least one solution to our set of requirements, while baryon-antibaryon scattering has to vanish. By identifying the quark lines as corresponding to specific types of quarks, we can analyze specific meson-meson and meson-baryon scattering reactions and decide whether or not they are allowed by the absence of exotic states and duality.

However, before we do this, we have to ask ourselves whether the duality diagrams are mathematically equivalent to our previous set of assumptions or whether they add some extra ingredients which were not present before. The answer to these questions is not easy. It is clear that extra ingredients are added, but it can be shown that these ingredients are fairly weak and they do not add much strength to our original assumptions. For example, a very clear additional assumption which is being made here is the following: Previously, when we claimed that no exotic amplitudes were allowed, we referred to amplitudes corresponding to SU(3) representations larger than the octet for mesons and larger than the decuplet for baryons. We did not specify the quark content of the particular states which are exchanged. Now, when we draw the duality diagrams we forbid all states of two quarks and two antiquarks in mesonic channels and all states of four quarks plus one antiquark in baryonic channels even if such states happen to belong to a non-exotic SU(3) representation. For example, we can have a two quark plus two antiquark state in an SU(3) octet. Such a state would normally be considered as non-exotic since it is in the octet, but within the framework of the quark model and for the purpose of drawing duality diagrams it will be considered as exotic and it will be forbidden. This is clearly an extra assumption that was not made before and it looks like a very strong assumption. It turns out, however, that in most cases this extra assumption can be shown to be equivalent to certain combinations of SU(3) symmetry, factorization and other assumptions that are not specific to the quark model.

In those cases where duality and the absence of exotic amplitudes lead to

a unique solution of the bootstrap equation (such as in the octet-octet scattering case discussed in Sec. XVII) the duality diagrams automatically give the same unique solution, since they are obviously consistent with the assumption of duality and absence of exotics and since they must give at least one solution. This solution is, therefore, the same as the unique solution which we have obtained before. In cases where duality and the absence of exotics do not lead to unique solutions and allow one or more free parameters (such as in the case of meson-baryon octet-octet scattering) the duality diagrams are capable of choosing one solution among the many possibilities. In the case of meson-baryon scattering the duality diagrams are doing precisely this.

Duality diagrams can be drawn for processes having more than two particles in the final state. In those cases they serve to illustrate clearly the generalization of the duality concept for a multiparticle amplitude. Figure 30a shows a duality diagram for the process  $M+B \rightarrow M+M+B$ . We see that all the exchanged particles in all channels are non-exotic, namely: whenever a baryon can be exchanged we have only one quark line and one antiquark line. The duality diagram for this process can describe any one of the five ordinary exchange diagrams shown in Figs. 30b-30f. Every one of these diagrams shows a possible mechanism of exchanging mesons or baryons in the various channels and every one of these mechanisms is a possible contributor to the production of the three particles in the final state. What the duality diagram (Fig. 30a) tells us is that every single one of these possibilities, when summed over all possible intermediate states, is sufficient to describe the entire process. Thus the possibility of a double meson exchange shown in Fig. 30d is sufficient to describe the process  $M+B \rightarrow M+M+B$  and there is no need to consider s-channel baryons in addition. On the other hand, the possibility of having s-channel baryons which decay to a meson and a baryon while the meson then decays again to two mesons, when summed over all possible intermediate baryons and mesons, is also sufficient in order to describe the entire process. Every one of these possibilities corresponds to the same duality diagram.

Another interesting lesson that we can learn from the duality diagrams is related to the question of higher order corrections. If we would like to discuss the possibility of inserting mass corrections on external legs, or propagator corrections on internal exchanged Reggeons, or the contributions of box diagrams, we can draw the duality diagrams corresponding to every one of these cases. Figure 31 shows that the duality diagrams corresponding to all of these cases as well as to the vertex corrections and several other corrections are identical. In every one of them we have the usual external lines plus one closed internal loop corresponding to one closed internal quark line. Consequently, every one of these diagrams by itself when summed over all possible intermediate states gives the

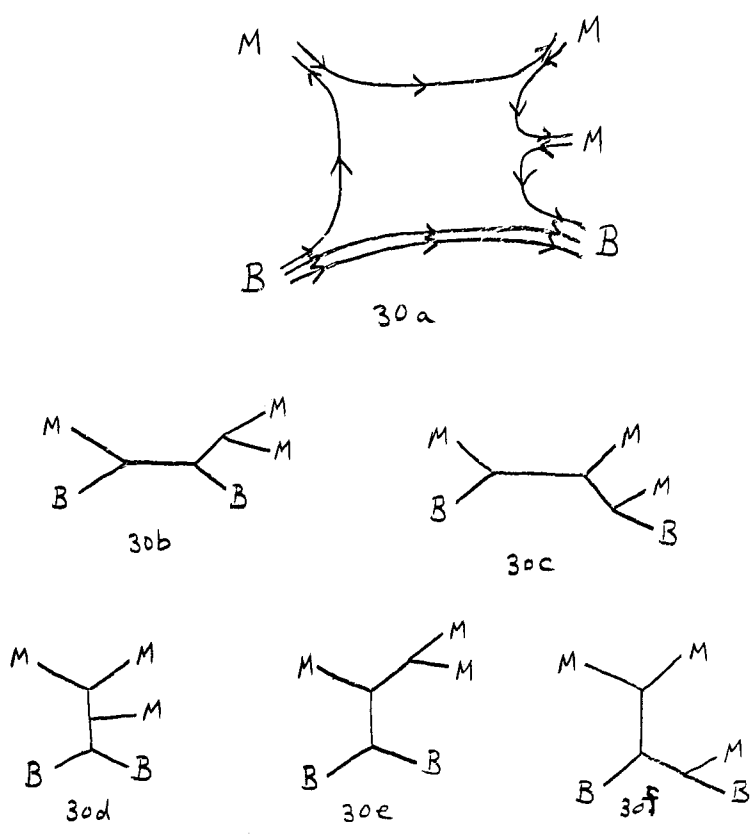


Figure 30.

(a) Duality diagram for  $M+B \rightarrow M+M+B$ ; (b) - (f) the various possible exchange mechanisms for the same process.



complete description of this particular correction. If we would add the contributions of two or more types of such corrections we will commit double counting. Again, the duality diagrams serve as a tool for telling us which diagrams are only providing us with alternative descriptions of the same situation and which diagrams can be safely added to each other from the point of view of duality. This last remark about higher order corrections will be meaningful, of course, only if and when we have some kind of a theory which will enable us to calculate the hadronic amplitude, starting from some fundamental amplitudes such as the Veneziano formula or some other formula. Attempts in this direction have been suggested and we will very briefly mention them in Sec. XXXIV. All that we want to point out here is that, regardless of the particular type of theory that we use, if we believe in duality, we should not add any of these corrections to each other and we should consider only one of them as sufficient for describing the entire set of corrections.

In the next section we shall discuss some of the experimental implication of the duality diagrams, but let us now summarize what, if anything, we have learned from them. As a mathematical tool they are simply a gadget for seeing in a very clear and simple way what duality means in terms of the internal quantum numbers of the system or in terms of the quark model. In many cases (some of which we shall describe in the following section) the duality diagrams help us to calculate very quickly selection rules which would be discovered otherwise only by fairly elaborate calculations. We have also mentioned that the duality diagrams assume a little bit more than we have assumed, so far, namely, a specific form of non-exotic states. They exclude a slightly larger group of states than the usual SU(3) type of assumption concerning the absence of exotics.

We must emphasize, however, that from the physics point of view the duality diagrams add almost nothing to our previous set of assumptions; they do not teach us any new fundamental principle here, they do not suggest any new theoretical idea and they should be considered only as a tool for quick calculations and as an easy way of seeing which descriptions of the amplitudes can be built from each other. All of these remarks are true, of course, only to the extent that duality diagrams as well as the relation between the quark model and duality are purely mathematical. If quarks happen to exist, then the duality diagrams are much more fundamental and they presumably describe the particular way in which the physical quarks interact with each other, annihilate each other and behave in the real world. We do not dare to speculate that this is indeed the case, and we therefore regard the duality diagrams only as a convenient mathematical tool with no new physical input except for some minor extra ingredients of the quark model or SU(3).

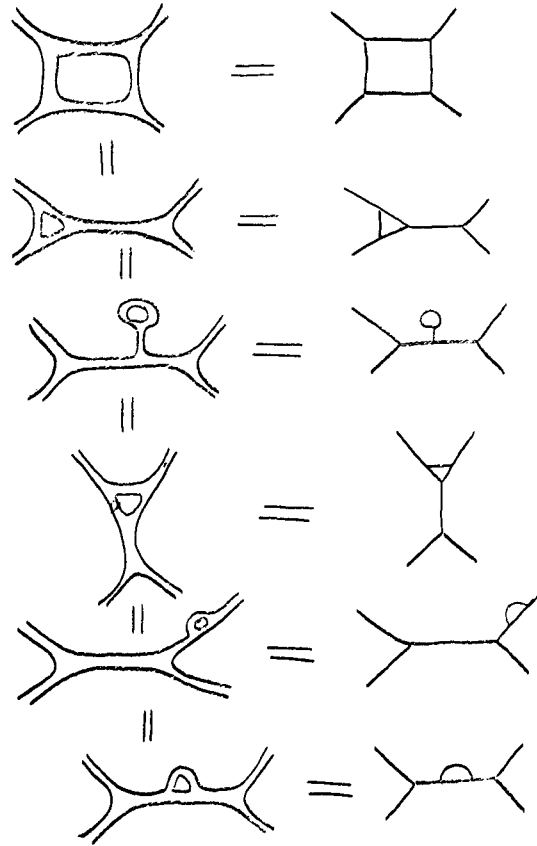


Fig. 31.

Box diagrams, propagator corrections, vertex corrections, tadpoles, etc. are all described by the same duality diagram.

### XXIII. DUALITY DIAGRAMS AND PURELY REAL AMPLITUDES

The basic assumption which leads to the introduction of duality diagrams is the assumption of the absence of exotic states. This assumption is relevant only to the imaginary part of the amplitude. We have already stated that the absence of exotic amplitudes is simply a combination of (i) absence of exotic resonances, (ii) resonance dominance. But resonance dominance is valid only for the imaginary part in a local or in a semi-local sense, and therefore the absence of exotic amplitudes is valid only for the imaginary part. We therefore conclude that if a certain process corresponds to an illegal duality diagram, namely - it cannot be described by a duality diagram which obeys all our diagram rules, then the imaginary part of its amplitude (and not the entire amplitude) will have to vanish.

A simple example which really does not necessitate duality diagrams is  $K^0 p \rightarrow K^+ n$ . In this process the antiquark of the K meson cannot annihilate any of the quarks of the proton and therefore we cannot draw any duality diagram corresponding to this reaction. The reaction is therefore forbidden by the duality diagrams and we will have a vanishing imaginary part. But we have already found before that this process will have no imaginary parts; it follows very simply from the observation that this process has exotic s-channel quantum numbers and therefore its imaginary part vanishes. The duality diagrams teach us nothing new in this case.

There are other cases, however, in which the s-channel is not exotic and the duality diagram is still forbidden. These are precisely those cases in which the duality diagram does add some information. As an example let us consider the process  $K^- p \rightarrow \pi^- \Sigma^+$ . This process does not involve exotic quantum numbers either in the s-channel or in the t-channel. However, if we try to draw a duality diagram for it, we immediately see that it cannot be drawn in a legal way. The reason can be explained in the following manner: The antiquark of the incoming meson has to annihilate one of the quarks of the incoming baryon. The antiquark of the outgoing meson must be related to one of the quarks of the outgoing baryon. But the quark of the incoming meson and the quark of the outgoing meson must be identical (Fig. 29b). This cannot happen, however, in  $K^- p \rightarrow \pi^- \Sigma^+$  since the quark of the  $K^-$  meson is a  $\lambda$  quark while the quark of the  $\pi^-$  meson is an n quark. Consequently there is no way to draw a legal duality diagram for  $K^- p \rightarrow \pi^- \Sigma^+$ . This means that the duality diagrams predict that at high energies and small angles (where we would expect the diagrams to be relevant) the imaginary part of the amplitude of this process vanishes. Similar predictions<sup>27</sup> can be derived for other processes and we shall not discuss all of them here.

Two interesting questions have to be raised with respect to predictions

such as this one. First, what is the particular ingredient of the duality diagrams that led us to a prediction which cannot be directly obtained from the absence of exotic amplitudes? Second, are these predictions consistent with experiment?

The answer to the first question can be stated in the following way. We shall show here that from duality, the absence of exotic states, and factorization we can almost (but not quite) show that the process  $K^- p \rightarrow \pi^- \Sigma^+$  is forbidden. This can be done in the following way. Let us consider  $K^- \pi^- \rightarrow \pi^- K^-$  (Fig. 32a). In this case the s-channel is exotic and therefore the imaginary part of the amplitude vanishes. In the t-channel we can exchange a  $K^*$  and a  $K^{**}$  meson. The vanishing of the imaginary part of the amplitude means that the  $K^*$  meson and the  $K^{**}$  meson contributions must cancel each other and we therefore get  $\alpha_{K^*} = \alpha_{K^{**}}$  and  $\beta_{K^*K\pi}^2 = \beta_{K^{**}K\pi}^2$ . If we then consider the process  $p\Sigma^+ \rightarrow \Sigma^+p$  (Fig. 32b) we find a

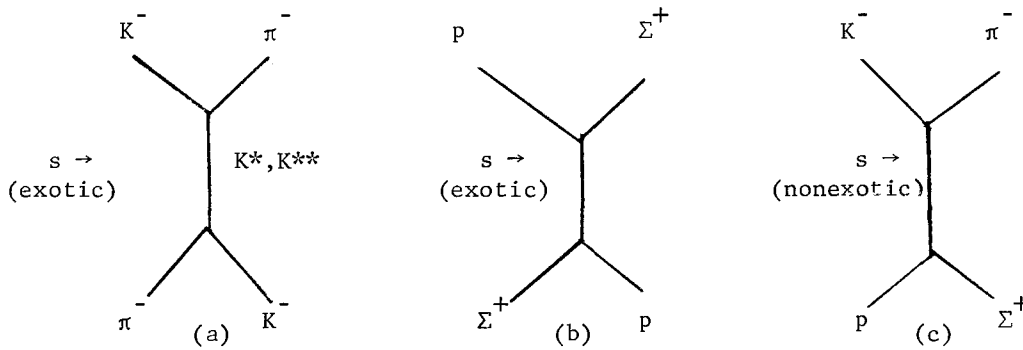


Fig. 32. Duality and the absence of exotics in  $K^- \pi^- \rightarrow \pi^- K^-$  and  $p\Sigma^+ \rightarrow \Sigma^+p$ , together with factorization are equivalent (up to a sign) to  $\text{Im}(K^- p \rightarrow \pi^- \Sigma^+) = 0$ .

similar situation: in the s-channel the quantum numbers are exotic and the imaginary part of the amplitude has to vanish. This, from the t-channel point of view, will happen only by cancellations of trajectories. The leading contributing trajectories are again  $K^*$  and  $K^{**}$  and again the cancellation will follow if and only if  $\alpha_{K^*} = \alpha_{K^{**}}$  and  $\beta_{K^*p\Sigma}^2 = \beta_{K^{**}p\Sigma}^2$ . Let us now return to the process  $K^- p \rightarrow \pi^- \Sigma^+$  (Fig. 32c). Here, again, the leading trajectories are  $K^*$  and  $K^{**}$ . Their degeneracy is guaranteed by the two other processes that we have discussed here and the residue functions which appear are  $\beta_{K^*K\pi} \beta_{K^*p\Sigma}$  and  $\beta_{K^{**}K\pi} \beta_{K^{**}p\Sigma}$ . These two residue functions must be equal, except for a sign, according to our previous analysis of  $K^- \pi^-$  scattering and  $p\Sigma^+$  scattering and the only assumption made here, in addition to duality and the absence of exotic states, is factorization (even SU(3) is not assumed). We, therefore, find that the contribution of the  $K^*$  and  $K^{**}$  trajectories

to the imaginary part of  $K^- p \rightarrow \pi^- \Sigma^+$  will either precisely cancel each other or will add with a constructive interference. This is as far as we can go without the duality diagrams and this is as far as we can learn from assuming only duality, absence of exotic amplitudes and factorization. What the duality diagram adds in this particular case is the choice between the two possible signs, a choice which determines that it is a relative negative sign between the two contributions which occurs here and the full imaginary part of the  $K^- p \rightarrow \pi^- \Sigma^+$  amplitude has to vanish. We, therefore, see that duality diagrams do add extra information but not as much as it would seem before analyzing carefully the possibility of using other reactions and factorization.

We now have to answer the second question, namely, how well do these predictions of the duality diagrams do when compared with experiment. This is very difficult to answer because most of the predictions only state that the imaginary parts of various amplitudes vanish, while the real parts can have any values. Experimentally, what we measure are always combinations of the real and the imaginary parts and it is very difficult to separate them from each other in order to find out whether the imaginary part indeed vanishes. The imaginary part can be isolated only in several indirect ways. One possibility is to measure polarization. If an amplitude is purely real, there will be no polarization. However, this is an extremely sensitive way of testing this prediction since a small imaginary part (contributing for example 10% of the entire cross section) can easily lead to polarization of the order of 30%. A second indirect way of testing the prediction is to consider specific phenomenological models such as the exchange of several Regge trajectories and possibly Regge cuts, trying to analyze the entire data for a given process in terms of the specific phenomenological model, and then - if the phenomenological model is successful, we can calculate the imaginary part of the amplitude from the model, assuming that the model reproduces correctly most of the properties of the physical amplitude. This way is even more indirect because it involves theoretical assumptions which cannot be verified.

The present situation of the predictions of duality diagrams is that in those cases where polarization measurements are available, the agreement is, at best, poor and in some cases disastrous. Comparisons of the second kind, namely, comparisons by using specific models are more rare and the situation is not so clearly negative.

When we ask, however, whether these predictions of the absence of polarization, etc. really follow from duality diagrams alone the answer is no! The situation here is very similar to the situation that we had in Sec. XVI when we discussed several failures of the exchange degeneracy hypothesis. There, also, we found inconsistency with experiment but the inconsistency occurred between experi-

ment and theoretical predictions which could also be based on much simpler models, which have nothing to do with duality. We have already stated there that we could easily blame the failures on the inadequacy of the Regge pole models as distinguished from Regge cuts model. We know that this is a very weak excuse, but this happens to be the correct phenomenological situation. We therefore mention here, again, that the duality diagrams suffer from the same disadvantage of the entire set of exchange degeneracy predictions, namely, they are subject to modification and to much weakening as a result of our phenomenological ignorance.

#### XXIV. TWO COMPLEMENTARY DESCRIPTIONS AT EVERY POINT

Our next assumption is much stronger than anything that we have discussed so far. We have already emphasized several times that duality states that hadronic scattering amplitudes can be described either as a sum of s-channel resonances or a sum of t-channel exchanges. Finite energy sum rules or global duality tell us that the two descriptions should "balance" each other numerically only when we integrate the amplitude over a sufficiently large energy region. In the case of the finite energy sum rule we have to integrate the resonance contributions from  $\nu = 0$  to  $\nu = N$  where  $N$  is a sufficiently large energy value such that above it, Regge behavior holds to the desired accuracy.

A much stronger assumption would be to demand that the sum of resonances in the s-channel and the sum of trajectories in the t-channel balance each other at any given point. The finite energy sum rules, according to such an assumption, will be correct not only as sum rules for an integrated amplitude but also in a differential form. One may take the integrand of the FESR at any given energy value, and it would be balanced by the derivative of the right hand side of the sum rule, namely, by the sum of Regge exchanges at this particular point. This is an extremely strong assumption which would mean that every single resonance and every single feature in the s-channel is reproduced by a sufficiently complicated set of exchanges in the t-channel and vice versa.

The trouble with such an assumption is that if we leave it at this point, it is very difficult to prove it or disprove it. Mathematically, it is almost always possible to construct a sufficiently complicated picture in the t-channel, for example, that will reproduce all the s-channel experimental features to their last detail. If we really want we can even reproduce the features of the  $\Delta(1236)$  resonance by sufficiently crazy set of exchanges which will dominate  $\pi N$  scattering at a c.m. energy of 1236 MeV. It will be totally useless, but mathematically possible, to do such an exercise. We remember, however, that simplicity is one of our most important criteria for the use of the duality hypothesis and we therefore would like the two complementary descriptions to be fairly simple. That is

immediately excluded in the case of the  $\Delta(1236)$  resonance. It is clear that any combination of t-channel exchanges that may reproduce the properties of this resonance will be so horrible and so artificial that we would not use it for any sensible physical description of the amplitude. This essentially indicates that we cannot expect to have two complementary descriptions at every point, both of which are simple.

The question which remains to be seen is, therefore, where between the two extremes of global duality and strict local duality we really stand. We clearly do not have two complementary descriptions which are simple at every point in all cases. On the other hand we may have two simple complementary descriptions over relatively narrow energy regions in some processes and perhaps even at every point in some other specific processes. The next few sections will be devoted to this question and we shall try to see to what extent we can push the idea that simple descriptions in both channels are valid over small energy regions.

This is the place to define, at least in a loose way, some of the concepts usually used in the literature. "Strict local duality" is what we refer to, when we discuss the two complementary descriptions which are supposed to be valid at every single point. "Semi-local duality" means that the duality hypothesis in its simple form is valid over relatively small energy regions but not necessarily point by point. How local is "semi-local" we shall discuss in Sec. XXIX.

One crucial theoretical question concerning local duality we have already answered in Sec. VI and VII: this is the question of whether it is indeed possible, even in principle, for s-channel resonances to reproduce the properties of t-channel trajectories and vice versa. The answer to this question was positive and this means that the central question concerning the validity of local duality is a pure experimental question and not a question of possible inconsistency with some fundamental principle.

## XXV. LOCAL DUALITY

When we talk about local duality we refer to the assumption of the previous section (that we have two complementary descriptions at every point), but we usually also refer to the extra assumption that no exotic amplitudes exist in any channel. This extra assumption which was so useful and so crucial in the discussion of global duality also adds an extra strength to the assumption of local duality. It says that if in the t-channel we have an exotic amplitude, it will have to vanish not in an average sense, but point by point. That requires that in the s-channel we have cancellations which are true not only in an average sense, but point by point. Thus, if we consider a process like  $\pi\pi$  scattering with  $I_t = 2$  in the t-channel, at relatively low energies (such as  $(s)^{\frac{1}{2}} < 2$  BeV) we cannot claim that the s-channel

contribution of the  $\rho$  meson cancels the contribution of the  $f^0$  meson, since they do not appear precisely at the same energy. The  $\rho$  and  $f$  terms can cancel each other only in an average sense, integrated over the entire region from threshold to some point above the  $f^0$  mass. In order to obey local duality we will have to assume that every one of them is cancelled by a certain partner at the same energy. Similar situations will occur in many other processes and we shall discuss in the next few sections how well they are obeyed experimentally. Let us emphasize here again that local duality without the additional assumption of the absence of exotic amplitudes cannot be ruled out simply because it is always possible to construct sufficiently complicated mathematical structures that will obey it. Local duality plus the absence of exotic amplitudes is already a very meaningful statement which can be compared with experiment and can be, in principle and in practice, ruled out because it predicts the vanishing of a specific amplitude at every given point over a large energy range and this can be checked experimentally. We will see, in general, in the next few sections that local duality in its strict sense is absolutely wrong but that semi-local duality in the sense of averaging over a region of several hundred MeV, at least in some cases, seems plausible and it is conceivable that, in general, it is not far from the truth.

#### XXVI. INFINITELY RISING, INFINITELY MANY, TRAJECTORIES

Before we get to the discussion of experimental tests of local duality we have to emphasize that it is at this point that we have led ourselves into the situation of demanding an infinite number of infinitely rising Regge trajectories in any given channel. The trajectories have to be infinitely rising if we want resonances to exist and to dominate the amplitude at arbitrarily large energies. At every given point there have to be a large number of resonances and for an arbitrarily high energy there have to be an arbitrarily large numbers of such resonances if we want these resonances to cancel each other and obey all the required properties of local duality. Another way of saying this is the following: We need that a large number of s-channel resonances will reproduce precisely point by point all the properties of a t-channel exchange. But one of the properties of a t-channel exchange is a pole at a specific value of  $t$ , a pole which is not possessed by any single s-channel resonance. The only way for the s-channel resonances to produce such a pole is if we have an infinite number of them and the infinite sum diverges at the particular  $t$ -value of the pole while it does not diverge at other  $t$ -values. The same mechanism will enable a number of t-channel exchanges to produce a pole in the variable  $s$ . We therefore see that eventually, as we go to higher and higher energies, we need infinitely many trajectories which are infinitely rising. We do not, at this point, demand that these trajectories



are linear. This will have to be so only in specific models such as the Veneziano model and we shall come to it later in these notes. We only have to demand that the trajectories rise indefinitely. As far as we know, in order to obey local duality they can rise in various forms other than linear and no principle related to duality will be violated. It is, of course, impossible to answer experimentally whether or not we have infinitely rising, infinitely many trajectories since at any given moment, we have only a finite number of known resonances. Moreover, it is possible that the many resonances expected at sufficiently high energy will overlap and will be impossible to resolve from each other. In fact, even if these resonances do not exist, it is perfectly reasonable to use an approximation of a sum of such resonances (provided that it is simple enough) for the physical amplitude. There is no harm in approximating a smooth physical amplitude in which no resonances were directly observed by a sum of a large number of resonances, as long as the requirements which lead to such a sum of resonances have predictive power which leads to predictions which can be tested experimentally. We, therefore, conclude that as far as the question of having many resonances at large energies is concerned, the test of this possibility and the test of such theoretical models is not to look for such resonances (since even if they exist, they probably will never be found) but to look for predictions of a model which assumes such sums of resonances, and to see whether these predictions are verified experimentally.

#### XXVII. LOCAL DUALITY: THE $\sigma$ AND $\rho'$ MESONS

One of the most interesting predictions of local duality which is also a very convenient place for demonstrating its predictive power is the case of  $\pi\pi$  scattering. As we have already mentioned in Sec. XXV,  $\pi\pi$  scattering at low energies in the isotopic spin amplitude  $I_t = 2$  has to vanish. This vanishing has to be true at any given energy and therefore it can occur from the s-channel point of view only by cancellations, point by point, of various s-channel isotopic spin amplitudes. The absence of exotic states which is assumed here prevents us from having  $I_s = 2$  amplitudes and therefore the  $I_s = 1$  and  $I_s = 0$  amplitudes are the ones which have to cancel each other precisely at every energy. This means, for example, that at the position of the  $\rho$  meson there should be an  $I = 0$  amplitude equal in magnitude and with an appropriate sign so as to cancel the contribution of the  $\rho$  meson in the  $I_t = 2$  projection. This can happen only if we have an isotopic spin zero meson, degenerate with the  $\rho$  meson in mass, and with approximately the same coupling to the  $\pi\pi$  system. Such a meson has been observed in analysis of the  $\pi\pi$  phase shifts as obtained from extrapolating  $\pi N \rightarrow \pi\pi N$  data to the pole of the exchanged pion. This meson which is sometimes called  $\sigma$  and sometimes called  $\epsilon$ , presumably does have

a mass approximately equal to the  $\rho$  meson mass and a width which is at least as large as the  $\rho$  width and perhaps several times larger. While we cannot claim here an exact cancellation, it is amusing to see that we do have an  $I = 0$  meson very close to the  $\rho$  meson according to the prediction of local duality.

This happy state of affairs does not continue to hold, unfortunately, when we go to the mass of the  $f^0$  meson. At the mass of the  $f^0$  meson we need some  $I = 1$  meson to cancel the  $f^0$  contribution in the  $I_t = 2$  amplitude. Such a meson which is usually referred to as the  $\rho'$  meson should have a mass of 1250 MeV and a coupling to  $\pi\pi$  approximately equal to that of the  $f$  meson. Various searches for this meson in photoproduction and in  $\pi N$  collisions have failed and the present upper limits for the production of this meson are extremely small.<sup>29</sup> The chances are that such a meson does not exist. The absence of the  $\rho'$  meson at 1250 MeV should be regarded as an explicit failure of local duality and the absence of exotic amplitudes. This, by itself, should come as no surprise since we have already indicated that it would be very peculiar if the simple t-channel description would be true, point by point, over the entire low energy region. The question which remains to be answered, however, is why was the local duality assumption so successful in the case of the  $\rho$  meson, namely - why do we have a degenerate pair of mesons around 750 MeV? Is this an accident or is this really a consequence of local duality? It is very difficult to answer this question in a definite way. Arguments for the existence of a  $\sigma$  meson somewhere in the neighborhood of the  $\rho$  meson can be derived from sum rules which have nothing to do with duality such as the Adler sum rule for  $\pi\pi$  scattering.<sup>30</sup> We shall not get into a detailed discussion of this point here but we shall only emphasize that the mass equality between the  $\rho$  and  $\sigma$  mesons has been previously predicted on totally different grounds, while the presence of  $\rho'$  meson degenerate with the  $f^0$  is not a result of these considerations. We can, therefore, claim that local duality fails here, that the existence of the  $\sigma$  meson, from the point of view of local duality, is an accident, and that this meson is required by other considerations such as a combination of global duality assumptions and the Adler sum rule.

One point which is extremely important is that we have derived here the prediction for the existence of the  $\rho'$  meson at 1250 MeV from local duality alone without ever mentioning the Veneziano formula. The absence of this meson therefore indicates that local duality is too strong an assumption. Anything which we will assume in addition to local duality, clearly will not enable us to save the situation here. Only models which will avoid assuming local duality may be consistent with experiment at this point. The absence of the  $\rho'$  is therefore a piece of evidence against local duality and it is a piece of evidence against the Veneziano formula only to the extent that the Veneziano formula uses local duality. It is not a special property of the Veneziano formula.

XXVIII. LOCAL DUALITY:  $\pi N \rightarrow \pi \Delta$

Another case where we can apply the assumption of local duality and the absence of exotic states to a relatively simple reaction is the process  $\pi N \rightarrow \pi \Delta$ . This is perhaps the simplest process which can be performed experimentally and which allows an exotic  $I_t = 2$  t-channel amplitude. In the s-channel we can have  $I_s = 1/2$  and  $I_s = 3/2$  and if we demand that the  $I_t = 2$  amplitude vanishes point by point through the low energy region, we shall have to find cancellations between the  $I_s = 1/2$  and  $I_s = 3/2$  terms. The cancellations should occur point by point and, in particular, whenever we have an  $N^*$  resonance with  $I = 1/2$  we should also have a resonance with  $I = 3/2$  with an appropriate coupling to the process  $\pi N \rightarrow \pi \Delta$  so as to cancel in the  $I_t = 2$  amplitude. This is clearly wrong for resonances such as the nucleon, the  $\Delta$  (both below threshold for this process), the Roper resonance and the  $D_{13}$  (1520) resonance. The question that we ask here is whether this may be true at higher energies such as in the region of 1680 MeV resonances where we do have both  $I = 1/2$  and  $I = 3/2$  resonances in the s-channel. We know that cancellations between  $I = 1/2$  and  $I = 3/2$  do occur at higher energies, since we know experimentally that the double charge exchange is very weak in the forward direction at high energies in this process. The question which interests us here is at what energy this property of the amplitude begins to be true, and down to what energy in the resonance region we can still observe it. In order to answer this we have to have a phase shift analysis for the process  $\pi^- p \rightarrow \pi^+ \Delta^-$  and we have to consider specific helicity amplitudes or partial wave amplitudes as a function of energy and see whether or not the two s-channel isospins precisely cancel each other in the appropriate  $I_t = 2$  amplitude.

There is one experimental difficulty in performing the phase shift analysis for this process. The difficulty, peculiarly enough, comes from duality. Even if we would have enormous statistics in an experiment on  $\pi N \rightarrow \pi \Delta$ , we will have great difficulties in identifying those events which indeed correspond to a  $\Delta$  in the final state. The experimentalists, of course, observe  $\pi N \rightarrow \pi N$  and they have to isolate the  $\Delta$  events in the Dalitz plot for the final state. In energies such as the one discussed here, namely, around 1500 to 1800 MeV, there is a substantial overlap between the two  $\Delta$  bands in the Dalitz plot. Prior to the duality days this would lead to no difficulties. One would assume Breit-Wigner forms for the two  $\Delta$ 's with, possibly, a relative phase between them and then one would fit the entire Dalitz plot distribution with a sum of these two resonances and find the amplitudes for producing any one of them. Duality tells us, among other things, that we should never add the contribution of the two  $\Delta$ 's in the two bands. We should perhaps multiply them (particularly if we believe in the Veneziano formula) or do various

other things but we should certainly not add them because that would commit double counting. Duality therefore prevents the experimentalist, even if he has fantastic statistics, from isolating the  $\Delta$  in a proper way in his sample of events.

This difficulty prevents us from reaching any definite strong conclusions concerning the question of  $\pi N \rightarrow \pi \Delta$ . However, some qualitative remarks can be made on the basis of a preliminary phase shift analysis that was done on this process.<sup>31</sup> This phase shift analysis essentially ignores the fundamental question that we have discussed here but we believe that as far as its qualitative features, namely, the sign of the various amplitudes and the general order of magnitude, the results should not change much. Details will clearly change, when and if we learn how to analyze the Dalitz plot properly and how to isolate the  $\Delta$ -events. The results for the  $I_t = 2$  amplitude in the t-channel and for the four different helicity amplitude of the process  $\pi^- p \rightarrow \pi^+ \Delta^-$  are shown<sup>32</sup> in Fig. 33. We see that the  $I_t = 2$  amplitude does not vanish point by point. It is remarkable, however, that in the region from 1500 MeV to 1800 MeV the contribution of this amplitude in all cases changes sign and the integral over this region, to a good approximation, vanishes. This is particularly interesting in view of the fact that for different t-values the signs of specific contributions of the various regions change, but they change in such a way that if one term becomes negative, another becomes positive and vice versa.<sup>32</sup> We can certainly claim that over a region of several hundred MeV's in this energy domain, we have a certain amount of cancellations. On the other hand, we can certainly claim that strict local duality is definitely not obeyed here, since the amplitude does not vanish point by point, and since the resonances in the 1500 MeV region are not cancelled by any isospin 3/2 states at that point. The phenomenon that we observe here is basically that whatever happens in the 1500 MeV region is normally cancelled by the contents of the amplitudes in the region of 1600 to 1700 MeV. The conclusion is, again, that strict local duality is false, but that semi-local duality is not such a bad approximation. Let us emphasize again that stronger conclusions can be drawn only when we are able to handle the  $\Delta$ -separation properly in this process, and that this problem by itself, will require a much better understanding of duality for the low energy region.

#### XXIX. HOW LOCAL IS "LOCAL"?

We have seen in the last two sections (and we can see it in many other examples) that strict local duality is simply inconsistent with experiment. We have also claimed that semi-local duality is not so bad. In this section we shall try to answer the question of how local is "local" or rather - how local is "semi-local", namely, over what energy region do we have to integrate, normally, in order to get agreement between the predictions of semi-local duality and experiment. In

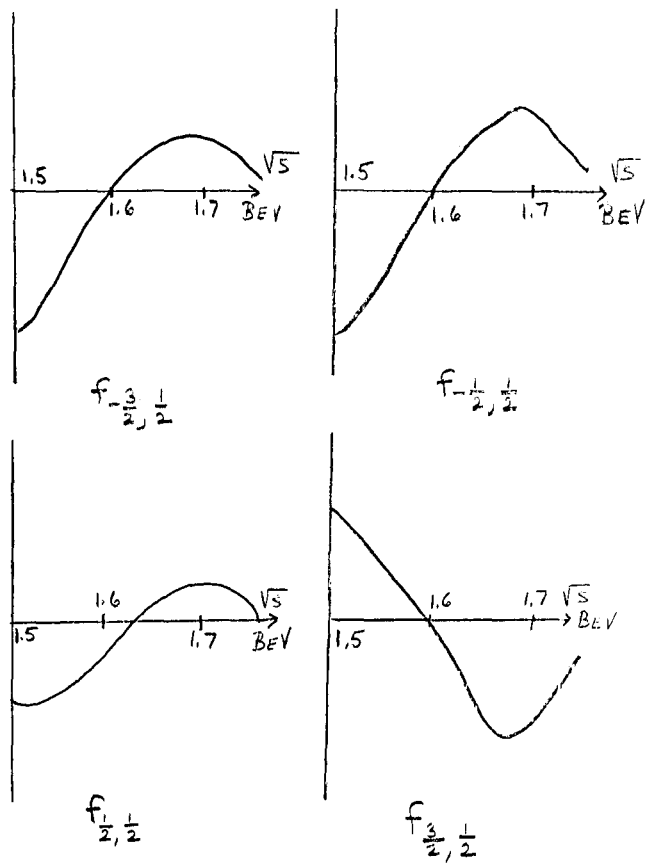


Fig. 33.

Helicity amplitudes for  $\pi N \rightarrow \pi \Delta$  at  $t=0$  (from reference 32)

the case of  $\pi N \rightarrow \pi \Delta$  it was clearly a region of several hundred MeV and in the case of  $\pi\pi$  scattering, in order to balance the  $f$  meson contribution, we have to associate it with the nearest  $I = 1$  mesons which could be either the  $\rho$  meson or the  $g$  meson. In that case, therefore, the domain of integration should also be of the order of magnitude of several hundred MeV and it will perhaps be slightly larger than in the  $\pi N \rightarrow \pi \Delta$  case. The general feeling that one gets by considering such processes, as well as by the  $\pi N$  example of Fig. 2, is that the process of averaging the resonance contribution by the extrapolated Regge trajectories is probably valid when done over ranges of several hundred MeV. This is much weaker than one would expect on the basis of strict local duality but it is much much stronger than one would ever dare to imagine before the days of duality or finite energy sum rules. No one would ever expect Regge pole theory to give any results in any average sense for the energy region below 2 BeV. Now we claim, and we have several interesting cases to support our claim, that when integrated over regions of several hundred MeV, in the low energy region, the extrapolated Regge contributions give approximately correct results in many cases.

The answer to our question of how local is "semi-local" would therefore be (i) global duality is probably a little bit too weak, (ii) strict local duality is certainly wrong. (iii) Regions of several hundreds MeV are normally sufficient for performing the semi-local average.

### XXX. FROM LOCAL DUALITY TO THE VENEZIANO FORMULA

In the last few paragraphs we have discussed the possibility that duality may be correct in a local or a semi-local way. One feature that duality should possess, if it is true on a local basis, is that a partial wave analysis of the contributions of the  $t$ -channel trajectories should exhibit all the appropriate  $s$ -channel resonances in any given process at any given point. We have seen in Secs. VI and VII that it is quite possible that  $s$ -channel resonances are produced by partial wave analysis of the  $t$ -channel exchanges and vice versa. However, there are a number of problems which remain open here. First of all, in order to ensure the proper co-existence of the  $s$ -channel poles and the  $t$ -channel poles we have to ensure that our dual amplitude obeys the requirements of crossing symmetry. Furthermore, we have to make sure that our  $t$ -channel exchanges are such that by partial wave analysis in the  $s$ -channel we will get only the  $s$ -channel resonances that we want and we should not get any unwanted resonances such as low mass resonances in very high partial waves (ancestors). Several other diseases could easily emerge from a careless partial wave analysis of the contributions of the  $t$ -channel exchanges, and although we have demonstrated in Secs. VI and VII that it is conceivable that duality in general and local duality in particular may be true,

one would really like to have an explicit working model which obeys these assumptions, even though such a model may have nothing to do with reality. Such a model would enable us to prove that duality is (at least theoretically) self consistent and that it may be formulated in a way that does not lead to unwanted resonances or to violation of the crossing properties. What one would like to have is therefore a closed expression which would allow us to express a hadronic scattering amplitude either as a sum of poles in one channel or as a sum of poles in the other channel in a manner that will prevent us from adding the poles in the two channels. Moreover, we would like our closed expression to obey crossing symmetry, to produce no unwanted resonances and to possess no exotic amplitudes in any channel. Such an expression can be constructed in several ways and in any of these ways it will have most of the wanted properties, but it will violate some other properties that we would like hadronic amplitudes to possess. (such as finite resonance widths or unitarity). The simplest closed form for a dual resonance model which (i) possesses crossing symmetry, (ii) has infinitely rising trajectories in all channels, (iii) obeys duality and (iv) does not lead to any unwanted singularities (ancestors) is the Veneziano formula. We shall discuss this formula in the next section. Here we would only add that the Veneziano formula is constructed on the basis of local duality, crossing symmetry and the narrow resonance approximation. Consequently, it cannot possibly succeed in explaining experimental results which are inconsistent with any of these ingredients. Since we have already seen that local duality in its strict form is experimentally inadequate, we should not expect the simplest Veneziano form to be a true picture or a good approximation of nature. It is clear that in the same way that local duality has to be corrected in one way or the other, the Veneziano formula can, at best, be a first step towards a correct theory and it is certainly not a correct theory by itself. We emphasize this before getting into any discussion of the formula itself since this should be clear, independent of the particular form of the Veneziano expression. Let us not forget that before writing the formula we have already encountered in our logical development failures such as the absence of the existence of the  $\rho'$  meson or the inaccuracy of strict local duality in  $\pi N \rightarrow \pi \Delta$ . These and other experimental difficulties accompany us as we start discussing the Veneziano formula, quite independent of its particular form.

### XXXI. THE VENEZIANO FORMULA

The two major characteristic properties of a dual resonance formula such as the Veneziano formula<sup>33</sup> are the following:

1. It has poles in the s-channel and poles in the t-channel in such a way that sums of an infinite number of s-channel poles can be re-expressed in terms of an infinite number of t-channel poles while every one of these sums by itself gives the complete amplitude (let us assume, for simplicity, that the u-channel is exotic and no poles in u exist).

2. The contributions of these poles should have the property that as we go to large s or large t, the amplitude obeys Regge behavior.

The simplest way of obtaining the Veneziano formula is according to a simple derivation due to Goebel. According to this approach we consider a set of poles in the variable s (note that we are using a narrow resonance approximation and therefore the poles would be on the real s axis). The poles in s would sit on Regge trajectories  $\alpha(s)$ . Let us suppose that we have poles for  $\alpha(s) = 1, 2, 3, \dots$ . Similarly, in the t-channel we have a trajectory  $\alpha(t)$  which gives us poles in those t-values corresponding to  $\alpha(t) = 1, 2, \dots$ . The poles in s should occur for all t-values corresponding to positive integer values of  $\alpha(s)$  and the poles in t should correspond to all s-values for any positive integer value of  $\alpha(t)$ . We, therefore, get the picture shown in Fig. 34 in which the s-t plane is covered by one set of parallel lines describing the positions of poles in s and a set of perpendicular lines describing the positions of the poles in t. The simplest expression that will have poles for every positive integer value of  $\alpha(s)$  is, of course,  $\Gamma(1-\alpha(s))$ . Similarly,  $\Gamma(1-\alpha(t))$  is capable of reproducing all the necessary poles in the variable t. If we now take the product of the two gamma functions we have a simple formula which has all the poles in s and all the poles in t, except that it has one unwanted feature. It has double poles at every point in which two positive integer values of  $\alpha(s)$  and  $\alpha(t)$  intersect. We want to remove these double poles since we do not expect such a phenomenon to occur in the physical hadronic amplitude. The simplest way to remove them is to multiply the product of the two gamma functions by another function which vanishes at every intersection. This could be easily done if we add a third set of lines along which  $[\alpha(s)+\alpha(t)]$  is equal to a given positive integer and consider the expression  $V(s,t) = \Gamma[1-\alpha(s)]\Gamma[1-\alpha(t)]/\Gamma[1-\alpha(s)-\alpha(t)]$ . This expression has poles in all the appropriate values of  $\alpha(s)$ , poles in all the appropriate values of  $\alpha(t)$  and all the double poles in the intersection points are removed by the gamma function in the denominator. The only feature that we got from this expression without really demanding it, is that it vanishes on all points on the diagonal lines, which are not intersection points. In the center of each square in Fig. 34 we should have a region in which our expression vanishes!



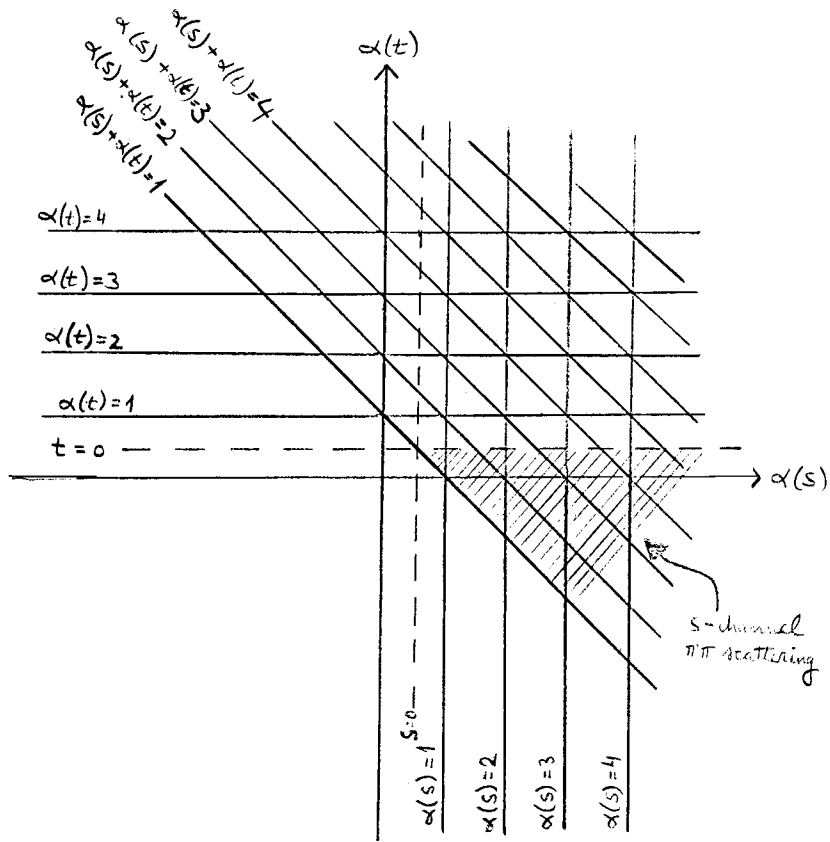


Fig. 34.

Goebel's derivation of the Veneziano formula (see text) .

Until now we have only shown that we have the correct set of poles in the s-channel and t-channel and that this set of poles provides us with an expression which does not add the pole terms of the two channels. What remains to be demanded is that as we go to large s or large t we have Regge behavior in these variables, respectively. In order to verify this, we have to study the asymptotic behavior of our function as  $s \rightarrow \infty$ . It is very easy to see that the asymptotic behavior will be of the general form  $[\alpha(s)]^{\alpha(t)}$ . This does not necessarily correspond to Regge behavior, namely to  $s^{\alpha(t)}$ . Regge behavior will be guaranteed in this case only if  $\alpha(s)$  is linearly related to s, namely, if our trajectory in the s-channel is linear. A similar condition holds for the trajectory in the t-channel,  $\alpha(t)$ . Only if this trajectory is linear in t we shall have Regge behavior as  $t \rightarrow \infty$ . We therefore conclude that our expression which has all the correct poles has to be supplemented by one requirement, namely, the requirement that the infinitely rising trajectories  $\alpha(s)$  and  $\alpha(t)$  are linear.

Note that since we are using the narrow resonance approximation, the Regge behavior will be correct only in an average sense. Along the real s-axis we clearly have poles which are equally spaced all the way to infinity and when we talk about Regge behavior as  $s \rightarrow \infty$  we really refer to an average Regge behavior. In other words - we have Regge behavior as we go along a ray which forms an arbitrarily small angle with the real axis and is therefore slightly removed from the actual positions of the resonances. In the real world, of course, the resonances have finite widths and the corresponding poles are therefore removed from the real s-axis. In that case Regge behavior can be true along the real s-axis.

We have, therefore, constructed here a formula possessing the proper s-channel and t-channel poles and having Regge behavior in all channels. The formula does not have any poles in u and it therefore corresponds to processes in which the u-channel is exotic, such as  $\pi^+ \pi^-$  elastic scattering. If we would like to discuss the entire family of  $\pi\pi \rightarrow \pi\pi$  reactions, we should add to the expression  $V(s,t)$  extra terms of the forms  $V(t,u)$  and  $V(s,u)$ . A combination of such terms which have the correct isospin properties will then provide us with a Veneziano formula for  $\pi\pi$  scattering. For other processes among spinless particles, one can always construct the appropriate formulae that will have all the required properties that we have assumed at the beginning of this section.

The theoretical importance of the Veneziano formula stems from the fact that this was the first explicit expression which showed that the requirement of duality is self-consistent and does not necessarily lead to any unwanted features such as unwanted poles, etc. Whether or not the Veneziano formula has anything to do with the actual physical hadronic amplitude remains to be seen. We shall discuss this briefly in the next sections, but a definite answer is not found yet. What is clear,

however, is that at least one important unrealistic assumption was made in the formula. This is the assumption of zero width for all resonances. This assumption by itself immediately leads to a violation of unitarity and to other related difficulties. It is clear that both from the theoretical point of view of preserving unitarity and from the experimental point of view of being able to discuss resonances with finite widths, we must be able to correct this. We shall return to this problem but let us immediately state here, that this question is not solved yet and therefore the route from the mathematical expression which demonstrates that duality is possible towards a physical theory which can be directly compared with experiment, is still not open.

Some other points concerning the Veneziano formula that should be mentioned here are the following:

1. The Pomeranchuk trajectory cannot be included in any simple way in the Veneziano formula. It is impossible to add the Pomeranchuk trajectory in any channel without producing exotic resonances in other channels. In constructing a Veneziano-like term, the Pomeranchuk contribution will therefore have to be added in some fashion, as was done in our discussion of two component amplitudes in Sec. XI. It is conceivable, however, that this term can emerge as a result of incorporating unitarity in an appropriate way into the Veneziano expression.

2. The Veneziano formula is clearly an explicit example of an exact resonance dominance case. The entire amplitude is given in the Veneziano approximation by a sum of poles and there is no part in the amplitude which is not accounted for by the contribution of these resonances. The question of resonance dominance and its experimental validity is therefore very relevant to the question of whether or not the Veneziano formula has something to do with the physical world. From that point of view, the Veneziano formula is supported by our observations of Sec. XIII that resonances do indeed dominate amplitudes which do not have Pomeranchuk contributions.

3. The Veneziano formula can be modified by adding several terms usually referred to as satellites. The general form of such a satellite for  $V(s,t)$  is  $\Gamma[n-\alpha(s)]\Gamma[m-\alpha(t)]/\Gamma[p-\alpha(s)-\alpha(t)]$ . If we add a sufficient number of satellites we can have a certain amount of freedom in choosing the parameters of the different terms. The relative strength of the satellites is not determined a priori, and since every one of them obeys the requirements that we started with, so will any linear combination of them. It is important to note that by playing with various combinations of satellites we can cancel certain poles. In such a case we abandon strict local duality and remain only with some kind of an average duality. Every satellite by itself does obey strict local duality, but combinations of satellites can be constructed in such a way that specific poles will disappear and only the

average contributions will have all the appropriate properties. In such a way we could invent, for example,  $\pi\pi$  scattering formulae which do not have a strong  $\rho'$  meson, but the price we pay for it is losing most of our predictive power by including the free parameters of the satellite. On the other hand, one could also claim that there is no theoretical reason a priori to prefer one term over the others or to choose the possibility of having no satellites over the possibility of having many of them.

4. The generalization of the Veneziano formula to cases in which there is more than one helicity amplitude is very difficult. No explicit expression which obeys all the necessary conditions, including Fermion Regge trajectories in certain channels and Boson Regge trajectories in other channels, have been constructed so far. In particular, there is no satisfactory expression for  $\pi N$  scattering yet. This spin complication may be a technicality. On the other hand, it may indicate that the formula cannot exist on any level higher than the most simple case of spinless external particle. We do not know whether this is the case or not.

#### XXXII. THE VENEZIANO FORMULA FOR n-POINT AMPLITUDES

The generalization of the Veneziano formula to processes with multi-particle final states such as 5-point functions or, in general, n-point functions was studied by a large number of authors.<sup>34</sup> We shall not attempt here a detailed discussion of this problem, since on one hand they are extensively discussed in many review articles that have appeared recently, and on the other hand, they cannot be covered in the short space available to us here. Let us only remark that these formulae have enormous theoretical importance, since they are crucial for solving two of the main difficulties of the Veneziano formula for the 4-point amplitude. In addition, they are, of course, needed if one is to discuss experimental situations with 5, 6 or more external particles.

The relevance of the n-point function to the 4-point function stems from the fact that the unitarization of the Veneziano formula for the 4-point amplitude necessitates integration over intermediate states of any number of particles and such intermediate states can be computed only if we have an appropriate n-point formula. It is also relevant to the spin difficulty in the 4-point Veneziano formula, because it is conceivable that an external particle with spin which appears in a given 4-point function can be constructed from a number of spinless particles in the n-point function. For example, the formula for  $\pi\rho \rightarrow \pi\rho$  could, in principle, be constructed from the 6-point function where we consider the particular case in which two pairs of external  $\pi$  mesons happen to correspond to physical  $\rho$  mesons. If we had an appropriate 6-point function with all the correct properties, then  $\pi\rho \rightarrow \pi\rho$  would simply be one special case of such a 6-point function.

The explicit constructions that were made so far, are valid only for the extremely degenerate case of spinless external particles, trajectories with intercept  $\alpha(0) < 0$ , and complete degeneracy of all external masses. The isospin properties or any other internal symmetry question were not yet solved in complete generality with respect to the n-point Veneziano function. These are very unfortunate aspects of the problem, particularly since the isospin question or, in general, the internal symmetry question plays such a crucial role in duality, in view of the importance of the absence of exotic states. Furthermore, experimentally, most interesting cases in which duality can be tested correspond to trajectories having  $\alpha(0) > 0$  and therefore the particular case which was studied, so far, is completely unrealistic. No one has succeeded in demonstrating explicitly whether the difficulties which prevents us from developing a complete n-point function which is relevant to realistic cases are purely technical difficulties which can be encountered by sufficient clever mathematical manipulations, or that for other situations it is impossible to construct a self-consistent n-point function. These questions will have to be answered in the near future.

Another question to which the construction of an n-point function is relevant is the question of the dependence of a 4-point amplitude on the masses of the external particles. The masses of the external particles are normally not a variable of the problem. However, in some specific cases such as amplitudes in which one of the external particles is a weak or an electromagnetic current and also in cases in which the external particles can be different particles with the same quantum numbers, one would like to study the amplitude as a function of one or more of its external masses. This, again, can be most probably solved if we fully understand the n-point function, since an external particle with a variable mass can always be considered as some combination of two or more external particles in a multi-particle formula. By changing the appropriate sub-energy variable we could study the dependence of the amplitude on the external mass in a given 4-point function.

We shall not comment here any more on the technicalities related to the construction of the n-point Veneziano function and we refer the reader to Ref. 34 for details.

### XXXIII. PHENOMENOLOGY AND THE VENEZIANO FORMULA

We have emphasized in Sec. XXXI that the Veneziano formula is too theoretical to be applied directly to experiments since it is based on the zero width approximation and it violates unitarity - two properties which are foreign to experimental amplitudes. However, even without solving completely the question of introducing finite widths or forcing the amplitude to obey the unitarity condition

in all channels, one could try to apply the Veneziano formula to specific phenomenological questions in specific kinematic domains. This can be done, for example, by constructing trajectories which are not strictly linear and which have an imaginary part which allows a finite width for the resonances along the trajectory. No way of doing this in a crossing symmetric manner which also preserves Regge behavior was suggested so far. However, if we are interested in experimental comparison in one specific channel or one restricted kinematical domain, we do not necessarily have to insist, for the time being, that we have a fully crossing symmetric expression, or that Regge behavior is valid in all directions. We may hope that by approximating our trajectories by a simple form with an appropriate imaginary part we can reach a contact with experimental data. A large number of attempts to fit various 4-point and 5-point processes with such Veneziano expressions were carried out and we shall discuss only a few of them here.

But before discussing any quantitative fits, let us emphasize one point which we find extremely interesting and puzzling. We have indicated in Sec. XXXI that the only qualitative property of the Veneziano amplitude that we did not demand to begin with, is the existence of regions in the  $s$ - $t$  plane where the amplitude vanishes. These regions correspond to those diagonal lines in Fig. 34 which are between two intersection points. The diagonal lines provide the Veneziano formula with a way of preventing double poles. This is not the only possible way to do it, but it is the particular way that the formula chooses. Those diagonal zeros predict, however, that if we are able to study the physical amplitude over a region of the  $s$ - $t$  plane, in addition to the poles which correspond to the vertical and horizontal lines in Fig. 34, we should also observe zeros corresponding to the diagonal lines! In order to study such an amplitude in a region of the  $s$ - $t$  plane we may look at specific Dalitz plots. However, in order to observe the effect that we are looking for, we should consider a Dalitz plot for the decay of a state with a definite spin parity into three particles. Furthermore, our Dalitz plot should include at least two vertical and two horizontal lines corresponding to resonance regions, so as to enable us to have at least one region within the Dalitz plot in which we should look for this zero. It is very hard to find a case in which all of these conditions are satisfied. For example, the decay of  $\eta \rightarrow 3\pi$  or  $\omega \rightarrow 3\pi$  do not provide us with a Dalitz plot which is large enough. Lovelace has pointed out<sup>35</sup> that there is one case in which we do have a sufficiently large Dalitz plot with a state with well defined spin parity decaying into three pions. This is the case of  $\bar{p}n$  annihilation at rest into three pions. The  $\bar{p}n$  system, at rest, is experimentally known to be in an S-wave and can easily be shown to possess the quantum numbers of the  $\pi$  meson. We, therefore, have a process very similar to  $\pi\pi$  elastic scattering, except that one of the external "pions" has a

mass of 1.88 BeV corresponding to the threshold center of mass energy of the  $\bar{p}n$  system. The Dalitz plot for this decay which is shown in Fig. 35 is sufficiently large so that we can see the regions of the  $\rho$  meson and the  $f^0$  meson in the two variables, and it is the only place in which we can easily see the explicit presence of the "hole" or the "vacancy" predicted by the diagonal zero in the Veneziano amplitude. Remarkably enough, it turns out<sup>36</sup> that there is an enormous "hole" with a complete absence of any events, precisely in the expected place at the center of the Dalitz plot for this decay. This remarkable fact which is very significant statistically, was not explained prior to the Lovelace analysis. Experimentally it is even more significant that we would ever dare to expect, even if we believed that the Veneziano formula is the correct expression for the amplitude. There is a substantial region in the Dalitz plot in which not a single event exists. Further inspection of the Dalitz plot indicates, unfortunately, that a simple Veneziano term cannot explain the experimental observations. In particular, some kind of a  $\rho'$  meson seems to be necessary in order to explain the observations but such a  $\rho'$  does not exist. Moreover, at least two terms (including one satellite) are necessary and a priori we do not know what should be the relative strength of these terms. All of these problems, however, do not diminish the surprising success of the qualitative prediction of the formula, and we believe that one should not be too disturbed by the quantitative difficulties at the present stage. In this connection we might add that by considering the 5-point function and treating the  $\bar{p}$  and the  $n$  as particles, it has been possible<sup>37</sup> to correlate the two coefficients of the two necessary terms in the  $\bar{p}n \rightarrow 3\pi$  amplitude which are needed in order to fit the experimental data for this Dalitz plot (Fig. 35). It would be extremely interesting to see if a similar hole is observed in the middle of the Dalitz plot for the process  $\bar{p}n \rightarrow KK\pi$  which is not yet available.

Another set of interesting predictions from a 5-point Veneziano formula was obtained by Törnquist and Petersson.<sup>38</sup> They have made a large number of assumptions, some of which we believe to be fairly unreasonable. However, after making these assumptions with which one could argue, they have succeeded in fitting an incredible amount of experimental data on the process  $K^-p \rightarrow \pi^+\pi^-\Lambda$  with only one parameter (which determines the overall magnitude of the process). The data that they fit (Figs. 36-38) include energy dependence, angular distributions, momentum distributions, cross sections for specific channels, invariant mass plots, etc. All of these data are fitted with one parameter and in spite of the fact that many many assumptions are made, we consider these fits as extremely interesting. Some of the assumptions which are made and which are not very reliable include ignoring the spins of the baryon (since no appropriate spin treatment has been proposed yet for the Veneziano formula and particularly for the 5-point function), and choosing

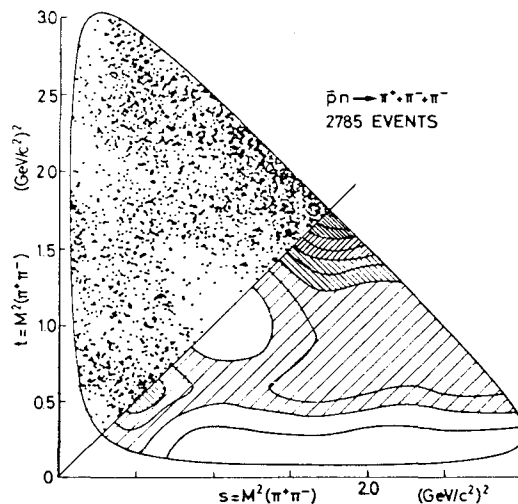


Fig. 35

The  $\bar{p}n \rightarrow \pi^+ \pi^- \pi^-$  Dalitz plot (References 35, 36).

specific channels in the 5-point functions which are inconsistent with the duality diagrams. We are not sure that the duality diagrams should be obeyed. However, the channels chosen by Törnquist and Petersson, especially for some sub-processes such as  $\bar{K}p \rightarrow \pi Y_1^*$ , are related by SU(3) to exotic amplitudes, either in the s-channel or in the t-channel. Such amplitudes might exist experimentally, as we have mentioned before, but we believe that one would not like to pursue the entire question of duality if strong exotic amplitudes exist, since most of the relevant predictions of duality are completely lost, including predictions which are used by Törnquist and Petersson in their fits, such as exchange degeneracy. We therefore feel (and in that respect we agree with Törnquist and Petersson) that while their fit should not be accepted as the final word on this process, it is sufficiently remarkable to be considered as a good starting point for studying the phenomenology of 5-point processes using various modifications of the Veneziano formula.

Other fits to physical processes were performed for  $\pi\pi \rightarrow \pi\pi$  (for off-mass shell pions) as well as for  $\pi K \rightarrow \pi K$ . These were extensively reviewed by Lovelace<sup>39</sup> and we do not wish to return to them here.

One extremely important lesson that we learned from the phenomenological Veneziano fits to various processes is the following: Experimentally, one observes in almost any high energy bubble chamber experiment a large number of invariant mass plots which do not look at all as if they are dominated by resonances. That might be considered as evidence against the resonance dominance assumption and against the entire spirit of the resonance dominance model which is one of the fundamental

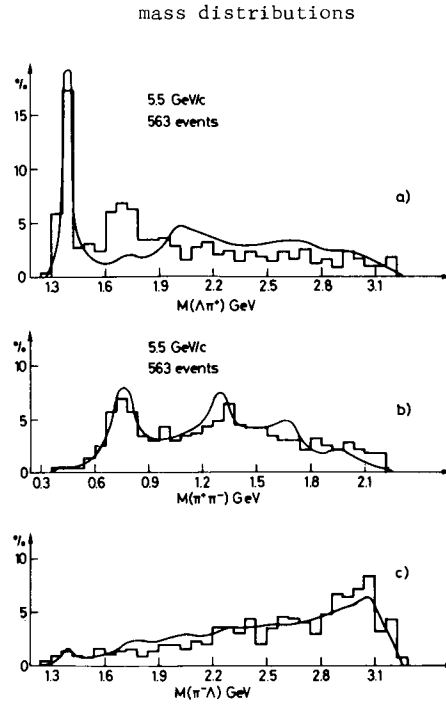
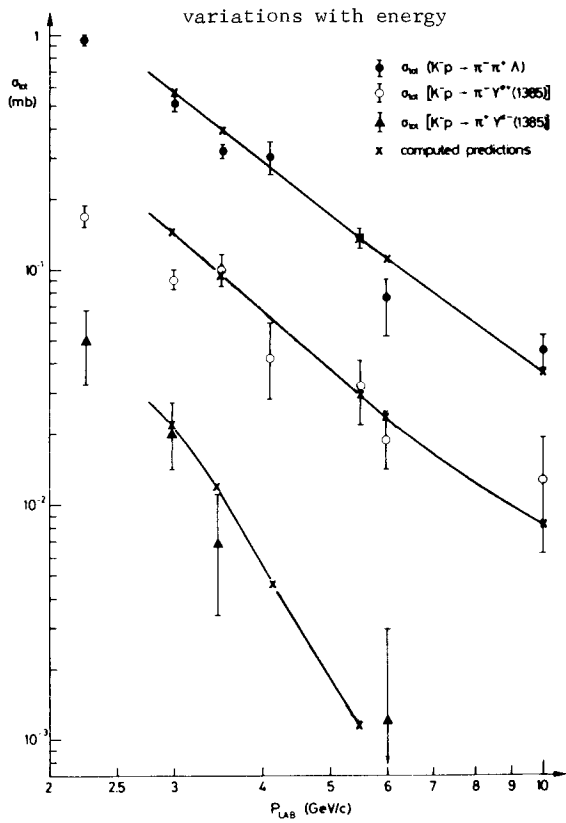


aspects of duality. However, the Veneziano formula is, of course, an extreme case of resonance dominance as it tells us that the entire amplitude is given in all channels by resonances alone. It is, therefore, extremely interesting to observe the fits in Figs. 36-38 as well as similar other fits for other processes that were suggested, and to notice that in these fits the theoretical curve is obtained by a sum of resonances with no background at all, and it does not look any different from those invariant mass plots which would normally be considered as indicating very few, if any, resonances. The lesson is, therefore, that a fairly smooth invariant mass plot which indicates only one or two clear resonances could very often be fitted very well as a combination of 4, 5, or 6 resonances and the fact that experimentally these are not resolved does not mean that the theoretical assumption of resonance dominance is invalid for these processes. It, of course, does not mean the contrary: if we do not see the resonances, it does not mean that they do exist. but we should not jump into negative conclusions in this case.

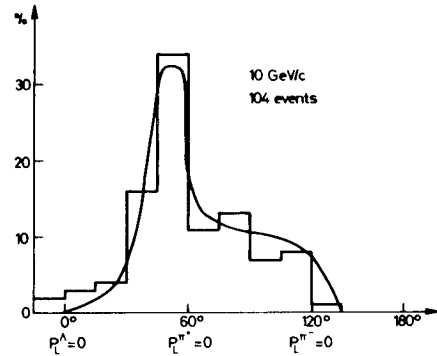
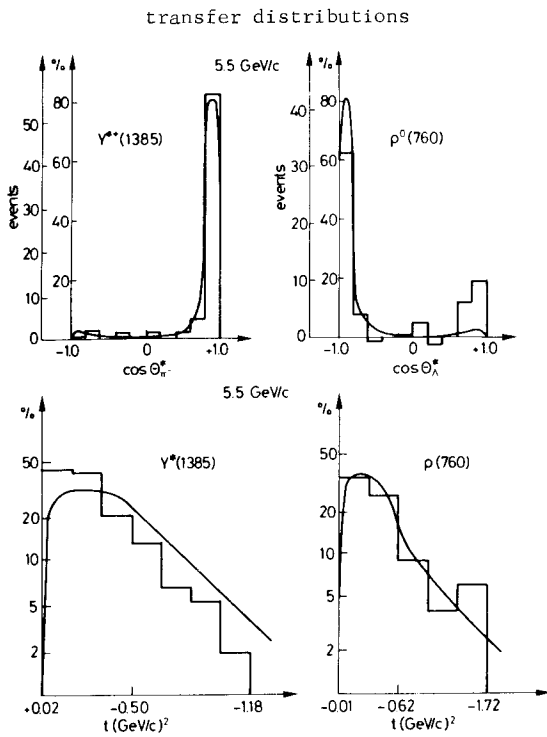
While there is no theoretical foundation for performing phenomenological Veneziano fits, in view of the unitarity problems, etc., one should probably continue to pursue this line of attack and to study additional experimental questions in terms of ad hoc modified Veneziano expressions. We should do this in order to see whether the qualitative aspects and the approximate quantitative aspects of hadronic amplitudes resemble various features of the Veneziano formula. In particular, we would assign extreme importance to further tests on the question of the existence of the zeros which are so special and so unique to the Veneziano formula and we would also ask ourselves whether the dependence of the 4-point amplitudes on the external masses can be answered appropriately in additional cases by Veneziano terms. Another crucial point which has to be answered and to which we do not have a satisfactory answer, so far, is how necessary are the satellites. Even if the Veneziano formula is true, it is not clear that it is simple. This is similar to the situation in Regge theory. It is probably true that we can fit the data by a sufficient number of Regge poles, but it is extremely important to know whether we can fit the data by one or two Regge poles in every process. Similarly, even if the general Veneziano formula is correct, it will become useful and meaningful only if we can fit most processes by one or two Veneziano terms and do not have to use a large number of satellites. All of these questions can be perhaps answered by a sufficiently careful study of various phenomenological situations.

#### XXXIV. THE FUNDAMENTAL THEORETICAL DIFFICULTIES OF THE VENEZIANO FORMULA

We have already mentioned that the unitarization of the Veneziano formula is a difficult problem which has to be answered before we accept it as a step toward a final theory for hadronic interactions. Similarly, (and these are quite



longitudinal phase space  
with angular distribution



angular distributions

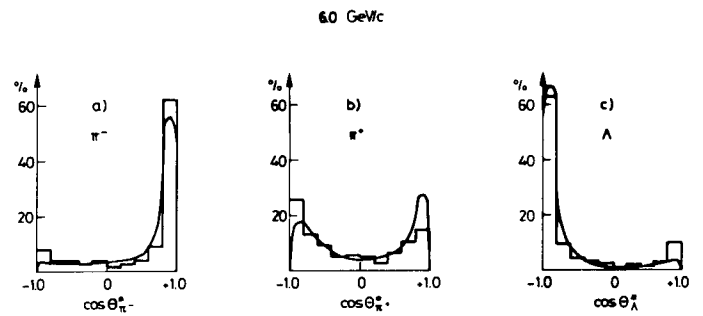


Fig. 36.

Veneziano fits to  $K^-p \rightarrow \pi^+ \pi^- \Lambda$  (Reference 38).

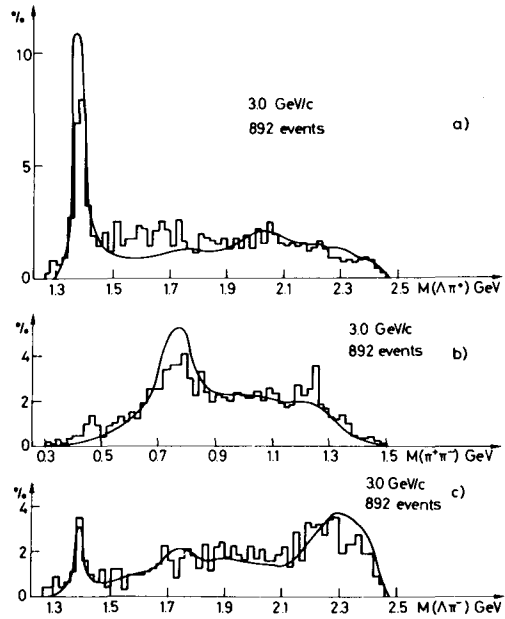


Fig. 37.

Veneziano fits to  $K^-p \rightarrow \pi^+\pi^-\Lambda$  (Reference 38).

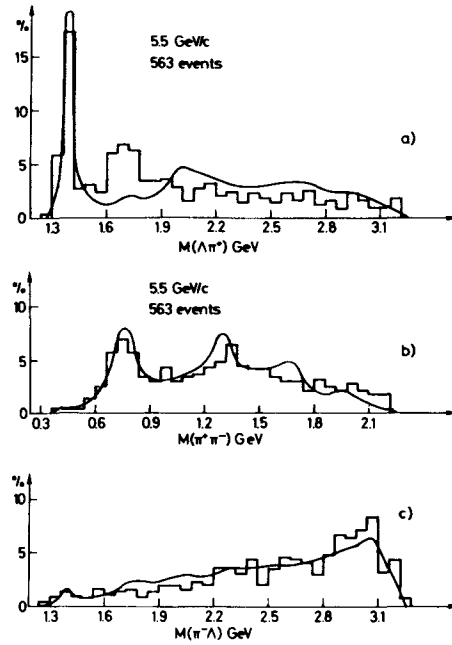


Fig. 38.

Veneziano fits to  $K^-p \rightarrow \pi^+\pi^-\Lambda$  (Reference 38).

related problems) one has to impose the requirement of factorization at every pole of the formula. Another theoretical problem, which we have mentioned, is the question of introducing spin in an appropriate way into the formula. To these we have to add the question of the Pomeranchuk trajectory and the question of whether or not we can have trajectories with  $\alpha(0) > 0$  in a construction of the n-point function.

The most optimistic point of view that one could take would be the following. The Veneziano formula is similar in a way to a Born term in perturbation theory. The Born term in perturbation theory does not obey unitarity, it has only a simple singularity structure, it has poles but no cuts, it does not have any kind of a Pomeranchuk contribution in any sense, and it provides us only with the first step towards a theory rather than with the complete picture. Similarly, it is conceivable that the simple Veneziano expression is a "Born term" in some kind of a theory of strong interactions, namely, it is possible that if we learn to iterate the simple Veneziano formula in an appropriate way by computing all possible diagrams with multi-particle terms in the intermediate level, we would be able to construct a series of terms, every one of which belonging to some expansion, and the full expansion could perhaps obey unitarity and all the other requirements and supply us with a theory for hadronic processes. Such a program is extremely ambitious. Nevertheless, several authors<sup>40</sup> have undertaken to start such a program and studied several properties which will be required for the final amplitude, had we succeeded in building it in such a way. Among the various interesting properties that were found, so far, we could mention the problem of the enormous degeneracy of states in the spectrum of hadrons which is imposed by the unitarity and the factorization requirements.

#### XXXV. OPEN PROBLEMS

We shall summarize our review of duality and its various aspects by listing some of the most interesting and crucial open problems which we have encountered during our discussion.

We should try to understand in detail the relation between duality, the absence of exotic states and the quark model. This is the first time that we have a bootstrap scheme which is very intimately related with the possible existence of fundamental building blocks - the quarks. Both the mathematical aspect as well as the possibility of the existence of concrete quarks should be pursued in this connection.

The complete failure of duality and the absence of exotic states in the baryon-antibaryon case should also be studied very carefully. As we have emphasized, we do not believe that this failure is sufficient to lead us to throw away the

entire scheme. This failure may be trying to teach us some fundamental thing on the nature of baryons and their construction or their properties. It is also possible that this catastrophe is trying to teach us something about the specific way in which duality and the absence of exotic amplitudes are broken.

The phenomenological question of a proper way of introducing Regge cuts into the description of hadronic processes should, of course, be studied quite independent of duality. However, in the context of duality it has special importance and we should try to understand this as well. In particular, one should study the possibility that the cuts are added to the poles in order to implement the requirements of the absorption model, and that from the s-channel point of view duality tells us that this is reflected by a dominance of the peripheral resonances.

Another aspect which should be studied is, of course, the various possibilities of starting from the Veneziano formula and continuing towards a theory of hadronic processes. These attempts, according to which the Veneziano formula is the Born term of a new theory of strong interactions, should be pursued in spite of the fact that some of the forecast has been fairly pessimistic. The ambitious goal of these attempts is too important.

For experimentalists there is another question which is extremely crucial and which will have to be answered. This is the question of finding a correct practical way of analyzing processes with three or more particles in the final state. The simple case of overlapping resonances in the Dalitz plot has become totally obscure and complicated with the introduction of duality. Previously, the custom was to add two Breit-Wigner formulae for the two overlapping resonances (possible with some phase) and to try to fit the Dalitz plot with this assumption. Duality says that this is illegal and that double counting is committed in this way, but duality does not provide us with any explicit simple way of replacing the old-fashioned way of analyzing Dalitz plots. The Veneziano formula could be one way of doing this but this is a specific model which goes far beyond the basic assumptions and notions of duality. It is true that, theoretically, it would be enough to consider all resonances in one of the variables and forget about the resonances in the other variable, but simplicity requires in many cases that we consider only one or two resonances in every one of the variables and then the question of the overlap is too difficult to solve in simple terms. We certainly owe the experimentalists an answer to this question, but the last two years have shown that this answer is not easy to get.

One other question which deserves attention is the large number of symmetry or quasi-symmetry principles which have been accumulated and which all have some grain of truth. One can easily see that it is impossible to implement all of these symmetry principles simultaneously without running into inconsistencies. How to

correlate and lead these symmetries to co-existence remains to be seen. For example, the  $\rho$  meson is related by the quark model or by SU(6) symmetry to the  $\pi$  meson and its octet, since they are the S-wave quark-antiquark system or the 35 representation of SU(6). The  $\rho$  meson is related somehow to the  $A_1$  meson by chiral symmetry in which they both belong to the same representation. Even mass relations between the two mesons can be obtained in such a way ( $m_{A_1} = (2)^{\frac{1}{2}} m_{\rho}$ ). On the other hand, duality relates the  $\rho$  trajectory to the  $f^0$  trajectory or the  $A_2$  trajectory because of exchange degeneracy, and strict local duality relates the  $\rho$  meson to the  $\sigma$  meson since they are needed to cancel each other in the specific mass of 750 MeV in  $\pi\pi$  scattering. Thus we see that the  $\rho$  meson is related to pseudoscalar mesons, to scalar mesons, to tensor mesons and to the axial vector mesons by various symmetry principles and every one of these principles even leads to mass relations. Exchange degeneracy is essentially a mass relation between the two trajectories, the  $\rho$  and the  $\pi$  are related by SU(6) or quark model symmetry breaking, the  $\rho$  and  $A_1$  are related by the Weinberg mass relation and the  $\rho$  and the  $\sigma$  should be degenerate by local duality. It is clear that it is very difficult to construct some global theory which will have all these symmetry properties incorporated in it. On the other hand, it is also clear that every single one of these symmetries is meaningful in one sense or the other. Clearly, the quark model, SU(6), chiral symmetry, exchange degeneracy and duality are at least approximately true. It should, therefore, be extremely interesting to try to incorporate all of these ideas into some overall symmetry scheme with an appropriate way of breaking, which will provide us with the specific partial symmetries that we have listed here.

## REFERENCES

1. K. Igi and S. Matsuda, Phys. Rev. Letters 18, 625 (1967); A. Logunov, L.D. Soloviev and A.N. Tavkhelidze, Phys. Letters 24B, 181 (1967).
2. R. Dolen, D. Horn and C. Schmid, Phys. Rev. 166, 1768 (1968).
3. See e.g. Proceedings of the Regge Cut Conference, Madison, Wisconsin (1969); M. Ross, invited talk at the Irvine Regge Pole Conference, December (1969); Chan Hong Mo, Rapporteur talk, Proceedings of the Vienna Conference (1968); H. Harari, Review talk, Proceedings of the Liverpool Electron-Photon Conference (1969).
4. See e.g., S. Matsuda and K. Igi, Phys. Rev. Letters 19, 928 (1967); S.Y. Chu and D.P. Roy, Phys. Rev. Letters 20, 958 (1968); G.V. Dass and C. Michael, Phys. Rev. Letters 20, 1066 (1968); F.J. Gilman, H. Harari and Y. Zarmi, Phys. Rev. Letters 21, 323 (1968); K.V. Vasavada and K. Raman, Phys. Rev. Letters 21, 577 (1968); R. Aviv and D. Horn, Phys. Rev. Letters 21, 704 (1968); A. Bietti et al., Phys. Letters 26B, 457 (1968); P. di-Vecchia et al., Phys. Letters 27B, 296 (1968); V. Barger and R.J.N. Phillips, Phys. Rev. Letters 21, 865 (1968) and Phys. Letters 29B, 503 (1969); J.D. Jackson and C. Quigg, Phys. Letters 29B, 236 (1969).
5. H. Harari and Y. Zarmi, Phys. Rev. (in print); H. Harari, Phys. Rev. Letters 22, 562 (1969).
6. J. Shapiro, Phys. Rev. 179, 1345 (1969).
7. C. Schmid, Phys. Rev. Letters 20, 689 (1968).
8. C.B. Chiu and A. Kotanski, Nucl. Phys. B7, 615 (1968).
9. V. Barger and D. Cline, Phys. Rev. Letters 16, 913 (1966); V. Barger and M. Olsson, Phys. Rev. 151, 1123 (1966).
10. C.B. Chiu and A.V. Stirling, Nuovo Cimento 56A, 805 (1968); H. Harari and Y. Zarmi, Ref. 5.
11. A. Donnachie and R.G. Kirsopp, Nucl. Phys. B10, 433 (1969).
12. H. Harari, Phys. Rev. Letters 20, 1395 (1968).
13. P.G.O. Freund, Phys. Rev. Letters 20, 235 (1968).
14. H. Harari and Y. Zarmi, Ref. 5.
15. H.G. Hilpert et al., Contributed paper to the Liverpool Electron-Photon Conference (1969).
16. H.W. Atherton et al., Fast Antiproton Group, CERN preprint, May 1969
17. A. Boyarsky et al., Contributed papers to the Liverpool Electron-Photon Conference (1969).
18. R.C. Arnold, Phys. Rev. Letters 14, 657 (1965).
19. F.J. Gilman, Phys. Rev. (to be published).

20. D. Cline, J. Matos and D.D. Reeder, Phys. Rev. Letters 23, 1318 (1969).
21. K.W. Lai and J. Louie, Contributed paper to the Irvine Regge-Pole Conference December (1969).
22. V. Barger and L. Durand, III, Phys. Rev. Letters 19, 1295 (1967); M. Le Bellac, Phys. Letters 25B, 524 (1967); M. Aderholz et al., Phys. Letters 27B, 174 (1968).
23. C.B. Chiu and J. Finkelstein, Phys. Letters 27B, 510 (1968).
24. A. Schwimmer, Phys. Rev. 184, 1508 (1969).
25. J.L. Rosner, Phys. Rev. Letters 21, 950 (1968).
26. H.J. Lipkin, Nucl. Phys. B9, 349 (1969).
27. H. Harari, Phys. Rev. Letters 22, 562 (1969).
28. J.L. Rosner, Phys. Rev. Letters 22, 689 (1969).
29. See e.g., A. Silverman, Review talk, Proceedings of the Liverpool Electron-Photon Conference (1969).
30. S.L. Adler, Phys. Rev. 140, B736 (1965); F.J. Gilman and H. Harari, Phys. Rev. 165, 1803 (1967).
31. A. Brody et al., Contributed paper to the Vienna Conference (1968).
32. A. Kerman and H.K. Shepard, Riverside preprint (1969).
33. G. Veneziano, Nuovo Cimento 57A, 190 (1968).
34. Chan Hong Mo, Phys. Letters 28B, 425 (1969); K. Bardakci and H. Ruegg, Phys. Letters 28B, 306 (1969); Chan Hong Mo and T.S. Tsun, Phys. Letters 28B, 485 (1969); M.A. Virasoro, Phys. Rev. Letters 22, 37 (1969); C. Goebel and B. Sakita, Phys. Rev. Letters 22, 257 (1969); Z. Koba and H.B. Nielsen, Nucl. Phys. B10, 633 (1969).
35. C. Lovelace, Phys. Letters 28B, 264 (1968).
36. P. Anninos et al., Phys. Rev. Letters 20, 402 (1968).
37. H.R. Rubinstein, E.J. Squires and N. Chaichian, Phys. Letters 30B, 189 (1969).
38. B. Petersson and N.A. Törnquist, Nucl. Phys. B13, 629 (1969).
39. C. Lovelace, Review talk at the Argonne Conference on  $\pi\pi$  Interactions (1969).
40. K. Kikkawa, B. Sakita and M.A. Virasoro, Phys. Rev. 184, 170 (1969); S. Fubini and G. Veneziano, Nuovo Cimento (in print)



